

Arthritis & Rheumatology

An Official Journal of the American College of Rheumatology
www.arthritisrheum.org and wileyonlinelibrary.com

Editor

Daniel H. Solomon, MD, MPH, *Boston*

Deputy Editors

Richard J. Bucala, MD, PhD, *New Haven*

Mariana J. Kaplan, MD, *Bethesda*

Peter A. Nigrovic, MD, *Boston*

Co-Editors

Karen H. Costenbader, MD, MPH, *Boston*

David T. Felson, MD, MPH, *Boston*

Richard F. Loeser Jr., MD, *Chapel Hill*

Social Media Editor

Paul H. Sufka, MD, *St. Paul*

Journal Publications Committee

Shervin Assassi, MD, MS, *Chair, Houston*

Adam Berlinberg, MD, *Denver*

Deborah Feldman, PhD, *Montreal*

Meenakshi Jolly, MD, MS, *Chicago*

Donnamarie Krause, PhD, OTR/L, *Las Vegas*

Uyen-Sa Nguyen, MPH, DSc, *Fort Worth*

Michelle Ormseth, MD, *Nashville*

R. Hal Scofield, MD, *Oklahoma City*

Editorial Staff

Jane S. Diamond, MPH, *Managing Editor, Atlanta*

Ilani S. Lorber, MA, *Assistant Managing Editor, Atlanta*

Lesley W. Allen, *Senior Manuscript Editor, Atlanta*

Kelly Barraza, *Manuscript Editor, Atlanta*

Jessica Hamilton, *Manuscript Editor, Atlanta*

Sara Omer, *Manuscript Editor, Atlanta*

Emily W. Wehby, MA, *Manuscript Editor, Atlanta*

Stefanie L. McKain, *Editorial Coordinator, Atlanta*

Brittany Swett, *Assistant Editor, Boston*

Will Galanis, *Production Editor, Boston*

Associate Editors

Marta Alarcón-Riquelme, MD, PhD, *Granada*

Heather G. Allore, PhD, *New Haven*

Neal Basu, MD, PhD, *Glasgow*

Edward M. Behrens, MD, *Philadelphia*

Bryce Binstadt, MD, PhD, *Minneapolis*

John Carrino, MD, MPH, *New York*

Lisa Christopher-Stine, MD, MPH,
Baltimore

Andrew Cope, MD, PhD, *London*

Nicola Dalbeth, MD, FRACP, *Auckland*

Brian M. Feldman, MD, FRCPC, MSc, *Toronto*

Richard A. Furie, MD, *Great Neck*

J. Michelle Kahlenberg, MD, PhD,
Ann Arbor

Benjamin Leder, MD, *Boston*

Yvonne Lee, MD, MMSc, *Chicago*

Katherine Liao, MD, MPH, *Boston*

Bing Lu, MD, DrPH, *Boston*

Anne-Marie Malfait, MD, PhD, *Chicago*

Stephen P. Messier, PhD,
Winston-Salem

Janet E. Pope, MD, MPH, *FRCPC,
London, Ontario*

Christopher T. Ritchlin, MD, MPH,
Rochester

William Robinson, MD, PhD,
Stanford

Georg Schett, MD, *Erlangen*

Sakae Tanaka, MD, PhD, *Tokyo*

Maria Trojanowska, PhD, *Boston*

Betty P. Tsao, PhD, *Charleston*

Fredrick M. Wigley, MD, *Baltimore*

Advisory Editors

Abhishek Abhishek, MD, PhD,
Nottingham

Ayaz Aghayev, MD, *Boston*

Tom Appleton, MD, PhD, *London,
Ontario*

Joshua F. Baker, MD, MSCE,
Philadelphia

Bonnie Bermas, MD, *Dallas*

Jamie Collins, PhD, *Boston*

Christopher Denton, PhD, FRCP, *London*

Anisha Dua, MD, MPH, *Chicago*

John FitzGerald, MD, *Los Angeles*

Nilig Haroon, MD, PhD, *Toronto*

Monique Hinchcliff, MD, MS,
New Haven

Hui-Chen Hsu, PhD, *Birmingham*

Vasileios Kyttaris, MD, *Boston*

Carl D. Langefeld, PhD,
Winston-Salem

Rik Lories, MD, PhD, *Leuven*

Suresh Mahalingam, PhD, *Southport,
Queensland*

Dennis McGonagle, FRCPI, PhD, *Leeds*

Aridaman Pandit, PhD, *Utrecht*

Kevin Winthrop, MD, MPH, *Portland*

Julie Zikherman, MD, *San Francisco*

AMERICAN COLLEGE OF RHEUMATOLOGY

David R. Karp, MD, PhD, *Dallas*, **President**

Kenneth G. Saag, MD, MSc, *Birmingham*, **President-Elect**

Douglas White, MD, PhD, *La Crosse*, **Treasurer**

Deborah Desir, MD, *New Haven*, **Secretary**

Steven Echard, IOM, CAE, *Atlanta*, **Executive Vice-President**

© 2021 American College of Rheumatology. All rights reserved. No part of this publication may be reproduced, stored or transmitted in any form or by any means without the prior permission in writing from the copyright holder. Authorization to copy items for internal and personal use is granted by the copyright holder for libraries and other users registered with their local Reproduction Rights Organization (RRO), e.g. Copyright Clearance Center (CCC), 222 Rosewood Drive, Danvers, MA 01923, USA (www.copyright.com), provided the appropriate fee is paid directly to the RRO. This consent does not extend to other kinds of copying such as copying for general distribution, for advertising or promotional purposes, for creating new collective works or for resale. Special requests should be addressed to: permissions@wiley.com

Access Policy: Subject to restrictions on certain backfiles, access to the online version of this issue is available to all registered Wiley Online Library users 12 months after publication. Subscribers and eligible users at subscribing institutions have immediate access in accordance with the relevant subscription type. Please go to onlinelibrary.wiley.com for details.

The views and recommendations expressed in articles, letters, and other communications published in Arthritis & Rheumatology are those of the authors and do not necessarily reflect the opinions of the editors, publisher, or American College of Rheumatology. The publisher and the American College of Rheumatology do not investigate the information contained in the classified advertisements in this journal and assume no responsibility concerning them. Further, the publisher and the American College of Rheumatology do not guarantee, warrant, or endorse any product or service advertised in this journal.

Cover design: Todd Machen

©This journal is printed on acid-free paper.

Arthritis & Rheumatology

An Official Journal of the American College of Rheumatology
www.arthritisrheum.org and wileyonlinelibrary.com

VOLUME 73 • February 2021 • NO. 2

In This Issue	A17
Journal Club	A18
Clinical Connections	A19
Special Articles	
Review: Rheumatoid Arthritis Pathogenesis, Prediction, and Prevention: An Emerging Paradigm Shift <i>Kevin D. Deane and V. Michael Holers</i>	181
Editorial: Urinary Biomarkers in Lupus Nephritis: Are We There Yet? <i>Chi Chiu Mok and Chandra Mohan</i>	194
Online-Only Special Article	
American College of Rheumatology Guidance for the Management of Rheumatic Disease in Adult Patients During the COVID-19 Pandemic: Version 3 <i>Ted R. Mikuls, Sindhu R. Johnson, Liana Fraenkel, Reuben J. Arasaratnam, Lindsey R. Baden, Bonnie L. Bermas, Winn Chatham, Stanley Cohen, Karen Costenbader, Ellen M. Gravallese, Andre C. Kalil, Michael E. Weinblatt, Kevin Winthrop, Amy S. Mudano, Amy Turner, and Kenneth G. Saag</i>	e1
Rheumatoid Arthritis	
Health Assessment Questionnaire at One Year Predicts All-Cause Mortality in Patients With Early Rheumatoid Arthritis <i>Safoora Fatima, O. Schieir, M. F. Valois, S. J. Bartlett, L. Bessette, G. Boire, G. Hazlewood, C. Hitchon, E. C. Keystone, D. Tin, C. Thorne, V. P. Bykerk, and J. E. Pope, on behalf of the CATCH Investigators</i>	197
Obesity-Related Traits and the Development of Rheumatoid Arthritis: Evidence From Genetic Data <i>Bowen Tang, Huwenbo Shi, Lars Alfredsson, Lars Klareskog, Leonid Padyukov, and Xia Jiang</i>	203
Multiomics and Machine Learning Accurately Predict Clinical Response to Adalimumab and Etanercept Therapy in Patients With Rheumatoid Arthritis <i>Weiyang Tao, Arno N. Concepcion, Marieke Vianen, Anne C. A. Marijnissen, Floris P. G. J. Lafeber, Timothy R. D. J. Radstake, and Aridaman Pandit</i>	212
Osteoarthritis	
Patients' Preoperative Expectations of Total Knee Arthroplasty and Satisfaction With Outcomes at One Year: A Prospective Cohort Study <i>Gillian A. Hawker, Barbara L. Conner-Spady, Eric Bohm, Michael J. Dunbar, C. Allyson Jones, Bheeshma Ravi, Tom Noseworthy, Donald Dick, James Powell, Paulose Paul, and Deborah A. Marshall, on behalf of the BEST-Knee Study Team</i>	223
Clinical Images	
Repair of Bone Erosion With Effective Urate-Lowering Therapy in a Patient With Tophaceous Gout <i>Shota Sakaguchi</i>	231
Systemic Lupus Erythematosus	
An Autoimmunogenic and Proinflammatory Profile Defined by the Gut Microbiota of Patients With Untreated Systemic Lupus Erythematosus <i>Bei-di Chen, Xin-miao Jia, Jia-yue Xu, Li-dan Zhao, Jun-yi Ji, Bing-xuan Wu, Yue Ma, Hao Li, Xiao-xia Zuo, Wen-you Pan, Xiao-han Wang, Shuang Ye, George C. Tsokos, Jun Wang, and Xuan Zhang</i>	232
Association Between Urinary Epidermal Growth Factor and Renal Prognosis in Lupus Nephritis <i>Juan M. Mejia-Vilet, John P. Shapiro, Xiaolan L. Zhang, Cristino Cruz, Grant Zimmerman, R. Angélica Méndez-Pérez, Mayra L. Cano-Verduzco, Samir V. Parikh, Haikady N. Nagaraja, Luis E. Morales-Buenrostro, and Brad H. Rovin</i>	244
Effects of BAFF Neutralization on Atherosclerosis Associated With Systemic Lupus Erythematosus <i>Fanny Saidoune, Guillaume Even, Yasmine Lamri, Julie Chezel, Anh-Thu Gaston, Brigitte Escoubet, Thomas Papo, Nicolas Charles, Antonino Nicoletti, and Karim Sacre</i>	255
Association of Urinary Matrix Metalloproteinase 7 Levels With Incident Renal Flare in Lupus Nephritis <i>Guobao Wang, Liling Wu, Huanjuan Su, Xiaodan Feng, Meng Shi, Lingwei Jin, Manqiu Yang, Zhanmei Zhou, Cailing Su, Bihui Yang, Yajing Li, and Wei Cao</i>	265
Vasculitis	
Deficiency of Adenosine Deaminase 2 in Adults and Children: Experience From India <i>Aman Sharma, GRSNK Naidu, Vikas Sharma, Saket Jha, Aaadhar Dhooria, Varun Dhir, Prateek Bhatia, Vishal Sharma, Sagar Bhattad, K. G. Chengappa, Vikas Gupta, Durga Prasanna Misra, Pallavi Pimpale Chavan, Sourabh Malaviya, Rajkiran Dudam, Bhawari Sharma, Sathish Kumar, Rajesh Bhojwani, Pankaj Gupta, Vikas Agarwal, Kusum Sharma, Manphool Singhal, Manish Rathi, Ritambhara Nada, Ranjana W. Minz, Ved Chaturvedi, Amita Aggarwal, Rohini Handa, Alice Grossi, Marco Gattorno, Zhengping Huang, Jun Wang, Ramesh Jois, V. S. Negi, Raju Khubchandani, Sanjay Jain, Juan I. Arostegui, Eugene P. Chambers, Michael S. Hershfield, Ivona Aksentijevich, Qing Zhou, and Pui Y. Lee</i>	276
Temporal Arteritis Revealing Antineutrophil Cytoplasmic Antibody-Associated Vasculitides: A Case-Control Study <i>Laure Delaval, Maxime Samson, Flora Schein, Christian Agard, Ludovic Tréfond, Alban Deroux, Henry Dupuy, Cyril Garrouste, Pascal Godmer, Cédric Landron, François Maurier, Guillaume le Guenno, Virginie Rieu, Julien Desblache, Cécile-Audrey Durel, Laurence Jousset-Mahr, Hassan Kassem, Grégory Pugnet, Vivane Queyrel, Laure Swiader, Daniel Blockmans, Karim Sacré, Estibaliz Lazaro, Luc Mouthon, Olivier Aumaitre, Pascal Cathébras, Loïc Guillevin, and Benjamin Terrier, on behalf of the French Vasculitis Study Group and French Study Group for Giant Cell Arteritis</i>	286
Clinical Images	
Spondylitis as a Rare Manifestation of Granulomatosis With Polyangiitis <i>Matthias H. Busch, Joop P. Aendekerk, Astrid M. L. Oude Lashof, and Pieter van Paassen</i>	294

Systemic Sclerosis

- Hemodynamic Response to Treatment and Outcomes in Pulmonary Hypertension Associated With Interstitial Lung Disease Versus Pulmonary Arterial Hypertension in Systemic Sclerosis: Data From a Study Identifying Prognostic Factors in Pulmonary Hypertension Associated With Interstitial Lung Disease
Louis Chauvelot, Delphine Gamondes, Julien Berthiller, Ana Nieves, Sébastien Renard, Judith Catella-Chatron, Kais Ahmad, Laurent Bertoletti, Boubou Camara, Emmanuel Gomez, David Launay, David Montani, Jean-François Mornex, Grégoire Prévot, Olivier Sanchez, Anne-Marie Schott, Fabien Subtil, Julie Traclet, Ségolène Turquier, Sabrina Zeghmar, Gilbert Habib, Martine Reynaud-Gaubert, Marc Humbert, Vincent Cottin, The French Network for Pulmonary Arterial Hypertension, and The French Network for Rare Pulmonary Diseases (OrphaLung)..... 295
- Association of Autologous Hematopoietic Stem Cell Transplantation in Systemic Sclerosis With Marked Improvement in Health-Related Quality of Life
Nancy Maltez, Mathieu Puyade, Mianbo Wang, Pauline Lansiaux, Zora Marjanovic, Catney Charles, Russell Steele, Murray Baron, Ines Colmegna, Marie Hudson, and Dominique Farge, for the Canadian Scleroderma Research Group and the MATHEC-SFGMTC Network..... 305
- Cancer in Systemic Sclerosis: Analysis of Antibodies Against Components of the Th/To Complex
Christopher A. Mecoli, Brittany L. Adler, Qingyuan Yang, Laura K. Hummers, Antony Rosen, Livia Casciola-Rosen, and Ami A. Shah..... 315

Gout

- Brief Report: Calcium Pyrophosphate Dihydrate Crystal Deposition in Gouty Tophi
Hang-Korng Ea, Alan Gauffenic, Quang Dinh Nguyen, Nhu G. Pham, Océane Olivier, Vincent Frochot, Dominique Bazin, Nghia H. Le, Caroline Marty, Agnès Ostertag, Martine Cohen-Solal, Jean-Denis Laredo, Pascal Richette, and Thomas Bardin..... 324

Pediatric Rheumatology

- Imaging-Based Uveitis Surveillance in Juvenile Idiopathic Arthritis: Feasibility, Acceptability, and Diagnostic Performance
Saira Akbarali, Jugnoo S. Rahi, Andrew D. Dick, Kiren Parkash, Katie Etherton, Clive Edelsten, Xiaoxuan Liu, and Ameenat L. Solebo..... 330
- Tapering Canakinumab Monotherapy in Patients With Systemic Juvenile Idiopathic Arthritis in Clinical Remission: Results From a Phase IIIb/IV Open-Label, Randomized Study
Pierre Quartier, Ekaterina Alexeeva, Tamás Constantin, Vyacheslav Chasnyk, Nico Wulffraat, Karin Palmlblad, Carine Wouters, Hermine I. Brunner, Katherine Marzan, Rayfel Schneider, Gerd Horneff, Alberto Martini, Jordi Anton, Xiaoling Wei, Alan Slade, Nicolino Ruperto, and Ken Abrams, in collaboration with the Paediatric Rheumatology International Trials Organisation and the Paediatric Rheumatology Collaborative Study Group..... 336

Autoimmune Disease

- Incidence, Clinical Features, and Outcomes of Late-Onset Neutropenia From Rituximab for Autoimmune Disease
Reza Zonozi, Zachary S. Wallace, Karen Laliberte, Noah R. Huizenga, Jillian M. Rosenthal, Eugene P. Rhee, Frank B. Cortazar, and John L. Niles..... 347

Letters

- High Prevalence of New-Onset or Worsening Hepatitis C Virus-Related Musculoskeletal Symptoms After Beginning Direct-Acting Antiviral Therapy: A Challenging Novel Observation
Muhammad Haroon, Khurram Anis, Zara Khan, and Naila Nawaz..... 355
- Morning Stiffness and Neutrophil Circadian Disarming: Comment on the Article by Orange et al
Omer Nuri Pamuk and Sarfaraz Hasni..... 356
- Reply
Dana E. Orange, Nathalie E. Blachere, Mayu O. Frank, Salina Parveen, Edward F. DiCarlo, Serene Mirza, Tania Pannellini, Mark P. Figgie, Vivian P. Bykerk, Caroline S. Jiang, Ellen M. Gravalles, Ana-Maria Orbai, Sarah L. Mackie, and Susan M. Goodman..... 357
- Early-Onset Hydroxychloroquine Retinopathy and a Possible Relationship to Blood Levels: Comment on the Article by Petri et al
Naoto Yokogawa, Akiko Ohno-Tanaka, Masayuki Hashiguchi, Mikiko Shimizu, Hiroko Ozawa, Shinji Ueno, Kei Shinoda, and David J. Browning..... 358
- Reply
Michelle Petri, Marwa Elkhailifa, Laurence S. Magder, Jessica Li, and Daniel W. Goldman..... 359
- To Switch or Not Switch Febuxostat: Comment on the Article by FitzGerald et al
Chuanhui Xu..... 359

Cover image: The figure on the cover (from Chen et al, pages 232–243) shows the taxonomic tree of all differentially enriched species in the comparison of gut microbiota between systemic lupus erythematosus patients and healthy controls. Each circular sector filled by a different color represents a single phylum. Bar plots outside the central circle depict the group in which a specific species was enriched and how big the linear discriminant analysis score was for that species. Species that were observed to be increased in systemic lupus erythematosus patients and decreased after treatment are shown as large red dots.

In this Issue

Highlights from this issue of *A&R* | By Lara C. Pullen, PhD

Multimomics and Machine Learning Predict Response to Anti-TNF in RA Patients

Although rheumatologists consider methotrexate to be the mainstay of treatment for rheumatoid arthritis (RA), some patients do not respond to the drug. These patients are often prescribed tumor necrosis factor inhibitors (TNFi). **In this issue, Tao et al (p. 212)** report the results of their efforts to predict the response of RA patients to anti-TNF prior to treatment. They also sought a better understanding of the mechanism of how individual RA patients respond differently to anti-TNF treatment. Their findings not only shed light on the mechanism behind the responses but also suggest that machine learning models based on molecular signatures can accurately predict response prior to treatment with adalimumab (ADA) and etanercept (ETN).

The investigators found that the transcription signatures in peripheral blood mononuclear cells (PBMCs), monocytes, and CD4+ cells diverged in ADA and ETN responders, such that CD4+ T cells from ADA responders were enriched in the TNF signaling pathway. These results differ from those of previous studies of TNFi, in which relatively little overlap in differentially expressed genes was found. In the current study, the researchers

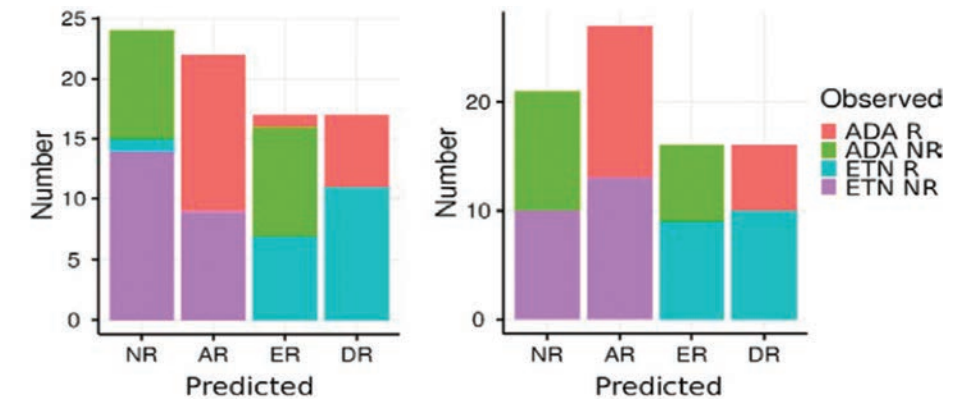


Figure 1. Machine learning prediction of 6-month response to ADA and ETN treatment using the best model based on gene expression data (left) and DNA methylation data (right).

noted very few differences in the monocyte differentially expressed gene pathways.

An analysis of the differentially methylated positions (DMPs) revealed that the DMPs of responders to ETN were hypermethylated, unlike those of responders to ADA. The investigators found divergent gene signatures associated with response to ADA and ETN and reproduced this divergence in multiple cell populations, a finding that suggests a potentially different mechanism of action between these 2 anti-TNF agents.

When they input the differential genes into machine learning models, the investigators were able to predict response to ADA and ETN with an overall accuracy of 85.9% and 79%, respectively. When they input DMPs into the models, they were able to reach an overall accuracy of 84.7% for ADA and 88% for ETN. The team performed a follow-up study that validated the high performance of the models and led them to conclude that their work can be used to pave the way for personalized anti-TNF therapy.

Presentation of DADA2 in Adults in India

Rheumatologists first identified deficiency of adenosine deaminase 2 (DADA2) as a monogenic syndrome of early-onset stroke and systemic vasculitis that mimics polyarteritis nodosa. **In this issue, Sharma et al (p. 276)** report the first case series of 33 patients from India diagnosed with DADA2 by adult and pediatric care providers. They intend for the case series to raise awareness about the syndrome and its presentation, particularly in adults. In their

article, the authors emphasize that nearly half of their confirmed cases presented during adulthood and, therefore, conclude that the onset of DADA2 is not restricted to young children.

The subjects in the cohort were diagnosed with DADA2 between April 2017 and March 2020. Eighteen subjects had experienced ≥ 1 stroke. While all symptomatic patients exhibited features of vasculitis, children were more likely to experience constitutional symptoms, anemia, and cutaneous and neurologic

involvement. The investigators also identified novel features of DADA2, including pancreatic infarction, focal myocarditis, and diffuse alveolar hemorrhage.

The researchers treated 25 of the patients with tumor necrosis factor inhibitors and found that all of the identified disease manifestations improved markedly after initiation of the treatment. Moreover, they were able to achieve disease remission in 19 patients. Two cases, however, were complicated by tuberculosis infection, and 2 deaths were reported.

Assessment of a New Approach to Imaging-Based Uveitis Surveillance in JIA

Children with juvenile idiopathic arthritis (JIA) must be regularly examined for uveitis to avoid visual morbidity from the most common extraarticular manifestation of the disease. Undiagnosed and untreated, the resulting poor

p. 330

vision can have a significantly negative effect on the child and on the adult they become. In this issue, Akbarali et al (p. 330) report the findings of their investigation into the feasibility, acceptability, and performance of optical coherence tomography (OCT) imaging-based diagnosis of uveitis. The investigators found that non-contact,

high-resolution imaging for JIA uveitis surveillance is feasible and acceptable for patients, and that it holds the promise of transforming pediatric practice. The imaging captures anterior chamber images, and although manual analysis of images is subject to interobserver and intraobserver variability, acquired images can be used to diagnose active inflammation with high levels of sensitivity and specificity.

This study was conducted in a quaternary care center and included 26 children 3–15 years of age, 12 of whom had active inflammation. All of the patients rated the acceptability of image acquisition as ≥ 8.5 on a scale

of 0–10. The time to acquire images ranged from 1.5 to 22 minutes. The researchers found a positive correlation between clinical assessment and image-based cell quantification. Sensitivity of anterior segment OCT manual image cell count for diagnosis of active inflammation was 92%, specificity was 86%, and negative predictive value was 92%. The authors acknowledge that further work is needed to determine the analytic and clinical validity of anterior segment OCT quantification of active inflammation and the clinical and cost-effectiveness of imaging-based disease monitoring.

Journal Club

A monthly feature designed to facilitate discussion on research methods in rheumatology.

Obesity-Related Traits and the Development of Rheumatoid Arthritis: Evidence from Genetic Data

Tang, et al. *Arthritis Rheumatol.* 2021;85:203–211

Obesity represents a state of low-grade inflammation in the human body and has been investigated as a risk factor for rheumatoid arthritis (RA) in prior population-based studies. However, it remains challenging to determine whether obesity causes RA, mainly owing to confounding and reverse causality, which prevail in conventional observational studies. To understand the underlying causal relationship, Tang and colleagues conducted a 2-sample Mendelian randomization (MR) study as well as a genetic correlation analysis, leveraging the largest genetic data set for 3 obesity-related traits (body mass index [BMI], waist-to-hip ratio [WHR], and WHR adjusted for BMI; $n = \sim 800,000$ participants) and RA (14,361 RA cases).

Linkage disequilibrium score regression and ρ -HESS, a statistical method to quantify local genetic correlation between pairs of traits, were applied to quantify the shared genetic components among 3 obesity phenotypes and RA, both globally (across the whole genome) and locally (restricted to a specific genomic region). Local genetic correlation enabled the authors to identify genomic regions that contribute to both traits when the overall genetic correlation is minimal. Mendelian randomization is a novel statistical tool that uses genetic variants as instrument variables to allow for causal inference between exposure and outcome.

Because genetic variants allocate randomly at conception and antecede disease occurrence, it is believed that MR is less susceptible to confounding and reverse causality than other observational epidemiologic methods.

Questions

1. What is currently known about the relationship between obesity and RA?
2. What is genetic correlation, how should the genetic correlation between pairs of traits be interpreted, and what is the difference between whole-genome genetic correlation and local genetic correlation?
3. Why did the authors choose MR to elucidate the relationship between obesity and RA? What are the advantages of MR over population-based studies?
4. What are the 3 basic assumptions for MR? How did the authors validate the model assumptions?
5. Do you think these genetic methods allow for a less biased inference regarding the potential causal relationship between obesity and RA?

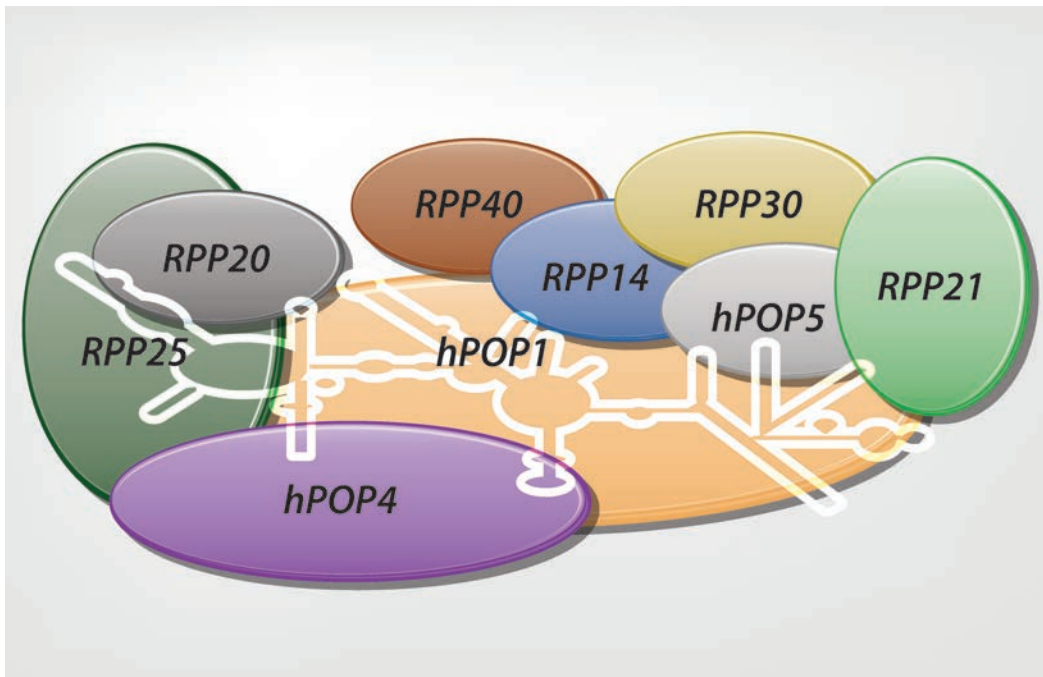
Clinical Connections

Cancer in Systemic Sclerosis: Analysis of Antibodies Against Components of the Th/To Complex

Mecoli et al, *Arthritis Rheumatol* 2021;85:315–323

CORRESPONDENCE

Livia Casciola-Rosen, PhD: lcr@jhmi.edu



KEY POINTS

- The majority of SSc patients with antibodies against Th/To have autoantibodies that recognize multiple protein components of this complex.
- The anti-Th/To clinical phenotype is characterized by limited cutaneous disease and pulmonary involvement.
- The presence of any Th/To autoantibody may have a protective effect against contemporaneous cancer.

SUMMARY

Important insights into the relationship between systemic sclerosis (SSc; scleroderma) and cancer have emerged over the past decade, demonstrating that both time and autoantibodies are critical filters in risk-stratifying SSc patients for malignancy. Anti-Th/To antibodies, which target at least 9 individual proteins of the complex (human POPI [hPOP1], hPOP4, hPOP5, RPP14, RPP20, RPP21, RPP25, RPP30, and RPP40), are a less common specificity in SSc cohorts.

In this study, Mecoli et al focused on the 4 most common autoantibodies of the Th/To complex (hPOP1, RPP25, RPP30, and RPP40). Their data shows that the clinical phenotype of this subgroup is characterized by limited cutaneous disease and pulmonary involvement. Interestingly, patients with autoantibodies to any of these 4 Th/To complex components are protected from cancer-associated SSc. Beyond a potential tool to use for cancer risk stratification in the clinical setting, these findings further expand the knowledge of the interface between autoimmunity and cancer.

An Autoimmunogenic and Proinflammatory Profile Defined by the Gut Microbiota of Patients With Untreated Systemic Lupus Erythematosus

Chen et al, *Arthritis Rheumatol* 2021;85:232–243

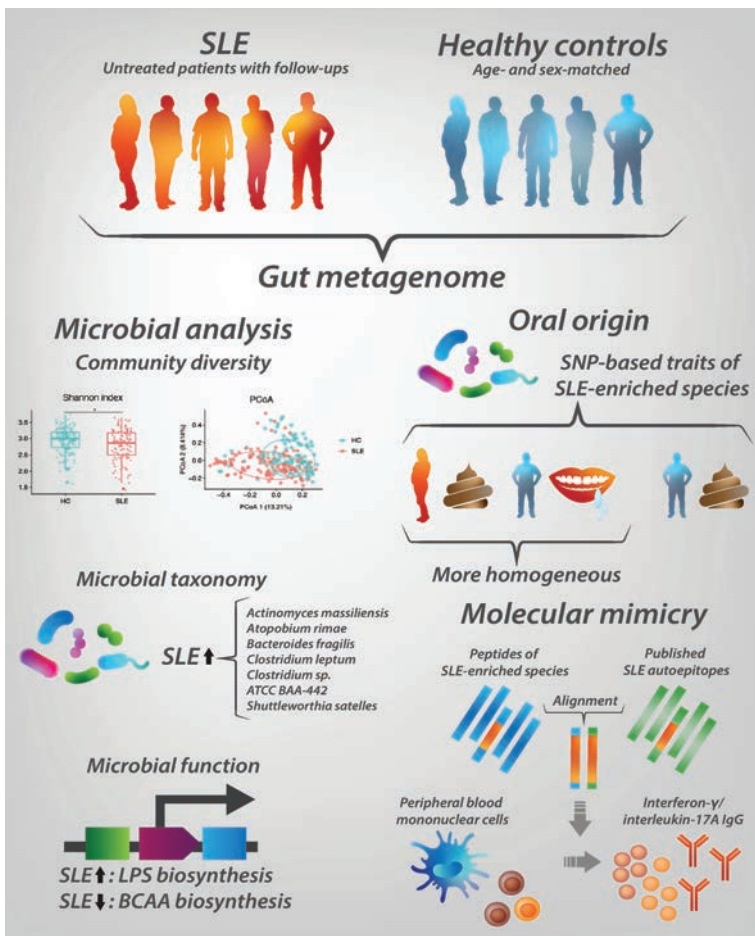
CORRESPONDENCE

Xuan Zhang, MD: zxpumch2003@sina.com

SUMMARY

Distinct patterns of gut microbiome dysbiosis have been reported in patients with systemic lupus erythematosus (SLE). However, it is not known why this disease-specific intestinal dysbiosis exists in people with SLE or how it contributes to disease pathogenesis. In a study by Chen et al, profiling of fecal metagenomes in lupus-prone mice and untreated SLE patients revealed disturbed gut microbiota and a dominant presence of several disease-specific species including *Atopobium rimae*, *Actinomyces massiliensis*, *Bacteroides fragilis*, *Clostridium leptum*, *Clostridium* species ATCC BAA-442, and *Shuttleworthia satelles*. Treatment with steroids and/or immunosuppressants resulted in suppression of these dominant species.

The observed changes in metabolic pathways, including branched chain amino acid (BCAA) and lipopolysaccharide (LPS) biosynthesis, suggest a role of gut microbiota-derived metabolites in disease development. Single-nucleotide polymorphism (SNP)-based analyses revealed that some SLE gut-enriched species originated from the oral cavity. Finally, peptides derived from SLE-dominant species mimic autoantigens. Specifically, the peptide YLYDGRIFI, from *Odoribacter splanchnicus*, mimics human SLE-specific autoantigen Sm B/B and the peptide DGQFCM, from *Akkermansia muciniphila*, mimics human Fas. These data provide an in-depth understanding of the gut microbiota characteristics in SLE patients and support microbiota-based interventions in the diagnosis and treatment of patients with SLE.



KEY POINTS

- Non-treated patients with SLE harbor specific gut microbiota which partially originates from the oral cavity.
- Microbial peptides defined by SLE-dominant species share molecular mimicry with human Sm and Fas epitopes.
- Metabolic products and molecular mimicry most probably contribute to disease pathogenesis and offer therapeutic opportunities.

REVIEW

Rheumatoid Arthritis Pathogenesis, Prediction, and Prevention: An Emerging Paradigm Shift

Kevin D. Deane  and V. Michael Holers 

Rheumatoid arthritis (RA) is currently diagnosed and treated when an individual presents with signs and symptoms of inflammatory arthritis (IA) as well as other features, such as autoantibodies and/or imaging findings, that provide sufficient confidence that the individual has RA-like IA (e.g., meeting established classification criteria) that warrants therapeutic intervention. However, it is now known that there is a stage of seropositive RA during which circulating biomarkers and other factors (e.g., joint symptoms) can be used to predict if and when an individual who does not currently have IA may develop future clinically apparent IA and classifiable RA. Indeed, the discovery of the “pre-RA” stage of seropositive disease has led to the development of several clinical trials in which individuals are studied to identify ways to delay or prevent the onset of clinically apparent IA/RA. This review focuses on several issues pertinent to understanding the prevention of RA. These include discussion of the pathogenesis of pre-RA development, prediction of the likelihood and timing of future classifiable RA, and a review of completed and ongoing clinical trials in RA prevention. Furthermore, this review discusses challenges and opportunities to be addressed to effect a paradigm shift in RA, where in the near future, proactive risk assessment focused on prevention of RA will become a public health strategy in much the same manner as cardiovascular disease is managed today.

Introduction

Rheumatoid arthritis (RA) is a common chronic autoimmune disease (1) that causes substantial morbidity and decreased quality of life as well as increased mortality and annual costs of billions of dollars (1). The current clinical management of seropositive RA (e.g., abnormalities of rheumatoid factor [RF] and/or antibodies to citrullinated protein antigens [ACPAs]) is focused on initiating treatment once an individual develops symptomatic and clinically identifiable inflammatory arthritis (IA) that may also be classifiable as RA by established criteria (2–4). Importantly, however, due to factors including an individual's delay in seeking care for symptoms, and delays of a referral to a specialist, the time between onset of symptoms and initiation of disease-modifying antirheumatic drug therapy is often increased beyond what is ideal, especially given that earlier diagnosis and treatment improves outcomes (5,6).

Furthermore, while new drugs and treat-to-target strategies have improved disease control, for many individuals, treatment does not return them to a “pre-RA” state (7). These factors, along with the high costs of managing RA, side effects of medication, and growing limits to access to rheumatologists worldwide (8), make RA a disease that in principle would benefit from preventive approaches.

Pathogenesis of RA: detectable autoimmunity before clinically apparent IA

For most individuals who develop seropositive RA, there is a period characterized by systemic elevations in RA-related autoantibody levels prior to the development of clinically apparent IA/RA, which is typically identified on physical examination as a swollen joint consistent with synovitis (9–15). A model of this development,

Supported by NIH grants AI-110498 and AI-101981.
Kevin D. Deane, MD, PhD, V. Michael Holers, MD: University of Colorado School of Medicine, Aurora.

Drs. Deane and Holers are investigators on an investigator-initiated grant with Janssen Research and Development. Dr. Deane has received consulting fees from Janssen, Inova Diagnostics, ThermoFisher, Bristol Myers Squibb, and

Microdrop (less than \$10,000 each). Dr. Holers has received consulting fees from Janssen, Bristol Myers Squibb, and Celgene (less than \$10,000 each).

Address correspondence to Kevin D. Deane, MD, PhD, 1775 Aurora Court, Mail Stop B-115, Denver, CO 80045. Email: kevin.deane@cuanschutz.edu.

Submitted for publication January 29, 2020; accepted in revised form June 18, 2020.

and a series of key case-control and prospective studies that have supported this model are included in Figure 1 and Table 1, respectively. These autoantibodies include multiple isotypes of RF and ACPAs, ACPA fine specificities (e.g., antibodies to citrullinated fibrinogen), and antibodies to carbamylated proteins and peptidyl-larginine deiminases (16–18).

Based on current data, it appears that this early stage of RA is characterized by early reactivity with a limited number of self-antigens, and limited systemic inflammation, that is followed by evolution over time of expanding innate and adaptive responses and tissue injury until some threshold is crossed and clinically apparent IA/RA develops. This model has been supported by findings of increases over time in the numbers and type of ACPAs (18–21), as well as expansion of other autoantibody systems and increasing systemic inflammation (e.g., cytokines) (22–24). Other processes that occur during this period include altered autoantibody glycosylation (25) and changes in cellular phenotypes such as T cell subsets (26). While not consistent across all studies, it appears that in many individuals, ACPAs precede RF and other autoantibodies (e.g., anti-carbamylated protein), which may indicate that ACPAs are reflective of the earliest breaks in tolerance (16,21), and that development of multiple types of autoantibodies is fundamentally related to a transition to clinically apparent disease.

Importantly, while expansion of autoimmunity and inflammation characterize this period, the key biologic pathways that drive initial autoimmunity and then a transition to a more pathogenic state and clinically identifiable IA/RA are not known. Moreover, many purported risk factors for RA have been identified only in individuals with clinically apparent articular RA; therefore, the role of these factors in the initiation and propagation of autoimmunity

and inflammation prior to clinically apparent IA/RA is not well understood. However, some risk factors that are associated with future risk of RA have been prospectively identified in pre-RA (for review, see ref. 27) (Table 2). In particular, for some individuals, interactions between tobacco smoke and the shared epitope may play an important role in these early processes and in increasing the risk of a transition from autoantibody positivity to clinically apparent IA/RA (20,28). In addition, many individuals with systemic elevations of RA-related autoantibodies have no evidence of synovitis on physical examination, imaging, or synovial biopsy (29,30). This finding strongly suggests that autoimmunity in these individuals is generated outside of the joints, with emerging evidence suggesting that this site may be mucosal (e.g., lungs, periodontium, or intestine) and related to the microbiome, and is an active area of investigation (for review, see ref. 31).

Nomenclature

Several terms, including “pre-RA,” “preclinical RA,” and “at-risk,” are commonly used to describe the period of development of RA before clinically apparent IA. Of these terms, “pre-RA” was suggested by a European League Against Rheumatism (EULAR) study group in 2014 (32). As such, we will use that term within this review. However, there are some caveats with regard to this term, including that the EULAR study group suggested it be applied only when individuals were later known to progress to clinically apparent RA. It is also not clear how to apply the term to individuals who may have clinically apparent IA even if it is not classifiable as RA, since those individuals are typically clinically treated as having RA. Additionally, as discussed in more detail below, as the understanding of pre-RA evolves, it is likely that

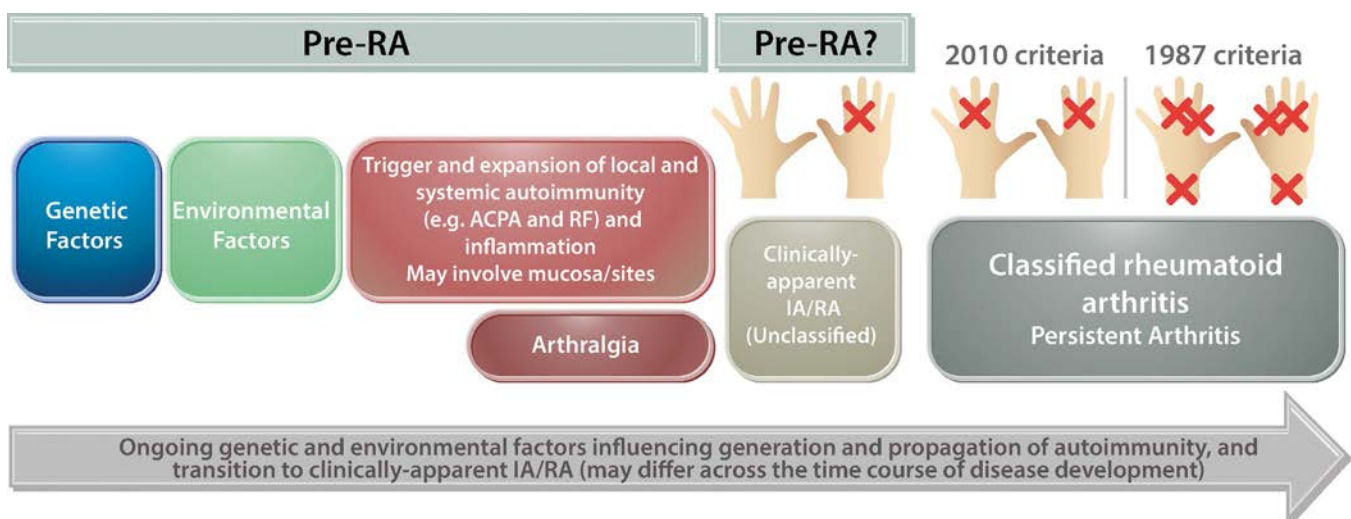


Figure 1. Model of rheumatoid arthritis (RA) development. In this model, genetic and environmental factors lead to the initiation and expansion of autoimmunity, which may progress to clinically apparent inflammatory arthritis (IA)/RA and classifiable RA. There is some controversy over whether the term “pre-RA” should be applied once clinically apparent IA is present if it is not classifiable as RA. ACPAs = antibodies to citrullinated protein antigens; RF = rheumatoid factor.

different terms to describe stages of RA will be needed that will facilitate research and clinical care, align with the biology of disease, and facilitate communication with individuals who may be evaluated for prevention.

Current prediction models for future RA

Multiple case-control studies have demonstrated that serum elevations of ACPAs and/or RF have high (often >80%) positive predictive values (PPVs) for future IA/RA (12,13,24) (Table 1). Moreover, while retrospective case-control studies may overestimate PPVs, in prospective studies that include ACPAs (with or without RF), symptoms, and other factors, PPVs for the development of IA/RA within 2–6 years ranged from ~30% to >70%, with the highest PPVs in subjects with high levels of autoantibodies, or dual positivity for ACPAs and RF (15,33).

As an example, in a Dutch study of 374 subjects with RF and/or ACPA positivity and joint symptoms but no IA on baseline physical examination, 131 individuals (35%) developed IA in a median of 12 months (29); furthermore, among individuals with a baseline high-risk score comprised of ACPAs, RF, and other factors, 74% developed IA/RA within 3 years. In addition, in a study in the UK of 100 ACPA-positive subjects with arthralgia, 50 (50%) developed IA/RA after a median of 7.9 months (33); furthermore, among individuals with a baseline high-risk score comprising examination findings, symptoms, genetic and autoantibody testing, and an abnormal power Doppler ultrasound finding, ~68% developed IA within 24 months.

Importantly, those 2 studies included 2 aspects of prediction: likelihood (i.e., will someone get IA?) and timing (i.e., when will they get IA?). As discussed below, these aspects can be used to counsel individuals who are facing decisions regarding their future risk of IA/RA, timing of clinical follow-up, and participating in a trial. Furthermore, these aspects support clinical trial design where it is essential to have accurate estimates of the expected number of “events” (i.e., incident IA/RA) within a given time frame.

Of note, markers of inflammation such as C-reactive protein level have been demonstrated to be elevated in pre-RA, although they have not been consistently helpful in improving prediction models (24,29,33); furthermore, while in conjunction with autoantibodies, cytokine/chemokine abnormalities have been shown to be useful in prediction (18,24), this has not yet been extensively validated.

Prevention: rationale, design, and existing studies

Rheumatologists are familiar with many “preventive” approaches in the care of individuals with RA. These include the prevention of worse joint damage in individuals with established RA, osteoporotic fractures, or future flares in individuals who have had acute gouty arthritis. Nevertheless, it is a relatively novel

concept to consider prevention of the first onset of clinically apparent manifestation of a disease.

Several factors have underpinned the development of clinical trials that have the “intent to prevent” (phrase courtesy of Marvin Fritzler) the onset of clinically apparent IA/RA. These factors include the predictive ability of autoantibodies, especially ACPAs, and improved identification of individuals with biomarker elevations through clinical care as well as approaches such as screening in populations at higher risk of RA, such as first-degree relatives (FDRs) of individuals with RA (15,34–36). It has also been observed that antimalarials may prevent future flares in palindromic rheumatism (37). Furthermore, findings of a “window of opportunity” in RA where earlier treatment in individuals with established IA may lead to improved outcomes and perhaps increases in drug-free remission suggest that the immune system may be more amenable to “normalization” if treated early (5).

Building on these factors, 2 clinical trials to prevent the first onset of clinically apparent IA have been completed. In one, 83 ACPA- and/or RF-positive individuals with arthralgia but without IA on physical examination were randomized (1:1) to receive either 2 doses of dexamethasone 100 mg intramuscularly 6 weeks apart or placebo (38). IA rates were not different between the study arms (20% versus 21%), although there was a decrease in autoantibody levels in treated individuals. In the Prevention of Clinically Manifest Rheumatoid Arthritis by B Cell-Directed Therapy in the Earliest Phase of the Disease (PRAIRI) study (39), 81 subjects with baseline ACPA and RF positivity and elevated C-reactive protein level (>0.6 mg/liter) were randomized (1:1) to receive either one dose of 1,000 mg rituximab or placebo, and all subjects received methylprednisolone 100 mg intravenously. The rates of IA were not significantly different between arms (34% in the treatment arm versus 40% in the placebo arm); however, the onset of IA was delayed such that 25% of the subjects in the treatment arm developed IA ~12 months later than those in the placebo group.

There are several other prevention studies underway. The Strategy for the Prevention of the Clinically Apparent Onset of RA (StopRA) study (40) in the US is randomizing individuals with ACPA levels ≥ 2 times normal to receive hydroxychloroquine versus placebo for 1 year; subjects are then followed up for an additional 2 years to assess the durability of response as well as to evaluate if treatment may result in a less aggressive form of IA/RA. Arthritis Prevention in the Preclinical Phase of RA with Abatacept (APPIRA) in the UK and Europe is randomizing individuals with ACPA levels >3 times normal or ACPAs plus RF, and inflammatory joint symptoms/arthralgia, to receive abatacept subcutaneously weekly versus placebo for 1 year, with an additional 1 year of follow-up (41). Other studies that have been launched include one using statins in autoantibody-positive subjects (42), and one using glucocorticoids and methotrexate in individuals with arthralgia and no evidence of IA on examination but who have “subclinical” IA on magnetic resonance imaging (43).

Table 1. Key longitudinal studies of pre-RA*

Author, year (ref.)	Country of origin/ population	Study type	Number of subjects and number with incident IA/RA	Key findings
del Puente et al, 1988 (9)	US/Akimel O'odham (Pima) people	Prospective cohort study	2,712 total; 70 (~2.6%) with incident IA/RA after up to 19 years of follow-up	The highest rate of development of RA (48 per 1,000 person-years) was in subjects with a baseline RF titer of >1:256
Aho et al, 2000 (10); and Aho et al, 1993 (74)	Finland	Retrospective biobank study	19,072 total; 124 with incident RA	Findings were reported in multiple publications and included elevations of IgG, RF, and antibodies to keratin and perinuclear factor (later determined to be varieties of ACPAs) prior to RA Incident RA was highest in subjects with RF positivity
Silman et al, 1992 (75)	UK	Prospective cohort study	370 unaffected FDRs from families with RA; 14 with incident RA	
Rantapää-Dahlqvist et al, 2003 (12)	Sweden	Retrospective biobank case-control study	83 cases with incident RA and 382 controls	At any time prior to a diagnosis of RA, anti-CCP2 was positive in ~34%, RF-IgA in ~34%, RF-IgM in 19%, and RF-IgG in 17% of subjects with RA. A combination of anti-CCP2 and RF-IgA positivity at any point in preclinical RA had a sensitivity of 21%, a specificity of 99%, and a PPV of 87% for future RA. Sensitivity and levels of autoantibodies were highest in the period <1.5 years prior to diagnosis.
Nielen et al, 2004 (13)	The Netherlands	Retrospective biobank case-control study	79 cases with incident RA and 2,138 controls	Overall, 49% of RA subjects were positive for anti-CCP1 or RF-IgM a median of 4.5 years prior to diagnosis. Using a 0–5-year window prior to diagnosis and comparison to controls, anti-CCP1 or RF-IgM positivity was ~36% sensitive and ~97% specific for RA, with a PPV of ~97%. Increased sensitivity, increased rates of simultaneous positivity for anti-CCP1 and RF-IgM, and higher levels were present in the most immediate pre-diagnosis period. Anti-CCP1 appeared to be positive prior to RF-IgM.
Majka et al, 2008 (14); Deane et al, 2010 (24); Ercan et al, 2010 (76); Kolfenbach et al, 2010 (17); Gan et al, 2015 (16); and Sokolove et al, 2012 (18)	US	Retrospective biobank case-control study	83 cases with incident RA and 83 controls	A series of studies were performed in this cohort demonstrating that: 1. RF and anti-CCP2 are elevated in 57% and 61% of subjects prior to a diagnosis of RA, respectively. Notably, younger subjects (<40 years) appeared to have a shorter duration of preclinical autoantibody positivity compared to older subjects (≥40 years). 2. An increasing number of abnormal cytokines/chemokines was associated with a shorter time to future diagnosis of RA in an age-dependent manner. 3. Pre-RA abnormalities of anti-CarP and anti-PAD antibodies, and abnormalities of glycosylation were present 4. A panel of elevated ACPA fine specificities and cytokines were ~58% sensitive and ~87% specific for onset of RA within 2 years
Karlson et al, 2009 (77)	US	Nested case-control study within the Nurses' Health Study and Women's Health Study	170 cases with incident RA and 506 controls	Soluble tumor necrosis factor receptor type II and interleukin-6 were elevated prior to a diagnosis of RA
Van de Stadt et al, 2013 (29)	The Netherlands	Prospective study of individuals presenting to rheumatology clinics	374 subjects with RF and/ or ACPA positivity but no IA at baseline; 131 with incident IA/RA after a median of 12 months	A score was developed assigning 1 point for each of the following that were present: positive FDR status, no alcohol consumption (use of alcohol was protective), symptoms starting <12 months prior, intermittent symptoms, symptoms in upper and lower extremities, visual analog pain score of ≥50 mm, morning stiffness ≥60 minutes, self-reported swelling in any joint; in addition, up to 4 points were assigned if both RF and ACPA were positive. In individuals with scores of ≥7, 74% developed IA/RA within 3 years

(Continued)

Table 1. (Cont'd)

Author, year (ref.)	Country of origin/ population	Study type	Number of subjects and number with incident IA/RA	Key findings
de Hair et al, 2013 (78)	The Netherlands	Prospective study of ACPA- and/or RF-positive subjects	55 subjects; 15 (27%) with incident IA after a median of 13 months	Nonsmokers and those with normal body weight had the lowest rates of progression to IA/RA
Ramos-Remus et al, 2015 (15)	Mexico	Prospective study of unaffected FDRs of patients with RA	819 FDRs; 17 (2.1%) with incident IA/RA over 5 years	ACPA positivity with or without concomitant RF positivity had PPVs of 58–64% for development of RA during follow-up
Rakieh et al, 2015 (33)	UK	Prospective study of ACPA (CCP2)-positive subjects with arthralgia referred to rheumatology clinics	100 ACPA-positive individuals; 50 with incident IA/RA after a median of 7.9 months	A score was developed assigning 1 point for each of the following: tender joints, morning stiffness >30 minutes, presence of the shared epitope, high levels of RF and/or ACPAs, and the presence of power Doppler ultrasound findings in ≥1 joint. In individuals with the highest scores (≥2), >41% developed IA/RA within 24 months; in individuals with scores of ≥4, 68% developed IA within 24 months.
Burgers et al, 2017 (79)	The Netherlands and Sweden	Prospective study of subjects with arthralgia	178 subjects with arthralgia meeting EULAR criteria for CSA at baseline; 44 (18%) developed incident IA/RA after a median of 16 weeks	This was a study to validate the EULAR definition for CSA (46). The presence of 3 or more of the following factors was ~84% sensitive and had a PPV of ~30% for IA/RA within 2 years: duration since onset of symptoms <1 year, symptoms in MCP joints, morning stiffness ≥60 minutes, more severe morning symptoms, having an FDR with RA, and on examination, difficulty making a fist and tenderness with an MCP squeeze. However, PPV for IA was much lower if the criteria were applied by a non-rheumatologist practitioner (PPV ~3%).
Gan et al, 2017 (80)	US	Prospective cohort study	35 ACPA (CCP3)-positive subjects with baseline IA identified through health-fair screenings; 14 with incident IA/RA after a mean of 2.6 years	Progression to IA/RA was associated with higher age, shared epitope positivity, and lower blood levels of omega-3 fatty acids
Tanner et al, 2019 (35)	Canada/Indigenous North Americans	Prospective cohort study	374 FDRs; 18 with incident IA/RA over ~5 years of follow-up	Highest rates of IA/RA (~97 per 1000 person-years) were in individuals positive for RF and ACPA at baseline, or who developed incident RF and/or ACPA positivity. The majority of RF- and/or ACPA-positive subjects did not develop IA/RA during followup, and a proportion (~70%) lost antibody positivity over time.

* RA = rheumatoid arthritis; IA = inflammatory arthritis; RF = rheumatoid factor; ACPAs = antibodies to citrullinated protein antigen; FDRs = first-degree relatives; anti-CCP2 = anti-cyclic citrullinated peptide 2; PPV = positive predictive value; anti-Carp = anti-carbamylated protein; anti-PAD = anti-peptidylarginine deiminase; EULAR = European League Against Rheumatism; CSA = clinically suspect arthralgia; MCP = metacarpophalangeal.

Paradigm shift to RA prevention: challenges and opportunities

While it represents a great advance that several clinical prevention trials in RA have been completed or are underway, challenges and opportunities remain in further advancing prevention (Table 3), and several of these are discussed below.

Improving prediction. Accurate prediction of future IA/RA is a critical aspect of prevention. While models to date have supported clinical trials, there are several important challenges. First, not all subjects with abnormalities of RA-related autoantibodies, even ACPAs, or other factors (e.g., articular symptoms) develop IA/RA within the time periods of prospective study (Table 1). This could be because retrospective studies have shown that autoantibodies may be elevated >10 years prior to RA diagnosis (12,21), and few prospective studies have been conducted that long. However, this also suggests that some individuals may develop RA-related autoimmunity and even some articular symptoms, yet never develop clinically apparent IA. Moreover, there is a growing understanding that RA-related autoantibody positivity may be lost over

Table 2. Purported genetic, environmental, and other risk and protective factors for future RA development evaluated in prospective studies or cross-sectional studies of at-risk individuals or individuals with pre-RA*

1. Genetic and familial risk factors
 - Shared epitope is associated with a higher risk of transition to RA in ACPA-positive individuals at baseline (33)
 - First-degree relative status increases the risk of progression to articular RA in an arthralgia cohort (29)
 - Certain populations are at high risk of RA, including populations indigenous to the Americas who have an ~5–7-fold increased risk of RA compared to non-indigenous populations (81)
2. Sex-related factors
 - Female sex, given that women have a 2–3-fold higher risk of RA compared to men (27)
 - Longer duration of breastfeeding and higher parity are protective (82)
 - Oral contraceptive use is associated with decreased autoantibody positivity in at-risk individuals without RA (first-degree relatives) (83)
3. Environmental (and potentially modifiable) factors (for review, see refs. 27 and 56)
 - Increased risk of RA
 - Tobacco exposure, especially long-duration and high-intensity smoking
 - Obesity
 - Inflammatory diet
 - Protective against RA
 - Moderate alcohol consumption
 - High fatty fish intake and intake of omega-3 fatty acids
4. Other
 - Lung disease (airways, parenchymal) is present in RA-related autoantibody-positive individuals and in some cases preceding articular RA (84)
 - Periodontal inflammation is present in RA-related autoantibody-positive individuals, and increased in comparison to controls (73)

* RA = rheumatoid arthritis; ACPA = antibodies to citrullinated protein antigen.

Table 3. Key challenges and opportunities in implementing prevention in RA*

1. Completion of ongoing clinical trials to learn the efficacy of the agents and approaches that are evaluated
2. Development of improved prediction models (including for seronegative RA)
3. Identification of relevant biologic pathways for prevention that may be unique to the pre-RA period
 - May be from ongoing or future trials and observational studies and include biology of nonarticular sites (e.g., mucosal sites)
 - Includes understanding of the pathophysiology of autoimmunity and joint symptoms in the absence of clearly definable IA
4. Effective strategies to identify individuals who are at sufficiently high risk of RA that preventive approaches may be considered
 - Incorporates accurate prediction models and individuals' preferences
 - May include public health awareness campaigns and broad population screening
5. Clear understanding of the role of imaging in diagnosis and management in pre-RA
6. Development of clear and informative nomenclature
 - Aligns with biology of disease
 - Effective in communicating with stakeholders
7. Optimization of stakeholder participation in prevention
 - Individuals at risk
 - Clinical rheumatologists
 - Research community
 - Funding agencies
 - Pharmaceutical, biotechnology, and diagnostic industries
 - Health care and insurance agencies
 - Governmental agencies that can implement policy around prevention

* RA = rheumatoid arthritis; IA = inflammatory arthritis.

time in at-risk individuals (35) (although in one study some individuals lost autoantibody positivity pre-RA yet still developed RA later [21]), or that autoantibodies may only be detectable after IA has developed (44). Furthermore, while there are multiple commercial assays for ACPAs available, they do not have the same diagnostic accuracies in established RA, and these differences may be more pronounced in pre-RA (45). Also, given that most biomarkers in RA have been developed in established disease, there may be additional discovery of biomarkers that are more appropriate for understanding pre-RA and in particular to identify transitions from benign to pathogenic autoimmunity.

Some additional challenges in prediction are that most prospective studies include autoantibody-positive subjects identified because they sought care for joint symptoms; therefore, studies are needed to understand prediction in individuals who have minimal joint symptoms, or who are asymptomatic, because these are the types of individuals who might be identified if population-based testing for RA biomarkers was performed. In addition, while most predictive models have primarily focused on autoantibodies, an entity termed “clinically suspect arthralgia” has been identified that uses a combination of self-reported symptoms and examination findings and has a PPV for future RA of ~30%, although in some scenarios, the PPV is much lower (~3%) (46). Furthermore, some models have used genetic factors instead of autoantibodies to estimate the

risk of seropositive as well as seronegative RA (47). As such, going forward, if diagnostic accuracy is sufficiently high, symptoms and other non-autoantibody factors may be used to identify individuals at sufficiently high risk of future RA that preventive interventions may be considered; importantly, these approaches may be especially helpful for the prediction of seronegative RA.

Physical examination has been the primary method to identify clinically apparent IA/RA; however, imaging is playing an increasing role in RA management to identify IA when examination findings are uncertain, as well as to follow up on response to therapy (48). Furthermore, imaging has been used to predict the development of future IA apparent on physical examination (33,48). However, if imaging is used to define IA that is not identifiable on examination (i.e., subclinical IA), that may change the approach to prevention where “treatable” IA is identified by imaging earlier than is possible by physical examination. While potentially beneficial, that approach could also lead to overtreatment, in particular because of the known high variability in interpreting images, and also because “synovitis” on imaging can be detected in symptom-free individuals from the general population (49,50). As such, it may be some time before the appropriate role of imaging is understood for use in defining the presence of current “actionable” disease in the absence of findings of IA on examination, as well as prediction and prevention in IA/RA.

In summary, prediction is a critical part of prevention, and it is important that existing clinical trials, ongoing natural history studies (e.g., of FDRs, indigenous North Americans, and the Dutch Lifelines study [15,34–36,51]) as well as future studies, optimize diagnostic accuracies of models for the likelihood and timing of future RA. These models should also account for cross-test interpretation, with consideration of a standardization of testing, similar to that done in autoantibody testing in type 1 diabetes mellitus (DM) (52,53). Specifically, one could envision a model, perhaps developed through advanced analytic techniques such as artificial intelligence/machine learning (54), that incorporates multiple dimensions including demographic characteristics, family history/genetics, environmental factors, autoantibodies and other biomarkers, symptoms, examination findings, and imaging to give accurate and clear information about an individual’s likelihood and timing of future RA. This could even be a 2-step model where a relatively inexpensive test (e.g., serum ACPA) could be evaluated first to determine an overall risk, and additional factors could then be assessed during follow-up to determine current clinical status, more specific level of risk, as well as potential timing of onset of disease (24). Furthermore, as discussed in more detail below, such a model could potentially identify what specific pathways should be targeted to prevent disease.

Novel targets for prevention. The current clinical trials in RA prevention are evaluating agents that have been used in established RA. This is in part because these agents have known efficacy, safety, and tolerability profiles in RA, and have regulatory agency support. These agents may also successfully be able to

alter antigen presentation, innate and adaptive responses (e.g., B and T cell interactions), expansion of autoantibodies (e.g., ACPA fine specificities and RF), and expansion of inflammation that appear critical in pre-RA development. However, these agents have been studied to determine their efficacy in established RA; therefore, it may be that they do not address key biologic pathways in pre-RA. Indeed, it may be that novel pathways, even mucosal-based ones, need to be targeted for effective prevention (31).

As such, it will be important to explore biologic pathways in pre-RA in conjunction with the existing (and future) clinical trials and other studies so that the next round of trials will target the most relevant pathways. To that end, a growing interest in using animal models to understand the mechanisms of “pre-disease” may provide the means to validate pathways identified in human studies, as well as potentially identify novel targets for prevention. For example, Jubair and colleagues have demonstrated in a murine model of arthritis that microbiome-directed interventions prior to the onset of IA can greatly diminish arthritis, even if administered after systemic autoimmunity has developed (55).

While results are conflicting and have not been evaluated in a randomized, prospective manner, there are a growing number of studies identifying lifestyle factors that may reduce the risk of RA. These include smoking cessation, a healthy diet (and likely one enriched in fish consumption and omega-3 fatty acids), weight loss, and increased exercise (for review, see ref. 56) (Table 2). Because these interventions may take years to yield beneficial effects, they may never be formally studied alone in interventional prevention trials. However, given the potentially broad beneficial effects, these factors may need to be included as “general” preventive recommendations in conjunction with other interventions; furthermore, they may be important to optimize risk/benefit ratios of interventions in individuals with only modest autoimmune abnormalities and risk of future RA.

Importantly, while precision/personalized medicine in the management of established RA has not yet reached fruition, one could envision that in pre-RA there may be an ability to identify a specific pathway for an individual that could be optimal to target, either pharmacologically and/or through lifestyle modifications, to optimize prevention.

Prevention trial design and duration of intervention. The current and completed trials for RA prevention are relatively simple—1:1 randomization comparing active drug and placebo. Furthermore, the interventions are of limited duration (e.g., in PRAIRI a single dose of rituximab was given). In addition, the primary outcome for these trials is the development of classifiable RA.

These approaches are appropriate in these early days of prevention to address safety and ethical concerns, costs, and the preferences of individuals who are participating in trials. The outcome of classifiable RA is also a clinically meaningful and agreed-upon disease state. In addition, the use of placebo is

important because the prediction of future RA is not perfect, and it is expected that a number of individuals, even those with high-risk features, may still not progress to clinically apparent IA/RA during the time period of a study, and therefore one needs to know if the study drug truly resulted in benefit.

However, for several reasons, the next round of prevention trials will likely have different designs. First, RA is a relatively rare disease and there are difficulties in finding individuals with pre-RA; furthermore, there are multiple possible pathways that may be addressed to delay or halt the development of RA. As such, adaptive trials may be considered, where multiple interventions can be tested within a single trial that can optimize small subject numbers (57). Second, instead of classifiable RA, trials may need to use other informative outcomes, such as levels of autoantibodies or cytokines/chemokines, especially since these outcomes may be able to shorten clinical trials given that outcomes of classifiable RA may take years to develop. Specifically, it appears that an important feature of the pathogenesis of pre-RA is expansion of ACPAs and new antibody formation (e.g., RF) and inflammation; as such, of interest for prevention is the efficacy of approaches to arrest the expansion of autoimmunity and inflammation, as well as to use biomarker levels to provide insights into the success of an intervention. For example, an intervention may be considered a success in an ACPA-positive individual who does not develop future abnormalities of RF.

Furthermore, it is important to consider whether there are symptoms and other impactful medical issues that have been identified prior to IA/RA and are potentially related to autoimmunity. Some of these features may be termed an “RA prodrome” and include arthralgia (the etiology of which in the absence of definable IA is as of yet unclear), functional limitations, fatigue, sleep abnormalities, work absences, mental health disorders, and potentially other nonarticular manifestations of autoimmunity such as lung and cardiovascular disease, and sicca symptoms (58–61). Understanding these potential non-IA manifestations of RA could impact the development of prevention approaches in RA, resulting in treatment of a current “autoimmune-opathy” and also prevention of future IA/RA—similar to the concept of treating a “diagnosis” of hypertension to prevent a future heart attack. These non-IA features could also be used as end points themselves. Nomenclature pertaining to pre-RA could also be expanded to include non-articular manifestations of disease.

Finally, it would be ideal if a time-limited intervention had lasting benefit for prevention; however, the development of IA/RA was only delayed in the rituximab-treated group in the PRAIRI study. As such, while the ongoing trials will further inform this issue, it may be that longer-term interventions are needed to more effectively delay or prevent IA/RA. This would be akin to statin treatment in hypercholesterolemia where the drug is continued indefinitely to provide long-term benefit. However, even if it takes a prolonged intervention to delay or halt the first appearance of IA, there may be substantial benefit in improved symptoms, and

reduced long-term damage and disability. Furthermore, while the issue of lead-time bias needs to be considered, it could be beneficial if the IA/RA that develops is a less-aggressive form that ultimately requires less expensive or toxic interventions for control; furthermore, earlier diagnosis and treatment of clinically apparent IA/RA enabled by closely following at-risk individuals could lead to improved outcomes. These issues should be evaluated as part of studies going forward.

Participation of individuals at risk of future RA. The current trials in RA prevention have used criteria to select individuals who are at high risk of RA within a relatively short time and combinations of autoantibody elevations and symptoms, with those subjects largely identified through clinics, although some studies include recruitment from FDR and general populations.

Selecting such high-risk individuals largely from clinics is reasonable for the first round of prevention trials to meet trial design and ethical requirements; furthermore, a trial can be spared from having to develop costly infrastructure to identify at-risk individuals through population-based approaches such as broad testing for autoantibodies. However, such approaches may identify individuals who are so far along in the development of RA that prevention is difficult to attain, as well as miss high-risk individuals who have few symptoms or lack access to clinical care. As such, in future trials additional inclusion criteria may be considered that have perhaps a lower (yet still definable and accurate) risk of RA, but also identify a stage of RA development that is more amenable to halt or a change to a more benign state. This could entail study design and enrollment strategies, such as broad population-based autoantibody testing, to identify individuals who may be asymptomatic and/or have only modest elevations of autoantibodies (Figure 2). Such trials may use “safer” interventions, such as low toxicity medications or lifestyle changes, yet still be effective if indeed the immune system is at stages of RA where only modest dysregulation is present and it is more amenable to remaining in or returning to a “normal” state. Importantly, RA would benefit from efforts similar to those in type 1 DM where networks such as Trialnet have been developed. Such networks include FDR and general population screening to create a pool of type 1 DM–related autoantibody–positive individuals who can readily be recruited for type 1 DM prevention trials such as the teplizumab study (62,63).

Another consideration is that individuals who seek clinical care for joint symptoms and are found to be in a pre-RA state may be more interested in participating in a prevention trial than someone who is at risk but is asymptomatic and/or has little understanding of what RA is—which may be the type of individual identified if broad population-based screening for RA risk was implemented. Informing these issues to some extent, there are studies that have explored “preferences” for prevention in at-risk individuals (64,65). General themes that have emerged include that at-risk individuals would like clarity around what RA is as a disease, their absolute risk of IA/RA, and to know that interventions are highly likely to

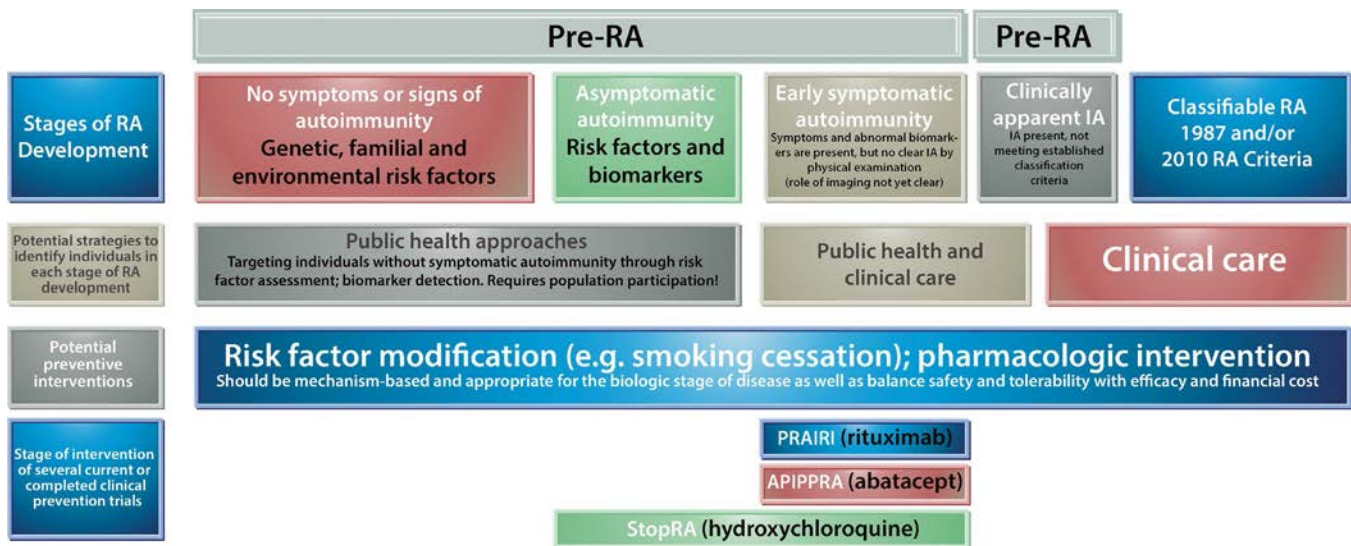


Figure 2. Strategies for identification and intervention for rheumatoid arthritis (RA) prevention. Differing approaches are needed based on the stage of RA development. There is some controversy over whether the term “pre-RA” should be applied once clinically apparent inflammatory arthritis (IA) is present if it is not classifiable as RA. PRAIRI = Prevention of Clinically Manifest Rheumatoid Arthritis by B Cell–Directed Therapy in the Earliest Phase of the Disease; APIPPRA = Arthritis Prevention in the Preclinical Phase with Abatacept; StopRA = Strategy for the Prevention of the Clinically Apparent Onset of RA.

be successful as well as well-tolerated and safe. Following this, if prevention is to be implemented in asymptomatic individuals, or those who are unaware of RA, there will need to be additional efforts to educate these populations about RA, and what screening and prevention may mean to their health. This will require broad public education about RA. These educational activities could be encompassed under a “rheumatology preventionist” (term courtesy of Frederick Miller). Importantly, a collateral benefit of increased prevention-related public awareness programs may be a reduction in delays in treatment for clinically apparent IA/RA (6). Notably, the aforementioned prevention trial of statins terminated early due to slow enrollment, which was in part due to subject reluctance to participate (ref. 42, and van Schaardenburg D: personal communication). This highlights the importance of fully understanding and addressing subjects’ preferences in order to complete robust clinical trials.

Importantly, having clear and informative nomenclature regarding pre-RA would help facilitate education of individuals who are at risk of RA as well as health care providers and other stakeholders (66). This may ultimately include nomenclature pertaining to nonarticular manifestations of RA. An example that may provide insights for RA is from type 1 DM where antibody-positive states, even in the absence of a need for insulin therapy, are now considered disease (67), with this designation facilitating education of individuals at risk of type 1 DM and the performance of interventional studies. Notably, International Statistical Classification of Diseases and Related Health Problems, Tenth Revision codes already exist for some aspects that could be applied to pre-RA, including ACPA positivity (R79.89) and family history of RA (Z82.61). A caveat is that naming a condition, or risk

of a future condition, may also have implications on an individual’s ability to obtain insurance coverage.

Participation of rheumatologists. Rheumatology practitioners will play a key near and long-term role in prevention because of their expertise in RA; furthermore, they are currently best positioned to identify individuals with joint symptoms and autoantibody abnormalities yet no clinically identifiable IA who are likely to be “first in line” for prevention. In addition, if “standard” RA medications are used in prevention, rheumatologists are best situated to work with individuals around the use, risks, and benefits of these agents. However, given that most rheumatology practices now entail treating individuals who have substantial illness and are already limited by provider shortages and long wait times (8), practice patterns may have to change to accommodate prevention. Furthermore, it may be that some aspects of prevention would ultimately be supported by primary care.

In addition, there will need to be new ways to evaluate and follow up individuals with pre-RA to gauge the effectiveness of an intervention, or even to know when an intervention could be tapered or stopped. These approaches have yet to be determined but will likely include joint examination although that may be less informative with regard to responses in individuals who have never developed clinically apparent IA; as such, follow-up may be more reliant on careful imaging, and assessment of informative biomarkers as well as subject-reported outcomes that quantify symptoms such as pain, stiffness, and swelling as well as nonarticular disease such as fatigue. These assessments could be accomplished through

wearables, mobile app or web-based (e.g., telemedicine), especially given the growing use of these platforms in RA (68).

Participation of other stakeholders. Other stakeholders critical to advancing prevention include epidemiologists, trialists and outcomes researchers, and translational and basic science researchers who can help discover new targets and implement informative clinical trials. Support from governmental funding and regulatory agencies is needed to promote prevention research. Similarly, pharmaceutical industry involvement is essential to support target identification and drug development, trials, and, importantly, to create sustainable business models that include prevention. The biotechnology and diagnostic industries will also need to support the development of platforms and biomarkers useful in predicting RA, as well as measuring outcomes. Finally, stakeholders need to include health care and insurance systems, and health economists and governmental agencies (e.g., US Preventive Services Taskforce) that can help enact screening and prevention into routine clinical care, and convince payors to implement prevention (69,70).

Current management of pre-RA

In terms of what can be done now for individuals with pre-RA, if an individual has sufficient symptoms and is autoantibody positive, there is a tendency to treat, even if clinically apparent IA is not identified. However, given that a number of individuals with symptoms and autoantibodies may not progress to IA, it is critical to perform trials to help guide the type and duration of interventions. If available, clinicians should consider referring appropriate individuals to clinical trials. If such referral is not possible, while not well-proven, recommendations for risk reduction could include tobacco cessation, exercise, a healthy body weight, and a Mediterranean-type diet that may also be broadly beneficial to other aspects of health (e.g., cardiovascular disease) (56,71). Recommendations on supplements should be avoided until more data are available; however, as several studies have shown that omega-3 levels and supplement intake are inversely associated with risk of increased autoantibody levels and progression to IA, this particular approach deserves additional study (72). In addition, while periodontal disease has been identified in pre-RA (73), and higher levels of perceived stress have been associated with incident IA/RA (60), more data are needed before interventions such as dental care and stress reduction are recommended as preventive interventions. Finally, and most importantly, subjects at risk of IA/RA should be counseled to seek medical attention if joint symptoms develop or worsen, and it is reasonable to advise periodic follow-up (perhaps annually) with a rheumatologist to evaluate the joints and offer ongoing counseling.

Conclusions

The understanding of pre-RA, and an ability to predict the development of future IA/RA, has advanced to where trials to prevent IA/RA have been completed, with others underway. The findings from these trials, and other studies evaluating the natural history of RA, will provide important knowledge for future preventive trials as well as potentially clinical care, moving the field in the near future to a paradigm where RA, and soon other autoimmune rheumatic diseases, may follow similar models where an at-risk state can be identified and approached with an “intent to prevent.”

AUTHOR CONTRIBUTIONS

Drs. Deane and Holers drafted the article, revised it critically for important intellectual content, and approved the final version to be published.

REFERENCES

- Smolen JS, Aletaha D, Barton A, Burmester GR, Emery P, Firestein GS, et al. Rheumatoid arthritis [review]. *Nat Rev Dis Primers* 2018;4:18001.
- Singh JA, Saag KG, Bridges SL Jr, Akl EA, Bannuru RR, Sullivan MC, et al. 2015 American College of Rheumatology guideline for the treatment of rheumatoid arthritis. *Arthritis Rheumatol* 2016;68:1–26.
- Arnett FC, Edworthy SM, Bloch DA, McShane DJ, Fries JF, Cooper NS, et al. The American Rheumatism Association 1987 revised criteria for the classification of rheumatoid arthritis. *Arthritis Rheum* 1988;31:315–24.
- Aletaha D, Neogi T, Silman AJ, Funovits J, Felson DT, Bingham CO III, et al. 2010 rheumatoid arthritis classification criteria: an American College of Rheumatology/European League Against Rheumatism collaborative initiative. *Arthritis Rheum* 2010;62:2569–81.
- Burgers LE, Raza K, van der Helm-van Mil AH. Window of opportunity in rheumatoid arthritis: definitions and supporting evidence: from old to new perspectives. *RMD Open* 2019;5:e000870.
- Stack RJ, Nightingale P, Jinks C, Shaw K, Herron-Marx S, Horne R, et al. Delays between the onset of symptoms and first rheumatology consultation in patients with rheumatoid arthritis in the UK: an observational study. *BMJ Open* 2019;9:e024361.
- Gul HL, Eugenio G, Rabin T, Burska A, Parmar R, Wu J, et al. Defining remission in rheumatoid arthritis: does it matter to the patient? A comparison of multi-dimensional remission criteria and patient reported outcomes. *Rheumatology (Oxford)* 2020;59:613–21.
- Battafarano DF, Ditmyer M, Bolster MB, Fitzgerald JD, Deal C, Bass AR, et al. 2015 American College of Rheumatology workforce study: supply and demand projections of adult rheumatology workforce, 2015–2030. *Arthritis Care Res (Hoboken)* 2018;70:617–26.
- Del Puente A, Knowler WC, Pettitt DJ, Bennett PH. The incidence of rheumatoid arthritis is predicted by rheumatoid factor titer in a longitudinal population study. *Arthritis Rheum* 1988;31:1239–44.
- Aho K, Palosuo T, Heliövaara M, Knekt P, Alha P, von Essen R. Anti-filaggrin antibodies within “normal” range predict rheumatoid arthritis in a linear fashion. *J Rheumatol* 2000;27:2743–6.
- Silman AJ, Ollier B, Mageed RA. Rheumatoid factor detection in the unaffected first degree relatives in families with multicase rheumatoid arthritis. *J Rheumatol* 1991;18:512–5.
- Rantapää-Dahlqvist S, de Jong BA, Berglin E, Hallmans G, Wadell G, Stenlund H, et al. Antibodies against cyclic citrullinated peptide



- and IgA rheumatoid factor predict the development of rheumatoid arthritis. *Arthritis Rheum* 2003;48:2741–9.
13. Nielen MM, van Schaardenburg D, Reesink HW, van de Stadt RJ, van der Horst-Bruinsma IE, de Koning MH, et al. Specific autoantibodies precede the symptoms of rheumatoid arthritis: a study of serial measurements in blood donors. *Arthritis Rheum* 2004;50:380–6.
 14. Majka DS, Deane KD, Parrish LA, Lazar AA, Baron AE, Walker CW, et al. Duration of preclinical rheumatoid arthritis-related autoantibody positivity increases in subjects with older age at time of disease diagnosis. *Ann Rheum Dis* 2008;67:801–7.
 15. Ramos-Remus C, Castillo-Ortiz JD, Aguilar-Lozano L, Padilla-Ibarra J, Sandoval-Castro C, Vargas-Serafin CO, et al. Autoantibodies in prediction of the development of rheumatoid arthritis among healthy relatives of patients with the disease. *Arthritis Rheumatol* 2015;67:2837–44.
 16. Gan RW, Trouw LA, Shi J, Toes RE, Huizinga TW, Demoruelle MK, et al. Anti-carbamylated protein antibodies are present prior to rheumatoid arthritis and are associated with its future diagnosis. *J Rheumatol* 2015;42:572–9.
 17. Kolfenbach JR, Deane KD, Derber LA, O'Donnell CI, Gilliland WR, Edison JD, et al. Autoimmunity to peptidyl arginine deiminase type 4 precedes clinical onset of rheumatoid arthritis. *Arthritis Rheum* 2010;62:2633–9.
 18. Sokolove J, Bromberg R, Deane KD, Lahey LJ, Derber LA, Chandra PE, et al. Autoantibody epitope spreading in the pre-clinical phase predicts progression to rheumatoid arthritis. *PLoS One* 2012;7:e35296.
 19. Kokkonen H, Mullazehi M, Berglin E, Hallmans G, Wadell G, Ronnelid J, et al. Antibodies of IgG, IgA and IgM isotypes against cyclic citrullinated peptide precede the development of rheumatoid arthritis. *Arthritis Res Ther* 2011;13:R13.
 20. Kokkonen H, Brink M, Hansson M, Lassen E, Mathsson-Alm L, Holmdahl R, et al. Associations of antibodies against citrullinated peptides with human leukocyte antigen-shared epitope and smoking prior to the development of rheumatoid arthritis. *Arthritis Res Ther* 2015;17:125.
 21. Kelmenson LB, Wagner BD, McNair BK, Frazer-Abel A, Demoruelle MK, Bergstedt DT, et al. Timing of elevations of autoantibody isotypes prior to diagnosis of rheumatoid arthritis. *Arthritis Rheumatol* 2020;72:251–61.
 22. Verheul MK, Böhringer S, van Delft MA, Jones JD, Rigby WF, Gan RW, et al. Triple positivity for anti-citrullinated protein autoantibodies, rheumatoid factor, and anti-carbamylated protein antibodies conferring high specificity for rheumatoid arthritis: implications for very early identification of at-risk individuals. *Arthritis Rheumatol* 2018;70:1721–31.
 23. Kokkonen H, Söderström I, Rocklöv J, Hallmans G, Lejon K, Dahlqvist SR. Up-regulation of cytokines and chemokines predates the onset of rheumatoid arthritis. *Arthritis Rheum* 2010;62:383–91.
 24. Deane KD, O'Donnell CI, Hueber W, Majka DS, Lazar AA, Derber LA, et al. The number of elevated cytokines and chemokines in preclinical seropositive rheumatoid arthritis predicts time to diagnosis in an age-dependent manner. *Arthritis Rheum* 2010;62:3161–72.
 25. Hafkenschied L, de Moel E, Smolik I, Tanner S, Meng X, Jansen BC, et al. N-linked glycans in the variable domain of IgG anti-citrullinated protein antibodies predict the development of rheumatoid arthritis. *Arthritis Rheumatol* 2019;71:1626–33.
 26. Hunt L, Hensor EM, Nam J, Burska AN, Parmar R, Emery P, et al. T cell subsets: an immunological biomarker to predict progression to clinical arthritis in ACPA-positive individuals. *Ann Rheum Dis* 2016;75:1884–9.
 27. Deane KD, Demoruelle MK, Kelmenson LB, Kuhn KA, Norris JM, Holers VM. Genetic and environmental risk factors for rheumatoid arthritis. *Best Pract Res Clin Rheumatol* 2017;31:3–18.
 28. Klareskog L, Stolt P, Lundberg K, Källberg H, Bengtsson C, Grunewald J, et al. A new model for an etiology of rheumatoid arthritis: smoking may trigger HLA-DR (shared epitope)-restricted immune reactions to autoantigens modified by citrullination. *Arthritis Rheum* 2006;54:38–46.
 29. Van de Stadt LA, Witte BI, Bos WH, van Schaardenburg D. A prediction rule for the development of arthritis in seropositive arthralgia patients. *Ann Rheum Dis* 2013;72:1920–6.
 30. De Hair MJ, van de Sande MG, Ramwadhoebe TH, Hansson M, Landewé R, van der Leij C, et al. Features of the synovium of individuals at risk of developing rheumatoid arthritis: implications for understanding preclinical rheumatoid arthritis. *Arthritis Rheumatol* 2014;66:513–22.
 31. Holers VM, Demoruelle MK, Kuhn KA, Buckner JH, Robinson WH, Okamoto Y, et al. Rheumatoid arthritis and the mucosal origins hypothesis: protection turns to destruction [review]. *Nat Rev Rheumatol* 2018;14:542–57.
 32. Gerlag DM, Raza K, van Baarsen LG, Brouwer E, Buckley CD, Burmester GR, et al. EULAR recommendations for terminology and research in individuals at risk of rheumatoid arthritis: report from the Study Group for Risk Factors for Rheumatoid Arthritis. *Ann Rheum Dis* 2012;71:638–41.
 33. Rakeh C, Nam JL, Hunt L, Hensor EM, Das S, Bissell LA, et al. Predicting the development of clinical arthritis in anti-CCP positive individuals with non-specific musculoskeletal symptoms: a prospective observational cohort study. *Ann Rheum Dis* 2015;74:1659–66.
 34. Kolfenbach JR, Deane KD, Derber LA, O'Donnell C, Weisman MH, Buckner JH, et al. A prospective approach to investigating the natural history of preclinical rheumatoid arthritis (RA) using first-degree relatives of probands with RA. *Arthritis Rheum* 2009;61:1735–42.
 35. Tanner S, Dufault B, Smolik I, Meng X, Anaparti V, Hitchon C, et al. A prospective study of the development of inflammatory arthritis in the family members of Indigenous North American people with rheumatoid arthritis. *Arthritis Rheumatol* 2019;71:1494–503.
 36. Kim SK, Bae J, Lee H, Kim JH, Park SH, Choe JY. Greater prevalence of seropositivity for anti-cyclic citrullinated peptide antibody in unaffected first-degree relatives in multicase rheumatoid arthritis-affected families. *Korean J Intern Med* 2013;28:45–53.
 37. Gonzalez-Lopez L, Gamez-Nava JI, Jhangri G, Russell AS, Suarez-Almazor ME. Decreased progression to rheumatoid arthritis or other connective tissue diseases in patients with palindromic rheumatism treated with antimalarials. *J Rheumatol* 2000;27:41–6.
 38. Bos WH, Dijkmans BA, Boers M, van de Stadt RJ, van Schaardenburg D. Effect of dexamethasone on autoantibody levels and arthritis development in patients with arthralgia: a randomised trial. *Ann Rheum Dis* 2010;69:571–4.
 39. Gerlag DM, Safy M, Majjer KI, Tang MW, Tas SW, Starmans-Kool MJ, et al. Effects of B cell directed therapy on the preclinical stage of rheumatoid arthritis: the PRAIRI study. *Ann Rheum Dis* 2019;78:179–85.
 40. National Institute of Allergy and Infectious Diseases, sponsor. Strategy to prevent the onset of clinically-apparent rheumatoid arthritis (StopRA). [Clinicaltrials.gov identifier: NCT02603146](https://clinicaltrials.gov/ct2/show/study/NCT02603146); 2020.
 41. Al-Laith M, Jasencova M, Abraham S, Bosworth A, Bruce IN, Buckley CD, et al. Arthritis prevention in the pre-clinical phase of RA with abatacept (the APIPPRA study): a multi-centre, randomised, double-blind, parallel-group, placebo-controlled clinical trial protocol. *Trials* 2019;20:429.
 42. Amsterdam Rheumatology & immunology Center, sponsor. Statins to prevent rheumatoid arthritis (STAPRA). [Netherlands Trial Register: NL5036](https://www.trialsregister.nl/ct2/show/study/NL5036); 2020.

43. Leiden University Medical Centre, sponsor. Treat early arthralgia to reverse or limit impending exacerbation to rheumatoid arthritis (TREAT EARLIER). Netherlands Trial Register: NL4599; 2020.
44. Barra L, Bykerk V, Pope JE, Haraoui BP, Hitchon CA, Thorne JC, et al. Anticitrullinated protein antibodies and rheumatoid factor fluctuate in early inflammatory arthritis and do not predict clinical outcomes. *J Rheumatol* 2013;40:1259–67.
45. Demoruelle MK, Parish MC, Derber LA, Kolfenbach JR, Hughes-Austin JM, Weisman MH, et al. Performance of anti-cyclic citrullinated peptide assays differs in subjects at increased risk of rheumatoid arthritis and subjects with established disease. *Arthritis Rheum* 2013;65:2243–52.
46. Van Steenberg HW, Aletaha D, Beart-van de Voorde LJ, Brouwer E, Codreanu C, Combe B, et al. EULAR definition of arthralgia suspicious for progression to rheumatoid arthritis. *Ann Rheum Dis* 2017;76:491–6.
47. Chibnik LB, Keenan BT, Cui J, Liao KP, Costenbader KH, Plenge RM, et al. Genetic risk score predicting risk of rheumatoid arthritis phenotypes and age of symptom onset. *PloS One* 2011;6:e24380.
48. Zabotti A, Finzel S, Baraliakos X, Aouad K, Ziade N, Iagnocco A. Imaging in the preclinical phases of rheumatoid arthritis. *Clin Exp Rheumatol* 2020;38:536–42.
49. Mangnus L, van Steenberg HW, Reijniere M, van der Helm-van Mil AH. Magnetic resonance imaging-detected features of inflammation and erosions in symptom-free persons from the general population. *Arthritis Rheumatol* 2016;68:2593–602.
50. Brulhart L, Alpizar-Rodriguez D, Nissen MS, Zufferey P, Ciobotariu I, Fleury G, et al. Ultrasound is not associated with the presence of systemic autoimmunity or symptoms in individuals at risk for rheumatoid arthritis. *RMD Open* 2019;5:e000922.
51. Van Zanten A, Arends S, Roozendaal C, Limburg PC, Maas F, Trouw LA, et al. Presence of anticitrullinated protein antibodies in a large population-based cohort from the Netherlands. *Ann Rheum Dis* 2017;76:1184–90.
52. Bonifacio E, Yu L, Williams AK, Eisenbarth GS, Bingley PJ, Marcovina SM, et al. Harmonization of glutamic acid decarboxylase and islet antigen-2 autoantibody assays for national institute of diabetes and digestive and kidney diseases consortia. *J Clin Endocrinol Metab* 2010;95:3360–7.
53. Meroni PL, Biggoggero M, Pierangeli SS, Sheldon J, Zegers I, Borghi MO. Standardization of autoantibody testing: a paradigm for serology in rheumatic diseases [review]. *Nat Rev Rheumatol* 2014;10:35–43.
54. Nelson CA, Butte AJ, Baranzini SE. Integrating biomedical research and electronic health records to create knowledge-based biologically meaningful machine-readable embeddings. *Nat Commun* 2019;10:3045.
55. Jubair WK, Hendrickson JD, Severs EL, Schulz HM, Adhikari S, Ir D, et al. Modulation of inflammatory arthritis in mice by gut microbiota through mucosal inflammation and autoantibody generation. *Arthritis Rheumatol* 2018;70:1220–33.
56. Zaccardelli A, Friedlander HM, Ford JA, Sparks JA. Potential of lifestyle changes for reducing the risk of developing rheumatoid arthritis: is an ounce of prevention worth a pound of cure? *Clin Ther* 2019;41:1323–45.
57. Bayar MA, le Teuff G, Koenig F, Le Deley MC, Michiels S. Group sequential adaptive designs in series of time-to-event randomised trials in rare diseases: a simulation study. *Stat Methods Med Res* 2020;29:1483–98.
58. Stack RJ, van Tuyl LH, Sloots M, van de Stadt LA, Hoogland W, Maat B, et al. Symptom complexes in patients with seropositive arthralgia and in patients newly diagnosed with rheumatoid arthritis: a qualitative exploration of symptom development. *Rheumatology (Oxford)* 2014;53:1646–53.
59. Maradit-Kremers H, Crowson CS, Nicola PJ, Ballman KV, Roger VL, Jacobsen SJ, et al. Increased unrecognized coronary heart disease and sudden deaths in rheumatoid arthritis: a population-based cohort study. *Arthritis Rheum* 2005;52:402–11.
60. Polinski KJ, Bemis EA, Feser M, Seifert J, Demoruelle MK, Striebich CC, et al. Perceived stress and inflammatory arthritis: a prospective investigation in the Studies of the Etiologies of Rheumatoid Arthritis cohort. *Arthritis Care Res (Hoboken)* 2020;72:1766–71.
61. Marrie RA, Walld R, Bolton JM, Sareen J, Walker JR, Patten SB, et al. Rising incidence of psychiatric disorders before diagnosis of immune-mediated inflammatory disease. *Epidemiol Psychiatr Sci* 2019;28:333–42.
62. Greenbaum CJ, Speake C, Krischer J, Buckner J, Gottlieb PA, Schatz DA, et al. Strength in numbers: opportunities for enhancing the development of effective treatments for type 1 diabetes-the Trial-Net experience. *Diabetes* 2018;67:1216–25.
63. Herold KC, Bundy BN, Long SA, Bluestone JA, DiMeglio LA, Dufort MJ, et al. An anti-CD3 antibody, teplizumab, in relatives at risk for type 1 diabetes. *N Engl J Med* 2019;381:603–13.
64. Sparks JA, Iversen MD, Yu Z, Tiedman NA, Prado MG, Kroouze RM, et al. Disclosure of personalized rheumatoid arthritis risk using genetics, biomarkers, and lifestyle factors to motivate health behavior improvements: a randomized controlled trial. *Arthritis Care Res (Hoboken)* 2018;70:823–33.
65. Falahee M, Finckh A, Raza K, Harrison M. Preferences of patients and at-risk individuals for preventive approaches to rheumatoid arthritis. *Clin Ther* 2019;41:1346–54.
66. Raza K, Holers VM, Gerlag D. Nomenclature for the phases of the development of rheumatoid arthritis. *Clin Ther* 2019;41:1279–85.
67. Bonifacio E, Mathieu C, Nepom GT, Ziegler AG, Anhalt H, Haller MJ, et al. Rebranding asymptomatic type 1 diabetes: the case for autoimmune β cell disorder as a pathological and diagnostic entity. *Diabetologia* 2017;60:35–8.
68. Luo D, Wang P, Lu F, Elias J, Sparks JA, Lee YC. Mobile apps for individuals with rheumatoid arthritis: a systematic review. *J Clin Rheumatol* 2019;25:133–41.
69. Calonge N. Developing evidence-based screening recommendations, with consideration for rheumatology. *Rheum Dis Clin North Am* 2014;40:787–95.
70. Irargorri N, Hazlewood G, Manns B, Bojke L, Spackman E, on behalf of the PROMPT study group. A model to determine the cost-effectiveness of screening psoriasis patients for psoriatic arthritis. *Arthritis Care Res (Hoboken)* doi: <https://onlinelibrary.wiley.com/doi/epdf/10.1002/acr.24110>. E-pub ahead of print.
71. Liu X, Tedeschi SK, Barbhayya M, Leatherwood CL, Speyer CB, Lu B, et al. Impact and timing of smoking cessation on reducing risk of rheumatoid arthritis among women in the Nurses' Health Studies. *Arthritis Care Res (Hoboken)* 2019;71:914–24.
72. Gan RW, Demoruelle MK, Deane KD, Weisman MH, Buckner JH, Gregersen PK, et al. Omega-3 fatty acids are associated with a lower prevalence of autoantibodies in shared epitope-positive subjects at risk for rheumatoid arthritis. *Ann Rheum Dis* 2017;76:147–52.
73. Mankia K, Cheng Z, Do T, Hunt L, Meade J, Kang J, et al. Prevalence of periodontal disease and periodontopathic bacteria in anti-cyclic citrullinated protein antibody-positive at-risk adults without arthritis. *JAMA Netw Open* 2019;2:e195394.
74. Aho K, von Essen R, Kurki P, Palosuo T, Heliövaara M. Antikeratin antibody and antiperinuclear factor as markers for subclinical rheumatoid disease process. *J Rheumatol* 1993;20:1278–81.

75. Silman AJ, Hennessy E, Ollier B. Incidence of rheumatoid arthritis in a genetically predisposed population. *Br J Rheumatol* 1992;31:365–8.
76. Ercan A, Cui J, Chatterton DE, Deane KD, Hazen MM, Brintnell W, et al. Aberrant IgG galactosylation precedes disease onset, correlates with disease activity, and is prevalent in autoantibodies in rheumatoid arthritis. *Arthritis Rheum* 2010;62:2239–48.
77. Karlson EW, Chibnik LB, Tworoger SS, Lee IM, Buring JE, Shadick NA, et al. Biomarkers of inflammation and development of rheumatoid arthritis in women from two prospective cohort studies. *Arthritis Rheum* 2009;60:641–52.
78. De Hair MJ, Landewe RB, van de Sande MG, van Schaardenburg D, van Baarsen LG, Gerlag DM, et al. Smoking and overweight determine the likelihood of developing rheumatoid arthritis. *Ann Rheum Dis* 2013;72:1654–8.
79. Burgers LE, Siljehult F, Brinck RM, van Steenberg HW, Landewe RB, Rantapää-Dahlqvist S, et al. Validation of the EULAR definition of arthralgia suspicious for progression to rheumatoid arthritis. *Rheumatology (Oxford)* 2017;56:2123–8.
80. Gan RW, Bemis EA, Demoruelle MK, Striebich CC, Brake S, Feser ML, et al. The association between ω -3 fatty acid biomarkers and inflammatory arthritis in an anti-citrullinated protein antibody positive population. *Rheumatology (Oxford)* 2017;56:2229–36.
81. Ferucci ED, Templin DW, Lanier AP. Rheumatoid arthritis in American Indians and Alaska Natives: a review of the literature. *Semin Arthritis Rheum* 2005;34:662–7.
82. Ren L, Guo P, Sun QM, Liu H, Chen Y, Huang Y, et al. Number of parity and the risk of rheumatoid arthritis in women: a dose-response meta-analysis of observational studies. *J Obstet Gynaecol Res* 2017;43:1428–40.
83. Bhatia SS, Majka DS, Kittelson JM, Parrish LA, Ferucci ED, Deane KD, et al. Rheumatoid factor seropositivity is inversely associated with oral contraceptive use in women without rheumatoid arthritis. *Ann Rheum Dis* 2007;66:267–9.
84. Demoruelle MK, Weisman MH, Simonian PL, Lynch DA, Sachs PB, Pedraza IF, et al. Brief report: airways abnormalities and rheumatoid arthritis-related autoantibodies in subjects without arthritis: early injury or initiating site of autoimmunity? *Arthritis Rheum* 2012;64:1756–61.

EDITORIAL

Urinary Biomarkers in Lupus Nephritis: Are We There Yet?

Chi Chiu Mok¹  and Chandra Mohan² 

Lupus nephritis (LN) is a major cause of end-stage renal disease (ESRD) in the younger population (1). There is marked ethnic disparity in the burden of renal disease in patients with systemic lupus erythematosus (SLE), with the highest prevalence observed in Africans, Hispanics, and Asians (2). In a US registry study, 73% of patients with LN who developed ESRD were African Americans and Hispanic Americans (3). Early identification of renal disease in SLE is important. Current screening for LN relies on urine tests for proteins (determination of the urinary protein-to-creatinine [P/Cr] ratio) and the presence of active sediments, along with calculation of the estimated glomerular filtration rate (eGFR). Albeit simple and noninvasive, these urine tests are neither sensitive nor specific for differentiating LN from other glomerulopathies or distinguishing active inflammation from chronic scarring in the kidneys. The gold standard for the diagnosis and prognostic stratification of LN remains a renal biopsy, which is invasive and contraindicated in a proportion of patients.

Urinary biomarkers appear to be more promising than serum markers, because they arise directly from the inflamed kidney tissue. An ideal urinary biomarker for LN activity should be specific for SLE and for renal involvement in the disease. It should be sensitive to change and show good correlation with renal activity as assessed serially on the basis of histologic features. Moreover, it should be more sensitive than conventional measures of the urinary P/Cr and urinary sediments in detecting a renal flare, surfacing before the development of proteinuria, and should be able to distinguish renal disease activity from chronicity. Finally, the assay test must be easy to perform, inexpensive, and have a short turnaround time to aid in therapeutic decisions.

Candidate proteins that include urinary cytokines, chemokines, adhesion molecules, and growth factors have been identified based on their relationship to the pathophysiology of LN and have been studied in cross-sectional and longitudinal studies (4). Examples are monocyte chemoattractant protein 1, neutrophil gelatinase B-associated lipocalin, tumor necrosis factor–like weak inducer of apoptosis, and interferon- γ -inducible protein 10. More

recently, utilization of nonbiased, high-throughput proteomics screening techniques offer the feasibility of carrying out simultaneous evaluation of a large number of proteins (5). In a systematic review, more than 28 candidate biomarker proteins in SLE were identified using mass spectrometry (MS)-based nontargeted proteomics approaches, which typically uncover high-abundance proteins (6). Affinity-based techniques, such as antibody-based or aptamer-based arrays, enable simultaneous interrogation of >1,000 low-abundance candidate proteins. In recent studies, proteins whose urinary levels were significantly elevated in patients with SLE when compared to healthy controls were verified by enzyme-linked immunosorbent assay (ELISA) in independent cohorts, involving multiple ethnicities (7,8).

Although these proteomics screening techniques have sped up the discovery of potential biomarkers for LN, we are not far away from the starting line. No urinary biomarkers have been extensively validated to justify their routine clinical use in LN (9). An important clinical dilemma is the differentiation between residual activity and damage in LN, manifesting as persistent proteinuria without overt symptoms or serologic evidence of active lupus. When a renal biopsy is not feasible, clinical judgment relies on circumstantial evidence, such as observed trends in the urinary P/Cr, serum albumin level, renal function, and other clinical parameters, which often do not correlate with histologic features (9). As new biomarkers require validation in terms of their sensitivity and specificity for predicting a renal flare, a large number of longitudinal samples, with short follow-up intervals, from LN cohorts are needed, because flares are difficult to predict. Moreover, the assay for candidate proteins has to be standardized and validated across different cohorts for attainment of consistent cutoff values bearing clinical relevance. The cost and time investment for collecting substantial numbers of samples at closely timed intervals over years is a major challenge. Markers for prognostic stratification require rigorous validation of their additive value in predicting renal response to therapy.

¹Chi Chiu Mok, MD, FRCP: Tuen Mun Hospital, Hong Kong, China; ²Chandra Mohan, MD, PhD: University of Houston, Houston, Texas.

No potential conflicts of interest relevant to this article were reported.

Address correspondence to Chi Chiu Mok, MD, FRCP, Tuen Mun Hospital, Department of Medicine, Block H, Tsing Chung Koon Road, Tuen Mun, New Territories, Hong Kong SAR, China. Email: ccmok2005@yahoo.com.

Submitted for publication August 10, 2020; accepted in revised form August 25, 2020.

In a study reported in this issue of *Arthritis & Rheumatology*, Wang et al (10) investigated the association of urinary matrix metalloproteinase 7 (MMP-7) levels with renal flares in LN. In a cross-sectional analysis of 88 patients with active LN, it was demonstrated that the urinary MMP-7 level was significantly higher than that in patients with active extrarenal SLE, non-SLE glomerular diseases, or healthy controls. The levels of urinary MMP-7 correlated better with renal histologic activity than with conventional lupus serologic measurements or levels of proteinuria. Although deposition of MMP-7 protein predominantly in tubular cells was demonstrated in LN kidney biopsy samples, there was no relationship between the urinary MMP-7 level and renal histologic chronicity index. These data suggest that the urinary MMP-7 level is a specific marker for LN and a good surrogate for LN activity. An added merit of this study is the demonstration in a longitudinal cohort of LN patients that a rise in urinary MMP-7 level occurred earlier than did an increase in proteinuria.

A closer look at the fluctuation in the urinary P/Cr and urinary MMP-7/Cr levels in individual patients who had renal flares revealed a higher sensitivity of the novel urinary MMP-7 marker in predicting a flare in the majority of patients. However, there were several patients in whom the urinary MMP-7 level either did not increase with a flare or rose only during or after a renal flare. Given the small number of patients who experienced a flare ($n = 15$) and the fixed 2-month interval of urine sampling, several uncertainties remain, including the optimal cutoff value for urinary MMP-7, absolute or percentage increase in its level, the duration of its elevation that warrants close monitoring or even preemptive treatment, and the clinical utility of the urinary MMP-7 measurement in patients of other ethnicities.

In this same issue of *Arthritis & Rheumatology*, Mejia-Vilet et al (11) reported on their study of the relationship between the urinary epidermal growth factor (EGF) level and progression of chronic kidney disease in several cohorts of patients with LN. This biomarker was identified by MS-based proteomics screening in a discovery cohort and validated by immunoblotting and ELISA. In a cross-sectional analysis, urinary EGF levels were significantly lower in patients with active LN than in patients with nonrenal SLE, patients with inactive SLE, and non-SLE controls. In the 3 groups of SLE patients, there was a trend toward lower urinary EGF levels in patients with a history of LN. Coupled with the inverse correlation between the urinary EGF level and renal histologic chronicity index instead of activity index, the lower levels of urinary EGF appear to be related to underlying kidney damage attributable to LN rather than to active glomerular inflammation. Longitudinal analysis showed that a lower level of urinary EGF, which correlated positively with the eGFR, at the time of renal flare was associated with further renal function decline at 2 years.

The study by Mejia-Vilet and colleagues (11) is a pilot study that validates the urinary EGF level as a biomarker for kidney reserve in LN. Although the urinary EGF level is not specific for

SLE, it may be a surrogate marker for residual nephron mass in patients with kidney diseases. However, the study was limited by a lack of analytic data to show an earlier decline in urinary EGF levels in advance of the eGFR, partly because of the long sample-collection interval (6 months) between visits in the longitudinal cohorts. While it is reasonable to not augment treatment in LN patients who have low nephron reserve, the flip side of the argument is to treat those with residual activity more aggressively, with the aim of retarding progression to ESRD. As a reduced urinary EGF level does not reflect LN activity, it still has to be interpreted in conjunction with other clinical parameters. Nevertheless, the urinary EGF level is a potential outcome biomarker for assessing the efficacy of novel antifibrotic and nephroprotective strategies in future clinical trials of chronic kidney disease (12). Again, the optimal cutoff value and the amount of change in urinary EGF level over time that would prove clinically useful for guiding treatment decisions requires further evaluation in prospective clinical trials of LN and other glomerular diseases.

These 2 studies in this issue of *Arthritis & Rheumatology* advance our repertoire of potential urinary biomarkers in LN. Combining biomarkers of active glomerular inflammation and renal scarring may strengthen their utility in reflecting concurrent renal histopathologic features and in predicting treatment responses and outcomes in patients with LN. Taking into account all of the recent insights from MS-based and affinity-based proteomics, as well as the burgeoning list of urinary biomarkers reported in the LN literature, we are now faced with several dozen biomarker candidates. These studies have been executed in independent silos, utilizing limited sample sizes with patients of 1 or 2 ethnicities, and with varying definitions for "active" LN, renal flare, and metrics for tracking disease longitudinally in LN. Given these variances, whether biomarkers identified in 1 study will successfully translate to other cohorts remains unknown.

As a field, advances are warranted in 2 dimensions. From the technical perspective, both targeted and nontargeted proteomics are still evolving disciplines that have yet to attain the capacity to scan the human proteome exhaustively (in contrast to the optimal performance of contemporary genomics and transcriptomics). Until this happens, new, and hopefully better, biomarkers will continue to be reported in the coming years, which would require rigorous validation.

Second, efforts are needed to standardize the definitions of the metrics used to define disease progression in LN that should be used when the relative performance of different biomarker candidates are being compared. Having defined these standardized metrics, biomarker candidates and panels constructed using these proteins warrant systematic testing in well-characterized patient cohorts drawn from multiple ethnicities. The statistical approaches to construct biomarker panels are not limiting. Likewise, current technical approaches to devise point-of-care testing kits to quickly assay urinary biomarkers are also not limiting (13). The steady trickle of newer protein biomarkers that outperform

proteinuria in predicting LN flares raises hope that LN diagnostics will morph substantially in the coming decade.

AUTHOR CONTRIBUTIONS

Drs. Mok and Mohan drafted the article, revised it critically for important intellectual content, and approved the final version to be published.

REFERENCES

1. Sim JJ, Bhandari SK, Batech M, Hever A, Harrison TN, Shu YH, et al. End-stage renal disease and mortality outcomes across different glomerulonephropathies in a large diverse US population. *Mayo Clin Proc* 2018;93:167–78.
2. Dall'Era M, Cisternas MG, Snipes K, Herrinton LJ, Gordon C, Helmick CG. The incidence and prevalence of systemic lupus erythematosus in San Francisco County, California: the California Lupus Surveillance Project. *Arthritis Rheumatol* 2017;69:1996–2005.
3. Hiraki LT, Lu B, Alexander SR, Shaykevich T, Alarcón GS, Solomon DH, et al. End-stage renal disease due to lupus nephritis among children in the US, 1995–2006. *Arthritis Rheum* 2011;63:1988–97.
4. Soliman S, Mohan C. Lupus nephritis biomarkers. *Clin Immunol* 2017;185:10–20.
5. Aljaberi N, Bennett M, Brunner HI, Devarajan P. Proteomic profiling of urine: implications for lupus nephritis. *Expert Rev Proteomics* 2019;16:303–13.
6. Nicolaou O, Kousios A, Hadjisavvas A, Lauwerys B, Sokratous K, Kyriacou K. Biomarkers of systemic lupus erythematosus identified using mass spectrometry-based proteomics: a systematic review. *J Cell Mol Med* 2017;21:993–1012.
7. Vanarsa K, Soomro S, Zhang T, Strachan B, Pedroza C, Nidhi M, et al. Quantitative planar array screen of 1000 proteins uncovers novel urinary protein biomarkers of lupus nephritis. *Ann Rheum Dis* 2020;79:1349–61.
8. Stanley S, Vanarsa K, Soliman S, Habazi D, Pedroza C, Gidley G, et al. Comprehensive aptamer-based screening identifies a spectrum of urinary biomarkers of lupus nephritis across ethnicities. *Nat Commun* 2020;11:3131.
9. Mok CC. Biomarkers for lupus nephritis: a critical appraisal [review]. *J Biomed Biotechnol* 2010;2010:638413.
10. Wang G, Wu L, Su H, Feng X, Shi M, Jin L, et al. Association of urinary matrix metalloproteinase 7 levels with incident flare in lupus nephritis. *Arthritis Rheumatol* doi: <http://onlinelibrary.wiley.com/doi/10.1002/art.41506/abstract>. E-pub ahead of print.
11. Mejia-Vilet JM, Shapiro JP, Zhang X, Cruz C, Zimmerman G, Méndez-Pérez RA, et al. Association between urinary epidermal growth factor and renal prognosis in lupus nephritis. *Arthritis Rheumatol* doi: <http://onlinelibrary.wiley.com/doi/10.1002/art.41507/abstract>. E-pub ahead of print.
12. Ruiz-Ortega M, Rayego-Mateos S, Lamas S, Ortiz A, Rodrigues-Diez RR. Targeting the progression of chronic kidney disease. *Nat Rev Nephrol* 2020;16:269–88.
13. Lei R, Huo R, Mohan C. Current and emerging trends in point-of-care urinalysis tests. *Expert Rev Mol Diagn* 2020;20:69–84.

Health Assessment Questionnaire at One Year Predicts All-Cause Mortality in Patients With Early Rheumatoid Arthritis

Safoora Fatima,¹ O. Schieir,² M. F. Valois,³ S. J. Bartlett,³ L. Bessette,⁴ G. Boire,⁵ G. Hazlewood,⁶ C. Hitchon,⁷ E. C. Keystone,² D. Tin,⁸ C. Thorne,⁸ V. P. Bykerk,⁹ and J. E. Pope,¹⁰ on behalf of the CATCH Investigators

Objective. Higher self-reported disability (high Health Assessment Questionnaire [HAQ] score) has been associated with hospitalizations and mortality in established rheumatoid arthritis (RA), but associations in early RA are unknown.

Methods. Patients with early RA (symptom duration <1 year) enrolled in the Canadian Early Arthritis Cohort who initiated disease-modifying antirheumatic drugs and had completed HAQ data at baseline and 1 year were included in the study. Discrete-time proportional hazards models were used to estimate crude and multi-adjusted associations of baseline HAQ and HAQ at 1 year with all-cause mortality in each year of follow-up.

Results. A total of 1,724 patients with early RA were included. The mean age was 55 years, and 72% were women. Over 10 years, 62 deaths (3.6%) were recorded. Deceased patients had higher HAQ scores at baseline (mean \pm SD 1.2 \pm 0.7) and at 1 year (0.9 \pm 0.7) than living patients (1.0 \pm 0.7 and 0.5 \pm 0.6, respectively; $P < 0.001$). Disease Activity Score in 28 joints (DAS28) was higher in deceased versus living patients at baseline (mean \pm SD 5.4 \pm 1.3 versus 4.9 \pm 1.4) and at 1 year (mean \pm SD 3.6 \pm 1.4 versus 2.8 \pm 1.4) ($P < 0.001$). Older age, male sex, lower education level, smoking, more comorbidities, higher baseline DAS28, and glucocorticoid use were associated with mortality. Contrary to HAQ score at baseline, the association between all-cause mortality and HAQ score at 1 year remained significant even after adjustment for confounders. For baseline HAQ score, the unadjusted hazard ratio (HR) was 1.46 (95% confidence interval [95% CI] 1.02–2.09), and the adjusted HR was 1.25 (95% CI 0.81–1.94). For HAQ score at 1 year, the unadjusted HR was 2.58 (95% CI 1.78–3.72), and the adjusted HR was 1.75 (95% CI 1.10–2.77).

Conclusion. Our findings indicate that higher HAQ score and DAS28 at 1 year are significantly associated with all-cause mortality in a large early RA cohort.

INTRODUCTION

Rheumatoid arthritis (RA) is a common progressive inflammatory condition affecting 1% of the population (1,2). It causes damage to the synovial joints but also has several systemic manifestations and sequelae of disease (3). It may affect several organ

systems, including cardiac, pulmonary, ocular, skin, and hematologic, thereby increasing the risk of multiple associated complications. RA is associated with poor physical function, worsening quality of life, and increased morbidity and mortality, especially due to cardiovascular disease complications (4–12). Several studies have found patients with RA to have a higher mortality

The Canadian Early Arthritis Cohort (CATCH) study was independently designed and is implemented by the investigators. It has been financially supported through unrestricted research grants from Amgen, Pfizer Canada, AbbVie, Medexus, Inc., Eli Lilly, Merck Canada, Sandoz Canada Biopharmaceuticals, Hoffmann-La Roche, Janssen Biotech, UCB Canada, Bristol Myers Squibb Canada, and Sanofi Genzyme.

¹Safoora Fatima, MD: University of Western Ontario Schulich School of Medicine and Dentistry, London, Ontario, Canada; ²O. Schieir, PhD, E. C. Keystone, MD: University of Toronto, Toronto, Ontario, Canada; ³M. F. Valois, PhD, S. J. Bartlett, PhD: McGill University, Montreal, Quebec, Canada; ⁴L. Bessette, MD: CHU de Québec-Université Laval, Laval, Quebec, Canada; ⁵G. Boire, MD: Centre Intégré Universitaire de Santé et de Services Sociaux de l'Estrie, CHU de Sherbrooke, and Université de Sherbrooke, Sherbrooke, Quebec, Canada; ⁶G. Hazlewood, MD, PhD:

University of Calgary, Calgary, Alberta, Canada; ⁷C. Hitchon, MD: University of Manitoba, Winnipeg, Manitoba, Canada; ⁸D. Tin, BScPhm, C. Thorne, MD: Southlake Regional Health Centre, Newmarket, Ontario, Canada; ⁹V. P. Bykerk, MD: University of Toronto, Toronto, Ontario, Canada, and Hospital for Special Surgery and Weill Cornell Medical College, New York, New York; ¹⁰J. E. Pope, MD: University of Western Ontario Schulich School of Medicine and Dentistry and St. Joseph's Health Care London, London, Ontario, Canada.

No potential conflicts of interest relevant to this article were reported.

Address correspondence to J. E. Pope, MD, St. Joseph's Health Care London, 268 Grosvenor Street, London, Ontario N6A 4V2, Canada. Email: janet.pope@sjhc.london.on.ca.

Submitted for publication April 19, 2020; accepted in revised form August 27, 2020.

risk than the general population (13,14). Recognizing predictors of mortality and morbidity is important from a clinical, research, and public health perspective as it provides valuable information to help make decisions, whether it be monitoring treatment responses, analyzing outcomes in research studies, or assessing the burden of disease.

The Health Assessment Questionnaire (HAQ) disability index is a tool commonly used in RA to measure disability using the patient's self-reported functional assessment (15). The HAQ has 8 categories, scored on a scale of 0 (no problem) to 3 (unable to perform) per category, leading to a final score between 0 and 3, with 0 representing no self-reported functional impairment and 3 representing severe functional impairment. It is a valid and reliable tool used to monitor the impact of disease severity and activity and assess change in function with treatment. In older studies, HAQ was found to be associated with hospitalizations and mortality in established RA (16–21). Another study by Farragher et al in 2007 found that early functional disability as measured by HAQ predicted cardiovascular and all-cause mortality, though that study included patients with any inflammatory polyarthritis (22). In the present study, we analyzed how well the HAQ predicted future all-cause mortality specifically in patients with early RA.

PATIENTS AND METHODS

Data were obtained from the Canadian Early Arthritis Cohort (CATCH). CATCH is a multicenter, prospective incident cohort study of patients with early RA who have follow-up assessments at fixed intervals, including disease activity measures (Disease Activity Score in 28 joints using the erythrocyte sedimentation rate or C-reactive protein level [DAS28-ESR/CRP] [23]), comorbidity profile, and laboratory testing. Ethics approval was previously obtained from each of the 19 participating CATCH sites across Canada. Written informed consent was obtained from participants at study enrollment, and the study was conducted in accordance with the Declaration of Helsinki. See Appendix A for a list of the CATCH investigators.

The study inclusion criteria consisted of the following: adults with early RA, defined as a duration of symptoms of fixed swelling of <1 year, who were enrolled between 2007 and 2017, initiated treatment with ≥ 1 disease-modifying antirheumatic drug (DMARD), and had completed HAQ data at baseline and at 1 year. Patients were excluded from analysis for the following reasons: age <18 years, missing age, no completed HAQ at baseline or 12 months, or no treatment with ≥ 1 DMARD/biologic agent in the first year of follow-up. Patients who were lost to follow-up were recorded, and forms completed for deceased patients included the date and cause of death.

Baseline characteristics, including sociodemographic variables, RA characteristics, treatment, and comorbidities were obtained and compared between patients who died over the follow-up period (deceased patients) and living patients. Data

on comorbidities were collected using the Rheumatic Disease Comorbidity Index (RDCI), which has been validated for RA, as well as for osteoarthritis, systemic lupus erythematosus, and fibromyalgia (24). The RDCI weighs co-existing medical conditions and yields a final score of 0–9, where higher scores indicate a higher burden of disease (25). Baseline characteristics were expressed using descriptive statistics, *t*-tests, and chi-square tests. Survival analyses were conducted using discrete-time proportional hazards models where crude and multi-adjusted associations of baseline HAQ and HAQ at 1 year with all-cause mortality were calculated in each year of follow-up.

RESULTS

This study included 1,724 patients with early RA. Their mean age was 55 years, and 72% were women. Initially, the cohort included a total of 3,195 study participants. Seventy-one patients were excluded due to age <18 years or missing age, 1,334 were excluded due to missing completed HAQ at baseline or at 12 months, and an additional 66 patients were excluded because they did not receive ≥ 1 DMARD/biologic agent in first year of treatment (Figure 1). Thus, the total number of participants in the study was 1,724.

There were 62 deaths (3.6%) recorded over the 10-year follow up period. Baseline characteristics comparing deceased and living patients are outlined in Table 1. There were statistically significant differences in age (older age in the deceased group), sex (lower

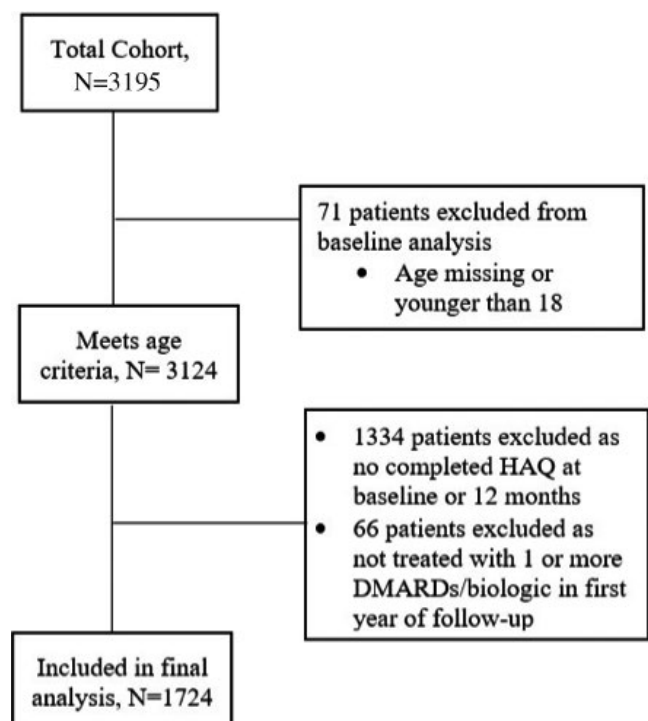


Figure 1. Flow chart of study participants included and the reasons for exclusion. HAQ = Health Assessment Questionnaire; DMARDs = disease-modifying antirheumatic drugs.

Table 1. Baseline characteristics of the patients with early RA*

	All (n = 1,724)	Living (n = 1,662)	Deceased (n = 62)	P
Length of follow-up, years	5.2 ± 2.7	5.2 ± 2.7	4.9 ± 2.4	0.3119
Sociodemographic and lifestyle factors				
Age, years	55 ± 15	54 ± 15	68 ± 9	<0.0001
Sex, no. (%) female	1,242 (72)	1,210 (73)	32 (52)	0.0003
Race, no. (%)				
White or European	1,467 (85)	1,412 (85)	55 (89)	0.4154
Aboriginal	74 (4)	70 (4)	4 (6)	0.3929
Education higher than high school degree, no. (%)	950 (55)	927 (56)	23 (37)	0.0127
No. (%) employed/no. (%) retired	938 (54)/476 (28)	924 (56)/435 (26)	14 (23)/41 (66)	<0.0001/<0.0001
Income <\$50,000, no. (%)†‡	367 (38)	352 (37)	15 (60)	0.0046
Current smoker, no. (%)	304 (18)	287 (17)	17 (27)	0.0402
Rheumatic Disease Comorbidity Index (range 0–9)	1.2 ± 1.3	1.2 ± 1.3	2.2 ± 1.6	<0.0001
RA characteristics				
Symptom duration, months	5.8 ± 3.0	5.8 ± 3.0	6.0 ± 3.3	0.5955
Met RA criteria, no. (%)	1,542 (89)	1,485 (89)	57 (92)	0.5154
Seropositivity in first year, no. (%)§	1,121 (75)	1,078 (75)	43 (78)	0.6000
TJC68	12 ± 9	12 ± 9	12 ± 10	0.6139
SJC66	9 ± 8	9 ± 8	11 ± 8	0.1532
TJC28	8 ± 7	8 ± 7	9 ± 6	0.5507
SJC28	7 ± 6	7 ± 6	9 ± 6	0.0581
ESR, mm/hour	26.5 ± 22.1	26.1 ± 21.9	37.3 ± 25.8	0.0002
CRP, mg/dl	14.6 ± 18.7	14.3 ± 18.6	22.7 ± 20.3	0.0009
DAS28-ESR/CRP				
Baseline	4.9 ± 1.4	4.9 ± 1.4	5.4 ± 1.3	0.0119
1 year	2.8 ± 1.4	2.8 ± 1.4	3.6 ± 1.4	<0.0001
CDAI	26.1 ± 14.3	26.1 ± 14.3	28.4 ± 13.3	0.2152
HAQ (range 0–3)				
Baseline	1.0 ± 0.7	1.0 ± 0.7	1.2 ± 0.7	0.0364
1 year	0.5 ± 0.6	0.5 ± 0.6	0.9 ± 0.7	<0.0001
RA treatment, no. (%)				
Baseline				
Any DMARDs	1,534 (89)	1,478 (89)	56 (90)	0.6814
MTX	1,210 (70)	1,164 (70)	46 (74)	0.4823
MTX in combination	696 (40)	670 (40)	26 (42)	0.7982
Biologics	36 (2)	34 (2)	2 (3)	0.5234
MTX route of administration				
Oral	741 (61)	709 (61)	32 (70)	0.2373
Subcutaneous	469 (39)	455 (39)	14 (30)	
Oral glucocorticoids	480 (28)	454 (27)	26 (42)	0.0117
1 year				
Any DMARDs	1,624 (94)	1,567 (94)	57 (92)	0.4373
MTX	1,343 (78)	1,299 (78)	44 (71)	0.1803
MTX in combination	814 (47)	792 (48)	22 (35)	0.0595
Biologics	206 (12)	196 (12)	10 (16)	0.3014
MTX route of administration				
Oral	672 (50)	648 (50)	24 (55)	0.5431
Subcutaneous	671 (50)	651 (50)	20 (45)	
Oral glucocorticoids	221 (13)	205 (12)	16 (26)	0.0018

* Except where indicated otherwise, values are the mean ± SD. RA = rheumatoid arthritis; TJC68 = tender joint count in 68 joints; SJC66 = swollen joint count in 66 joints; ESR = erythrocyte sedimentation rate; CRP = C-reactive protein; DAS28-ESR/CRP = Disease Activity Score in 28 joints using the ESR or CRP; CDAI = Clinical Disease Activity Index; HAQ = Health Assessment Questionnaire; DMARDs = disease-modifying antirheumatic drugs; MTX = methotrexate.

† Includes "Do not wish to answer" response and uncombined income.

‡ Data were missing for 44% of the patients.

§ Data were missing for 14% of the patients.

percentage of women in the deceased group), education (lower education level and less employment in the deceased group), smoking (higher percentage of smokers in the deceased group) and RDCI (higher comorbidity index in the deceased group). Treatments given were similar between the 2 groups, except that glucocorticoid use was higher in the deceased group.

HAQ scores and DAS28 scores were higher in deceased patients compared to living patients, both at baseline and at 1 year. These differences were statistically significant at 1 year with $P < 0.001$. Patients in the deceased group had a mean ± SD baseline HAQ score of 1.2 ± 0.7 and a 1-year HAQ score of 0.9 ± 0.7 . In comparison, living patients had a mean ± SD HAQ

Table 2. Unadjusted survival model: association of each covariate with all-cause mortality in the patients with early RA*

Baseline variable	Unadjusted HR (95% CI)
Sociodemographic and lifestyle factors	
Age (years)†	1.10 (1.07–1.13)
Female†	0.37 (0.22–0.62)
White	1.01 (0.46–2.24)
Aboriginal	1.71 (0.61–4.76)
Education level higher than high school degree†	0.48 (0.28–0.82)
Current smoker†	1.81 (1.01–3.24)
Comorbidity (RDCI 0–9)†	1.60 (1.36–1.87)
RA characteristics	
Symptom duration (months)	0.99 (0.91–1.08)
Seropositivity in first year	1.11 (0.55–2.23)
DAS28-ESR/CRP†	1.26 (1.06–1.51)
Oral glucocorticoid use†	1.75 (1.03–2.98)

* RA = rheumatoid arthritis; HR = hazard ratio; 95% CI = 95% confidence interval; RDCI = Rheumatic Disease Comorbidity Index; DAS28-ESR/CRP = Disease Activity in 28 joints using the erythrocyte sedimentation rate or C-reactive protein level.

† Age, male sex, lower education level, smoking, more comorbidities, higher baseline disease activity, and glucocorticoid use were associated with all-cause mortality in unadjusted survival models.

score of 1.0 ± 0.7 at baseline and 0.5 ± 0.6 at 1 year. Mean \pm SD DAS28 scores in deceased patients were 5.4 ± 1.3 at baseline and 3.6 ± 1.4 at 1 year, whereas DAS28 scores in living patients were 4.9 ± 1.4 at baseline and 2.8 ± 1.4 at 1 year.

In an unadjusted survival model, the following covariates were associated with all-cause mortality: older age, male sex, lower education level, smoking, more comorbidities, higher baseline DAS28, higher HAQ scores, and glucocorticoid use (Tables 2 and 3). HAQ scores at both baseline and at 1 year were significantly associated with all-cause mortality, with an unadjusted hazard ratio (HR) of 1.46 (95% confidence interval [95% CI] 1.02–2.09) and 2.58 (95% CI 1.78–3.72), respectively (model 1 in Table 3).

In a multivariate discrete-time survival model, HAQ scores at baseline and at 1 year were compared to all-cause mortality adjusting for age, sex, comorbidities, disease activity, smoking, education level, seropositivity, symptom duration, and glucocorticoid use (Table 3). Contrary to HAQ at baseline, the association

between all-cause mortality and HAQ at 1 year remained significant after adjusting for the variables listed above (for baseline HAQ, adjusted HR 1.32 [95% CI 0.85–2.04]; for HAQ at 1 year, adjusted HR 1.87 [95% CI 1.6–3.02]).

DISCUSSION

This study showed that in patients with early RA, HAQ scores adjusted for confounders at 1 year but not at baseline were significantly associated with all-cause mortality. The literature shows that higher disease activity, as reflected by the DAS28, is associated with increased disability, as measured by the HAQ. Taken together, this association and the findings of the present study suggest that poorer disease control (high DAS28) within the first year of treatment of RA may lead to increased disability (high HAQ scores), which in turn may contribute to higher mortality. This finding may indicate that RA patients who do not have a good response to treatment in the first year have higher subsequent mortality.

Additionally, this study showed that in RA patients, mortality was independently associated with older age, male sex, lower education level, smoking, more comorbidities, higher baseline disease activity, glucocorticoid use, and higher HAQ scores. These findings are helpful in a clinical setting, as they can guide physician–patient discussions with regard to risk factors associated with prognosis, prescribing glucocorticoids, counselling on smoking cessation, monitoring treatment responses, and focusing on patient education. However, these interventions would need to be tested to determine if they change the risk of mortality. With regard to glucocorticoid use, although it is independently associated with mortality, higher disease activity often requires more glucocorticoids; thus, both factors may drive higher mortality. From a physician perspective, this would mean prescribing as much glucocorticoids as necessary (as an adjunct to other treatments) to better control disease activity but also prescribing as little as possible to avoid adverse effects.

This study has several strengths. It has good power given a large sample size consisting of 1,724 patients with early RA, even though only 3.6% of the patients died during the follow-up

Table 3. Multivariable discrete-time survival models: comparing baseline HAQ versus HAQ at 1 year with all-cause mortality in the patients with early RA*

	Baseline HAQ, HR (95% CI)	HAQ at 1 year, HR (95% CI)†
Model 1: crude (time + HAQ)	1.46 (1.02–2.09)	2.58 (1.78–3.72)
Model 2: adjusted for age and sex	1.37 (0.96–1.95)	2.40 (1.63–3.52)
Model 3: adjusted for model 2 + DAS28 and RDCI	1.25 (0.81–1.94)	1.75 (1.10–2.77)
Model 4: adjusted for model 3 + education, smoking, seropositivity, symptom duration, and oral glucocorticoid use	1.32 (0.85–2.04)	1.87 (1.16–3.02)
Model 5: adjusted for model 3 + smoking and symptom duration only	1.30 (0.84–2.00)	1.73 (1.09–2.74)

* HAQ = Health Assessment Questionnaire; HR = hazard ratio; 95% CI = 95% confidence interval; DAS28 = Disease Activity Score in 28 joints; RDCI = Rheumatic Disease Comorbidity Index.

† All-cause mortality was associated with high HAQ score at 1 year even after adjusting for age, sex, comorbidities, disease activity, smoking, education, seropositivity, symptom duration, and glucocorticoid use in adjusted survival models.

period. Moreover, it had a long duration (from 2007 to 2017) with variable length of follow-up, which is helpful to capture deaths over time, as is important in a mortality study. There was very little loss to follow up. Death summaries were completed at each site. Furthermore, CATCH has 19 study sites across Canada, and the demographic characteristics of the patients in CATCH are similar to those in population-based studies, suggesting good external validity and generalizability (2,26). From a methods perspective, the use of multivariate analysis models adjusted for potential confounders produced more accurate models with adjustment for important factors associated with mortality, such as age and sex.

Some potential confounders may not have been adjusted for. Examples of these could include variable access to advanced therapies, other comorbidities not included in the standardized comorbidity questionnaire, and the severity of comorbidities. Other important factors associated with mortality may not have been collected, as this is not the primary reason for the CATCH cohort. Finally, we recognize that though HAQ score predicts mortality, this could be true for poor function in the general population without RA. It is noted that in both the groups who eventually died during the observational period and the ones who were still alive, the HAQ score improved on average, but to a lesser extent in the deceased group. Also, the interplay between disease activity and self-reported function may be complex (27). Disease activity may be associated with the reversible component of the HAQ, while damage and other comorbidities are associated with the irreversible component of the HAQ. Patients with higher HAQ scores who have other conditions, such as fibromyalgia and osteoarthritis, do worse, and the measure is subjective, in that a patient may report marked impairment of activities of daily living despite a lack of disease activity and damage. We did not adjust for pain and depression, which may alter mortality risk (27–30).

There are several reasons high HAQ scores are associated with increased mortality. Disease activity and damage could be important associations. However, comorbidities could be the cause of death, and patients with early RA with comorbidities have less chance of remission and more functional impairment at 1 year than those without any comorbidities, as has been shown in the CATCH early RA cohort (31).

In summary, this study showed that higher HAQ scores at 1 year were significantly associated with all-cause mortality in early RA. Future research can separate the interplay between disease activity, which is also associated with mortality both at baseline and after treatment (at 1 year), and other factors, such as damage and patient perceptions of function and comorbidities.

AUTHOR CONTRIBUTIONS

All authors were involved in drafting the article or revising it critically for important intellectual content, and all authors approved the final version to be published. Dr. Pope had full access to all of the data in the study and takes responsibility for the integrity of the data and the accuracy of the data analysis.

Study conception and design. Fatima, Schieir, Valois, Bykerk, Pope.

Acquisition of data. Fatima, Schieir, Valois, Bessette, Boire, Hitchon, Keystone, Tin, Thorne, Bykerk, Pope.

Analysis and interpretation of data. Fatima, Schieir, Valois, Bartlett, Bessette, Boire, Hazlewood, Hitchon, Keystone, Tin, Thorne, Bykerk, Pope.

REFERENCES


- Alamanos Y, Voulgari PV, Drosos AA. Incidence and prevalence of rheumatoid arthritis, based on the 1987 American College of Rheumatology criteria: a systematic review. *Semin Arthritis Rheum* 2006;36:182–8.
- Widdifield J, Paterson JM, Bernatsky S, Tu K, Tomlinson G, Kuriya B, et al. The epidemiology of rheumatoid arthritis in Ontario, Canada. *Arthritis Rheumatol* 2014;66:786–93.
- Jenkins JK, Hardy KJ, McMurray RW. The pathogenesis of rheumatoid arthritis: a guide to therapy. *Am J Med Sci* 2002;323:171–80.
- Avina-Zubieta JA, Thomas J, Sadatsafavi M, Lehman AJ, Lacaille D. Risk of incident cardiovascular events in patients with rheumatoid arthritis: a meta-analysis of observational studies. *Ann Rheum Dis* 2012;71:1524–9.
- Sparks JA, Chang SC, Liao KP, Lu B, Fine AR, Solomon DH, et al. Rheumatoid arthritis and mortality among women during 36 years of prospective follow-up: results from the Nurses' Health Study. *Arthritis Care Res (Hoboken)* 2016;68:753–62.
- Barnabe C, Sun Y, Boire G, Hitchon CA, Haraoui B, Thorne JC, et al. Heterogeneous disease trajectories explain variable radiographic, function and quality of life outcomes in the Canadian Early Arthritis Cohort (CATCH). *PLoS One* 2015;10:e0135327.
- Sherer Y, Shoenfeld Y. Mechanisms of disease: atherosclerosis in autoimmune diseases. *Nat Clin Pract Rheumatol* 2006;2:99–106.
- Innala L, Möller B, Ljung L, Magnusson S, Smedby T, Södergren A, et al. Cardiovascular events in early RA are a result of inflammatory burden and traditional risk factors: a five year prospective study. *Arthritis Res Ther* 2011;13:R131.
- Symmons DP, Gabriel SE. Epidemiology of CVD in rheumatic disease, with a focus on RA and SLE [review]. *Nat Rev Rheumatol* 2011;7:399.
- McInnes IB, Schett G. The pathogenesis of rheumatoid arthritis. *N Engl J Med* 2011;365:2205–19.
- Young A, Dixey J, Cox N, Davies P, Devlin J, Emery P, et al. How does functional disability in early rheumatoid arthritis (RA) affect patients and their lives? Results of 5 years of follow-up in 732 patients from the Early RA Study (ERAS). *Rheumatology (Oxford)* 2000;39:603–11.
- Pincus T, Callahan LF, Sale WG, Brooks AL, Payne LE, Vaughn WK. Severe functional declines, work disability, and increased mortality in seventy-five rheumatoid arthritis patients studied over nine years. *Arthritis Rheum* 1984;27:864–72.
- Gabriel SE, Crowson CS, O'Fallon WM. Mortality in rheumatoid arthritis: have we made an impact in 4 decades? *J Rheumatol* 1999;26:2529–33.
- Gonzalez A, Kremers HM, Crowson CS, Nicola PJ, Davis JM III, Thorneau TM, et al. The widening mortality gap between rheumatoid arthritis patients and the general population. *Arthritis Rheum* 2007;56:3583–7.
- Maska L, Anderson J, Michaud K. Measures of functional status and quality of life in rheumatoid arthritis: Health Assessment Questionnaire Disability Index (HAQ), Modified Health Assessment Questionnaire (MHAQ), Multidimensional Health Assessment Questionnaire (MDHAQ), Health Assessment Questionnaire II (HAQ-II), Improved Health Assessment Questionnaire (Improved HAQ), and Rheumatoid Arthritis Quality of Life (RAQoL). *Arthritis Care Res (Hoboken)* 2011;63 Suppl 11:S4–13.

16. Pincus T, Sokka T. Quantitative target values of predictors of mortality in rheumatoid arthritis as possible goals for therapeutic interventions: an alternative approach to remission or ACR20 responses? *J Rheumatol* 2001;28:1723–34.
17. Sokka T, Pincus T. Markers for work disability in rheumatoid arthritis. *J Rheumatol* 2001;28:1718–22.
18. Wolfe F, Zwiilich SH. The long-term outcomes of rheumatoid arthritis: a 23-year prospective, longitudinal study of total joint replacement and its predictors in 1,600 patients with rheumatoid arthritis. *Arthritis Rheum* 1998;41:1072–82.
19. Yelin E, Trupin L, Wong B, Rush S. The impact of functional status and change in functional status on mortality over 18 years among persons with rheumatoid arthritis. *J Rheumatol* 2002;29:1851–7.
20. Wolfe F, Michaud K, Gefeller O, Choi HK. Predicting mortality in patients with rheumatoid arthritis. *Arthritis Rheum* 2003;48:1530–42.
21. Jacobsson LT, Turesson C, Nilsson JÅ, Petersson IF, Lindqvist E, Saxne T, et al. Treatment with TNF blockers and mortality risk in patients with rheumatoid arthritis. *Ann Rheum Dis* 2007;66:670–5.
22. Farragher TM, Lunt M, Bunn DK, Silman AJ, Symmons DP. Early functional disability predicts both all-cause and cardiovascular mortality in people with inflammatory polyarthritis: results from the Norfolk Arthritis Register. *Ann Rheum Dis* 2007;66:486–92.
23. Prevoe ML, van't Hof MA, Kuper HH, van Leeuwen MA, van de Putte LB, van Riel PL. Modified disease activity scores that include twenty-eight-joint counts: development and validation in a prospective longitudinal study of patients with rheumatoid arthritis. *Arthritis Rheum* 1995;38:44–8.
24. Michaud K, Wolfe F. Comorbidities in rheumatoid arthritis. *Best Pract Res Clin Rheumatol* 2007;21:885–906.
25. England BR, Sayles H, Mikuls TR, Johnson DS, Michaud K. Validation of the rheumatic disease comorbidity index. *Arthritis Care Res (Hoboken)* 2015;67:865–72.
26. Humphreys JH, Verstappen SM, Hyrich KL, Chipping JR, Marshall T, Symmons DP. The incidence of rheumatoid arthritis in the UK: comparisons using the 2010 ACR/EULAR classification criteria and the 1987 ACR classification criteria. Results from the Norfolk Arthritis Register. *Ann Rheum Dis* 2013;72:1315–20.
27. Aletaha D, Smolen J, Ward MM. Measuring function in rheumatoid arthritis: identifying reversible and irreversible components. *Arthritis Rheum* 2006;54:2784–92.
28. Ang DC, Choi H, Kroenke K, Wolfe F. Comorbid depression is an independent risk factor for mortality in patients with rheumatoid arthritis. *J Rheumatol* 2005;32:1013–9.
29. Li N, Chan E, Peterson S. The economic burden of depression among adults with rheumatoid arthritis in the United States. *J Med Econ* 2019;22:372–8.
30. Wolfe F, Ablin J, Baker JF, Diab R, Guymer EK, Littlejohn GO, et al. All-cause and cause-specific mortality in persons with fibromyalgia and widespread pain: an observational study in 35,248 persons with rheumatoid arthritis, non-inflammatory rheumatic disorders and clinical fibromyalgia. *Semin Arthritis Rheum* 2020;50:1457–64.
31. Hitchon CA, Boire G, Haraoui B, Keystone E, Pope J, Jamal S, et al, on behalf of the CATCH Investigators. Self-reported comorbidity is common in early inflammatory arthritis and associated with poorer function and worse arthritis disease outcomes: results from the Canadian Early Arthritis Cohort. *Rheumatology (Oxford)* 2016;55:1751–62.

APPENDIX A: THE CATCH INVESTIGATORS

The CATCH investigators include the following: Murray Baron, Louis Bessette, Gilles Boire, Vivian Bykerk, Ines Colmegna, Sabrina Fallavollita, Derek Haaland, Paul Haraoui, Glen Hazlewood, Carol Hitchon, Shahin Jamal, Raman Joshi, Ed Keystone, Bindu Nair, Peter Panopoulos, Janet Pope, Laurence Rubin, Carter Thorne, Edith Villeneuve, and Michel Zimmer.

Obesity-Related Traits and the Development of Rheumatoid Arthritis: Evidence From Genetic Data

Bowen Tang,¹  Huwenbo Shi,² Lars Alfredsson,¹ Lars Klareskog,¹ Leonid Padyukov,¹ and Xia Jiang³

Objective. To investigate the association between obesity-related traits and risk of rheumatoid arthritis (RA).

Methods. We conducted genetic correlation analysis and a 2-sample Mendelian randomization (MR) study, using genome-wide genetic data based on >850,000 individuals of European ancestry. Summary statistics were collected from the largest genome-wide association study conducted to date for body mass index (BMI; $n = 806,810$), waist-to-hip ratio (WHR; $n = 697,734$), WHR adjusted for BMI (WHRadjBMI; $n = 694,649$), and RA ($n_{\text{case}} = 14,361$, $n_{\text{control}} = 43,923$). We conducted cross-trait linkage disequilibrium score regression and ρ -HESS analyses to quantify genetic correlation between pairs of traits (causal overlap). For each obesity-related exposure, we utilized independent, genome-wide significant single-nucleotide polymorphisms ($P < 5 \times 10^{-9}$) as instruments to perform MR analysis (causal relationship). We interrogated the causal relationship both in the general population and in a sex-specific manner and calculated odds ratios (ORs) and 95% confidence intervals (95% CIs). Sensitivity analyses were performed to validate MR model assumptions.

Results. Despite a negligible overall genetic correlation between the 3 obesity-related traits and RA, we found significant local genetic correlations at several regions on chromosome 6 (positions 28–29M, 30–35M, and 50–52M), highlighting a shared genetic basis. We further observed an increased risk of RA per SD increment (4.8 kg/m²) in genetically predicted BMI (OR 1.22 [95% CI 1.09–1.37]). The effect was consistent across sensitivity analyses and comparable between sexes (OR 1.22 [95% CI 1.04–1.44] in male subjects and 1.19 [95% CI 1.04–1.36] in female subjects). However, we did not find evidence supporting a causal role of either WHR (OR 0.98 [95% CI 0.84–1.14]) or WHRadjBMI (OR 0.90 [95% CI 0.79–1.04]) in RA.

Conclusion. Genetically predicted BMI significantly increases RA risk. Future studies are needed to understand the biologic mechanisms underlying this link.

INTRODUCTION

Rheumatoid arthritis (RA) is a chronic autoimmune inflammatory joint disease that is more prevalent in Nordic countries and among women (1). Although genome-wide association study meta-analysis (meta-GWAS) has revealed >100 RA-associated genetic loci and large-scale epidemiologic investigations have identified several environmental risk factors, the mechanistic developmental processes of RA remain incompletely understood (2).

Obesity represents a state of low-grade inflammation and has been considered as a potential risk factor for RA (3). Three meta-analyses of longitudinal studies based on >400,000 subjects have jointly demonstrated higher body mass index (BMI)

to be significantly associated with a 3–12% increased risk of RA (4–6). A sex-specific effect has also been observed, in which BMI heightens RA risk to a greater extent in women, with an odds ratio (OR) of 1.12 per 5 kg/m² increment (95% confidence interval [95% CI] 1.07–1.18) than in men (OR 0.90 per 5 kg/m² increment [95% CI 0.81–1.01]) (4). In addition to BMI, researchers have proposed that abdominal obesity, commonly measured by waist circumference (WC) and/or waist-to-hip ratio (WHR), can serve as more appropriate indicators of RA risk (7). A significant yet modest elevation of RA risk (2–5%) among individuals with higher WC has been reported (7,8).

Unlike genetic components, environmental triggers are usually difficult to pinpoint. Results from epidemiologic studies

Dr. Jiang's work was supported by a starting grant from the Swedish Research Council.

¹Bowen Tang, MSc, Lars Alfredsson, PhD, Lars Klareskog, PhD, Leonid Padyukov, PhD: Karolinska Institutet, Stockholm, Sweden; ²Huwenbo Shi, PhD: Harvard University, Boston, Massachusetts; ³Xia Jiang, PhD: Harvard University, Boston, Massachusetts, and Karolinska Institutet, Stockholm, Sweden.

No potential conflicts of interest relevant to this article were reported.

Address correspondence to Xia Jiang, PhD, Karolinska Institutet, Department of Clinical Neuroscience, tomtebodavägen 18A, Solna, Stockholm 17177, Sweden. Email: xia.jiang@ki.se.

Submitted for publication April 15, 2020; accepted in revised form September 3, 2020.

can be affected by measurement error, confounding, and reverse causality. For example, chronic inflammation during the long preclinical course of RA may lead to lifestyle changes that result in altered body composition (9), complicating efforts to elucidate the observed obesity–RA relationship. Mendelian randomization (MR) is a novel statistical tool that uses genetic variants as instrumental variables (IVs) to make causal inferences between exposure(s) and outcome(s), based on the fact that allocation of genetic variants at meiosis is independent of confounders and always prior to disease onset; results are therefore less susceptible to confounding and reverse causation (10). Three important model assumptions need to be satisfied for MR to yield unbiased estimates, i.e., that IVs are robustly associated with exposure (relevance), affect outcome only through exposure (exclusion restriction), and are not associated with confounders in the exposure–outcome relationship (exchangeability) (10).

To date, only 1 MR study of BMI and RA has been reported (11). This study used a small number of index single-nucleotide polymorphisms (SNPs) ($n_{IV} = 65$), had limited samples for outcome ($n_{RA} = 7,480$), and lacked sensitivity analyses to verify model assumptions. Recent genetic discoveries related to several obesity-related traits including BMI, WHR, and WHR adjusted for BMI (WHRadjBMI), involving hundreds of thousands of participants (12), have provided an unprecedented opportunity to explore a causal relationship between these factors and RA. In the current study, we substantially extended previous findings by incorporating summary statistics from the largest meta-GWAS conducted on exposures ($n > 699,000$; $n_{IV} > 600$) and outcome ($n_{RA} = 14,361$; $n_{control} = 43,923$) to date. We performed the analysis both in the general population and in male and female populations separately. In addition, to explore a causal relationship, we quantified genetic correlation, a measure of shared genetic overlap, between obesity-related traits and RA.

MATERIALS AND METHODS

We carried out the current study using a 2-sample MR design, which extracts IV–exposure and IV–outcome associations from 2 independent non-overlapping populations (13) (for a conceptual framework, see Supplementary Figure 1, on the *Arthritis & Rheumatology* website at <http://onlinelibrary.wiley.com/doi/10.1002/art.41517/abstract>).

IV–exposure. We selected index SNPs from the largest meta-GWAS conducted to date on human anthropometric traits, meta-analyzing UK Biobank (UKB) and Genetic Investigation of Anthropometric Traits Consortium data totaling ~700,000 individuals (806,810 participants for BMI, 697,734 for WHR, and 694,649 for WHRadjBMI), all of European ancestry (12). In the original meta-GWAS, to identify independent genetic association signals, a clumping strategy of $P < 5 \times 10^{-9}$ and a linkage

disequilibrium window of ± 5 Mb ($r^2 > 0.05$) were first applied to obtain clumping-based loci, followed by a proximal joint and conditional analysis to determine primary and secondary hits (additional independent signals conditioning on the primary signals) within each clumping-based locus. The GWAS was conducted both in the general population and by sex.

We performed MR analyses using primary signals only (670 BMI-associated index SNPs, 316 WHR-associated index SNPs, and 346 WHRadjBMI-associated index SNPs) as well as primary and secondary signals combined (806, 382, and 463 index SNPs for BMI, WHR, and WHRadjBMI, respectively). We further extracted IV–exposure associations in men and women separately.

IV–outcome. IV–outcome associations were obtained from a meta-GWAS of 18 cohorts totaling 14,361 RA cases and 43,923 controls of European ancestry (14) (Supplementary Table 1, on the *Arthritis & Rheumatology* website at <http://onlinelibrary.wiley.com/doi/10.1002/art.41517/abstract>). To our knowledge, none of the participants in these 18 studies overlapped with participants in the exposure meta-GWAS.

We matched our IVs (primary and secondary SNPs for the 3 obesity-related exposures) with summary data from outcome GWAS (RA meta-GWAS). Finally, 793 SNPs for BMI, 372 SNPs for WHR, and 445 SNPs for WHRadjBMI were available (Supplementary Tables 2–4, <http://onlinelibrary.wiley.com/doi/10.1002/art.41517/abstract>). Overall, we were able to capture >96% of IVs, a virtually complete coverage.

Genome-wide genetic data. MR leverages information on a small number of index SNPs. To quantify genetic correlation between exposures and outcome, we further obtained full sets of summary-level genome-wide genetic data (~10 million SNPs) for each of the 3 obesity-related exposures and for RA.

Statistical analysis. *Genetic correlation analyses.* To investigate causal overlap, we first assessed genome-wide pairwise genetic correlation for each exposure and outcome, using linkage disequilibrium score regression (LDSC), an approach that leverages GWAS summary association statistics and LD to estimate genetic correlation (15). Genome-wide genetic correlations estimated by LDSC measure correlation of SNP effect sizes across all SNPs in the genome. It is possible that even though 2 traits show negligible overall genetic correlation, specific genomic regions contribute to both traits. We therefore examined local genetic correlation using ρ -HESS, an algorithm that partitions the whole genome into 1,703 regions based on LD patterns in European populations and quantifies correlation between pairs of traits due to genetic variation restricted to specific regions (16). Taking into account multiple tests, P values of 1.1×10^{-3} (0.05/45) and 2.9×10^{-5} (0.05/1,703) were applied as significant thresholds for LDSC and ρ -HESS, respectively.

Mendelian randomization analyses. To investigate a causal relationship between obesity and RA, we conducted a 2-sample MR applying several approaches. A random-effects inverse variance-weighted method (IVW), an MR-Egger regression, and an MR pleiotropy residual sum and outlier (MR-PRESSO) test were used. The random-effects IVW pools the estimate from each genetic variant (IV) and calculates a precise causal estimation assuming all genetic variants are valid, or are invalid in such a way that the overall pleiotropy is balanced to be zero (17). MR-Egger regression is robust even if all variants are invalid, and its intercept can be adopted as a test of unbalanced pleiotropy (17). MR-PRESSO detects pleiotropic outlier variants and provides outlier-corrected estimations (18). Given the major role of the HLA region in immunity, inflammation, and RA etiology (19) and to control for potential pleiotropy, we performed all analysis excluding SNPs from this region (chromosome 6: 2.9–3.3M).

Sensitivity analyses. To verify MR model assumptions, we performed additional sensitivity analyses. For each index SNP, we searched the National Human Genome Research Institute-European Bioinformatics Institute Catalog of Human Genome-Wide Association Studies for potential associations with confounding traits and conducted analyses with these SNPs excluded. To ascertain whether our estimation was driven by any individual SNP with a large effect, we carried out leave-one-out analysis in which we removed one SNP at a time and performed IVW on the remaining SNPs.

The statistical power of our study was calculated using an algorithm described by Brion et al (20). After correction for tests on 3 exposures, associations with *P* values of <0.017 (0.05/3) were considered statistically significant; *P* values between 0.017 and <0.05 were considered to be suggestive of significance. All analyses were performed using LDSC software (15), ρ -HESS software (16), and TwoSampleMR in R 3.6.0 software (21).

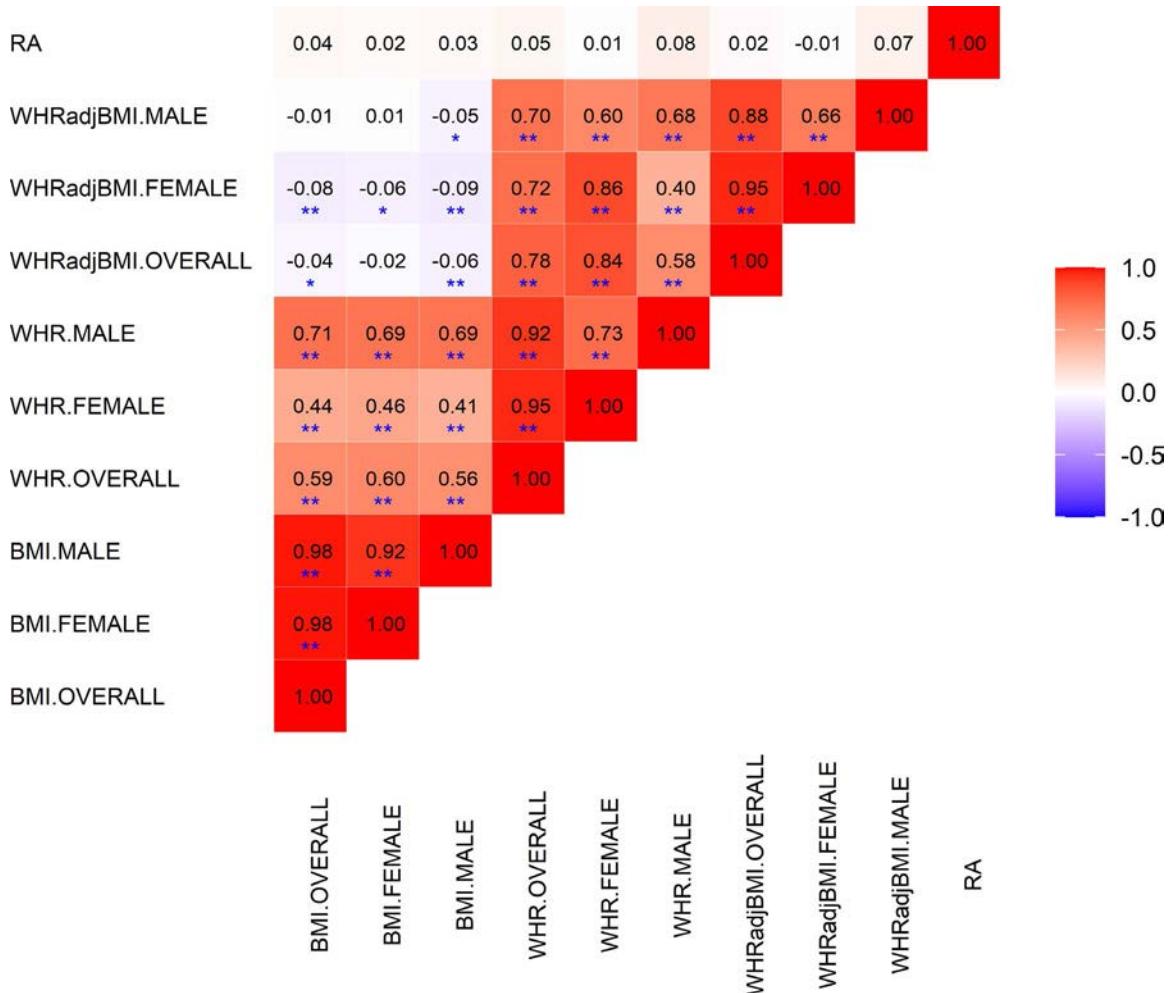


Figure 1. Cross-trait genetic correlation between obesity-related traits and rheumatoid arthritis (RA). The point estimate of genetic correlation is shown within each box, with the color of the box representing the magnitude of correlation. * = *P* < 0.05 (suggestive for statistical significance); ** = *P* (Bonferroni-corrected) < 1.1×10^{-3} . WHRadjBMI = waist-to-hip ratio adjusted for body mass index.

RESULTS

Our results indicated that obesity-related traits were strongly genetically correlated with one another. Within each trait, there was a high degree of shared genetic similarity between men and women (r_g 0.92 [95% CI 0.90–0.94] for BMI, 0.73 [95% CI 0.69–0.77] for WHR, and 0.66 [95% CI 0.62–0.70] for WHRadjBMI). Across traits, BMI and WHR shared a common genetic basis, with an overall correlation of 0.59 (95% CI 0.55–0.63) (r_g 0.46 [95% CI 0.41–0.51] in women and 0.69 [95% CI 0.66–0.72] in men). However, for WHRadjBMI, in which the effect of BMI was removed from WHR, we observed minimal correlation with BMI (r_g ranging from –0.09 to 0.01), as expected. These results illustrate the challenge of studying obesity-related traits alone and without a genetic context, as their effects are difficult to dissect. We did not

find evidence of a shared genetic basis of BMI, WHR, or WHRadjBMI with RA either overall or in the male or the female population. All estimates were close to 0 (r_g ranging from –0.01 to 0.08, all $P > 0.05$), suggesting negligible genetic correlations (Figure 1).

Despite an absence of genome-wide genetic correlation, obesity-related exposures and RA might still share pleiotropic risk loci. As shown in Figure 2, when partitioning the genome into 1,703 regions, we observed significant local genetic correlation in several regions of chromosome 6 (positions 28.0–29.0M, 30.7–35.5M, and 50.3–52.3M) and chromosome 19 (positions 9.2–11.3M). When performing separate analyses by sex, we found additional shared regions on chromosomes 8 (positions 75.4–76.5M) and 16 (positions 27.4–29.1M) in women.

Motivated by the findings of local genetic correlations, we explored the causal relationships between different measures of

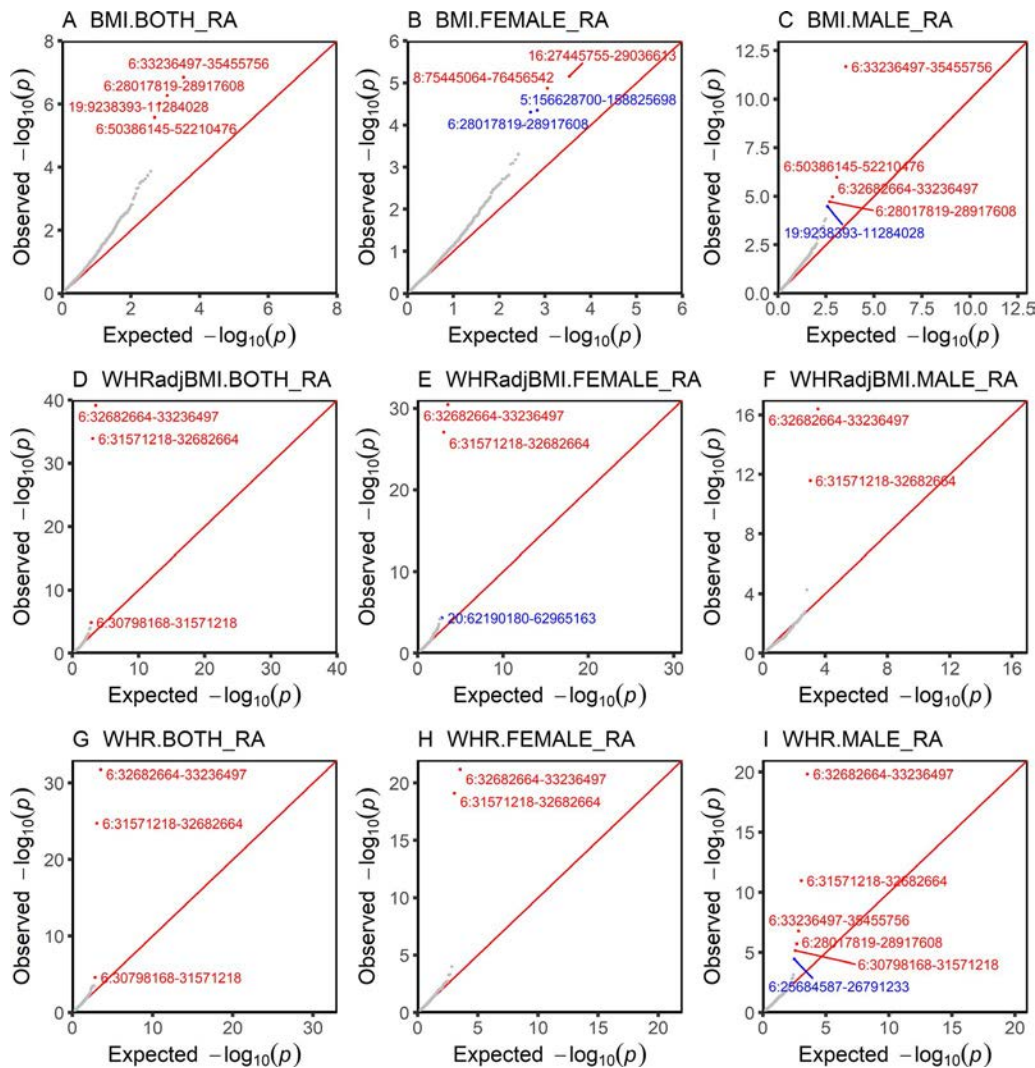


Figure 2. Local genetic correlation between obesity-related traits and rheumatoid arthritis (RA). Plots show region-specific P values for the local genetic covariance between RA and body mass index (BMI), waist-to-hip ratio (WHR), and WHR adjusted for BMI (WHRadjBMI) overall (both) and in female and male subjects analyzed separately. Each dot presents a specific genomic region. Red indicates significance after multiple corrections ($P < 3 \times 10^{-5}$ [0.05/1,703 regions compared]); blue indicates nominal significance under an arbitrary threshold of $P < 5 \times 10^{-5}$.

obesity and RA through MR analysis. With our current sample size for outcome ($n = 58,284$; 24% cases) and assuming phenotypic variance of the exposures explained by IVs to be 4–8% (Supplementary Table 5, on the *Arthritis & Rheumatology* website at <http://onlinelibrary.wiley.com/doi/10.1002/art.41517/abstract>), our study had sufficient power to detect associations of 15% increase in risk of RA with BMI (98% power), WHR (86% power), and WHRadjBMI (96% power). The power remained acceptable in an analysis restricted to women (which had 80% power to detect a 15% increase in risk of RA associated with BMI or WHR or a 10% increase in risk of RA associated with WHRadjBMI) and decreased only slightly in an analysis restricted to men (80% power to detect a 15% increase in risk of RA associated with BMI or a 25% increase in risk of RA associated with WHR or WHRadjBMI). Since results from our ρ -HESS analysis revealed significant correlations with the HLA region and given the complexity of that region (19), we performed all MR analysis excluding SNPs from the HLA region.

We found strong evidence supporting the notion of a causal relationship between BMI and RA. As shown in Table 1, we observed a 20% increased risk of RA per SD increment (4.8 kg/m²) in BMI (OR using random-effects IVW 1.22 [95% CI 1.09–1.37]). The effect was not altered in analyses using MR-PRESSO (OR 1.20 [95% CI 1.07–1.34 excluding 1 outlier] and was only slightly attenuated in analyses using MR-Egger (OR 1.13 [95% CI 0.83–1.54]), but without any apparent sign of pleiotropy (P for MR-Egger intercept = 0.43). Sensitivity analysis with additional removal of SNPs associated with potential confounding traits, including smoking, education level, type 2 diabetes, and others (Supplementary Table 2, <http://onlinelibrary.wiley.com/doi/10.1002/art.41517/abstract>) revealed similar results of even more

pronounced magnitude (Table 2) (OR [95% CI] 1.27 [1.12–1.45], 1.44 [0.94–2.22], and 1.24 [1.10–1.41] in analyses using IVW, MR-Egger, and MR-PRESSO, respectively). Leave-one-out analysis demonstrated that the observed risk effect was not driven by outlying variants (Supplementary Table 6, <http://onlinelibrary.wiley.com/doi/10.1002/art.41517/abstract>).

In contrast, we did not find any association between genetically predicted WHR and RA, with overall effects that were close to 1.00 and nonsignificant (OR [95% CI] 0.98 [0.84–1.14], 0.91 [0.60–1.37], and 0.93 [0.81–1.07] by IVW, MR-Egger, and MR-PRESSO, respectively) (Table 1). Results from sensitivity analyses removing IVs associated with potential confounders remained consistent (OR [95% CI] 1.05 [0.87–1.26], 0.94 [0.54–1.63], and 1.02 [0.87–1.21] by IVW, MR-Egger, and MR-PRESSO, respectively) (Table 2). Leave-one-out analysis did not identify any outlying variant (Supplementary Table 7, <http://onlinelibrary.wiley.com/doi/10.1002/art.41517/abstract>).

Our findings imply a causal role of BMI, but not WHR, in the development of RA. Given the complex interrelationships between obesity-related measurements and to validate our results, we investigated WHRadjBMI, a residual component of WHR in which the effect of BMI is removed. We anticipated observing a null or even reduced effect of WHRadjBMI on RA after eliminating the positive association of BMI from the null association of WHR. As expected, we did not observe any increased effect of WHRadjBMI on RA, with effect sizes that were either close to or slightly lower than 1.00 (OR [95% CI] 0.90 [0.79–1.04] by IVW, 0.92 [0.68–1.25] by MR-Egger, and 0.86 [0.77–0.97] by MR-PRESSO) (Table 1 and Supplementary Table 8, on the *Arthritis & Rheumatology* website at <http://onlinelibrary.wiley.com/doi/10.1002/art.41517/abstract>).

Table 1. Association between genetically predicted obesity-related traits and risk of rheumatoid arthritis in a primary analysis excluding SNPs located in the HLA region*

Parameter, MR approach	SNPs at $P < 5 \times 10^{-9}$ (primary + secondary GWAS hits)			SNPs at $P < 5 \times 10^{-9}$ (primary GWAS hits)		
	OR (95% CI)	P	P for heterogeneity or pleiotropy	OR (95% CI)	P	P for heterogeneity or pleiotropy
BMI ($n = 790/660$)						
Random-effects IVW	1.22 (1.09–1.37)	6.1×10^{-4}	<0.001	1.21 (1.08–1.37)	1.6×10^{-3}	<0.001
MR-Egger	1.13 (0.83–1.54)	0.43	0.60	1.11 (0.81–1.54)	0.51	0.57
MR-PRESSO (detected outliers 1/NA)	1.20 (1.07–1.34)	1.5×10^{-3}	–	1.21 (1.08–1.37)	1.7×10^{-3}	–
WHR ($n = 369/310$)						
Random-effects IVW	0.98 (0.84–1.14)	0.78	<0.001	0.96 (0.82–1.13)	0.62	<0.001
MR-Egger	0.91 (0.60–1.37)	0.66	0.71	0.96 (0.62–1.49)	0.85	0.99
MR-PRESSO (detected outliers 2/2)	0.93 (0.81–1.07)	0.31	–	0.92 (0.79–1.08)	0.32	–
WHRadjBMI ($n = 441/335$)						
Random-effects IVW	0.90 (0.79–1.04)	0.15	<0.001	0.85 (0.73–0.98)	0.02	<0.001
MR-Egger	0.92 (0.68–1.25)	0.60	0.90	0.99 (0.71–1.38)	0.95	0.31
MR-PRESSO (detected outliers 5/3)	0.86 (0.77–0.97)	0.01	–	0.83 (0.72–0.94)	5.6×10^{-3}	–

* N values (number of single-nucleotide-polymorphisms [SNPs]) for body mass index (BMI), waist-to-hip ratio (WHR), and WHR adjusted for BMI (WHRadjBMI) and numbers of detected outliers in the Mendelian randomization pleiotropy residual sum and outlier (MR-PRESSO) analyses are for the analysis of primary + secondary genome-wide association study (GWAS) hits/analysis of primary SNPs only. OR = odds ratio; 95% CI = 95% confidence interval; IVW = inverse variance-weighted method; NA = not applicable.

Table 2. Association between genetically predicted obesity-related traits and risk of rheumatoid arthritis in a sensitivity analysis excluding genetic instruments in the HLA region or associated with confounding traits*

Parameter, MR approach	SNPs at $P < 5 \times 10^{-9}$ (primary + secondary GWAS hits)			Primary SNPs at $P < 5 \times 10^{-9}$		
	OR (95% CI)	<i>P</i>	<i>P</i> for heterogeneity or pleiotropy	OR (95% CI)	<i>P</i>	<i>P</i> for heterogeneity or pleiotropy
BMI (n = 696/582)						
Random-effects IWV	1.27 (1.12–1.45)	2.4×10^{-4}	<0.001	1.28 (1.11–1.46)	4.5×10^{-4}	<0.001
MR-Egger	1.44 (0.94–2.22)	0.10	0.55	1.44 (0.88–2.33)	0.14	0.62
MR-PRESSO (detected outliers 1/2)	1.24 (1.10–1.41)	6.9×10^{-4}	–	1.30 (1.14–1.49)	1.2×10^{-4}	–
WHR (n = 307/255)						
Random-effects IWV	1.05 (0.87–1.26)	0.61	<0.001	1.03 (0.86–1.24)	0.75	2.0×10^{-3}
MR-Egger	0.94 (0.54–1.63)	0.82	0.68	1.13 (0.61–2.11)	0.70	0.76
MR-PRESSO (detected outliers 2/1)	1.02 (0.87–1.21)	0.77	–	1.05 (0.88–1.26)	0.58	–
WHRadjBMI (n = 348/258)						
Random-effects IWV	0.92 (0.78–1.09)	0.34	<0.001	0.85 (0.71–1.01)	0.06	0.01
MR-Egger	0.98 (0.66–1.46)	0.93	0.74	1.19 (0.72–1.97)	0.49	0.16
MR-PRESSO (detected outliers 4/2)	0.85 (0.74–0.97)	0.02	–	0.80 (0.68–0.94)	0.01	–

* N values (number of SNPs) for BMI, WHR, and WHRadjBMI and numbers of detected outliers in the MR-PRESSO analyses are for the analysis of primary + secondary GWAS hits/analysis of primary SNPs only. See Table 1 for definitions.

RA occurs in women 2–3 times more frequently than in men. To better understand this sex disparity, we performed sex-specific analyses that were restricted to BMI and WHR. As shown in Table 3, we found comparable effects of BMI between men and women, by IWV (OR 1.22 [$P = 1.5 \times 10^{-2}$] and 1.19 [$P = 1.2 \times 10^{-2}$], respectively) and MR-PRESSO (OR 1.19 [$P = 1.4 \times 10^{-2}$] and 1.19 [$P = 1.2 \times 10^{-2}$] respectively), with no indications of pleiotropy (P for MR-Egger intercept = 0.62 in men and 0.40 in women). The results were consistent in sensitivity analyses in which IVs associated with potential confounders were removed (OR 1.29 [$P = 9.2 \times 10^{-3}$] and 1.28 [$P = 3.0 \times 10^{-3}$], respectively) (Table 4). For WHR, we found an increased but nonsignificant effect of WHR among men and a slightly reduced effect among women. Our sex-specific results for WHR should be interpreted with caution given the large variations in point estimates of results from the main and sensitivity analyses (only 79 IVs for WHR in men), and substantial

pleiotropy indicated in women (P for MR-Egger intercept = 0.08 in main analysis, 0.04 in sensitivity analysis).

We performed additional sensitivity analyses with restriction to only primary association signals (which are believed to be stronger IVs) (Tables 1 and 2). The results were not substantially different when different sets of IVs were used.

DISCUSSION

In the present study, we leveraged the largest genetic data set for 3 obesity-related traits (BMI, WHR, and WHRadjBMI) published to date, together with the largest GWAS addressing the outcome of interest, to understand causal overlaps and causal relationships between obesity and risk of RA. We found a modest but significant shared genetic basis between obesity-related exposures and RA on several genomic regions. We further identified a pronounced causal effect of BMI in the development of

Table 3. Association between genetically predicted obesity-related traits and risk of rheumatoid arthritis by sex, excluding genetic instruments in the HLA region*

Parameter, MR approach	SNPs at $P < 5 \times 10^{-9}$ (primary + secondary GWAS hits) in men			SNPs at $P < 5 \times 10^{-9}$ (primary + secondary GWAS hits) in women		
	OR (95% CI)	<i>P</i>	<i>P</i> for heterogeneity or pleiotropy	OR (95% CI)	<i>P</i>	<i>P</i> for heterogeneity or pleiotropy
BMI (n = 237/299)						
Random-effects IWV	1.22 (1.04–1.44)	1.5×10^{-2}	<0.001	1.19 (1.04–1.36)	1.2×10^{-2}	<0.001
MR-Egger	1.11 (0.71–1.72)	0.65	0.62	1.03 (0.71–1.48)	0.89	0.40
MR-PRESSO (detected outliers 4/NA)	1.19 (1.04–1.37)	1.4×10^{-2}	–	1.19 (1.04–1.36)	1.2×10^{-2}	–
WHR (n = 7/249)						
Random-effects IWV	1.22 (0.94–1.59)	0.13	0.001	0.86 (0.76–0.97)	1.4×10^{-2}	0.01
MR-Egger	1.11 (0.41–2.97)	0.84	0.84	1.08 (0.81–1.44)	0.59	0.08
MR-PRESSO (detected outliers 1/2)	1.16 (0.90–1.49)	0.25	–	0.83 (0.74–0.93)	2.0×10^{-3}	–

* N values (number of SNPs) for BMI, WHR, and WHRadjBMI and numbers of detected outliers in the MR-PRESSO analyses are for the analysis of primary + secondary GWAS hits/analysis of primary SNPs only. See Table 1 for definitions.

Table 4. Association between genetically predicted obesity-related traits and risk of rheumatoid arthritis by sex, in a sensitivity analysis excluding genetic instruments in the HLA region or associated with confounding traits*

Parameter, MR approach	SNPs at $P < 5 \times 10^{-9}$ (primary + secondary GWAS hits) in men			SNPs at $P < 5 \times 10^{-9}$ (primary + secondary GWAS hits) in women		
	OR (95% CI)	<i>P</i>	<i>P</i> for heterogeneity or pleiotropy	OR (95% CI)	<i>P</i>	<i>P</i> for heterogeneity or pleiotropy
BMI (n = 198/247)						
Random-effects IWW	1.29 (1.06–1.55)	9.2×10^{-3}	<0.001	1.28 (1.09–1.50)	3.0×10^{-3}	<0.001
MR-Egger	1.25 (0.73–2.12)	0.42	0.90	1.83 (1.01–3.32)	0.05	0.22
MR-PRESSO (detected outliers 4/NA)	1.25 (1.06–1.46)	6.9×10^{-3}	–	1.28 (1.09–1.50)	3.0×10^{-3}	–
WHR (n = 59/203)						
Random-effects IWW	1.23 (0.92–1.63)	0.16	0.02	0.87 (0.75–1.01)	0.06	0.01
MR-Egger	0.94 (0.34–2.64)	0.91	0.61	1.28 (0.86–1.93)	0.23	0.04
MR-PRESSO (detected outliers 1/2)	1.14 (0.88–1.49)	0.32	–	0.83 (0.72–0.95)	8.1×10^{-3}	–

* N values (number of SNPs) for BMI, WHR, and WHRadjBMI and numbers of detected outliers in the MR-PRESSO analyses are for the analysis of primary + secondary GWAS hits/analysis of primary SNPs only. See Table 1 for definitions.

RA and observed that the effect of obesity on risk of RA is similar between women and men.

The present results are in accordance with findings from earlier epidemiologic investigations. Reports from 3 meta-analyses have described a dose-response relationship between BMI and RA (4–6). Specifically, a linear relationship with risk ratio for RA of 1.13 per 5-kg/m² increment in BMI has been described (4), a result that is strongly supported by our finding of an increased risk of RA with genetically predicted BMI fitting a linear model. However, studies exploring the association of WC/WHR with RA are lacking. To our knowledge, only 2 population-based studies have examined WC and RA risk. One prospective study based on the Danish Diet, Cancer and Health cohort of 55,037 subjects has shown a modestly increased RA risk per 5-cm WC increment in both men (OR 1.04 [95% CI 0.69–1.57]) and women (OR 1.05 [95% CI 1.01–1.09]) (8). Similar results were found in a case-control study of 557 RA cases and 1,671 controls (OR 1.02 per 1-cm increase [95% CI 1.01–1.04]) (7). However, these findings are not supported by our current MR study, which showed no evidence of a causal relationship between WHR and RA. When we assessed the association of RA risk with WHRadjBMI-RA, thus removing the effect of BMI from WHR, our finding of a negative WHRadjBMI-RA association further confirmed the validity of our results. It is thus reasonable to assume that conventional epidemiologic settings could not eliminate the confounding of BMI from WC/WHR, and the findings of studies exploring a relationship of WC/WHR to RA are likely to be confounded by the effect of BMI.

Our results extend findings from a previous MR study that also demonstrated a positive association between genetically predicted BMI and RA (11). However, compared to that study, which utilized 68 SNPs as instruments and 7,480 RA cases as outcomes, our current study has several advantages. We significantly improved statistical power by incorporating >600 index SNPs as IVs based on a sample of >600,000 individuals for the exposure, as well as the largest meta-GWAS on the outcome RA. We carefully checked and

controlled for bias arising from population stratification by restricting participants to individuals of European ancestry. We interrogated not only BMI but also an indicator of abdominal fat distribution (WHR) and did not find compelling evidence of a causal role of WHR. Finally, we conducted additional sensitivity analyses to verify MR model assumptions. We selected the most significant independent SNPs identified by the largest GWAS on obesity (primary signals at a stringent GWAS *P* threshold of 5×10^{-9}), so all were robustly associated with the exposure of interest, guaranteeing the “relevance” assumption. We excluded SNPs located in the HLA region or associated with potential confounders of the exposure-outcome relationship, to satisfy “exclusion restriction” assumptions. The consistent results observed across different approaches lend further support for a putative causal relationship between BMI and RA.

Biologic mechanisms linking BMI to RA remain largely unknown, though with several well-documented assumptions. Obesity, especially the accumulation of visceral fat, contributes to a chronic low-grade proinflammatory state (22). Adipocytes act as an active endocrine/paracrine organ that secretes a number of adipokines involved in the regulation of inflammation and autoimmunity (9,23). For example, leptin, an adipokine produced by adipocytes, up-regulates phagocytic function and secretion of proinflammatory cytokines, such as tumor necrosis factor, interleukin-6 (IL-6), and IL-12, in monocyte/macrophages and modifies T cell differentiation toward a proinflammatory state (24). Thus, leptin has been suggested to play a role in the pathogenesis of RA (25). Although we hypothesized the inflammatory nature of adiposity as an underlying etiology for RA risk, we did not identify an association with WHR. BMI has been found to be highly correlated with excess fat mass ($r = 0.94$) and abdominal visceral fat ($r = 0.71$) (26), while WHR poorly predicted the accumulation of visceral fat (27,28), which may account for our significant findings with BMI but not with WHR. Moreover, studies have suggested that local adipose, such as articular adipose or infrapatellar fat pad, plays a pivotal role in the pathologic process

of RA. Articular adipose tissue secretes a large amount of inflammation-related factors (e.g., IL-6, IL-8, adipokines) and intensifies pathogenic activities of rheumatoid fibroblast-like synoviocytes (29). Finally, higher BMI is associated with an increased level of estradiol (30,31), and estrogens are suggested to have proinflammatory effects (32). Although the exact role of sex hormones in the development of RA remains to be elucidated, their involvement has been confirmed (33).

Overall, our study demonstrates a putative causal relationship between BMI and risk of RA, which provides novel insights into the disease mechanism of RA and suggests an actionable prevention strategy. However, the study had some limitations that should be taken into account. First, due to limited data, we were not able to examine RA subtypes characterized by anti-citrullinated antibody status. The current RA GWAS summary statistics were based on a mix of 88.1% seropositive, 9.3% seronegative, and 2.6% unknown-status cases. Studies have demonstrated differing effects of BMI in the 2 distinct RA subtypes (34,35), and future MR analyses should be designed to explore these.

Moreover, explaining and understanding the sex disparity underlying RA remains challenging, as confounding by sex and by interaction of sex with the underlying genetics in both RA and obesity is likely. Obesity-related traits are highly correlated across men and women, with most IVs shared by both sexes. It is thus difficult to obtain sex-specific IVs. For RA, unfortunately, the meta-GWAS was performed without adjustment for sex to maximize statistical power; in that large-scale genotyping collaboration across multiple countries and institutions (14), additional covariates besides blood samples were not collected (Okada Y: personal communication). Our sex-specific analysis should be interpreted with caution.

Additionally, because the genetic code is fixed at conception, MR typically compares groups of the population having different trajectories in their distribution of exposure over time. Our analyses can therefore be interpreted as assessing the impact of long-term elevated BMI. However, we acknowledge that incomplete information about how genetic variant changes the distribution of exposure across the life course may bias the results: if genetic associations with exposure vary over time, then MR estimates based on genetic associations with the exposure measured at a single time point can be unreliable. This was, however, a minor issue in our study; although an earlier age-stratified GWAS identified 15 loci with age-specific effects, these SNPs, which exert time-varying effects on BMI, were small in amount and with modest variations across age groups (36).

Of note, despite the many solutions proposed to satisfy MR model assumptions, these falsification strategies can only detect that an assumption is violated but cannot ever confirm that it holds. For example, current identification of IV–confounder associations relies heavily on conventional techniques (genome-wide scan) and established knowledge (through literature review and the National Human Genome Research Institute–European

Bioinformatics Institute GWAS catalog). We can never be certain that all IVs associated with confounders of the exposure–outcome relationship were excluded; the association might remain to be identified or the SNP may be associated with an underlying risk factor that is unrecognized.

Future studies may include individual-level data to investigate genetic risk score–based approaches and to test, for example, the imbalance in measured covariates across levels of the proposed instruments. Finally, there should be additional efforts to increase generalizability as almost all current MR studies in RA have been conducted in European adult populations (age >18 years). Future investigations should also use MR analysis to explore treatment strategy and prognosis of RA, in addition to disease onset.

ACKNOWLEDGMENTS

We are grateful to all investigators who shared genome-wide summary statistics and to Dr. Stephen Burgess for insightful suggestions in interpreting MR results with time-varying exposure.

AUTHOR CONTRIBUTIONS

All authors were involved in drafting the article or revising it critically for important intellectual content, and all authors approved the final version to be published. Dr. Jiang had full access to all of the data in the study and takes responsibility for the integrity of the data and the accuracy of the data analysis.

Study conception and design. Tang, Jiang.

Acquisition of data. Tang, Jiang.

Analysis and interpretation of data. Tang, Shi, Alfredsson, Klareskog, Padyukov, Jiang.

REFERENCES

- Kiadaliri AA, Kristensen LE, Englund M. Burden of rheumatoid arthritis in the Nordic region, 1990–2015: a comparative analysis using the Global Burden of Disease Study 2015. *Scand J Rheumatol* 2018;47:1–101.
- Malmstrom V, Catrina AI, Klareskog L. The immunopathogenesis of seropositive rheumatoid arthritis: from triggering to targeting [review]. *Nat Rev Immunol* 2017;17:60–75.
- Hedstrom AK, Klareskog L, Alfredsson L. Interplay between obesity and smoking with regard to RA risk. *RMD Open* 2019; 5:e000856.
- Feng J, Chen Q, Yu F, Wang Z, Chen S, Jin Z, et al. Body mass index and risk of rheumatoid arthritis: a meta-analysis of observational studies. *Medicine (Baltimore)* 2016;95:e2859.
- Feng X, Xu X, Shi Y, Liu X, Liu H, Hou H, et al. Body mass index and the risk of rheumatoid arthritis: an updated dose-response meta-analysis. *Biomed Res Int* 2019;2019:3579081.
- Qin B, Yang M, Fu H, Ma N, Wei T, Tang Q, et al. Body mass index and the risk of rheumatoid arthritis: a systematic review and dose-response meta-analysis. *Arthritis Res Ther* 2015;17:86.
- Ljung L, Rantapaa-Dahlqvist S. Abdominal obesity, gender and the risk of rheumatoid arthritis: a nested case-control study. *Arthritis Res Ther* 2016;18:277.
- Linauskas A, Overvad K, Symmons D, Johansen MB, Stengaard-Pedersen K, de Thurah A. Body fat percentage, waist circumference, and obesity as risk factors for rheumatoid arthritis: a Danish cohort study. *Arthritis Care Res (Hoboken)* 2019;71:777–86.

9. Stavropoulos-Kalinoglou A, Metsios GS, Koutedakis Y, Kitas GD. Obesity in rheumatoid arthritis. *Rheumatology (Oxford)* 2010;50: 450–62.
10. Davies NM, Holmes MV, Smith GD. Reading Mendelian randomisation studies: a guide, glossary, and checklist for clinicians. *BMJ* 2018;362:k601.
11. Bae SC, Lee YH. Causal association between body mass index and risk of rheumatoid arthritis: a Mendelian randomization study. *Eur J Clin Invest* 2019;49:e13076.
12. Pulit SL, Stoneman C, Morris AP, Wood AR, Glastonbury CA, Tyrrell J, et al. Meta-analysis of genome-wide association studies for body fat distribution in 694,649 individuals of European ancestry. *Hum Mol Genet* 2019;28:166–74.
13. Hartwig FP, Davies NM, Hemani G, Smith GD. Two-sample Mendelian randomization: avoiding the downsides of a powerful, widely applicable but potentially fallible technique. *Int J Epidemiol* 2016;45:1717–26.
14. Okada Y, Wu D, Trynka G, Raj T, Terao C, Ikari K, et al. Genetics of rheumatoid arthritis contributes to biology and drug discovery. *Nature* 2014;506:376–81.
15. Bulik-Sullivan B, Finucane HK, Anttila V, Gusev A, Day FR, Loh PR, et al. An atlas of genetic correlations across human diseases and traits. *Nat Genet* 2015;47:1236–41.
16. Shi H, Mancuso N, Spendlove S, Pasaniuc B. Local genetic correlation gives insights into the shared genetic architecture of complex traits. *Am J Hum Genet* 2017;101:737–51.
17. Burgess S, Thompson SG. Interpreting findings from Mendelian randomization using the MR-Egger method. *Eur J Epidemiol* 2017;32:377–89.
18. Verbanck M, Chen CY, Neale B, Do R. Detection of widespread horizontal pleiotropy in causal relationships inferred from Mendelian randomization between complex traits and diseases. *Nat Genet* 2018;50:693–8.
19. Weyand CM, Goronzy JJ. Association of MHC and rheumatoid arthritis: HLA polymorphisms in phenotypic variants of rheumatoid arthritis. *Arthritis Res Ther* 2000;2:212–6.
20. Brion MJ, Shakhbazov K, Visscher PM. Calculating statistical power in Mendelian randomization studies. *Int J Epidemiol* 2012;42:1497–501.
21. Hemani G, Zheng J, Elsworth B, Wade KH, Haberland V, Baird D, et al. The MR-Base platform supports systematic causal inference across the human phenome. *Elife* 2018;7:e34408.
22. Ibrahim MM. Subcutaneous and visceral adipose tissue: structural and functional differences. *Obes Rev* 2010;11:11–8.
23. Lago F, Dieguez C, Gómez-Reino J, Gualillo O. Adipokines as emerging mediators of immune response and inflammation. *Nat Clin Pract Rheumatol* 2007;3:716–24.
24. Matarese G, Moschos S, Mantzoros CS. Leptin in immunology. *J Immunol* 2005;174:3137–42.
25. Tian G, Liang JN, Wang ZY, Zhou D. Emerging role of leptin in rheumatoid arthritis. *Clin Exp Immunol* 2014;177:557–70.
26. Bouchard C. BMI, fat mass, abdominal adiposity and visceral fat: where is the ‘beef’? *Int J Obes (Lond)* 2007;31:1552–3.
27. Van der Kooy K, Leenen R, Seidell JC, Deurenberg P, Droop A, Bakker CJ. Waist-hip ratio is a poor predictor of changes in visceral fat. *Am J Clin Nutr* 1993;57:327–33.
28. Busetto L, Baggio MB, Zurlo F, Carraro R, Digirolamo M, Enzi G. Assessment of abdominal fat distribution in obese patients: anthropometry versus computerized tomography. *Int J Obes Relat Metab Disord* 1992;16:731–6.
29. Kontny E, Plebanczyk M, Lisowska B, Olszewska M, Malyk P, Maslinski W. Comparison of rheumatoid articular adipose and synovial tissue reactivity to proinflammatory stimuli: contribution to adipocytokine network. *Ann Rheum Dis* 2012;71:262–7.
30. Rohrmann S, Shiels MS, Lopez DS, Rifai N, Nelson WG, Kanarek N, et al. Body fatness and sex steroid hormone concentrations in US men: results from NHANES III. *Cancer Causes Control* 2011;22:1141–51.
31. McTiernan A, Wu L, Chen C, Chlebowski R, Mossavar-Rahmani Y, Modugno F, et al. Relation of BMI and physical activity to sex hormones in postmenopausal women. *Obesity* 2006;14: 1662–77.
32. Cutolo M, Sulli A, Capellino S, Villaggio B, Montagna P, Pizzorni C, et al. Anti-TNF and sex hormones. *Ann N Y Acad Sci* 2006; 1069:391–400.
33. Alpízar-Rodríguez D, Pluchino N, Canny G, Gabay C, Finckh A. The role of female hormonal factors in the development of rheumatoid arthritis. *Rheumatology (Oxford)* 2016;56:1254–63.
34. Wesley A, Bengtsson C, Elkan AC, Klareskog L, Alfredsson L, Wedrén S, et al. Association between body mass index and anti-citrullinated protein antibody-positive and anti-citrullinated protein antibody-negative rheumatoid arthritis: results from a population-based case-control study. *Arthritis Care Res (Hoboken)* 2013;65:107–12.
35. Pedersen M, Jacobsen S, Klarlund M, Pedersen BV, Wiik A, Wohlfahrt J, et al. Environmental risk factors differ between rheumatoid arthritis with and without auto-antibodies against cyclic citrullinated peptides. *Arthritis Res Ther* 2006;8:R133.
36. Winkler TW, Justice AE, Graff M, Barata L, Feitosa MF, Chu S, et al. The influence of age and sex on genetic associations with adult body size and shape: a large-scale genome-wide interaction study [corrected and republished in *PLoS Genet* 2016 Jun;12:e1006166]. *PLoS Genet* 2015;11:e1005378.

Multiomics and Machine Learning Accurately Predict Clinical Response to Adalimumab and Etanercept Therapy in Patients With Rheumatoid Arthritis

Weiyang Tao, Arno N. Concepcion, Marieke Vianen, Anne C. A. Marijnissen, Floris P. G. J. Lafeber, Timothy R. D. J. Radstake, and Aridaman Pandit 

Objective. To predict response to anti-tumor necrosis factor (anti-TNF) prior to treatment in patients with rheumatoid arthritis (RA), and to comprehensively understand the mechanism of how different RA patients respond differently to anti-TNF treatment.

Methods. Gene expression and/or DNA methylation profiling on peripheral blood mononuclear cells (PBMCs), monocytes, and CD4+ T cells obtained from 80 RA patients before they began either adalimumab (ADA) or etanercept (ETN) therapy was studied. After 6 months, treatment response was evaluated according to the European League Against Rheumatism criteria for disease response. Differential expression and methylation analyses were performed to identify the response-associated transcription and epigenetic signatures. Using these signatures, machine learning models were built by random forest algorithm to predict response prior to anti-TNF treatment, and were further validated by a follow-up study.

Results. Transcription signatures in ADA and ETN responders were divergent in PBMCs, and this phenomenon was reproduced in monocytes and CD4+ T cells. The genes up-regulated in CD4+ T cells from ADA responders were enriched in the TNF signaling pathway, while very few pathways were differential in monocytes. Differentially methylated positions (DMPs) were strongly hypermethylated in responders to ETN but not to ADA. The machine learning models for the prediction of response to ADA and ETN using differential genes reached an overall accuracy of 85.9% and 79%, respectively. The models using DMPs reached an overall accuracy of 84.7% and 88% for ADA and ETN, respectively. A follow-up study validated the high performance of these models.

Conclusion. Our findings indicate that machine learning models based on molecular signatures accurately predict response before ADA and ETN treatment, paving the path toward personalized anti-TNF treatment.

INTRODUCTION

Rheumatoid arthritis (RA) is a chronic autoimmune disease leading to joint inflammation and destruction (1,2). To date, conventional synthetic disease-modifying antirheumatic drugs (csDMARDs), such as methotrexate, are typically given as a first-line treatment to patients with RA in an attempt to achieve a state of low disease activity. Upon failure or loss of efficacy of csDMARDs, patients are switched to biologic DMARDs (bDMARDs), such as tumor necrosis factor inhibitors (TNFi) (3). Currently, there are different biologic TNFi, including adalimumab (ADA) and etanercept

(ETN), available for clinical use (4). ADA is the first fully human therapeutic anti-TNF monoclonal antibody, while ETN is a recombinant human TNF receptor (p75)–Fc fusion protein that competitively inhibits TNF (5). Although these TNFi have revolutionized the treatment of RA, ~30% of patients do not respond well to their initial anti-TNF therapy (4). Treatment failure elevates the risk of adverse events such as infections and puts additional socioeconomic burden on the patients (3,6). Thus, there is a strong unmet need to predict response to TNFi.

To predict treatment response, it is crucial to identify reliable predictors. Katchamart et al (1) and Callaghan et al (4) reviewed 18

Supported by AbbVie. Mr. Tao's work was supported by a China Scholarship Council Fellowship (201606300050). Dr. Pandit's work was supported by the Netherlands Organization for Scientific Research (grant 016.Veni.178.027).

Weiyang Tao, MSc, Arno N. Concepcion, BA, Marieke Vianen, BA, Anne C. A. Marijnissen, PhD, Floris P. G. J. Lafeber, PhD, Timothy R. D. J. Radstake, MD, PhD, Aridaman Pandit, PhD: University Medical Center Utrecht and Utrecht University, Utrecht, The Netherlands.

Drs. Radstake and Pandit contributed equally to this work.

No potential conflicts of interest relevant to this article were reported.

Address correspondence to Timothy R. D. J. Radstake, MD, PhD or to Aridaman Pandit, PhD, Heidelberglaan 100, 3584 CX Utrecht, The Netherlands. Email: T.R.D.J.Radstake@umcutrecht.nl or A.Pandit@umcutrecht.nl.

Submitted for publication March 11, 2020; accepted in revised form September 1, 2020.

and 154 studies, respectively, and identified several potential predictors of RA remission and response to biologic therapy, including age, sex, disease duration, disease activity, smoking status, and concomitant methotrexate therapy, among others (1,4). Vastesaeger et al (7) developed a matrix tool based on 6 predictors (sex, Health Assessment Questionnaire, presence of comorbidities, age, tender joint count, and erythrocyte sedimentation rate) to predict remission and low disease activity in RA patients treated with golimumab (anti-TNF) therapy. More recently, Ganhão et al (8) examined this matrix tool in real-world RA patients receiving anti-TNF therapy and corroborated the idea of this tool for the prediction of remission. Those studies, however, 1) did not illustrate the biologic mechanisms that underlie this differential response to the TNFi, and 2) did not examine potential treatment responses to different TNFi.

At the cellular and tissue level, RA is characterized by the chronic infiltration of immune cells in the synovial membrane (9). To understand biologic processes associated with anti-TNF response, several transcriptomic and epigenetic studies have been conducted using the synovium and blood from patients with RA (10–19). Those studies have demonstrated that transcriptomic and epigenetic profiling have the potential to predict response to anti-TNF therapies before treatment. Despite the promising predictive potential, we still lack molecular insights into the predictive power of different cell types involved in the anti-TNF response.

Most studies focus on predicting response to one TNFi, and cannot predict if the patients who fail to respond to one TNFi will respond to another known TNFi (20). The gene signature used for predicting response has been shown to be unique for different TNFi (17). Thus, it is crucial to investigate the role of different cell types, especially immune cells, in RA patients receiving different anti-TNF therapies to reveal the biologic process of specific anti-TNF response.

Building upon the previous studies, we performed transcriptomic and epigenetic profiling of immune cell types and whole PBMCs, along with deep clinical profiling of RA patients, to generate cell-specific profiles that can predict response to 2 TNFi—ADA and ETN—prior to treatment initiation.

PATIENTS AND METHODS

Patients in this study were selected from the BiOCURA cohort at the University Medical Center Utrecht (18). BiOCURA is an observational cohort in which patients with RA who are eligible for treatment both with TNFi agents (ADA, ETN, infliximab, golimumab, and certolizumab pegol) and with non-TNFi agents (tocilizumab, abatacept, and rituximab) were enrolled and followed up for 12 months after the initiation of treatment. All csDMARDs (methotrexate, hydroxychloroquine, leflunomide, and glucocorticoids) were allowed concomitantly with the bDMARD. Patients’

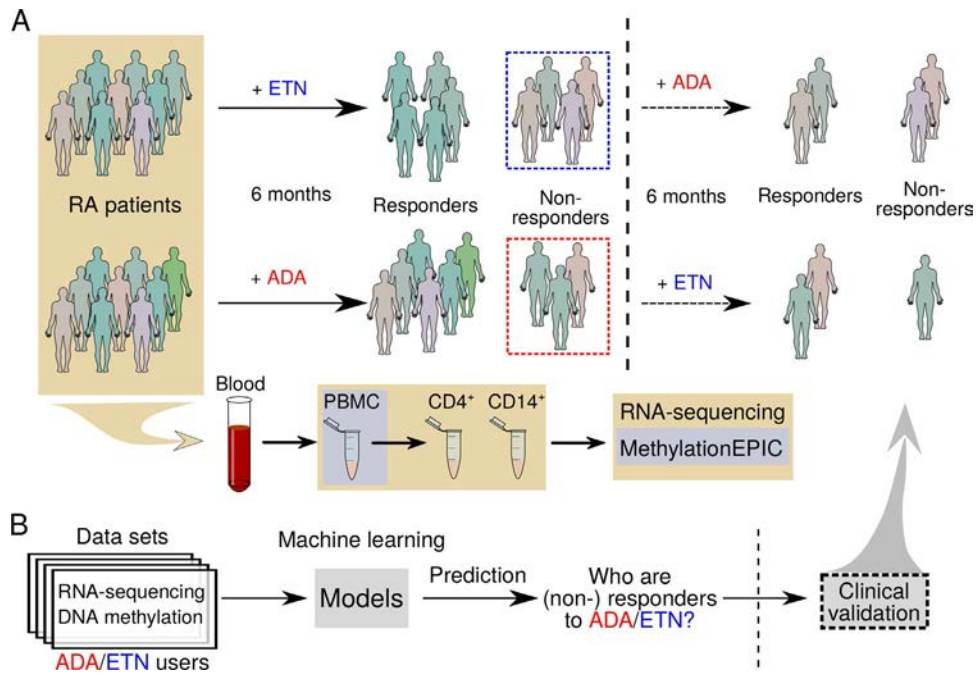


Figure 1. Flow chart showing the study methods. **A**, Blood samples were obtained from patients with rheumatoid arthritis (RA) at baseline, and patients were treated with subcutaneous adalimumab (ADA) or etanercept (ETN) for 6 months. Peripheral blood mononuclear cells (PBMCs) were isolated for RNA sequencing and DNA methylation profiling. CD4+ T cells and CD14+ monocytes were then isolated for RNA sequencing. Patients were classified as responders or nonresponders according to European League Against Rheumatism criteria at the end of month 6. Patients who did not respond to ADA were switched to ETN, and patients who did not respond to ETN were switched to ADA, for 6 months and treatment responses were observed. **B**, RNA sequencing data sets and DNA methylation data sets were used to build machine learning models to predict treatment responses at baseline.

responses were evaluated based on the Disease Activity Score in 28 joints (DAS28) at baseline and after 6 months of treatment according to European League Against Rheumatism (EULAR) criteria (21). (For the patients with a follow-up duration of <6 months, response evaluation was based on DAS28 at baseline and at the last visit, which showed that all of these patients were nonresponders to either ADA or ETN).

Stratified random sampling was carried out to retain 80 of 212 patients with RA who were treated with either ADA or ETN alone and were followed up for ≥ 6 months (for responders) in this study for further analysis. We first isolated peripheral blood mononuclear cells (PBMCs) from these patients prior to ADA or ETN treatment (Figure 1A). Then genome-wide gene expression and DNA methylation profiling were performed on these PBMCs, using RNA sequencing and an Infinium MethylationEPIC Bead-Chip kit, respectively. (RNA sequencing data and DNA methylation data can be accessed at GEO accession no. GSE138747). RNA sequencing on CD14+ monocytes and CD4+ T cells isolated from the PBMCs were performed to gain more insights into different responses to anti-TNF. Using the gene expression and DNA methylation signatures, we then built and internally validated machine learning models to predict response to ADA and ETN (Figure 1B). Finally, 9 patients were used to externally validate the prediction that was made by the machine learning models. A detailed description of the methods conducted in this study can be

found in the Supplementary Methods, available on the *Arthritis & Rheumatology* website at <http://onlinelibrary.wiley.com/doi/10.1002/art.41516/abstract>.

RESULTS

Demographic and disease characteristics of the patients. The characteristics of the patients are summarized in Table 1 and Supplementary Table 1, available on the *Arthritis & Rheumatology* website at <http://onlinelibrary.wiley.com/doi/10.1002/art.41516/abstract>. Eighty patients with RA were selected from the BiOCURA study (18), of which 38 (47.5%) and 42 (52.5%) were treated with ADA (ADA cohort) and ETN (ETN cohort), respectively. In each cohort ~70% of the patients were women. At baseline, the mean ages of the patients in the ADA cohort and the ETN cohort were 53.34 years and 54.27 years, respectively. After 6 months of treatment, 11, 9, and 18 patients showed good, moderate, and no response, respectively, to ADA, while 11, 8, and 23 patients showed good, moderate, and no response, respectively, to ETN. No significant difference was observed between the cohorts in terms of either age, sex, smoking status, weight, height, alcohol use, rheumatoid factor positivity, anti-cyclic citrullinated peptide (anti-CCP) positivity, bDMARD exposure, hemoglobin, leukocyte, and thrombocyte counts at baseline, or drug response rate after 6 months of treatment (Supplementary Table 1).

Table 1. Demographic and baseline clinical characteristics of the RA patients in the ADA and ETN cohorts*

	ADA		ETN	
	Nonresponder (n = 18)	Responder (n = 20)	Nonresponder (n = 23)	Responder (n = 19)
Sex, no.				
Female	13	14	16	13
Male	5	6	7	6
Smoking, no.				
Never	4	5	10	5
Stopped	8	10	8	12
Yes	6	5	5	2
RF, no.				
Negative	9	5	6	5
Positive	9	15	17	14
Anti-CCP, no.				
Negative	6	5	5	4
Positive	12	15	18	15
bDMARD naive, no.				
No	10	6	13	5
Yes	8	14	10	14
Age, years	53.4 ± 11.6	53.3 ± 13.2	56.95 ± 9.51	51.03 ± 11.31
Weight, kg	79.23 ± 15.51	81.91 ± 16.87	81.55 ± 15.56	81.27 ± 18.73
Height, cm	173.56 ± 9.06	175.8 ± 11.27	173.57 ± 12.42	173.11 ± 6.91
Alcohol use, units/week	3.39 ± 4.64	3.5 ± 4.29	5.13 ± 7.12	4.22 ± 5.04
Hemoglobin count, gm/dl	8.45 ± 0.77	8.44 ± 0.74	8.60 ± 0.74	8.39 ± 0.60
Leukocyte count x 10 ⁹ /liter	9.59 ± 4.61	7.42 ± 2.15	8.02 ± 1.94	7.53 ± 2.01
Thrombocyte count x 10 ⁹ /liter	296.88 ± 51.38	261.15 ± 62.53	278.22 ± 57.11	289.06 ± 70.2

* There were no significant differences, determined by Fisher's exact test for categorical variables and by Welch's 2-sample *t*-test for continuous variables, between responders and nonresponders in either the adalimumab (ADA) or etanercept (ETN) cohort. Except where indicated otherwise, values are the mean ± SD. RF = rheumatoid factor; anti-CCP = anti-cyclic citrullinated peptide; bDMARD = biologic disease-modifying antirheumatic drug.

To increase statistical power, we combined patients with good response and those with moderate response, and designated them as responders. Thus, 53% of patients receiving ADA (20 of 38) and 45% of patients receiving ETN (19 of 42) were considered to be responders. No significant difference was observed between responders and nonresponders at baseline for clinical parameters in either cohort (Table 1).

Distinct gene signatures of responders to ADA and ETN. We first studied the molecular signatures of circulating PBMCs and identified 549 differentially expressed genes (DEGs) (nominal $P < 0.05$) between ADA responders and nonresponders (Figure 2A and Supplementary Figure 1, available on the *Arthritis & Rheumatology* website at <http://onlinelibrary.wiley.com/doi/10.1002/art.41516/abstract>). Similarly, we identified 460 DEGs

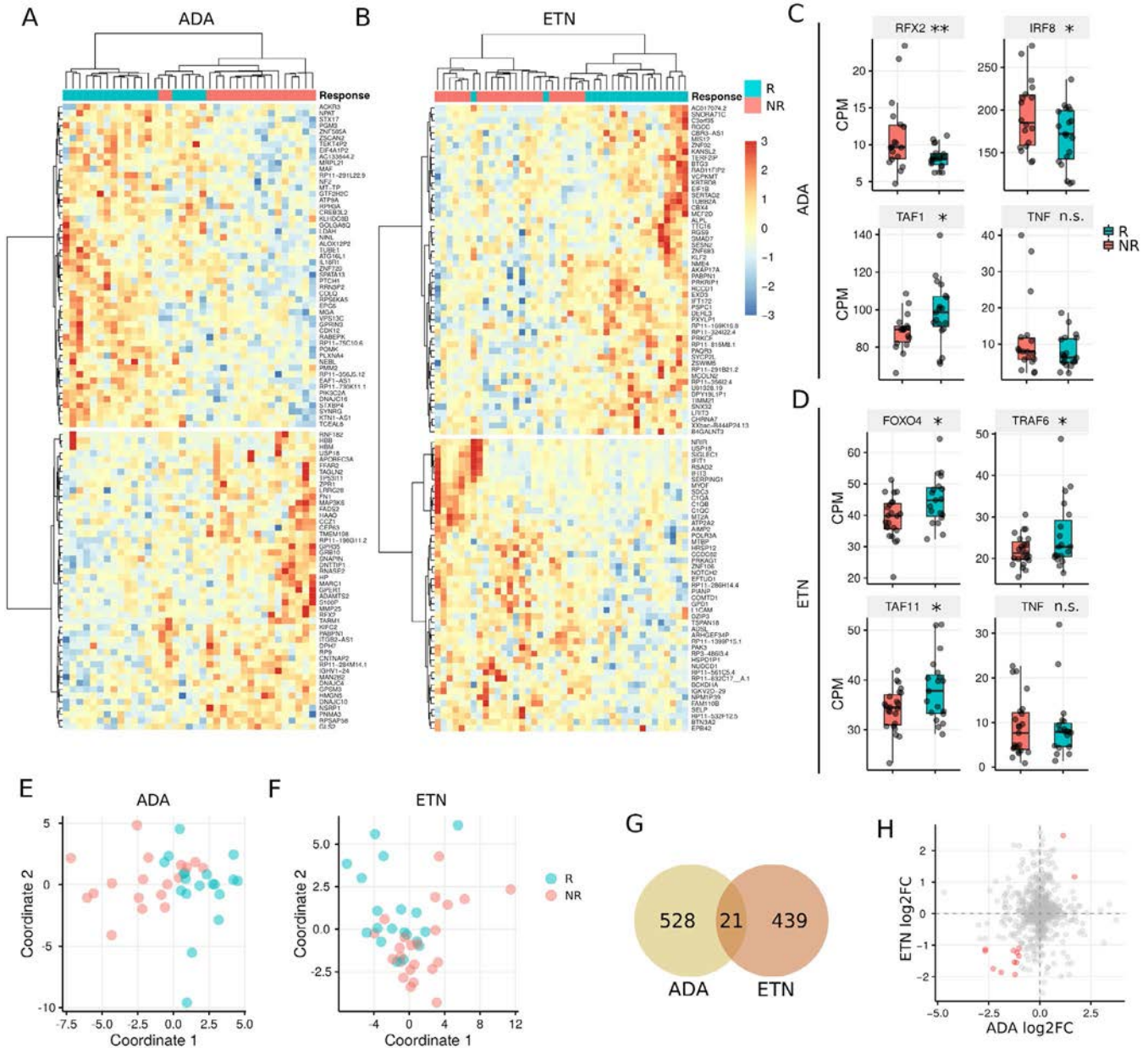


Figure 2. Differences between gene expression in PBMCs from responders (R) versus nonresponders (NR) to ADA or ETN. **A** and **B**, Heatmaps showing the top 100 differentially expressed genes (DEGs) in PBMCs from responders versus nonresponders to ADA (**A**) and ETN (**B**). **C** and **D**, Expression of example DEGs in responders and nonresponders to ADA (**C**) and ETN (**D**). Data are shown as box plots in the style of Tukey. Each box represents the 25th to 75th percentiles. Lines inside the boxes represent the median. Whiskers outside the boxes represent the lowest and highest data points excluding the outliers. The outliers are determined by 1.5-interquartile range criteria. Circles represent individual patients. **E** and **F**, Multidimensional scaling plots based on gene expression data showing clusters of patient response to ADA (**E**) and ETN (**F**). **G**, Venn diagram showing the overlap in DEGs between patients receiving ADA and patients receiving ETN. **H**, Scatterplot showing differences in fold change (FC) in RNA expression for DEGs in the ADA cohort and the ETN cohort. * = $P < 0.05$; ** = $P < 0.01$. CPM = count per million; NS = not significant (see Figure 1 for other definitions). Color figure can be viewed in the online issue, which is available at <http://onlinelibrary.wiley.com/doi/10.1002/art.41516/abstract>.

between ETN responders and nonresponders (Figure 2B and Supplementary Figure 1). For the ADA cohort, genes involved in DNA and nucleotide binding, such as RFX2, IRF8, and TAF1, were differentially expressed between responders and nonresponders. Similarly, in the ETN cohort, genes involved in DNA and nucleotide binding such as FOXO4 and TAF11, and TNF receptor signaling, such as TRAF6, were differentially expressed between responders and nonresponders (Figures 2C and D). Interestingly, the expression of TNF was not associated with the response to either ADA or ETN (both $P > 0.05$) (Figures 2C and D).

Multidimensional scaling analysis performed using DEGs showed that we can differentiate between responders and nonresponders in each cohort (Figures 2A, B, E, and F). Since both ADA and ETN are TNFi, we checked the overlap in DEGs identified from the 2 cohorts. Notably, only 2% of DEGs (21 of 988)

overlapped between the 2 cohorts, and even fewer genes were differentially expressed in the same direction (Figures 2G and H). Taken together, these results suggest that responses to ADA and ETN are defined by distinct gene signatures.

Distinct DNA methylation profiles in responders to ETN and responders to ADA.

Genome-wide DNA methylation analysis of PBMCs from the same patients identified 16,141 and 17,026 differentially methylated positions (DMPs) of CpG sites (nominal $P < 0.05$) associated with response to ADA and ETN, respectively (Figures 3A and B and Supplementary Figure 2, available on the *Arthritis & Rheumatology* website at <http://online.library.wiley.com/doi/10.1002/art.41516/abstract>). These DMPs are distributed on or near 7,719 and 7,850 genes, with an average of 2.09 and 2.17 DMPs per gene for the ADA and ETN cohorts,

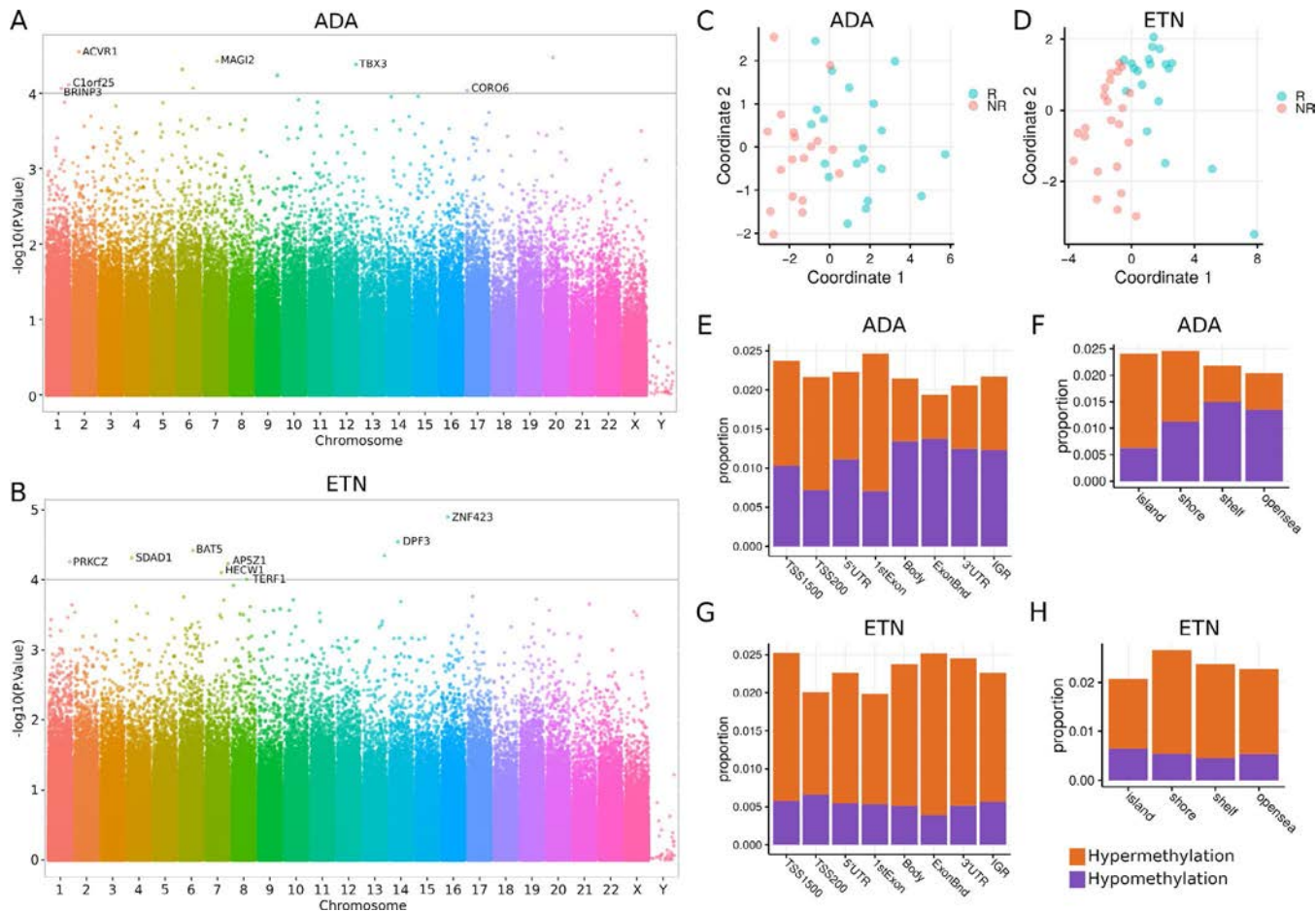


Figure 3. Differentially methylated positions (DMPs) associated with response to ADA and ETN in PBMCs. **A** and **B**, Manhattan plots showing the $-\log_{10}$ -transformed P values for CpG sites in the DNA methylation profiling for response to ADA (**A**) and ETN (**B**). Gene names are shown for genes in which any CpG site reached a significance level of $P < 10^{-4}$. The corresponding probes are shown in Supplementary Figure 2, available on the *Arthritis & Rheumatology* website at <http://onlinelibrary.wiley.com/doi/10.1002/art.41516/abstract>. **C** and **D**, Multidimensional scaling plots, based on DNA methylation data, showing clusters of patients classified as responders or nonresponders to ADA (**C**) and ETN (**D**). **E** and **G**, Distribution of gene region features where DMPs associated with response to ADA (**E**) and to ETN (**G**) were located. TSS1500 = 200–1,500 bases upstream of the transcription start site (TSS); TSS200 = 0–200 bases upstream of the TSS; 5'UTR = 5'-untranslated region; ExonBnd = exon boundary; IGR = intergenic region. **F** and **H**, Distribution of area related to CpG island where DMPs associated with response to ADA (**F**) and ETN (**H**) were located. island = CpG island; shore = 0–2 kb from island; shelf = 2–4 kb from island; opensea = the rest of the area. See Figure 1 for other definitions. Color figure can be viewed in the online issue, which is available at <http://onlinelibrary.wiley.com/doi/10.1002/art.41516/abstract>.

respectively. Multidimensional scaling plots showed clear differences between responders and nonresponders for both ETN and ADA using these DMPs (Figures 3C and D). Approximately 46%

($n = 7,424$) of the DMPs were hypermethylated in ADA responders, while a drastically higher fraction of DMPs (76.3%; $n = 12,994$) were hypermethylated in ETN responders. We found more

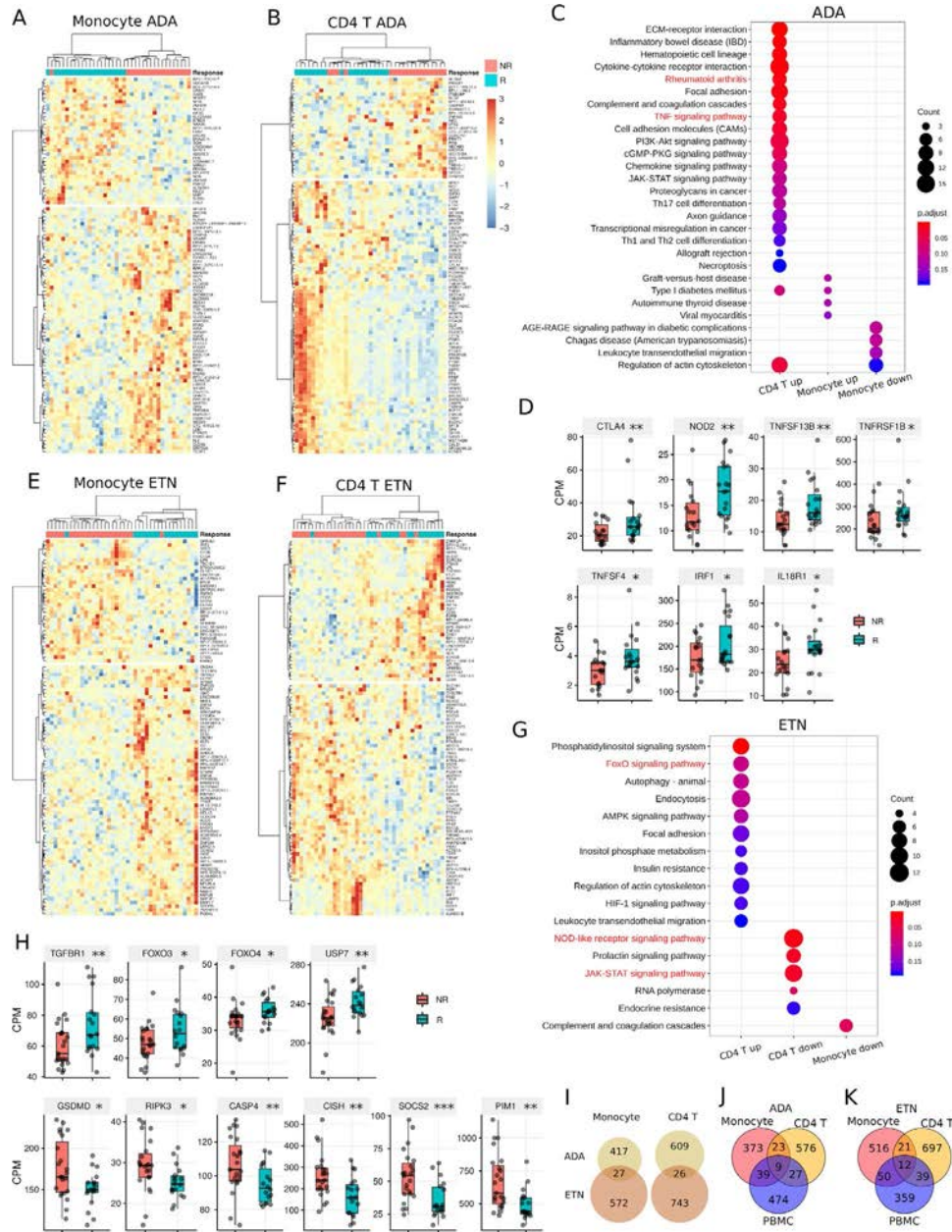


Figure 4. Differences between gene expression in monocytes and CD4+ T cells from responders (R) versus nonresponders (NR) to ADA and ETN. **A** and **B**, Heatmaps showing the top 100 differentially expressed genes (DEGs) in monocytes (**A**) and CD4+ T cells (**B**) from responders versus nonresponders to ADA. **C**, KEGG pathways enriched by the DEGs associated with ADA response in monocytes and CD4+ T cells. **D**, Expression of ADA response-associated DEGs involved in RA and the tumor necrosis factor (TNF) signaling pathway in CD4+ T cells. **E** and **F**, Heatmaps showing the top 100 DEGs associated with ETN response in monocytes (**E**) and CD4+ T cells (**F**). **G**, KEGG pathways enriched by the DEGs associated with ETN response in monocytes and CD4+ T cells. **H**, Expression of ETN response-associated DEGs involved in FoxO signaling, NOD-like receptor signaling, and JAK/STAT signaling pathways in CD4+ T cells. **I**, Venn diagrams showing the overlap between ADA response-associated DEGs and ETN response-associated DEGs in monocytes and CD4+ T cells. **J** and **K**, Venn diagrams showing the overlap between ADA response-associated DEGs (**J**) and ETN response-associated DEGs (**K**) in monocytes, CD4+ T cells, and PBMCs. In **D** and **H**, data are shown as box plots in the style of Tukey. Each box represents the 25th to 75th percentiles. Lines inside the boxes represent the median. Whiskers outside the boxes represent the lowest and highest data points excluding the outliers. The outliers are determined by 1.5-interquartile range criteria. Circles represent individual patients. * = $P < 0.05$; ** = $P < 0.01$; *** = $P < 0.001$. CPM = count per million (see Figure 1 for other definitions). Color figure can be viewed in the online issue, which is available at <http://onlinelibrary.wiley.com/doi/10.1002/art.41516/abstract>.

hypermethylated DMPs in the upstream and promoter regions of genes (Figure 3E) and on CpG islands (Figure 3F) in ADA responders. In contrast, globally more hypermethylated DMPs were found in ETN responders (Figures 3G and H). Thus, on the epigenetic level, we observed a distinct hypermethylation pattern between ADA and ETN responders, suggesting the role of epigenetics in defining response to ADA and to ETN in PBMCs.

TNF signaling signatures in CD4+ T cells from responders to ADA. Since we found different gene signatures defining response to ADA or ETN, we hypothesized that different cell types may contribute to the response to ADA or ETN. Therefore, we performed RNA sequencing on 2 major innate and adaptive immune cell types, monocytes and CD4+ T cells, that are known to be involved in RA pathogenesis. Monocytes and CD4+ T cells were isolated from PBMCs from the same patients. Differential gene expression analyses identified 444 and 635 DEGs (nominal $P < 0.05$) between responders and nonresponders to ADA in monocytes and CD4+ T cells, respectively (Figures 4A and B and Supplementary Figures 3A and B, available on the *Arthritis & Rheumatology* website at <http://onlinelibrary.wiley.com/doi/10.1002/art.41516/abstract>). Notably, the expression of genes associated with RA and the TNF signaling pathway, such as CTLA4, TNFSF13B, TNFRSF1B, TNFSF4, IRF1, and IL18R1, was higher in CD4+ T cells from ADA responders than those from ADA nonresponders (Figures 4C and D). These genes were not differentially expressed between monocytes from responders and those from nonresponders to ADA (data not shown), suggesting that CD4+ T cells showed clearer molecular “TNF signaling” signatures associated with response to ADA compared to monocytes.

Similarly, 599 and 769 DEGs were associated with response to ETN in monocytes and CD4+ T cells, respectively (Figures 4E and F and Supplementary Figures 3C and D). In CD4+ T cells from responders to ETN, genes in the FoxO signaling pathway, such as FOXO3, FOXO4, TGFBR1, and USP7, were up-regulated, while genes in the NOD-like receptor signaling pathway, such as GSDMD, RIPK3, and CASP4, and the JAK/STAT signaling pathway, such as CISH, SOCS2, and PIM1, were down-regulated (Figures 4G and H). Notably, very few pathways were differential in the monocytes from both the ADA and ETN cohorts (Figures 4C and G).

Consistent with the finding in PBMCs, the expression of TNF in both CD4+ T cells and monocytes was not associated with the response to either ADA or ETN (data not shown), and the DEGs associated with response to ADA and ETN showed little overlap in both monocytes and CD4+ T cells (Figure 4I). Comparing the DEGs identified from different cells, we found that each exhibited unique gene signatures (Figures 4J and K), suggesting a necessity to study different cell populations to identify which cells were involved in differentiating the response to anti-TNF therapy (Figures 4J and K).

Accurate prediction of clinical response by machine learning models.

In addition to understanding the mechanisms of how RA patients respond differently to ETN or ADA therapy, the ultimate goal of this study was to predict which therapy is effective for which patients before commencing therapy. To this aim, we built machine learning models based on random forest algorithms, exploiting the transcriptome signatures from monocytes, CD4+ T cells, and PBMCs, and methylation signatures from PBMCs (see Supplementary Methods, available on the *Arthritis & Rheumatology* website at <http://onlinelibrary.wiley.com/doi/10.1002/art.41516/abstract>). The model based on DEGs of PBMCs (“PBMC RNA” ADA model) showed the highest overall accuracy of predicting response to ADA among other models (ADA models). More specifically, these ADA models reached overall accuracy of 80.3%, 72.7%, 85.9%, and 84.7% using DEGs on monocytes, CD4+ T cells, PBMCs, and DMPs of PBMCs, respectively. The true-positive rates of these models ranged from 76.0% to 90.0%, and the true-negative rates ranged from 70.0% to 89.0% (Figure 5A).

The overall accuracy of the models for ETN therapy (ETN models) ranged from 73.3% to 79.0% using DEGs of different cell subsets and reached as high as 88% using DMPs of PBMCs (Figure 5B). For the ETN models using DEGs, the model based on gene expression of CD4+ T cells (“CD4 RNA” ETN model) showed the highest overall accuracy (79.0%) and nearly equal true-positive (78.1%) and true-negative (82.0%) rates. These results suggest that we can accurately predict the clinical response before ADA and ETN treatment using molecular signatures-based machine learning models, although the prediction accuracy of these molecular signatures differs between cell types and treatments, underlining the need to study more than one drug, cell type, or epigenetic layer.

Further, we predicted the response to ADA and ETN for all patients included in this study using the best models using gene expression data (“PBMC RNA” ADA model and “CD4 RNA” ETN model) and DNA methylation data (“PBMC DNA” ADA and ETN models) (Figures 5C and D). Interestingly, both the RNA models and the DNA models predict that ~30% of patients will not respond to either ADA or ETN, which is consistent with the clinical observation that 30% of patients do not respond well to their first anti-TNF therapy (4). In addition, ~50% of patients respond well to either ADA or ETN. To test whether these predictions were reliable, we followed up the patients who failed to respond to the first round of ADA or ETN treatment and were switched to the other treatment (either ETN or ADA) for 6 months (Figure 1A). Finally, data for 9 patients (including 4 patients receiving ADA therapy and 5 patients receiving ETN therapy) were used to validate the reliability of the prediction. We found remarkably high prediction accuracy of our models, with response to switched treatment correctly predicted in 88.9% ($n = 8$) and 77.8% ($n = 7$) of the patients by the RNA models and DNA models, respectively (Figure 5E).

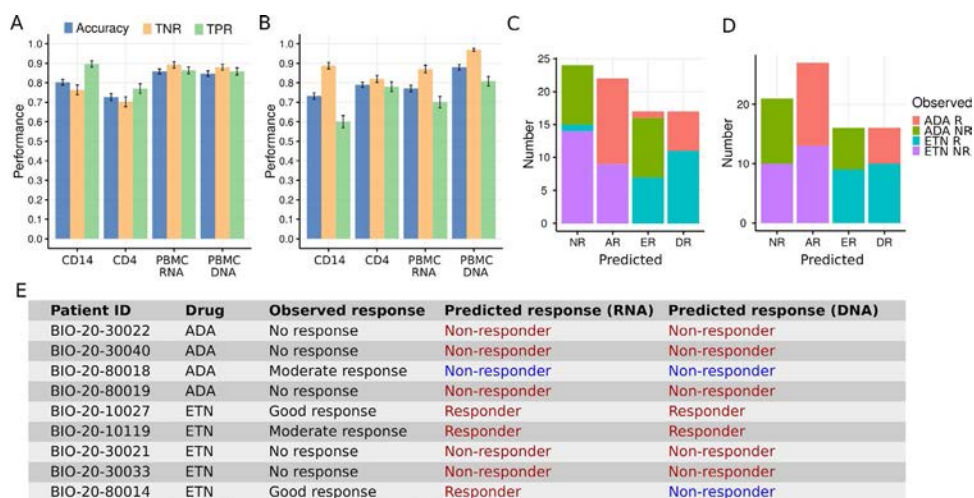


Figure 5. Machine learning models of the prediction of RA patients' response to ADA and ETN therapy. **A** and **B**, Accuracy, true-negative rate (TNR), and true-positive rate (TPR) of machine learning models based on gene expression signatures (CD14, CD4, and PBMC RNA) and DNA methylation signatures (PBMC DNA) for the prediction of 6-month response to ADA (**A**) and ETN (**B**). Bars show the mean ± SEM from cross-validation analysis. **C** and **D**, Machine learning prediction of 6-month response to ADA and ETN treatment using the best model based on gene expression data (**C**) and DNA methylation data (**D**). R = responder; NR = nonresponder; AR = responder to ADA only; ER = responder to ETN only; DR = double responder (response to both ADA and ETN). **E**, Validation of machine learning prediction by 6-month-follow-up drug-switched study (see Figure 1). The last 2 columns are predictions made by the best machine learning models based on gene expression data and DNA methylation data, respectively. Correct predictions are shown in red. See Figure 1 for other definitions. Color figure can be viewed in the online issue, which is available at <http://onlinelibrary.wiley.com/doi/10.1002/art.41516/abstract>.

DISCUSSION

To date, methotrexate is still generally accepted as the mainstay of treatment for RA. When methotrexate fails, however, treatment schemes are basically followed on a trial-and-error basis. Hence, it may take a considerable amount of time before RA patients receive the therapeutic regimen that fits them best. Similarly, the different TNFi agents do not have the same beneficial clinical effect in all patients. This observed effect underlies the reason that a second or even a third TNFi can induce clinically meaningful effects upon failure of the first. As a result, being able to predict which TNFi would be effective and should be the first choice of treatment would be highly beneficial in reducing the time to effective treatment, which has been extensively proven to be a paramount factor in achieving long-standing disease remission. Hence, by using a deep molecular approach followed by machine-learning algorithms, we aimed to predict the response to TNFi, and to provide support for decision-making regarding choice of TNFi, by comparing ADA and ETN.

In general, the overlap of DEGs identified in previous studies of TNFi is relatively low (17). This discrepancy might be due to multiple factors, including small sample sizes, different response classification criteria, different durations of treatment, low detection power of microarrays, and existence of biologically divergent signatures between different anti-TNF therapies or between different cell populations. For example, the expression of CD11c (ITGAX) in monocytes was previously associated with response to ADA in RA patients (22), but was recently shown to have no association

with response to ADA or ETN when tested in whole blood samples in a large patient cohort (23). Therefore, in our study we deliberately included patients with the same clinical characteristics in both cohorts and performed transcriptomic and epigenetic profiling of multiple cell populations using recently developed techniques, i.e., RNA sequencing and a MethylationEPIC BeadChip kit.

We found divergent gene signatures associated with response to ADA and ETN, and this divergence of gene signatures was reproduced in multiple cell populations, suggesting a potentially different action of mechanism between these 2 anti-TNF agents. As a result, we found that the majority of the patients did not respond to both ADA and ETN but had the potential to respond to one of the drugs. Since ADA is an anti-TNF monoclonal antibody, while ETN is a TNF receptor–Fc fusion protein, the genetic and epigenetic differences between individual patients thus determine the drug response. Given such different molecular signatures, ADA and ETN should be studied and considered differently in the future although both are TNFi.

DNA methylation has been shown to play an important role in the progression of RA (24–26). To our knowledge, only one previous study investigated DNA methylation on whole blood for response to ETN using a HumanMethylation450 BeadChip kit, which examines ~450,000 CpG sites in the human genome (19). In that study, Plant et al identified 5 DMPs (cg04857395, cg26401028, cg16426293, cg03277049, and cg12226028) associated with response to ETN in whole blood (19). In the present study, we used the more recently developed MethylationEPIC BeadChip, which examines >850,000 CpG sites, and did not find

any of the sites reported by Plant et al to be differentially expressed in PBMCs from patients in the ADA treatment cohort (P values ranged from 0.1 to 0.8) and ETN cohort (P values ranged from 0.5 to 0.9). There are several potential reasons for this. First, different cells were studied in both studies. In other words, Plant et al interrogated DNA methylation in whole blood cells, while we studied the PBMCs. Second, the criteria used to determine whether a patient had a good response or no response differed between the studies. Plant et al defined a good response as a DAS28 of <2.6 and a nonresponse as an improvement in the DAS28 of <0.6 or as an end point DAS28 of >5.1 after 3 months of ETN treatment (19). In contrast, in our study, the EULAR criteria (21) were applied after 6 months of ADA or ETN treatment, as described in Patients and Methods. More importantly, only the patients with an extreme response phenotype, either good response or nonresponse, were included in the study by Plant et al (19). Therefore, it is essential to use a set of reliable and consistent criteria when identifying and comparing the molecular signatures associated with response to anti-TNF therapies in different studies.

To the best of our knowledge, this is the first study in which paired multicellular and multiomics data have been used to investigate molecular determinants of response to TNFi. However, there are some limitations, which we discuss below. The majority of the DEGs and DMPs identified in this study were not significant after correcting for multiple hypothesis testing, likely due to patient heterogeneity. Thus, we combined the gene expression/methylation signatures identified using nominal P values to build machine learning models to improve the prediction of response. We achieved high accuracy using the RNA models and/or DNA model to predict response to ADA and ETN. These models were further validated by a follow-up study, which shows a reliable application prospect to guide clinical decision-making. However, one may argue that the responsiveness of these patients may be affected by the previous TNFi treatment.

It is still unknown how the responsiveness to a TNFi is affected by prior treatment with another TNFi, and our current data cannot completely address this question. In clinical practice, patients who failed to respond to a TNFi would not be recommended to receive the same treatment, at least in the near future, suggesting that the responsiveness to a particular TNFi is relatively stable. However, patients who fail to respond to one TNFi are frequently treated with another TNFi, based on an assumption that the response to a TNFi is not affected by prior treatment regimens. Our results support this assumption, as we found that response to a second TNFi treatment could be predicted to a certain extent based on baseline gene signatures measured prior to failure to respond to the first treatment. However, further studies are needed to assess the stability of response, to explore the reasons why some TNFi work in some patients and not in others, and to ultimately apply such predictions in clinical practice.

To further determine whether the signatures we identified were robust or dependent upon a subset of patient samples, we

performed additional tests as described below. We performed jackknife resampling iterations, where 20% of the samples in each group were removed in each iteration, and then we repeated the entire analysis using the randomly retained 80% of the remaining samples (see Supplementary Methods, available on the *Arthritis & Rheumatology* website at <http://onlinelibrary.wiley.com/doi/10.1002/art.41516/abstract>). We performed 1,000 such iterations and found that most DEGs and DMPs identified in the original analysis were re-identified in $>50\%$ of the jackknife resampling iterations (Supplementary Figure 4, available on the *Arthritis & Rheumatology* website at <http://onlinelibrary.wiley.com/doi/10.1002/art.41516/abstract>). As an additional control, we shuffled the sample identity (i.e., whether the patient was a responder or non-responder) to mix samples between groups. Such mislabeling of the samples between groups should not provide us with genes/methylation sites that are consistently differential between different iterations. Indeed, we found that most of the DEGs and DMPs were not consistently re-identified (most DEGs and DMPs were consistent in $<25\%$ of such iterations) (Supplementary Figure 4).

Using the DEGs and DMPs consistently identified in $>50\%$ of jackknife resampling iterations, we found clear patient clusters, methylation patterns, and response prediction ability similar to those shown in Figures 2–5 (Supplementary Figure 5, available on the *Arthritis & Rheumatology* website at <http://onlinelibrary.wiley.com/doi/10.1002/art.41516/abstract>). Based on models built upon the features identified after jackknife down sampling or random sample shuffling (Supplementary Figure 6, available on the *Arthritis & Rheumatology* website at <http://onlinelibrary.wiley.com/doi/10.1002/art.41516/abstract>), we found that models created after jackknife down sampling were much better than those based on genes obtained by random sample shuffling. The jackknife down sampling models were comparable to the models shown in Figure 5, suggesting that the selected features in our final models are informative. Thus, the molecular signatures identified were robust and were clearly dependent on the response status of the patients.

Examination of overlapping between DEGs and corresponding genes illustrated that in both the ADA treatment cohort and the ETN treatment cohort, >100 genes were differentially expressed, with ≥ 1 CpG site differentially methylated (Supplementary Table 2, available on the *Arthritis & Rheumatology* website at <http://onlinelibrary.wiley.com/doi/10.1002/art.41516/abstract>). Interestingly, compared to DMPs with smaller variability in methylation levels (static DMPs), DMPs with larger variability in methylation levels (dynamic DMPs) were more correlated with the expression of corresponding genes (Supplementary Figure 6, available on the *Arthritis & Rheumatology* website at <http://onlinelibrary.wiley.com/doi/10.1002/art.41516/abstract>). So, the gene expression is weakly regulated by DNA methylation, especially when the CpG sites are less dynamic.

This study also had some limitations. As a subset of BioCURA, the patients included in this study did not all complete 6 months of treatment. More specifically, 4 patients discontinued

treatment prior to month 3, and 18 patients discontinued treatment between month 3 and month 6. All of these patients were determined to be nonresponders based on the EULAR criteria using DAS28 at baseline and DAS28 at the last visit prior to month 6. Some patients may have shown response after a longer period of treatment, but in this study they were classified as nonresponders due to the study design and follow-up criteria. The second limitation is that since this is an observational cohort, the ratios of responders to nonresponders does not represent the actual response ratio observed in patients. We selected for a comparable number of responders and nonresponders to allow enough samples in each group. Future studies should be conducted on larger cohorts of patients representing actual response ratios, but ensuring a sufficient number of patients in each group.

In conclusion, we systemically studied, for the first time, transcription and/or DNA methylome signatures associated with response to different TNFi in PBMCs, monocytes, and CD4+ T cells from patients with RA. We found that transcription signatures in ADA and ETN responders are divergent in PBMCs, and this phenomenon was reproduced in monocytes and CD4+ T cells. Besides, DMPs of responders to ETN but not to ADA were strongly hypermethylated. Finally, machine learning models based on these molecular signatures could accurately predict response before ADA and ETN treatment, paving the path toward personalized treatment strategies with TNFi.

ACKNOWLEDGMENTS

We thank Chiara Angiolilli for valuable suggestions and comments on the manuscript. We thank Katja Coeleveld, Kim van der Wurff-Jacobs, and Dorien van de Berg for bio-banking, Karin A. L. Schrijvers-te-Brake, Annemiek Sloeserwij, and Joke Nijdeken for facilitating the acquisition of data, and the Society for Rheumatology Research Utrecht (SRU) for including patients. We are grateful to all of the patients who participated in this study.

AUTHOR CONTRIBUTIONS

All authors were involved in drafting the article or revising it critically for important intellectual content, and all authors approved the final version to be published. Dr. Pandit had full access to all of the data in the study and takes responsibility for the integrity of the data and the accuracy of the data analysis.

Study conception and design. Tao, Lafeber, Radstake, Pandit.

Acquisition of data. Concepcion, Vianen, Marijnissen, Radstake, Pandit.

Analysis and interpretation of data. Tao, Pandit.

ROLE OF THE STUDY SPONSOR

AbbVie had no role in the study design or in the collection, analysis, or interpretation of the data, the writing of the manuscript, or the decision to submit the manuscript for publication. Publication of this article was not contingent upon approval by AbbVie.

REFERENCES

- Katchamart W, Johnson S, Lin HJ, Phumethum V, Salliot C, Bombardier C. Predictors for remission in rheumatoid arthritis patients: a systematic review. *Arthritis Care Res (Hoboken)* 2010;62:1128–43.
- Van der Helm-van Mil AH, Huizinga TW, de Vries RR, Toes RE. Emerging patterns of risk factor make-up enable subclassification of rheumatoid arthritis. *Arthritis Rheum* 2007;56:1728–35.
- Chen YF, Jobanputra P, Barton P, Jowett S, Bryan S, Clark W, et al. A systematic review of the effectiveness of adalimumab, etanercept and infliximab for the treatment of rheumatoid arthritis in adults and an economic evaluation of their cost-effectiveness. *Health Technol Asses* 2006;10:3310.
- Callaghan CA, Boyter AC, Mullen AB, McRorie ER. Biological therapy for rheumatoid arthritis: is personalised medicine possible? *Eur J Hosp Pharm* 2014;21:229–37.
- Weinblatt ME, Keystone EC, Furst DE, Moreland LW, Weisman MH, Birbara CA, et al. Adalimumab, a fully human anti-tumor necrosis factor α monoclonal antibody, for the treatment of rheumatoid arthritis in patients taking concomitant methotrexate: the ARMADA trial. *Arthritis Rheum* 2003;48:35–45.
- Listing J, Strangfeld A, Kary S, Rau R, von Hinueber U, Stoyanova-Scholz M, et al. Infections in patients with rheumatoid arthritis treated with biologic agents. *Arthritis Rheum* 2005;52:3403–12.
- Vastesaeger N, Kutzbach AG, Amital H, Pavelka K, Lazaro MA, Moots RJ, et al. Prediction of remission and low disease activity in disease-modifying antirheumatic drug-refractory patients with rheumatoid arthritis treated with golimumab. *Rheumatology (Oxford)* 2016;55:1466–76.
- Ganhão S, Bernardes M, Lucas R, Fonseca JE, Rosa-Gonçalves D, Madeira N, et al. Remission and low disease activity matrix tools: results in real-world rheumatoid arthritis patients under anti-TNF α therapy. *Acta Reumatol Port* 2019; Special Issue:107–9.
- Klareskog L, Catrina AI, Paget S. Rheumatoid arthritis. *Lancet* 2009;373:659–72.
- Kraan TC, Wijbrandts CA, van Baarsen LG, Rustenburg F, Baggen JM, Verweij CL, et al. Responsiveness to anti-tumour necrosis factor α therapy is related to pretreatment tissue inflammation levels in rheumatoid arthritis patients. *Ann Rheum Dis* 2008;67:563–6.
- Van der Pouw Kraan TC, van Gaalen F, Huizinga TW, Pieterman E, Breedveld FC, Verweij CL. Discovery of distinctive gene expression profiles in rheumatoid synovium using cDNA microarray technology: evidence for the existence of multiple pathways of tissue destruction and repair. *Genes Immun* 2003;4:187–96.
- Lindberg J, Wijbrandts CA, van Baarsen LG, Nader G, Klareskog L, Catrina A, et al. The gene expression profile in the synovium as a predictor of the clinical response to infliximab treatment in rheumatoid arthritis. *PLoS One* 2010;5:e11310.
- Lindberg J, af Klint E, Catrina AI, Nilsson P, Klareskog L, Ulfgren AK, et al. Effect of infliximab on mRNA expression profiles in synovial tissue of rheumatoid arthritis patients. *Arthritis Res Ther* 2006;8:R179.
- Badot V, Galant C, Toukap AN, Theate I, Maudoux AL, van den Eynde BJ, et al. Gene expression profiling in the synovium identifies a predictive signature of absence of response to adalimumab therapy in rheumatoid arthritis. *Arthritis Res Ther* 2009;11:R57.
- Dennis G, Holweg CT, Kummerfeld SK, Choy DF, Setiadi AF, Hackney JA, et al. Synovial phenotypes in rheumatoid arthritis correlate with response to biologic therapeutics. *Arthritis Res Ther* 2014;16:R90.
- Aterido A, Canete JD, Tornere J, Blanco F, Fernandez-Gutierrez B, Perez C, et al. A combined transcriptomic and genomic analysis identifies a gene signature associated with the response to anti-TNF therapy in rheumatoid arthritis. *Front Immunol* 2019;10:1459.
- Toonen EJ, Gilissen C, Franke B, Kievit W, Eijbsbouts AM, den Broeder AA, et al. Validation study of existing gene expression signatures for anti-TNF treatment in patients with rheumatoid arthritis. *PLoS One* 2012;7:e33199.

18. Cuppen BV, Rossato M, Fritsch-Stork RD, Concepcion AN, Linn-Rasker SP, Bijlsma JW, et al. RNA sequencing to predict response to TNF-inhibitors reveals possible mechanism for nonresponse in smokers. *Expert Rev Clin Immu* 2018;14:623–33.
19. Plant D, Webster A, Nair N, Oliver J, Smith S, Eyre S, et al. Differential methylation as a biomarker of response to etanercept in patients with rheumatoid arthritis. *Arthritis Rheumatol* 2016;68:1353–60.
20. Kekow J, Mueller-Ladner U, Schulze-Koops H. Rituximab is more effective than second anti-TNF therapy in rheumatoid arthritis patients and previous TNF α blocker failure. *Biologics* 2012;6:191–9.
21. Franssen J, van Riel PL. The Disease Activity Score and the EULAR response criteria. *Clin Exp Rheumatol* 2005;23:S93–9.
22. Stuhlmüller B, Haupl T, Hernandez MM, Grutzkau A, Kuban RJ, Tandon N, et al. CD11c as a transcriptional biomarker to predict response to anti-TNF monotherapy with adalimumab in patients with rheumatoid arthritis. *Clin Pharmacol Ther* 2010;87:311–21.
23. Smith SL, Eyre S, Yarwood A, Hyrich K, Morgan AW, Wilson AG, et al. Investigating CD11c expression as a potential genomic biomarker of response to TNF inhibitor biologics in whole blood rheumatoid arthritis samples. *Arthritis Res Ther* 2015;17:359.
24. Araki Y, Mimura T. The mechanisms underlying chronic inflammation in rheumatoid arthritis from the perspective of the epigenetic landscape [review]. *J Immunol Res* 2016;2016:6290682.
25. Ai RZ, Laragione T, Hammaker D, Boyle DL, Wildberg A, Maeshima K, et al. Comprehensive epigenetic landscape of rheumatoid arthritis fibroblast-like synoviocytes. *Nat Commun* 2018;9:1921.
26. Nair N, Wilson AG, Barton A. DNA methylation as a marker of response in rheumatoid arthritis [review]. *Pharmacogenomics* 2017;18:1322–32.

Patients' Preoperative Expectations of Total Knee Arthroplasty and Satisfaction With Outcomes at One Year: A Prospective Cohort Study

Gillian A. Hawker,¹ Barbara L. Conner-Spady,² Eric Bohm,³ Michael J. Dunbar,⁴ C. Allyson Jones,⁵ Bheeshma Ravi,¹ Tom Noseworthy,² Donald Dick,⁵ James Powell,² Paulose Paul,⁵ and Deborah A. Marshall,² on behalf of the BEST-Knee Study Team

Objective. To assess the relationship between patients' expectations for total knee arthroplasty (TKA) and satisfaction with surgical outcome.

Methods. This prospective cohort study recruited patients with knee osteoarthritis (OA) ages ≥ 30 years who were referred for TKA at 2 hip/knee surgery centers in Alberta, Canada. Those who received primary, unilateral TKA completed questionnaires pre-TKA to assess TKA expectations (17-item Hospital for Special Surgery [HSS] TKA Expectations questionnaire) and contextual factors (age, sex, Western Ontario and McMaster Universities Osteoarthritis Index pain score, Knee Injury and Osteoarthritis Outcome Score physical function short form [KOOS-PS], 8-item Patient Health Questionnaire depression scale, body mass index [BMI], comorbidities, and prior joint replacement), and 1-year post-TKA to assess overall satisfaction with TKA results. Using multivariate logistic regression, we examined the relationship between TKA expectations (HSS TKA outcomes considered to be very important) and postoperative satisfaction (very satisfied versus somewhat satisfied versus dissatisfied). Adjusted odds ratios (ORs) and 95% confidence intervals (95% CIs) were calculated.

Results. At 1 year, 1,266 patients with TKA (92.1%) reported their TKA satisfaction (mean \pm SD age 67.2 ± 8.8 years, 60.9% women, and mean BMI 32.6 kg/m^2); 74.7% of patients were very satisfied, 17.1% were somewhat satisfied, and 8.2% were dissatisfied. Controlling for other factors, an expectation of TKA to improve patients' ability to kneel was associated with lower odds of satisfaction (adjusted OR 0.725 [95% CI 0.54–0.98]). An expectation of TKA to improve psychological well-being was associated with lower odds of satisfaction for individuals in the lowest tertile of pre-TKA KOOS-PS scores (adjusted OR 0.49 [95% CI 0.28–0.84]), but higher odds for those in the highest tertile (adjusted OR 2.37 [95% CI 1.33–4.21]).

Conclusion. In patients with TKA, preoperative expectations regarding kneeling and psychological well-being were significantly associated with the level of TKA satisfaction at 1 year. Ensuring that patients' expectations are achievable may enhance appropriate provision of TKA.

INTRODUCTION

Total knee arthroplasty (TKA) is the most commonly performed orthopedic surgery (1,2). In 2014, 680,150 primary TKA surgeries were performed in the US to treat knee osteoarthritis

(OA), and the numbers are growing (3). Although regarded as a highly effective surgical option for advanced knee OA, ~20% of patients report dissatisfaction with their surgical results (4). Greater understanding of the preoperative determinants of postoperative satisfaction has potential to assist in appropriate selection of

Supported by an operating grant from the Canadian Institutes of Health Research (grant MOP-312807).

¹Gillian A. Hawker, MD, MSc, Bheeshma Ravi, MD, PhD: University of Toronto, Toronto, Ontario, Canada; ²Barbara L. Conner-Spady, PhD, Tom Noseworthy, MD, MSc, MPH, James Powell, MD, Deborah A. Marshall, PhD: University of Calgary Cumming School of Medicine, Calgary, Alberta, Canada; ³Eric Bohm, MD, MSc: Concordia Hip and Knee Institute and University of Manitoba, Winnipeg, Manitoba, Canada; ⁴Michael J. Dunbar, MD, MPH: Dalhousie University and Queen Elizabeth II Health Sciences Centre, Nova Scotia Health Authority, Halifax, Nova Scotia, Canada; ⁵C. Allyson Jones, PhD, Donald Dick, MD, Paulose Paul, MD: University of Alberta, Edmonton, Alberta, Canada.

Dr. Hawker has received research support as the Sir John and Lady Eaton Professor and Chair of Medicine for the University of Toronto. Dr. Marshall has received research support through a Canada Research Chair in Health Systems and Services Research (2008–2018) and is currently supported as the Arthur J. E. Child Chair in Rheumatology. No other disclosures relevant to this article were reported.

Address correspondence to Gillian A. Hawker, MD, MSc, University of Toronto, Department of Medicine, 6 Queen's Park Crescent West, 3rd Floor, Toronto, Ontario M5S 3H2, Canada. Email: g.hawker@utoronto.ca.

Submitted for publication April 21, 2020; accepted in revised form August 25, 2020.

surgical candidates, and thus improves patient outcomes and the use of valuable health resources (5).

Cross-sectional studies have found that patients with unmet expectations following TKA are more likely to be dissatisfied with their surgical results, even after controlling for improvements in pain and function (6–9). However, a relationship between patients' preoperative expectations of TKA and postoperative satisfaction has not been confirmed (9–12). In a prior systematic review (13), of 5 studies identified (14–18), none of the studies found a significant relationship between preoperative expectations and postoperative satisfaction. A subsequent study (19), which assessed preoperative expectations with the validated Hospital for Special Surgery (HSS) TKA Expectations Scale (20), identified no relationship between pre-TKA HSS summary scores and postoperative satisfaction, but relationships with specific expectations on the HSS scale were not examined. Thus, it remains unclear whether patients' preoperative expectations for TKA—and specifically whether they are realistic, and thus achievable—are modifiable determinants of postoperative satisfaction.

With a view to improving the appropriateness of TKA for knee OA, the present study examined the contribution of preoperative, patient-reported TKA expectations (items on the HSS Knee Expectations scale) to TKA satisfaction 1 year following primary unilateral TKA for knee OA. We hypothesized that patients with knee OA with preoperative expectations of TKA that were unrealistic, and thus unachievable, would be less likely to be satisfied with their TKA results.

PATIENTS AND METHODS

Study setting and design. This prospective cohort study recruited patients with knee OA who were referred to a surgeon regarding elective TKA at 2 orthopedic hip and knee centralized intake clinics in Alberta, Canada between October 2014 and September 2016. Patients age ≥ 30 years who were able to read and comprehend English and were determined by a surgeon to have primary knee OA on physical examination and imaging were eligible. Individuals with inflammatory arthritis were excluded. To examine the effects of age and sex on knee OA, recruitment continued until there were at least 200 men and women in each of 3 age groups (30–59 years, 60–69 years, and 70 years). All 45 surgeons at the clinics agreed to participate, and all surgeons and patients provided written informed consent.

Assessments. After providing informed consent, and prior to surgeon consultation, patients completed a standardized questionnaire to assess sociodemographic characteristics (level of education, income status, living situation, employment status) and prior joint replacement of a hip or the other knee. Those who proceeded to TKA completed a second questionnaire following

a mandatory preoperative education session to assess knee OA symptom severity (Western Ontario and McMaster Universities Osteoarthritis Index [WOMAC] pain scale and Knee Injury and Osteoarthritis Outcome Score physical function short form [KOOS-PS]) (21–23); depressed mood (Patient Health Questionnaire 8-item depression scale [PHQ-8]) (24); height/weight to calculate body mass index (BMI); number of physician-diagnosed health conditions for which they were receiving treatment (25); and musculoskeletal comorbidity (pain or stiffness in the hips, contralateral knee, or lower back). Participants were asked to indicate all OA therapies “ever tried”: acetaminophen, oral or topical nonsteroidal antiinflammatory drugs, opioid analgesics (pain killers with codeine, e.g., Tylenol #1, 2, 3, Percocet, oxycodone, or MS Contin), and joint injection (i.e., cortisone, hyaluronic acid), exercise informally or in an exercise program, and physiotherapy. The participants' age and sex were obtained from clinic records. TKA expectations were assessed using the HSS TKA Expectations Questionnaire (20). For each of the 17 TKA items, participants were asked to answer the question “How important are these expectations in the treatment of your knee arthritis?” using a 5-point Likert scale (very important, somewhat important, a little important, I do not expect this, and this does not apply to me).

One year after surgery, participants completed another questionnaire to reassess knee pain symptoms (WOMAC pain, KOOS-PS), assess the occurrence of surgical complications (open-ended text), and determine overall satisfaction with TKA results (Self-Administered Patient Satisfaction Scale for Primary Hip and Knee Arthroplasty [26] on a 4-point Likert scale: very dissatisfied, somewhat dissatisfied, somewhat satisfied, and very satisfied), and whether TKA expectations had been met (on a 4-point Likert scale: definitely not; probably not; yes, probably; and yes, definitely). Participant-reported complications were verified against the patients' electronic health records. Questionnaires were completed online, by interview, or on paper according to patient preference.

Statistical analysis. After assessing distributions for normality, variables were calculated using proportions, means, and medians as appropriate. KOOS-PS scores were reverse coded so that for both KOOS-PS and WOMAC pain higher scores indicated greater severity. Comorbid conditions were summed and categorized as 0–1, 2, and ≥ 3 . Recommended OA treatment was defined as weight loss if overweight or obese, formal or informal exercise, including via physical therapy, and analgesics. The HSS summary score was calculated by summing the scale scores and normalizing to 0–100, where higher scores indicated greater expectations of TKA.

TKA expectations were defined as outcomes on the HSS TKA questionnaire that participants indicated were very important (yes/no). Covariates were patient factors previously associated with TKA outcome: age, sex, employment status, WOMAC

Table 1. Baseline characteristics of study participants by level of overall satisfaction with TKA results at 1-year follow-up*

Presurgical patient characteristics	Total sample (n = 1,266)	Dissatisfied (n = 104)	Somewhat satisfied (n = 217)	Very satisfied (n = 945)
Sociodemographic characteristics				
Age, years	67.2 ± 8.8	65.7 ± 8.0	67.0 ± 8.3	67.4 ± 9.0
Female, no. (%)	771 (60.9)	55 (52.9)	131 (60.4)	585 (61.9)
White, no./no. assessed (%)	1,139/1,247 (91.3)	94/102 (92.2)	192/215 (89.3)	853/930 (91.7)
Postsecondary education, no. (%)	694/1,246 (55.7)	65 (63.7)	118 (55.7)	511 (54.8)
Annual income >\$60,000, no. (%)	486/1,086 (44.8)	41 (45.05)	86 (47.0)	359 (44.2)
Living with others, no. (%)	997/1,257 (79.6)	82 (79.6)	171 (79.2)	744 (79.7)
Employed for pay (full or part time), no. (%)	393/1,251 (31.4)	34 (33.0)	63 (29.3)	296 (31.7)
Joint symptoms (higher scores worse)				
WOMAC pain (0–20)	11.6 ± 3.5	11.6 ± 3.3	11.4 ± 3.5	11.6 ± 3.5
KOOS PS-SF (0–100) (n = 1,201)	53.2 ± 17.3	53.7 ± 17.8	53.0 ± 17.1	53.2 ± 17.3
Prior joint replacement, hip or knee, no. (%)	213/1,243 (17.1)	18 (17.65)	40 (18.5)	155 (16.8)
Prior OA therapies, no. (%)				
Weight loss if overweight or obese	1,158 (91.5)	100 (96.15)	192 (88.5)	866 (91.6)
Exercise/physiotherapy	999 (80.1)	80 (76.9)	169 (79.0)	750 (80.7)
Analgesic therapies	1180 (94.8)	93 (90.3)	208 (97.2)	879 (94.8)
All of the above	876 (70.5)	73 (70.9)	146 (68.5)	657 (71.0)
Health status				
PHQ-8/24, median (interquartile range)	5 (2–10)	6 (3–11)	5 (2–11)	5 (2–10)
BMI, kg/m ² (n = 1,991)	32.55 ± 6.3	32.4 ± 5.7	32.0 ± 6.0	32.7 ± 6.4
Comorbid conditions, no. (%)				
0–1	750/1,244 (60.3)	60 (58.2)	125 (58.2)	565 (61.0)
2	303 (24.4)	27 (26.2)	55 (25.6)	221 (23.9)
3+	191 (15.3)	16 (15.5)	35 (16.3)	140 (15.1)
One or both hips troublesome, no. (%)	298/1,243 (24.0)	35 (37.6)	61 (28.5)	202 (21.6)††
Both knees troublesome, no. (%)	625/1,243 (50.3)	45 (48.4)	91 (42.5)	489 (52.2)††
Patient-reported TKA expectations				
HSS expectations/100, median (interquartile range)	85.3 (75.0–92.65)	86.8 (75.7–94.1)	85.3 (75.0–92.6)	85.3 (75.0–92.65)
HSS subscales, considered the outcome very important, no. (%)				
Improve ability to walk	1,211/1,253 (96.65)	99 (95.2)	205 (96.2)	907 (96.9)
Relieve pain	1,180/1,263 (93.4)	99 (95.2)	204 (94.4)	877 (93.0)
Improve ability to go down stairs	1,100/1,262 (87.2)	92 (88.5)	187 (86.6)	821 (87.5)
Improve ability to go up stairs	1,084/1,261 (86.0)	90 (86.5)	185 (86.7)	809 (86.0)
Perform daily activities	1,041 (82.4)	91 (87.5)	175 (81.0)	775 (82.1)
Change position (e.g., get up from chair)	1,001/1,259 (79.5)	82 (78.85)	168 (77.8)	751 (80.0)
Participate in recreational activities	944/1,261 (74.9)	75 (72.1)	159 (73.6)	710 (75.45)
Remove the need for walking aids	839/1,255 (66.85)	67 (65.05)	138 (64.2)	634 (67.7)
Improve ability to interact with others (e.g., care for someone)	838/1,262 (66.4)	74 (71.15)	151 (69.9)	613 (65.1)
Enjoy psychological well-being	831/1,256 (66.2)	76 (73.1)	144 (67.3)	611 (65.1)
Improve ability to exercise or participate in sports	802/1,260 (63.65)	65 (62.5)	135 (62.5)	602 (64.0)
Improve ability to take public transit or drive	794/1,262 (62.9)	71 (68.3)	134 (62.3)	589 (62.5)
Improve ability to kneel	761/1,261 (60.4)	68 (65.4)	142 (65.7)	551 (58.55)
Make the knee/leg straight	749/1,256 (59.6)	68 (65.4)	128 (59.5)	553 (59.0)
Improve ability to squat	700/1,262 (55.5)	60 (57.7)	128 (59.3)	512 (54.35)
Improve sexual activity	450/1,251 (36.0)	40 (38.5)	74 (34.7)	336 (36.0)
Be employed for monetary reimbursement	370/1,251 (29.6)	33 (32.7)	62 (29.1)	275 (29.35)

* Except where indicated otherwise, values are the mean ± SD. Higher scores for the Patient Health Questionnaire 8-item depression scale (PHQ-8) indicate more depressive symptoms. Denominator is shown when response is <100%. TKA = total knee arthroplasty; WOMAC = Western Ontario and McMaster Universities Osteoarthritis Index; KOOS-PS-SF = Knee injury and Osteoarthritis Outcome Score physical function short form; OA = osteoarthritis; BMI = body mass index; HSS = Hospital for Special Surgery.

pain, KOOS function, PHQ-8 depressed mood, BMI, number of non-musculoskeletal comorbid conditions and musculoskeletal comorbidities (27); and prior joint replacement of a hip or other knee. The primary ordinal outcome was participants' level of satisfaction with TKA based on responses to the overall satisfaction

subscale: very satisfied versus somewhat satisfied versus somewhat or very dissatisfied. Secondary outcomes included occurrence of a complication, defined as revision, manipulation, infection, or patellar resurfacing (yes/no); and expectations definitely met (yes/no) at 1 year post-TKA.

Preoperative characteristics, TKA expectations, and secondary outcomes were compared by level of TKA satisfaction using the chi-square test, Student's *t*-test, and Wilcoxon's rank sum test, as appropriate. Collinearity of variables was assessed using a variance inflation factor of >4 and tolerance value of <0.25 (28). Due to lack of variability in responses or collinearity, TKA expectations regarding using stairs, squatting, walking, and pain relief were excluded from multivariate analyses. After confirming the assumption of proportional odds, multivariate logistic regression was used to fit the cumulative logit model for the relationship between patients' TKA expectations, as defined, and our primary outcome. As the degree to which participants' expectations might be achievable may depend on their pre-TKA level of physical disability, we also assessed for interactions between TKA expectations and KOOS-PS scores.

Variable selection for multivariate modeling was based on a univariate screen; those variables associated with overall satisfaction at a *P* value of less than or equal to 0.25 were included in the multivariate model (model 1). Occurrence of a TKA complication (any/none) was then added to the model to assess for any effects on our exposures of interest (model 2). In a secondary analysis, we replaced individual expectations with the HSS summary score in model 1. *P* values less than 0.05 (2-sided) were considered significant. All statistical analyses were performed using SAS version 9.4.

The study was approved by the Research Ethics Boards of the Universities of Alberta (PRO-00051108) and Calgary (REB 14-1294), and from Women's College Hospital (REB 2014-0092) at the University of Toronto. The BEST-Knee Study Team members are listed in Appendix A.

RESULTS

Description of the cohort. Of the 1,374 eligible, consenting patients with knee OA who completed preoperative assessments and underwent primary, elective TKA, 1,272 completed the 1-year follow-up assessment, and 1,266 (92.1%) provided information on their overall level of TKA satisfaction.

Preoperative characteristics of the cohort. The demographic and clinical characteristics of the cohort are shown in Table 1. The mean \pm SD age of the participants was 67.2 \pm 8.8 years, and 60.9% were women. Most patients self-identified as white (91.3%); 55.7% had received postsecondary education, 44.8% reported an annual household income >\$60,000, and 31.4% were employed. The mean \pm SD WOMAC pain score and KOOS-PS score were 11.6 \pm 3.5 and 53.2 \pm 17.3, respectively; 17.1% had undergone a prior hip or contralateral knee replacement. More than two-thirds (70.5%) had used recommended knee OA therapies. The median PHQ-8 score was 5 (interquartile range 2–10). The mean \pm SD BMI was 32.55 \pm 6.3 kg/m²; 13.3% had a BMI of \geq 40. More than one-third (39.7%) had \geq 2 non-musculoskeletal comorbid conditions; 24.0% reported symptoms in the hips, 25.8% in the lower back, and 50.3% in both knees.

The median HSS TKA expectations summary score was 85.3 (interquartile range 75.0–92.65), indicating overall high expectations for TKA. Nearly all participants indicated that improved ability to perform daily activities, walk, go up and down stairs, and reduce their knee pain were very important (>80%). Most also indicated that it was very important that TKA improve their ability to change position, e.g., get up from a chair (79.5%) and participate in recreational activities (74.9%), but more variability was observed in the proportion indicating other outcomes as very important such as exercise or participation in sports (63.7%), kneeling (60.4%), improvement of psychological well-being (66.2%), and engaging in sexual activity (36.0%).

Patient-reported outcomes at 1-year post-TKA. At follow-up, 28 patients (2.2%) reported having experienced a TKA complication, and 3 additional participants underwent revision TKA due to unrelated trauma (1 hip fracture, 2 car accidents) (Table 2). Including these individuals, 945 participants (74.7%) were very satisfied, 217 (17.1%) were somewhat satisfied, 73 (5.8%) were somewhat dissatisfied, and 31 (2.45%) were very dissatisfied with their overall TKA results.

Table 2. TKA complications and patient-reported expectations met by overall satisfaction 1-year postsurgery*

Measure	Total sample (n = 1,266)	Dissatisfied (n = 104)	Somewhat satisfied (n = 217)	Very satisfied (n = 945)
Complications, no. (%)				
Revision TKA	13 (1.0)	9 (8.65)	3 (1.4)	1 (0.1)†
Manipulation under anesthesia	10 (0.8)	6 (5.8)	1 (0.5)	3 (0.3)†
Infection (not requiring revision)	2 (0.2)	1 (1.0)	–	1 (0.1)
Patellar resurfacing	3 (0.2)	3 (2.9)	–	–
Any	28 (2.2)	19 (18.3)	4 (1.8)	5 (0.5)†
Expectations of TKA met, no. (%)				
Definitely yes	836 (66.0)	3 (2.9)	68 (31.3)	765 (81.0)†
Probably yes	325 (25.7)	10 (9.6)	142 (65.4)	173 (18.3)
Probably/definitely not	103/1,265 (8.1)‡	91 (87.5)	7 (3.2)	6 (0.6)

* TKA = total knee arthroplasty.

† *P* < 0.001 for comparison of level of satisfaction.

‡ Data on the expectations of TKA met, probably/definitely not, were available for 1,265 patients.

Table 3. Relationship of preoperative TKA expectations to postoperative satisfaction 1 year after surgery (n = 1,157)*

	Unadjusted OR (95% CI)	Model 1 adjusted OR (95% CI)†	Model 2 adjusted OR (95% CI)‡
Covariates			
Age, per year	1.01 (0.99–1.03)§	1.01 (1.00–1.03)	1.01 (1.00–1.03)
Sex, male	0.83 (0.64–1.07)§	0.85 (0.64–1.13)	0.81 (0.61–1.08)
Employed for pay	1.04 (0.80–1.37)	–	–
WOMAC pain, per unit increase	1.01 (0.97–1.04)	–	–
KOOS-PS, per unit increase	1.10 (0.99–1.01)	–	–
PHQ-8 depressed mood, per 10-point increase	0.80 (0.64–0.98)§	0.72 (0.55–0.95)	0.55 (0.41–0.74)
BMI, per 5 kg/m ² increase	1.05 (0.95–1.16)§	1.34 (1.04–1.63)	1.45 (1.11–1.89)
No. comorbid conditions (referent = 0)	–	–	–
1 condition	1.38 (0.99–1.92)	–	–
2 conditions	1.06 (0.75–1.50)	–	–
3+ conditions	1.08 (0.73–1.62)	–	–
Hip symptoms (yes)	0.59 (0.45–0.78)§	0.59 (0.43–0.80)	0.59 (0.43–0.81)
Contralateral knee symptoms (yes)	1.35 (1.04–1.74)§	1.40 (1.05–1.85)	1.38 (1.04–1.83)
Prior joint replacement hip or knee	0.91 (0.65–1.26)	–	–
HSS expectations (outcome is very important)			
Perform daily activities	0.90 (0.65–1.26)	–	–
Change position, e.g., get up from chair	1.11 (0.82–1.51)	–	–
Participate in recreational activities	1.13 (0.85–1.51)	–	–
Remove the need for walking aids	1.15 (0.88–1.49)	–	–
Improve ability to interact with others	0.79 (0.60–1.03)§	0.79 (0.57–1.09)	0.80 (0.58–1.11)
Enjoy psychological well-being	–	–	–
Lowest tertile of KOOS-PS	0.61 (0.39–0.97)§	0.49 (0.28–0.84)	0.49 (0.285–0.85)
Middle tertile of KOOS-PS	0.67 (0.41–1.08)§	0.73 (0.41–1.32)	0.73 (0.42–1.215)
Highest tertile of KOOS-PS	1.53 (0.94–2.51)§	2.37 (1.33–4.21)	2.65 (1.48–4.75)
Improve ability to exercise or participate in sports	1.07 (0.82–1.38)	–	–
Improve ability to take public transit or drive	0.91 (0.70–1.18)	–	–
Improve ability to kneel	0.75 (0.57–0.97)§	0.725 (0.54–0.98)	0.705 (0.52–0.96)
Make the knee/leg straight	0.89 (0.69–1.15)	–	–
Improve sexual activity	0.99 (0.76–1.29)	–	–
Be employed for pay	0.95 (0.72–1.25)	–	–
HSS expectations summary score	1.00 (0.99–1.01)	–	–

* For all models, the dependent variable was overall satisfaction (modeling very satisfied versus somewhat satisfied versus somewhat/very dissatisfied). 95% CI = 95% confidence interval; WOMAC = Western Ontario and McMaster Universities Osteoarthritis Index; PHQ-8 = Patient Health Questionnaire 8-item depression scale; BMI = body mass index; HSS = Hospital for Special Surgery.

† Model 1 includes all covariates significant in univariate analysis at $P \leq 0.25$.

‡ Model 2 consists of model 1 plus the addition of occurrence of a complication.

§ $P \leq 0.25$ for the relationship of the variable with level of satisfaction, thus eligible for inclusion in multivariate models.

¶ A significant interaction was found between expectations for well-being and pre-total knee arthroplasty (pre-TKA) Knee Injury and Osteoarthritis Outcome Score physical function shortform (KOOS-PS) score (P for interaction < 0.001); thus, unadjusted odds ratios (ORs) are shown by tertile of pre-TKA KOOS PS values (lowest to highest reflects least to most pre-TKA disability).

Two-thirds (66.0%) reported that their surgical expectations had been definitely met, 25.7% reported they had been somewhat met, and 8.1% reported that they had not been met. Having TKA expectations definitely met was associated with significantly greater overall satisfaction (81.0% were very satisfied, 31.3% were somewhat satisfied, and only 2.9% were dissatisfied; $P < 0.001$). Occurrence of a TKA complication was associated with lower overall satisfaction; of the 28 patients with a complication, 5 (17.9%) were very satisfied, 4 (14.3%) were somewhat satisfied, and 18 (64.3%) were dissatisfied; $P < 0.001$.

Relationship of pre-TKA expectations to post-TKA satisfaction. Unadjusted and adjusted odds ratios (ORs) and 95% confidence intervals (95% CIs) for exposures of interest are shown in Table 3. In univariate analyses, age, sex,

depressed mood, BMI, hip and contralateral knee complaints, and expectations of TKA to improve patients' ability to interact with others and to kneel were associated with post-TKA satisfaction ($P \leq 0.25$), and thus these variables were eligible for inclusion in the multivariable model. A significant interaction was also found between expectations for improved psychological well-being and pre-TKA disability (KOOS-PS scores).

In multivariate modeling, a greater BMI (adjusted OR per 5 kg/m² increase 1.34 [95% CI 1.04–1.63]) and contralateral knee complaints (adjusted OR 1.40 [95% CI 1.05–1.85]) were associated with higher odds of overall satisfaction with TKA results, while the odds were reduced in patients with depressed mood (adjusted OR per 10-point increase in PHQ-8 score 0.72 [95% CI 0.55–0.95]), symptomatic hips (adjusted OR 0.59 [95% CI 0.43–0.80]), and those who expected TKA to improve their ability to kneel (adjusted OR 0.725 [95% CI 0.54–0.98]). Additionally,

expectations for TKA to improve well-being were associated with lower odds of satisfaction in participants with less pre-TKA disability (adjusted OR for lowest KOOS-PS tertile pre-TKA 0.49 [95% CI 0.28–0.84]), but higher odds of satisfaction in those with greater disability (adjusted OR for uppermost KOOS-PS tertile 2.37 [95% CI 1.33–4.21]). Controlling for these variables, no relationship was found between patient age, sex, and expectations for improved ability to interact with others and post-TKA satisfaction.

Addition of TKA complications to the model showed that complications were associated with significantly lower odds of satisfaction (adjusted OR 0.04 [95% CI 0.01–0.11]), but the above-noted relationships between expectations and satisfaction remained. When individual expectations were replaced with the HSS summary score, no relationship was found between expectations and post-TKA satisfaction (adjusted OR 1.00 [95% CI 0.99–1.01]).

DISCUSSION

In a large cohort of patients who underwent primary elective TKA, we examined the relationship between preoperative patient-reported TKA expectations and level of satisfaction with TKA results after 1-year. TKA expectations were defined as those TKA outcomes deemed very important by the patient. Including patients who experienced a TKA complication, 75% of our TKA recipients were very satisfied at follow-up, 17% were somewhat satisfied, and 8% were dissatisfied with their results. Controlling for other preoperative patient factors that may affect TKA outcome, we found that an expectation of TKA to improve ability to kneel was associated with lower odds of satisfaction. Expectations of TKA to improve psychological well-being were also associated with lower odds of satisfaction, but only among those with less pre-TKA disability (lower KOOS-PS scores). Among participants with high pre-TKA disability, the expectation of TKA to improve well-being was associated with higher odds of satisfaction. No relationship was found between summary HSS scores and post-TKA satisfaction. Given that setting appropriate patient expectations preoperatively is a critical component of obtaining informed consent for any operative procedure, we believe these findings are important.

Consistent with prior studies that have assessed preoperative expectations for TKA using the HSS Expectations Scale (7,29,30), we found that TKA expectations, as we defined them, were highest for pain relief and basic functional improvements, e.g., walking and using stairs, but more variable for other outcomes. We had hypothesized that patients with unrealistic (unachievable) expectations would be less likely to report satisfaction. However, the achievability of specific expectations is likely to be influenced by contextual factors. Consistent with this, the odds of being satisfied with one's TKA results given high expectations for TKA to improve psychological well-being

varied based on level of preoperative disability, as measured using the KOOS-PS scale. A possible explanation for this finding is that psychological well-being means different things to knee OA patients at different stages of OA progression. To individuals with advanced knee OA, psychological well-being may be linked more strongly to pain, sleep, and mood, which are generally improved with TKA. For individuals with less pain or disability preoperatively, psychological well-being may refer more to their ability to participate in valued recreational activities, like sport or travel, which may be harder to achieve as a result of TKA and thus less likely to lead to satisfaction with results. Taken together, our findings suggest that a one size fits all approach will not work. The achievability of patients' expectations for TKA must be evaluated in the context of both clinical and psychological factors.

Almost two-thirds of our cohort participants also had expectations that TKA would improve their ability to kneel. Others have similarly found that a desire to kneel was a motivation for TKA (31,32). These findings are consistent with the importance of kneeling to the performance of many daily activities, some occupations, and many religious and cultural observances (e.g., prayer) (33). However, research to date indicates that 60–80% of primary TKA patients report difficulty or an inability to kneel after TKA (34–40). Identified barriers to kneeling post-TKA include pain and other sensory changes (e.g., numbness around the incision, patient fear of harming the prosthesis, and lack of information about kneeling after TKA). Whether or not improved ability to kneel is an unrealistic expectation of TKA is unclear. Despite the high importance placed on kneeling by patients with knee OA, little research has been conducted to identify modifiable determinants of ability to kneel after TKA, including the effects of prosthesis type, surgical technique, postoperative management, and patient factors (e.g., fear of kneeling). Our results indicate a critical need for research to address these knowledge gaps.

Only 66% of our participants reported that their TKA expectations had been definitely met. While 75.6% of participants whose expectations had been met were very satisfied with their TKA results, only 4.6% of those with unmet expectations were similarly satisfied. These findings are consistent with prior cross-sectional studies of TKA recipients and provide additional support for the need to incorporate patients' expectations of surgery in TKA decision-making (6,7,11,19,41,42).

Our findings are consistent with those of others who have found a negative relationship between depressed mood and musculoskeletal comorbidities and TKA outcome (27,43–45). However, interestingly, while concomitant OA symptoms in the hips were associated with lower odds of being satisfied, the presence of contralateral knee symptoms were associated with high odds of satisfaction. A potential explanation for these findings is that the index replacement enables off-loading of the contralateral knee but not the hips. Finally, while

others have linked higher BMI to risk for complications following TKA (46–48), despite the high prevalence of obesity in our cohort, we found no evidence that individuals with a greater BMI were at lower odds of being satisfied with their TKA results, before or after controlling for the occurrence of TKA complications.

The strengths of our study include the large sample with broad representation by age and sex, recruited from regional orthopedic surgical intake clinics; the 45 surgeons practicing at these clinics perform ~60% of knee replacements in the province. Patients' expectations and post-TKA satisfaction were assessed using validated questionnaires. We examined overall level of expectations as well as the effects of specific expectations for TKA. We focused on patients with knee OA, who represent the majority of TKA recipients, and on primary TKA, for which postoperative satisfaction has been variable. Given our focus on improving patient appropriateness for TKA, we were interested in preoperative predictors of post-TKA satisfaction. However, we assessed and controlled for occurrence of complications in secondary analyses.

Our study also had some limitations. Our cohort was predominantly white; thus, results may not be generalizable to TKA recipients of other racial or ethnic backgrounds. Operative and postoperative factors may also contribute to achievement of patients' TKA expectations and thus satisfaction, but were not assessed (4). For example, better perioperative pain management may enable greater adherence to postoperative rehabilitation and thus influence the ability to kneel postoperatively. We investigated interactions between expectations and preoperative self-reported function, but other factors, such as age and sex, may also impact the relationship of expectations to satisfaction. The observational nature of our study precludes determination of cause and effect relationships. Finally, while our sample was large and diverse, our research was conducted in a single Canadian province and thus findings may not be generalizable to other settings.

In conclusion, in this study of knee OA patients undergoing primary TKA, after controlling for known patient-related preoperative predictors of TKA outcome, patients' expectations of TKA with respect to postoperative ability to kneel and achieve psychological well-being were strongly related to postoperative satisfaction. Attention to patient's expectations of TKA, and whether or not they are achievable, has potential to improve patient outcomes and the use of valuable health care resources.

ACKNOWLEDGMENTS

We would like to thank the participating study surgeons at the Edmonton Bone and Joint Centre: Drs. Gordon Arnett, Robert Balyk, Jeffery Bury, John Cinats, Donald Dick, D'Arcy Durand, Lee Ekert, Don Glasgow, Robert Glasgow Sr. (deceased), Gordon Golpen, Ben Herman, Catherine Hui, Lary Hunka, Hongxing Jiang, William C.

Johnson (deceased), Frank Kortbeek, Guy Lavoie, Mitch Lavoie, Paul K. Leung, James Mahood, Edward Masson, Richard McLeod, James McMillan (deceased), Greg O'Connor, David Otto, Carlo Panaro, Paulose Paul, Gordon Russell, Don Weber, Colleen Weeks, and Andrea Woo (FP, screening); Jane Squire Howden (clinic staff); and Anne-Marie Adachi, Jessica Beatty, Shakib Rahman, and Braden Woodhouse (research staff). We would also like to thank the participating study surgeons from the Alberta Hip & Knee Clinic: Drs. Greg Abelseth, Kelley De Souza, John Donaghy, Paul Duffy, Kelly Johnston, Robert Korley, Raul Kuchinad, Michael Monument, Maureen O'Brien, James Powell, Shannon Puloski, Ed Rendall, Alex Rezansoff, Raj Sharma, James Stewart, Scott Timmerman, and Jason Werle; Tanya Reczek (clinic staff); Jeffrey Depew (research staff); Bukky Dada (Department of Community Health Sciences, University of Calgary); and Ian Stanaitis (Women's College Hospital/University of Toronto).

AUTHOR CONTRIBUTIONS

All authors were involved in drafting the article or revising it critically for important intellectual content, and all authors approved the final version to be published. Dr. Hawker had full access to all of the data in the study and takes responsibility for the integrity of the data and the accuracy of the data analysis.

Study conception and design. Hawker, Conner-Spady, Bohm, Dunbar, Jones, Ravi, Noseworthy, Marshall.

Acquisition of data. Dick, Powell, Paul, Marshall.

Analysis and interpretation of data. Hawker.

REFERENCES

1. Cram P, Lu X, Kates SL, Singh JA, Li Y, Wolf BR. Total knee arthroplasty volume, utilization, and outcomes among Medicare beneficiaries, 1991–2010. *JAMA* 2012;308:1227–36.
2. Healthcare Cost and Utilization Project (HCUP). HCUP: fast stats—most common operations during inpatient stays. URL: www.hcup-us.ahrq.gov/faststats/national/inpatientcommonprocedures.jsp?year1=2014&characteristic1=0&included1=1&year2=2008&characteristic2=54&included2=1&expansionInfoState=hide&dataTablesState=hide&definitionsState=hide&exportState=hide.
3. Sloan M, Premkumar A, Sheth NP. Projected volume of primary total joint arthroplasty in the US, 2014 to 2030. *J Bone Joint Surg Am* 2018;100:1455–60.
4. Kahlenberg CA, Nwachukwu BU, McLawhorn AS, Cross MB, Cornell CN, Padgett DE. Patient satisfaction after total knee replacement: a systematic review. *HSS J* 2018;14:192–201.
5. Lawson EH, Gibbons MM, Ko CY, Shekelle PG. The appropriateness method has acceptable reliability and validity for assessing overuse and underuse of surgical procedures. *J Clin Epidemiol* 2012;65:1133–43.
6. Dunbar MJ, Richardson G, Robertsson O. I can't get no satisfaction after my total knee replacement: rhymes and reasons. *Bone Joint J* 2013;95-b Suppl A:148–52.
7. Scott CE, Bugler KE, Clement ND, MacDonald D, Howie CR, Biant LC. Patient expectations of arthroplasty of the hip and knee. *J Bone Joint Surg Br* 2012;94:974–81.
8. Husain A, Lee GC. Establishing realistic patient expectations following total knee arthroplasty. *J Am Acad Orthop Surg* 2015;23:707–13.
9. Hamilton DF, Lane JV, Gaston P, Patton JT, Macdonald D, Simpson AH, et al. What determines patient satisfaction with surgery? A prospective cohort study of 4709 patients following total joint replacement. *BMJ Open* 2013;3:e002525.
10. Clement ND, Macdonald D, Burnett R. Predicting patient satisfaction using the Oxford knee score: where do we draw the line? *Arch Orthop Trauma Surg* 2013;133:689–94.

11. Bourne RB, Chesworth BM, Davis AM, Mahomed NN, Charron KD. Patient satisfaction after total knee arthroplasty: who is satisfied and who is not? *Clin Orthop Relat Res* 2010;468:57–63.
12. Judge A, Arden NK, Kiran A, Price A, Javaid MK, Beard D, et al. Interpretation of patient-reported outcomes for hip and knee replacement surgery: identification of thresholds associated with satisfaction with surgery. *J Bone Joint Surg Br* 2012;94:412–8.
13. Haanstra TM, van den Berg T, Ostelo RW, Poolman RW, Jansma EP, Cuijpers P, et al. Systematic review: do patient expectations influence treatment outcomes in total knee and total hip arthroplasty? *Health Qual Life Outcomes* 2012;10:152.
14. Vissers MM, de Groot IB, Reijman M, Bussmann JB, Stam HJ, Verhaar JA. Functional capacity and actual daily activity do not contribute to patient satisfaction after total knee arthroplasty. *BMC Musculoskelet Disord* 2010;11:121.
15. Mannion AF, Kampfen S, Munzinger U, Kramers-de Quervain I. The role of patient expectations in predicting outcome after total knee arthroplasty. *Arthritis Res Ther* 2009;11:R139.
16. Lingard EA, Sledge CB, Learmonth ID. Patient expectations regarding total knee arthroplasty: differences among the United States, United Kingdom, and Australia. *J Bone Joint Surg Am* 2006;88:1201–7.
17. Arden NK, Kiran A, Judge A, Biant LC, Javaid MK, Murray DW, et al. What is a good patient reported outcome after total hip replacement? *Osteoarthritis Cartilage* 2011;19:155–62.
18. Brokelman R, van Loon C, van Susante J, van Kampen A, Veth R. Patients are more satisfied than they expected after joint arthroplasty. *Acta Orthop Belg* 2008;74:59–63.
19. Clement ND, MacDonald D, Patton JT, Burnett R. Post-operative Oxford knee score can be used to indicate whether patient expectations have been achieved after primary total knee arthroplasty. *Knee Surg Sports Traumatol Arthrosc* 2015;23:1578–90.
20. Mancuso CA, Sculco TP, Wickiewicz TL, Jones EC, Robbins L, Warren RF, et al. Patients' expectations of knee surgery. *J Bone Joint Surg Am* 2001;83:1005–12.
21. Bellamy N. Pain assessment in osteoarthritis: experience with the WOMAC osteoarthritis index. *Semin Arthritis Rheum* 1989;18 Suppl 2:14–7.
22. Bellamy N, Buchanan WW, Goldsmith CH, Campbell J, Stitt LW. Validation study of WOMAC: a health status instrument for measuring clinically important patient relevant outcomes to antirheumatic drug therapy in patients with osteoarthritis of the hip or knee. *J Rheumatol* 1988;15:1833–40.
23. Perruccio AV, Lohmander LS, Canizares M, Tennant A, Hawker GA, Conaghan PG, et al. The development of a short measure of physical function for knee OA KOOS-Physical Function Shortform (KOOS-PS): an OARSI/OMERACT initiative. *Osteoarthritis Cartilage* 2008;16:542–50.
24. Kroenke K, Strine TW, Spitzer RL, Williams JB, Berry JT, Mokdad AH. The PHQ-8 as a measure of current depression in the general population. *J Affect Disord* 2009;114:163–73.
25. Sangha O, Stucki G, Liang MH, Fossel AH, Katz JN. The Self-Administered Comorbidity Questionnaire: a new method to assess comorbidity for clinical and health services research. *Arthritis Rheum* 2003;49:156–63.
26. Mahomed N, Gandhi R, Daltroy L, Katz JN. The self-administered patient satisfaction scale for primary hip and knee arthroplasty. *Arthritis* 2011;2011:591253.
27. Zhang L, Lix LM, Ayilara O, Sawatzky R, Bohm ER. The effect of multimorbidity on changes in health-related quality of life following hip and knee arthroplasty. *Bone Joint J* 2018;100-B:1168–74.
28. Freund R, Wilson W. Regression analysis: statistical modeling of a response variable. First ed. San Diego (CA): Academic Press; 1998.
29. Judge A, Cooper C, Arden NK, Williams S, Hobbs N, Dixon D, et al. Pre-operative expectation predicts 12-month post-operative outcome among patients undergoing primary total hip replacement in European orthopaedic centres. *Osteoarthritis Cartilage* 2011;19:659–67.
30. Cross M, Lapsley H, Barcenilla A, Parker D, Coolican M, March L. Patient expectations of hip and knee joint replacement surgery and postoperative health status. *Patient* 2009;2:51–60.
31. Van Zaanen Y, van Geenen RC, Pahlplatz TM, Kievit AJ, Hoozemans MJ, Bakker EW, et al. Three out of ten working patients expect no clinical improvement of their ability to perform work-related knee-demanding activities after total knee arthroplasty: a multicenter study. *J Occup Rehabil* 2019;29:585–94.
32. Neuprez A, Delcour JP, Fatemi F, Gillet P, Crielaard JM, Bruyère O, et al. Patients' expectations impact their satisfaction following total hip or knee arthroplasty. *PLoS One* 2016;11:e0167911.
33. Mulholland SJ, Wyss UP. Activities of daily living in non-Western cultures: range of motion requirements for hip and knee joint implants. *Int J Rehabil Res* 2001;24:191–8.
34. Blackburn J, Wylde V, Greenwood R, Blom AW, Levy A. The effect of numbness on outcome from total knee replacement. *Ann R Coll Surg Engl* 2017;99:385–9.
35. Hassaballa M, Artz N, Weale A, Porteous A. Alteration in skin sensation following knee arthroplasty and its impact on kneeling ability: a comparison of three common surgical incisions. *Knee Surg Sports Traumatol Arthrosc* 2012;20:1983–7.
36. Sharkey PF, Miller AJ. Noise, numbness, and kneeling difficulties after total knee arthroplasty: is the outcome affected? *J Arthroplasty* 2011;26:1427–31.
37. Palmer SH, Servant CT, Maguire J, Parish EN, Cross MJ. Ability to kneel after total knee replacement. *J Bone Joint Surg Br* 2002;84:220–2.
38. Kim TK, Kwon SK, Kang YG, Chang CB, Seong SC. Functional disabilities and satisfaction after total knee arthroplasty in female Asian patients. *J Arthroplasty* 2010;25:458–64.
39. Schai PA, Gibbon AJ, Scott RD. Kneeling ability after total knee arthroplasty: perception and reality. *Clin Orthop Relat Res* 1999;367:195–200.
40. Wylde V, Artz N, Howells N, Blom AW. Kneeling ability after total knee replacement [review]. *EFORT Open Rev* 2019;4:460–7.
41. Noble PC, Conditt MA, Cook KF, Mathis KB. The John Insall Award: patient expectations affect satisfaction with total knee arthroplasty. *Clin Orthop Relat Res* 2006;452:35–43.
42. Conner-Spady BL, Bohm E, Loucks L, Dunbar MJ, Marshall DA, Noseworthy TW. Patient expectations and satisfaction 6 and 12 months following total hip and knee replacement. *Qual Life Res* 2020;29:705–19.
43. Lingard EA, Katz JN, Wright EA, Sledge CB. Predicting the outcome of total knee arthroplasty. *J Bone Joint Surg Am* 2004;86-a:2179–86.
44. Lopez-Olivo MA, Landon GC, Siff SJ, Edelstein D, Pak C, Kallen MA, et al. Psychosocial determinants of outcomes in knee replacement. *Ann Rheum Dis* 2011;70:1775–81.
45. Fisher DA, Dierckman B, Watts MR, Davis K. Looks good but feels bad: factors that contribute to poor results after total knee arthroplasty. *J Arthroplasty* 2007;22 Suppl 2:39–42.
46. Jarvenpaa J, Kettunen J, Kroger H, Miettinen H. Obesity may impair the early outcome of total knee arthroplasty. *Scand J Surg* 2010;99:45–9.
47. Núñez M, Lozano L, Núñez E, Segur JM, Sastre S, Maculé F, et al. Total knee replacement and health-related quality of life:

factors influencing long-term outcomes. *Arthritis Rheum* 2009;61:1062–9.

48. Malinzak RA, Ritter MA, Berend ME, Meding JB, Olberding EM, Davis KE. Morbidly obese, diabetic, younger, and unilateral joint arthroplasty patients have elevated total joint arthroplasty infection rates. *J Arthroplasty* 2009;24:84–8.

APPENDIX A: THE BEST-KNEE STUDY TEAM

Members of the BEST-Knee Study Team are as follows: Drs. Gillian A. Hawker, Deborah A. Marshall, Eric Bohm, Michael J. Dunbar, Peter Faris, C. Allyson Jones, Tom Noseworthy, Bheeshma Ravi, and Linda Woodhouse.

DOI 10.1002/art.41509

Clinical Images: Repair of bone erosion with effective urate-lowering therapy in a patient with tophaceous gout



The patient, a 61-year-old man with an 18-year history of gout (untreated for the first 13 years), presented to our hospital with left knee pain. Physical examination revealed inflammatory changes in the left knee, large subcutaneous (SC) nodules in the first metatarsophalangeal (MTP) joints bilaterally, and enlargement of the left Achilles tendon. The large SC nodules had progressed during the last 5 years, despite treatment with allopurinol having been initiated. The serum uric acid level was 5.9 mg/dl, and the C-reactive protein level was elevated (5.8 mg/dl). Radiography of the feet revealed bone erosion, overhanging calcified edges in both first MTP joints, and spurs in both first metatarsal bones with soft tissue thickening (**arrows in A**). Steroid injection in the left knee improved pain. Synovial fluid aspiration revealed urate crystals. A diagnosis of rheumatoid arthritis was excluded based on the patient's medical history, as well as physical examination and laboratory findings. Treatment with topiroxostat 40 mg/day was initiated, with the daily dosage increased to 80 mg after 1 month and to 120 mg after a further 1 month, followed by the addition of benzbromarone (100 mg daily), and the serum uric acid level was maintained in a range of 4.0–6.0 mg/dl. After 30 months of treatment, the size of the gouty tophi had decreased. The erosion involving the proximal aspect of the first MTP joints had decreased, and the surrounding bone cortex had thickened (**arrows in B**). In patients with chronic tophaceous gout, osteoblast-associated bone resorption and enhanced osteoclastogenesis due to monosodium urate monohydrate (MSU) crystals induce bone erosion (1,2). Profound urate-lowering response (serum urate level <1 mg/dl) to treatment with pegloticase leads to dissolution of MSU crystals and healing of bone erosions (3). As seen in this patient, urate-lowering therapy with a xanthine oxidase inhibitor plus a uricosuric drug can also lead to repair of bone erosion.

1. Dalbeth N, Smith T, Nicolson B, Clark B, Callon K, Naot D, et al. Enhanced osteoclastogenesis in patients with tophaceous gout: urate crystals promote osteoclast development through interactions with stromal cells. *Arthritis Rheum* 2008;58:1854–65.
2. Bouchard L, de Médicis R, Lussier A, Naccache PH, Poubelle PE. Inflammatory microcrystals alter the functional phenotype of human osteoblast-like cells in vitro: synergism with IL-1 to overexpress cyclooxygenase-2. *J Immunol* 2002;168:5310–7.
3. Dalbeth N, Doyle AJ, McQueen FM, Sundry J, Baraf HS. Exploratory study of radiographic change in patients with tophaceous gout treated with intensive urate-lowering therapy. *Arthritis Care Res (Hoboken)* 2014;66:82–5.

Shota Sakaguchi, MD 
Sanzai Hospital
Saito, Japan

factors influencing long-term outcomes. *Arthritis Rheum* 2009;61:1062–9.

48. Malinzak RA, Ritter MA, Berend ME, Meding JB, Olberding EM, Davis KE. Morbidly obese, diabetic, younger, and unilateral joint arthroplasty patients have elevated total joint arthroplasty infection rates. *J Arthroplasty* 2009;24:84–8.

APPENDIX A: THE BEST-KNEE STUDY TEAM

Members of the BEST-Knee Study Team are as follows: Drs. Gillian A. Hawker, Deborah A. Marshall, Eric Bohm, Michael J. Dunbar, Peter Faris, C. Allyson Jones, Tom Noseworthy, Bheeshma Ravi, and Linda Woodhouse.


DOI 10.1002/art.41509

Clinical Images: Repair of bone erosion with effective urate-lowering therapy in a patient with tophaceous gout






The patient, a 61-year-old man with an 18-year history of gout (untreated for the first 13 years), presented to our hospital with left knee pain. Physical examination revealed inflammatory changes in the left knee, large subcutaneous (SC) nodules in the first metatarsophalangeal (MTP) joints bilaterally, and enlargement of the left Achilles tendon. The large SC nodules had progressed during the last 5 years, despite treatment with allopurinol having been initiated. The serum uric acid level was 5.9 mg/dl, and the C-reactive protein level was elevated (5.8 mg/dl). Radiography of the feet revealed bone erosion, overhanging calcified edges in both first MTP joints, and spurs in both first metatarsal bones with soft tissue thickening (**arrows in A**). Steroid injection in the left knee improved pain. Synovial fluid aspiration revealed urate crystals. A diagnosis of rheumatoid arthritis was excluded based on the patient's medical history, as well as physical examination and laboratory findings. Treatment with topiroxostat 40 mg/day was initiated, with the daily dosage increased to 80 mg after 1 month and to 120 mg after a further 1 month, followed by the addition of benzbromarone (100 mg daily), and the serum uric acid level was maintained in a range of 4.0–6.0 mg/dl. After 30 months of treatment, the size of the gouty tophi had decreased. The erosion involving the proximal aspect of the first MTP joints had decreased, and the surrounding bone cortex had thickened (**arrows in B**). In patients with chronic tophaceous gout, osteoblast-associated bone resorption and enhanced osteoclastogenesis due to monosodium urate monohydrate (MSU) crystals induce bone erosion (1,2). Profound urate-lowering response (serum urate level <1 mg/dl) to treatment with pegloticase leads to dissolution of MSU crystals and healing of bone erosions (3). As seen in this patient, urate-lowering therapy with a xanthine oxidase inhibitor plus a uricosuric drug can also lead to repair of bone erosion.

1. Dalbeth N, Smith T, Nicolson B, Clark B, Callon K, Naot D, et al. Enhanced osteoclastogenesis in patients with tophaceous gout: urate crystals promote osteoclast development through interactions with stromal cells. *Arthritis Rheum* 2008;58:1854–65.
2. Bouchard L, de Médicis R, Lussier A, Naccache PH, Poubelle PE. Inflammatory microcrystals alter the functional phenotype of human osteoblast-like cells in vitro: synergism with IL-1 to overexpress cyclooxygenase-2. *J Immunol* 2002;168:5310–7.
3. Dalbeth N, Doyle AJ, McQueen FM, Sundry J, Baraf HS. Exploratory study of radiographic change in patients with tophaceous gout treated with intensive urate-lowering therapy. *Arthritis Care Res (Hoboken)* 2014;66:82–5.

Shota Sakaguchi, MD 
Sanzai Hospital
Saito, Japan

An Autoimmunogenic and Proinflammatory Profile Defined by the Gut Microbiota of Patients With Untreated Systemic Lupus Erythematosus

Bei-di Chen,¹  Xin-miao Jia,¹ Jia-yue Xu,² Li-dan Zhao,¹ Jun-yi Ji,³ Bing-xuan Wu,¹ Yue Ma,² Hao Li,⁴ Xiao-xia Zuo,⁵ Wen-you Pan,⁶ Xiao-han Wang,⁷ Shuang Ye,⁸ George C. Tsokos,⁴  Jun Wang,² and Xuan Zhang¹ 

Objective. Changes in gut microbiota have been linked to systemic lupus erythematosus (SLE), but knowledge is limited. Our study aimed to provide an in-depth understanding of the contribution of gut microbiota to the immunopathogenesis of SLE.

Methods. Fecal metagenomes from 117 patients with untreated SLE and 52 SLE patients posttreatment were aligned with 115 matched healthy controls and analyzed by whole-genome profiling. For comparison, we assessed the fecal metagenome of MRL/lpr mice. The oral microbiota origin of the gut species that existed in SLE patients was documented by single-nucleotide polymorphism–based strain-level analyses. Functional validation assays were performed to demonstrate the molecular mimicry of newly found microbial peptides.

Results. Gut microbiota from individuals with SLE displayed significant differences in microbial composition and function compared to healthy controls. Certain species, including the *Clostridium* species ATCC BAA-442 as well as *Atopobium rimae*, *Shuttleworthia satelles*, *Actinomyces massiliensis*, *Bacteroides fragilis*, and *Clostridium leptum*, were enriched in SLE gut microbiota and reduced after treatment. Enhanced lipopolysaccharide biosynthesis aligned with reduced branched chain amino acid biosynthesis was observed in the gut of SLE patients. The findings in mice were consistent with our findings in human subjects. Interestingly, some species with an oral microbiota origin were enriched in the gut of SLE patients. Functional validation assays demonstrated the proinflammatory capacities of some microbial peptides derived from SLE-enriched species.

Conclusion. This study provides detailed information on the microbiota of untreated patients with SLE, including their functional signatures, similarities with murine counterparts, oral origin, and the definition of autoantigen-mimicking peptides. Our data demonstrate that microbiome-altering approaches may offer valuable adjuvant therapies in SLE.

INTRODUCTION

Systemic lupus erythematosus (SLE), characterized by chronic inflammation and multiple organ damage, is a prototypical autoimmune disease resulting from loss of self tolerance and

sustained autoantibody production. The pathogenesis of autoimmunity in SLE has not yet been fully elucidated. Beyond genetic factors and among environmental triggers, microbiota have drawn the attention of investigators, but a complete understanding of the mechanisms involved is missing (1).

Supported by the National Natural Science Foundation of China (grants 81788101, 81630044, and 81801627), the Chinese Academy of Medical Science Innovation Fund for Medical Sciences (grants CIFS2016-12M-1-003, 2017-12M-1-008, 2017-12M-3-011, and 2016-12M-1-008), the Beijing Capital Health Development Fund (grant 2020-2-4019), the Medical Epigenetics Research Center of Chinese Academy of Medical Sciences (grant 2017PT 31035), the National Key Science and Technology Project of China (grant 2018YFC2000500), the Fundamental Research Funds for the Central Universities, Peking Union Medical College (grant 3332018026), and the Chinese Academy of Sciences Strategic Priority Research Program (grant XDB29020000) and Key Research Program (grant KFZD-SW-219).

¹Bei-di Chen, BS, Xin-miao Jia, PhD, Li-dan Zhao, MD, Bing-xuan Wu, BS, Xuan Zhang, MD: Department of Rheumatology, Clinical Immunology Center, State Key Laboratory of Complex Severe and Rare Diseases, Peking Union Medical College Hospital, Chinese Academy of Medical Science, and Peking Union Medical College, Beijing, China; ²Jia-yue Xu, PhD, Yue Ma, PhD, Jun Wang, PhD: Chinese Academy of Sciences and University of Chinese

Academy of Sciences, Beijing, China; ³Jun-yi Ji, BS: Tsinghua University, Beijing, China; ⁴Hao Li, PhD, George C. Tsokos, MD: Beth Israel Deaconess Medical Center and Harvard Medical School, Boston, Massachusetts; ⁵Xiao-xia Zuo, MD: Xiangya Hospital and Central South University, Changsha, China; ⁶Wen-you Pan, MD: Huaian First People's Hospital and Nanjing Medical University, Huaian, China; ⁷Xiao-han Wang, MD: Anyang District Hospital, Anyang, China; ⁸Shuang Ye, MD: Renji Hospital and Shanghai Jiaotong University School of Medicine, Shanghai, China.

Ms Chen and Drs. Jia and Xu contributed equally to this work.

No potential conflicts of interest relevant to this article were reported.

Address correspondence to Xuan Zhang, MD, 1 Shuai-Fu-Yuan, Dong-Cheng District, Beijing, China, 100730 (email: zxpumch2003@sina.com); or to Jun Wang, PhD, No. 1 Beichen West Road, Chaoyang District, Beijing, China, 100101 (email: junwang@im.ac.cn); or to George C. Tsokos, MD, 330 Brookline Avenue, Boston, MA 02115 (email: gtsokos@bidmc.harvard.edu).

Submitted for publication July 14, 2020; accepted in revised form August 27, 2020.

Microbiota residing in the gastrointestinal tract are affected by factors like diet and geography (2). There are complex interactions between microbiota and the host, and the establishment of gut microbiota is closely implicated with the development and function of the host immune system (3). Disturbed gut microbiota, in which the microbial configuration of gut content is significantly different from that of healthy subjects, was found in several autoimmune diseases, including rheumatoid arthritis (RA) (4), ankylosing spondylitis (5), and Behçet's disease (6). Recent reports have described increased growth of certain bacteria in the gut of SLE patients (7–10), which suggests a possible link between gut bacterial imbalance and SLE development. Different cellular and molecular mechanisms have been proposed to explain the contribution of microbiota to the expression of autoimmunity, including aberrant microbial translocation, antigen mimicry, and disturbed immune responses dictated by microbial metabolites (11–13).

Early reports on the microbiota found in the gut of SLE patients were based on 16S ribosomal RNA (rRNA) gene amplicon sequencing. With the evolution of technology, shotgun metagenomic sequencing can provide better genomic coverage with detailed functional information (14). We applied shotgun metagenomic profiling to assess individuals with untreated SLE, and our results demonstrate the expansion of unique species that define peptides mimicking known autoantigens that are able to instigate inflammation. In addition, we show that the gut microbiota in SLE patients can originate from the mouth and that they share metabolic, rather than taxonomic, features with the gut microbiota of MRL/lpr lupus-prone mice, the classic SLE mouse model (15).

MATERIALS AND METHODS

Study design. This study was approved by the Institutional Review Board of Peking Union Medical College (PUMC) Hospital (ethics review no. JS-1239). Written informed consent was obtained from all human subjects. For this study, 117 individuals with untreated SLE, who had not received any steroids or immunosuppressive drugs for the last 3 months, were recruited from PUMC. All patients met the American College of Rheumatology revised criteria for SLE (16). The SLE Disease Activity Index 2000 (SLEDAI-2K) (17) was used to evaluate disease activity. Investigators also enrolled 115 sex- and age-matched healthy controls. Subjects were excluded if they had 1) antibiotic treatment within 3 months before sample collection, 2) current evidence of any acute or chronic inflammatory or infectious diseases, 3) severe major systemic disease, including malignancy, or 4) any other autoimmune disease. All participants were of Han Chinese ethnicity. Clinical data were collected within 1 week prior to fecal sample collection. Both data and first sample collection were completed before these untreated SLE patients began receiving therapy.

Demographic characteristics and clinical meta-data are listed in Supplementary Table 1, available on the *Arthritis & Rheumatology* website at <http://onlinelibrary.wiley.com/doi/10.1002/art.41511/abstract>. Among the SLE patients who had already initiated therapy at the time of sample and data collection, the medications being administered included steroids (73.1%; prednisone or methylprednisolone), hydroxychloroquine (78.8%), and immunosuppressive drugs (44.2%; mycophenolate mofetil, cyclophosphamide, leflunomide, or methotrexate).

For the animal studies, 5–6-week-old female MRL/lpr mice ($n = 9$) and age-matched female MRL/MpJ mice ($n = 11$) were purchased from SLAC Laboratory or the Institute of Laboratory Animal Sciences. The mice were housed in a specific pathogen-free environment at PUMC Hospital according to the institutional husbandry standard until 17 weeks of age, at which point their fecal samples were collected. The protocol for animal experiments was approved by the Institutional Animal Care and Use Committee of PUMC Hospital, and the study was conducted in accordance with institutional guidelines.

Sample collection and processing. Fecal samples were collected in a sterile stool container, frozen at -80°C within 2 hours of sample collection, and then transported in dry ice prior to extraction (Novogene Bioinformatics Technology) using a TIANGEN kit according to the manufacturer's instructions. Agarose gel electrophoresis was used to monitor DNA purity and integrity. Samples with an optical density at 260/280 nm of between 1.8 and 2.0 and a DNA level of $>1 \mu\text{g}$ were used for library construction.

Shotgun sequencing and metagenomic analyses. DNA from fecal samples was extracted and sequenced on an Illumina HiSeq platform, and paired-end reads of 250-bp nucleotides were generated. To ensure comparability, 28 and 24 million paired-end reads, for human samples and mouse samples, respectively, were randomly extracted from the preprocessed data in each direction. After quality control (KneadData), DNA reads were assessed for taxonomic and functional differences using MetaPhlan2 annotations (18). Diversity analyses were performed using R program version 3.5.1, and taxonomic and functional differences were analyzed using LEfSe metagenomic discovery analysis (19). StrainPhlan strain-level analyses for the oral origin of gut microbiota in SLE patients were based on the single-nucleotide polymorphisms (SNPs) found for each species from the sequencing data. Raw data from metagenomic sequencing are available in the Sequence Read Archive under BioProject ID PRJNA532888 (human cohort) and PRJNA591036 (mice).

Molecular mimicry analysis. *Extraction of epitopes.* Autoantigen epitopes that were reported to trigger autoimmune reactions in SLE patients were identified from the Immune Epitope Database (IEDB) (<http://www.iedb.org/>). The amino acid sequences of these epitopes were mapped using

BLAST (20) to the protein sequences of the species that were significantly abundant in SLE gut microbiota selected by LEfSe analysis. Only results with both identity and coverage of $\geq 80\%$ were considered for further experimental examination.

Enzyme-linked immunospot (ELISpot) assay. Heparinized blood samples were obtained from participants with SLE at PUMC Hospital. Patient peripheral blood mononuclear cells (PBMCs) were isolated by Ficoll-Hypaque density gradient centrifugation. Interferon- γ (IFN γ) and interleukin-17A (IL-17A) ELISpot assays were performed using a Human ELISpot^{plus} kit (MabTech) according to the manufacturer's instructions. Briefly, 96-well MultiScreen Filter Plates (Millipore) precoated with capture antibody were washed 5 times with phosphate buffered saline (PBS) and blocked with 10% fetal bovine serum (FBS) for at least 30 minutes at room temperature before use. Duplicates of $2-5 \times 10^5$ PBMCs per well were plated with different peptides and incubated overnight for 20–24 hours. Human anti-HLA-DR microbeads (Miltenyi Biotec) were used to eliminate HLA-DR-positive cells from PBMCs, and the numbers of cells plated in these groups were controlled to ensure that the same amounts were used for all groups before cell sorting. Plates were then washed 5 times with PBS, and then 1 $\mu\text{g/ml}$ of anti-human IFN γ monoclonal antibody (mAb) (7-B6-1-Biotin) or 0.5 $\mu\text{g/ml}$ of anti-human IL-17A mAb (MT504-Biotin) was added and incubated for 2 hours.

Each plate was then washed 5 times with PBS and incubated for 1 hour with streptavidin-horseradish peroxidase, followed by being washed 5 times with PBS and developed with 0.45 μm -filtered tetramethylbenzidine substrate for 10–20 minutes. The reaction was stopped by rinsing extensively with deionized water, and plates were left to dry. Antigen-specific IgG ELISpot assays were performed using a Human IgG ELISpot^{BASIC} kit (MabTech). PBMCs were first prestimulated with a mixture of 1 $\mu\text{g/ml}$ of R848 and 10 ng/ml of recombinant human IL-2 for 96 hours, promoting the ability of memory B cells to secrete detectable IgG. The ELISpot plates were coated with anti-human IgG (mAb MT91/145) overnight at 4°C. After washing and blocking with 10% FBS, duplicates of $2-5 \times 10^5$ PBMCs were plated in the coated ELISpot plates for 36 hours. Plates were washed with PBS, and then 1 $\mu\text{g/ml}$ of biotinylated peptides were added and incubated for 2 hours. Subsequent operations were consistent with the above processes. Plates were finally scanned and enumerated using an ImmunoSpot plate reader (Cellular Technology Limited). Each well was scored positive if the number of spot-forming cells detected was at least twice the number found in the negative control (randomly synthesized peptides).

Statistical analysis. Significantly enriched taxa and pathways between different groups were ascertained by LEfSe analyses. Wilcoxon's rank sum tests and Kruskal-Wallis tests were used to determine the significance of differences in alpha diversity between 2 groups and among multiple groups, respectively. In order to

determine significant differences in the distribution of gut microbiota between groups, permutational multivariate analysis of variance (PERMANOVA) was conducted, using the function "adonis" in the R package vegan (permutation number 999). Fisher's exact test was used for the determination of whether the SLE or healthy control fecal samples had a higher homology with the oral samples in a specific species. One-way ANOVA of repeated measures was utilized to calculate significant differences in the results of ELISpot assays between the groups. The tests listed above were conducted using either R version 3.5.1 or GraphPad Prism version 7.0. All statistical analyses in our study were performed using a 2-sided test.

RESULTS

Diversity analysis of SLE gut microbiota and association with clinical indices. To characterize the signatures of the microbiota found in the gut of SLE patients, fecal samples from 117 individuals with untreated SLE and 115 age- and sex-matched healthy controls were analyzed using metagenomic shotgun sequencing. Clinical information for the study population is summarized in Supplementary Table 1, available on the *Arthritis & Rheumatology* website at <http://onlinelibrary.wiley.com/doi/10.1002/art.41511/abstract>. Fecal samples from 52 patients who were willing to provide a second sample after treatment were also collected for comparison. Disease activity in these patients as measured by the most widely used disease activity index in SLE, the SLEDAI-2K (17), was significantly decreased following treatment ($P < 0.0001$) (Supplementary Figure 1, available on the *Arthritis & Rheumatology* website at <http://onlinelibrary.wiley.com/doi/10.1002/art.41511/abstract>). Fecal DNA was sequenced on an Illumina HiSeq platform, and a minimum of 56 million reads after quality filtering and removal of host DNA were obtained for each sample and then analyzed using MetaPhlan2 (21) and HUMAnN2 (22) to derive data on microbial composition and function. Among all 284 samples, 597 species and 512 MetaCyc pathways were obtained.

Shannon diversity index scores (considering both microbial richness and evenness), but not the number of species observed, were significantly lower in patients with untreated SLE compared to healthy controls ($P = 0.016$) (Figure 1A and Supplementary Figure 2A, available on the *Arthritis & Rheumatology* website at <http://onlinelibrary.wiley.com/doi/10.1002/art.41511/abstract>). Shannon diversity index scores continued to decrease after effective treatment ($P = 0.044$) (Supplementary Figure 2B). Intriguingly, the primary source of decline in Shannon index scores was observed in the SLE subgroup with lupus nephritis (adjusted $P = 0.006$) (Figure 1B). The reduction in Shannon diversity index scores could also be partly attributable to a decrease in scores in the SLE subgroup who had a shorter disease duration (within 1 year) and those who were negative for anti-double-stranded DNA (anti-dsDNA) antibodies (adjusted $P = 0.027$ and 0.038, respectively) (Supplementary Figure 2C).

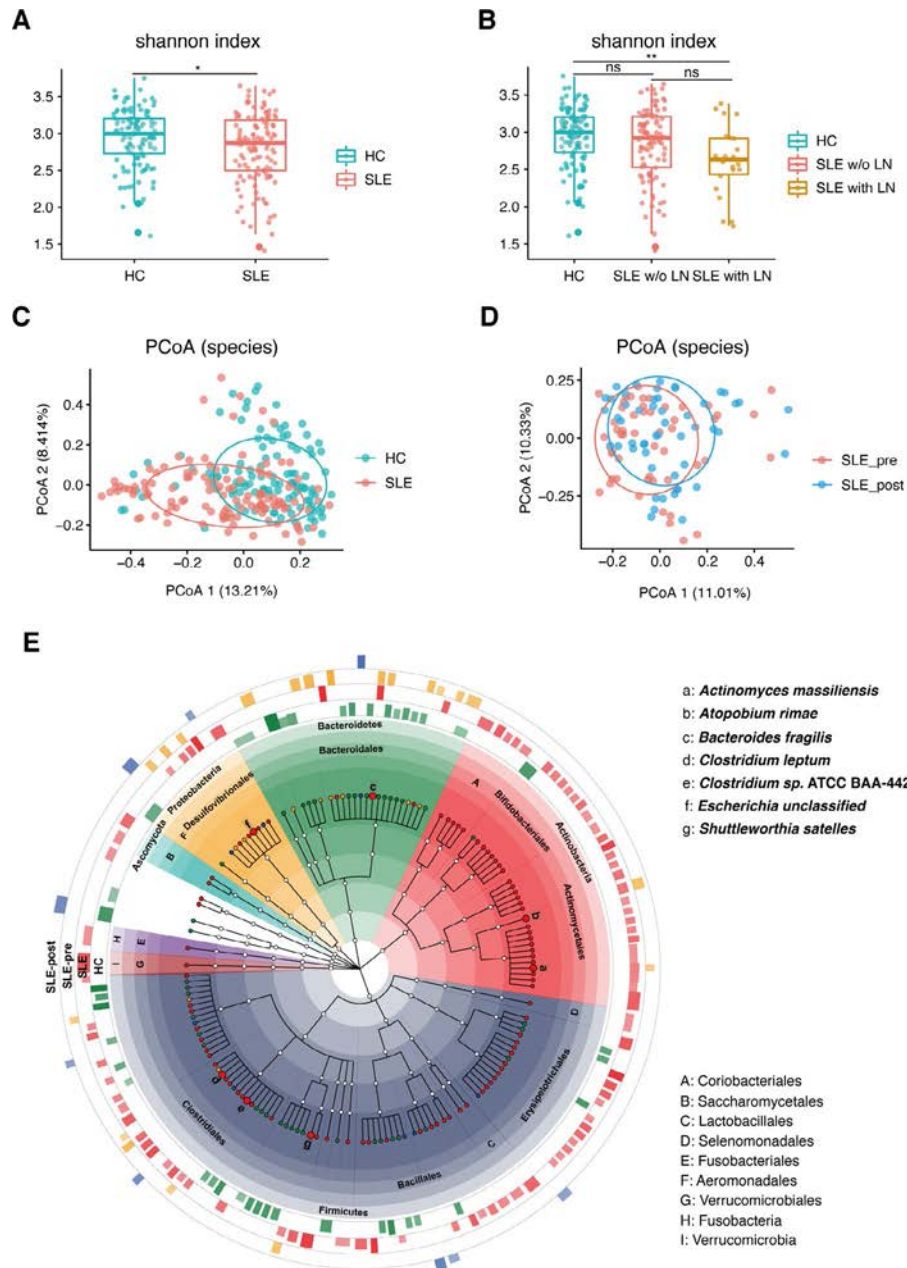


Figure 1. Taxonomic analyses of the fecal microbiota in patients with systemic lupus erythematosus (SLE). **A** and **B**, Alpha diversity analyses of Shannon diversity index scores in 115 healthy controls (HCs) compared to 117 SLE patients (**A**) and in 115 healthy controls compared to 22 SLE patients with lupus nephritis (LN) and 95 SLE patients without lupus nephritis (**B**). Data are shown as box plots. Each box represents the upper and lower interquartile range. Lines inside the boxes represent the median. Lines outside the boxes represent the 95% confidence interval for the medians. Each symbol represents an individual fecal sample. * = $P < 0.05$; ** = $P < 0.01$, by 2-tailed Wilcoxon's rank sum test and Kruskal-Wallis test for multiple group comparisons. **C** and **D**, Beta diversity analyses of Bray–Curtis similarity index scores of microbial species (sp.) between 115 healthy controls and 117 SLE patients (**C**) and between 52 pre-treatment (SLE_pre) and post-treatment (SLE_post) fecal samples from SLE patients (**D**). **E**, Taxonomic tree of all differentially enriched species. Each circular sector filled by a different color represents a single phylum. Bar plots outside the central circle depict the group in which a specific species was enriched and how big the linear discriminant analysis score was for that species. Species that were observed to be increased in SLE patients and decreased after treatment are shown as large red dots. NS = not significant; PCoA = principal coordinates analysis.

Analysis of Bray–Curtis distance based on species-level composition (using β diversity analysis) revealed different microbiota profiles between SLE patients and healthy controls (R^2 with the function *adonis* = 0.030, $P = 0.001$) (Figure 1C and

Supplementary Table 2, available on the *Arthritis & Rheumatology* website at <http://onlinelibrary.wiley.com/doi/10.1002/art.41511/abstract>). A trend that was more similar to the control group was demonstrated in the distribution of posttreatment samples only

(R^2 with the function *adonis* = 0.014, P = 0.086) (Figure 1D and Supplementary Figure 2D), partially due to the high within-group variability in SLE samples (Supplementary Figure 2E), an observation also reported by other investigators (8). Clinical indices, including scores for the severity of lupus nephritis, malar rash, arthritis, disease activity, and disease duration and levels of anti-dsDNA antibody, anti-Sm antibody, and anti-RNP antibody could not alone explain the taxonomic variation in the SLE samples (Supplementary Table 3, available on the *Arthritis & Rheumatology* website at <http://onlinelibrary.wiley.com/doi/10.1002/art.41511/abstract>). Further analyses that included SLE-related clinical parameters revealed a significant correlation between the platelet counts and creatinine levels in the blood of SLE patients and the variation in SLE gut microbiota (R^2 with the function *adonis* = 0.018, P = 0.045 for platelet count; R^2 with the function *adonis* = 0.019, P = 0.037 for creatinine level) (Supplementary Figure 3A and Supplementary Table 4, available on the *Arthritis & Rheumatology* website at <http://onlinelibrary.wiley.com/doi/10.1002/art.41511/abstract>). Levels of creatinine also correlated significantly with

gut microbiota variation in all study participants (R^2 with the function *adonis* = 0.008, P = 0.037) (Supplementary Figure 3B).

Taxonomic and functional signatures in SLE gut microbiota. To elucidate the key microbial taxa that contribute to the variation of SLE gut microbiota, linear discriminant analysis (LDA) of effect size, which was ascertained using LefSe metagenomic discovery analysis, was performed to determine the relative abundance of taxa using a cutoff LDA value of >2.0 (19). Correlations between the relative abundance of species that were significantly differentiated and clinical meta-data were also determined, using Spearman's correlation coefficients with 95% confidence intervals (95% CIs) (Supplementary Figure 4, available on the *Arthritis & Rheumatology* website at <http://onlinelibrary.wiley.com/doi/10.1002/art.41511/abstract>), and only taxa that were differently distributed between SLE patients and healthy controls were included.

Seven marker species were found to be enriched in SLE patients and reduced after treatment, including *Clostridium* species ATCC BAA-442 as well as *Atopobium rimae*, *Shuttleworthia satelles*, *Actinomyces massiliensis*, *Bacteroides fragilis*,

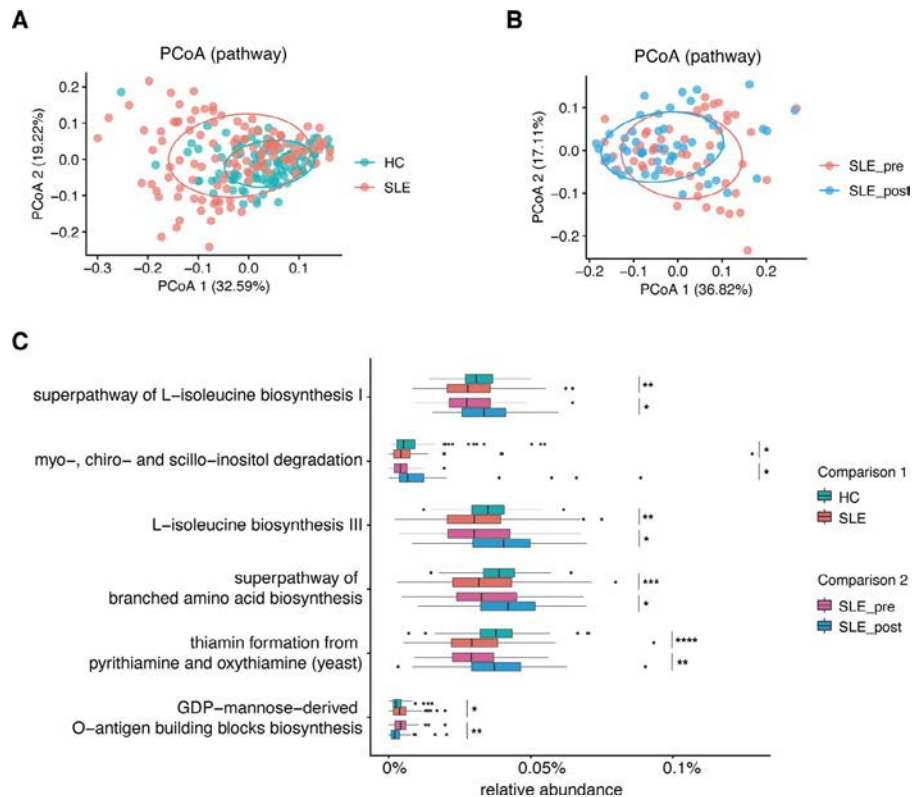


Figure 2. Functional analyses of the fecal microbiota in patients with SLE. **A** and **B**, Beta diversity analyses of Bray-Curtis similarity index scores of microbial pathways between 117 SLE patients and 115 healthy controls (**A**) and between 52 SLE patients pretreatment and 52 SLE patients posttreatment (**B**). **C**, Microbial pathways that were significantly different between SLE patients and healthy controls (Comparison 1) and pathways that were reversed in fecal samples from SLE patients following treatment (Comparison 2) that were evaluated using linear discriminant analysis effect size analysis, which was ascertained using LefSe metagenomic discovery analysis. In **C**, data are shown as box plots. Each box represents the upper and lower interquartile range. Lines inside the boxes represent the median. Lines outside the boxes represent the 95% confidence interval for the medians. Each symbol represents an individual fecal sample. * = P < 0.05; ** = P < 0.01; *** = P < 0.001; **** = P < 0.0001. See Figure 1 for definitions. Color figure can be viewed in the online issue, which is available at <http://onlinelibrary.wiley.com/doi/10.1002/art.41511/abstract>.

Clostridium leptum, and an unclassified *Escherichia* (Figure 1E and Supplementary Tables 5 and 6, available on the *Arthritis & Rheumatology* website at <http://onlinelibrary.wiley.com/doi/10.1002/art.41511/abstract>). Among these species, the relative abundance of *Clostridium* species ATCC BAA-442 positively correlated with the SLEDAI score ($R = 0.196$, [95% CI 0.010–0.369], $P = 0.034$). In addition to the aforementioned species, *Lactobacillus salivarius* was enriched in SLE patients and positively correlated with SLEDAI scores ($R = 0.228$ [95% CI 0.043–0.398], $P = 0.013$) and disease duration ($R = 0.198$ [95% CI 0.011–0.371], $P = 0.033$). *Ruminococcus gnavus* was the most discriminative species enriched in patients with lupus nephritis, followed by *Clostridium nexile*, *Olsenella uli*, *Actinomyces johnsonii*, *Staphylococcus aureus*, and *Enterococcus avium* (Supplementary Figure 5, available on the *Arthritis & Rheumatology* website at <http://onlinelibrary.wiley.com/doi/10.1002/art.41511/abstract>).

HUMAN2 was used to generate the functional profile of gut microbiota, and it was found that microbial pathways differed substantially in SLE patients compared to those in healthy

controls (R^2 with the function *adonis* = 0.047, $P = 0.001$) (Figure 2A). Functional patterns also changed significantly after treatment ($R^2 = 0.023$, $P = 0.029$) (Figure 2B). The superpathways of GDP-mannose-derived O-antigen building blocks biosynthesis were increased in SLE patients and then reduced following treatment (Figure 2C and Supplementary Tables 7 and 8, available on the *Arthritis & Rheumatology* website at <http://onlinelibrary.wiley.com/doi/10.1002/art.41511/abstract>). The relative abundances of 5 other pathways were lower in SLE patients and were significantly reversed after treatment (Figure 2C). Among them, 3 pathways were associated with branched chain amino acids (BCAAs), including the superpathways of branched amino acid biosynthesis, L-isoleucine biosynthesis I, and L-isoleucine biosynthesis III.

Shared microbial changes between SLE patients and lupus-prone mice.

Metagenomic profiling was further performed in lupus-prone MRL/lpr mice (15). This analysis included fecal samples from 9 female MRL/lpr mice and 11 female MRL/MpJ mice (the control strain) at 17 weeks of age, the time of

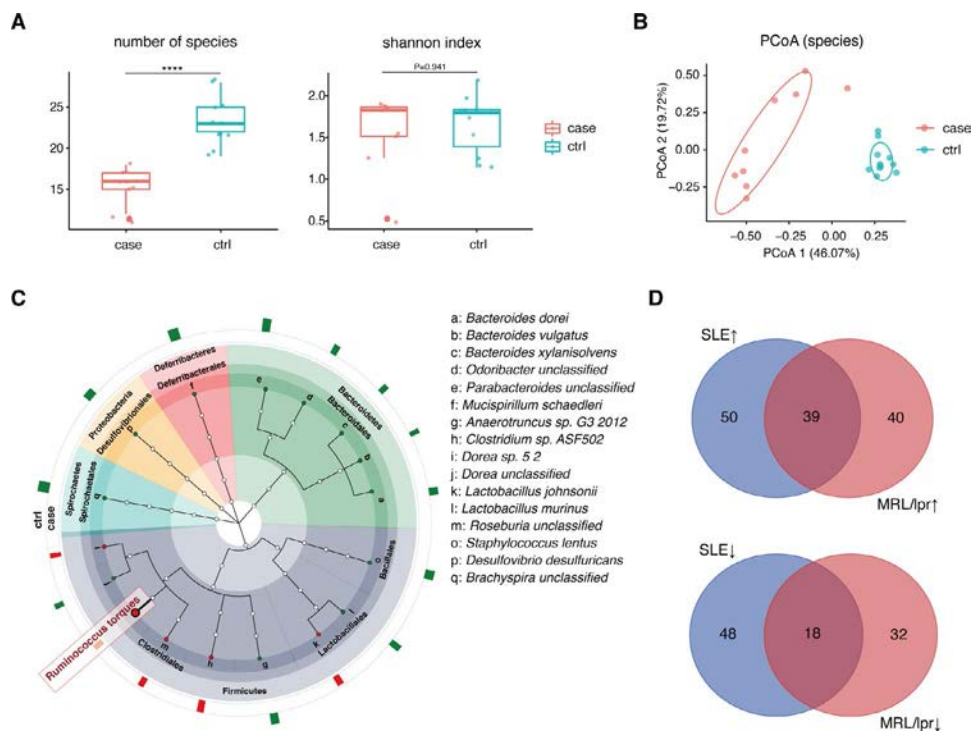


Figure 3. Metagenomic analyses of the fecal microbiota in MRL/lpr mice. **A**, Alpha diversity, characterized by the number of species and Shannon diversity index scores, in 17-week-old MRL/lpr mice (case) ($n = 9$) and MRL/MpJ mice (control [ctrl]) ($n = 11$). Data are shown as box plots. Each box represents the upper and lower interquartile range. Lines inside the boxes represent the median. Lines outside the boxes represent the 95% confidence interval for the medians. Each symbol represents a single mouse. **** = $P < 0.0001$ by Wilcoxon's 2-tailed rank sum test. **B**, Beta diversity analyses of the Bray–Curtis similarity index of microbial species between MRL/lpr mice and MRL/MpJ mice. Permutational multivariate analysis of variance was performed with a permutation number of 999, and significance levels are shown on plots. **C**, Taxonomic tree of all differentially enriched species. Each circular sector filled by a different color represents a single phylum. Bar plots outside the central circle depict the group in which a specific species was enriched and how big the linear discriminant analysis score was. Phyla and orders are labeled on the plot. Species that were increased in both SLE patients and MRL/lpr mice are shown as large red dots with the species name in boldface. **D**, Venn plots showing the overlap between MetaCyc pathways enriched with SLE gut microbiota and those enriched with MRL/lpr mouse gut microbiota, as well as the overlap between MetaCyc pathways with decreased SLE gut microbiota and decreased MRL/lpr mouse gut microbiota. See Figure 1 for other definitions. Color figure can be viewed in the online issue, which is available at <http://onlinelibrary.wiley.com/doi/10.1002/art.41511/abstract>.

peak disease development. From all 20 samples, each with 48 million reads, 48 species and 383 MetaCyc pathways were obtained. The number of species observed was notably decreased in mice with lupus ($P = 0.0002$), while the Shannon diversity index showed no noticeable difference ($P = 0.941$) (Figure 3A). The β diversity among mice with lupus was significantly different from that among control mice (R^2 with the function *adonis* = 0.406, $P = 0.001$),

with more dispersed β diversity in lupus samples compared to controls (Figure 3B).

Taxonomic analysis revealed 5 up-regulated species and 12 down-regulated species in MRL/lpr mice (Figure 3C). Among these species, *Ruminococcus torques* was increased in the fecal samples from both SLE patients and mice with lupus. The genus *Desulfovibrio* was decreased whereas *Blautia* was increased in

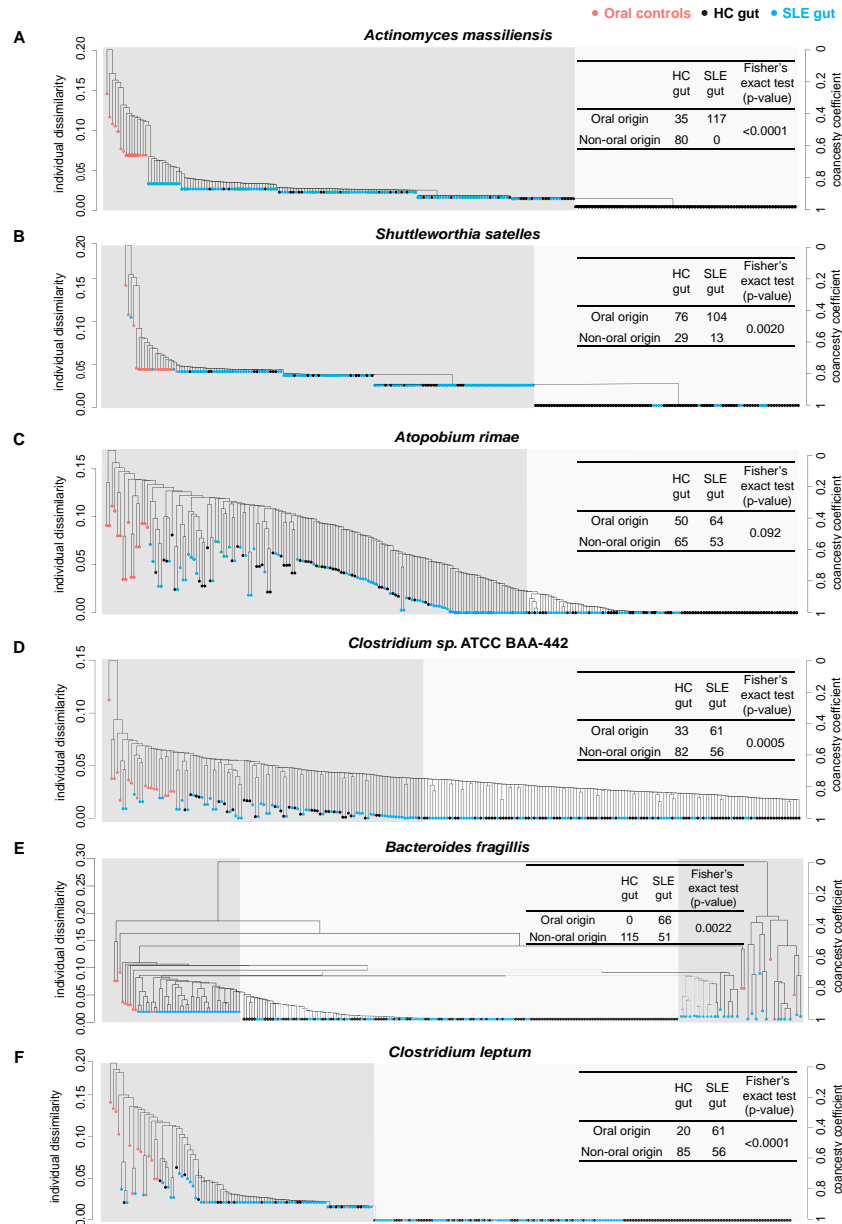


Figure 4. Oral origin of enriched species in patients with SLE. Phylogenetic trees of the 3 marker species related to oral inflammation (A–C) and the other 3 marker species with definite phylogeny (D–F), based on the single-nucleotide polymorphisms from each species in 16 oral samples from an independent healthy cohort, 115 fecal samples from healthy controls, and 117 fecal samples from SLE patients, are shown. Each point represents a single sample, and the color of the points denotes the grouping (red for oral samples from healthy controls, black for fecal samples from healthy controls, and blue for fecal samples from SLE patients). Ancestor oral branches are shown on the left with a dark gray–shaded background, and outliers are shown on the right with a light gray–shaded background. Significance levels were calculated using Fisher's exact test, with detailed information included in the panels as tables. See Figure 1 for definitions. Color figure can be viewed in the online issue, which is available at <http://onlinelibrary.wiley.com/doi/10.1002/art.41511/abstract>.

the gut of both SLE patients and MRL/lpr mice. Intriguingly, SLE patients and mice with lupus shared a lot more signatures in pathway analysis based on DNA reads. Among all 383 coexisting pathways, 39 were commonly enriched, whereas 18 were commonly reduced (Figure 3D and Supplementary Tables 9 and 10, available on the *Arthritis & Rheumatology* website at <http://onlinelibrary.wiley.com/doi/10.1002/art.41511/abstract>). Pathways of L-arginine and L-ornithine biosynthesis, tryptophan biosynthesis, menaquinol biosynthesis, palmitoleate and oleate biosynthesis, and phosphatidylglycerol biosynthesis, as well as purine nucleotide salvage and degradation, were discovered to be positively correlated with lupus. Conversely, pathways of peptidoglycan biosynthesis and BCAA biosynthesis were found to be negatively correlated with lupus.

Oral origin of gut microbes in SLE patients. Among the 7 marker species that were enriched in the gut of SLE patients and decreased after treatment, *A massiliensis*, *S satelles*, and *A rimae* were species initially isolated from the human oral cavity and found to be closely related to oral inflammation (23–25). Thus, their enrichment in the gut lumen of SLE patients implies a possible translocation from the oral cavity. To confirm this hypothesis,

a strain-level analysis of those species was carried out based on SNPs using the salivary metagenome from another healthy cohort (n = 16) (4) and the fecal metagenome of our healthy controls and our SLE cohort. Phylogenetic trees were constructed for not only the oral inflammation-related species, but also other marker species (Figures 4A–F). The exact number of gut samples that clustered with oral samples was calculated, using samples from both the SLE patients and healthy controls. The strains of *A massiliensis*, *S satelles*, *Clostridium* species ATCC BAA-442, *B fragilis*, and *C leptum* in the oral samples had a closer relationship to those in the gut of SLE patients compared to those in the gut of healthy controls, indicating that the enriched species in the gut microbiota of SLE patients partly came from the oral microbiota. The enrichment of various oral species in the feces of SLE patients compared to that of healthy controls suggests an increased overall transmission rate of salivary microbes to the gut in SLE.

Molecular mimicry of microbial peptides from SLE-enriched species. The fact that microbial peptides can trigger autoimmune responses by mimicking autoantigens has been proposed as a critical mechanism by which gut microbiota could affect SLE development (26). In order to unveil some new microbial

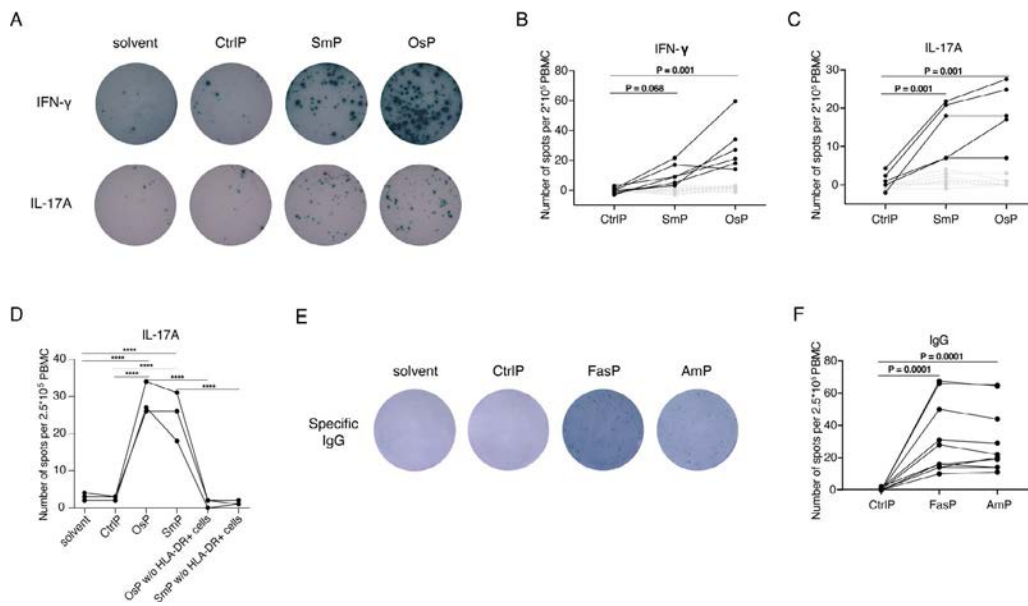


Figure 5. Molecular mimicry of species enriched with systemic lupus erythematosus (SLE) gut microbiota. **A–D**, Peripheral blood mononuclear cells (PBMCs) obtained from 21 SLE patients were plated in enzyme-linked immunospot (ELISpot) plates and stimulated by different peptides (SmP [ILQDGRIFI from Sm B/B ’], OsP [LYDGRIFI from *Odoribacter sp*], and CtrlP [a randomly synthesized peptide, ILKEPVHGV]). The numbers of interferon- γ (IFN- γ)-producing cells and interleukin-17A (IL-17A)-producing cells were then detected by ELISpot. Examples of the ELISpot results are shown in **A**. The number of spots detected for the existence of IFN γ -producing cells (**B**) and IL-17A-producing cells (**C**) in different peptide stimulation groups and for the existence of IL-17A-producing cells in the absence or presence of HLA-DR-positive cells (n = 3) (**D**) were determined. **E** and **F**, PBMCs obtained from 23 SLE patients were first prestimulated with a mixture of R848 and recombinant IL-2 for 96 hours, and then plated in the ELISpot plates for 36 hours to produce IgG. The cells that produced IgG capable of binding the peptides (FasP [DGQFCH from Fas], AmP [DGQFCM from *Akkermansia muciniphila*], and CtrlP [a randomly synthesized peptide, DTYESE]) were then detected. Examples of IgG ELISpot results are shown (**E**), as is the number of spots detected for the existence of peptide-specific IgG-producing cells (**F**). **** = $P < 0.0001$. In **B**, **C**, **D**, and **F**, black circles and solid lines represent the samples that were reactive with autoimmune and microbial peptides; gray circles and broken lines represent those that were not reactive. All spots were counted by subtracting the spot number of the solvent controls. Significant differences were calculated by one-way analysis of variance and only included samples that were reactive for the autoepitopes. Color figure can be viewed in the online issue, which is available at <http://onlinelibrary.wiley.com/doi/10.1002/art.41511/abstract>.

peptides that may accentuate SLE, autoantigen peptides that were demonstrated to trigger autoimmune responses in SLE patients from the IEDB were retrieved, including those confirmed by T or B cell assays, and then compared to the genome sequences of species enriched in patients with untreated SLE or species that were decreased after treatment.

To identify mimicry peptides with autoimmunogenic ability, new cohorts of SLE patients and healthy controls were recruited, and PBMCs were collected for analysis. Using ELISpot assay, we demonstrated that the peptide YLYDGRIFI of the IS66 family transposase from *Odoribacter splanchnicus*, similar to the autoepitope ILQDGRIFI of human Sm B/B' antigen presented to T cells by HLA-DR (27), was capable of increasing levels of IFN γ and IL-17A secretion from the PBMCs of a subgroup of anti-Sm-positive SLE patients (6 of 21 [IFN γ] and 5 of 21 [IL-17A]) (Figures 5A and B). Although *O splanchnicus* was not enriched in SLE patients, it was significantly reduced after treatment (Supplementary Figure 6A, available on the *Arthritis & Rheumatology* website at <http://onlinelibrary.wiley.com/doi/10.1002/art.41511/abstract>). To further explore whether the proinflammatory cytokine-producing ability could be attributed to non-specific stimulation or whether it might be dependent on the presentation of HLA, we eliminated HLA-DR-positive cells from the PBMCs and found that the residual cells no longer secreted IL-17A when challenged with either YLYDGRIFI or ILQDGRIFI (Figure 5C). However, PBMCs from some healthy controls also were able to trigger the secretion of inflammatory cytokines (Supplementary Figure 6B).

Peptide DGQFCM, mimicking the extracellular part DGQFCH of human Fas (28), was from *Akkermansia muciniphila*, an enriched species in SLE patients (Supplementary Figure 6C). This peptide was capable of specifically binding to IgG produced by the memory B cells from a subgroup of SLE patients (10 of 23) (Supplementary Figures 5D and E), but showed little ability to bind to IgG produced by memory B cells from healthy controls (1 of 7). To support the potential immunopathogenic role of *A muciniphila* in SLE, the fecal abundance of this species has been shown to be positively correlated with the blood levels of IgA and IgM and the erythrocyte sedimentation rate (ESR), all characteristics of inflammation, in SLE patients (Supplementary Table 4, available on the *Arthritis & Rheumatology* website at <http://onlinelibrary.wiley.com/doi/10.1002/art.41511/abstract>).

DISCUSSION

Deep metagenomic shotgun sequencing revealed substantial alterations in the gut microbiota and autoimmunogenic signatures of patients with SLE. We found significantly reduced alpha diversity of SLE gut microbiota, which has been previously reported using amplicon sequencing (8). Further reductions in microbial diversity observed in the SLE patients after treatment was probably a result of the type of medication used, as some therapies commonly

used to treat patients with SLE (such as steroids, methotrexate, and leflunomide) can inhibit the growth of certain gut bacteria and have previously been associated with reduced diversity of gut microbiota (29,30). In spite of the large within-group variability, a distinct taxonomic distribution pattern was still observed in SLE patients compared to healthy controls. The fact that posttreatment gut microbial composition in SLE patients was more similar to that in healthy controls demonstrated a recovery of gut microbiota linked with disease improvement. Serum creatinine levels were found to explain the microbial variations, and patients with lupus nephritis had much lower alpha diversity of the gut, both supporting an interplay between renal function and gut ecology in SLE (31). Despite the fact that PERMANOVA is one of the most commonly used methods for analyzing the variance of distance matrices of microbiota, it is noteworthy that this method is sensitive to assumptions and that it might lead to false-positive results.

Several marker species that were enriched in SLE patients who had not received treatment were found to be decreased in SLE patients after treatment, indicating that these species might be involved in disease etiology. The abundance of *Clostridium* species ATCC BAA-442 positively correlated with SLEDAI score. It can metabolize daidzein, an isoflavone that has been previously shown to ameliorate the inflammation of lupus-prone mice by binding to estrogen receptor β (32), into *O*-demethylangolensin (33), and thus may contribute to SLE by reducing daidzein. A subgroup of strains from *B fragilis*, another marker species, can produce specific *B fragilis* toxins capable of increasing gut permeability (34) and activating Th17 response (35). An expansion of *R gnavus* was previously reported in patients with lupus nephritis, and antibodies against its lipoglycan in SLE serum were associated with disease activity and anti-dsDNA antibody levels (8). *R gnavus* was also among the most increased species in patients with lupus nephritis in our cohort, accentuating its role in renal damage.

We further identified changed metabolic pathways implicated in SLE development from our metagenomic data. For instance, the biosynthesis of O-antigen, the outermost domain of lipopolysaccharide (LPS), was increased in SLE patients and decreased after treatment. An increased O-antigen synthesis indicates elevated LPS levels in the gut, consistent with the elevated serum LPS levels observed in serum from SLE patients (36). In contrast, pathways related to the biosynthesis of BCAAs, a group of metabolites capable of attenuating adaptive immunity (37), were reduced in SLE patients and restored after treatment.

Metagenomic data on mice with lupus were analyzed and found to corroborate findings in SLE patients. *R torques*, the species enriched in both lupus patients and mice with lupus, is an effective mucin degrader that has been reported to be increased in patients with inflammatory bowel disease (38). Although *R torques* has not yet been implicated in the expression of SLE, its role in degrading mucin makes it a potential contributor to lupus by impairing the gut barrier. The small number of species that changed in both SLE patients and lupus-prone mice

could be due to the limited overlapping microbes present in human and specific pathogen-free mice. Therefore, it was intriguing that the functional changes in SLE patients and lupus-prone mice had a higher proportion of overlapping microbes. Pathways related to the synthesis of arginine, ornithine, tryptophan, menaquinols, palmitoleate, oleate, and phosphatidylglycerol, as well as pathways of purine nucleotide salvage and degradation, were all enriched in both lupus patients and mice with lupus. Arginine can be metabolized into inflammation-related metabolites, including ornithine and nitric oxide (39). Tryptophan metabolites such as indoles, kynurenine, and tryptamine are the ligands of aryl hydrocarbon receptor that mediate gut barrier protection and inflammation reduction (40). Palmitoleate and oleate are both monounsaturated fatty acids with antiinflammatory ability in macrophages, neutrophils, and endothelial cells (41). The metabolites associated with these pathways may either contribute to the development of lupus-related autoimmunity or represent a reflection of altered microbial metabolism resulting from aberrant lupus immunopathology. These exciting but hard-to-interpret findings justify advanced fecal and serum metabolomic profiling, exploration of local pathologic tissues, and in-depth mechanism investigation.

Oral dysbiosis has recently been observed in SLE patients (42,43). Although there has been evidence of increased microbial transmission from the oral cavity to the gut in patients with RA (44), a similar finding has not been reported in SLE patients yet. Among the marker species enriched in the gut of patients with SLE and reduced following treatment, we discovered 3 pathogens initially associated with oral inflammation. Salivary metagenomic data of healthy subjects from our previous cohort (4) were included to perform the SNP-based analyses. By investigating whether our SLE or control gut samples were more similar to the independent oral samples from the healthy subjects, we provided evidence of increased microbial transmission along the gastrointestinal tract of most of our marker species in SLE patients compared to healthy controls. These findings implicate a damaged barrier in the upper gastrointestinal tract in SLE patients, making it easier for the transmissible oral species to colonize the gut.

By sequencing alignment and *in vitro* experiments, we identified 2 microbial peptides that triggered immune activation via molecular mimicry. Microbial peptide YLYDGRIFI defined by *O. splanchnicus*, mimicking the Sm epitope confirmed by T cell assays, stimulated PBMCs from patients with SLE to secrete IFN γ and IL-17A in an HLA-DR-dependent manner. Sm antibody is the most specific autoantibody found in SLE patients thus far, and IFN γ and IL-17A have long been implicated in the pathogenesis of SLE (45). Although the immune cells from healthy subjects could also be stimulated by this peptide, it is rational to postulate that SLE patients had a better chance of being exposed to this peptide because of impaired gut integrity (8). For example, *Enterococcus gallinarum* was detected in the liver biopsy tissue from

SLE patients and was proved to cross the gut barrier and induce autoimmunity in mice with lupus (12).

We also discovered that the peptide DGQFCM from *A muciniphila*, which had a similar sequence with a Fas autoepitope, could bind to IgG secreted by the memory B cells from SLE patients, but not those of healthy controls (46). *A muciniphila* is a commonly known probiotic, though its gut enrichment has been reported in multiple sclerosis, and it has been shown as capable of stimulating Th1 differentiation (47). *A muciniphila* has been shown to be enriched in the SLE gut and has been shown to be positively correlated with the blood levels of IgA and IgM and the ESR. Although the clinical significance of Fas antibodies is not clear in SLE, it has been reported that these antibodies are present in the sera of some SLE patients (28) and capable of promoting apoptosis in both lymphocytes and keratinocytes (48,49). Our experiments on the molecular mimicry of the newly found microbial peptides in SLE patients were still preliminary, especially given the fact that we did not validate them *in vivo* as was the case in the study of molecular mimicry between human Ro60 and the microbial orthologs from *Bacteroides thetaiotaomicron* (50). Further mechanistic studies are needed to explore the exact mechanisms by which *O. splanchnicus* and *A muciniphila* contribute to the pathogenesis of SLE.

Taken together, our large-scale gut metagenomic study of patients with SLE who had not been recently treated, and our investigation of SLE patients after treatment and of lupus-prone mice, suggest a disturbed gut microbiota with a distinct functional profile in SLE patients and propose the possibility that 2 autoantigen-cross-reacting peptides from SLE-enriched species are able to incite the production of inflammatory cytokines or combine with SLE-related autoantibodies. Furthermore, the possibility that some gut-enriched species originate from the mouth in patients with SLE but not healthy subjects may represent an equally serious contributor to the development of gut inflammation and autoimmune pathology. Complete characterization of the role of the alimentary tract microbiota in patients with SLE should offer innocuous adjunct therapeutic modalities.

ACKNOWLEDGMENTS

We thank PUMC Hospital and the study participants. We also thank Yan-ping Wei, Ya-ran Zhang, Wen-xiu Mo, Xin-yue Xiao, and Xian-da Xie for the collection of fecal samples.

AUTHOR CONTRIBUTIONS

All authors were involved in drafting the article or revising it critically for important intellectual content, and all authors approved the final version to be published. Dr. Zhang had full access to all of the data in the study and takes responsibility for the integrity of the data and the accuracy of the data analysis.

Study conception and design. Tsokos, J. Wang, Zhang.

Acquisition of data. Chen, Zhao, Zuo, Pan, X.-h. Wang, Ye, Zhang.


Analysis and interpretation of data. Chen, Jia, Xu, Zhao, Ji, Wu, Ma, Li, Tsokos, J. Wang, Zhang.

REFERENCES

- Tsokos GC. Autoimmunity and organ damage in systemic lupus erythematosus [review]. *Nat Immunol* 2020;21:605–14.
- He Y, Wu W, Zheng HM, Li P, McDonald D, Sheng HF, et al. Regional variation limits applications of healthy gut microbiome reference ranges and disease models [letter]. *Nat Med* 2018;24:1532–5.
- Pronovost GN, Hsiao EY. Perinatal interactions between the microbiome, immunity, and neurodevelopment. *Immunity* 2019;50:18–36.
- Zhang X, Zhang D, Jia H, Feng Q, Wang D, Liang D, et al. The oral and gut microbiomes are perturbed in rheumatoid arthritis and partly normalized after treatment. *Nat Med* 2015;21:895–905.
- Zhou C, Zhao H, Xiao XY, Chen BD, Guo RJ, Wang Q, et al. Metagenomic profiling of the pro-inflammatory gut microbiota in ankylosing spondylitis. *J Autoimmun* 2019;107:102360.
- Ye Z, Zhang N, Wu C, Zhang X, Wang Q, Huang X, et al. A metagenomic study of the gut microbiome in Behcet's disease. *Microbiome* 2018;6:135.
- Li Y, Wang H, Li X, Li H, Zhang Q, Zhou H, et al. Disordered intestinal microbes are associated with the activity of systemic lupus erythematosus. *Clin Sci (Lond)* 2019;133:821–38.
- Azzouz D, Omarbekova A, Heguy A, Schwudke D, Gisch N, Rovin BH, et al. Lupus nephritis is linked to disease-activity associated expansions and immunity to a gut commensal. *Ann Rheum Dis* 2019;78:947–56.
- He Z, Shao T, Li H, Xie Z, Wen C. Alterations of the gut microbiome in Chinese patients with systemic lupus erythematosus. *Gut Pathog* 2016;8:64.
- Hevia A, Milani C, Lopez P, Cuervo A, Arbolea S, Duranti S, et al. Intestinal dysbiosis associated with systemic lupus erythematosus. *mBio* 2014;5:e01548-14.
- Zhao Z, Ren J, Dai C, Kannapell CC, Wang H, Gaskin F, et al. Nature of T cell epitopes in lupus antigens and HLA-DR determines autoantibody initiation and diversification. *Ann Rheum Dis* 2019;78:380–90.
- Vieira SM, Hiltensperger M, Kumar V, Zegarra-Ruiz D, Dehner C, Khan N, et al. Translocation of a gut pathobiont drives autoimmunity in mice and humans. *Science* 2018;359:1156–61.
- Yin Y, Choi SC, Xu Z, Perry DJ, Seay H, Croker BP, et al. Normalization of CD4+ T cell metabolism reverses lupus. *Sci Transl Med* 2015;7:274ra18.
- Franzosa EA, Hsu T, Sirota-Madi A, Shafquat A, Abu-Ali G, Morgan XC, et al. Sequencing and beyond: integrating molecular 'omics' for microbial community profiling [review]. *Nat Rev Microbiol* 2015;13:360–72.
- Perry D, Sang A, Yin Y, Zheng YY, Morel L. Murine models of systemic lupus erythematosus. *J Biomed Biotechnol* 2011;2011:271694.
- Hochberg MC, for the Diagnostic and Therapeutic Criteria Committee of the American College of Rheumatology. Updating the American College of Rheumatology revised criteria for the classification of systemic lupus erythematosus [letter]. *Arthritis Rheum* 1997;40:1725.
- Gladman DD, Ibanez D, Urowitz MB. Systemic lupus erythematosus disease activity index 2000. *J Rheumatol* 2002;29:288–91.
- Truong DT, Franzosa EA, Tickle TL, Scholz M, Weingart G, Pasolli E, et al. MetaPhlan2 for enhanced metagenomic taxonomic profiling. *Nat Methods* 2015;12:902–3.
- Segata N, Izard J, Waldron L, Gevers D, Miropolsky L, Garrett WS, et al. Metagenomic biomarker discovery and explanation. *Genome Biol* 2011;12:R60.
- Altschul SF, Gish W, Miller W, Myers EW, Lipman DJ. Basic local alignment search tool. *J Mol Biol* 1990;215:403–10.
- Segata N, Waldron L, Ballarini A, Narasimhan V, Jousson O, Huttenhower C. Metagenomic microbial community profiling using unique clade-specific marker genes. *Nat Methods* 2012;9:811–4.
- Franzosa EA, McIver LJ, Rahnvard G, Thompson LR, Schirmer M, Weingart G, et al. Species-level functional profiling of metagenomes and metatranscriptomes. *Nat Methods* 2018;15:962–8.
- Hsiao WW, Li KL, Liu Z, Jones C, Fraser-Liggett CM, Fouad AF. Microbial transformation from normal oral microbiota to acute endodontic infections. *BMC Genomics* 2012;13:345.
- Colombo AP, Boches SK, Cotton SL, Goodson JM, Kent R, Haffajee AD, et al. Comparisons of subgingival microbial profiles of refractory periodontitis, severe periodontitis, and periodontal health using the human oral microbe identification microarray. *J Periodontol* 2009;80:1421–32.
- Vielkind P, Jentsch H, Eschrich K, Rodloff AC, Stingy CS. Prevalence of *Actinomyces* spp. in patients with chronic periodontitis. *Int J Med Microbiol* 2015;305:682–8.
- Chen B, Sun L, Zhang X. Integration of microbiome and epigenome to decipher the pathogenesis of autoimmune diseases. *J Autoimmun* 2017;83:31–42.
- Talken BL, Schafermeyer KR, Bailey CW, Lee DR, Hoffman RW. T cell epitope mapping of the Smith antigen reveals that highly conserved Smith antigen motifs are the dominant target of T cell immunity in systemic lupus erythematosus. *J Immunol* 2001;167:562–8.
- Takata-Tomokuni A, Ueki A, Shiwa M, Isozaki Y, Hatayama T, Katsuyama H, et al. Detection, epitope-mapping and function of anti-Fas autoantibody in patients with silicosis. *Immunology* 2005;116:21–9.
- Jackson MA, Verdi S, Maxan ME, Shin CM, Zierer J, Bowyer RC, et al. Gut microbiota associations with common diseases and prescription medications in a population-based cohort. *Nat Commun* 2018;9:2655.
- Maier L, Pruteanu M, Kuhn M, Zeller G, Telzerow A, Anderson EE, et al. Extensive impact of non-antibiotic drugs on human gut bacteria. *Nature* 2018;555:623–8.
- Mu Q, Zhang H, Liao X, Lin K, Liu H, Edwards MR, et al. Control of lupus nephritis by changes of gut microbiota. *Microbiome* 2017;5:73.
- Hong Y, Wang T, Huang C, Cheng W, Lin B. Soy isoflavones supplementation alleviates disease severity in autoimmune-prone MRL-*lpr/lpr* mice. *Lupus* 2008;17:814–21.
- Hur HG, Beeger RD, Heinze TM, Lay JO Jr, Freeman JP, Dore J, et al. Isolation of an anaerobic intestinal bacterium capable of cleaving the C-ring of the isoflavonoid daidzein. *Arch Microbiol* 2002;178:8–12.
- Wick EC, Rabizadeh S, Albesiano E, Wu X, Wu S, Chan J, et al. Stat3 activation in murine colitis induced by enterotoxigenic *Bacteroides fragilis*. *Inflamm Bowel Dis* 2014;20:821–34.
- Chung L, Orberg ET, Geis AL, Chan JL, Fu K, Shields CE, et al. *Bacteroides fragilis* toxin coordinates a pro-carcinogenic inflammatory cascade via targeting of colonic epithelial cells. *Cell Host Microbe* 2018;23:203–14.
- Ogunrinde E, Zhou Z, Luo Z, Alekseyenko A, Li QZ, Macedo D, et al. A link between plasma microbial translocation, microbiome, and autoantibody development in first-degree relatives of systemic lupus erythematosus patients. *Arthritis Rheumatol* 2019;71:1858–68.
- Ikeda K, Kinoshita M, Kayama H, Nagamori S, Kongpracha P, Umemoto E, et al. Slc3a2 mediates branched-chain amino-acid-dependent maintenance of regulatory T cells. *Cell Rep* 2017;21:1824–38.
- Png CW, Linden SK, Gilshenan KS, Zoetendal EG, McSweeney CS, Sly LI, et al. Mucolytic bacteria with increased prevalence in IBD mucosa augment in vitro utilization of mucin by other bacteria. *Am J Gastroenterol* 2010;105:2420–8.
- Popolo A, Adesso S, Pinto A, Autore G, Marzocco S. L-Arginine and its metabolites in kidney and cardiovascular disease. *Amino Acids* 2014;46:2271–86.

40. Gao J, Xu K, Liu H, Liu G, Bai M, Peng C, et al. Impact of the gut microbiota on intestinal immunity mediated by tryptophan metabolism. *Front Cell Infect Microbiol* 2018;8:13.
41. De Souza CO, Vannice GK, Neto JC, Calder PC. Is palmitoleic acid a plausible nonpharmacological strategy to prevent or control chronic metabolic and inflammatory disorders? [review] *Mol Nutr Food Res* 2018;62:1700504.
42. Van der Meulen TA, Harmsen HJ, Vila AV, Kurilshikov A, Liefers SC, Zhernakova A, et al. Shared gut, but distinct oral microbiota composition in primary Sjogren's syndrome and systemic lupus erythematosus. *J Autoimmun* 2019;97:77–87.
43. Correa JD, Calderaro DC, Ferreira GA, Mendonca SM, Fernandes GR, Xiao E, et al. Subgingival microbiota dysbiosis in systemic lupus erythematosus: association with periodontal status. *Microbiome* 2017;5:34.
44. Schmidt TS, Hayward MR, Coelho LP, Li SS, Costea PI, Voigt AY, et al. Extensive transmission of microbes along the gastrointestinal tract. *Elife* 2019;8:e42693.
45. Katsuyama T, Tsokos GC, Moulton VR. Aberrant T cell signaling and subsets in systemic lupus erythematosus [review]. *Front Immunol* 2018;9:1088.
46. Hamilton JA, Li J, Wu Q, Yang P, Luo B, Li H, et al. General approach for tetramer-based identification of autoantigen-reactive B cells: characterization of La- and snRNP-reactive B cells in autoimmune BXD2 mice. *J Immunol* 2015;194:5022–34.
47. Cekanaviciute E, Yoo BB, Runia TF, Debelius JW, Singh S, Nelson CA, et al. Gut bacteria from multiple sclerosis patients modulate human T cells and exacerbate symptoms in mouse models. *Proc Natl Acad Sci U S A* 2017;114:10713–8.
48. Bijl M, Horst G, Limburg PC, Kallenberg CG. Anti-CD3-induced and anti-Fas-induced apoptosis in systemic lupus erythematosus (SLE). *Clin Exp Immunol* 2001;123:127–32.
49. Herrera-Esparza R, Villalobos R, Bollain YG, Ramirez-Sandoval R, Sanchez-Rodriguez SH, Pacheco-Tovar G, et al. Apoptosis and redistribution of the Ro autoantigen in Balb/c mouse like in subacute cutaneous lupus erythematosus. *Clin Dev Immunol* 2006;13:163–6.
50. Greiling TM, Dehner C, Chen X, Hughes K, Iniguez AJ, Boccitto M, et al. Commensal orthologs of the human autoantigen Ro60 as triggers of autoimmunity in lupus. *Sci Transl Med* 2018;10:eaan2306.

Association Between Urinary Epidermal Growth Factor and Renal Prognosis in Lupus Nephritis

Juan M. Mejia-Vilet,¹  John P. Shapiro,² Xiaolan L. Zhang,² Cristino Cruz,¹ Grant Zimmerman,² R. Angélica Méndez-Pérez,¹ Mayra L. Cano-Verduzco,¹ Samir V. Parikh,² Haikady N. Nagaraja,³ Luis E. Morales-Buenrostro,¹ and Brad H. Rovin²

Objective. To evaluate the role of urinary epidermal growth factor (EGF) as a biomarker of chronic kidney damage in lupus nephritis (LN).

Methods. A proteomics approach was used to identify urinary EGF as a biomarker of interest in a discovery cohort of patients with LN. The expression of urinary EGF was characterized in 2 large multiethnic LN cohorts, and the association between urinary EGF levels at the time of flare and kidney outcomes was evaluated in a subset of 120 patients with long-term follow-up data. For longitudinal studies, the expression of urinary EGF over time was determined in 2 longitudinal cohorts of patients with LN from whom serial urine samples were collected.

Results. Discovery analysis showed the urinary EGF levels as being low in patients with active LN (median peptide count 8.4, interquartile range [IQR] 2.8–12.3 in patients with active LN versus median 48.0, IQR 45.3–64.6 in healthy controls). The peptide sequence was consistent with that of proEGF, and this was confirmed by immunoblotting. The discovery findings were verified by enzyme-linked immunosorbent assay. Patients with active LN had a significantly lower level of urinary EGF compared to that in patients with active nonrenal systemic lupus erythematosus (SLE), patients with inactive SLE, and healthy kidney donors (each $P < 0.05$). The urinary EGF level was inversely correlated with the chronicity index of histologic features assessed in kidney biopsy tissue (Spearman's $r = -0.67$, $P < 0.001$). Multivariate survival analysis showed that the urinary EGF level was associated with time to doubling of the serum creatinine level (DSCr), a marker of future end-stage kidney disease (ESKD) (hazard ratio 0.88, 95% confidence interval 0.77–0.99, $P = 0.045$). Patients whose LN symptoms progressed to DSCr and those who experienced progression to ESKD had a lower urinary EGF level at the time of flare, and urinary EGF levels decreased over the 12 months following flare. All patients who experienced progression to ESKD were identified based on a urinary EGF cutoff level of <5.3 ng/mg.

Conclusion. Urinary EGF levels are correlated with histologic kidney damage in patients with LN. Low urinary EGF levels at the time of flare and decreasing urinary EGF levels over time are associated with adverse long-term kidney outcomes.

INTRODUCTION

Lupus nephritis (LN) affects 40–60% of systemic lupus erythematosus (SLE) patients (1). Kidney involvement in SLE greatly

increases morbidity and mortality, with 10–20% of patients experiencing progression to end-stage kidney disease (ESKD) over 5–10 years (2,3). At present, there is a paucity of recognized biomarkers that can be used to detect early and progressive kidney

Presented by Dr. Mejia-Vilet in partial fulfillment of the requirements for a PhD degree at the National Autonomous University of Mexico, Mexico City, Mexico.

The contents of this article are solely the responsibility of the authors and do not necessarily represent the official views of the National Center for Advancing Translational Sciences or the NIH.

Supported by the Mexican National Council for Science and Technology (Conacyt) (FOSSIS grant 2017-2-289663 to Dr. Mejia-Vilet), National Institute of Arthritis and Musculoskeletal and Skin Diseases, NIH (grant RO1-AR-071947 to Dr. Rovin), National Center for Advancing Translational Sciences, NIH (grant UL1-TR-002733), and The Ohio State University Center for Clinical and Translational Science (research voucher to Mr. Shapiro).

¹Juan M. Mejia-Vilet, MD, MSc, Cristino Cruz, MS, R. Angélica Méndez-Pérez, MD, Mayra L. Cano-Verduzco, MD, Luis E. Morales-Buenrostro, MD, PhD: Instituto Nacional de Ciencias Médicas y Nutrición Salvador Zubirán,

Mexico City, Mexico; ²John P. Shapiro, MS, Xiaolan L. Zhang, MD, Grant Zimmerman, MD, Samir V. Parikh, MD, Brad H. Rovin, MD: The Ohio State University Wexner Medical Center, Columbus; ³Haikady N. Nagaraja, PhD: The Ohio State University, Columbus.

Dr. Mejia-Vilet and Mr. Shapiro contributed equally to this work.

Dr. Rovin has received consulting fees, speaking fees, and/or honoraria from AstraZeneca, Aurinia, Bristol Myers Squibb, Callidatis, ChemoCentryx, EMD Serono, Janssen, MorphoSys, Novartis, Omeros, and Retrophin (less than \$10,000 each). No other disclosures relevant to this article were reported.

Address correspondence to Brad H. Rovin, MD, The Ohio State University Medical Center, Division of Nephrology, Department of Internal Medicine, 395 West 12th Avenue, Ground Floor Doan Office, Columbus, OH 43210. Email: Rovin.1@osu.edu.

Submitted for publication April 14, 2020; accepted in revised form August 7, 2020.

damage and to predict prognosis in LN patients (4). During an unbiased urine proteomics survey designed to discover candidate urinary biomarkers of LN damage, we observed significantly decreased levels of pro-epidermal growth factor (proEGF) in several LN patients compared to healthy controls.

EGF is a globular protein synthesized in the kidney, specifically in the glomerulus, loop of Henle, and distal convoluted tubule (5–7). While EGF is absent or minimally detectable in plasma, it is detectable in the urine of normal healthy individuals. Urinary EGF levels have been found to be correlated with intrarenal EGF messenger RNA (mRNA) expression and have been reported to be decreased in several kidney diseases (6). An association between low urinary EGF levels and the degree of interstitial fibrosis and progressive chronic kidney disease was observed in patients with IgA nephropathy (8–10), diabetic kidney disease (11–13), Alport syndrome (14) and other glomerular and nonglomerular diseases (6, 15–18). Therefore, this study aimed to understand the relationship between urinary EGF levels, histopathologic features of the kidney, and renal outcomes in patients with LN.

PATIENTS AND METHODS

Study design. Candidate LN biomarkers were identified using a shotgun urine proteomics approach and subsequently verified in a large cross-sectional cohort of patients with LN, followed by validation and characterization in longitudinal cohorts of patients undergoing treatment and follow-up for active LN. Biomarker discovery was conducted at Ohio State University (OSU). Biomarkers were verified in a cross-sectional LN cohort comprising patients from OSU and from Mexico City. The behavior of biomarkers over time was assessed in 2 prospective longitudinal cohorts, the Mexican LN cohort and a cohort from the Ohio SLE Study. All patients met at least 4 of the American College of Rheumatology classification criteria for SLE (19) and had biopsy-proven LN.

The study was approved by the OSU Institutional Review Board and the Instituto Nacional de Ciencias Médicas y Nutrición Salvador Zubirán Research and Ethics Review Board. All patients signed informed consent to participate in the study.

Study subjects. Discovery proteomics analysis followed by verification with immunoblotting and an in-house proEGF enzyme-linked immunosorbent assay (ELISA) were performed using urine samples collected at the time of LN flare in a subset of patients ($n = 36$) from the Ohio SLE Study (20). Healthy volunteers were recruited as controls ($n = 36$).

Further verification of the discovery findings was done by assessing samples of urine collected from patients on the day of kidney biopsy (obtained prior to the procedure) for the diagnosis of LN flare. In all patients, active LN was defined histologically by the presence of immune complex deposits and associated inflammatory lesions, according to the 2003 International Society

of Nephrology/Renal Pathology Society (ISN/RPS) classification of LN (21). This kidney biopsy cohort consisted of 29 patients with LN from Ohio (not those in the Ohio SLE Study cohort) and 124 patients with LN from Mexico. Urine from 49 patients with SLE (renal or nonrenal) but with no or mild disease activity (based on a score of <6 on the SLE Disease Activity index 2000 [SLEDAI-2K] [22]) and from 22 patients with active nonrenal SLE (SLEDAI-2K score of ≥ 6 , with 4 points assessed for organ involvement) served as disease controls. Ten healthy kidney donors who provided urine samples prior to kidney donation were included as normal healthy controls. All samples were centrifuged within 30 minutes of collection and stored frozen at -70°C .

To evaluate urinary EGF expression over time and in response to therapy, 2 longitudinal cohorts of patients with LN were studied: 1) a prospective cohort of 91 patients with active LN from Mexico, followed up for a median of 27 months (range 14–44 months), and 2) 28 patients with active LN and 23 patients with active nonrenal SLE from the Ohio SLE Study cohort, with a median follow-up time of 110 months (range 56–180 months) (20). A subgroup of 17 patients who presented with active LN and who had an estimated glomerular filtration rate (eGFR) below $30 \text{ ml/minute}/1.73 \text{ m}^2$ was studied to evaluate urinary EGF behavior during severe acute kidney injury.

Finally, to evaluate the intraindividual coefficients of variation for the measurement of EGF in the urine, the levels of urinary EGF were measured in 4 urine samples from 13 healthy controls. These serial samples were obtained over 56 days (on days 0, 7, 28, and 56).

Urine proteomics. Urine from LN patients and healthy individuals was incubated for 16 hours at 4°C in polystyrene plates. After washing with phosphate buffered saline (PBS) and NH_3HCO_3 , trypsin was added for protein digestion and peptides were collected. Samples were analyzed by reversed-phase high-performance liquid chromatography (HPLC) (Dionex Ultimate 3000 capillary/nano HPLC system) and liquid chromatography tandem mass spectrometry (LC-MS/MS) with a ThermoFisher LTQ Orbitrap XL mass spectrometer equipped with micro/nanospray ionization sources (Michrom Bioresources). HPLC separations were carried out at a flow rate of 2 ml/minute on a $0.2 \text{ mm} \times 150 \text{ mm}$ C18 column (5 mm, 300A; Michrom Bioresources). The mobile phases consisted of HPLC grade water and acetonitrile with 50 mM acetic acid added as an ion-pairing reagent. A 10–35% gradient was run over 30 minutes, followed by a 35–90% gradient run over 15 minutes. The heated capillary temperature and electrospray voltage were set at 175°C and 2.0 kV , respectively.

Data analysis was performed using Proteome Discoverer version 1.4 (Thermo Scientific). Data were searched against a Uniprot Human database that included common contaminants. Variable modifications included oxidation on methionine ($+15.995 \text{ Da}$), and identified peptides were filtered to a 1% false discovery rate.

Protein identification by Western blotting. Proteins revealed by LC-MS/MS were further characterized by immunoblotting. In this study, we specifically examined urinary expression of EGF. Urine (18 μ l) was mixed with 6 μ l loading dye, run on 4–12% Bis-Tris gel (unreduced), and transferred to a nitrocellulose blotting membrane. The membrane was blocked for 1 hour with 2% casein in PBS plus 0.05% Tween 20 (PBST). An anti-EGF antibody (MAB236; R&D Systems) was diluted in 2% casein in PBST and incubated overnight. After washing in PBST, a secondary antibody in 2% casein in PBST was added for 1 hour. After rinsing in PBST, an enhanced chemiluminescence substrate (Pierce ECL Western blotting substrate) was added for 1 minute, and the film was then developed.

ProEGF ELISA. A goat anti-proEGF antibody (AF4289; R&D Systems) was used both for capture and detection of proEGF. Anti-proEGF was biotinylated with EZ-link NHS-PEG4-biotin (ThermoFisher Scientific). Recombinant human EGF (4289-EG; R&D Systems) was used as a standard. Plates were coated overnight with capture anti-proEGF and urine was diluted as needed in PBS plus 1% bovine serum albumin, followed by incubation for 2 hours. Biotinylated anti-proEGF was then added, followed by incubation for 2 hours, and streptavidin-horseradish peroxidase and tetramethylbenzidine substrate were added, with incubation for 20 minutes each. The plates were read at an optical density of 450 nm.

Plasma and urinary EGF ELISAs. A commercial EGF ELISA (DuoSet DY236; R&D Systems) was used to measure EGF in the urine, in accordance with the manufacturer's recommendations. Samples were diluted 1:10 to 1:200 and run in duplicate, yielding intraassay and interassay coefficients of variation below 10% at both centers. The values obtained were normalized to the levels of urinary creatinine excretion (urinary EGF/Cr). Urinary EGF/Cr values were \log_{10} -transformed for all analyses.

Variable and outcome definitions. All clinical data were collected prospectively from the OSU, Ohio SLE Study, and Mexican cohort databases. Kidney biopsy samples were classified according to the ISN/RPS criteria for LN (21), and were scored using the National Institutes of Health renal activity index and chronicity index for histologic features (23,24). Each component of the activity and chronicity indexes was evaluated as a percentage of affected glomeruli, tubules, or interstitium, and based on these percentages, each component was classified as not present (<5% of the affected region), mild (present in 6–25% of the affected region), moderate (present in 26–50% of the affected region), or severe (present in >50% of the affected region), as recently revised (24).

Renal outcomes included the number of patients who developed a 30% reduction in the eGFR, doubling of serum creatinine level (DSCr), or progression to ESKD. Stable renal function was defined as either an eGFR of no lower than 80% of the baseline

eGFR or the best eGFR attained in the first 12 months after treatment for an LN flare.

Statistical analysis. Clinical variables at the time of flare are presented as numbers and relative frequencies or as the median with interquartile range (IQR). Pearson's correlations between urinary EGF/Cr levels and histologic variables were computed, and in some cases (as noted), Spearman's correlations between \log_{10} -transformed data were used to describe associations. The associations between at-flare parameters and time to renal outcomes were assessed by Cox regression analysis. We constructed nested Cox proportional hazards models to evaluate the additive effect of the urinary EGF/Cr levels for goodness of fit, with generalized R^2 and likelihood ratio tests.

For the longitudinal analysis, linear mixed models were fitted to evaluate the association between repeated urinary EGF/Cr measurements and long-term outcomes. Modeling included \log_{10} -EGF/Cr values as the dependent variable. Fixed effects in the model included the outcome group, months of follow-up, and their interaction, as well as age, sex, and the eGFR course over repeated measurements. Subjects were included as random effects in the model. Least-squares estimates of the mean (with 95% confidence intervals [95% CIs]) were obtained and plotted against the duration of follow-up. Diagnostics of the final model included the evaluation of the distribution of the standardized residuals and the homogeneity of the residual variance among outcome groups. Individual regression coefficients were obtained for the urinary EGF/Cr levels, eGFR, measurement of proteinuria, and levels of anti-double-stranded DNA antibodies and complement, with correlations assessed using Pearson's correlation coefficients.

All statistical analyses were performed with IBM SPSS version 24.0 and GraphPad Prism version 6. *P* values less than 0.05 were considered statistically significant.

RESULTS

Reduced urinary levels of proEGF revealed by LC-MS/MS in patients with LN compared to healthy controls.

Using LC-MS/MS, urinary proEGF peptide counts were found to be markedly lower in several of the patients with LN compared to healthy controls ($P = 0.001$) (Supplementary Figure 1A, available on the *Arthritis & Rheumatology* website at <http://online.library.wiley.com/doi/10.1002/art.41507/abstract>). Importantly, the peptides identified aligned within the sequence of proEGF. No peptides were detected from inside the mature EGF protein (Supplementary Figure 2, available on the *Arthritis & Rheumatology* website at <http://onlinelibrary.wiley.com/doi/10.1002/art.41507/abstract>).

To corroborate this finding, Western blotting with specific proEGF and EGF antibodies was done using urine samples from

Table 1. Characteristics of the study patients included in the cross-sectional and longitudinal analyses*

	Cross-sectional analysis			Longitudinal analysis		
	Active LN (n = 153)	Active nonrenal SLE (n = 23)†	Inactive/mildly active SLE (n = 49)	Healthy kidney donors (n = 10)	Active LN Mexican cohort (n = 91)	Active LN Ohio SLE Study cohort (n = 28)
Age, years	32 (25–39)	43 (32–49)	43 (32–50)	39 (27–47)	32 (25–40)	32 (27–44)
Female, no. (%)	137 (90)	22 (96)	46 (94)	6 (60)	85 (93)	25 (89)
Race, no. (%)						
Caucasian	13 (9)	18 (78)	0	0	0	14 (50)
African American	13 (9)	5 (22)	0	0	0	12 (43)
Mexican-Mestizo	124 (80)	0	49 (100)	10 (100)	91 (100)	0
Other	3 (2)	0	0	0	0	2 (7)
Creatinine, mg/dl	1.1 (0.7–2.0)	0.7 (0.6–0.8)	0.7 (0.6–0.8)	0.8 (0.6–1.0)	1.2 (0.7–2.2)	1.1 (0.9–1.6)
eGFR, ml/minute/1.73 m ²	68 (36–111)	103 (87–122)	104 (89–120)	110 (93–122)	64 (28–109)	74 (43–97)
Proteinuria, mg/mg	3.2 (1.9–4.9)	0.1 (0.0–0.1)	0.1 (0.1–0.2)	0.0 (0.0–0.1)	3.2 (2.2–5.0)	1.6 (1.0–2.7)
Anti-dsDNA positive, no. (%)	116 (76)	20 (87)	36 (73)	0	76 (84)	22 (79)
Low C3, no. (%)	112 (73)	16 (70)	11 (22)	0	67 (74)	21 (75)
Low C4, no. (%)	127 (83)	18 (78)	24 (49)	0	78 (86)	22 (79)
SLEDAI-2K score	16 (14–22)	17 (9–24)	0 (0–4)	0	16 (14–22)	22 (18–28)
Classification of LN, no. (%)						
Class II	3 (2)	0	0	0	1 (1)	0
Class III ± class V‡	50 (33)	0	0	0	30 (33)	10 (36)
Class IV ± class V‡	84 (55)	0	0	0	55 (60)	18 (64)
Class V	16 (10)	0	0	0	5 (6)	0
Kidney biopsy histologic score						
Activity index (scale 0–24)	4 (1–9)	NA	NA	NA	4 (1–8)	NA
Chronicity index (scale 0–12)	4 (3–6)	NA	NA	NA	4 (3–6)	NA

* Except where indicated otherwise, values are the median (interquartile range). LN = lupus nephritis; SLE = systemic lupus erythematosus; eGFR = estimated glomerular filtration rate; anti-dsDNA = anti-double-stranded DNA; SLEDAI-2K = SLE Disease Activity Index 2000; NA = not applicable.

† Patients in this group were also followed up in the longitudinal analysis.

‡ Class III or class IV LN may occur alone or in combination with class V LN.

LN patients and healthy controls. We found that the protein bands corresponded to proEGF and not the mature EGF protein (Supplementary Figure 1B, <http://onlinelibrary.wiley.com/doi/10.1002/art.41507/abstract>). These findings verify that proEGF is the dominant form of EGF excreted into the urine.

Reduced urinary levels of proEGF revealed by ELISA in patients with LN. We developed an ELISA for urinary proEGF and measured proEGF in the same urine samples as used for proteomics analysis. The urinary proEGF levels measured by ELISA recapitulated the pattern seen with quantitative MS (data not shown). Because most previous studies that have evaluated urinary EGF used commercial ELISAs, which are reported to measure mature EGF (8–11), we simultaneously assessed the same urine samples using both our proEGF ELISA and a commercial ELISA for mature EGF. The commercial EGF ELISA results were highly correlated with the proEGF ELISA results ($r^2 = 0.911$, $P < 0.001$) (Supplementary Figure 3, available on the *Arthritis & Rheumatology* website at <http://onlinelibrary.wiley.com/doi/10.1002/art.41507/abstract>), suggesting that the antibodies used in commercial ELISAs cross-react with proEGF. Therefore, for the remainder of this discussion, urinary EGF is taken to mean urinary proEGF.

Association of urinary EGF levels with LN activity levels and histologic features. Because urine proteomics is a discovery technique that was applied to only a small number of patients, the urinary EGF/Cr level was measured in a large cross-sectional cohort of patients with active LN, to better characterize its expression in the general LN population (Table 1). Urinary EGF/Cr levels in patients with active LN were compared to those in urine samples from patients with active nonrenal SLE, patients with inactive or mildly active SLE, and healthy kidney donors.

Urinary EGF/Cr levels were lower in patients with active LN (median 6.9 ng/mg, IQR 3.4–12.2) compared to patients with active

nonrenal SLE (median 18.2 ng/mg, IQR 10.8–27.5), patients with inactive or mildly active SLE (median 16.6 ng/mg, IQR 7.1–22.3), and healthy kidney donors (median 16.8 ng/mg, IQR 16.0–17.9). Within all groups, urinary EGF/Cr levels were lower in patients with a history of LN as compared to patients who had never had kidney involvement (Figure 1 and Supplementary Table 1, available on the *Arthritis & Rheumatology* website at <http://onlinelibrary.wiley.com/doi/10.1002/art.41507/abstract>). There were no detectable EGF levels in plasma samples from any of these patients (data not shown). The differences among patients with active LN, patients with active nonrenal SLE, patients with inactive/mildly active SLE, and healthy kidney donors remained statistically significant after accounting for total proteinuria levels (Supplementary Figure 4, available on the *Arthritis & Rheumatology* website at <http://onlinelibrary.wiley.com/doi/10.1002/art.41507/abstract>).

Urinary EGF/Cr levels positively correlated with the eGFR in patients at the time of flare (Pearson's $r = 0.656$, $P < 0.001$), and negatively correlated with the kidney biopsy histologic chronicity index (Spearman's $r = -0.669$, $P < 0.001$) and with all of its components, including glomerular sclerosis (Pearson's $r = -0.539$, $P < 0.001$), interstitial fibrosis (Pearson's $r = -0.654$, $P < 0.001$), and tubular atrophy (Pearson's $r = -0.665$, $P < 0.001$) (Figures 2A–D). In contrast, there was no correlation between the urinary EGF/Cr levels and the histologic renal activity index (Spearman's $r = -0.165$, $P = 0.074$). In the group with active LN, urinary EGF/Cr levels decreased for every 1-point increase in the chronicity index when the index was above 1 (Supplementary Table 2, available on the *Arthritis & Rheumatology* website at <http://onlinelibrary.wiley.com/doi/10.1002/art.41507/abstract>).

Association between urinary EGF levels at the time of LN flare and renal outcomes. The association between urinary EGF/Cr levels at the time of LN flare and occurrence of DSCr was assessed in 120 patients with active LN who had >12 months of follow-up data. These patients were treated with

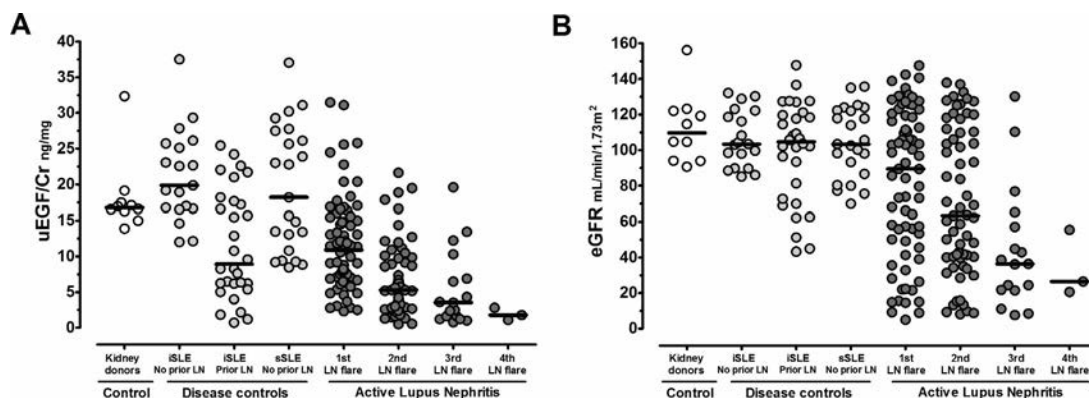


Figure 1. Urinary epidermal growth factor levels normalized to the levels of urinary creatinine excretion (uEGF/Cr) (A) and estimated glomerular filtration rate (eGFR) (B) in all groups of patients according to their history of lupus nephritis (LN) compared to healthy kidney donors and disease controls. Symbols represent individual subjects; horizontal lines indicate the median. iSLE = inactive or mildly active systemic lupus erythematosus; sSLE = active nonrenal SLE.

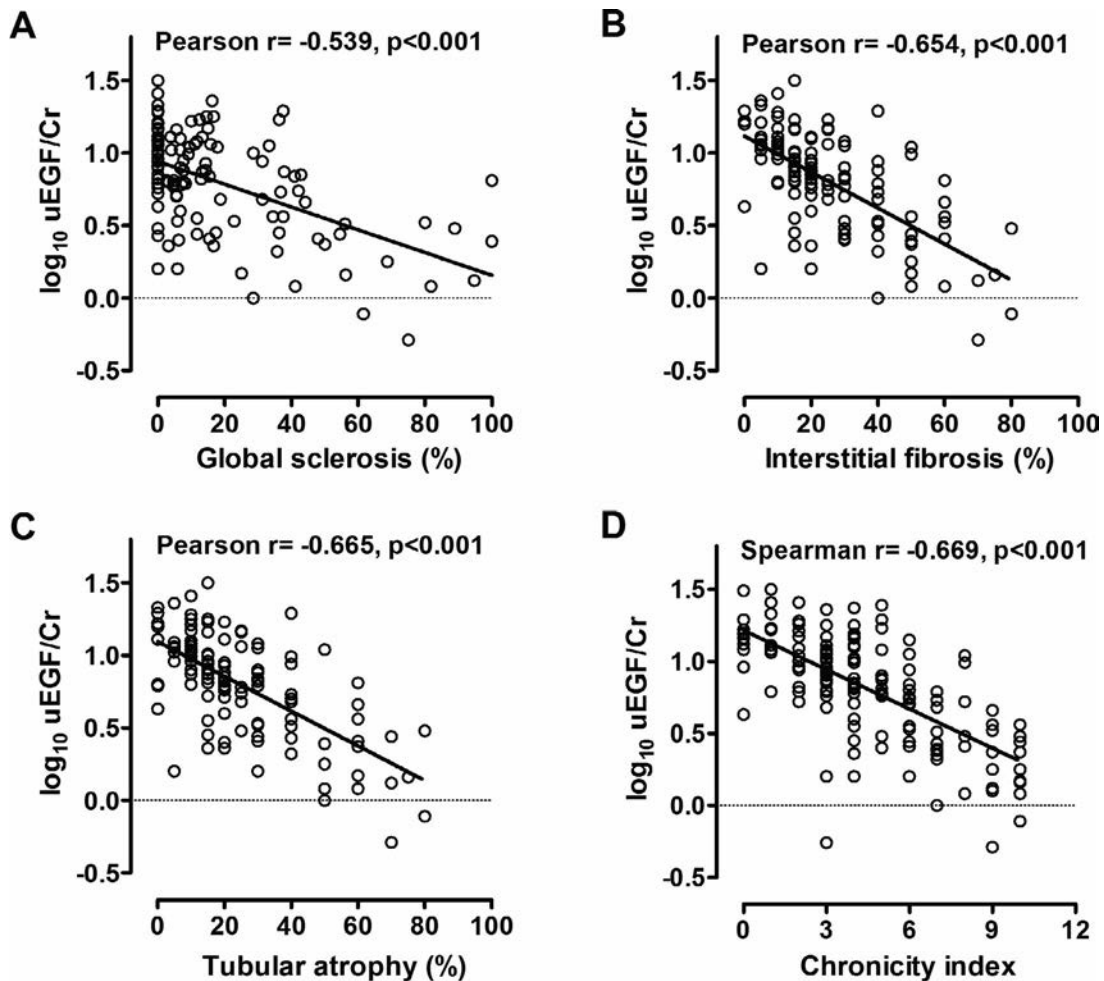


Figure 2. Correlation between urinary epidermal growth factor (EGF) levels and the histologic chronicity index (D) as well as its components, including global sclerosis (A), interstitial fibrosis (B), and tubular atrophy (C), assessed in kidney biopsy samples from patients with active lupus nephritis. Urinary EGF levels were normalized to the levels of urinary creatinine excretion (uEGF/Cr). Spearman's and Pearson's correlation coefficients were used for these analyses.

glucocorticoids in conjunction with either mycophenolate mofetil (MMF) (65% of patients), intravenous cyclophosphamide (27% of patients), calcineurin inhibitor plus MMF (5% of patients), or azathioprine (3% of patients). Over a median follow-up of 26 months (IQR 17–35 months), 32 patients (27%) experienced DSCr.

In univariate Cox regression analysis, age, eGFR, proteinuria levels, urinary EGF/Cr levels, and the histologic chronicity index were associated with the time to DSCr. In multivariate analysis, age (hazard ratio [HR] 0.93, 95% CI 0.88–0.98), urinary EGF/Cr levels (HR 0.88, 95% CI 0.77–0.99), and the histologic chronicity index (HR 1.19, 95% CI 1.01–1.40) were each significantly associated with the time to DSCr (Supplementary Table 3, available on the *Arthritis & Rheumatology* website at <http://onlinelibrary.wiley.com/doi/10.1002/art.41507/abstract>). The time-dependent area under the curve for the urinary EGF/Cr level in relation to time to DSCr was 0.82. A urinary EGF/Cr level of <5.3 ng/mg at the time of flare had 81% sensitivity and 77% specificity to predict DSCr within 2 years.

In order to evaluate the additive effect of the urinary EGF/Cr level at the time of flare on the prognostic yield of clinical and histologic variables to predict the time to DSCr, we constructed nested Cox regression models. The addition of the urinary EGF/Cr level at the time of flare to all of the evaluated models improved the model fit, and its contribution was always significant (Table 2).

Longitudinal expression of urinary EGF. To assess the course of the urinary EGF/Cr levels over time, we evaluated 91 patients (Mexican LN cohort) whose urine samples were collected prospectively at the time of flare and during follow-up at 6 and 12 months (Table 1). Over 27 months of follow-up (range 14–44 months), 64 patients (70%) maintained stable renal function (eGFR within 20% of the baseline eGFR), 23 patients (25%) experienced DSCr, and 14 patients (15%) experienced progression to ESKD. In this longitudinal cohort, the individual slopes of the \log_{10} -transformed urinary EGF/Cr levels positively correlated with the slopes of the \log_{10} -transformed eGFRs (Pearson's

Table 2. Comparison of nested models of hazards for time to doubling of the serum creatinine level*

Model	HR	95% CI	P	LR test	P	Model R ²
Model 0: age + sex				–	–	0.054
Age, per year	0.95	0.91–0.99	0.012			
Sex, female vs. male	2.00	0.47–8.42	0.347			
Model 1: age + sex + proteinuria				Model 1 vs. Model 0	0.031	0.100
Age, per year	0.95	0.91–0.99	0.014			
Sex, female vs. male	1.57	0.36–6.76	0.548			
Proteinuria, per mg/mg	1.12	1.02–1.24	0.021			
Model 1': age + sex + proteinuria + urinary EGF/Cr				Model 1' vs. Model 1	<0.001	0.230
Age, per year	0.94	0.90–0.98	0.007			
Sex, female vs. male	1.79	0.41–7.88	0.442			
Proteinuria, per mg/mg	1.09	0.97–1.23	0.139			
Urinary EGF/Cr, per ng/mg	0.77	0.69–0.87	<0.001			
Model 2: age + sex + eGFR				Model 2 vs. Model 0	<0.001	0.242
Age, per year	0.93	0.89–0.98	0.005			
Sex, female vs. male	1.88	0.44–8.03	0.397			
eGFR, per 10 ml/minute/1.73 m ²	0.79	0.72–0.87	<0.001			
Model 2': age + sex + eGFR + uEGF/Cr				Model 2' vs. Model 2	<0.001	0.275
Age, per year	0.93	0.89–0.98	0.003			
Sex, female vs. male	2.28	0.53–9.84	0.269			
eGFR, per 10 ml/minute/1.73 m ²	0.89	0.79–0.99	0.035			
Urinary EGF/Cr, per ng/mg	0.83	0.73–0.95	0.005			
Model 3: age + sex + proteinuria + eGFR + chronicity index				Model 3 vs. Model 0	<0.001	0.346
Age, per year	0.94	0.89–0.98	0.008			
Sex, female vs. male	1.44	0.33–6.38	0.632			
Proteinuria, per mg/mg	1.06	0.94–1.20	0.372			
eGFR, per 10 ml/minute/1.73 m ²	0.87	0.78–0.98	0.017			
Chronicity index	1.28	1.09–1.50	0.002			
Model 3': age + sex + proteinuria + eGFR + chronicity index + urinary EGF/Cr				Model 3' vs. Model 3	0.019	0.372
Age, per year	0.93	0.88–0.98	0.005			
Sex, female vs. male	1.82	0.41–8.19	0.433			
Proteinuria, per mg/mg	1.05	0.92–1.19	0.470			
eGFR, per 10 ml/minute/1.73 m ²	0.92	0.82–1.03	0.134			
Chronicity index	1.19	1.01–1.40	0.040			
Urinary EGF/Cr, per ng/mg	0.88	0.77–0.99	0.045			

* HR = hazard ratio; 95% CI = 95% confidence interval; LR = likelihood ratio; eGFR = estimated glomerular filtration rate (calculated using the CKD-EPI [Chronic Kidney Disease Epidemiology Collaboration] equation); EGF/Cr = urinary epidermal growth factor level normalized to the levels of urinary creatinine excretion.

$r = 0.494$, $P < 0.001$) (Supplementary Figure 5, available on the *Arthritis & Rheumatology* website at <http://onlinelibrary.wiley.com/doi/10.1002/art.41507/abstract>). There was an independent association between the course of urinary EGF/Cr levels, loss of 30% of kidney function, DSCr, and progression to ESKD (Figures 3A–F).

Urinary EGF/Cr values at the time of flare and at 6 and 12 months of follow-up were compared between the groups with stable kidney function and those who developed adverse kidney outcomes (Supplementary Table 4, available on the *Arthritis & Rheumatology* website at <http://onlinelibrary.wiley.com/doi/10.1002/art.41507/abstract>). The urinary EGF/Cr started at a lower level and decreased further in patients who progressed to develop adverse kidney outcomes. Interestingly, the urinary EGF/Cr levels also decreased over the first 6 months following LN flare in patients with stable kidney function, but then plateaued.

As the lower limit of the 95% CI for urinary EGF/Cr levels at 12 months was 5.3 ng/mg in patients with stable

renal function in the Mexican longitudinal cohort, we further validated whether this cutoff was associated with progression to ESKD in 28 patients with active LN and 23 patients with active nonrenal SLE from the Ohio SLE Study cohort. All 7 patients who experienced progression to ESKD in this cohort had a progressive decrease in the urinary EGF/Cr level to <5.3 ng/mg (Supplementary Figure 6, available on the *Arthritis & Rheumatology* website at <http://onlinelibrary.wiley.com/doi/10.1002/art.41507/abstract>). Only 3 (14%) of 21 patients who did not progress to ESKD had a urinary EGF/Cr level of <5.3 ng/mg on follow-up. All patients with active nonrenal SLE had a urinary EGF/Cr level of >5.3 ng/mg.

Urinary EGF levels in patients with severe LN and acute kidney injury. We assessed the urinary EGF/Cr level in a subset of 17 patients from the Mexican longitudinal cohort who presented with a severe LN flare and an eGFR

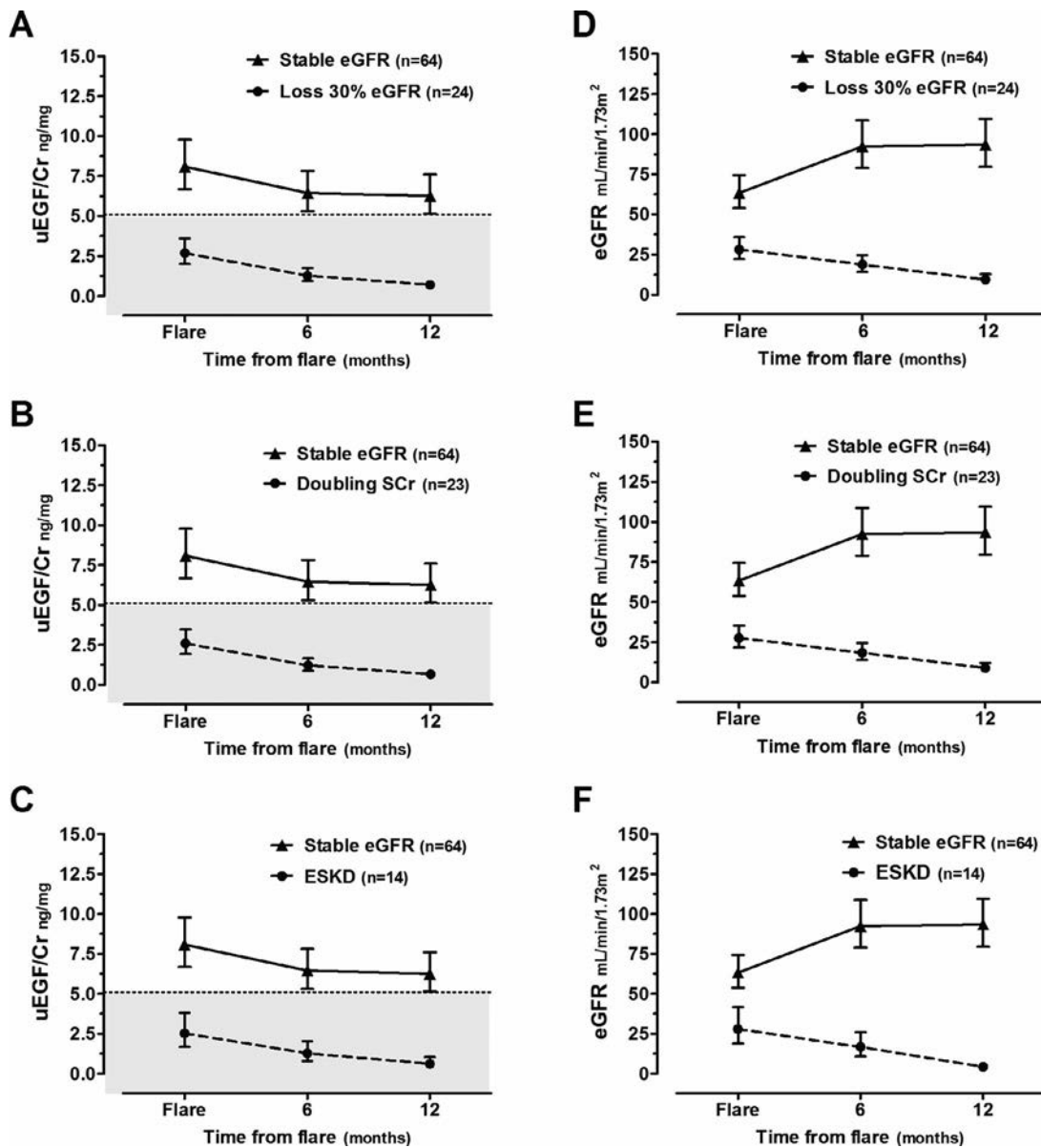


Figure 3. Urinary epidermal growth factor (EGF) levels (A–C) and estimated glomerular filtration rate (D–F) over time after diagnosis and treatment of lupus nephritis (LN) flare in patients from the Mexican cohort. The time course of urinary EGF levels normalized to the levels of urinary creatinine excretion (uEGF/Cr) and time course of the eGFR in LN patients who went on to have a 30% decline in eGFR (A and D), who experienced a doubling of their serum creatinine levels (SCr) (B and E), or who developed end-stage kidney disease (ESKD) (C and F) are shown. Results are the estimated mean with 95% confidence intervals from linear mixed modeling. The broken horizontal line with gray-shaded area in A–C indicates values below the cutoff of 5.3 ng/mg.

of <30 ml/minute/1.73 m². All patients received immunosuppressive treatment. As shown in Figures 4A and B, those patients whose eGFR recovered to >50 ml/minute/1.73 m² had a significantly higher urinary EGF/Cr level at the time of flare (median 4.8 ng/mg, 95% CI 3.3–7.7; $P = 0.001$) and over the follow-up when compared to patients who persistently had an eGFR of <30 ml/minute/1.73 m² or patients who experienced progression to ESKD (median 2.3 ng/mg, 95% CI 1.1–3.9 ng/mg).

Variability in urinary EGF levels in longitudinal samples. The median intraindividual coefficient of variation for urinary EGF levels in patients with active nonrenal SLE from the Ohio SLE Study cohort was 11% (range 8–28%). To determine whether this intraindividual variability represented assay or biologic variability, we evaluated the urinary EGF/Cr levels in 4 urine samples from 13 healthy controls obtained over 56 days (days 0, 7, 28, and 56). The median intraindividual variability in the urinary EGF/CR levels in this group was 10.6% (IQR 8.9–17.7%, range 4.0–28.8%).

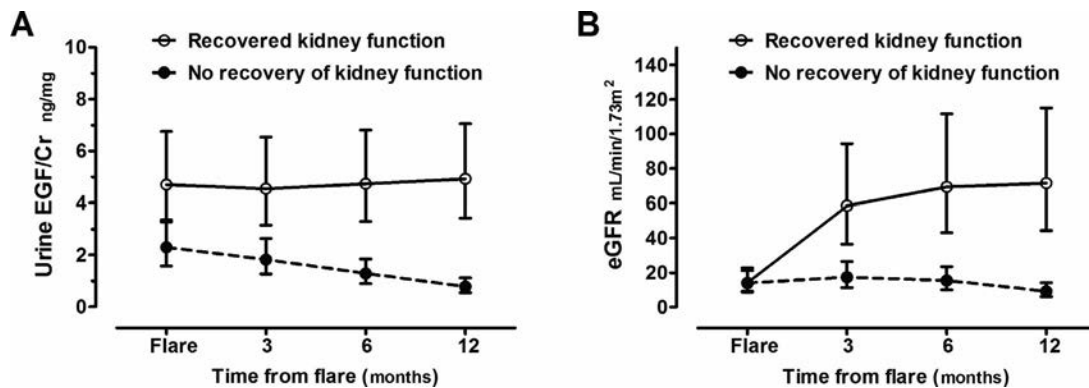


Figure 4. Urinary epidermal growth factor levels normalized to the levels of urinary creatinine excretion (uEGF/Cr) (A) and estimated glomerular filtration rate (eGFR) (B) over time after occurrence of a severe lupus nephritis flare, according to whether the patients did or did not recover kidney function. At presentation, all patients had impaired renal function, with an eGFR of <30 mL/minute/ m^2 . Results are the mean with 95% confidence intervals.

DISCUSSION

In this study, we found that proEGF peptides are diminished in the urine of patients with active LN, and we corroborated this finding in a large multiethnic population by ELISA. The urinary EGF/Cr measurement is derived from the kidneys, and the value correlates with components of the histologic chronicity index assessed on kidney biopsy samples. Moreover, the urinary EGF/Cr level is associated with long-term kidney prognosis in patients with LN. The course of the urinary EGF/Cr level over time reflects the course of kidney function, and a low baseline value and/or progressive decline in the urinary EGF/Cr level is associated with progressive loss of kidney function, forecasting a higher risk of adverse renal outcomes in LN patients.

EGF was originally identified in the 1950s as a factor derived from a larger pre-protein (1,168–1,207 amino acids in length) resulting from proteolytic cleavage (25,26). The highest EGF mRNA levels in the body are found in the kidneys (27) and correlate with the excretion of EGF in the urine. In contrast, EGF is not detectable, or is present in very low concentrations, in human plasma (28,29). Renal EGF is mainly expressed by the epithelial cells of the thick ascending limb of the loop of Henle and the distal tubule, and its expression has been shown to be reduced in chronic kidney diseases (6), including diabetic kidney disease (12,30,31).

Although human mature EGF in urine has been described in previous reports (31), we showed that peptides found in urine from patients with LN corresponded to the precursor proEGF protein. In urine peptidomic studies in rats and humans with diabetic kidney disease, the peptide sequence of urine EGF corresponded to that of the immature proEGF protein (12). Consistently, immunohistochemistry studies have shown abundant proEGF in human kidneys, but only minor staining for the mature EGF protein (32). Most of the studies that demonstrated reduced urinary EGF/Cr protein levels in diabetic kidney disease (11,13,33), IgA nephropathy (5,8,10,34), and Alport syndrome

(14) measured urinary EGF levels with a similar commercial antibody as was used herein. Our findings suggest that this antibody is not specific for mature EGF and cross-reacts with proEGF. Therefore, the urinary EGF protein detected in the urine of patients with LN, and probably in those with other forms of kidney disease, is actually proEGF.

Urinary EGF is not a biomarker of kidney function that is specific for LN. As reported for other kidney diseases (8–18), we found that urinary EGF/Cr levels correlated inversely with the histologic equivalents of chronic renal damage, including glomerular sclerosis, interstitial fibrosis, and tubular atrophy, as well as the combination of these components, also known as the histologic chronicity index. An inverse correlation between the urinary EGF/Cr and chronic kidney damage has also been observed in several other glomerular disease cohorts (the European Renal cDNA Bank [ERCB], Clinical Phenotyping Resource and Biobank Core [C-PROBE], Nephrotic Syndrome Study Network [NEPTUNE], and Peking University-IgA Nephropathy [PKU-IgAN] Consortium), some of which included patients with lupus (6).

Urinary EGF/Cr levels at the time of LN flare were independently associated with progressive loss of kidney function. When combined with other biomarkers of kidney function at the time of flare, such as proteinuria, the eGFR, and the histologic chronicity index, the addition of urinary EGF/Cr levels improved the prognostic value of these variables. The association of baseline urinary EGF/Cr levels with adverse kidney outcomes has also been demonstrated in other glomerular disease cohorts (6), patients with Alport syndrome (14), and patients with diabetic kidney disease (11–13).

However, urinary EGF/Cr levels over the clinical course of a disease have rarely been explored. We demonstrated that the course of the urinary EGF/Cr level after treatment for LN is a predictor of subsequent kidney function. As such, a low baseline urinary EGF/Cr level and/or a progressive decrease in its level is associated with progressive loss of kidney function and adverse

long-term kidney outcomes. This supports the idea that the urinary EGF/Cr level may serve as an additional biomarker of chronic kidney damage in LN, thereby expanding the list of currently recognized biomarkers.

Because the urinary EGF/Cr level can be measured by ELISA, testing is readily adaptable to the clinical laboratory. For clinical use, we suggest that the urinary EGF/Cr level be measured at the time of an LN flare, and then repeated after resolution of the LN flare, to establish a baseline level in the absence of any acute changes that may occur during active disease.

We envision several applications for the urinary EGF/Cr level in the management of patients with LN. For patients who have an LN flare and acute kidney injury, the urinary EGF/Cr level at the time of flare, and its behavior after flare, may help differentiate patients who are likely to recover kidney function from those who are unlikely to recover kidney function, and this could help influence treatment choice, intensity, and persistence. Because of the ability of nephrons to hyper-filter, remaining nephrons can compensate for a considerable loss (up to 50%) of nephron mass (35), allowing the serum creatinine levels and the eGFR to remain in the normal laboratory range. The urinary EGF/Cr level may be able to identify patients with chronic kidney damage before the serum creatinine level increases and the eGFR falls. Similarly, patients in remission after even 1 episode of active LN often have sustained chronic kidney damage that is not obvious from the serum creatinine level or eGFR. Serial monitoring of the urinary EGF/Cr level in quiescent LN may provide a means of keeping track of silent histologic damage, alerting the clinician that such patients, for example, may need closer monitoring after exposure to nephrotoxic medications or require dose adjustment of drugs excreted by the kidneys.

Finally, the serum creatinine level and eGFR do not accurately reflect kidney function in patients with very low or high muscle mass. In such cases, the urinary EGF/Cr level may give a more accurate picture of the extent of chronic kidney damage.

There is no diurnal variation in urinary EGF excretion, and its rate of excretion is similar when sampled on consecutive days, supporting its measurement in spot urine samples (36,37). However, it is also worth noting that over the long term, the intraindividual variability in the urinary EGF/Cr level can be up to 28%. Intraindividual variability of this biomarker has been reported in previous studies in patients with chronic kidney disease (38) and patients with IgA nephropathy (39). Therefore, in the monitoring of repeat samples in the same subject, changes in the urinary EGF/Cr level can only be considered significant when they vary by at least 30%.

A major limitation of this study is that we did not have repeat kidney biopsy samples available to corroborate the correlation of urinary EGF/Cr levels with increasing histologic kidney damage over time. Moreover, the interval between samples in patients with lupus was too large to adequately evaluate the biomarker variability in this population, although we hypothesize that the variability may be similar to that observed in healthy individuals. Finally,

interobserver agreement between nephropathologists in both centers was not assessed.

In summary, this proteomics-based approach to biomarker discovery in LN found urinary EGF/Cr levels to be a potential biomarker of kidney damage. Unlike an increased serum creatinine level at the time of flare, which may reflect either acute kidney injury or chronic kidney damage, reduced urinary EGF/Cr levels at the time of flare are reflective of the severity of chronic kidney damage. Low levels of urinary EGF/Cr at the time of flare, and falling levels over time, are associated with poor long-term kidney outcomes.

AUTHOR CONTRIBUTIONS

All authors were involved in drafting the article or revising it critically for important intellectual content, and all authors approved the final version to be published. Dr. Rovin had full access to all of the data in the study and takes responsibility for the integrity of the data and the accuracy of the data analysis.

Study conception and design. Mejia-Vilet, Shapiro, Parikh, Rovin.

Acquisition of data. Mejia-Vilet, Shapiro, Zhang, Cruz, Zimmerman, Méndez-Pérez, Cano-Verduzco, Parikh, Rovin.


Analysis and interpretation of data. Mejia-Vilet, Méndez-Pérez, Nagaraja, Morales-Buenrostro, Rovin.

REFERENCES

- Mejia-Vilet JM, Rovin BH. Epidemiology and management of lupus nephritis. In: Wallace D, Hahn B, editors. *Dubois' lupus erythematosus and related syndromes*. Elsevier; 2018. p. 727–44.
- Mok CC, Kwok RC, Yip PS. Effect of renal disease on the standardized mortality ratio and life expectancy of patients with systemic lupus erythematosus. *Arthritis Rheum* 2013;65:2154–60.
- Tektonidou MG, Dasgupta A, Ward MM. Risk of end-stage renal disease in patients with lupus nephritis, 1971–2015: a systematic review and Bayesian meta-analysis. *Arthritis Rheumatol* 2016;68:1432–41.
- Birmingham DJ, Merchant M, Waikar SS, Nagaraja H, Klein JB, Rovin BH. Biomarkers of lupus nephritis histology and flare: deciphering the relevant amidst the noise. *Nephrol Dial Transplant* 2017;32:i71–9.
- Gesualdo L, di Paolo S, Calabró A, Milani S, Maiorano E, Ranieri E, et al. Expression of epidermal growth factor and its receptor in normal and diseased human kidney: an immunohistochemical and in situ hybridization study. *Kidney Int* 1996;49:656–65.
- Ju W, Nair V, Smith S, Zhu L, Shedden K, Song PX, et al. Tissue transcriptome-driven identification of epidermal growth factor as a chronic kidney disease biomarker. *Sci Transl Med* 2015;7:316ra193.
- Salido EC, Yen PH, Shapiro LJ, Fisher DA, Barajas L. In situ hybridization of prepro-epidermal growth factor mRNA in the mouse kidney. *Am J Physiol* 1989;256:F632–8.
- Segarra-Medrano A, Carnicer-Caceres C, Valtierra-Carmeno N, Agraz-Pamplona I, Ramos-Terrades N, Escalante EJ, et al. Value of urinary levels of interleukin-6, epidermal growth factor, monocyte chemoattractant protein type 1 and transforming growth factor β 1 in predicting the extent of fibrosis lesions in kidney biopsies of patients with IgA nephropathy. *Nefrología* 2017;37:531–8.
- Ranieri E, Gesualdo L, Petrarulo F, Schena FP. Urinary IL-6/EGF ratio: a useful prognostic marker for the progression of renal damage in IgA nephropathy. *Kidney Int* 1996;50:1990–2001.
- Torres DD, Rossini M, Manno C, Mattace-Raso F, d'Altri C, Ranieri E, et al. The ratio of epidermal growth factor to monocyte chemotactic

- peptide-1 in the urine predicts renal prognosis in IgA nephropathy. *Kidney Int* 2008;73:327–33.
11. Wu L, Li XQ, Chang DY, Zhang H, Li JJ, Wu SL, et al. Associations of urinary epidermal growth factor and monocyte chemoattractant protein-1 with kidney involvement in patients with diabetic kidney disease. *Nephrol Dial Transplant* 2020;35:291–7.
 12. Betz BB, Jenks SJ, Cronshaw AD, Lamont DJ, Cairns C, Manning JR, et al. Urinary peptidomics in a rodent model of diabetic nephropathy highlights epidermal growth factor as a biomarker for renal deterioration in patients with type 2 diabetes. *Kidney Int* 2016;89:1125–35.
 13. Satirapoj B, Dispan R, Radinahamed P, Kitiyakara C. Urinary epidermal growth factor, monocyte chemoattractant protein-1 or their ratio as predictors for rapid loss of renal function in type 2 diabetic patients with diabetic kidney disease. *BMC Nephrol* 2018;19:246.
 14. Li B, Zhang Y, Wang F, Nair V, Ding F, Xiao H, et al. Urinary epidermal growth factor as a prognostic marker for the progression of Alport syndrome in children. *Pediatr Nephrol* 2018;33:1731–9.
 15. Wu L, Li XQ, Goyal T, Eddy S, Kretzler M, Ju WJ, et al. Urinary epidermal growth factor predicts renal prognosis in antineutrophil cytoplasmic antibody-associated vasculitis. *Ann Rheum Dis* 2018;77:1339–44.
 16. Azukaitis K, Ju W, Kirchner M, Nair V, Smith M, Fang Z, et al. Low levels of urinary epidermal growth factor predict chronic kidney disease progression in children. *Kidney Int* 2019;96:214–21.
 17. Gipson DS, Trachtman H, Waldo A, Gibson KL, Eddy S, Dell KM, et al. Urinary epidermal growth factor as a marker of disease progression in children with nephrotic syndrome. *Kidney Int Rep* 2019;5:414–25.
 18. Bartoli F, Penza R, Aceto G, Niglio F, d'Addato O, Pastore V, et al. Urinary epidermal growth factor, monocyte chemoattractant protein-1, and β 2-microglobulin in children with ureteropelvic junction obstruction. *J Pediatr Surg* 2011;46:530–6.
 19. Hochberg MC. Updating the American College of Rheumatology revised criteria for the classification of systemic lupus erythematosus [letter]. *Arthritis Rheum* 1997;40:1725.
 20. Rovin BH, Song H, Birmingham DJ, Hebert LA, Yu CY, Nagaraja HN. Urine chemokines as biomarkers of human systemic lupus erythematosus activity. *J Am Soc Nephrol* 2005;16:467–73.
 21. Weening JJ, d'Agati VD, Schwartz MM, Seshan SV, Alpers CE, Appel GB, et al. The classification of glomerulonephritis in systemic lupus erythematosus revisited. *Kidney Int* 2004;65:521–30.
 22. Gladman DD, Ibanez D, Urowitz MB. Systemic Lupus Erythematosus Disease Activity Index 2000. *J Rheumatol* 2002;29:288–91.
 23. Austin HA III, Muenz LR, Joyce KM, Antonovych TA, Kullick ME, Klippel JH, et al. Prognostic factors in lupus nephritis: contribution of renal histologic data. *Am J Med* 1983;75:382–91.
 24. Bajema IM, Wilhelmus S, Alpers CE, Bruijn JA, Colvin RB, Cook HT, et al. Revision of the International Society of Nephrology/Renal Pathology Society classification for lupus nephritis: clarification of definitions, and modified National Institutes of Health activity and chronicity indices. *Kidney Int* 2018;93:789–96.
 25. Gray A, Dull TJ, Ullrich A. Nucleotide sequence of epidermal growth factor cDNA predicts a 128,000-molecular weight protein precursor. *Nature* 1983;303:722–5.
 26. Mroczkowski B, Reich M, Whittaker J, Bell GI, Cohen S. Expression of human epidermal growth factor precursor cDNA in transfected mouse NIH 3T3 cells. *Proc Natl Acad Sci U S A* 1988;85:126–30.
 27. Hirata Y, Orth DN. Epidermal growth factor (urogastrone) in human tissues. *J Clin Endocrinol Metab* 1979;48:667–72.
 28. Callegari C, Laborde NP, Buenaflor G, Nascimento CG, Brasel JA, Fisher DA. The source of urinary epidermal growth factor in humans. *Eur J Appl Physiol Occup Physiol* 1988;58:26–31.
 29. Oka Y, Orth DN. Human plasma epidermal growth factor/ β -urogastrone is associated with blood platelets. *J Clin Invest* 1983;72:249–59.
 30. Mount CD, Lukas TJ, Orth DN. Purification and characterization of epidermal growth factor (β -urogastrone) and epidermal growth factor fragments from large volumes of human urine. *Arch Biochem Biophys* 1985;240:33–42.
 31. Lindenmeyer MT, Kretzler M, Boucherot A, Berra S, Yasuda Y, Henger A, et al. Interstitial vascular rarefaction and reduced VEGF-A expression in human diabetic nephropathy. *J Am Soc Nephrol* 2007;18:1765–76.
 32. Kajikawa K, Yasui W, Sumiyoshi H, Yoshida K, Nakayama H, Ayhan A, et al. Expression of epidermal growth factor in human tissues: immunohistochemical and biochemical analysis. *Virchows Arch A Pathol Anat Histopathol* 1991;418:27–32.
 33. Mathiesen ER, Nexø E, Hommel E, Parving HH. Reduced urinary excretion of epidermal growth factor in incipient and overt diabetic nephropathy. *Diabet Med* 1989;6:121–6.
 34. Stangou M, Alexopoulos E, Papagianni A, Pantzaki A, Bantis C, Dovas S, et al. Urinary levels of epidermal growth factor, interleukin-6 and monocyte chemoattractant protein-1 may act as predictor markers of renal function outcome in immunoglobulin A nephropathy. *Nephrology* 2009;14:613–20.
 35. Sharma A, Mucino MJ, Ronco C. Renal functional reserve and renal recovery after acute kidney injury. *Nephron Clin Pract* 2014;127:94–100.
 36. Dailey GE, Kraus JW, Orth DN. Homologous radioimmunoassay for human epidermal growth factor (urogastrone). *J Clin Endocrinol Metab* 1978;46:929–36.
 37. Nakamura K, Imai Y, Matuzaki F. Human epidermal growth factor (urogastrone) in human fluids detected by radioreceptor assay. *Nihon Nainbunpi Gakkai Zasshi* 1983;59:1587–96.
 38. Segarra A, Martinez C, Carnicer C, Perich C, Jatem E, Martin M. Analytical and biological variability of urinary epidermal growth factor-to-creatinine ratio in patients with chronic kidney disease and healthy volunteers. *Clin Lab* 2019;65:190304.
 39. Segarra A, Carnicer C, Jatem E, Martin M, Molina M, Perich C, et al. Accuracy of urinary epidermal growth factor to creatinine ratio to predict 24-hour urine epidermal growth factor and interstitial kidney fibrosis in patients with IgA nephropathy. *Clin Lab* 2019;65:181122.

Effects of BAFF Neutralization on Atherosclerosis Associated With Systemic Lupus Erythematosus

Fanny Saidoune,¹ Guillaume Even,² Yasmine Lamri,¹ Julie Chezel,³ Anh-Thu Gaston,² Brigitte Escoubet,⁴ Thomas Papo,³ Nicolas Charles,¹ Antonino Nicoletti,² and Karim Sacre³ 

Objective. Cardiovascular disease (CVD) is the leading cause of death in systemic lupus erythematosus (SLE). B cells play a key role in the pathogenesis of lupus, and anti-BAFF therapy has been approved for use in SLE. Since mature B cells also promote atherosclerosis, we undertook this study to evaluate, in a mouse model and in SLE patients, whether BAFF neutralization has an atheroprotective effect in SLE.

Methods. The effect of BAFF on atherosclerosis associated with lupus was investigated in the atherosclerosis/lupus-prone apolipoprotein E–knockout D227K mouse model and in a cohort of SLE patients. Mice were treated with a blocking anti-BAFF monoclonal antibody (mAb), while fed a standard chow diet. Carotid plaque and carotid intima-media thickness were assessed by ultrasound at baseline and during follow-up in SLE patients who were asymptomatic for CVD.

Results. Anti-BAFF mAb in ApoE^{-/-} D227K mice induced B cell depletion, efficiently treated lupus, and improved atherosclerosis lesions (21% decrease; $P = 0.007$) in mice with low plasma cholesterol levels but worsened the lesions (17% increase; $P = 0.06$) in mice with high cholesterol levels. The atheroprotective effect of the BAFF–BAFF receptor signaling inhibition on B cells was counterbalanced by the proatherogenic effect of the BAFF–TACI signaling inhibition on macrophages. In SLE patients, blood BAFF levels were associated with subclinical atherosclerosis ($r = 0.26$, $P = 0.03$). Anti-BAFF mAb treatment had a differential effect on the intima-media thickness progression in SLE patients depending on body mass index.

Conclusion. Depending on the balance between lipid-induced and B cell–induced proatherogenic conditions, anti-BAFF could be detrimental or beneficial, respectively, to atherosclerosis development in SLE.

INTRODUCTION

Accelerated atherosclerosis is now recognized as the main cause of death in patients with systemic lupus erythematosus (SLE) (1), but the increased prevalence of premature atherosclerosis in SLE is not fully explained by traditional cardiovascular risk factors such as age, smoking status, hypertension, or dyslipidemia (2–6). While we have previously shown that lupus immunopathogenesis may promote accelerated atherosclerosis (7),

the mechanisms by which SLE might contribute to this remain elusive.

Lupus disease is dependent on the generation of autoreactive antibodies by B cells (8,9). Strong evidence points to BAFF, a cytokine required for maturation and survival of B-2 cells, as playing a key role in lupus (10). Constitutive overexpression of BAFF leads to a lupus-like phenotype in mice that are not genetically lupus-prone (11). In humans, circulating BAFF levels are elevated in as many as 50% of SLE patients, and a large 2-year longitudinal

Supported by the French CRC 2017 Ministère de la Santé (number 17-068) and the Agence Nationale de la Recherche (JCJC SVSE1 2011 BASILE and JCJC CE17 2015 BATTI). Dr. Saidoune's work was supported by research grants from the Ministère de la Recherche, Association Nationale de la Recherche et de la Technologie-Conventions Industrielles de Formation par la Recherche, and from DHU Fire (Bourse Emergence 4). Dr. Chezel's work was supported by a research grant from the Fondation pour la Recherche Médicale (DEA20170638077).

¹Fanny Saidoune, PhD, Yasmine Lamri, PhD, Nicolas Charles, PhD: Centre de Recherche sur l'Inflammation, INSERM UMR1149, CNRS ERL8252, Laboratoire d'Excellence Inflamex, Université de Paris, Paris, France; ²Guillaume Even, PhD, Anh-Thu Gaston, PhD, Antonino Nicoletti, PhD: Université de Paris, INSERM U1148, Laboratoire d'Excellence

Inflamex, Paris, France; ³Julie Chezel, MD, Thomas Papo, MD, Karim Sacre, MD PhD: Centre de Recherche sur l'Inflammation, INSERM UMR1149, CNRS ERL8252, Laboratoire d'Excellence Inflamex, Université de Paris, Hôpital Bichat–Claude-Bernard, AP-HP, Paris, France; ⁴Brigitte Escoubet, MD, PhD: Université de Paris, Hôpital Bichat–Claude-Bernard, AP-HP, Paris, France.

Drs. Charles and Nicoletti contributed equally to this work.

Dr. Saidoune has received research support from GlaxoSmithKline France. No other disclosures relevant to this article were reported.

Address correspondence to Karim Sacre, MD, PhD, Department of Internal Medicine, Bichat Hospital, AP-HP, 46 Rue Henri Huchard, 75018 Paris, France. Email: karim.sacre@bch.aphp.fr.

Submitted for publication February 5, 2020; accepted in revised form August 6, 2020.

study documented a significant correlation between BAFF levels and clinical disease activity (12,13). Moreover, belimumab, a B cell-depleting monoclonal antibody (mAb) that targets BAFF, was shown to reduce SLE disease activity, prevent flares, and reduce glucocorticoid use in a large international, multicenter, randomized, placebo-controlled phase III trial (14,15). Belimumab was the first biologic therapy approved by the Food and Drug Administration for use in SLE.

While B cells were initially considered as atheroprotective immune cells, recent studies have challenged this view with the demonstration that B-2 cells comprise proatherogenic cells (16–18). Accordingly, atherosclerosis-prone mice in which hematopoietic cells did not express the receptor for the pro-B-2 BAFF cytokine displayed a significant reduction in atherosclerotic lesion development (18,19). Therefore, targeting BAFF signaling and B-2 cells may represent an interesting therapeutic option to treat both SLE and atherosclerosis. The aim of our study was to test this hypothesis using a new mouse model with dual susceptibility to lupus and atherosclerosis (untreated or treated with an anti-BAFF therapy) as well as in a cohort of SLE patients in whom we monitored carotid plaques, B cells, and BAFF levels.

SUBJECTS AND METHODS

Study participants. Seventy-three consecutive patients with SLE followed up at the Department of Internal Medicine, Bichat Hospital, University of Paris were enrolled between January 2012 and January 2013. All patients fulfilled the American College of Rheumatology criteria for SLE (20). Exclusion criteria consisted of known coronary disease or symptoms suggestive of cardiovascular disease (CVD; angina, arrhythmia, congestive heart failure, stroke, or peripheral arterial disease). The local ethics committee approved the study (Institutional Review Board IRB 00006477 of HUPNVS, AP-HP). All patients provided written informed consent. Patient characteristics are detailed in the Supplementary Methods (available on the *Arthritis & Rheumatology* website at <http://onlinelibrary.wiley.com/doi/10.1002/art.41485/abstract>).

Mice. Female apolipoprotein E-knockout mice were purchased from The Jackson Laboratory, and ApoE^{-/-} D227K (Qa-1^{D22K/D227K}) mice were generated as previously described (21). All mice were on a C57BL/6J background and were maintained and fed a standard chow diet in the animal facility of Unité 1148, Institut National de la Santé et de la Recherche Médicale (INSERM), Bichat Hospital. In vivo BAFF neutralization was performed on 12-week-old ApoE^{-/-} D227K mice by intraperitoneal injection once every 2 weeks with 100 µg mouse anti-BAFF mAb (Armenian hamster IgG1, clone 10F4B; provided by GlaxoSmith-Kline) or isotype control (Hamster IgG; Innovative Research). For each experiment, mice were euthanized at 40 weeks of age by intraperitoneal injection of 100 mg/kg ketamine HCl and 20 mg/kg

xylazine, followed by exsanguination. Mice were used in accordance with the French and European guidelines and approved by the ethical committee and by the Department of Research of the French government under study proposal number 5339 (APAFIS no. 5339-2017122818274866v6).

Cell, tissue, and plasma analyses. Human and mouse cell suspensions were analyzed by flow cytometry. Mouse atherosclerotic lesions were measured as previously described (21). Mouse kidney lesions were characterized by immunofluorescence. IgG anti-double-stranded DNA (anti-dsDNA), IgG anti-phosphorylcholine (anti-PC), and BAFF were quantified by enzyme-linked immunosorbent assay. Detailed methods are available in the Supplementary Methods (<http://onlinelibrary.wiley.com/doi/10.1002/art.41485/abstract>).

Statistical analysis. After normal distribution testing (D'Agostino-Pearson test or Shapiro-Wilk test depending on sample size), differences between groups were analyzed using Student's unpaired *t*-test, unless otherwise indicated. Two-way analysis of variance was used to compare 2 independent variables in 2 groups. Correlations were analyzed using Spearman's or Pearson's correlation coefficient test. Data are represented either as the mean ± SEM or as median and interquartile ranges. All analyses were performed with GraphPad Prism, version 6. All tests were 2-tailed, and *P* values less than 0.05 were considered significant.

RESULTS

Association of lupus phenotype and accelerated atherosclerosis in ApoE^{-/-} D227K mice with the expansion of B cells in secondary lymphoid organs and aortic adventitia. In order to obtain a model of lupus-associated atherosclerosis, ApoE^{-/-} D227K mice were generated by crossing lupus-prone Qa-1^o (D227K) mice (22) with atherosclerosis-prone ApoE^{-/-} mice. We first investigated whether B cells were modified in ApoE^{-/-} D227K mice and then compared the spleen cells between 40-week-old ApoE^{-/-} mice and ApoE^{-/-} D227K mice. As previously reported (21), CD19+ B cells in ApoE^{-/-} D227K mice were expanded compared to ApoE^{-/-} mice, with no difference in the overall percentages of T cells, dendritic cells, monocyte/macrophages, or neutrophils in the spleen (Figure 1A). Among B cells, the proportions of germinal center B cells (I-A/I-E+GL7^{high}) and follicular B cells (CD21+IgM^{low}) were significantly increased (Figure 1B). Consistent with this observation, plasma BAFF levels were higher in ApoE^{-/-} D227K mice compared to ApoE^{-/-} mice (Figure 1C).

Concomitantly, ApoE^{-/-} D227K mice displayed a lupus-like phenotype with raised levels of IgG directed against dsDNA in serum and increased IgG and complement C3 deposition in renal glomeruli (Figures 1D and E), and they developed significantly larger aortic plaques than did the ApoE^{-/-} mice (Figure 1F).

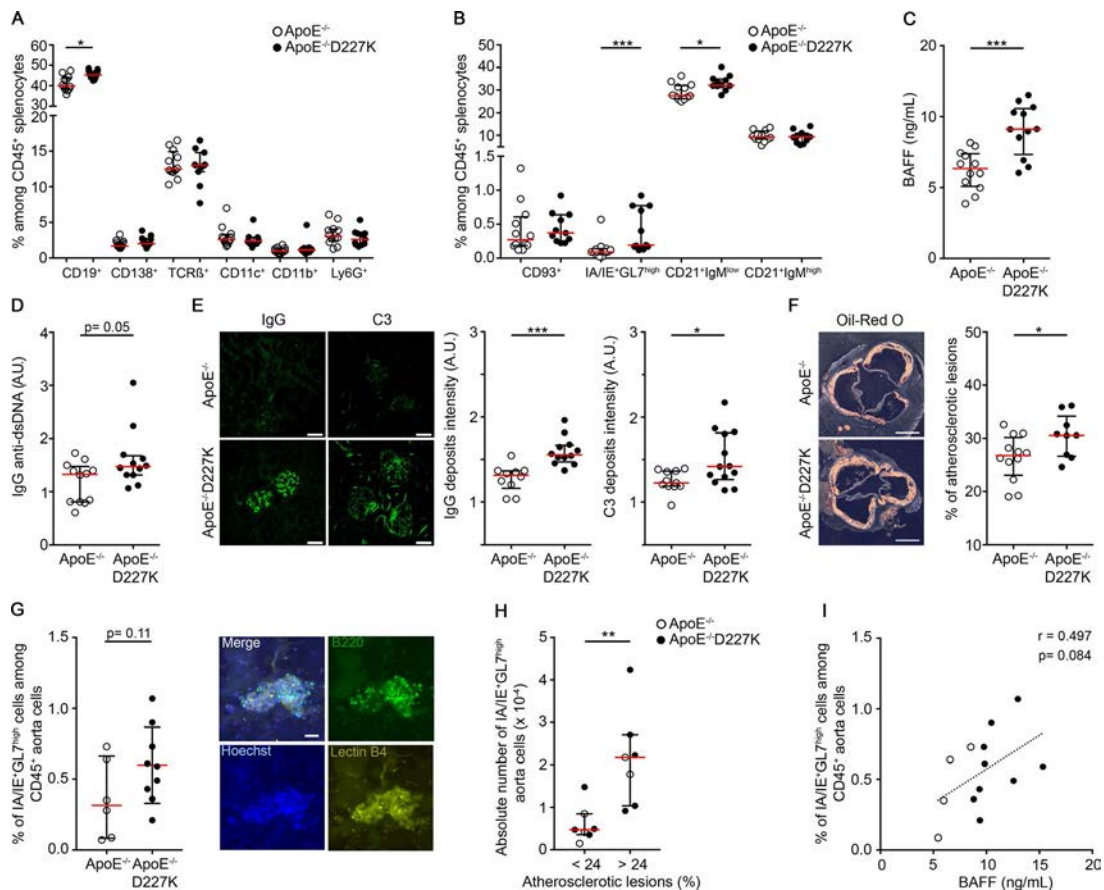


Figure 1. Expansion of B cells in secondary lymphoid organs and aortic adventitia are associated with a lupus phenotype and accelerated atherosclerosis in ApoE^{-/-} D227K mice. **A**, Proportions of B cells (CD19+), plasmacytes (CD138+), T cells (T cell receptor β -positive [TCR β +]), dendritic cells (CD11c+), monocytes (CD11b+), and neutrophils (Ly6G+) among CD45+ living cells in the spleens of ApoE^{-/-} mice (n = 12) and ApoE^{-/-} D227K mice (n = 11), determined by flow cytometry. **B**, Proportions of immature B cells (CD93+), germinal center B cells (I-A/I-E+GL7^{high}), follicular B cells (CD21+IgM^{low}), and marginal zone B cells (CD21+IgM^{high}) among CD45+ splenocytes. **C**, Plasma BAFF levels. **D**, Levels of anti-double-stranded DNA (anti-dsDNA) IgG in plasma. **E**, Immunofluorescence staining for IgG and C3 glomerular deposits in kidneys, and the corresponding quantification. Bars = 50 μ m. **F**, Oil red O staining in the aortic root, and quantification of the percentage of atherosclerotic lesions 400 μ m from the appearance of the cusp in ApoE^{-/-} mice (n = 12) and ApoE^{-/-} D227K mice (n = 9). Bars = 500 μ m. **G**, Proportions of germinal center B cells among CD45+ living cells in digested whole aorta of ApoE^{-/-} mice (n = 6) and ApoE^{-/-} D227K mice (n = 9), and immunofluorescence staining of B cell cluster (B-220+) in the whole adventitia (aortic arch) supplied by isolectin B4+ blood vessels. Bar = 50 μ m. **H**, Absolute numbers of germinal center B cells in the aorta of mice according to percentage of atherosclerotic lesions in an aortic root sample obtained 600 μ m from the cusp. In **A–H**, Symbols represent individual mice; horizontal and vertical bars show the median and interquartile range. **I**, Correlation between plasma BAFF levels and the proportion of germinal center B cells in the aorta. * = $P < 0.05$; ** = $P < 0.01$; *** = $P < 0.001$.

Additionally, the percentage of I-A/I-E+GL7^{high} B cells, organized in clusters in the aortic adventitia, was increased in the aorta of ApoE^{-/-} D227K mice and was associated with both severity of atherosclerotic lesions and higher plasma BAFF levels (Figures 1G–I). These data suggest that atherogenesis in ApoE^{-/-} D227K mice is accelerated and associated with a BAFF-driven expansion of I-A/I-E+GL7^{high} B cells and lupus-like phenotype.

Reduction of lupus-like disease activity through neutralizing anti-BAFF, but with no detectable effect on atherosclerosis, in ApoE^{-/-} D227K mice. To investigate the role of BAFF in accelerated atherosclerosis associated with lupus, we treated ApoE^{-/-} D227K mice being fed a standard chow diet for 28

weeks with a neutralizing anti-mouse BAFF mAb hamster antibody (clone 10F4). Mice treated with anti-BAFF mAb had similar body weights and levels of total cholesterol and plasma triglyceride, compared to mice treated with control mAb (Supplementary Table 2, <http://onlinelibrary.wiley.com/doi/10.1002/art.41485/abstract>). In ApoE^{-/-} D227K mice, anti-BAFF mAb treatment induced an efficient and sustained B cell (CD19+) depletion over time in peripheral blood (Figure 2A). As expected, the complete BAFF neutralization (Figure 2B) resulted in a robust reduction of B cells (CD19+) in both the lymph nodes and the spleen (Figure 2C). Among B cells, plasma cells (CD138+), germinal center B cells (I-A/I-E+GL7^{high}), follicular B cells (CD21+IgM^{low}), and marginal zone B cells (CD21+IgM^{high}) were dramatically reduced (Figure 2D).

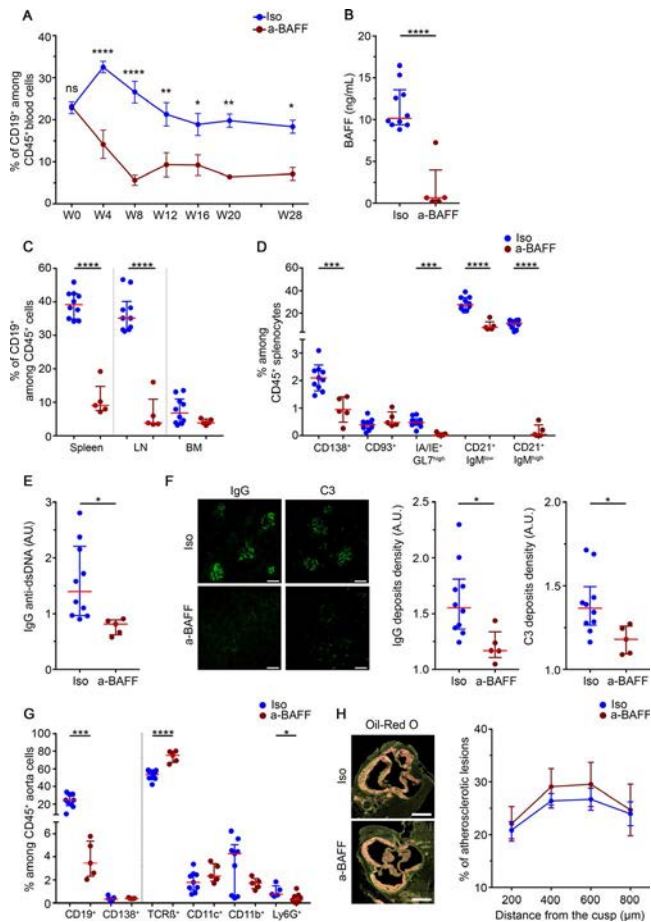


Figure 2. Neutralizing anti-BAFF dramatically dampens B cells in secondary and tertiary lymphoid organs, efficiently treats lupus, but has no apparent effect on atherosclerosis in ApoE^{-/-} D227K mice. **A**, Proportions of total B cells (CD19⁺) among CD45⁺ living leukocytes in the peripheral blood of ApoE^{-/-} D227K mice treated with isotype control (Iso; n = 10) or with anti-BAFF antibody (a-BAFF; n = 5). Proportions were determined by flow cytometry prior to the first injection (week 0 [W0]) and at 4, 8, 12, 16, 20, 28 weeks after the first injection. **B**, Plasma BAFF levels. **C**, Proportions of total B cells among CD45⁺ living cells in the spleen, lymph nodes (LNs), and bone marrow (BM), determined by flow cytometry. **D**, Proportions of plasmacytes (CD138⁺), immature B cells (CD93⁺), germinal center B cells (I-A/I-E+GL7^{high}), follicular B cells (CD21+IgM^{low}), and marginal zone B cells (CD21+IgM^{high}) among CD45⁺ splenocytes. **E**, Levels of anti-dsDNA IgG in plasma. **F**, Immunofluorescence staining for IgG and C3 glomerular deposits in kidneys, and the corresponding quantification. Bars = 50 μ m. **G**, Proportions of B cells (CD19⁺), plasmacytes (CD138⁺), T cells (TCR β ⁺), dendritic cells (CD11c⁺), monocytes (CD11b⁺), and neutrophils (Ly6G⁺) among CD45⁺ living cells in digested whole aorta of ApoE^{-/-} D227K mice treated with isotype control (n = 9) or anti-BAFF antibody (n = 5). **H**, Oil red O staining in the aortic root, and quantification of the percentage of atherosclerotic lesions 200 μ m, 400 μ m, 600 μ m, and 800 μ m from the appearance of the cusp. Bars = 500 μ m. In **A** and **H**, values are the mean \pm SEM. In **B-G**, Symbols represent individual mice; horizontal and vertical bars show the median and interquartile range. * = $P < 0.05$; ** = $P < 0.01$; *** = $P < 0.001$; **** = $P < 0.0001$. See Figure 1 for other definitions. Color figure can be viewed in the online issue, which is available at <http://onlinelibrary.wiley.com/doi/10.1002/art.41485/abstract>.

Anti-BAFF mAb treatment did not alter numbers of T cells, dendritic cells, monocyte/macrophages, or neutrophils in the spleen (Supplementary Figure 2A, <http://onlinelibrary.wiley.com/doi/10.1002/art.41485/abstract>). We confirmed in our mouse model that neutralization of BAFF was highly effective as a lupus treatment. Indeed, ApoE^{-/-} D227K mice treated with anti-BAFF mAb had a profound decrease in serum anti-dsDNA antibody levels and markedly reduced IgG and C3 deposition in renal glomeruli (Figures 2E and F). However, despite an almost complete depletion of B cells in the aorta wall (Figure 2G and Supplementary Figure 2B), a significant reduction of B-2 cells and a corresponding increase of B-1 cells in the spleen (Supplementary

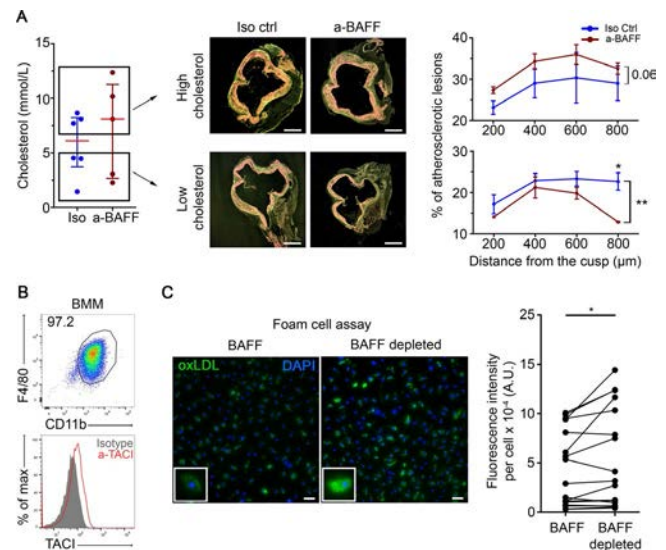


Figure 3. Efficacy of neutralizing anti-BAFF on atherosclerosis in ApoE^{-/-} D227K mice depends on plasma cholesterol levels. **A**, Plasma cholesterol levels in ApoE^{-/-} D227K mice treated with isotype control (n = 6) or anti-BAFF antibody (n = 5). The low cholesterol group (mean \pm SEM cholesterol level 3.16 ± 1.35 mmol/liter) and high cholesterol group (9.182 ± 1.78 mmol/liter) included 2 and 3 anti-BAFF monoclonal antibody-treated mice, respectively, and 3 isotype controls each. P values indicate the difference between isotype control and anti-BAFF antibody groups, and between low and high cholesterol groups. Symbols represent individual mice; horizontal and vertical bars show the median and interquartile range. Oil red O staining in the aortic root, and quantification of the mean \pm SEM percentage of atherosclerotic lesions at 200 μ m, 400 μ m, 600 μ m, and 800 μ m from the appearance of the cusp are shown. Bars = 500 μ m. **B**, Proportion of macrophages (F4/80+CD11b⁺) among living cells after 10 days in mouse bone marrow-derived macrophage (BMM) culture, determined by flow cytometry. TAC1 expression on BMMs is shown. **C**, Foam cell formation assay in BMMs. BMMs were stimulated with 400 μ g/ml oxidized low-density lipoprotein (ox-LDL) and 10% plasma drawn from ApoE^{-/-} D227K mice, which was or was not depleted of BAFF in vitro. Lipid droplets in cells were visualized by oil red O staining and counterstained with DAPI. A representative field and cell (inset) per condition and the corresponding quantification of fluorescence intensity per cell are shown. Bars = 50 μ m. * = $P < 0.05$; ** = $P < 0.01$. See Figure 2 for other definitions. Color figure can be viewed in the online issue, which is available at <http://onlinelibrary.wiley.com/doi/10.1002/art.41485/abstract>.

Figure 2C), along with a decrease in IgG antibodies specific for the oxidized low-density lipoprotein (ox-LDL) anti-PC antibodies in serum (Supplementary Figure 2D), anti-BAFF mAb treatment had no measurable effect on plaque formation and thus on atherosclerosis associated with lupus (Figure 2H).

Enhanced foam cell formation through BAFF neutralization. In contrast to findings of previous studies on anti-CD20-treated and BAFF receptor (BAFF-R)-knock-out mouse models of atherosclerosis (16–19,23), and although it had a prominent effect on B cells, neutralization of BAFF did not reduce atherosclerotic lesions in ApoE^{-/-} D227K mice. To further increase complexity, anti-BAFF antibody treatment may actually increase atherosclerosis in ApoE^{-/-} mice through the inhibition of a TACI-mediated atheroprotective effects on macrophages (24). In the latter study, mice were fed an atherogenic high-fat diet and displayed plasma cholesterol levels that were ~6 times higher than those observed in ApoE^{-/-} D227K mice (mean ± SD total cholesterol 39.8 ± 2.3 mmol/liter versus 7.19 ± 4.4 mmol/liter) (24).

We hypothesized that the effect of BAFF neutralization on atherosclerosis might differ according to cholesterol levels

prior to treatment. We grouped ApoE^{-/-} D227K mice based on plasma cholesterol levels, defining high and low cholesterol groups (Figure 3A). After anti-BAFF mAb treatment, atherosclerosis lesions improved in the ApoE^{-/-} D227K mice that had low plasma cholesterol levels (21% decrease; $P = 0.007$) and worsened in mice with high cholesterol levels (17% increase; $P = 0.06$) (Figure 3A). Interestingly, the beneficial effect of the anti-BAFF mAb treatment on atherosclerosis was not reproduced when given to ApoE^{-/-} mice with low cholesterol (Supplementary Figure 3, <http://onlinelibrary.wiley.com/doi/10.1002/art.41485/abstract>), indicating that this effect was not solely related to the plasma cholesterol level but, presumably, to the lupus-prone background of the ApoE^{-/-} D227K mice.

Since anti-BAFF mAb treatment contributed to the atherogenesis in ApoE^{-/-} D227K mice with high cholesterol, we investigated the impact of BAFF depletion on foam cell formation in vitro. We confirmed the expression of the TACI receptor on bone marrow-derived macrophages (24,25) (Figure 3B) and found that BAFF depletion (Supplementary Figure 4, <http://onlinelibrary.wiley.com/doi/10.1002/art.41485/abstract>) significantly increased the ox-LDL-dependent macrophage differentiation into foam cells (Figure 3C), strongly suggesting that BAFF neutralization

Table 1. Characteristics of the SLE patients*

	All (n = 73)	No carotid plaque (n = 51)	Carotid plaque (n = 22)	P
Age, mean ± SD years	40.4 ± 10.5	36.9 ± 8	48.4 ± 11.2	<0.01
Female sex	66 (90.4)	45 (88.2)	21 (95.5)	NS
Hypertension	18 (24.7)	5 (9.8)	13 (59.1)	<0.01
Smoker	24 (32.9)	17 (33.3)	7 (31.8)	NS
LDL cholesterol, mean ± SD gm/liter	0.95 ± 0.4	0.94 ± 0.37	0.98 ± 0.47	NS
10-year risk of heart attack, mean ± SD %†	1.7 ± 3.6	1 ± 1.6	3.3 ± 5.9	<0.05
BMI >25 kg/m ²	35 (47.9)	19 (37.3)	16 (72.3)	<0.05
eGFR <60 ml/minute/1.73 m ² ‡	11 (15)	4 (7.8)	7 (31.8)	<0.05
Proteinuria/creatininuria, mean ± SD mg/mmoles	70 ± 195.1	61.8 ± 188.8	89.7 ± 212.7	NS
Duration of SLE, mean ± SD years	12.2 ± 9.5	10.9 ± 7.5	15.2 ± 12.6	NS
SELENA-SLEDAI score, mean ± SD	2.3 ± 3	2.5 ± 3	1.9 ± 3	NS
Lupus nephritis§	41 (56.2)	25 (49)	16 (72.7)	NS
aPL antibodies¶	25 (34.2)	19 (37.3)	6 (27.3)	NS
APS	12 (16.4)	7 (13.7)	5 (22.7)	NS
Cumulative time of steroid treatment, mean ± SD years	8.3 ± 6.6	7.5 ± 6	10.2 ± 7.6	NS
Cumulative dose of steroid treatment, mean ± SD gm	40.4 ± 26.6	38.5 ± 23.9	46.9 ± 34.7	NS
Receiving steroid treatment at study time	49 (67.1)	35 (68.6)	14 (63.6)	NS
Steroid dosage at study time, mean ± SD mg/day	9.7 ± 7.1	9.1 ± 5.1	11.2 ± 10.5	NS
Other treatment, at study time				
Hydroxychloroquine	71 (97.3)	50 (98)	21 (95.5)	NS
Immunosuppressive therapy#	49 (67.1)	32 (62.7)	17 (77.3)	NS
Antiplatelet therapy	10 (13.7)	5 (9.8)	5 (22.7)	NS
Statins	13 (17.8)	6 (11.8)	7 (31.8)	NS

* Except where indicated otherwise, values are the number (%) of patients. Carotid plaque was defined as an internal carotid wall thickness of >1.5 mm. SLE = systemic lupus erythematosus; NS = not significant; LDL = low-density lipoprotein; BMI = body mass index; eGFR = estimated glomerular filtration rate; SELENA-SLEDAI = Safety of Estrogens in Lupus Erythematosus National Assessment version of the SLE Disease Activity Index; aPL = antiphospholipid; APS = antiphospholipid syndrome.

† Calculated using the Framingham equation.

‡ Calculated using the Modification of Diet in Renal Disease equation.

§ Class III or class IV.

¶ Including lupus anticoagulant, anticardiolipin, and anti-β₂-glycoprotein I antibodies.

Including cyclophosphamide, azathioprine, mycophenolate mofetil, and methotrexate.

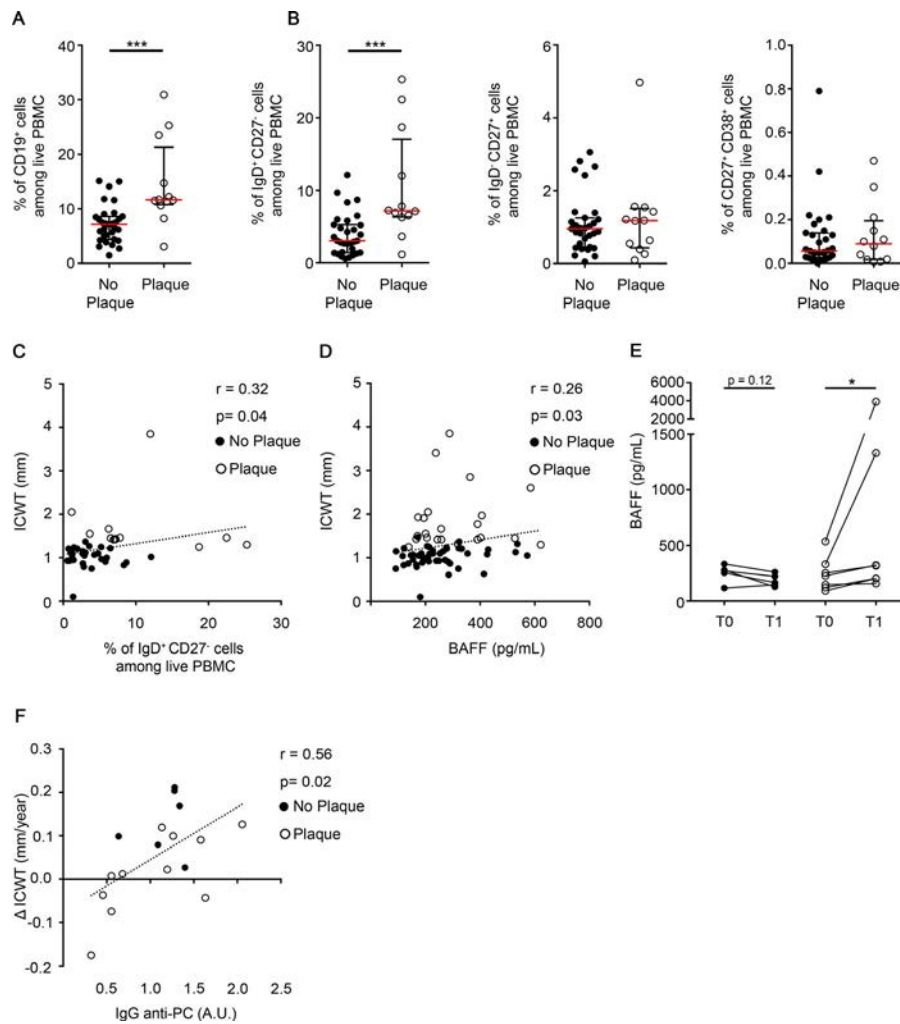


Figure 4. CD19+IgD+CD27⁻ B cells, BAFF, and IgG anti-phosphorylcholine (anti-PC) antibodies in systemic lupus erythematosus (SLE) patients are associated with atherosclerosis. **A**, Proportions of B cells (CD19⁺) among living peripheral blood mononuclear cells (PBMCs), determined by flow cytometry and analyzed in SLE patients with carotid plaque ($n = 12$) and those without carotid plaque ($n = 31$). Carotid plaque was defined by an internal carotid wall thickness (ICWT) of >1.5 mm. **B**, Proportions of CD19⁺ cell subsets in PBMCs (preswitch [IgD+CD27⁻], postswitch [IgD-CD27⁺], and plasmablast cells [CD27+CD38⁺]) in the patients described in **A**. **C**, Correlation between frequency of preswitch B cells and ICWT in SLE patients with carotid plaque ($n = 12$) and those without ($n = 29$). **D**, Correlation between plasma BAFF levels and ICWT in SLE patients with carotid plaque ($n = 22$) and those without ($n = 51$). **E**, Plasma BAFF levels in 7 patients in whom carotid plaque had developed between the first vascular assessment (T0) and the follow-up vascular assessment (T1) (open circles) and in 5 patients who exhibited no progression in subclinical atherosclerosis between the first and second assessments (solid circles). The onset of carotid plaque during follow-up in SLE patients was associated with an increase of 171% (mean \pm SEM $+675.8 \pm 1,236$ pg/ml; $P = 0.01$) in plasma BAFF levels between the first and second vascular assessments, while the lack of progression in subclinical atherosclerosis tended to be associated with a decrease in BAFF of 12% (mean \pm SEM -66 ± 65.5 pg/ml; $P = 0.12$). **F**, Correlation between plasma levels of IgG anti-PC antibodies measured at baseline and ICWT progression during follow-up in SLE patients with carotid plaque ($n = 11$) and those without carotid plaque ($n = 6$). In **A** and **B**, symbols represent individual patients; horizontal and vertical bars show the median and interquartile range. * = $P < 0.05$; *** = $P < 0.001$. Color figure can be viewed in the online issue, which is available at <http://onlinelibrary.wiley.com/doi/10.1002/art.41485/abstract>.

in vivo in a high-cholesterol environment may lead to increased foam cell formation and subsequent increased plaque formation (Figure 3A).

Taken together, these data suggest a contrasting effect of BAFF on atherosclerosis, enhancing atherogenesis in a B cell/BAFF-R-dependent manner on the one hand and promoting atheroprotection in a macrophage/TACI-dependent manner on the other hand.

Correlation of CD19+IgD+CD27⁻ B cells, BAFF, and IgG anti-PC antibodies with subclinical atherosclerosis in SLE patients. Next, we studied human atherosclerosis associated with SLE. We first analyzed the prevalence of subclinical atherosclerosis in a cohort of 73 SLE patients (mean \pm SD age 40.4 ± 10.5 years, 90.4% female) without known CVD (Table 1). Ultrasound was performed at baseline and identified carotid plaque (i.e., a local internal carotid artery wall thickness [ICWT] of >1.5 mm [26]) in

22 SLE patients (30.1%), despite a very low risk for cardiovascular events (CVEs) according to the Framingham score (27) (mean \pm SD 1.7 \pm 3.6%). As expected, age, hypertension, Framingham score, overweight, and chronic kidney disease were associated with subclinical atherosclerosis in SLE (Table 1).

Interestingly, the frequency of CD19+ B cells in peripheral blood was significantly higher in SLE patients with carotid plaque compared to SLE patients without plaque (Figure 4A). Among B cells, increased proportions of the CD19+IgD+CD27- preswitch B cell subset were associated with carotid plaque and correlated positively with ICWT in SLE (Figures 4B and C). In addition, serum BAFF levels correlated positively with ICWT (Figure 4D).

We next analyzed the occurrence of carotid plaques over time in SLE patients. Among the 51 SLE patients without carotid plaque at baseline, 27 had a second vascular ultrasound

performed at a mean \pm SD of 3.3 \pm 1.4 years after the first evaluation. Ultrasound revealed new carotid plaque in 10 cases (37%), corresponding to a rate of 1 plaque per 7.1 SLE patients per year. The 10-year cardiovascular risk did not significantly differ between SLE patients in whom carotid plaque occurred during follow-up and those with no new carotid plaque (mean \pm SD 2.4 \pm 3 versus 0.8 \pm 0.7; $P = 0.471$). However, an increase in plasma BAFF levels over time was associated with the onset of carotid plaque, and a steady level of plasma BAFF levels was associated with a lack of progression of subclinical atherosclerosis (Figure 4E). Moreover, progression of ICWT in SLE patients during follow-up positively correlated with anti-PC IgG antibody levels measured in serum at baseline (Figure 4F).

Contrasting effect of anti-BAFF treatment on intima-media thickness progression in SLE patients.

During a 16-month period, 3 of 73 SLE patients in our cohort received belimumab. Belimumab induced a robust reduction both in plasma BAFF levels and in IgD+CD27- preswitch B cell frequency measured in peripheral blood (Figures 5A and B), which was associated with better control of SLE activity as assessed by the Safety of Estrogens in Lupus Erythematosus National Assessment version of the SLE Disease Activity Index (28) in all 3 cases.

Despite a homogeneous effect of belimumab on the B cells in all 3 patients, subclinical atherosclerosis progression was heterogeneous. Intima-media thickness, prospectively observed before and during treatment in 2 patients, strongly increased in patient 1, while slightly decreasing in patient 2 (Figure 5C). Interestingly, these 2 patients shared the same characteristics regarding SLE disease and risk of CVEs, with the exception of body mass index (BMI) (38.3 kg/m² for patient 1 and 21.4 kg/m² for patient 2, at the start of belimumab treatment) (Supplementary Table 3, <http://onlinelibrary.wiley.com/doi/10.1002/art.41485/abstract>). This observation suggests that despite a homogeneous impact on B cells, anti-BAFF treatment in SLE patients might have differential effects on atherosclerosis depending on BMI. Accordingly, the positive correlation of BAFF levels with ICWT that was observed in the cohort of SLE patients (Figure 4D) was lost when considering patients with a BMI of >25 kg/m² (Figure 5D). Furthermore, the decrease in plasma BAFF levels during belimumab treatment was associated with an in vitro increase in the ox-LDL-dependent macrophage differentiation into foam cells in patient 1 (BMI >25 kg/m²) but a decrease in patient 2 (BMI <25 kg/m²) (Figure 5E).

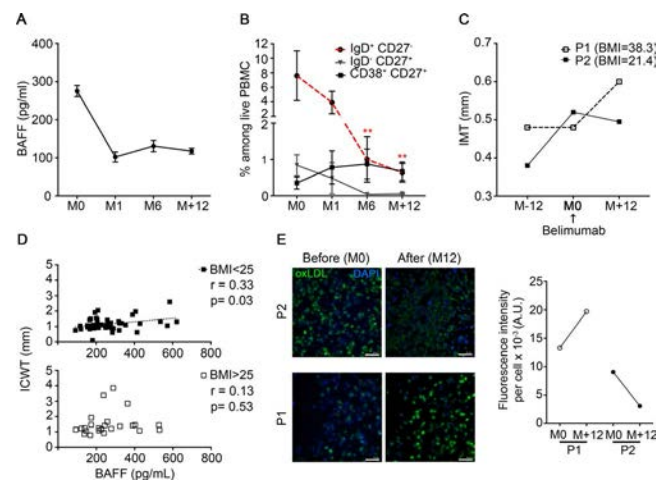


Figure 5. Opposite effect of neutralizing anti-BAFF on atherosclerosis according to body mass index (BMI) in SLE patients. **A**, Plasma BAFF levels in 3 SLE patients treated with belimumab (10 mg/kg once every 4 weeks) over time. BAFF was measured the day of first injection (month 0 [M0]) and at 1, 6, and >12 months after the first injection. **B**, Frequencies of CD19+ cell subsets in PBMCs (preswitch [IgD+CD27-], postswitch [IgD+CD27+], and plasmablast cells [CD27+CD38+]) in the patients described in **A**. **C**, Progression of intima-media thickness (IMT) measured >12 months before the first injection of belimumab, the day of first injection, and after >12 months of belimumab treatment in an SLE patient with high BMI (P1) and in an SLE patient with normal BMI (P2). **D**, Correlation between plasma BAFF levels and ICWT in SLE patients with a BMI of <25 kg/m² ($n = 46$) and those with a BMI of >25 kg/m² ($n = 24$). **E**, Foam cell formation assay on phorbol myristate acetate-induced macrophage-differentiated THP-1 cells stimulated with 2 μ g/ml oxidized low-density lipoprotein (ox-LDL) and 10% plasma obtained the day of first injection of belimumab and after >12 months of belimumab treatment in the 2 SLE patients described in **C**. A representative field per condition and the corresponding quantification of fluorescence intensity per cell are shown. Bars = 50 μ m. In **A** and **B**, values are the mean \pm SEM. ** = $P < 0.01$ versus month 0. See Figure 4 for other definitions. Color figure can be viewed in the online issue, which is available at <http://onlinelibrary.wiley.com/doi/10.1002/art.41485/abstract>.

DISCUSSION

Models for predicting CVEs in the general population (such as the Framingham model) underestimate the cardiovascular risk in SLE, at least partly because they do not incorporate important risk factors such as overweight, chronic kidney disease, or systemic inflammation (2,3,29). Despite the high

prevalence and early onset of CVEs, the mechanisms leading to accelerated atherosclerosis in SLE are still unclear, and the optimal cardiovascular prevention strategy has yet to be defined.

We hypothesized that SLE immune dysregulation may accelerate atherosclerosis and investigated the effect of BAFF neutralization on the development of atherosclerosis associated with lupus. Our data support the notion of an unexpected double-edged effect of BAFF neutralization on atherosclerosis development both in an atherosclerosis/lupus-prone mouse model and in SLE patients. Indeed, our findings strongly suggest that the disruption of BAFF–BAFF-R signaling on B cells has an atheroprotective effect, while the disruption of BAFF–TACI signaling on macrophages has a proatherogenic effect. In SLE, neutralizing BAFF using an anti-BAFF antibody may promote atherosclerosis by enhancing macrophage foam cell formation when proatherogenic conditions, such as dyslipidemia or overweight, are present. In contrast, neutralizing anti-BAFF antibodies might beneficially affect atherosclerosis development by depleting B cells when only proatherogenic B-2 cells are overrepresented (for a schematic view see Supplementary Figure 5, <http://onlinelibrary.wiley.com/doi/10.1002/art.41485/abstract>).

B cell and humoral responses are instrumental in the initiation and progression of atherosclerosis (30). Although initial studies indicated the atheroprotective potential of the B cells that rely on B-1 cells (31,32), more recent studies have identified T-dependent B cells (B-2 cells) as potent proatherogenic mediators in mouse models of atherosclerosis (16,17). Accordingly, the atheroprotective effect of disrupting BAFF–BAFF-R signaling that we observed could be attributed to the depletion of mature B cells, which was very similar to the data obtained on anti-CD20 antibody-treated mice (16–19,23). In ApoE^{-/-} D227K mice, anti-BAFF antibody treatment appeared to affect only the B-2 cell population, while the B-1 cells and other lymphocyte populations remained unaffected and anti-BAFF antibody treatment had no direct effect on plasma lipid concentrations.

Due to the fact that the treatment of atherosclerosis/lupus-prone mice with anti-BAFF neutralizing antibody may increase atherosclerosis, despite a similar reduction in mature B cells, we hypothesized that BAFF may have the capacity to affect atherosclerosis beyond changes in BAFF-R signaling and B cells. In addition to BAFF-R, BAFF binds to BCMA and TACI receptors (33). Our findings confirm that TACI is expressed on macrophages and that BAFF mediates atheroprotective effects through the TACI receptor. Disrupting BAFF–TACI signaling on macrophages enhances their differentiation into foam cells under conditions of hypercholesterolemia (in mice) and/or obesity (in humans). Although TACI is also bound by the alternative ligand APRIL (33), overexpression of APRIL in ApoE^{-/-} mice does not seem to affect atherosclerotic plaque size (34).

Our findings are consistent with those of a recent study showing that neutralization of BAFF leads to increased atherosclerotic plaque size in mouse models of atherosclerosis, through

a B cell-independent antiinflammatory property of BAFF on macrophages (24). In contrast to our study, no atheroprotective effect of anti-BAFF treatment was observed. Of note, mice in that study did not have lupus, were fed an atherogenic diet for 6 weeks, and displayed very high plasma cholesterol levels (>15 gm/liter). Such an extreme regimen may have obviated the beneficial effect of B cell depletion on atherosclerosis progression. On the other hand, since reduction of atherosclerosis has been observed in BAFF-R-deficient mice, anti-BAFF-R-treated mice, and anti-CD20 antibody-treated mice (16–19,23), the in-rebound increased soluble BAFF levels known to occur in such a condition might have also contributed to the atheroprotective effect (23). A recent study has demonstrated markedly decreased atherosclerosis in ApoE^{-/-} BAFF-transgenic mice that displayed extremely high levels of BAFF, consistent with the notion of overexpression of both soluble and membrane-bound forms of BAFF (35).

Overall, BAFF neutralization using mAb may actually increase atherosclerotic plaque size, when the beneficial effect of depletion of mature B-2 cells on both secondary lymphoid organs and aortic adventitia is counterbalanced by the detrimental effect of BAFF inhibition on the cholesterol-driven foam cell formation. Thus, depending on the balance between pathogenic B cells and proatherogenic conditions, such as excess body fat or abnormal cholesterol levels, anti-BAFF mAb might promote or protect against atherosclerosis. Of note, metabolic syndrome is highly prevalent in SLE, and overweight is a major contributor to atherosclerosis (3,36).

Our study has several limitations. First, a small number of mice were treated with anti-BAFF antibody. Our in vivo experimental design, however, included a larger number of mice in the anti-BAFF group. Unfortunately, most mice ($n = 7$) developed neutralizing antibodies against the anti-BAFF antibodies (which were Armenian hamster IgG1s) that prevented satisfactory B cell depletion. In the absence of sustained B cell depletion, we failed to detect a significant effect on the lupus phenotype in these mice. This group of mice was therefore not included in our report, since the data associated with these partially BAFF-depleted mice would bias the interpretation. Interestingly, the effects of BAFF neutralization on atherosclerosis in these mice indicate a contrasting effect of BAFF neutralization on atherosclerosis development, depending on individual cholesterol levels (Supplementary Figure 6, <http://onlinelibrary.wiley.com/doi/10.1002/art.41485/abstract>).

Second, the heterogeneity in plasma cholesterol levels was important in mice, despite a shared genetic background. The cholesterol levels, however, were normally distributed, and the fact that all mice were not issued from the same cage may have contributed to this distribution. In addition, such a distribution has already been reported in ApoE^{-/-} mice in the literature (37,38). In our study, cholesterol level was not associated with mouse weight and was independent of the treatment received (Supplementary Figure 7, <http://onlinelibrary.wiley.com/doi/10.1002/art.41485/abstract>). On the other hand, the distribution and overall modest level of cholesterol in our mouse model gave us the

opportunity to test the effect of BAFF neutralization on atherosclerosis according to cholesterol levels.

Third, atherosclerosis lesions were analyzed only at the aortic root and might not be representative of the entire aortic tree. In the present study, the entire aorta (besides the aortic root) was required for flow cytometry analysis and adventitial tertiary lymphoid organ staining (Figure 1G). It is nevertheless noteworthy that we previously demonstrated that ApoE^{-/-} D227K mice also had more severe atherosclerosis lesions than ApoE^{-/-} mice based on aorta en-face staining quantification (21).

In summary, despite the promising hypothesis of B cells as a therapeutic target for attenuating accelerated atherosclerosis associated with SLE, our study highlights a double-edged effect of BAFF neutralization on atherosclerosis development. The impact of BAFF-targeted immune therapy on CVD prevention in SLE should be carefully examined in long-term clinical studies.

ACKNOWLEDGMENTS

We are thankful to C. François for help with study organization and to Drs. J. F. Alexandra, M. P. Chauveheid, A. Dossier, and T. Goulenok for their help with patient screening. We acknowledge the invaluable help of the members of the cytometry core and the biochemistry core facilities of the INSERM U1149, of the morphology core facility of the INSERM U1152, and of the animal core facility of the INSERM U1148. We thank GlaxoSmithKline for providing the anti-BAFF mAb (IgG1; clone 10F4B).

AUTHOR CONTRIBUTIONS

All authors were involved in drafting the article or revising it critically for important intellectual content, and all authors approved the final version to be published. Dr. Sacre had full access to all of the data in the study and takes responsibility for the integrity of the data and the accuracy of the data analysis.

Study conception and design. Saidoune, Charles, Nicoletti, Sacre.

Acquisition of data. Saidoune, Even, Lamri, Chezel, Gaston, Escoubet, Papo, Charles, Nicoletti, Sacre.


Analysis and interpretation of data. Saidoune, Even, Lamri, Chezel, Gaston, Escoubet, Papo, Charles, Nicoletti, Sacre.

REFERENCES

1. Thomas G, Mancini J, Jourde-Chiche N, Sarlon G, Amoura Z, Harlé JR, et al. Mortality associated with systemic lupus erythematosus in France assessed by multiple-cause-of-death analysis. *Arthritis Rheumatol* 2014;66:2503–11.
2. Esdaile JM, Abrahamowicz M, Grodzicky T, Li Y, Panaritis C, Berger RD, et al. Traditional Framingham risk factors fail to fully account for accelerated atherosclerosis in systemic lupus erythematosus. *Arthritis Rheum* 2001;44:2331–7.
3. Sacre K, Escoubet B, Zennaro MC, Chauveheid MP, Gayat E, Papo T. Overweight is a major contributor to atherosclerosis in systemic lupus erythematosus patients at apparent low risk for cardiovascular disease: a cross-sectional controlled study. *Medicine (Baltimore)* 2015;94:e2177.
4. Sacre K, Escoubet B, Pasquet B, Chauveheid MP, Zennaro MC, Tubach F, et al. Increased arterial stiffness in systemic lupus erythematosus (SLE) patients at low risk for cardiovascular disease: a cross-sectional controlled study. *PLoS One* 2014;9:e94511.
5. Roman MJ, Shanker BA, Davis A, Lockshin MD, Sammaritano L, Simantov R, et al. Prevalence and correlates of accelerated atherosclerosis in systemic lupus erythematosus. *N Engl J Med* 2003;349:2399–406.
6. Bessant R, Hingorani A, Patel L, MacGregor A, Isenberg DA, Rahman A. Risk of coronary heart disease and stroke in a large British cohort of patients with systemic lupus erythematosus. *Rheumatology (Oxford)* 2004;43:924–9.
7. Clement M, Charles N, Escoubet B, Guedj K, Chauveheid MP, Caligiuri G, et al. CD4+CXCR3+ T cells and plasmacytoid dendritic cells drive accelerated atherosclerosis associated with systemic lupus erythematosus. *J Autoimmun* 2015;63:59–67.
8. Yanaba K, Bouaziz JD, Matsushita T, Magro CM, St. Clair EW, Tedder TF. B-lymphocyte contributions to human autoimmune disease. *Immunol Rev* 2008;223:284–99.
9. Sanz I, Lee FE. B cells as therapeutic targets in SLE [review]. *Nat Rev Rheumatol* 2010;6:326–37.
10. Vincent FB, Morand EF, Schneider P, Mackay F. The BAFF/APRIL system in SLE pathogenesis [review]. *Nat Rev Rheumatol* 2014;10:365.
11. Mackay F, Woodcock SA, Lawton P, Ambrose C, Baetscher M, Schneider P, et al. Mice transgenic for BAFF develop lymphocytic disorders along with autoimmune manifestations. *J Exp Med* 1999;190:1697–710.
12. Zhang J, Roschke V, Baker KP, Wang Z, Alarcón GS, Fessler BJ, et al. Cutting edge: a role for B lymphocyte stimulator in systemic lupus erythematosus. *J Immunol* 2001;166:6–10.
13. Stohl W, Metyas S, Tan SM, Cheema GS, Oamar B, Xu D, et al. B lymphocyte stimulator overexpression in patients with systemic lupus erythematosus: longitudinal observations. *Arthritis Rheum* 2003;48:3475–86.
14. Navarra SV, Guzmán RM, Gallacher AE, Hall S, Levy RA, Jimenez RE, et al. Efficacy and safety of belimumab in patients with active systemic lupus erythematosus: a randomised, placebo-controlled, phase 3 trial. *Lancet* 2011;377:721–31.
15. Furie R, Petri M, Zamani O, Cervera R, Wallace DJ, Tegzová D, et al. A phase III, randomized, placebo-controlled study of belimumab, a monoclonal antibody that inhibits B lymphocyte stimulator, in patients with systemic lupus erythematosus. *Arthritis Rheum* 2011;63:3918–30.
16. Ait-Oufella H, Herbin O, Bouaziz JD, Binder CJ, Uyttenhove C, Laurans L, et al. B cell depletion reduces the development of atherosclerosis in mice. *J Exp Med* 2010;207:1579–87.
17. Kyaw T, Tay C, Khan A, Dumouchel V, Cao A, To K, et al. Conventional B-2 B cell depletion ameliorates whereas its adoptive transfer aggravates atherosclerosis. *J Immunol* 2010;185:4410–9.
18. Kyaw TT, Tay C, Hosseini H, Kanellakis P, Gadowski T, MacKay F, et al. Depletion of B-2 but not B1a B Cells in BAFF receptor-deficient ApoE^{-/-} mice attenuates atherosclerosis by potentially ameliorating arterial inflammation. *PLoS One* 2012;7:e29371.
19. Sage AP, Tsiantoulas D, Baker L, Harrison J, Masters L, Murphy D, et al. BAFF receptor deficiency reduces the development of atherosclerosis in mice: brief report. *Arterioscler Thromb Vasc Biol* 2012;32:1573–6.
20. Hochberg MC. Updating the American College of Rheumatology revised criteria for the classification of systemic lupus erythematosus [letter]. *Arthritis Rheum* 1997;40:1725.
21. Clement M, Guedj K, Andreato F, Morvan M, Bey L, Khallou-Laschet J, et al. Control of the T follicular helper–germinal center B-cell axis by CD8⁺ regulatory T cells limits atherosclerosis and tertiary lymphoid organ development. *Circulation* 2015;131:560–70.
22. Kim HJ, Verbrinnen B, Tang X, Lu L, Cantor H. Inhibition of follicular T-helper cells by CD8⁺ regulatory T cells is essential for self tolerance. *Nature* 2010;467:328–32.
23. Kyaw T, Cui P, Tay C, Kanellakis P, Hosseini H, Liu E, et al. BAFF receptor mAb treatment ameliorates development and progression of atherosclerosis in hyperlipidemic ApoE^{-/-} mice. *PLoS One* 2013;8:e60430.

24. Tsiantoulas D, Sage AP, Göderle L, Ozsvar-Kozma M, Murphy D, Porsch F, et al. BAFF neutralization aggravates atherosclerosis. *Circulation* 2018;138:2263–73.
25. Allman WR, Dey R, Liu L, Siddiqui S, Coleman AS, Bhattacharya P, et al. TACI deficiency leads to alternatively activated macrophage phenotype and susceptibility to *Leishmania* infection. *Proc Natl Acad Sci U S A* 2015;112:E4094–103.
26. Touboul PJ, Hennerici MG, Meairs S, Adams H, Amarenco P, Bornstein N, et al. Mannheim carotid intima-media thickness and plaque consensus (2004–2006–2011): an update on behalf of the advisory board of the 3rd, 4th and 5th watching the risk symposia, at the 13th, 15th and 20th European Stroke Conferences, Mannheim, Germany, 2004, Brussels, Belgium, 2006, and Hamburg, Germany, 2011. *Cerebrovasc Dis* 2012;34:290–6.
27. D'Agostino RB Sr, Vasan RS, Pencina MJ, Wolf PA, Cobain M, Massaro JM, et al. General cardiovascular risk profile for use in primary care: the Framingham Heart Study. *Circulation* 2008;117:743–53.
28. Petri M, Kim MY, Kalunian KC, Grossman J, Hahn BH, Sammaritano LR, et al, for the OC-SELENA Trial. Combined oral contraceptives in women with systemic lupus erythematosus. *N Engl J Med* 2005;353:2550–8.
29. Mageau A, Timsit JF, Perrozzello A, Ruckly S, Dupuis C, Bouadma L, et al. The burden of chronic kidney disease in systemic lupus erythematosus: a nationwide epidemiologic study [review]. *Autoimmun Rev* 2019;18:733–7.
30. Tsiantoulas D, Diehl CJ, Witztum JL, Binder CJ. B cells and humoral immunity in atherosclerosis [review]. *Circ Res* 2014;114:1743–56.
31. Caligiuri G, Khallou-Laschet J, Vandaele M, Gaston AT, Delignat S, Mandet C, et al. Phosphorylcholine-targeting immunization reduces atherosclerosis. *J Am Coll Cardiol* 2007;50:540–6.
32. Caligiuri G, Nicoletti A, Poirier B, Hansson GK. Protective immunity against atherosclerosis carried by B cells of hypercholesterolemic mice. *J Clin Invest* 2002;109:745–53.
33. Mackay F, Schneider P. Cracking the BAFF code. *Nat Rev Immunol* 2009;9:491–502.
34. Moens SJ, van Leuven SI, Zheng KH, Havik SR, Versloot MV, van Duivenvoorde LM, et al. Impact of the B cell growth factor APRIL on the qualitative and immunological characteristics of atherosclerotic plaques. *PLoS One* 2016;11:e0164690.
35. Jackson SW, Scharping NE, Jacobs HM, Wang S, Chait A, Rawlings DJ. Cutting edge: BAFF overexpression reduces atherosclerosis via TACI-dependent B cell activation. *J Immunol* 2016;197:4529–34.
36. Parker B, Urowitz MB, Gladman DD, Lunt M, Bae SC, Sanchez-Guerrero J, et al. Clinical associations of the metabolic syndrome in systemic lupus erythematosus: data from an international inception cohort. *Ann Rheum Dis* 2013;72:1308–14.
37. Accad M, Smith SJ, Newland DL, Sanan DA, King LE, Linton MF, et al. Massive xanthomatosis and altered composition of atherosclerotic lesions in hyperlipidemic mice lacking acyl CoA:cholesterol acyltransferase 1. *J Clin Invest* 2000;105:711–9.
38. Liu B, Zhang Y, Wang R, An Y, Gao W, Bai L, et al. Western diet feeding influences gut microbiota profiles in apoE knockout mice. *Lipids Health Dis* 2018;17:159.

Association of Urinary Matrix Metalloproteinase 7 Levels With Incident Renal Flare in Lupus Nephritis

Guobao Wang,¹ Liling Wu,² Huanjuan Su,¹ Xiaodan Feng,³ Meng Shi,¹ Lingwei Jin,⁴ Manqiu Yang,¹ Zhanmei Zhou,¹ Cailing Su,¹ Bihui Yang,¹ Yajing Li,¹ and Wei Cao¹ 

Objective. Flares of lupus nephritis (LN) are frequent and associated with impaired renal prognosis. One major management obstacle in LN flare is the lack of effective methods to identify at-risk patients earlier in their disease course. This study was undertaken to test the utility of measurement of urinary matrix metalloproteinase 7 (MMP-7) for the dynamic surveillance of renal disease activity and prediction of renal flares in LN.

Methods. A prospective, 2-stage cohort study was performed in patients with LN. Urinary MMP-7 levels at the time of biopsy were evaluated in 154 patients with newly diagnosed LN in 2 independent cohorts. Urinary MMP-7 levels were assessed for correlation with renal histologic activity. Furthermore, after a minimum period of 12 months of renal disease remission, urinary MMP-7 levels were monitored bimonthly for 2 years in 65 patients with LN. The association between urinary MMP-7 levels and development of LN flare was analyzed.

Results. Urinary MMP-7 levels were elevated in patients with LN. A higher urinary MMP-7 level in LN was associated with greater renal histologic activity. As a marker for identifying LN patients with more severe renal histologic activity (i.e., a histologic activity index of ≥ 7), the level of urinary MMP-7 outperformed other clinical markers and improved their predictive performance, thus linking urinary MMP-7 levels to renal disease activity. Furthermore, among patients who had follow-up measurements of urinary MMP-7 after achievement of long-term remission of renal disease activity, an elevated urinary MMP-7 level during follow-up was independently associated with an increased risk of LN flare. This elevation in the urinary MMP-7 level hinted at the risk of an LN flare at an earlier time point prior to indications using conventional laboratory measures. Thus, use of the urinary MMP-7 level in conjunction with other clinical measures improved the prognostic value for prediction of an LN flare.

Conclusion. Urinary MMP-7 levels in LN are correlated with renal histologic activity. An elevated urinary MMP-7 level detected after achievement of long-term renal disease remission is associated with a higher risk of incident renal flare in patients with LN.

INTRODUCTION

Lupus nephritis (LN) is the most common cause of morbidity and mortality in patients with systemic lupus erythematosus (SLE) (1). LN has a flaring–remitting course, with patients often experiencing episodic active renal lesions (flares) that lead to cumulative renal damage (2,3). However, not all patients in whom remission

of renal disease activity occurs have an equal risk of renal flares. Investigations that can be applied to monitor renal disease activity longitudinally may provide a chance for prompt and necessary interventions to improve renal survival (4,5). Current surveillance of renal disease activity in LN is based on follow-up of its clinical evolution (6,7), with confirmation by assessment of renal histologic activity in serial kidney biopsy samples (8–10). Clearly, sensitive

Supported by the National Natural Science Foundation of China (grants 81922014 and 81870473 to Dr. Cao and grants 81870489 and 81670669 to Mr. Wang), Research Fund for Lin He's Academician Workstation of New Medicine and Clinical Translation (grant 19331203 to Mr. Jin), Medical Health Science and Technology Project of Zhejiang Provincial Health Commission (grant 2020358611 to Mr. Jin), and Wenzhou Science & Technology Bureau (grants Y20180499 and Y20190063 to Mr. Jin).

¹Guobao Wang, MS, Huanjuan Su, MS, Meng Shi, MD, PhD, Manqiu Yang, BS, Zhanmei Zhou, BS, Cailing Su, BS, Bihui Yang, MS, Yajing Li, BS, Wei Cao, MD, PhD: Nanfang Hospital, Southern Medical University, State Key Laboratory of Organ Failure Research, Guangzhou, China; ²Liling Wu, MD, PhD: Nanfang Hospital, Southern Medical University, Guangzhou, China, and Shenzhen Second People's Hospital, First Affiliated Hospital

of Shenzhen University, Shenzhen, China; ³Xiaodan Feng, MS: Guangzhou Development District Hospital, Guangzhou, China; ⁴Lingwei Jin, MS: The 2nd Affiliated Hospital & Yuying Children's Hospital of Wenzhou Medical University, Wenzhou, China.

Mr. Wang, Dr. Wu, Ms H. Su, and Mr. Feng contributed equally to this work.

No potential conflicts of interest relevant to this article were reported.

Address correspondence to Wei Cao, MD, PhD, Nanfang Hospital, Southern Medical University, Division of Nephrology, State Key Laboratory of Organ Failure Research, 1838 North Guangzhou Avenue, Guangzhou 510515, China. Email: sijaer@163.com.

Submitted for publication April 29, 2020; accepted in revised form August 25, 2020.

and noninvasive indicators are required to identify at-risk patients earlier in their disease course. Although several candidate clinical indicators have been identified up to now (11–13), only a few have been tested serially after long-term complete renal disease remission has been achieved and during periods leading up to a flare.

Matrix metalloproteinases (MMPs) comprise a family of zinc-containing proteinases and are crucial for tissue development and homeostasis (14). MMP-7 is one of the smallest secreted members of the MMP family. Activation of MMP-7 could increase the activity of other MMPs that have been postulated as potential biomarkers for disease progression in LN (15). In addition, MMP-7 has been implicated in cell proliferation and inflammation (16–19), both being features that characterize the active renal damage occurring in patients with LN, and MMP-7 is readily detected in the serum, urine, and various tissues including the kidneys (20–22). Elevated levels of MMP-7 in the serum and kidneys have been demonstrated in LN patients with active renal injury (20,23). Wnt/ β -catenin signaling, an upstream regulator of MMP-7 expression, is increasingly activated in the kidneys along with the development of LN (24). Urinary MMP-7, whose level is a reflection of renal Wnt/ β -catenin activity and MMP-7 expression, has been proposed as an indicator of the severity of renal damage in certain kidney diseases (22,25). Nevertheless, in human LN, the exact level of urinary MMP-7 and its relationship to renal disease activity have not yet been elucidated.

In the present study, we postulated that the urinary MMP-7 level may serve as an early predictor of LN flares. To test this hypothesis, a prospective, 2-stage cohort study was performed in patients with LN. We assessed the urinary MMP-7 level for direct correlation with histologic features of renal disease activity at the time of renal biopsy. Moreover, among patients who had been receiving long-term maintenance therapy and who were in complete clinical remission during maintenance, we monitored their urinary MMP-7 levels and determined the association between the urinary MMP-7 level over time and the risk of incident renal flare. Our findings demonstrate that tracking the urinary MMP-7 level longitudinally aids in the prediction of renal flares, and offers the potential to improve the efficacy of precision therapeutics in patients with LN.

PATIENTS AND METHODS

Study design and patients. This study was designed as a prospective, 2-stage cohort study (see Supplementary Figure 1, available on the *Arthritis & Rheumatology* website at <http://online.library.wiley.com/doi/10.1002/art.41506/abstract>). The study was approved by our local Institutional Ethics Review Board, and written informed consent was obtained from all subjects.

Stage I. Stage I of the study was performed in 2 independent cohorts of patients with LN from 3 tertiary university hospitals in 2 cities in China between 2014 and 2017. For the test cohort, we recruited 88 patients from a single hospital in Guangzhou. For the validation cohort, we recruited 66 patients from

other hospitals in Wenzhou and Guangzhou. All participants were individuals age 18 years or older who met the American College of Rheumatology updated criteria for the classification of SLE (26) and had biopsy-proven LN. Exclusion criteria included those who had undergone kidney transplantation, and those with overlap syndromes (i.e., diabetes, urinary tract infection, or other immune complex diseases). Renal biopsy was performed in all patients before the initiation of immunosuppressive therapy. Serum samples were collected from subjects early in the morning, during bed rest. Fresh urine samples were collected after the individual had woken up, on the day of biopsy, as previously described (27).

Thirty patients with extrarenal SLE, 40 patients with proteinuria due to nonproliferative glomerular diseases, and 20 healthy volunteers were included as controls. Nonproliferative glomerular diseases in the 40 patients consisted of minimal-change nephrotic disease (MCD) in 20 patients and thin basement membrane nephropathy (TBMN) in 20 patients, as previously described (12). Paired serum and urine samples were collected from the disease controls in the same manner as described above, before initiation of immunosuppressive therapy.

Stage II. In stage II of the study, from 2012 to 2019, 65 consecutive patients who had biopsy-proven class III/class IV with or without class V LN and who were followed up in 2 Guangzhou hospitals were recruited. All participants in the second stage of the study had achieved a renal response, as defined according to renal disease activity and clinical parameters described below, after receiving 6 months of induction therapy, and all had been in complete renal remission for at least 12 months during the period of maintenance therapy. At the time of enrollment, all subjects were taking mycophenolate mofetil (median dose 0.5 gm/day, interquartile range [IQR] 0.5–0.5 gm/day), prednisone (median dose 10 mg/day, IQR 10–15 mg/day), and hydroxychloroquine (median dose 0.2 gm/day). In addition, 43.1% of patients were taking renin-angiotensin system (RAS) blockers titrated to a blood pressure target of 130/80 mm Hg or lower. After enrollment, the mycophenolate mofetil dose was tapered off and then stopped. The prednisone dose was waned below 10 mg/day. There was no difference in the doses of prednisone and mycophenolate mofetil between the flare group and the no-flare group after enrollment. Participants were followed up for 2 years. Serum and urine samples were collected bimonthly.

All serum and urine samples were centrifuged at 2,500g for 10 minutes. The supernatants were stored at -80°C before being analyzed.

Histologic analysis. Renal biopsy samples were obtained from patients with LN. Normal kidney tissue adjacent to the site of a renal carcinoma was obtained from subjects as controls ($n = 10$). Sections from the kidney tissue were processed for hematoxylin and eosin, periodic acid-Schiff, and Masson's trichrome staining. LN was categorized according to the 2018 International Society of Nephrology/Renal Pathology Society

(ISN/RPS) LN classification system (2). Patients demonstrating features of class III/class IV LN in the presence of concomitant class V LN were categorized as having class III/class IV LN.

Disease activity. Renal pathologic activity was evaluated using the renal histologic activity index and histologic chronicity index in all kidney biopsy samples. Both indices were calculated using the 2018 National Institutes of Health scoring system for LN (score scales 0–24 for the activity index and 0–12 for the chronicity index) (2).

Clinical disease activity was determined using the following parameters (12,28): proteinuria (reference range 0–0.14 gm/day), active urinary sediment (reference range 0–5 red blood cells or white blood cells/high-power field), serum levels of creatinine (reference range 0.5–1.2 mg/dl), serum levels of C3 (reference range 0.9–1.8 gm/liter), serum levels of anti-double-stranded DNA (anti-dsDNA) antibodies (reference range 0–200 IU/liter), and serum levels of antinuclear antibodies (reference range 0–20 IU/liter).

Complete clinical remission of LN was defined as achievement of a normal estimated glomerular filtration rate (eGFR) (defined as >90 ml/minute/1.73 m²), presence of inactive urinary sediments, and a proteinuria level of <0.5 gm/day after 6 months of induction therapy (29). LN flare was defined as either an increase in the level of proteinuria to >0.5 gm/day or an increased level or recurrence of active urinary sediment or an elevation of >0.3 mg/dl in the serum creatinine level (3,5). The signs of active renal disease were persistent and present for at least 2 visits, 2 days apart.

Immunohistochemical analysis of kidney MMP-7 levels. Intrarenal expression of MMP-7 was determined in 2- μ m-thick sections of the kidney biopsy tissue using an anti-human MMP-7 antibody (1:100, AF907; R&D Systems) as previously described (30). The intensity of staining for MMP-7 was expressed as the ratio of integrated optical density to observed area.

All histologic analyses were performed by 2 independent nephropathologists (ZZ and CS) who were blinded with regard to the subjects' clinical data. Inter- and intraobserver reproducibility testing displayed good reliability (for interobserver agreement, intraclass correlation coefficient [ICC] 83.2%, 95% confidence interval [95% CI] 75.5–88.7%; for intraobserver agreement, ICC 90.8%, 95% CI 86–94.0%).

Enzyme-linked immunosorbent assay (ELISA) for MMP-7 in the serum and urine. Quantification of serum or urinary MMP-7 levels was performed using ELISAs as dictated by the manufacturer's protocol (DY907; R&D Systems). The values for MMP-7 levels in urine samples were standardized to those of urinary creatinine, with results expressed as ng/mg creatinine. Determination of the urinary MMP-7 level using this ELISA kit is accurate, as was confirmed using a spike/recovery assay (mean recovery rate ranging from 88% to 109% at different spiked levels) and linearity assay (mean recovery rate ranging from 92% to

105% at different dilutions). Confidence in the MMP-7 assay is further supported by the MMP-7 interassay variability (5.8%) and intraassay variability (2.6%). Finally, ELISA quantification of the MMP-7 level is inexpensive and rapid.

Statistical analysis. Continuous variables were expressed as the mean \pm SD or as the median with IQR, and categorical variables were presented as proportions. We used independent-sample *t*-tests, Mann-Whitney U tests, or Kruskal-Wallis tests to compare continuous variables, and chi-square tests to compare categorical variables. Correlations were determined using Pearson's correlation coefficients. In the correlation analyses, the urinary MMP-7 value was log-transformed to correct for dispersion of data. Participants in the LN cohorts in stage I were dichotomized according to the median level of renal histologic activity (median activity index of 7).

The association between the urinary MMP-7 level on the day of biopsy and higher renal histologic activity (activity index ≥ 7) in patients with LN was investigated using multiple logistic regression analyses, controlling for the effect of clinically important confounding variables, including sex, hypertension, use of RAS blockers, proteinuria, and serum levels of creatinine, C3, and anti-dsDNA on the day of biopsy. To compare the predictive performance of the urinary MMP-7 level with the predictive performance of other clinical indicators in identifying patients with higher renal histologic activity (activity index ≥ 7), an area under the receiver operating characteristics curve (AUC) was generated (31). The ICCs (with 95% CIs) for inter- and intraobserver reproducibility of the histologic analyses were determined (32).

Among the 65 patients with LN who had follow-up urinary MMP-7 measurements after having achieved complete renal disease remission for at least 12 months, the association between the urinary MMP-7 level and risk of incident LN flare (an increase in proteinuria to >0.5 gm/day) was determined using a multivariable time-dependent Cox proportional hazards model with adjustment for the aforementioned confounding variables (except for proteinuria). Repeated assessments of urinary MMP-7, serum C3, serum creatinine, and serum anti-dsDNA levels were time-dependent variables. Using C-statistics, the discriminatory capability of current clinical measures used in conjunction with the urinary MMP-7 level was compared with that of current clinical measures used alone (without urinary MMP-7).

Two-tailed *P* values of less than 0.05 were considered statistically significant. R program version 3.2.0 was used for all statistical analyses (The R Foundation; <http://www.R-project.org/>).

RESULTS

Characteristics of the patients. The 2-stage study design and distribution of participants are shown in Supplementary Figure 1 (<http://onlinelibrary.wiley.com/doi/10.1002/art.41506/abstract>). In stage I, 88 patients with LN from 1 hospital were enrolled in the

Table 1. Characteristics of the patients with LN by renal histologic activity in the test and validation cohorts in study stage I*

Characteristic	Test cohort		Validation cohort	
	AI <7 (n = 44)	AI ≥7 (n = 44)	AI <7 (n = 33)	AI ≥7 (n = 33)
On admission				
Age, mean ± SD years	35 ± 15	31 ± 10	33 ± 16	31 ± 12
Female	35 (79.5)	33 (75.0)	26 (78.8)	23 (69.7)
Hypertension	9 (20.5)	26 (59.1)	5 (15.2)	19 (57.6)
BMI, mean ± SD kg/m ²	21.8 ± 3.4	22.1 ± 3.1	21.7 ± 3.8	22.2 ± 3.4
Medication, RAS blockers	10 (22.7)	21 (47.7)	8 (24.2)	16 (45.5)
Day of biopsy				
LN classification†				
Class II	3 (6.8)	0 (0.0)	2 (6.1)	0 (0.0)
Class III	25 (56.8)	6 (13.6)	19 (57.6)	5 (15.2)
Class IV	4 (9.1)	38 (86.4)	4 (12.1)	28 (84.8)
Class V	12 (27.3)	0 (0.0)	8 (24.2)	0 (0.0)
Histologic AI (scale 0–24), median (IQR)	2 (2–4)	10 (8–12)	3 (2–5)	10 (8–13)
Histologic chronicity index (scale 0–12), median (IQR)	3 (2–5)	5 (4–6)	3 (2–3)	6 (4–8)
Proteinuria, median (IQR) gm/day	1.8 (1.9–3.1)	3.4 (2.7–6.7)	1.6 (0.8–3.1)	3.4 (2.6–6.2)
Serum creatinine, median (IQR) mg/dl	0.7 (0.6–0.9)	1.0 (0.8–1.5)	0.7 (0.5–1.1)	1.0 (0.8–1.4)
Serum C3, mean ± SD gm/liter	0.65 ± 0.35	0.44 ± 0.25	0.59 ± 0.28	0.43 ± 0.19
Serum ANA, median (IQR) IU/ml	152 (110–334)	155 (76–314)	266 (196–384)	266 (241–336)
Serum anti-dsDNA, median (IQR) IU/ml	268 (206–375)	283 (243–398)	149 (92–280)	155 (95–184)

* Except where indicated otherwise, values are the number (%) of patients with lupus nephritis (LN). AI = histologic renal activity index; BMI = body mass index; RAS = renin-angiotensin system; IQR = interquartile range; ANA = antinuclear antibody; anti-dsDNA = anti-double-stranded DNA.

† According to the 2018 International Society of Nephrology/Renal Pathology Society LN classification system.

test cohort. Table 1 provides the clinical and histologic characteristics of the patients in the test cohort, dichotomized according to the median renal histologic activity index (based on a median activity index of 7, IQR 2–10). Patients with greater histologic activity (activity index ≥7) had higher levels of proteinuria, higher serum creatinine levels, lower C3 levels, and more hypertension, and use of RAS blockers was more frequent among these patients compared to those with a renal histologic activity index of <7.

Sixty-six patients with LN from other hospitals were enrolled in the validation cohort, and the characteristics of these patients were similar to those in the test cohort (Table 1). Twenty age- and sex-matched volunteers (mean ± SD age 34 ± 12 years, 75% female) served as healthy controls. Disease controls consisted of patients with extrarenal SLE (n = 30), patients with MCD (n = 20), and patients with TBMN (n = 20) (characteristics are detailed in Supplementary Table 1, available on the *Arthritis & Rheumatology* website at <http://onlinelibrary.wiley.com/doi/10.1002/art.41506/abstract>). Renal biopsy was performed in all patients before the initiation of immunosuppressive therapy.

For stage II of the study, 65 patients with LN were recruited from 1 Guangzhou hospital. All patients had received maintenance therapy, and all had been in complete renal disease remission for at least 12 months during maintenance. Supplementary Table 2 (available on the *Arthritis & Rheumatology* website at <http://onlinelibrary.wiley.com/doi/10.1002/art.41506/abstract>) presents the characteristics of the patients at the time of enrollment, segregated by the renal flare status during 2 years of follow-up. There was no difference in patient characteristics between the flare and the no-flare groups.

Marked elevation in the urinary MMP-7 level in patients with LN.

In stage I, distribution of the urinary MMP-7 level on the day of biopsy was determined in the LN test cohort, disease controls, or healthy volunteers. As shown in Figure 1A, patients with LN had an elevated urinary MMP-7 level (median 5.14 ng/mg creatinine, IQR 2.80–11.67), as compared with healthy volunteers (median 1.09 ng/mg creatinine, IQR 0.66–1.82), patients with extrarenal SLE (median 1.33 ng/mg creatinine, IQR 0.99–2.29), patients with MCD (median 1.56 ng/mg creatinine, IQR 1.16–2.68), or patients with TBMN (median 1.38 ng/mg creatinine, IQR 0.87–2.71) (all $P < 0.001$).

The MMP-7 level in serum samples was assessed on the same day that urine samples were obtained. The serum MMP-7 level was slightly elevated in patients with LN compared with healthy volunteers and disease controls, but the magnitude of this elevation was trivial (fold change of <2) (Supplementary Table 1 [<http://onlinelibrary.wiley.com/doi/10.1002/art.41506/abstract>]). No correlation was observed between the urinary and serum MMP-7 levels in patients with LN ($r = 0.113$, $P = 0.292$) (Figure 1B).

We further examined the kidney expression of MMP-7 by immunohistochemical staining of renal biopsy tissue. MMP-7 was barely detectable in the normal kidneys from 10 healthy controls. However, the MMP-7 protein level was notably induced in renal biopsy samples from patients with LN (representative results shown in Figure 1C). MMP-7 was predominantly deposited in tubular cells in the kidneys of patients with LN (indicated by arrows in Figure 1C). Other than tubular cells, glomerular podocytes and parietal epithelial cells were also positive for MMP-7 staining. The

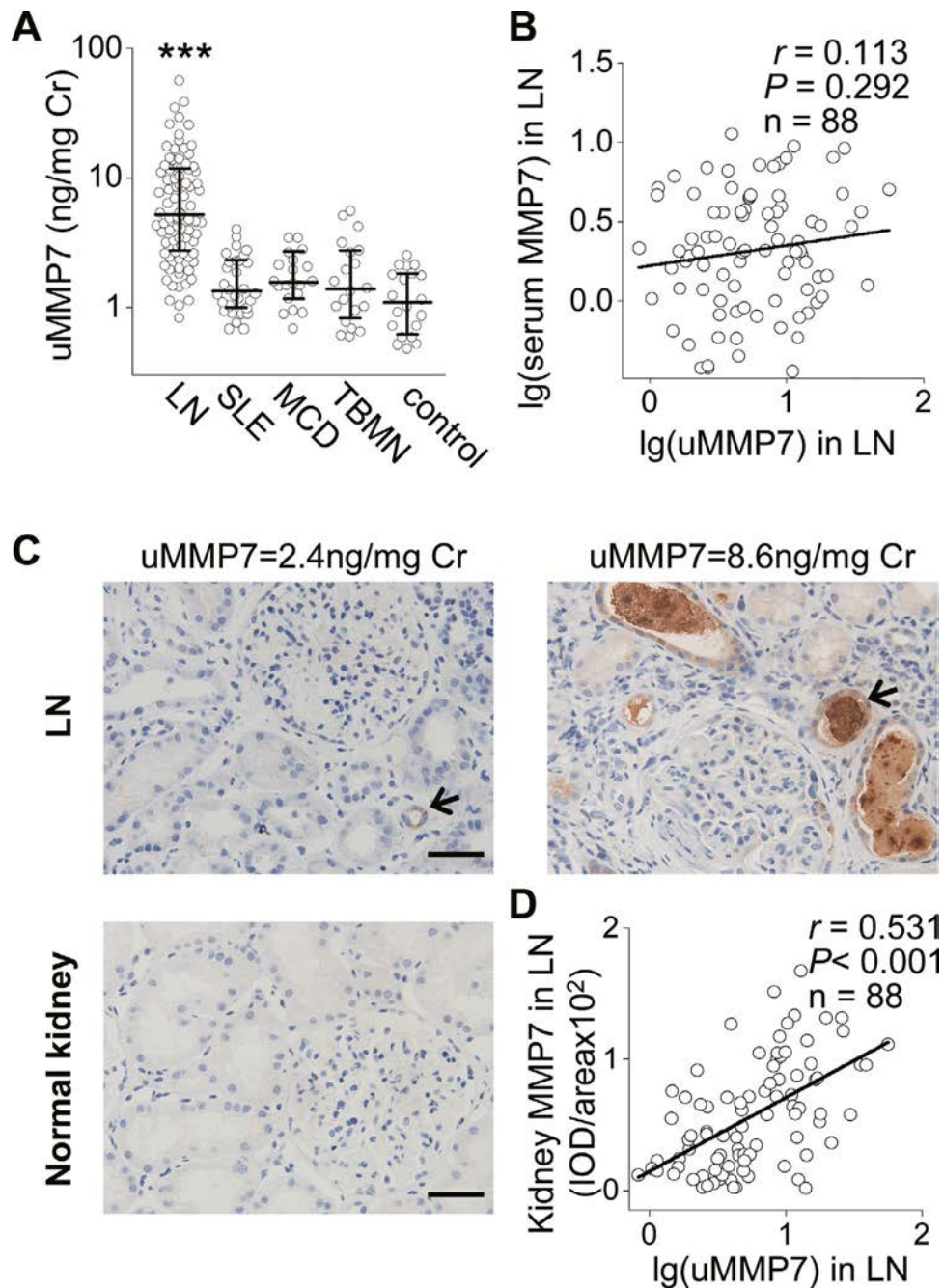


Figure 1. Marked elevation in the urinary matrix metalloproteinase 7 (uMMP-7) level in patients with lupus nephritis (LN). **A**, Urinary MMP-7 levels (normalized to the values for creatinine [Cr]) were determined in patients with LN (test cohort, stage I; $n = 88$), patients with extrarenal systemic lupus erythematosus (SLE) ($n = 30$), patients with minimal-change nephrotic disease (MCD) ($n = 20$), and patients with thin basement membrane nephropathy (TBMN) ($n = 20$) on the day of biopsy, and in healthy volunteers as controls ($n = 20$). Symbols represent individual subjects. Horizontal lines with bars show the median with interquartile range. *** = $P < 0.001$ versus controls, by Mann-Whitney U test. **B**, Correlations between urinary MMP-7 levels and serum MMP-7 levels in patients with LN were determined using Pearson's correlation analysis. **C**, Representative images show renal MMP-7 expression in kidney biopsy samples from patients with LN ($n = 88$) on the day of biopsy and in normal kidneys ($n = 10$). Values for urinary MMP-7 levels in patients with LN are shown at the top of each image. **Arrows** indicate positively stained renal tubules. Bars = 50 μm . **D**, Correlations between urinary MMP-7 levels and kidney MMP-7 levels in patients with LN were determined using Pearson's correlation analysis. IOD/area = ratio of integrated optical density to observed area.

urinary MMP-7 level on the day of biopsy positively correlated with kidney MMP-7 expression in patients with LN ($r = 0.531$, $P < 0.001$) (Figure 1D). Thus, an elevated urinary MMP-7 level reflects an increase in intrarenal MMP-7 expression.

Correlation between elevated urinary MMP-7 levels at the time of biopsy and greater renal histologic activity in patients with LN. MMP-7 has been demonstrated to be involved in cell proliferation and inflammation (16–18). Given that

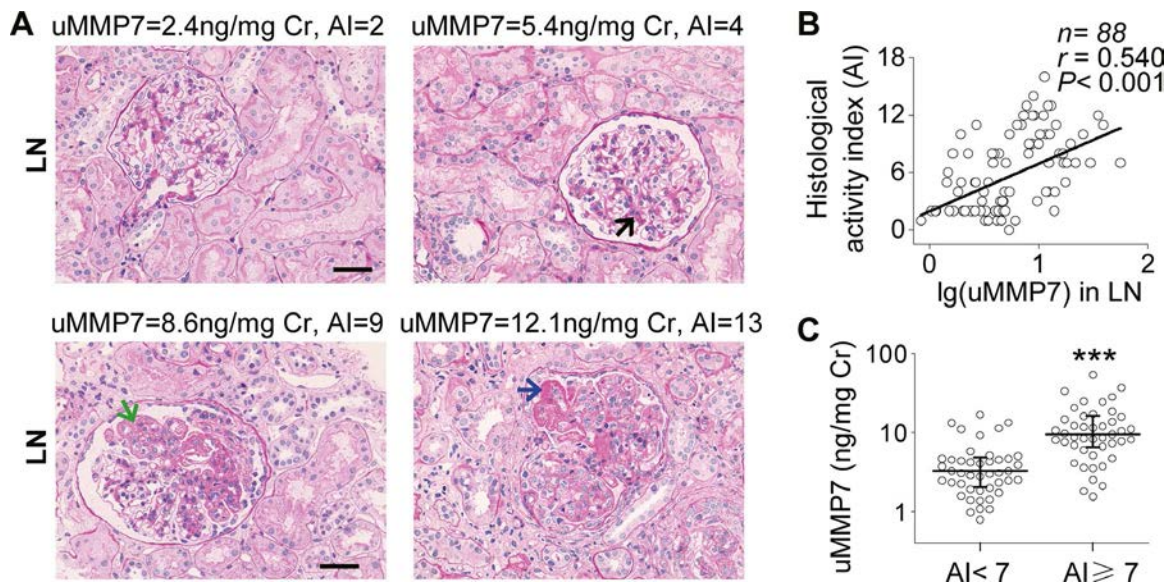


Figure 2. Correlation of elevated urinary MMP-7 levels at the time of biopsy with greater renal histologic activity in patients with LN. **A**, Representative images show active renal lesions in kidney biopsy specimens from patients with LN on the day of biopsy (test cohort, stage I; $n = 88$) according to different renal histologic activity indices (AIs). Lesions were visualized by periodic acid–Schiff staining. Values for urinary MMP-7 levels and AIs are shown at the top of each image. **Black arrow** indicates mesangial hypercellularity. **Green arrow** indicates endocapillary hypercellularity. **Blue arrow** indicates wire loop lesions. Bars = 50 μm . **B**, Correlations between urinary MMP-7 levels and renal AIs in patients with LN were determined using Pearson's correlation analysis. **C**, Urinary MMP-7 levels were compared between renal histologic AI groups dichotomized according to the median renal AI (AI ≥ 7 versus AI < 7). Symbols represent individual patients. Horizontal lines with bars show the median with interquartile range. *** = $P < 0.001$ versus AI < 7 group, by Mann-Whitney U test. See Figure 1 for other definitions.

the urinary MMP-7 level reflects kidney MMP-7 expression, we reasoned that the level of urinary MMP-7 was associated with the histopathologic extent of renal disease activity in LN. To test this hypothesis, the urinary MMP-7 levels on the day of biopsy were compared with the renal histologic activity or chronicity indices in the LN test cohort. Kidney sections were stained with periodic acid–Schiff to determine the renal histologic activity (representative micrographs shown in Figure 2A). The urinary MMP-7 level closely correlated with the renal histologic activity index ($r = 0.540$, $P < 0.001$) (Figure 2B), particularly in the hyaline deposits and the cellular/fibrocellular crescents (Supplementary Table 3, available on the *Arthritis & Rheumatology* website at <http://onlinelibrary.wiley.com/doi/10.1002/art.41506/abstract>). There was no correlation between the urinary MMP-7 level and the histologic chronicity index or its components (Supplementary Figure 2A and Supplementary Table 3 [<http://onlinelibrary.wiley.com/doi/10.1002/art.41506/abstract>]).

The urinary MMP-7 level was further compared between groups dichotomized according to renal histologic activity (based on a median activity index of 7). The urinary MMP-7 level was higher in those with greater renal histologic activity (activity index ≥ 7) compared with those with less renal histologic activity (activity index < 7) ($P < 0.001$) (Figure 2C). The incidence of more severe LN (activity index of ≥ 7) was greater in patients with higher urinary MMP-7 levels (Supplementary Figure 2B [<http://onlinelibrary.wiley.com/doi/10.1002/art.41506/abstract>]).

Subjects with a urinary MMP-7 level in the highest tertile of MMP-7 levels had a risk of more severe renal disease (renal histologic activity index of ≥ 7) that was 19 times greater than that in subjects in the lowest tertile, after adjustment for multiple variables (Supplementary Table 4, available on the *Arthritis & Rheumatology* website at <http://onlinelibrary.wiley.com/doi/10.1002/art.41506/abstract>).

For identification of LN patients with an activity index of ≥ 7 , the AUC for the predictive performance of the urinary MMP-7 level in the test cohort on the day of biopsy was 0.83 (Supplementary Figure 2C [<http://onlinelibrary.wiley.com/doi/10.1002/art.41506/abstract>]). This performance of the urinary MMP-7 level for identifying LN patients with an activity index of ≥ 7 was further verified in an independent validation cohort (AUC 0.82) (Supplementary Figure 2C). These AUCs for the predictive performance of the urinary MMP-7 level, in both the test cohort and the validation cohort, were superior to those for the predictive performance of other clinical measures (i.e., measurement of proteinuria, and serum levels of creatinine, C3, and anti-dsDNA antibodies) (Supplementary Figure 2C and Supplementary Table 5, available on the *Arthritis & Rheumatology* website at <http://onlinelibrary.wiley.com/doi/10.1002/art.41506/abstract>). Importantly, when the urinary MMP-7 level was combined with other clinical measures, the performance for identifying patients with LN with greater histologic activity was further improved (Supplementary Table 5). These results suggest that an increased urinary MMP-7 level was

associated with greater renal histologic activity, and thus may be useful for the prediction and management of LN in the presence of higher renal disease activity.

Association of an elevated urinary MMP-7 level during follow-up with the risk of incident LN flare. Increases in renal disease activity (renal flares) are frequently observed in patients with LN, having been observed in 27–66% of patients (3,10). Early diagnosis and appropriate therapies are critical for successful treatment of LN flares. In stage II of the study, among the 65 participants who had follow-up data on urinary MMP-7 levels (bimonthly for 2 years) after a minimum period of remission of renal disease activity of 12 months, we determined whether an elevated MMP-7 level during follow-up was associated with the development of LN flares.

LN flares were observed in 15 patients. Occurrence of an incident LN flare was independently associated with an elevated urinary MMP-7 level in multivariable analyses, regardless of the use of RAS blockers or the presence of hypertension (Figure 3). Moreover, we tested the incremental value (C-statistic) of adding the urinary MMP-7 level to traditional clinical measures in predicting incident LN flare. The C-statistic for incident LN flare during 2 years of follow-up increased with the addition of the urinary MMP-7 level (C-statistic 0.665 [95% CI 0.523–0.806] without urinary MMP-7 level versus 0.865 [95% CI 0.763–0.985] with urinary MMP-7 level) (Supplementary Table 6, available on the *Arthritis & Rheumatology* website at <http://onlinelibrary.wiley.com/doi/10.1002/art.41506/abstract>). A similar increase in the C-statistic for incident LN flare was observed when we used the cutoff point for MMP-7 levels (urinary MMP-7 level of 2.5 ng/mg creatinine) that was identified to achieve optimal discrimination in multivariable analyses (C-statistic 0.880) (Supplementary Figure 3, available on the *Arthritis & Rheumatology* website at <http://onlinelibrary.wiley.com/doi/10.1002/art.41506/abstract>).

Among the 15 subjects who had experienced renal flare during the follow-up, we further explored whether urinary MMP-7 levels could serve as an early predictor of LN flare. Changes in urinary MMP-7 levels and clinical measures in these 15 subjects before, during, and after renal flares were assessed (Figure 4A, and Supplementary Figure 4A on the *Arthritis & Rheumatology* website at <http://onlinelibrary.wiley.com/doi/10.1002/art.41506/abstract>). The urinary MMP-7 level increased in advance of LN flares at an earlier time point than was observed for changes in conventional clinical measures.

Among the clinical variables assessed, proteinuria (defined as an increase to >0.5 gm/day) was the best indicator of an LN flare in individuals in this cohort of 15 subjects with renal flare during follow-up. Therefore, we compared the predictive performance of the urinary MMP-7 level with the predictive performance of proteinuria at each time point in every individual patient before, during, and after a flare (Supplementary Figure 4B [<http://onlinelibrary.wiley.com/doi/10.1002/art.41506/abstract>]). All but 1 flare (93% of patients) occurred in patients with an elevated urinary MMP-7 level that was >2.5 ng/mg creatinine during follow-up. An elevated urinary MMP-7 level (defined as a urinary MMP-7 level of >2.5 ng/mg creatinine) hinted at the occurrence of an LN flare at an earlier time point (median 3 months, IQR 2–4 months) than that predicted with measurement of proteinuria (Figure 4B). Moreover, the urinary MMP-7 level declined with remission of LN (defined as achievement of a normal eGFR and proteinuria level of <0.5 gm/day) (5), whereas it stayed elevated in patients whose disease was not in remission during the follow-up (Figure 4C).

Of the 15 subjects who experienced flares, 5 underwent a repeat renal biopsy at the time of flare (characteristics of the patients at the time of the initial biopsy and time of the repeat biopsy are presented in Supplementary Table 7, available on the *Arthritis & Rheumatology* website at <http://onlinelibrary.wiley.com/doi/10.1002/art.41506/abstract>). Kidney biopsy samples from these 15 subjects were immunostained for MMP-7, and

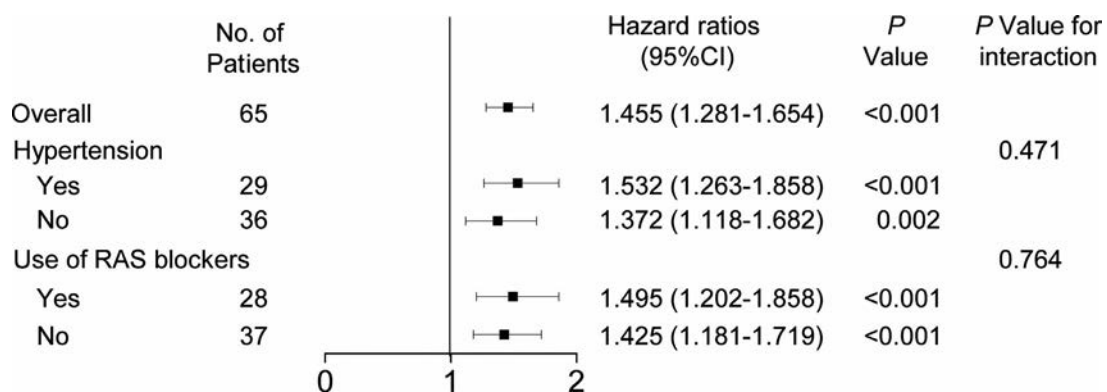


Figure 3. Association of urinary MMP-7 levels with subsequent incident LN flare. Associations were assessed in the total cohort of patients with LN and in subgroups of patients stratified according to the presence or absence of hypertension, and according to the use or lack of use of renin–angiotensin system (RAS) blockers. Whisker plots show the average hazard ratio with 95% confidence interval (95% CI). See Figure 1 for other definitions.

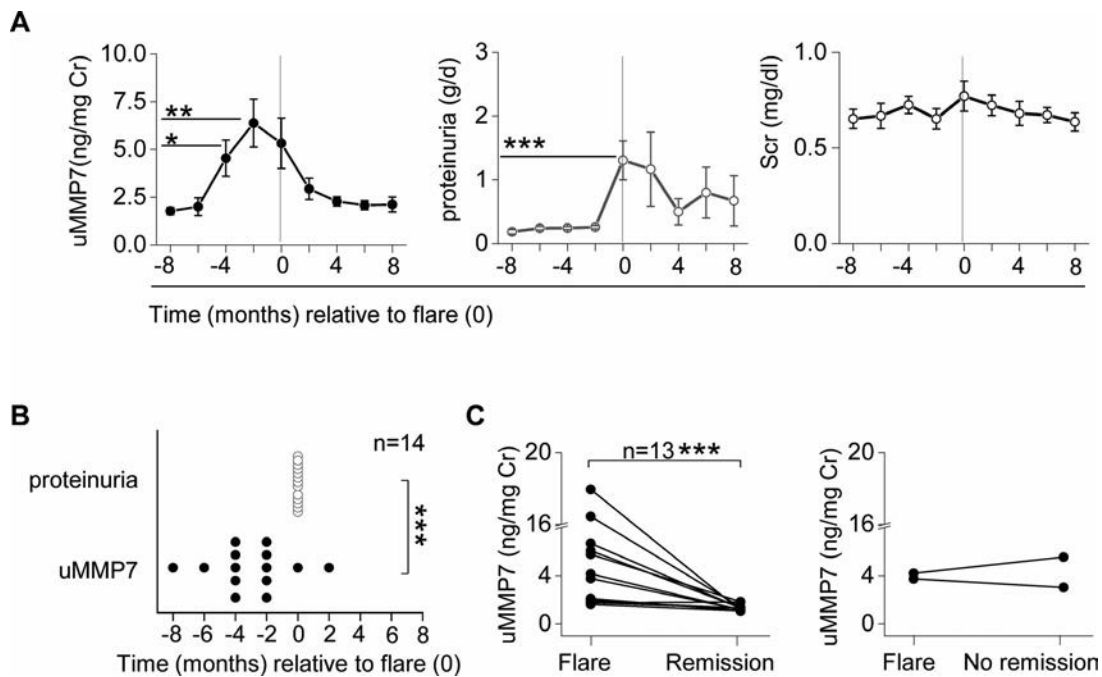


Figure 4. Evidence of elevated urinary MMP-7 levels during follow-up heralding LN flare in advance of clinical measures in patients with LN. **A**, Urinary MMP-7 levels were compared with conventional clinical measures, including levels of proteinuria and serum creatinine (Scr), before, during, and after an incident flare in patients with LN ($n = 15$). The vertical line at time 0 indicates the time of flare. Results are the mean \pm SEM. **B**, The time point at which an elevation in urinary MMP-7 level (defined as >2.5 ng/mg creatinine) or elevation in proteinuria (defined as an increase to >0.5 gm/day) was measured in patients with LN, showing that, compared to proteinuria, elevation in the urinary MMP-7 level heralds a renal flare at an earlier time point (median 3 months, interquartile range 2–4 months). **C**, The urinary MMP-7 level at the time of flare was compared with that at the end of follow-up, showing that the urinary MMP-7 level declines with LN remission (left) and remains stable in patients whose disease is not in remission (right). * = $P < 0.05$; ** = $P < 0.01$; *** = $P < 0.001$, by Mann-Whitney U test. See Figure 1 for other definitions.

the levels of urinary MMP-7 and renal histologic activity were determined in both renal biopsy samples (representative micrographs in Figure 5A and Supplementary Figure 5, available on the *Arthritis & Rheumatology* website at <http://onlinelibrary.wiley.com/doi/10.1002/art.41506/abstract>). As shown in Figure 5B, renal histologic activity was elevated at the time of LN flare (repeat biopsy sample) as compared with renal histologic activity at the time of diagnosis of LN (initial biopsy sample). The urinary MMP-7 level and kidney MMP-7 expression increased as the renal histologic activity progressed (Figures 5C and D).

DISCUSSION

In the present 2-stage study, we identified urinary MMP-7 as a promising predictor of renal flares in LN. We demonstrated elevated urinary MMP-7 levels in patients with LN. An elevated urinary MMP-7 level at the time of biopsy in patients with LN was independently associated with increased renal histologic activity, thereby linking the urinary MMP-7 level to renal disease activity. Furthermore, we found that an elevation in urinary MMP-7 level after renal remission had occurred was associated with incident renal flare. An elevated urinary MMP-7 level was predictive of LN flares before any clinical evidence indicative of renal dysfunction

and before any serologic measurements indicative of a flare. This association was independent of sex, traditional clinical measures, the presence of hypertension, and the use of RAS blockers. Inclusion of the urinary MMP-7 level into the current set of clinical measures improved the prognostic value for prediction of LN flares. Thus, longitudinal monitoring of urinary MMP-7 levels, especially when combined with clinical measures, may facilitate surveillance of renal disease activity and assist early prediction of LN flares.

An elevated urinary MMP-7 level typically has been attributed to exacerbated systemic inflammation or enhanced kidney injury (22,25). Although we found a slightly increased serum level of MMP-7 in subjects with newly diagnosed LN when compared with that in healthy volunteers, this elevation was trivial. Moreover, no correlation was observed between the serum and urinary MMP-7 levels. In contrast, kidney MMP-7 protein levels were markedly induced in these subjects with LN. MMP-7 protein has been shown to increase the release of Fas ligand in renal cells, thereby accelerating local cell injury and inflammation (18,33). Furthermore, we demonstrated that the urinary MMP-7 level positively correlated with kidney MMP-7 expression. Thus, elevated urinary MMP-7 levels in LN are unlikely to be simply the result of systemic inflammation, and may be related to active renal damage.

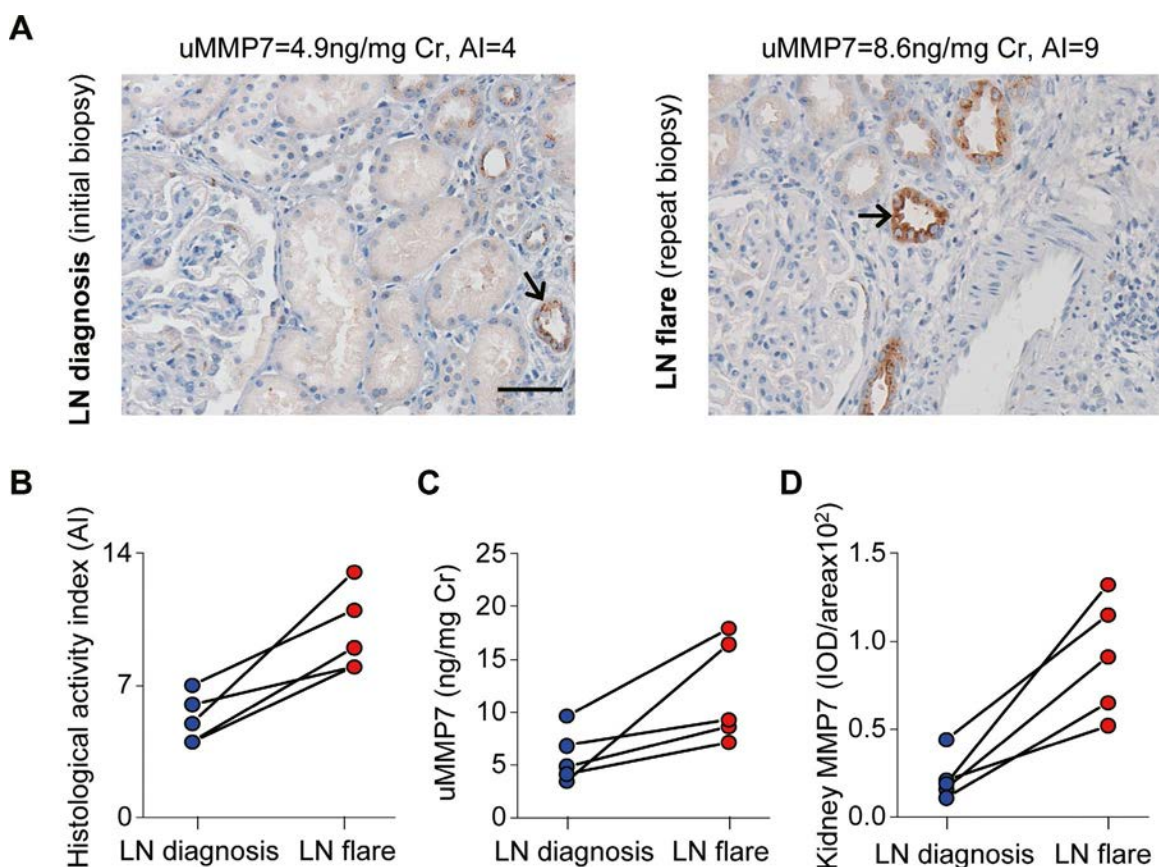


Figure 5. Correlation of the urinary MMP-7 level with renal histologic activity in patients with LN. **A**, Representative images show kidney MMP-7 expression at the time of diagnosis of LN (initial biopsy) and time of LN flare (repeat biopsy). Values for the urinary MMP-7 level and renal histologic activity index (AI) at the time of biopsy are shown at the top of each image. **Arrows** indicate positively stained renal tubules. Bar = 50 μ m. **B–D**, Renal AIs (**B**), urinary MMP-7 levels (**C**), and kidney MMP-7 expression (**D**) in each individual patient ($n = 5$) were compared between the time of diagnosis of LN and the time of LN flare. See Figure 1 for other definitions.

In fact, in our study, a higher urinary MMP-7 level was associated with greater renal histologic activity. The urinary MMP-7 level increased as renal histologic activity progressed. Measurement of urinary MMP-7 levels in conjunction with other clinical measures improved their accuracy in discriminating LN patients with greater renal histologic activity. A urinary MMP-7 cutoff level of 6.2 ng/mg creatinine (according to Youden index analysis) yielded good sensitivity and specificity for identifying LN patients with greater renal histologic activity. However, in clinical scenarios, the criteria for an optimal cutoff value should change according to the aim of the study. As for screening purposes, the urinary MMP-7 cutoff value that warranted the best combination of sensitivity (0.82) and false positive rate (0.20) was 4.94 ng/mg creatinine. The urinary MMP-7 level may therefore be a potential indicator of renal disease activity in LN.

Increases in renal disease activity (renal flares) occur frequently in patients with LN, and these flares are associated with impaired renal survival and increased patient exposure to treatment-related toxic effects (3). As not all patients are at equal risk of renal flares, early identification of patients at risk is highly cost-effective and

could reduce the risk of adverse renal outcomes (6,10,34). Multiple biomarkers have been explored recently as indicators of renal disease activity in LN. However, few have been tested serially during periods leading up to a flare (35).

In our prospective cohort of patients with LN, we demonstrated that despite long-term maintenance therapy, participants who had achieved complete remission of renal disease activity still had a high rate of renal flares. Patients at risk for flares cannot be predicted a priori with the use of clinical variables that are usually measured during outpatient follow-up. Importantly, monitoring of MMP-7 after renal remission could help to predict who is prone to flare. A rise in serially monitored urinary MMP-7 levels was associated with an increased risk of future renal flare. Everyone in our cohort with an elevated MMP-7 level above 2.5 ng/mg creatinine developed a renal flare at a median 3 months (IQR 2–4 months) later, as evidenced by the levels of proteinuria and serologic parameters. Furthermore, the urinary MMP-7 level added prognostic value to the clinical measures for predicting renal flares in all patients and in the subgroups of patients who had hypertension (the most prevalent comorbidity in LN) or who had taken

RAS blockers (the most prevalent treatment for LN). Reduction in dose and cessation of immunosuppressive therapy are the 2 most common events preceding the occurrence of renal flares. Thus, dynamic surveillance of the urinary MMP-7 level, especially in the period during tapering or withdrawal of immunosuppressive treatment, may facilitate the stratification of patients early in their disease course. Patients predicted to experience a flare would require more intensive monitoring and should be considered for continuation of treatment, while those predicted not to experience a flare may be candidates for withdrawal of immunosuppressive therapy.

In stage II, after a minimum period of 12 months of complete renal disease remission, participants had follow-up urinary MMP-7 measurements for 2 years. Therefore, the incidence of LN flare in our cohort was 23% during a median of 36 months after achieving complete renal disease remission, which is slightly higher than that reported in previous studies (18–20% for 36-month follow-up after LN remission) (36,37). However, flare rates may vary according to the race or population studied, the histologic classes of LN distributed, the immunosuppressive treatment, the sample size, and the definition of flare used, making direct comparisons difficult (3). This question will need to be examined in our ongoing serial studies with larger sample sizes and with longer durations of follow-up. In addition, the median time to flare was 28 months (IQR 23–36 months) after the first episode in this cohort, generally coinciding with a reduction in the number or doses of immunosuppressive agents, as previously reported (38).

Our conclusions are strengthened by the comparison of urinary MMP-7 levels directly with renal histologic activity both at the time of the initial kidney biopsy and at the repeat kidney biopsy, which empowers the urinary MMP-7 level as a promising diagnostic tool for renal disease activity in LN. Moreover, we utilized longitudinal assessments of the urinary MMP-7 level at regular intervals among patients who had achieved complete remission, and characterized the profiles of urinary MMP-7 levels as LN moves from quiescence to flares. This provides an opportunity to compare the dynamics of biomarker levels with changes in renal disease activity.

The study has some limitations. First, we did not have a disease control group comprising patients with diabetic nephropathy, nor did we include LN patients with diabetes. Therefore, the influence of diabetes in LN patients on the urinary MMP-7 level remains unclear and needs further investigation. Second, in these LN cohorts, we did not investigate the level of other MMPs (15,39) that are associated with kidney fibrosis. Finally, most patients included in our study were Chinese, and the majority were women. Therefore, future studies that enroll patients with other ethnic groups and include both sexes are needed to extend our results.

In summary, our study provides evidence that an elevation in the urinary MMP-7 level in LN is associated with increased renal disease activity. Close surveillance of the urinary MMP-7 level after achievement of remission of renal disease activity could be used to identify patients at risk of LN flare early in their disease course, thereby allowing more prompt and rational management strategies

that could lead to ascertainment of the optimal approach for achieving renal survival in patients with LN.

AUTHOR CONTRIBUTIONS

All authors were involved in drafting the article or revising it critically for important intellectual content, and all authors approved the final version to be published. Mr. Wang, and Drs. Wu and Cao had full access to all of the data in the study and take responsibility for the integrity of the data and the accuracy of the data analysis.

Study conception and design. Cao.

Acquisition of data. H. Su, Feng, Shi, Jin, M. Yang, Zhou, C. Su, B. Yang, Li.










Analysis and interpretation of data. Wang, Wu, Cao.

REFERENCES

1. Doria A, Iaccarino L, Ghirardello A, Zampieri S, Arienti S, Sarzi-Puttini P, et al. Long-term prognosis and causes of death in systemic lupus erythematosus. *Am J Med* 2006;119:700–6.
2. Bajema IM, Wilhelmus S, Alpers CE, Bruijn JA, Colvin RB, Cook HT, et al. Revision of the International Society of Nephrology/Renal Pathology Society classification for lupus nephritis: clarification of definitions, and modified National Institutes of Health activity and chronicity indices. *Kidney Int* 2018;93:789–96.
3. Sprangers B, Monahan M, Appel GB. Diagnosis and treatment of lupus nephritis flares: an update [review]. *Nat Rev Nephrol* 2012;8:709–17.
4. Fiehn C, Hajjar Y, Mueller K, Waldherr R, Ho AD, Andrassy K. Improved clinical outcome of lupus nephritis during the past decade: importance of early diagnosis and treatment. *Ann Rheum Dis* 2003;62:435–9.
5. De Rosa M, Azzato F, Toblli JE, de Rosa G, Fuentes F, Nagaraja HN, et al. A prospective observational cohort study highlights kidney biopsy findings of lupus nephritis patients in remission who flare following withdrawal of maintenance therapy. *Kidney Int* 2018;94:788–94.
6. Quintana LF, Jayne D. Sustained remission in lupus nephritis: still a hard road ahead. *Nephrol Dial Transplant* 2016;31:2011–8.
7. Kim AH, Strand V, Sen DP, Fu Q, Mathis NL, Schmidt MJ, et al. Association of blood concentrations of complement split product iC3b and serum C3 with systemic lupus erythematosus disease activity. *Arthritis Rheumatol* 2019;71:420–30.
8. Arriens C, Chen S, Karp DR, Saxena R, Sambandam K, Chakravarty E, et al. Prognostic significance of repeat biopsy in lupus nephritis: histopathologic worsening and a short time between biopsies is associated with significantly increased risk for end stage renal disease and death. *Clin Immunol* 2017;185:3–9.
9. Moroni G, Depetri F, Ponticelli C. Lupus nephritis: when and how often to biopsy and what does it mean? *J Autoimmun* 2016;74:27–40.
10. Gatto M, Zen M, Iaccarino L, Doria A. New therapeutic strategies in systemic lupus erythematosus management [review]. *Nat Rev Rheumatol* 2019;15:30–48.
11. Mejia-Vilet JM, Zhang XL, Cruz C, Cano-Verduzco ML, Shapiro JP, Nagaraja HN, et al. Urinary soluble CD163: a novel noninvasive biomarker of activity for lupus nephritis. *J Am Soc Nephrol* 2020;31:1335–47.
12. Shi M, Luo W, Feng X, Jin L, Yang M, Wu L, et al. Urinary angiotensinogen predicts renal disease activity in lupus nephritis. *Antioxid Redox Signal* 2019;31:1289–301.
13. Torres-Salido MT, Cortes-Hernandez J, Vidal X, Pedrosa A, Vilardell-Tarres M, Ordi-Ros J. Neutrophil gelatinase-associated

- lipocalin as a biomarker for lupus nephritis. *Nephrol Dial Transplant* 2014;29:1740–9.
14. Parrish AR. Matrix metalloproteinases in kidney disease: role in pathogenesis and potential as a therapeutic target. *Prog Mol Biol Transl Sci* 2017;148:31–65.
 15. Adamidis KN, Kopaka ME, Petraki C, Charitaki E, Apostolou T, Christodoulidou C, et al. Glomerular expression of matrix metalloproteinases in systemic lupus erythematosus in association with activity index and renal function. *Ren Fail* 2019;41:229–37.
 16. George SJ, Dwivedi A. MMPs, cadherins, and cell proliferation. *Trends Cardiovasc Med* 2004;14:100–5.
 17. Vandenbroucke RE, Vanlaere I, van Hauwermeiren F, van Wonterghem E, Wilson C, Libert C. Pro-inflammatory effects of matrix metalloproteinase 7 in acute inflammation. *Mucosal Immunol* 2014;7:579–88.
 18. Tsukinoki T, Sugiyama H, Sunami R, Kobayashi M, Onoda T, Maeshima Y, et al. Mesangial cell Fas ligand: upregulation in human lupus nephritis and NF- κ B-mediated expression in cultured human mesangial cells. *Clin Exp Nephrol* 2004;8:196–205.
 19. Ke B, Fan C, Yang L, Fang X. Matrix metalloproteinases-7 and kidney fibrosis [review]. *Front Physiol* 2017;8:21.
 20. Vira H, Pradhan V, Umare V, Chaudhary A, Rajadhyksha A, Nadkar M, et al. Role of MMP-7 in the pathogenesis of systemic lupus erythematosus (SLE). *Lupus* 2017;26:937–43.
 21. Reich HN, Landolt-Marticorena C, Boutros PC, John R, Wither J, Fortin PR, et al. Molecular markers of injury in kidney biopsy specimens of patients with lupus nephritis. *J Mol Diagn* 2011;13:143–51.
 22. Yang X, Chen C, Teng S, Fu X, Zha Y, Liu H, et al. Urinary matrix metalloproteinase-7 predicts severe AKI and poor outcomes after cardiac surgery. *J Am Soc Nephrol* 2017;28:3373–82.
 23. Berthier CC, Bethunaickan R, Gonzalez-Rivera T, Nair V, Ramanujam M, Zhang W, et al. Cross-species transcriptional network analysis defines shared inflammatory responses in murine and human lupus nephritis. *J Immunol* 2012;189:988–1001.
 24. Tveita AA, Rekvig OP. Alterations in Wnt pathway activity in mouse serum and kidneys during lupus development. *Arthritis Rheum* 2011;63:513–22.
 25. Zhou D, Tian Y, Sun L, Zhou L, Xiao L, Tan RJ, et al. Matrix metalloproteinase-7 is a urinary biomarker and pathogenic mediator of kidney fibrosis. *J Am Soc Nephrol* 2017;28:598–611.
 26. Hochberg MC. Updating the American College of Rheumatology revised criteria for the classification of systemic lupus erythematosus [letter]. *Arthritis Rheum* 1997;40:1725.
 27. Yamamoto T, Nakagawa T, Suzuki H, Ohashi N, Fukasawa H, Fujigaki Y, et al. Urinary angiotensinogen as a marker of intrarenal angiotensin II activity associated with deterioration of renal function in patients with chronic kidney disease. *J Am Soc Nephrol* 2007;18:1558–65.
 28. Yee CS, Farewell VT, Isenberg DA, Griffiths B, Teh LS, Bruce IN, et al. The use of Systemic Lupus Erythematosus Disease Activity Index-2000 to define active disease and minimal clinically meaningful change based on data from a large cohort of systemic lupus erythematosus patients. *Rheumatology (Oxford)* 2011;50:982–8.
 29. Bertsias GK, Tektonidou M, Amoura Z, Aringer M, Bajema I, Berden JH, et al. Joint European League Against Rheumatism and European Renal Association-European Dialysis and Transplant Association (EULAR/ERA-EDTA) recommendations for the management of adult and paediatric lupus nephritis. *Ann Rheum Dis* 2012;71:1771–82.
 30. Cao W, Jin L, Zhou Z, Yang M, Wu C, Wu L, et al. Overexpression of intrarenal renin-angiotensin system in human acute tubular necrosis. *Kidney Blood Press Res* 2016;41:746–56.
 31. DeLong ER, DeLong DM, Clarke-Pearson DL. Comparing the areas under two or more correlated receiver operating characteristic curves: a nonparametric approach. *Biometrics* 1988;44:837–45.
 32. Shrout PE, Fleiss JL. Intraclass correlations: uses in assessing rater reliability. *Psychol Bull* 1979;86:420–8.
 33. Miwa K, Asano M, Horai R, Iwakura Y, Nagata S, Suda T. Caspase 1-independent IL-1 β release and inflammation induced by the apoptosis inducer Fas ligand. *Nat Med* 1998;4:1287–92.
 34. Davidson A. What is damaging the kidney in lupus nephritis? [review]. *Nat Rev Rheumatol* 2016;12:143–53.
 35. Birmingham DJ, Merchant M, Waikar SS, Nagaraja H, Klein JB, Rovin BH. Biomarkers of lupus nephritis histology and flare: deciphering the relevant amidst the noise. *Nephrol Dial Transplant* 2017;32:i71–9.
 36. Ponticelli C, Moroni G. Flares in lupus nephritis: incidence, impact on renal survival and management. *Lupus* 1998;7:635–8.
 37. Shao SJ, Hou JH, Xie GT, Sun W, Liang DD, Zeng CH, et al. Improvement of outcomes in patients with lupus nephritis: management evolution in Chinese patients from 1994 to 2010. *J Rheumatol* 2019;46:912–9.
 38. Carlavilla A, Gutierrez E, Ortuno T, Morales E, Gonzalez E, Praga M. Relapse of lupus nephritis more than 10 years after complete remission. *Nephrol Dial Transplant* 2005;20:1994–8.
 39. Lesiak A, Narbutt J, Sysa-Jedrzejowska A, Lukamowicz J, McCauliffe DP, Wozniacka A. Effect of chloroquine phosphate treatment on serum MMP-9 and TIMP-1 levels in patients with systemic lupus erythematosus. *Lupus* 2010;19:683–8.

Deficiency of Adenosine Deaminase 2 in Adults and Children: Experience From India

Aman Sharma,¹  GSRSNK Naidu,¹ Vikas Sharma,¹ Saket Jha,² Aaadhar Dhooria,³ Varun Dhir,¹ 
Prateek Bhatia,¹ Vishal Sharma,¹  Sagar Bhattad,⁴ K. G. Chengappa,⁵  Vikas Gupta,⁶
Durga Prasanna Misra,⁷  Pallavi Pimpale Chavan,⁸ Sourabh Malaviya,⁹ Rajkiran Dudam,¹⁰ Banwari Sharma,¹¹
Sathish Kumar,¹² Rajesh Bhojwani,¹³ Pankaj Gupta,¹ Vikas Agarwal,⁷ Kusum Sharma,¹ Manphool Singhal,¹
Manish Rathi,¹ Ritambhra Nada,¹ Ranjana W. Minz,¹ Ved Chaturvedi,¹⁴ Amita Aggarwal,⁷  Rohini Handa,¹⁵
Alice Grossi,¹⁶ Marco Gattorno,¹⁷  Zhengping Huang,¹⁸  Jun Wang,¹⁹ Ramesh Jois,²⁰ V. S. Negi,⁵
Raju Khubchandani,⁸ Sanjay Jain,¹ Juan I. Arostegui,²¹  Eugene P. Chambers,²² Michael S. Hershfield,²³
Ivona Aksentijevich,²⁴ Qing Zhou,¹⁹ and Pui Y. Lee²⁵

Objective. Deficiency of adenosine deaminase 2 (DADA2) is a potentially fatal monogenic syndrome characterized by variable manifestations of systemic vasculitis, bone marrow failure, and immunodeficiency. Most cases are diagnosed by pediatric care providers, given the typical early age of disease onset. This study was undertaken to describe the clinical phenotypes and treatment response both in adults and in children with DADA2 in India.

Methods. A retrospective analysis of pediatric and adult patients with DADA2 diagnosed at various rheumatology centers across India was conducted. Clinical characteristics, diagnostic findings, and treatment responses were analyzed in all subjects.

Results. In total, 33 cases of DADA2 were confirmed in this cohort between April 2017 and March 2020. Unlike previous studies, nearly one-half of the confirmed cases presented during adulthood. All symptomatic patients exhibited features of vasculitis, whereas constitutional symptoms and anemia were more common in pediatric patients. Cutaneous and neurologic involvement were common, and 18 subjects had experienced at least one stroke. In addition, the clinical spectrum of DADA2 was expanded by recognition of novel features in these patients, including pancreatic infarction, focal myocarditis, and diffuse alveolar hemorrhage. Treatment with tumor necrosis factor inhibitors (TNFi) was initiated in 25 patients. All of the identified disease manifestations showed marked improvement after initiation of TNFi, and disease remission was achieved in 19 patients. Two cases were complicated by tuberculosis infection, and 2 deaths were reported.

Conclusion. This report presents the first case series of patients with DADA2 from India, diagnosed by adult and pediatric care providers. The findings raise awareness of this syndrome, particularly with regard to its presentation in adults.

INTRODUCTION

Adenosine deaminase 2 (ADA-2) is an extracellular enzyme secreted by activated monocytes, macrophages, and dendritic cells. Although its physiologic function is not entirely clear, ADA-2

promotes the differentiation of monocytes to macrophages and may also act as a growth factor for endothelial cells and hematopoietic cells (1–3). ADA-2 is encoded by the *ADA2* gene (previously known as *CECR1*, or cat eye syndrome chromosome region 1 gene) on chromosome 22q11.1 (4).

Dr. Arostegui's work was supported by the Spanish Ministry of Science, Innovation, and Universities co-financed by the European Regional Development Fund (grant RTI2018-096824-B-C21). Dr. Lee's work was supported by the National Institute of Arthritis and Musculoskeletal and Skin Diseases, NIH (grant K08-AR-074562), a Rheumatology Research Foundation Investigator Award, and the Boston Children's Hospital Faculty Career Development Award.

¹Aman Sharma, MD, FRCP, GSRSNK Naidu, DM, Vikas Sharma, DM, Varun Dhir, DM, Prateek Bhatia, MD, Vishal Sharma, DM, Pankaj Gupta, MD, Kusum Sharma, MD, Manphool Singhal, MD, Manish Rathi, DM, Ritambhra Nada, MD, Ranjana W. Minz, MD, Sanjay Jain, DM: Postgraduate Institute of Medical Education and Research, Chandigarh, India; ²Saket Jha, DM: Om Hospital

and Research Center, Kathmandu, Nepal; ³Aaadhar Dhooria, DM: Santokba Durlabhji Memorial Hospital, Jaipur, India; ⁴Sagar Bhattad, DM: Aster CMI Hospital, Bengaluru, India; ⁵K. G. Chengappa, DM, V. S. Negi, DM: Jawaharlal Institute of Postgraduate Medical Education and Research, Puducherry, India; ⁶Vikas Gupta, DM: Dayanand Medical College, Ludhiana, India; ⁷Durga Prasanna Misra, DM, Vikas Agarwal, DM, Amita Aggarwal, DM: Sanjay Gandhi Postgraduate Institute of Medical Sciences, Lucknow, India; ⁸Pallavi Pimpale Chavan, MD, Raju Khubchandani, MD: SRCC Children's Hospital, Mumbai, India; ⁹Sourabh Malaviya, MD: Medanta Hospital, Indore, India; ¹⁰Rajkiran Dudam, MD: Hyderabad Rheumatology Centre, Hyderabad, India; ¹¹Banwari Sharma, DM: Niramaya Healthcare, Jaipur, India; ¹²Sathish Kumar, MD: Christian Medical College, Vellore, India; ¹³Rajesh Bhojwani, MS: Santokba Durlabhji Memorial

An autoinflammatory disease known as deficiency of ADA-2 (DADA2) results from biallelic mutations in *ADA2* (5,6). Since its first description in 2014, case reports and series from different countries have expanded the clinical spectrum of the disease (7–11). Common clinical features of the disease include recurrent fever, skin ulcers, livedo reticularis, early-onset stroke, peripheral neuropathy, hypogammaglobulinemia, cytopenias, and elevated blood levels of acute-phase reactants (5–11). These features led to the recognition of DADA2 as a monogenic form of polyarteritis nodosa (PAN) that presents in early childhood. Although a few cases of DADA2 in adults have been described (6,12), little is known regarding the clinical manifestations and treatment outcomes in patients with adult-onset DADA2.

Anti-tumor necrosis factor (anti-TNF) therapy is the established treatment of choice for DADA2, and it has shown remarkable efficacy in preventing stroke (13). However, how other clinical manifestations respond to this treatment has not been described in detail, and there are cases that do not respond to TNF inhibitors (TNFi) (14). In the present report, we describe the clinical features, genotypes, and treatment outcomes in 33 patients with DADA2 in India. Unlike previous cases series, nearly one-half of the patients in our cohort were adults at the time of disease onset. We compare the clinical manifestations between patients presenting with DADA2 during childhood and those presenting with DADA2 in adulthood, and report the response of various clinical manifestations to TNFi.

PATIENTS AND METHODS

Subjects and study design. We conducted a retrospective analysis of patients diagnosed as having DADA2 at different rheumatology centers across India. To recruit the patients, a request was sent to all members of the Indian Rheumatology Association to contribute data on patients with DADA2 diagnosed at the respective centers. Diagnosis of DADA2 was established on the basis of findings from an ADA-2 enzyme activity assay and/or *ADA2* gene sequencing, depending on the logistic availability of the techniques at each center. The clinical details in all subjects, which included presenting manifestations, organ involvement, laboratory investigations, treatment approaches, and response to therapy, were documented by the health care providers. Results of tissue biopsy and radiographic imaging of the involved organs

were also collected, including findings from computed tomography (CT), magnetic resonance imaging (MRI), and angiography. Two of the patients in our cohort have been described in previous reports (14,15). Demographic characteristics, clinical data, and treatment outcomes in all of the study subjects are described in detail in Supplementary Table 1 (available on the *Arthritis & Rheumatology* website at <http://onlinelibrary.wiley.com/doi/10.1002/art.41500/abstract>).

Clinical remission was defined as the presence of the following features: 1) absence of active systemic inflammation, 2) absence of active organ-specific vasculitis, and 3) improvement or stabilization of prior organ damage related to DADA2. Treatment outcomes for each of the various individual manifestations were recorded as resolved (complete improvement), improved (partial improvement), persisting activity (ongoing activity), and relapse (recurrence after initial resolution) or new-onset features.

This study was approved by the Institute Ethics Committee of the Postgraduate Institute of Medical Education and Research in Chandigarh, India. A waiver of patient consent was granted by the Institute Ethics Committee for the retrospective analysis.

ADA-2 activity assay. Measurement of ADA-2 activity, as determined from the patients' plasma or dried plasma spots, was performed using spectrophotometric assay, as described previously (5,16). This assay quantifies the adenosine-dependent generation of ammonia in the presence of a selective inhibitor of ADA-1, EHNA (erythro-9-Amino- β -hexyl- α -methyl-9H-purine-9-ethanol hydrochloride). EHNA was purchased from Cayman Chemicals and all other reagents were purchased from Sigma-Aldrich. The kinetics of each reaction were analyzed using a Biotek Synergy Hybrid microplate reader.

ADA2 gene mutation analysis. Ten exons of the *ADA2* gene were amplified using KOD FX high success-rate DNA polymerase (product no. KFX-101), and the polymerase chain reaction product of each amplicon was purified using an Axygen AxyPrep DNA gel extraction kit (product no. AP-GX-250) in accordance with the manufacturer's instructions. Sanger sequencing of the *ADA2* gene was conducted as previously described (5,17). Results of Sanger sequencing were analyzed using Sequencher software, version 5.4.6 (Gene Codes Corporation).

Hospital, Jaipur, India; ¹⁴Ved Chaturvedi, DM: Sir Ganga Ram Hospital, New Delhi, India; ¹⁵Rohini Handa, MD: Indraprastha Apollo Hospital, New Delhi, India; ¹⁶Alice Grossi, PhD: IRCCS, Istituto Giannina Gaslini, UOSD Laboratory of Genetics and Genomics of Rare Diseases, Genoa, Italy; ¹⁷Marco Gattorno, MD: Centro Malattie Autoinfiammatorie e Immunodeficienze, IRCCS, Istituto Giannina Gaslini, Genoa, Italy; ¹⁸Zhengping Huang, MD: Guangdong Second Provincial General Hospital, Guangzhou, China; ¹⁹Jun Wang, BS, Qing Zhou, PhD: Zhejiang University, Zhejiang, China; ²⁰Ramesh Jois, MD: Vikram Hospital, Bengaluru, India; ²¹Juan I. Arostegui, MD, PhD: Hospital Clinic, Institut d'Investigacions Biomèdiques August Pi i Sunyer, Barcelona, Spain; ²²Eugene P. Chambers, MD: Vanderbilt University Medical Center and DADA2 Foundation, Nashville, Tennessee; ²³Michael S. Hershfield, MD: Duke University School of Medicine, Durham, North Carolina;

²⁴Ivona Aksentijevich, MD: National Human Genome Research Institute, NIH, Bethesda, Maryland; ²⁵Pui Y. Lee, MD, PhD: Boston Children's Hospital, Boston, Massachusetts.

Dr. Gattorno has received consulting fees, speaking fees, and/or honoraria from Novartis and Sobi (less than \$10,000 each). No other disclosures relevant to this article were reported.

Address correspondence to Aman Sharma, MD, FRCP, Clinical Immunology and Rheumatology Services, Department of Internal Medicine, Postgraduate Institute of Medical Education and Research, Madhya Marg, Sector 12, Chandigarh 160012, India. Email: amansharma74@yahoo.com.

Submitted for publication May 31, 2020; accepted in revised form August 20, 2020.

Structural modeling was performed using PyMOL and UCSF Chimera software (18). Construction of a pcDNA3.1 plasmid encoding wild-type or mutant ADA-2 with a C-terminal Myc tag was performed as previously described (17). The list of mutations and primer pairs used to generate mutant constructs are available in Supplementary Table 2 (available on the *Arthritis & Rheumatology* website at <http://onlinelibrary.wiley.com/doi/10.1002/art.41500/abstract>). Plasmids were transfected into 293T cells using Fugene 6 (Promega). ADA-2 expression in the cell lysates and ADA-2 activity in the culture medium were quantified after 3 days. Each mutant was analyzed in at least 3 independent experiments, and measurements were normalized to the activity of wild-type ADA-2.

Western blotting. ADA-2 protein was detected using a monoclonal antibody against Myc tag, as previously described (17). Transfected cells (5×10^5) were resuspended in 100 μ l of Laemmli buffer with 2-mercaptoethanol. Sodium dodecyl sulfate–polyacrylamide gel electrophoresis was performed using an 8% polyacrylamide gel. After transfer to a PVDF membrane and blocking with 5% dry milk, a primary antibody to Myc tag (clone 9E10; BioLegend) or to GAPDH (clone D4C6R; Cell Signaling Technology) was applied for 1 hour. Membranes were washed in Tris buffered saline with 0.1% Tween 20, and horseradish peroxidase–conjugated goat anti-mouse IgG (1:5,000; Cell Signaling Technology) was used for detection. Images were acquired using a Bio-Rad ChemiDoc system.

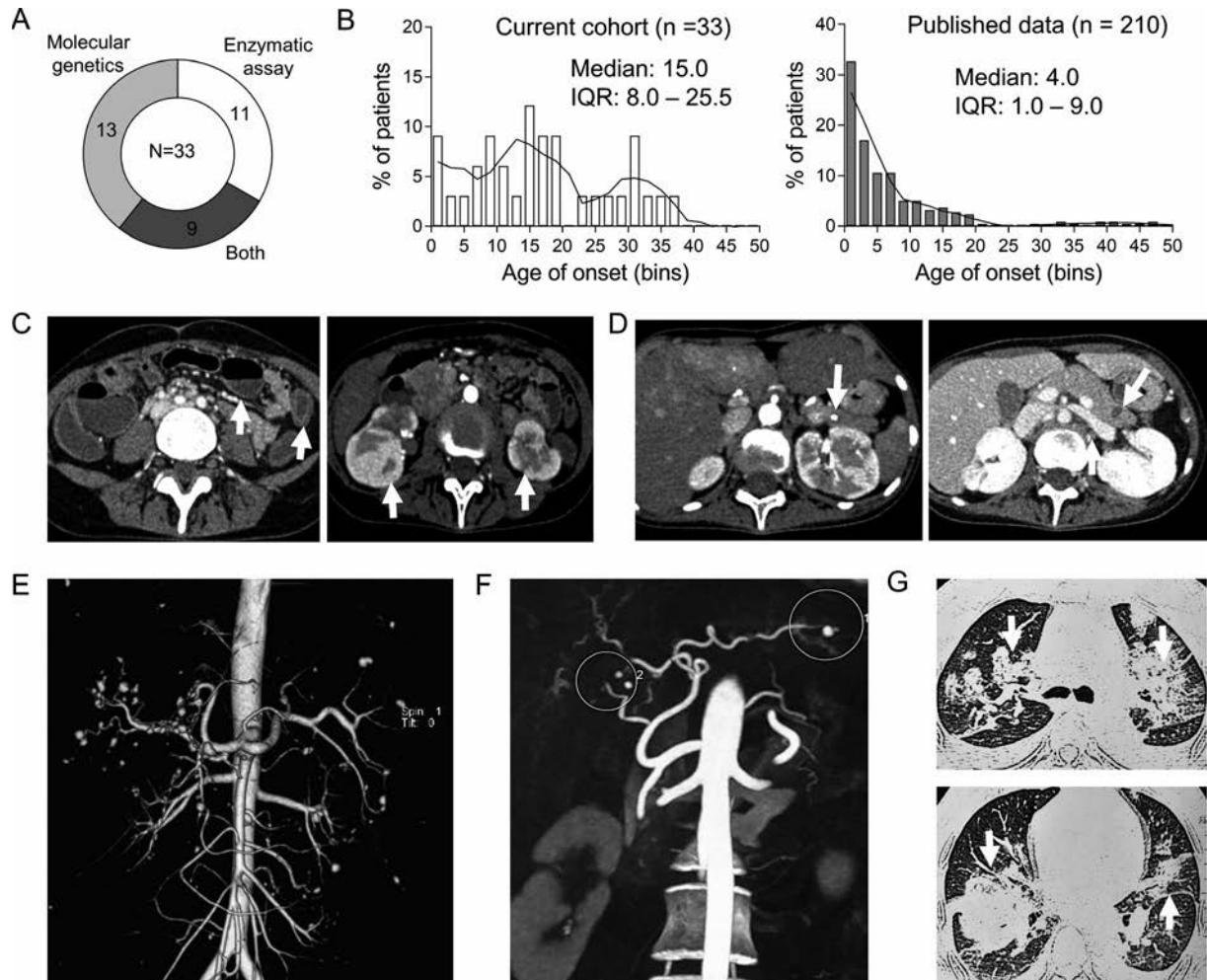


Figure 1. Clinical characteristics and disease manifestations in enrolled patients. **A**, Distribution of methods utilized to confirm the diagnosis of deficiency of adenosine deaminase 2 (DADA2) syndrome. **B**, Comparison of age at disease onset between the current cohort ($n = 33$) and previously reported cases ($n = 210$). The median with interquartile range (IQR) values for age at onset are indicated. **C–G**, Images illustrating clinical manifestations of DADA2, including small bowel obstruction and bilateral renal infarcts (arrows) in a 43-year-old man (on computed tomography [CT] scan) (**C**), a micro-aneurysm (arrow, left) and infarct (arrow, right) within the pancreatic body in a 17-year-old female subject (on CT scan) (**D**), aneurysms of the left lower intercostal artery and hepatic, splenic, renal, and mesenteric arteries in a 16-year-old male subject (on CT angiography, 3-dimensional reconstruction) (**E**), aneurysms of the right hepatic artery (circled area on left) and splenic artery (circled area on right) in a 17-year-old female subject (on CT angiography) (**F**), and bilateral consolidation and surrounding ground-glass opacities (arrows) in a 38-year-old man with diffuse alveolar hemorrhage (on CT scan) (**G**).

Statistical analysis. Values for continuous variables are presented as the median with interquartile range, whereas percentages and proportions are used for categorical variables. The differences between 2 groups were analyzed using the Mann-Whitney U test, and chi-square test was used for comparison of categorical variables. Multiple linear regression analysis was performed to predict the factors associated with delay in diagnosis. All tests were 2-sided, and *P* values less than 0.05 were considered significant. Statistical analyses were performed using Prism software, version 8.0 (GraphPad).

RESULTS

Patient characteristics. Between April 2017 and March 2020, a total of 124 patients were tested for DADA2 by enzymatic activity assay and/or *ADA2* gene mutation analysis. Of these 124 patients, we established the diagnosis of DADA2 in 33 patients from 28 unrelated families. Eighteen patients were from North India, 9 were from South India, 5 were from West India, and 1

was from Syria. Thirteen of the 18 northern India patients and 3 of the 5 western India patients belonged to the Agarwal/Jain community. All patients presented with features of systemic vasculitis, except for 1 infant who initially presented with pure red cell aplasia (PRCA) and 2 individuals who were diagnosed by means of screening of first-degree relatives of previously confirmed cases. Although these 2 subjects were asymptomatic at the time of diagnosis, both had a symptom history suggestive of DADA2, including manifestations such as skin vasculitis (*n* = 2) and central retinal artery occlusion (*n* = 1).

Biallelic mutations in *ADA2* were confirmed by sequencing of DNA from the 22 patients who submitted a blood sample. The remaining patients were diagnosed based on findings of near-absent *ADA2* activity in the plasma (Figure 1A). The demographic characteristics and clinical manifestations of the cohort are summarized in Table 1. Distinct from the typical childhood-onset pattern of DADA2 established by previous studies (median age at onset 4 years), 16 (48%) of 33 subjects in this cohort had disease onset during adulthood (age at onset >16 years), and the

Table 1. Demographic and clinical features of the study patients*

Clinical feature	Overall (<i>n</i> = 33)	Childhood-onset DADA2 (<i>n</i> = 17)	Adult-onset DADA2 (<i>n</i> = 16)	<i>P</i> †
Age at onset, median (range) years	15 (1–37)	8 (1–15)	25.5 (16–37)	–
Age at diagnosis, median (range) years	23 (1–51)	16 (1–46)	32.5 (16–51)	–
Time to diagnosis, median (range) months	52 (1–454)	101 (1–454)	33 (1–290)	0.241
Male, no. (%)	23 (69.7)	11 (64.7)	12 (75)	0.708
Skin involvement, no. (%)	24 (72.7)	12 (70.6)	12 (75)	1.0
Neurologic involvement, no. (%)	26 (78.8)	14 (82.4)	12 (75)	0.688
CNS involvement, no. (%)	22 (66.7)	13 (76.5)	9 (56.3)	0.282
Stroke	18 (54.5)	9 (52.9)	9 (56.3)	
Ischemic	9 (27.3)	5 (29.4)	4 (25)	
Hemorrhagic	4 (12.1)	2 (11.8)	2 (12.5)	
Both	5 (15.2)	2 (11.8)	3 (18.8)	
PNS involvement, no. (%)	13 (39.4)	6 (35.3)	7 (43.8)	0.728
Constitutional symptoms, no. (%)	18 (54.6)	12 (70.6)	6 (37.5)	0.037
Gastrointestinal involvement, no. (%)	15 (45.5)	10 (58.8)	5 (31.3)	0.166
Renal involvement, no. (%)	16 (48.5)	9 (52.9)	7 (43.8)	0.732
Hematologic involvement, no. (%)	10 (30.3)	8 (47.1)	2 (12.5)	0.031
Anemia	9 (27.3)	7 (41.2)	2 (12.5)	
Leukopenia	1 (3)	1 (5.9)	0 (0)	
Other manifestations, no./total assessed (%)				
Arthritis/arthralgia	10 (30.3)	6 (35.3)	4 (25)	0.465
Ocular involvement	6 (18.2)	5 (29.4)	1 (6.3)	0.085
Central retinal artery occlusion	4 (12.1)	3 (17.7)	1 (6.3)	0.601
Loss of peripheral pulses	3 (9.1)	2 (11.8)	1 (6.3)	1.0
Testicular pain‡	4/23 (17.4)	2/11 (18.2)	2/12 (16.7)	–
Pregnancy loss‡	2/10 (20)	NA	2/4 (50)	–
Laboratory abnormality, no./total assessed (%)§				
Elevated ESR	21/28 (75)	10/16 (62.5)	11/12 (91.7)	0.184
Elevated CRP	20/22 (90.5)	10/12 (83.3)	10/10 (100)	0.476
Positive for ANAs or ANCAs¶	3/26 (11.5)	1/15 (6.7)	2/11 (18.2)	0.556

* DADA2 = deficiency of adenosine deaminase 2; CNS = central nervous system; PNS = peripheral nervous system; NA = not applicable; ESR = erythrocyte sedimentation rate; CRP = C-reactive protein.

† Comparison between childhood-onset and adult-onset groups.

‡ Percentage is calculated only in the affected sex.

§ Among patients with results available.

¶ Antinuclear antibodies (ANAs) were tested in 26 patients, and antineutrophil cytoplasmic antibodies (ANCAs) were tested in 22 patients.

overall median age at onset was 15 years (Figure 1B). The median time to diagnosis from initial presentation was 52 months.

A multiple linear regression analysis was performed to predict the time to diagnosis of DADA2 in a model including sex, age at disease onset, constitutional symptoms, involvement of the central nervous system (CNS), peripheral nervous system, gastrointestinal tract system, renal system, skin, and joints, and presence of stroke and mesenteric ischemia. None of these variables was predictive of a delay in diagnosis among these patients (Supplementary Table 3, available on the *Arthritis & Rheumatology* website at <http://onlinelibrary.wiley.com/doi/10.1002/art.41500/abstract>).

Clinical features of patients with DADA2. Vasculitis that mimics polyarteritis nodosa (PAN) was the predominant phenotype in our cohort. The nervous system and skin were the most commonly involved organs, affecting 79% and 73% of patients, respectively (Table 1). More than one-half of the patient cohort had experienced at least one ischemic or hemorrhagic stroke. Constitutional symptoms were noted in 55% of patients. Other common organ-specific manifestations included those affecting the renal system (49%), gastrointestinal tract (46%), and joints (30%). Testicular pain was present in 17% of male patients, and pregnancy loss was noted in 2 of 10 female patients.

Figures 1C–F illustrate the protean clinical manifestations of DADA2 observed in the study patients, including small bowel obstruction, end-organ infarction, and visceral vessel aneurysms. Rare manifestations that have not been previously described in DADA2 and that were observed in our cohort, each found in 1 patient, included pancreatic infarct (Figure 1D), diffuse alveolar hemorrhage with respiratory failure (Figure 1G), and focal myocarditis with bradycardia (results not shown). Supplementary Table 1 (<http://onlinelibrary.wiley.com/doi/10.1002/art.41500/abstract>) provides further details on the major clinical manifestations of individual patients in our cohort.

Laboratory studies revealed anemia in 27% of patients, and leukopenia was noted in 1 subject. Hypogammaglobulinemia was not found in this cohort. Most patients had an elevated erythrocyte sedimentation rate (median 49 mm/hour, range 10–155 mm/hour) and elevated C-reactive protein level (median 42 mg/liter, range 0.39–140 mg/liter).

The frequencies of most of the DADA2 clinical features were similar between childhood-onset and adult-onset cases (Table 1). Univariate analyses showed that fewer patients with adult-onset DADA2 had constitutional symptoms (38% versus 71% of patients with childhood-onset DADA2; $P = 0.037$) and hematologic manifestations (12% versus 47% of patients with childhood-onset DADA2; $P = 0.031$).

The features of the disease in our patients were compared with those in published cohorts of patients with DADA2 and patients with PAN (see Supplementary Table 4, available on the *Arthritis & Rheumatology* website at <http://onlinelibrary.wiley.com/doi/10.1002/art.41500/abstract>). Overall, the

clinical features of our cohort resembled the described manifestations of DADA2, with only mild differences between adult and pediatric cases. CNS involvement appears to be a major distinguishing feature between DADA2 and PAN in adults. Whereas 56% of patients with adult-onset DADA2 in our cohort experienced at least one stroke, <5% of 384 patients with adult-onset PAN exhibited stroke or other CNS involvement in a previous study (19).

Radiographic and histopathologic results. CT scanning or MRI of the brain was performed in 22 patients, and abnormal findings were noted in all but 2 patients. Nine of the patients had only ischemic infarcts, 2 had only intracranial haemorrhage, and 5 exhibited both of these findings (concurrently in 2 cases and as separate events in 3 patients). Three cases displayed aneurysms of cerebral vessels (Figure 2A), and 1 showed meningeal enhancement and multiple hyperintensities on MRI suggestive of posterior reversible encephalitis syndrome (PRES) (Figure 2B). All patients except 1 underwent abdominal ultrasonography ($n = 28$) and/or abdominal CT ($n = 23$). Eight patients had renal infarcts (representative results from 1 patient in Figure 1C) and 1 patient had renal, splenic, and pancreatic infarcts (Figure 1D). Perinephric hematoma was noted in 2 patients. Hepatomegaly, splenomegaly, and fatty infiltration of the liver were noted in 3 patients each. Mesenteric lymphadenopathy was noted in 1 patient. Features of mesenteric ischemia were noted in 4 patients, and 1 patient had ascites. None of the patients had hepatic infarcts, focal nodular hyperplasia of the liver, or features of portal hypertension. Vascular aneurysms affecting various branches of the abdominal aorta were found in 9 patients (representative results from 2 patients in Figures 1E and F). Peripheral arterial narrowing or occlusion was noted in 3 patients (representative results from 1 patient in Figure 2C).

In total, 23 tissue biopsy samples were obtained from 20 patients. Overall, vasculitis of the small or medium vessels was noted in 16 patients (70%) and vasculopathy in 2 patients (9%). Among the 12 skin biopsy samples obtained, vasculitis was noted in 9 samples, whereas livedoid vasculopathy, septal panniculitis, and acne vulgaris were noted in 1 sample each. Among 5 intestinal biopsy samples, 2 showed vasculitis, whereas active ileitis was evident in 1 sample and ischemic enteritis in another sample. Gastrointestinal ulcerations were noted in 2 patients (representative results in Figure 2D). Four nerve biopsy samples were obtained, and all revealed evidence of vasculitis. A temporal artery biopsy sample from 1 patient showed active vasculitis, whereas a testicular biopsy sample from 1 male patient was inconclusive. Figures 2E and F show the presence of vasculitis and acute inflammation in the colonic biopsy sample from a patient with mesenteric ischemia. Taken together, these findings suggest that DADA2 is a mimic of PAN in adults as well as children.

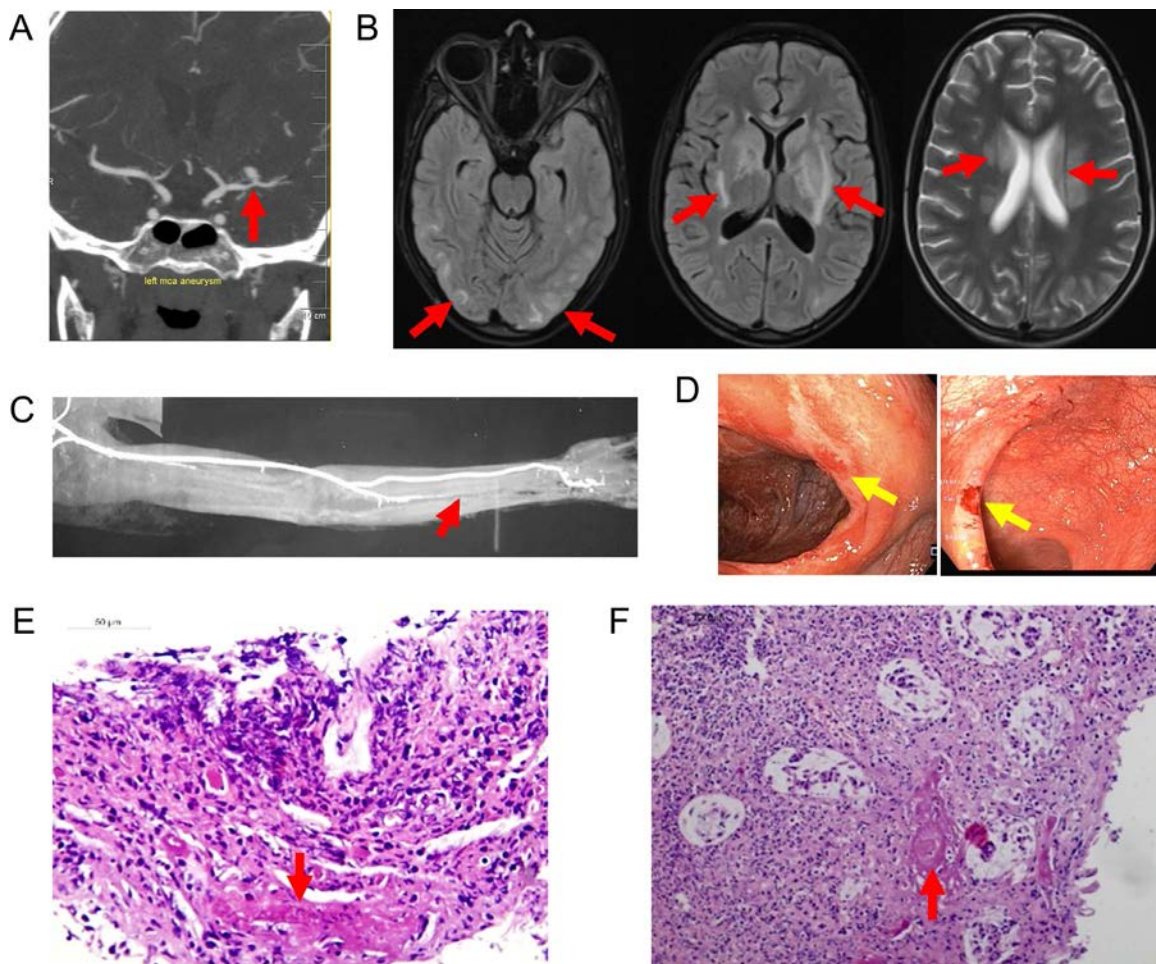


Figure 2. Radiographic and biopsy findings of end-organ damage in patients with DADA2. **A**, CT angiography of the intracerebral vessels in a 14-year-old male subject showing aneurysm (arrow) in the left middle cerebral artery (mca). **B**, Magnetic resonance imaging of the brain of a 17-year-old female subject showing areas of enhancement (arrows) in the bilateral parietal subcortical white matter (left), bilateral basal ganglia, internal and external capsules (middle), and centrum semiovale (right). **C**, CT angiography of the left upper limb of a 35-year-old female subject showing marked attenuation (arrow) of the distal half of the left ulnar artery. **D**, Endoscopy image of ulcers in the cecum (arrow, left) and rectum (arrow, right) of a 17-year-old female subject with gastrointestinal involvement. **E** and **F**, Images of hematoxylin and eosin-stained biopsy tissue (original magnification $\times 40$) from a 17-year-old female subject with mesenteric ischemia showing acute ulcer with fibrinoid necrosis of the arteriolar wall (arrow) with neutrophil debris indicating arteritis (**E**), and mucosal injury with moderate chronic inflammation in the lamina propria (arrow) along with acute vasculitis with thrombosis (**F**). See Figure 1 for other definitions.

ADA-2 activity and ADA2 gene mutations. Plasma ADA-2 activity was assessed in 20 patients, and all exhibited near-absent levels that were significantly lower than the levels found in carriers with 1 mutation (Figure 3A). Among the 22 patients with available data from genetic analyses, 16 patients were homozygous and 6 were compound heterozygous for pathogenic mutations in ADA2. Ten different ADA2 mutations were identified (Figure 3B), including 8 missense mutations and 2 splice-site mutations (see Supplementary Table 5, available on the *Arthritis & Rheumatology* website at <http://onlinelibrary.wiley.com/doi/10.1002/art.41500/abstract>). Most of these variants have been described previously (5–7,15,20–22). The p.G47R variant was the most common allele in this cohort, found in 18 of 22 patients. In a subgroup analysis of patients with genetic testing, there was

no difference in the clinical features or outcomes between patients with homozygous p.G47R alleles and patients with other mutations (data not shown). There was no difference in the clinical manifestations and treatment outcomes in patients with confirmed ADA2 mutations as compared to those who did not have available genetic data. There was also no statistically significant difference in the rate of genetic testing between adults and children. One patient possessed 2 novel variants, p.H112Y and p.G321A, which affect the same amino acid residues as those affected by the previously identified pathogenic variants p.H112Q and p.G321E (5,23). The p.H112Y variant was predicted to disrupt zinc ion coordination within the ADA2 structure, whereas p.G321A induced clashes with adjacent amino acids, as determined by structural modeling (Figure 3C). As confirmation of the

pathogenicity of the *ADA2* mutations in this cohort, in vitro expression of the missense variants in 293T cells showed detectable protein expression but reduced *ADA2* enzymatic activity in the supernatant (Figures 3D and E).

ADA2 mutations with residual enzymatic function (>3%) are associated with the vasculitis phenotype, whereas null mutations are found in patients with severe hematologic manifestations of DADA2 (14). A similar correlation was noted in our cohort, as 19 of 22 patients with a genetic diagnosis of DADA2 possessed at least one hypomorphic allele (G47R or L188V) with residual activity of >3% (Supplementary Tables 1 and 5 [http://onlinelibrary.wiley.com/doi/10.1002/art.41500/abstract]). Insertions/deletions with frameshift and nonsense mutations associated with hematologic compromise were not found in our patients.

Treatment and outcomes. Before the diagnosis of DADA2, most patients were treated with high-dose glucocorticoids (76% orally and 46% intravenously) (Figure 4A). In total, 70% of patients received one or more immunosuppressive agents, with the more common choices being cyclophosphamide (42%), azathioprine (24%), mycophenolate (21%), and methotrexate (18%). Five patients received aspirin, and 4 were given rituximab. The overall efficacy of these interventions was suboptimal, as the disease course in most patients appeared to be glucocorticoid-dependent, and many patients continued to have either persistent disease or relapse.

TNFi are widely considered the treatment of choice for the vasculitis/inflammatory phenotype of DADA2 (6,9,13). Once

the diagnosis of DADA2 was established, 25 patients in our cohort (76%) were started on a regimen of TNFi after ruling out the presence of tuberculosis infection. The fraction of patients who required treatment with glucocorticoids was reduced by about one-half, and most patients also discontinued the use of other immunosuppressive medications (Figure 4A). The initial choice of TNFi included adalimumab (n = 14), etanercept (n = 10), and infliximab (n = 1). One patient received all 3 agents sequentially, as well as golimumab. With the exclusion of this patient, the frequency of treatment with biosimilar TNFi was 75% (18 patients), whereas innovator products were given to 6 patients (25%).

In the TNFi-treated group, 1 patient died during the first admission when the diagnosis was established. She had severe intestinal vasculitis at baseline that was resistant to high-dose glucocorticoids and cyclophosphamide. Her gastrointestinal symptoms improved transiently after starting adalimumab, but the patient succumbed to sepsis 3 weeks later.

Three patients discontinued TNFi treatment. One patient discontinued treatment after 6 months, as she developed active pulmonary tuberculosis without evidence of active features of DADA2 at her last follow-up visit. Two patients discontinued TNFi after 3 months due to financial constraints. One of these patients initially responded well to adalimumab, but died due to gastrointestinal bleeding 4 months after discontinuing treatment, and the second patient had coronary artery disease requiring coronary angioplasty and stenting.

All 8 patients in the non-TNFi group were offered treatment with TNFi, but all refused. Two of these patients had no features

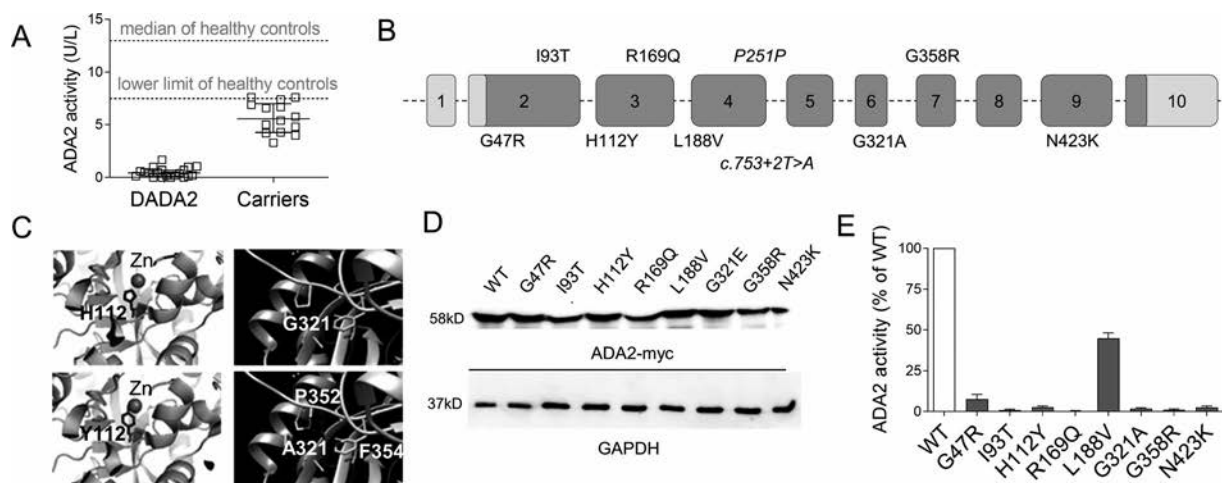


Figure 3. Confirmation of DADA2 by enzyme activity and genetic studies. **A**, Comparison of plasma ADA-2 activity between patients (n = 20) and carriers with monoallelic mutation (n = 8), using an established spectrophotometric assay. Horizontal lines with bars show the median with interquartile range. The median value and lower limit of normal in healthy controls (broken lines) was determined from >200 healthy individuals. **B**, Listing of mutations according to their exon location. **C**, Structural modeling illustrating disruption of zinc ion (Zn) coordination by the p.H112Y variant (left) and clashes with nearby amino acids (within 5 angstroms) induced by the p.G321A variant (right). **D**, Western blot analysis of cell lysates from 293T cells transfected with wild-type (WT) or mutant ADA-2 constructs. Top, Detection of ADA-2 using antibodies to Myc tag. Bottom, GAPDH loading control. **E**, Spectrophotometric quantification of ADA-2 activity in the medium of transfected 293T cells. Bars show the mean \pm SD from 3 independent experiments. See Figure 1 for other definitions.

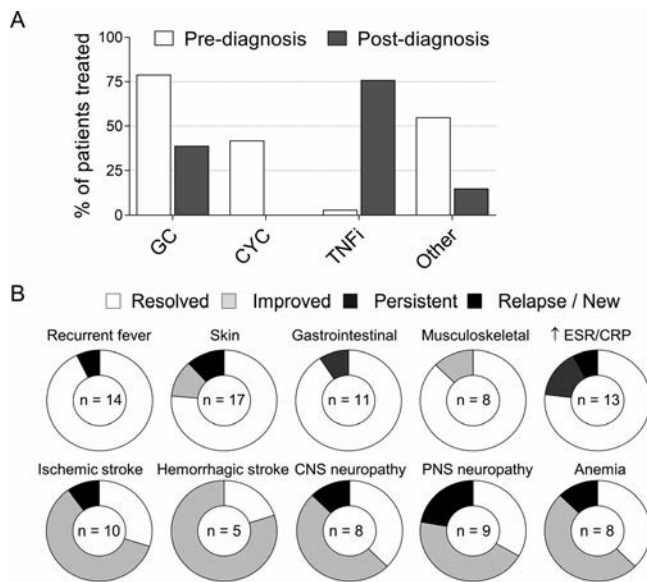


Figure 4. Therapeutic approaches and response to tumor necrosis factor inhibitors (TNFi) in patients with deficiency of adenosine deaminase 2 (DADA2). **A**, Medication usage in patients before and after confirmed diagnosis of DADA2. **B**, Quantification of treatment responses in 21 patients maintained on a regimen of TNFi. Other drugs included azathioprine, cyclosporin A, intravenous immunoglobulin, methotrexate, mycophenolate mofetil, rituximab, sulfasalazine, and thalidomide. GC = glucocorticoids; CYC = cyclophosphamide; ESR = erythrocyte sedimentation rate; CRP = C-reactive protein; CNS = central nervous system; PNS = peripheral nervous system.

of active disease, 2 had relapsing disease but could not afford treatment, 3 were in remission with other treatment regimens, and 1 was lost to follow-up.

Among the remaining 21 patients who continued to receive TNFi (11 with childhood-onset DADA2, 10 with adult-onset DADA2), clinical remission was achieved in 19 patients. The response of various organ manifestations to TNFi is shown in Figure 4B. All 10 categories of DADA2 features captured in our study either resolved or improved in most patients after treatment, with no notable differences 1) between adult and pediatric patients, 2) between the choices of TNFi, or 3) between innovator products and biosimilars. Notably, these 21 patients had a combined total of 22 ischemic or hemorrhagic stroke events prior to anti-TNF therapy, while 1 event to date occurred since the initiation of treatment.

Persistent or relapsing disease and new manifestations were noted in 2 patients. One patient had a relapse of cutaneous vasculitis and experienced new-onset foot drop while receiving biweekly adalimumab. These findings improved after adalimumab dosing was escalated to once weekly. The second patient developed recurrent strokes, relapsing cutaneous vasculitis, and neuropathy despite receiving treatment with multiple TNFi, including etanercept, adalimumab, golimumab, and infliximab. She had multiple relapses while receiving these medications, and her clinical course was further complicated by brief treatment cessation in the setting of active tuberculosis. Taken together, these data demonstrate

the overall efficacy of TNFi for manifestations of vasculitis in both adults and children with DADA2. Cases of relapsing disease and treatment discontinuation also highlight the challenge of treating this complex syndrome.

DISCUSSION

In this report, we describe the clinical characteristics, genetic findings, and treatment responses in 33 subjects with confirmed DADA2. This is the first case series on DADA2 from India. Our study demonstrates that onset of DADA2 is not restricted to young children, and highlights the need for health care providers to also recognize this monogenic syndrome in adults. Given the wide age range of disease onset, we suggest that DADA2 should also be considered in adult patients with PAN. Early diagnosis by sequencing or ADA-2 activity assay followed by initiation of anti-TNF treatment can significantly improve the morbidity of this potentially fatal disease.

DADA2 was first recognized as a monogenic syndrome of early-onset stroke and systemic vasculitis that mimics PAN (5,6). Subsequent studies have noted that about one-quarter of childhood PAN cases are due to DADA2 (9). The most striking difference between our patients and published cohorts is the age at disease onset (see Supplementary Table 4 [<http://onlinelibrary.wiley.com/doi/10.1002/art.41500/abstract>]). In a recent review of 161 patients with DADA2, 77% of patients had disease onset before the age of 10 years (24). Only a few adult cases have been described in the past and some had childhood disease onset with delayed diagnosis (6,12,25). In contrast, more than two-thirds of subjects in our cohort exhibited disease onset after age 10 years, and about one-third presented after age 20 years. The oldest subject in our cohort presented at age 37 years, with hemorrhagic stroke and skin ulcers. What triggers disease onset in DADA2 is not clear and some individuals with biallelic pathogenic variants can remain asymptomatic well into adulthood (6,12). Our cohort had a slight preponderance of male subjects, with 69% of the subjects being male, whereas the previous study had an equal sex distribution, as expected for an autosomal recessive disease (24). This discrepancy might reflect the health care-seeking behavior in our country.

Most of our patients exhibited features of PAN, and the frequency of various manifestations is within the range described in previous series (5–11). The clinical features are mostly comparable between childhood-onset and adult-onset cases, except for mild differences in the prevalence of constitutional symptoms and anemia. The findings of diffuse alveolar hemorrhage, pancreatic infarct, focal myocarditis, and PRES-like encephalopathy further expand the broad clinical spectrum of DADA2. A hallmark that distinguishes DADA2 from PAN is the prevalence of CNS disease. More than 50% of our patients had at least one episode of ischemic stroke or brain hemorrhage, compared to <5% with CNS involvement in classic PAN (19). Cytopenias and hypogammaglobulinemia are

also suggested to be additional features occurring frequently in DADA2 (5,26,27), although these features were generally absent in our patients, possibly due to referral bias, environmental differences, and/or additional genetic modifiers.

Severe hematologic manifestations associated with DADA2, such as neutropenia, pancytopenia, immune-mediated thrombocytopenia, and lymphoproliferative disorders, were not seen in our patients. This is consistent with the genotype–phenotype correlation recently described in DADA2: missense mutations with residual enzymatic activity (>3%) align with the vasculitis phenotype whereas variants with minimal residual function, including nonsense mutations and insertion/deletion mutations, are associated with severe hematologic compromise (14). Consistent with this view, 1 child in our cohort developed early-onset PRCA and was found to have homozygous G358R mutations, a variant that displays minimal residual enzymatic activity and was previously described in patients with PRCA and bone marrow failure syndrome (14,21).

Our understanding of the pathophysiology of DADA2 remains incomplete, as the function of ADA-2 awaits further clarification. To date, more than 80 pathogenic variants have been linked to DADA2 (24,28). The most common pathogenic variant in our cohort was p.G47R. The p.G47R variant is uncommon in the general population (minor allele frequency of 1×10^{-4} in the gnomAD database) but was found in ~1 of 10 individuals in the Georgian-Jewish community in Israel (6,29). Another interesting point noted in our cohort was the clustering of patients in the Agarwal/Jain community, with most of these patients carrying the p.G47R variant. This is an endogamous community, and genetic diseases like limb-girdle muscular dystrophy type 2A, megalencephalic leukodystrophy with cysts, and hereditary fructose intolerance have been reported in this community (30–33).

Even in the absence of randomized controlled trials, TNFi have emerged as the drug of choice for the treatment of DADA2 (6,9). A recent study by Ombrello and colleagues revealed a drastic reduction in stroke risk after initiation of TNFi (13). Based on this experience, we recommended initiation of TNFi in symptomatic patients immediately after the diagnosis of DADA2. We quantified the effects of TNFi on various disease manifestations and found remarkable improvement in all of the measured parameters. The use of glucocorticoids was reduced and treatment with other immunosuppressant agents, including cyclophosphamide and rituximab, was no longer necessary.

Our experience showed that biosimilar TNFi are effective for DADA2, although no direct comparison with innovator molecules is available. While clinical improvement was seen in most cases, dose escalation of adalimumab was required for disease control in 1 case, and another patient had relapsing disease despite trials with multiple TNFi. On the other hand, our data also illustrate the challenges of long-term TNFi therapy. Two patients developed active tuberculosis during treatment, and 1 died from overwhelming sepsis. In addition, several patients were either not able to

start a TNFi or discontinued treatment due to financial limitations. One patient experienced a relapse a few months after treatment cessation and succumbed to severe gastrointestinal hemorrhage.

The main limitation of our study is the retrospective nature of the study. Another limitation is the variability in diagnostic methods without complete information on ADA2 mutations and ADA-2 enzyme activity for all patients in our cohort. This could be attributed to logistic limitations at the different centers involved in the study. In addition, referral bias could have contributed to the paucity of hematologic and immunologic defects in our cohort, as all patients were recruited from rheumatology centers.

In this case series from India, we have described the clinical features, genetic findings, and treatment outcomes in patients with DADA2. We have shown that disease onset during adulthood is common, and that the clinical presentation may occur as late as the fourth decade of life. Rapid diagnosis and treatment with TNFi are important for a successful outcome.

ACKNOWLEDGMENTS

We thank the patients and volunteers for their participation. We thank N. Ganson and S. Kelly for providing assistance with developing the spectrophotometric assay for quantitation of ADA-2 activity, and H. Jee for technical assistance. We thank the DADA2 Foundation for providing a framework to connect patients, physicians, and researchers around the world.

AUTHOR CONTRIBUTIONS

All authors were involved in drafting the article or revising it critically for important intellectual content, and all authors approved the final version to be published. Dr. Aman Sharma had full access to all of the data in the study and takes responsibility for the integrity of the data and the accuracy of the data analysis.

Study conception and design. Aman Sharma, Naidu, Jain, Lee.

Acquisition of data. Aman Sharma, Naidu, Vikas Sharma, Jha, Dhooria, Dhir, Bhatia, Vishal Sharma, Bhattad, Chengappa, V. Gupta, Misra, Chavan, Malaviya, Dudam, Banwari Sharma, Kumar, Bhojwani, P. Gupta, Kusum Sharma, Singhal, Rathi, Nada, Minz, Chaturvedi, Aggarwal, Handa, Grossi, Gattorno, Huang, Wang, Jois, Negi, Khubchandani, Jain, Arostegui, Chambers, Hershfield, Aksentijevich, Zhou, Lee.




Analysis and interpretation of data. Aman Sharma, Naidu, Misra, Agarwal, Chambers, Zhou, Lee.

REFERENCES

1. Kaljas Y, Liu C, Skaldin M, Wu C, Zhou Q, Lu Y, et al. Human adenosine deaminases ADA1 and ADA2 bind to different subsets of immune cells. *Cell Mol Life Sci* 2017;74:555–70.
2. Zavialov AV, Engström A. Human ADA2 belongs to a new family of growth factors with adenosine deaminase activity. *Biochem J* 2005;391:51–7.
3. Zavialov AV, Gracia E, Glaichenhaus N, Franco R, Zavialov AV, Lauvau G. Human adenosine deaminase 2 induces differentiation of monocytes into macrophages and stimulates proliferation of T helper cells and macrophages. *J Leukoc Biol* 2010;88:279–90.
4. Riaz MA, Brinkman-Mills P, Nguyen T, Pan H, Phan S, Ying F, et al. The human homolog of insect-derived growth factor, CECR1, is a candidate gene for features of cat eye syndrome. *Genomics* 2000;64:277–85.

5. Zhou Q, Yang D, Ombrello AK, Zavialov AV, Toro C, Zavialov AV, et al. Early-onset stroke and vasculopathy associated with mutations in ADA2. *N Engl J Med* 2014;370:911–20.
6. Elkan PN, Pierce SB, Segel R, Walsh T, Barash J, Padeh S, et al. Mutant adenosine deaminase 2 in a polyarteritis nodosa vasculopathy. *N Engl J Med* 2014;370:921–31.
7. Nanthapaisal S, Murphy C, Omoyinmi E, Hong Y, Standing A, Berg S, et al. Deficiency of adenosine deaminase type 2: a description of phenotype and genotype in fifteen cases. *Arthritis Rheumatol* 2016;68:2314–22.
8. Batu ED, Karadag O, Taskiran EZ, Kalyoncu U, Aksentijevich I, Alikasifoglu M, et al. A case series of adenosine deaminase 2-deficient patients emphasizing treatment and genotype-phenotype correlations [letter]. *J Rheumatol* 2015;42:1532–4.
9. Caorsi R, Penco F, Grossi A, Insalaco A, Omenetti A, Alessio M, et al. ADA2 deficiency (DADA2) as an unrecognized cause of early onset polyarteritis nodosa and stroke: a multicentre national study. *Ann Rheum Dis* 2017;76:1648–56.
10. Sahin S, Adrovic A, Barut K, Ugurlu S, Turanli ET, Ozdogan H, et al. Clinical, imaging and genotypical features of three deceased and five surviving cases with ADA2 deficiency. *Rheumatol Int* 2018;38:129–36.
11. Gibson KM, Morishita KA, Dancey P, Moorehead P, Drogemoller B, Han X, et al. Identification of novel adenosine deaminase 2 gene variants and varied clinical phenotype in pediatric vasculitis. *Arthritis Rheumatol* 2019;71:1747–55.
12. Trotta L, Martelius T, Siitonen T, Hautala T, Hamalainen S, Juntti H, et al. ADA2 deficiency: clonal lymphoproliferation in a subset of patients [letter]. *J Allergy Clin Immunol* 2018;141:1534–7.
13. Ombrello AK, Qin J, Hoffmann PM, Kumar P, Stone D, Jones A, et al. Treatment strategies for deficiency of adenosine deaminase 2 [letter]. *N Engl J Med* 2019;380:582–4.
14. Lee PY, Kellner ES, Huang Y, Furutani E, Huang Z, Bainter W, et al. Genotype and functional correlates of disease phenotype in deficiency of adenosine deaminase 2 (DADA2). *J Allergy Clin Immunol* 2020;145:1664–72.
15. Sharma A, Naidu GSRSNK, Chattopadhyay A, Acharya N, Jha S, Jain S. Novel CECR1 gene mutations causing deficiency of adenosine deaminase 2, mimicking antiphospholipid syndrome. *Rheumatology (Oxford)* 2019;58:181–2.
16. Ben-Ami T, Revel-Vilk S, Brooks R, Shaag A, Hershfield M, Kelly SJ, et al. Extending the clinical phenotype of adenosine deaminase 2 deficiency. *J Pediatr* 2016;177:316–20.
17. Lee PY, Huang Y, Zhou Q, Schnappauf O, Hershfield M, Li Y, et al. Disrupted N-linked glycosylation as a disease mechanism in deficiency of ADA2. *J Allergy Clin Immunol* 2018;142:1363–5.
18. Pettersen EF, Goddard TD, Huang CC, Couch GS, Greenblatt DM, Meng EC, et al. UCSF Chimera: a visualization system for exploratory research and analysis. *J Comput Chem* 2004;25:1605–12.
19. Pagnoux C, Seror R, Henegar C, Mahr A, Cohen P, Guern VL, et al. Clinical features and outcomes in 348 patients with polyarteritis nodosa: a systematic retrospective study of patients diagnosed between 1963 and 2005 and entered into the French Vasculitis Study Group Database. *Arthritis Rheum* 2010;62:616–26.
20. Rama M, Duflos C, Melki I, Bessis D, Bonhomme A, Martin H, et al. A decision tree for the genetic diagnosis of deficiency of adenosine deaminase 2 (DADA2): a French reference centres experience. *Eur J Hum Genet* 2018;26:960–71.
21. Hashem H, Kumar AR, Müller I, Babor F, Bredius R, Dalal J, et al. Hematopoietic stem cell transplantation rescues the hematological, immunological, and vascular phenotype in DADA2. *Blood* 2017;130:2682–8.
22. Santiago TM, Zavialov A, Saarela J, Seppanen M, Reed AM, Abraham RS, et al. Dermatologic features of ADA2 deficiency in cutaneous polyarteritis nodosa. *JAMA Dermatol* 2015;151:1230–4.
23. Cipe FE, Aydogmus C, Serwas NK, Keskindemirci G, Boztug K. Novel mutation in CECR1 leads to deficiency of ADA2 with associated neutropenia. *J Clin Immunol* 2018;38:273–7.
24. Meyts I, Aksentijevich I. Deficiency of adenosine deaminase 2 (DADA2): updates on the phenotype, genetics, pathogenesis and treatment. *J Clin Immunol* 2018;38:569–78.
25. Springer JM, Gierer SA, Jiang H, Kleiner D, Deutch N, Ombrello AK, et al. Deficiency of adenosine deaminase 2 in adult siblings: many years of a misdiagnosed disease with severe consequences. *Front Immunol* 2018;9:1361.
26. Ozen S, Batu ED, Taskiran EZ, Ozkara HA, Unal S, Guleray N, et al. A monogenic disease with a variety of phenotypes: deficiency of adenosine deaminase 2. *J Rheumatol* 2020;47:117–25.
27. Schepp J, Proietti M, Frede N, Buchta M, Hübscher K, Restrepo JR, et al. Screening of 181 patients with antibody deficiency for deficiency of adenosine deaminase 2 sheds new light on the disease in adulthood. *Arthritis Rheumatol* 2017;69:1689–700.
28. Huang Z, Li T, Nigrovic PA, Lee PY. Polyarteritis nodosa and deficiency of adenosine deaminase 2: shared genealogy, generations apart [review]. *Clin Immunol* 2020;215:108411.
29. Karczewski KJ, Francioli LC, Tiao G, Cummings BB, Alfoldi J, Wang Q, et al. The mutational constraint spectrum quantified from variation in 141,456 humans. *Nature* 2020;581:434–43.
30. Khadilkar SV, Chaudhari CR, Dastur RS, Gaitonde PS, Yadav JG. Limb-girdle muscular dystrophy in the Agarwals: utility of founder mutations in CAPN3 gene. *Ann Indian Acad Neurol* 2016;19:108–11.
31. Ankala A, Kohn JN, Dastur R, Gaitonde P, Khadilkar SV, Hegde MR. Ancestral founder mutations in calpain-3 in the Indian Agarwal community: historical, clinical, and molecular perspective. *Muscle Nerve* 2013;47:931–7.
32. Gorospe JR, Singhal BS, Kainu T, Wu F, Stephan D, Trent J, et al. Indian Agarwal megalencephalic leukodystrophy with cysts is caused by a common MLC1 mutation. *Neurology* 2004;62:878–82.
33. Bijarnia-Mahay S, Movva S, Gupta N, Sharma D, Puri RD, Kotecha U, et al. Molecular diagnosis of hereditary fructose intolerance: founder mutation in a community from India. *JIMD Rep* 2015;19:85–93.

Temporal Arteritis Revealing Antineutrophil Cytoplasmic Antibody–Associated Vasculitides: A Case–Control Study

Laure Delaval,¹  Maxime Samson,² Flora Schein,³ Christian Agard,⁴ Ludovic Tréfond,⁵ Alban Deroux,⁶ Henry Dupuy,⁷ Cyril Garrouste,⁵ Pascal Godmer,⁸ Cédric Landron,⁹ François Maurier,¹⁰ Guillaume le Guenno,⁵ Virginie Rieu,⁵ Julien Desblache,¹¹ Cécile-Audrey Durel,¹²  Laurence Jousselein-Mahr,¹³ Hassan Kassem,¹⁴ Grégory Pugnet,¹⁵ Vivane Queyrel,¹⁶ Laure Swiader,¹⁷ Daniel Blockmans,¹⁸  Karim Sacré,¹⁹  Estibaliz Lazaro,⁷ Luc Mouthon,²⁰ Olivier Aumaître,⁵ Pascal Cathébras,³ Loic Guillevin,²⁰ and Benjamin Terrier,²⁰  on behalf of the French Vasculitis Study Group and French Study Group for Giant Cell Arteritis

Objective. Temporal arteritis (TA) is a typical manifestation of giant cell arteritis (GCA). Antineutrophil cytoplasmic antibody (ANCA)–associated vasculitides (AAVs) are rarely revealed by TA manifestations, leading to a risk of misdiagnosis of GCA and inappropriate treatments. This study was undertaken to describe the clinical, biologic, and histologic presentations and outcomes in cases of TA revealing AAV (TA-AAV) compared to controls with classic GCA.

Methods. In this retrospective case–control study, the characteristics of patients with TA-AAV were compared to those of control subjects with classic GCA. Log-rank test, with hazard ratios (HRs) and 95% confidence intervals (95% CIs), was used to assess the risk of treatment failure.

Results. Fifty patients with TA-AAV (median age 70 years) were included. Thirty-three patients (66%) presented with atypical symptoms of GCA (ear, nose, and throat involvement in 32% of patients, and renal, pulmonary, and neurologic involvement in 26%, 20%, and 16% of patients, respectively). Blood samples were screened for ANCAs at the time of disease onset in 33 patients, and results were positive in 88%, leading to a diagnosis of early TA-AAV in 20 patients. The diagnosis of AAV was delayed a median interval of 15 months in 30 patients. Compared to controls with GCA, patients with TA-AAV were younger (median age 70 years versus 74 years), were more frequently men (48% versus 30%), and had high frequencies of atypical manifestations and higher C-reactive protein levels (median 10.8 mg/dl versus 7.0 mg/dl). In patients with TA-AAV, temporal artery biopsy (TAB) showed fibrinoid necrosis and small branch vasculitis in 23% of patients each, whereas neither of these characteristics was evident in controls with GCA. Treatment failure–free survival was comparable between early TA-AAV cases and GCA controls, whereas those with delayed TA-AAV had a significantly higher risk of treatment failure compared to controls (HR 3.85, 95% CI 1.97–7.51; $P < 0.0001$).

Conclusion. TA-AAV should be considered diagnostically in cases of atypical manifestations of GCA, refractoriness to glucocorticoid treatment, or early relapse. Analysis of TAB specimens for the detection of small branch vasculitis and/or fibrinoid necrosis could be useful. Detection of ANCAs should be performed in cases of suspected GCA with atypical clinical features and/or evidence of temporal artery abnormalities on TAB.

¹Laure Delaval, MD: Centre de Référence des Maladies Auto-Immunes Systémiques Rares d'Ile-de-France, Hôpital Cochin, Paris, France; ²Maxime Samson, MD, PhD: Centre Hospitalier Universitaire (CHU) de Dijon Bourgogne, Dijon, France; ³Flora Schein, MD, Pascal Cathébras, MD: Hôpital Nord, Saint-Étienne, France; ⁴Christian Agard, MD, PhD: CHU de Nantes, Nantes, France; ⁵Ludovic Tréfond, MD, Cyril Garrouste, MD, Guillaume le Guenno, MD, Virginie Rieu, MD, Olivier Aumaître, MD, PhD: CHU de Clermont-Ferrand, Clermont-Ferrand, France; ⁶Alban Deroux, MD: CHU de Grenoble Alpes, Grenoble, France; ⁷Henry Dupuy, MD, Estibaliz Lazaro, MD, PhD: Hôpital Haut-Lévêque, Pessac, France; ⁸Pascal Godmer, MD: Centre Hospitalier Bretagne Atlantique, Vannes, France; ⁹Cédric Landron, MD: CHU de Poitiers, Poitiers, France; ¹⁰François Maurier, MD: Hôpitaux Privés de Metz, Metz, France; ¹¹Julien Desblache, MD: Centre Hospitalier de Pau, Pau, France; ¹²Cécile-Audrey Durel, MD: Hôpital Edouard Herriot and Hospices Civiles de Lyon, Lyon, France; ¹³Laurence Jousselein-Mahr, MD: Hôpital St. Antoine, AP-HP, Paris, France; ¹⁴Hassan

Kassem, MD: Centre Hospitalier Sud Essonne Dourdan-Etampes, Dourdan, France; ¹⁵Grégory Pugnet, MD, PhD: CHU de Toulouse, Toulouse, France; ¹⁶Vivane Queyrel, MD: Hôpital Pasteur 2, Nice, France; ¹⁷Laure Swiader, MD: CHU de Marseille, Hôpital de la Timone, Marseille, France; ¹⁸Daniel Blockmans, MD, PhD: University Hospital Gasthuisberg, Leuven, Belgium; ¹⁹Karim Sacré, MD, PhD: Hôpital Bichat-Claude Bernard, AP-HP, Paris, France; ²⁰Luc Mouthon, MD, PhD, Loic Guillevin, MD, PhD, Benjamin Terrier, MD, PhD: Centre de Référence des Maladies Auto-Immunes Systémiques Rares d'Ile-de-France, Hôpital Cochin, and Université Paris Descartes, Paris, France.

No potential conflicts of interest relevant to this article were reported.

Address correspondence to Benjamin Terrier, MD, PhD, Hôpital Cochin, Department of Internal Medicine, 27 Rue du Faubourg St. Jacques, 75679 Paris Cedex 14, France. Email: benjamin.terrier@aphp.fr.

Submitted for publication August 22, 2019; accepted in revised form August 20, 2020.

INTRODUCTION

The 2012 International Chapel Hill Consensus Conference classified vasculitis according to several defining characteristics, including the size of the affected vessels (1). Giant cell arteritis (GCA), whose onset usually occurs in individuals after age 50 years, is the most frequent non-necrotizing granulomatous vasculitis involving large vessels (2). In contrast, antineutrophil cytoplasmic antibody (ANCA)-associated vasculitides (AAVs) are a group of necrotizing vasculitides that predominantly affect small vessels (i.e., the capillaries, venules, arterioles, and small arteries) and that are associated with the presence of myeloperoxidase (MPO) or proteinase 3 (PR3) ANCA (1,3).

Temporal artery biopsy (TAB) is a technique that is frequently performed for the diagnosis of GCA, with results showing temporal artery abnormalities in 50–80% of cases (4,5). However, in a study of 354 patients with positive findings on TAB, the diagnosis of AAV was retained in 3 cases (0.8%) (6). G n reau et al reported that systemic necrotizing vasculitis was diagnosed on the basis of TAB findings in 1.4% of patients with suspected GCA, and on the basis of inflammation of the temporal artery in 4.5% of TAB specimens (7). Likewise, rare reports have described AAVs that were revealed by manifestations of temporal arteritis (TA-AAV), including granulomatosis with polyangiitis (GPA) (8–10), microscopic polyangiitis (MPA) (11–13), and eosinophilic granulomatosis with polyangiitis (EGPA) (14–16). Nevertheless, the therapeutic management strategy and prognosis may strongly differ between GCA and AAVs, thereby supporting the notion that these diseases should not be misdiagnosed.

In the present study, we aimed to describe the clinical, biologic, and histologic presentations and outcomes in patients with TA-AAV, and performed a case–control study to identify features suggestive of AAV in the setting of TA manifestations, especially cephalic manifestations.

PATIENTS AND METHODS

Patients. We conducted a French nationwide, retrospective multicenter study that included patients who had been seen in several departments of internal medicine and rheumatology in France (19 sites) and Belgium (1 site) from January 2000 to February 2017. The study was supported by the French Vasculitis Study Group and French Study Group for Large Vessel Vasculitis. Patients whose initial clinical presentation was suggestive of TA, i.e., abnormal TAB findings and/or cephalic manifestations, but whose final diagnosis was an AAV were included (designated TA-AAV). Patients whose TAB findings revealed no abnormalities were included if they had cephalic symptoms suggestive of TA (i.e., headache, scalp tenderness, and/or jaw claudication) and had signs and symptoms fulfilling the American College of Rheumatology (ACR) 1990 criteria for GCA (2). Patients were diagnosed as having an AAV if they fulfilled the ACR 1990 criteria for the classification of vasculitis (3) and/or the European Medicines

Agency algorithm (17) and/or the definitions from the 2012 Chapel Hill Consensus Conference (1) for GPA, MPA, or EGPA. This study was conducted in compliance with the Good Clinical Practice protocol and the principles of the Declaration of Helsinki. The study was approved by a local ethics committee, and the requirement for informed consent was waived by the committee.

Clinical, laboratory, morphologic, and pathologic assessments. For each patient, clinical, biologic, and pathologic data were retrospectively collected from the time of diagnosis of TA, throughout the diagnosis of AAV, and up until the last follow-up. Clinical and biologic assessments included evaluation of clinical manifestations, serum C-reactive protein (CRP) levels, blood cell counts, ANCA titers and specificity (against PR3 or MPO), TAB findings, and treatment characteristics.

Response to therapy and outcome. The patients' response to therapy was evaluated by physicians in charge of the patients during the routine follow-up, and the treatment response data were retrospectively reviewed. Remission was defined as the absence of clinical and morphologic manifestations attributable to active disease and normalization of acute-phase reactant levels.

Control group. TA-AAV cases were compared to controls, comprising patients with TA, i.e., patients with GCA fulfilling the ACR 1990 criteria for GCA (2), who were without any evidence of an AAV. Controls were randomly selected from the GCA databases of 2 French vasculitis centers (Cochin Hospital and Dijon University Hospital), with a distribution ratio of 1 case for every 2 controls. We compared the clinical, biologic, and histologic features of all subjects at the time of diagnosis of TA.

Statistical analysis. Data are presented as the mean \pm SD or median with interquartile range (IQR), as appropriate, for continuous variables, and as the frequency (expressed as a percentage) for qualitative variables. Quantitative variables were compared using Student's *t*-test or the nonparametric Mann-Whitney test, and categorical variables were compared using the chi-square test or Fisher's exact test. Kaplan-Meier curves were plotted to describe the treatment failure-free survival rate, and the log-rank test, with hazard ratios (HRs) and 95% confidence intervals (95% CIs), was used to compare the curves. All analyses were performed using SAS software, version 9.4 and GraphPad Prism version 5.0. All statistical tests were 2-sided, and the significance of differences was set at *P* values less than or equal to 0.05.

RESULTS

Clinical, biologic, and pathologic characteristics of TA-AAV cases that were suggestive of TA at initial presentation. Fifty patients with TA-AAV (24 men and 26 women; median age 70 years [IQR 64–75 years]) were included.

The clinical, biologic, and pathologic characteristics observed in the TA-AAV cases are summarized in Table 1. Clinical manifestations at baseline included cephalic symptoms in 44 patients (88%), constitutional symptoms in 42 (84%), polymyalgia rheumatica in 15 (30%), cough in 15 (30%), and visual manifestations in 6 (12%) (i.e., visual loss and diplopia in 3 patients each). All patients with TA-AAV who did not have cephalic symptoms had temporal artery inflammation detectable on TAB. Conversely, all patients without a positive TAB finding had cephalic symptoms highly suggestive of TA, and this was associated with constitutional symptoms and increased acute-phase reactant levels in 70%. Thirty-three patients (66%) presented initially with symptoms atypical of classic GCA, including ear, nose, and throat (ENT) involvement in 16 (32%), renal involvement (renal failure, proteinuria, and/or

hematuria) in 13 (26%), lung involvement (nodules, intraalveolar hemorrhage, or consolidation) in 10 (20%), peripheral neuropathy in 9 (18%), abdominal pain and cutaneous manifestations in 5 (10%) each, episcleritis in 2, and cardiac involvement in 3 (i.e., 1 patient with myocardial infarction and 2 patients with pericarditis). At the time of initial presentation, 17 patients with atypical features were considered to have TA-AAV, along with 3 patients who had classic cephalic symptoms but were positive for ANCA. Overall, 20 patients were classified as having early TA-AAV. For the remaining 30 patients, the diagnosis of TA-AAV was delayed, whereas atypical features were present in 16 patients since baseline.

ANCA were screened in blood samples from 33 patients (66%) at the time of initial presentation, and 29 patients (88%) were found to be positive for ANCA (targeting MPO in 62%

Table 1. Baseline clinical, biologic, and pathologic features of the patients with TA-AAV compared to controls with GCA*

	TA-AAV cases			GCA controls (n = 100)	P†	
	All (n = 50)	Early diagnosis (n = 20)	Delayed diagnosis (n = 30)		Early diagnosis vs. controls	Delayed diagnosis vs. controls
Demographics						
Age, median (IQR) years	70 (64–75)	66.5 (63–71)	71.5 (65–78)	74 (66–82)	0.008	0.22
Female	26 (52)	9 (45)	17 (57)	70 (70)	0.04	0.19
Clinical manifestations						
Constitutional symptoms	42 (84)	18 (90)	24 (80)	82 (82)	0.52	0.79
Asthenia	39 (78)	16 (80)	23 (77)	79 (79)	1.00	0.80
Fever	27 (54)	11 (55)	16 (53)	45 (45)	0.47	0.53
Weight loss	23 (46)	10 (50)	13 (43)	55 (55)	0.81	0.30
Night sweats	11 (22)	6 (30)	5 (17)	21 (21)	0.39	0.80
Cephalic symptoms	44 (88)	17 (85)	27 (90)	97 (97)	0.06	0.14
Headache	34 (68)	12 (60)	22 (73)	82 (82)	0.04	0.30
Jaw claudication	22 (44)	7 (35)	15 (50)	33 (33)	1.00	0.13
Scalp tenderness	22 (44)	9 (45)	13 (43)	45 (45)	1.00	1.00
No temporal pulse	8 (16)	3 (15)	5 (17)	17 (17)	1.00	1.00
Lung involvement	10 (20)	6 (30)	4 (13)	0 (0)	<0.0001	0.002
Visual manifestation	6 (12)	0 (0)	6 (20)	23 (23)	0.01	0.80
Episcleritis	2 (4)	2 (10)	0	1 (1)	0.01	1.00
Polymyalgia rheumatica	15 (30)	5 (25)	10 (33)	32 (32)	0.11	1.00
Peripheral arthralgias	17 (34)	7 (35)	10 (33)	15 (15)	0.05	0.03
Renal involvement	13 (26)	8 (40)	5 (17)	0 (0)	<0.0001	0.0005
ENT involvement	16 (32)	10 (50)	6 (20)	0 (0)	<0.0001	<0.0001
Peripheral neuropathy	9 (18)	6 (30)	3 (10)	0 (0)	<0.0001	0.01
Cutaneous lesions	5 (10)	3 (15)	2 (7)	0 (0)	0.004	0.05
GI involvement	5 (10)	3 (15)	2 (7)	3 (3)	0.06	0.33
Cardiac involvement	3 (6)	2 (10)	1 (3)	2 (2)	0.13	0.55
CNS involvement	2 (4)	1 (5)	1 (3)	3 (3)	0.52	1.00
Pachymeningitis	1 (2)	1 (5)	0	0 (0)	0.17	1.00
CRP, median (IQR) mg/dl	10.8 (6.5–16.4)	13.9 (8.3–17)	9.8 (6–15.2)	7.0 (4.4–12.6)	0.02	0.46
Abnormalities on TAB‡						
Mononuclear cell infiltrates	22 (71)	6 (55)	16 (80)	44 (79)	0.13	1.00
Granulomatous inflammation	4 (13)	0 (0)	4 (20)	21 (38)	0.01	0.18
Disruption of the internal elastic lamina	14 (45)	4 (36)	10 (50)	36 (64)	0.10	0.30
Giant cells	9 (29)	1 (9)	8 (40)	31 (55)	0.007	0.30
Small branch vasculitis	7 (23)	3 (27)	4 (20)	0 (0)	0.003	0.004
Fibrinoid necrosis	7 (23)	3 (27)	4 (20)	0 (0)	0.003	0.004

* Except where indicated otherwise, values are the number (%) of the patients or the number of patients/total number assessed (%). IQR = interquartile range; ENT = ear, nose, and throat; GI = gastrointestinal; CNS = central nervous system; CRP = C-reactive protein.

† By Fisher's exact test.

‡ Temporal artery biopsy (TAB) was performed in 42 of 50 patients with temporal arteritis revealing antineutrophil cytoplasmic antibody-associated vasculitis (TA-AAV) and in 94 of 100 controls with giant cell arteritis (GCA).

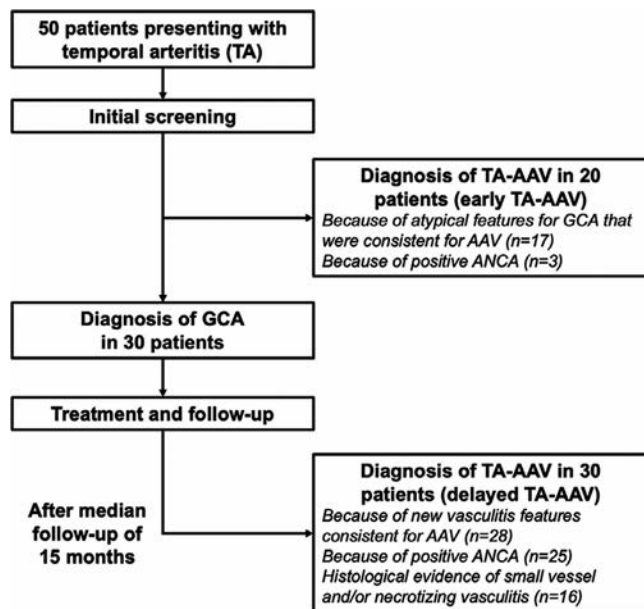


Figure 1. Flow chart of study distribution of patients with temporal arteritis revealing antineutrophil cytoplasmic antibody (ANCA)-associated vasculitis (TA-AAV). GCA = giant cell arteritis.

and targeting PR3 in 38%). Based on these findings, 20 patients were diagnosed as having early TA-AAV, while 9 patients were still diagnosed as having GCA because of the absence of symptoms suggestive of AAV (Figure 1). Abnormal TAB findings, i.e., presence of inflammatory infiltrates, were observed in 31 (74%) of 42 patients, and among these patients, the TAB findings revealed, a posteriori, some features atypical of GCA in 13 patients (42%), i.e., fibrinoid necrosis (Figure 2) and small branch vasculitis (Figure 3) in 7 patients (23%) each.

Characteristics of TA-AAV cases at diagnosis of AAV.

Diagnosis of TA-AAV was made at the time of initial presentation in 20 patients (40%) (designated early TA-AAV), and during follow-up after a median time of 15 months (IQR 9–46 months) in 30 patients (60%) (designated delayed TA-AAV). Among those with delayed TA-AAV, the diagnosis was made because of refractory disease in 13 patients (43%) or after vasculitis relapse in 17 patients (57%). Twenty-six patients (87%) were receiving treatment with glucocorticoids at a median dose of 22.5 mg/day (IQR 7–36 mg/day). The patients' characteristics at the time of AAV diagnosis are summarized in Table 2.

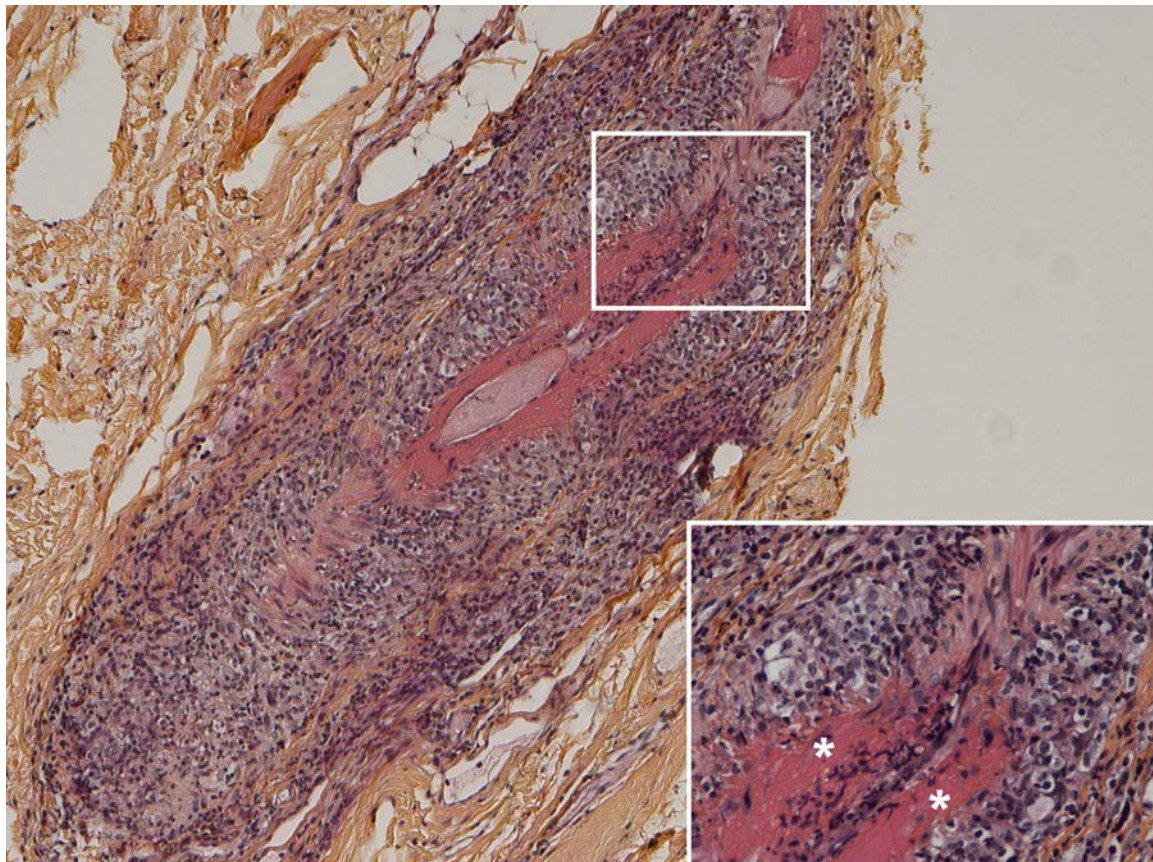


Figure 2. Representative temporal artery biopsy (TAB) specimen from a patient with temporal arteritis revealing antineutrophil cytoplasmic antibody-associated vasculitis, showing fibrinoid necrosis. **Inset** shows a higher-magnification view of the boxed area on the TAB specimen, indicating sites of necrotizing panarteritis with an inflammatory infiltrate rich in macrophages, lymphocytes, epithelioid cells, and some eosinophils in contact with a band of fibrinoid necrosis (**asterisks**) with pycnotic debris. Original magnification $\times 100$; $\times 400$ in **inset**. The image was provided courtesy of Claire Toquet, MD, PhD (Service d'Anatomie et Cytologie Pathologique, Hôtel-Dieu, CHU Nantes, Nantes, France).

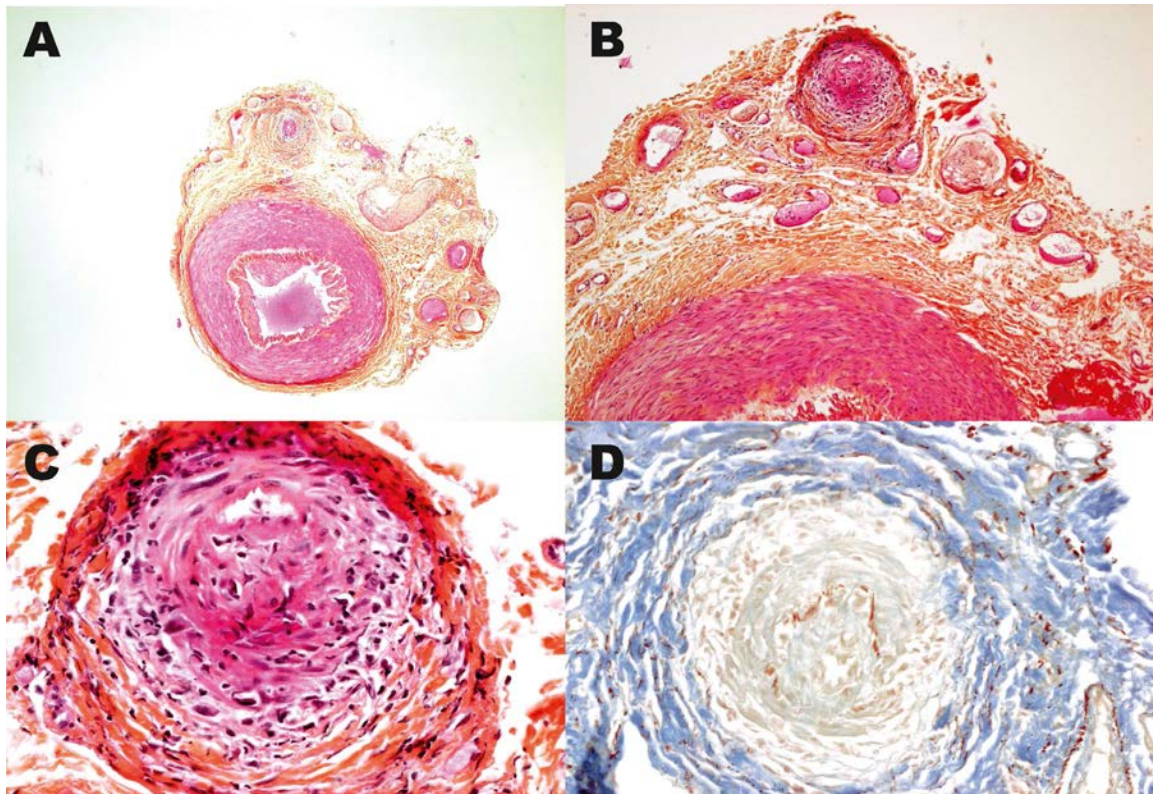


Figure 3. Representative temporal artery biopsy (TAB) specimen from a patient with temporal arteritis revealing antineutrophil cytoplasmic antibody–associated vasculitis, showing small branch vasculitis. Analysis of the TAB specimen reveals the absence of intimal or medial inflammatory infiltrate (**A**), with small branch necrotizing vasculitis evident on hematoxylin–eosin–safran staining (**B** and **C**) and orcein staining (**D**). Original magnification $\times 4$ in **A**; $\times 10$ in **B**; $\times 40$ in **C** and **D**. The images were provided courtesy of Jean-Louis Kemeny, MD, PhD (CHU de Clermont-Ferrand, Clermont-Ferrand, France). Color figure can be viewed in the online issue, which is available at <http://onlinelibrary.wiley.com/doi/10.1002/art.41527/abstract>.

The delayed TA-AAV population presented at baseline with constitutional symptoms in 24 patients (80%) and cephalic symptoms in 27 patients (90%). All 3 patients without cephalic symptoms had temporal artery inflammation evident on TAB. Sixteen (53%) of the 30 patients had symptoms atypical of classic GCA: ENT involvement in 6, renal involvement in 3, lung involvement in 3, peripheral neuropathy in 3, and cutaneous manifestations in 2. Furthermore, additional features developed during the follow-up before AAV had been diagnosed: recurrence of constitutional symptoms in 21 (70%) and cephalic symptoms in 11 (37%), ENT involvement in 14 (47%), lung involvement in 12 (40%), peripheral neuropathy in 12 (40%), renal involvement in 7 (23%), and cutaneous involvement in 7 (23%).

Among the patients with a delayed diagnosis of TA-AAV, the phenotype of the AAV diagnosis was GPA in 67% of patients and MPA in 27% of patients, contrasting with a frequency of ANCA positivity in the delayed diagnosis group of 72% for the MPO-ANCA specificity and 24% for the PR3-ANCA specificity (including 9 patients with GPA and 8 patients with MPA positive for MPO-ANCAs, and 6 patients with GPA positive for PR3-ANCAs). In patients with a delayed diagnosis of AAV, histologic evidence of an AAV was available from a site other than the temporal artery in 10 patients (33%). Four of the 5 patients without ANCAs had

histologic evidence of an AAV, and 1 had a very suggestive clinical presentation (i.e., ENT involvement, purpura, and rapidly progressive glomerulonephritis).

Case-control study of TA-AAV cases versus GCA controls. To identify whether TA-AAV patients exhibited peculiar manifestations at the time of initial presentation as compared to the classic manifestations of TA (i.e., GCA), we performed a case-control study comparing the 50 patients with TA-AAV to the 100 control patients with GCA, and within the TA-AAV group, we distinguished between early TA-AAV ($n = 20$) and delayed TA-AAV ($n = 30$). Comparisons of the characteristics of the patients in these groups are summarized in Table 1. Compared to GCA controls, patients with early TA-AAV were younger and less frequently female. Moreover, fewer patients with an early diagnosis of TA-AAV had headaches or visual manifestations, but more of them had lung involvement, episcleritis, peripheral arthralgias, renal and ENT involvement, peripheral neuropathy, and cutaneous lesions. CRP levels were higher in patients with early TA-AAV compared to GCA controls. Findings from TAB showed that granulomatous inflammation and giant cells were less frequent, and small branch vasculitis and fibrinoid necrosis were more frequent, in patients with early TA-AAV compared to GCA controls.

Characteristics of the patients with a delayed diagnosis of TA-AAV were more comparable to those of the GCA controls at baseline. However, extracephalic symptoms and findings on TAB were also the main differences between patients with delayed TA-AAV and control patients with classic GCA (Table 1). Differences remained the same, except for differences in the distribution of age and sex and frequency of episcleritis, when only those with abnormal TAB findings were compared between the TA-AAV group (n = 31) and GCA control group (n = 54) (data not shown).

Therapeutic management of cases and controls.

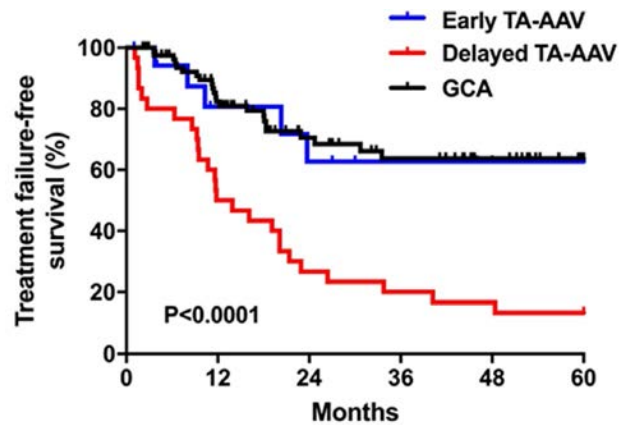
Patients with early TA-AAV were treated with glucocorticoids in all cases, in combination with immunosuppressive agents as first-line therapy in 14 patients (including 10 receiving cyclophosphamide, 2 receiving rituximab, and 2 receiving methotrexate). In contrast, all patients with delayed TA-AAV received glucocorticoids alone, similar to all controls with classic GCA.

Outcomes in cases and controls. To compare the prognosis of TA-AAV compared to GCA, we analyzed treatment failure-free survival rates in patients with TA-AAV and early diagnosis of AAV, patients with delayed diagnosis of TA-AAV, and GCA

Table 2. Characteristics of the patients at the time of diagnosis of AAV*

	Early TA-AAV (n = 20)	Delayed TA-AAV (n = 30)
Delay from TA to AAV diagnosis, median (IQR) months	-	15 (9-46)
Type of AAV		
GPA	11 (55)	20 (67)
MPA	8 (4)	8 (27)
EGPA	1 (5)	2 (7)
Clinical manifestations		
Constitutional symptoms	18 (90)	21 (7)
Cephalic symptoms	17 (85)	11 (37)
ENT involvement	10 (50)	14 (47)
Lung involvement	6 (30)	12 (40)
Ocular manifestations	3 (15)	7 (23)
Peripheral neuropathy	6 (30)	12 (40)
Renal involvement	8 (40)	7 (23)
Cutaneous lesions	3 (15)	7 (23)
Gastrointestinal involvement	3 (15)	2 (7)
Pachymeningitis	1 (5)	3 (10)
C-reactive protein, median (IQR) mg/dl	13.9 (8.3-17)	3.7 (1.9-8.4)
ANCA positive		
All ANCA	19 (95)	25 (83)
MPO-ANCA	10 (53)	18 (72)
PR3-ANCA	9 (47)	6 (24)
Prednisone at AAV diagnosis		
Taking prednisone	-	26 (87)
Dose, median (IQR) mg/day	-	22.5 (7-36)

* Except where indicated otherwise, values are the number (%) of patients. AAV = antineutrophil cytoplasmic antibody (ANCA)-associated vasculitis; TA = temporal arteritis; IQR = interquartile range; GPA = granulomatosis with polyangiitis; MPA = microscopic polyangiitis; EGPA = eosinophilic granulomatosis with polyangiitis; ENT = ear, nose, and throat; MPO = myeloperoxidase; PR3 = proteinase 3.



	P value	Hazard ratio (95% CI)
Early TA-VAA vs. GCA	0.83	1.10 (0.41-2.98)
Delayed TA-VAA vs. GCA	<math>< 0.0001</math>	3.85 (1.97-7.51)

Figure 4. Treatment failure-free survival in patients with early or delayed diagnosis of temporal arteritis revealing antineutrophil cytoplasmic antibody-associated vasculitis (TA-AAV) compared to patients with giant cell arteritis (GCA) as controls. Patients with delayed TA-AAV had a significantly higher risk of treatment failure compared to GCA controls, as indicated by the hazard ratio. 95% CI = 95% confidence interval. Color figure can be viewed in the online issue, which is available at <http://onlinelibrary.wiley.com/doi/10.1002/art.41527/abstract>.

controls. Treatment failure-free survival was comparable between those with early TA-AAV and GCA controls. In contrast, those with delayed TA-AAV had a significantly higher risk of treatment failure compared to GCA controls (HR 3.85, 95% CI 1.97-7.51; $P < 0.0001$) (Figure 4). This latter finding was frequently the reason that the diagnosis of TA-AAV was delayed.

DISCUSSION

In addition to GCA, the manifestations of TA may, on rare occasions, reveal the presence of medium-sized and small-sized vessel vasculitides. The consequences of such a potential misdiagnosis could be detrimental, since therapeutic management and outcomes strongly differ between these diseases. With the aim of attaining an early diagnosis of TA-AAV, we have described herein the clinical presentation and outcomes of TA-AAV in comparison to the typical profile of classic GCA.

Compared to GCA controls, patients with TA-AAV were slightly younger, were more frequently men, had a high frequency of atypical manifestations of large vessel vasculitis, and had higher CRP levels. At the patient level, because of their lack of specificity, demographic differences and higher CRP levels cannot be used to confirm a diagnosis of TA-AAV. On the other hand, two-thirds of TA-AAV patients presented with manifestations atypical of GCA, such as mononeuritis multiplex, lung involvement, ENT

involvement, or renal involvement. These manifestations were commonly underestimated, because cephalic symptoms were at the forefront of the initial presentation, whereas cranial symptoms and headache are not typical of AAVs (18), except in the case of pachymeningitis, which remains a rare manifestation of the disease (10,13). For these reasons, the diagnosis of TA-AAV is more challenging than it looks.

Detection of ANCAs using antigen-specific immunoassays was the most frequent abnormality observed that led to the final diagnosis of TA-AAV. The majority of TA-AAV patients presented with a GPA phenotype, whereas the majority of ANCAs detected were directed against MPO. There is a large variability in the detection of ANCAs with the use of indirect immunofluorescence testing in older patients, which could lead to false-positive findings, contrasting with the high diagnostic performance of immunoassays for PR3-ANCAs and MPO-ANCAs to discriminate AAV from disease controls (19). Recently, a revised international consensus on testing of ANCAs proposed that ANCA measurement should use antigen-specific immunoassays as the primary screening method (20), especially in all patients with suspected GCA, to avoid false-positive and false-negative results.

TAB could be a useful tool in challenging situations. The TAB findings were frequently abnormal in patients with cephalic symptoms, regardless of whether they had a diagnosis of GCA or AAV, suggesting that TAB could be contributive to the diagnosis of systemic vasculitides whatever the underlying diagnosis (7). In some cases, the TAB findings did not reveal temporal artery abnormalities, but all of these patients had cephalic symptoms and a clinical presentation suggestive of GCA. In our study, histologic findings that could be highly suggestive of small vessel vasculitis included the presence of necrotizing vasculitis or small branch vasculitis (21), contrasting with the absence of granulomatous inflammation and/or giant cells, but these abnormalities lacked sensitivity for a diagnosis of TA-AAV. In contrast, neither small branch vasculitis nor fibrinoid necrosis were noted in any TAB specimen from the GCA controls, thus showing that these findings could represent a major red flag when analyzing TAB specimens. Indeed, in a study by Cavazza et al (6), a pattern typical of small vessel vasculitis without ANCA positivity was reported in 9% of patients. Nevertheless, in our study, the patients who were considered as having TA-AAV all met the criteria for AAV and not for other small vessel vasculitides, including immune complex small vessel vasculitis. However, the absence of a centralized review of the TAB findings represents a limitation of our study, which could have led to underestimation of the number of histologic abnormalities consistent with typical characteristics of an AAV. Overall, atypical manifestations and TAB findings in those cases of suspected GCA should alert physicians to the possibility of a diagnosis of TA-AAV, in whom the clinical and therapeutic management would be different.

Based on the initial presentation and follow-up of patients, we could distinguish patients with an early diagnosis of TA-AAV

from those with a delayed diagnosis of TA-AAV. Delayed diagnosis of TA-AAV was made after a median time of 15 months because of the development of refractory disease or a vasculitis relapse, as these patients had been followed up according to the protocol for classic GCA, while those with early diagnosis of TA-AAV had a similar treatment failure-free survival rate as that in patients with GCA. These findings show that the prognosis of TA-AAV is poor when initial treatment is not appropriate, and suggest that TA-AAV should be considered in any cases of GCA with refractoriness to glucocorticoid treatment or early relapse. Such distinction is of major importance, since cyclophosphamide or rituximab would be preferentially used to treat TA-AAV (22,23), whereas tocilizumab or methotrexate would be preferentially considered as second-line therapies in GCA (24–26). To illustrate the diagnostic and therapeutic challenge in patients with a potential diagnosis of TA-AAV or GCA with ANCA positivity, a small study previously analyzed the relevance of ANCAs during GCA, especially to estimate ANCA frequency and its impact on disease outcome. Thirty percent of GCA patients were positive for ANCAs, but the majority had positive results from indirect immunofluorescence without any positive result from antigen-specific immunoassays. Moreover, ANCA positivity seemed predictive of premature disease relapse (mean interval 15.8 months versus 28.5 months in ANCA-negative patients) (27).

Fourteen of the 30 patients whose diagnosis of TA-AAV was delayed did not have any extracranial feature suggestive of AAV at the time of initial presentation. For those patients, close monitoring during follow-up is necessary, and reconsideration of the initial diagnosis should be mentioned in those cases in which a lack of treatment response occurs. Some patients who had features that are atypical for GCA at baseline were still considered as having GCA because of the predominance of cephalic manifestations and temporal artery inflammation on TAB, with a diagnosis of AAV only during follow-up. It is therefore very important to consider any atypical features as red flags for the diagnosis of GCA, and this should immediately raise some concerns leading to discussion of an alternative diagnosis. To help physicians diagnose TA-AAV, we identified some clinical and biologic red flags from our study, including those identified by screening for atypical manifestations and among these patients, screening for ANCAs, as well as careful reading of TAB specimens in all patients with TA. The presence of features that are atypical for GCA should prompt careful consideration of an alternative diagnosis and prompt screening for ANCAs and further careful review of the TAB readings.

Finally, despite its inherent limitations related to the small number of patients studied and its retrospective design, our study represents a large compilation of AAV patients presenting with cephalic manifestations. As a limitation, data from the GCA controls were obtained from 2 French vasculitis centers, and not from any of the centers where the patients with TA-AAV were recruited. Furthermore, controls were not matched to patients by age or sex, but this choice was made voluntarily in this hypothesis of demographic

differences between groups. Moreover, centralized review of the TAB readings was not possible and could represent a limitation of the study because of the difficulty in distinguishing between fibrinoid necrosis and laminar necrosis (6). Given the aim of this study, and since ANCA testing is performed in patients with suspected GCA, we considered it mandatory that patients be ANCA-negative in order to receive a diagnosis of GCA. Lastly, diagnosis of AAV was based on the presence of robust features, especially typical manifestations of AAV, positive findings for PR3- or MPO-ANCAs, and/or histologic evidence of an AAV in a site other than the temporal artery, and 1 of the main outcomes we assessed was the relapse of the disease requiring the initiation of new treatment lines.

In conclusion, TA-AAV should be considered in cases in which the manifestations are atypical of GCA and in cases in which manifestations of GCA are present along with glucocorticoid refractoriness or early relapse. In these cases, TAB could be useful, especially when showing small branch vasculitis and/or fibrinoid necrosis. In addition, detection of ANCAs using antigen-specific immunoassays should be performed in cases of suspected GCA with clinically atypical features and abnormal findings on TAB.

ACKNOWLEDGMENTS

We thank the following colleagues who provided patients for the study: Drs. Emilie Berthoux, Pierre Charles, Pascal Cohen, Antoine Dossier, Mikael Ebbo, Vincent Grobost, Matthieu Groh, Isabelle Guichard, Antoine Néel, and Odile Souchaud. In addition, we thank Dr. Claire Toquet (Service d'Anatomie et Cytologie Pathologique, Hôtel-Dieu, CHU Nantes, Nantes, France) and Dr. Jean-Louis Kemeny (CHU de Clermont-Ferrand, Clermont-Ferrand, France) for providing the illustrations.

AUTHOR CONTRIBUTIONS

All authors were involved in drafting the article or revising it critically for important intellectual content, and all authors approved the final version to be published. Dr. Terrier had full access to all of the data in the study and takes responsibility for the integrity of the data and the accuracy of the data analysis.

Study conception and design. Delaval, Terrier.

Acquisition of data. Delaval, Samson, Schein, Agard, Tréfond, Deroux, Dupuy, Garrouste, Godmer, Landron, Maurier, Le Guenno, Rieu, Desblache, Durel, Jousselin-Mahr, Kasseem, Pugno, Queyrel, Swiader, Blockmans, Sacré, Lazaro, Mouthon, Aumaître, Cathébras, Guillevin, Terrier.

Analysis and interpretation of data. Delaval, Terrier.

REFERENCES

- Jennette JC, Falk RJ, Bacon PA, Basu N, Cid MC, Ferrario F, et al. 2012 revised International Chapel Hill Consensus Conference nomenclature of vasculitides. *Arthritis Rheum* 2013;65:1–11.
- Hunder GG, Bloch DA, Michel BA, Stevens MB, Arend WP, Calabrese LH, et al. The American College of Rheumatology 1990 criteria for the classification of giant cell arteritis. *Arthritis Rheum* 1990;33:1122–8.
- Bloch DA, Michel BA, Hunder GG, McShane DJ, Arend WP, Calabrese LH, et al. The American College of Rheumatology 1990 criteria for the classification of vasculitis: patients and methods. *Arthritis Rheum* 1990;33:1068–73.
- Gonzalez-Gay MA, Garcia-Porrúa C, Llorca J, Gonzalez-Louzao C, Rodriguez-Ledo P. Biopsy-negative giant cell arteritis: clinical spectrum and predictive factors for positive temporal artery biopsy. *Semin Arthritis Rheum* 2001;30:249–56.
- Salvarani C, Cantini F, Hunder GG. Polymyalgia rheumatica and giant-cell arteritis. *Lancet Lond Engl* 2008;372:234–45.
- Cavazza A, Muratore F, Boiardi L, Restuccia G, Pipitone N, Pazzola G, et al. Inflamed temporal artery: histologic findings in 354 biopsies, with clinical correlations. *Am J Surg Pathol* 2014;38:1360–70.
- Généreau T, Lortholary O, Pottier MA, Michon-Pasturel U, Ponge T, de Wazières B, et al. Temporal artery biopsy: a diagnostic tool for systemic necrotizing vasculitis. *Arthritis Rheum* 1999;42:2674–81.
- Vermeulen JP, Mahowald ML. A case of Wegener's granulomatosis presenting with jaw claudication. *J Rheumatol* 1984;11:707–9.
- Garrouste C, Sailler L, Astudillo L, Lavayssière L, Cointault O, Borel C, et al. Fulminant alveolar hemorrhage: evolution of giant cell arteritis to ANCA-positive vasculitis? *Rev Med Interne* 2008;29:232–5. In French.
- McCarthy A, Farrell M, Hedley-Whyte T, McGuone D, Kavanagh E, McNally S, et al. Granulomatosis with polyangiitis masquerading as giant cell arteritis [letter]. *J Neurol* 2013;260:1661–3.
- Fujii K, Tsutsumi T, Takaoka K, Osugi Y, Ando S, Koyama Y. A concomitant case of giant cell arteritis and microscopic polyangiitis with hemoperitoneum by rupture of the gastroepiploic artery. *Mod Rheumatol* 2012;22:934–8.
- Chirinos JA, Tamariz LJ, Lopes G, Carpio FD, Zhang X, Milikowski C, et al. Large vessel involvement in ANCA-associated vasculitides: report of a case and review of the literature. *Clin Rheumatol* 2004;23:152–9.
- Morinaga A, Ono K, Komai K, Yamada M. Microscopic polyangiitis presenting with temporal arteritis and multiple cranial neuropathies. *J Neurol Sci* 2007;256:81–3.
- Endo T, Katsuta Y, Kimura Y, Kikuchi A, Aramaki T, Takano T, et al. A variant form of Churg-Strauss syndrome: initial temporal non-giant cell arteritis followed by asthma. Is this a distinct clinicopathologic entity? *Hum Pathol* 2000;31:1169–71.
- Amato MB, Barbas CS, Delmonte VC, Carvalho CR. Concurrent Churg-Strauss syndrome and temporal arteritis in a young patient with pulmonary nodules. *Am Rev Respir Dis* 1989;139:1539–42.
- Buhaescu I, Williams A, Yood R. Rare manifestations of Churg-Strauss syndrome: coronary artery vasospasm, temporal artery vasculitis, and reversible monocular blindness - a case report. *Clin Rheumatol* 2009;28:231–3.
- Watts R, Lane S, Hanslik T, Hauser T, Hellmich B, Koldingsnes W, et al. Development and validation of a consensus methodology for the classification of the ANCA-associated vasculitides and polyarteritis nodosa for epidemiological studies. *Ann Rheum Dis* 2007;66:222–7.
- Comarmond C, Cacoub P. Granulomatosis with polyangiitis (Wegener): clinical aspects and treatment [review]. *Autoimmun Rev* 2014;13:1121–5.
- Damoiseaux J, Csernok E, Rasmussen N, Moosig F, van Paassen P, Baslund B, et al. Detection of antineutrophil cytoplasmic antibodies (ANCAs): a multicentre European Vasculitis Study Group (EUVAS) evaluation of the value of indirect immunofluorescence (IIF) versus antigen-specific immunoassays. *Ann Rheum Dis* 2017;76:647–53.
- Bossuyt X, Tervaert JW, Arimura Y, Blockmans D, Flores-Suárez LF, Guillevin L, et al. Position paper: revised 2017 international consensus on testing of ANCAs in granulomatosis with polyangiitis and microscopic polyangiitis [review]. *Nat Rev Rheumatol* 2017;13:683–92.
- Lie JT, on behalf of the American College of Rheumatology Subcommittee on Classification of Vasculitis. Illustrated histopathologic classification criteria for selected vasculitis syndromes. *Arthritis Rheum* 1990;33:1074–87.
- Jones RB, Furuta S, Tervaert JW, Hauser T, Luqmani R, Morgan MD, et al. Rituximab versus cyclophosphamide in ANCA-associated

renal vasculitis: 2-year results of a randomised trial. *Ann Rheum Dis* 2015;74:1178–82.

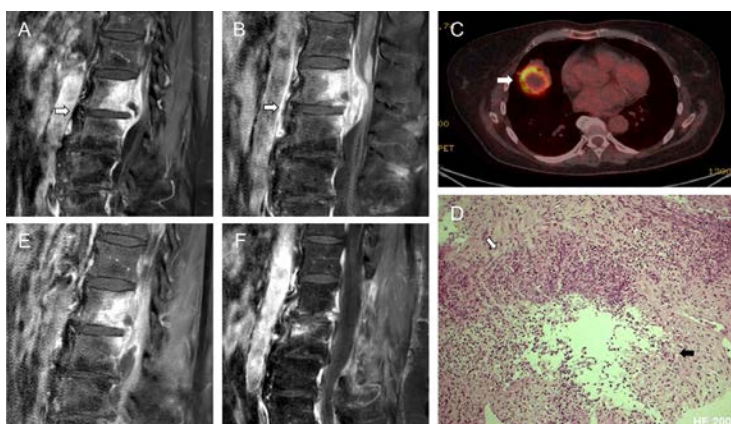
23. Stone JH, Merkel PA, Spiera R, Seo P, Langford CA, Hoffman GS, et al. Rituximab versus cyclophosphamide for ANCA-associated vasculitis. *N Engl J Med* 2010;363:221–32.
24. Stone JH, Tuckwell K, Dimonaco S, Klearman M, Aringer M, Blockmans D, et al. Trial of tocilizumab in giant-cell arteritis. *N Engl J Med* 2017;377:317–28.
25. Villiger PM, Adler S, Kuchen S, Wermelinger F, Dan D, Fiege V, et al. Tocilizumab for induction and maintenance of remission in giant cell

arteritis: a phase 2, randomised, double-blind, placebo-controlled trial. *Lancet Lond Engl* 2016;387:1921–7.

26. Hoffman GS, Cid MC, Hellmann DB, Guillevin L, Stone JH, Schousboe J, et al. A multicenter, randomized, double-blind, placebo-controlled trial of adjuvant methotrexate treatment for giant cell arteritis. *Arthritis Rheum* 2002;46:1309–18.
27. Gil H, Mauny F, Meaux-Ruault N, Magy-Bertrand N, Roncato-Saberan M, Hafsaoui C, et al. Valeur des anticorps anticytoplasme des polynucléaires neutrophiles dans la maladie de Horton. *Rev Med Interne* 2008;29:780–4.

DOI 10.1002/art.41565

Clinical Images: Spondylitis as a rare manifestation of granulomatosis with polyangiitis





The patient, a 62-year old woman who had a known disc herniation in 2005, was admitted to the tertiary care center for lumbar spondylitis (at L2–L3) with epidural involvement seen on magnetic resonance imaging (MRI) (**A**). An infectious cause was suspected, and with empirical antibiotic treatment, clinical and imaging features improved. Three weeks after finishing antibiotic treatment, the patient was readmitted due to increasing pain. MRI showed progressive spondylitis with epidural abscess formation (**B**). Furthermore, the radiologist noted the intact intervertebral L2–L3 disc (**arrows in A and B**), which is considered a typical finding for tuberculous spondylitis (1). Fluorodeoxyglucose–positron emission tomography/computed tomography revealed a cavitating lung lesion (**arrow in C**). Blood, lung, and tissue cultures, polymerase chain reaction, tuberculosis (TB) skin test, and interferon- γ release test results were negative. Tissue biopsy at L2–L3 showed early necrotizing granulomatous inflammation with abundant infiltration of neutrophils (**white arrow in D**) and histiocytes (**black arrow in D**). Based on these findings, TB treatment was preemptively initiated while mycobacterial cultures were still pending. The patient's condition appeared to stabilize, but 3 weeks later she was readmitted with peripheral polyneuropathy, most likely due to tuberculostatic toxicity. Mycobacterial cultures were negative, but caudal compression had worsened (**E**). Additional testing was positive for antineutrophil cytoplasmic antibodies against proteinase 3 (PR3-ANCA) (38 IU/ml [normal <2]). Necrotizing granulomatous inflammation and PR3-ANCA positivity are hallmarks of granulomatosis with polyangiitis (GPA) (2). ANCA positivity can also occur in TB (3), but without any evidence of active TB, GPA was diagnosed. Treatment with methylprednisolone (1,000 mg/day for 3 days), followed by oral prednisone in tapering doses and cyclophosphamide (2–3 mg/kg/day) was initiated; treatment was switched to azathioprine (3 mg/kg/day) after 3 months. Symptoms improved, PR3-ANCA was no longer present, and imaging showed marked improvement with minimal residual radiologic abnormalities of L3 and the L2–L3 disc (**F**). Though extremely rare, this case illustrates that inflammatory spondylitis can be a manifestation of GPA.

We thank Dr. Myrurgia Abdul Hamid for the histopathologic images.

1. De Vuyst D, Vanhoenacker F, Gielen J, Bernaerts A, De Schepper AM. Imaging features of musculoskeletal tuberculosis [review]. *Eur Radiol* 2003;13:1809–19.
2. Jennette JC, Falk RJ, Andrassy K, Bacon PA, Churg J, Gross WL, et al. Nomenclature of systemic vasculitides: proposal of an international consensus conference [review]. *Arthritis Rheum* 1994;37:187–92.
3. Teixeira L, Mahr A, Jauregui F, Noël LH, Nunes H, Lefort A, et al. Low seroprevalence and poor specificity of antineutrophil cytoplasmic antibodies in tuberculosis. *Rheumatology (Oxford)* 2005;44:247–50.

Matthias H. Busch, MD 
 Joop P. Aendekerk, MD 
 Astrid M. L. Oude Lashof, MD, PhD
 Pieter van Paassen, MD, PhD
 Maastricht University Medical Center
 Maastricht, The Netherlands

Hemodynamic Response to Treatment and Outcomes in Pulmonary Hypertension Associated With Interstitial Lung Disease Versus Pulmonary Arterial Hypertension in Systemic Sclerosis: Data From a Study Identifying Prognostic Factors in Pulmonary Hypertension Associated With Interstitial Lung Disease

Louis Chauvelot,¹  Delphine Gamondes,² Julien Berthiller,³ Ana Nieves,⁴ Sébastien Renard,⁵ Judith Catella-Chatron,⁶ Kais Ahmad,¹ Laurent Bertoletti,⁶ Boubou Camara,⁷ Emmanuel Gomez,⁸ David Launay,⁹ David Montani,¹⁰ Jean-François Mornex,¹ Grégoire Prévot,¹¹ Olivier Sanchez,¹² Anne-Marie Schott,⁴ Fabien Subtil,¹³ Julie Traclet,¹ Ségolène Turquier,¹ Sabrina Zeghmar,¹ Gilbert Habib,⁵ Martine Reynaud-Gaubert,⁴ Marc Humbert,¹⁰ Vincent Cottin,¹  The French Network for Pulmonary Arterial Hypertension, and The French Network for Rare Pulmonary Diseases (OrphaLung)

Objective. Patients with systemic sclerosis and both pulmonary hypertension and interstitial lung disease (SSc–PH–ILD) generally carry a worse prognosis than patients with SSc and pulmonary arterial hypertension (SSc–PAH) without ILD. There is no evidence of the efficacy of PAH therapies in SSc–PH–ILD. We undertook this study to compare survival of and response to treatment in patients with SSc–PH–ILD and those with SSc–PAH.

Methods. We analyzed 128 patients (66 with SSc–PH–ILD and 62 with SSc–PAH) from 15 centers, in whom PH was diagnosed by right-sided heart catheterization; they were prospectively included in the PH registry. All patients received PAH-specific therapy. Computed tomography of the chest was used to confirm or exclude ILD.

Results. At baseline, patients with SSc–PH–ILD had less severe hemodynamic impairment than those with SSc–PAH (pulmonary vascular resistance 5.7 Wood units versus 8.7 Wood units; $P = 0.0005$) and lower diffusing capacity for carbon monoxide (median 25% [interquartile range (IQR) 18%, 35%] versus 40% [IQR 31%, 51%]; $P = 0.0005$). Additionally, patients with SSc–PH–ILD had increased mortality (8.1% at 1 year, 21.2% at 2 years, and 41.5% at 3 years) compared to those with SSc–PAH (4.1%, 8.7%, and 21.4%, respectively; $P = 0.04$). Upon treatment with PAH-targeted therapy, no improvement in the 6-minute walk distance was observed in either group. Improvement in the World Health Organization functional class was observed less frequently in patients with SSc–ILD–PH compared to those with SSc–PAH (13.6% versus 33.3%; $P = 0.02$). Hemodynamics improved similarly in both groups.

Conclusion. ILD confers a worse prognosis to SSc–PH. Response to PAH-specific therapy is clinically poor in SSc–PH–ILD but was not found to be hemodynamically different from the response observed in SSc–PAH.

INTRODUCTION

The leading cause of death in systemic sclerosis (SSc) is pulmonary involvement (1), either pulmonary hypertension (PH)

or interstitial lung disease (ILD). Pulmonary arterial hypertension (PAH), or group 1 PH in which the precapillary pulmonary vascular bed is the predominant site of disease (2,3), ultimately leads to right ventricular failure and death. The prevalence of PH in SSc is

¹Louis Chauvelot, MD, Kais Ahmad, MD, Jean-François Mornex, MD, PhD, Julie Traclet, MD, Ségolène Turquier, MD, Sabrina Zeghmar, MS, Vincent Cottin, MD, PhD: Hospices Civils de Lyon, Centre de Référence National des Maladies Pulmonaires Rares, Centre de Compétence de l'Hypertension Pulmonaire, Hôpital Louis Pradel, UMR 754, INRAE, Université Claude Bernard Lyon 1, OrphaLung, RespiFil, and ERN-LUNG, Lyon, France; ²Delphine Gamondes, MD: Hospices Civils de Lyon and Hôpital Louis Pradel, Lyon, France; ³Julien Berthiller, MS: Hospices Civils de Lyon, Université Claude Bernard Lyon 1, and

Health Services and Performance Research (HESPER) EA7425, Lyon, France; ⁴Ana Nieves, MD, Anne-Marie Schott, MD, PhD, Martine Reynaud-Gaubert, MD, PhD: Centre de Compétences des Maladies Pulmonaires Rares and Hôpital Nord, AP-HM, Marseille, France; ⁵Sébastien Renard, MD, Gilbert Habib, MD, PhD: Hôpital de la Timone, AP-HM, Marseille, France; ⁶Judith Catella-Chatron, MD, Laurent Bertoletti, MD, PhD: INSERM U1059 and CHU de Saint-Etienne, Saint-Etienne, France; ⁷Boubou Camara, MD: Clinique Universitaire de Pneumologie and CHU de Grenoble Alpes, Grenoble, France; ⁸Emmanuel

~5% in recent series (4,5), with approximately two-thirds of SSc patients diagnosed as having PAH (SSc-PAH) and one-third diagnosed as having PH-ILD (SSc-PH-ILD). SSc-PAH generally carries a worse prognosis than idiopathic PAH (6–9).

In SSc, PH can be due to several mechanisms: precapillary PH in the setting of isolated PAH, pulmonary venoocclusive disease, chronic lung disease (especially ILD), chronic thromboembolic PH, or postcapillary PH secondary to chronic disease of the left side of the heart (2). Classifying SSc patients into a discrete PH group has therapeutic implications but may be challenging (10) due to overlapping features and lack of a precise definition of group 3 PH.

Clinically significant ILD, present in approximately one-third of SSc patients with SSc (11), is characterized by a predominant pattern of nonspecific interstitial pneumonia and significantly contributes to mortality (12). The extent of ILD present at the time of computed tomography (CT) scan is associated with disease progression and mortality (13). The severity of functional alterations and a decline in serial measurement of forced vital capacity (FVC) are also predictive of a poor outcome (13,14).

ILD and PH may be related in patients with SSc (SSc-PH-ILD). The extent of ILD at the time of CT scan does not seem to be associated with hemodynamic severity of PH (15). However, SSc-PH-ILD may carry a worse prognosis than SSc-PAH (16–19). PH may be present in approximately one-third of patients with SSc-ILD (20).

Although treatment is recommended in SSc-PAH, similar to that for idiopathic PAH (2), data regarding the efficacy of PAH-specific therapies in SSc-PH-ILD patients are scarce. Immunosuppressive therapy used to treat ILD does not affect the outcome of SSc-PH (21). In a retrospective study of 70 patients with SSc-PH-ILD, PAH-specific therapies were not associated with clinical benefit, and prognosis was poor, with only 39% survival at 2 years and 21% at 3 years (22); however, no comparison to PAH was available. According to another study, initiation of prostanoid therapy within 6 months of the diagnosis was associated with improved transplant-free survival (16). In the present study, we compared the survival of and response to PAH therapy in patients with SSc-PH-ILD and those with SSc-PAH.

PATIENTS AND METHODS

Patient population. Data were extracted from the French prospective PH registry, which enrolls PH patients ≥ 18 years old. Among these patients, PH was suspected based on systematic annual screening tests recommended for patients with asymptomatic SSc (2), or based on the presence of dyspnea, fatigue, chest pain, lower limb edema, or syncope/presyncope, and was confirmed by right-sided heart catheterization (RHC). In addition to participating in the PH registry, patients with SSc-PH-ILD (with ILD at baseline CT scan, according to the opinion of the investigators [LC and VC]) were further included in the Pulmonary Hypertension in Interstitial Lung Disease (HYPID) and HYPID-2 consecutive observational studies (ClinicalTrials.gov identifiers: NCT01443598 and NCT02799771, respectively), which aimed to identify prognostic factors in PH associated with ILD. Five of the patients with SSc-PH-ILD have been reported previously (18). Our SSc-PAH group consisted of all consecutive cases with SSc-PAH (group 1) that were included in the French PH registry within the same time period, at 4 large centers.

Informed consent was obtained from all patients in the PH registry and the HYPID and HYPID-2 cohorts. The present study was approved by the institutional review board of the Hospices Civils de Lyon (approved December 6, 2017). The Comité National d'Informatique et Liberté (CNIL), the committee dedicated to privacy, information technology, and civil rights in France, approved the reference methodology MR03 that was used to collect and analyze registry data (approval no. 17-215). The HYPID and HYPID-2 studies were approved by the CNIL and the Comité de Protection des Personnes (approved January 5, 2011) and the institutional review board (approval CEPRO 2016-021).

Inclusion criteria. Patients were included in the present study if they fulfilled all of the following criteria: age ≥ 18 years; diagnosis of SSc according to the American College of Rheumatology/European League Against Rheumatism 2013 criteria (23); precapillary PH demonstrated by RHC, with a mean pulmonary artery pressure (PAP) of ≥ 25 mm Hg, a mean pulmonary vascular resistance (PVR) of >3 Wood units, and a mean pulmonary

Gomez, MD: CHU de Nancy, Vandœuvre-lès-Nancy, France; ⁹David Launay, MD, PhD: Université de Lille, CHU de Lille, and Centre de Référence des Maladies Systémiques et Auto-Immunes Rares, Lille, France; ¹⁰David Montani, MD, PhD, Marc Humbert, MD, PhD: Hôpital Bicêtre, AP-HP, Centre de Référence de l'Hypertension Pulmonaire, INSERM U999, and Université Paris-Saclay, Paris, France; ¹¹Grégoire Prévot, MD: Centre de Compétences des Maladies Pulmonaires Rares, CHU de Toulouse, and Hôpital Larrey, Toulouse, France; ¹²Olivier Sanchez, MD, PhD: Hôpital Européen Georges Pompidou, AP-HP, Centre de Compétences des Maladies Pulmonaires Rares, Université Paris Descartes, INSERM U1140, Paris, France; ¹³Fabien Subtil, MD: Université de Lyon, Université Claude Bernard Lyon 1, CNRS UMR 5558, Villeurbanne, France, and Hospices Civils de Lyon, Lyon, France.

Drs. Reynaud-Gaubert and Humbert contributed equally to this work.

Dr. Montani has received consulting fees, speaking fees, and/or honoraria from Actelion, Bayer, Bristol Myers Squibb, GlaxoSmithKline, MSD, and Pfizer (less than \$10,000 each) and research support from Actelion and Bayer. Dr.

Mornex has received consulting fees, speaking fees, and/or honoraria from Actelion and GlaxoSmithKline (less than \$10,000 each) and research support from Actelion and GlaxoSmithKline. Dr. Humbert has received consulting fees, speaking fees, and/or honoraria from Actelion, Bayer, GlaxoSmithKline, Merck, and United Therapeutics (less than \$10,000 each) and research support from Bayer and GlaxoSmithKline. Dr. Cottin has received consulting fees, speaking fees, and/or honoraria from Actelion, Boehringer Ingelheim, Bayer/MSD, Gilead, GlaxoSmithKline, Novartis, Roche, Promedior, Celgene, and Galápagos (less than \$10,000 each) and research support from Actelion, Boehringer Ingelheim, Roche, and Sanofi. No other disclosures relevant to this article were reported.

Address correspondence to Vincent Cottin, MD, PhD, Centre de Référence National des Maladies Pulmonaires Rares, Service de Pneumologie, Hôpital Louis Pradel, 28 Avenue Doyen Lepine, F-69677 Lyon Cedex, France. Email: vincent.cottin@chu-lyon.fr.

Submitted for publication September 4, 2019; accepted in revised form August 27, 2020.

artery wedge pressure (PAWP) of <15 mm Hg; no evidence of chronic thromboembolic PH; ≥ 1 CT scan of the chest available for review; pulmonary function tests available at baseline; and receipt of ≥ 1 dose of targeted PAH treatment shortly after PH diagnosis. Patients with postcapillary PH or probable pulmonary venoocclusive disease, according to published criteria (24), were excluded. As the French PH registry was designed before the 2018 revision of the PH definition, PH was defined by a mean PAP of ≥ 25 mm Hg rather than by >20 mm Hg.

To ensure that patients were assigned to the correct group (with/without ILD), the most recent chest CT scan that was available was reviewed. If the most recent CT scan showed no evidence of ILD, patients were classified as SSc-PAH. If it showed evidence of ILD, the CT scan obtained at the time of PH diagnosis was reviewed. If ILD was already present in the CT scan at the time of PH diagnosis, patients were classified as SSc-PH-ILD, regardless of physiologic alteration. Otherwise, in instances in which ILD appeared >1 year after the onset of PH, patients were classified as SSc-PAH and censored for survival analysis on the day of ILD diagnosis, defined as the date that the first CT scan showed ILD.

Evaluations. Prospective baseline evaluation included World Health Organization (WHO) functional class assessment, pulmonary function tests, 6-minute walk test, and RHC. Presence of comorbidities was recorded. Chronic kidney disease, defined by a glomerular filtration rate of <60 ml/minute/1.73 m², was recorded as present or absent by the investigators (LC and VC).

All CT scans were reviewed by a pneumologist and a radiologist with expertise in ILD, for the presence of ILD, extent of ILD (13), and classification of the ILD pattern by consensus. This review was not possible for 3 patients because CT images could not be retrieved, although radiologist reports were available and confirmed ILD. Patients were assigned to the SSc-PH-ILD and SSc-PAH groups according to the presence or absence of ILD, respectively (Figure 1).

Follow-up prospective investigations included WHO functional class, 6-minute walk test, long-term supplemental oxygen, and RHC data. The follow-up visit used in the analysis was the first visit to include at least an RHC or a 6-minute walk test within 1 year after beginning PAH-specific treatment.

Statistical analysis. Results are expressed as the mean \pm SD or the median (interquartile range [IQR]) for continuous variables and as numbers with percentages for categorical variables. The hypothesis of normal distribution was verified by Kolmogorov-Smirnov test and, graphically, using a histogram.

Categorical variables were compared using a chi-square test or Fisher's exact test. Continuous variables were compared using Student's *t*-test or the nonparametric Wilcoxon test, depending on the normality of the distribution. Overall survival curves were obtained using the Kaplan-Meier method, and subgroups were

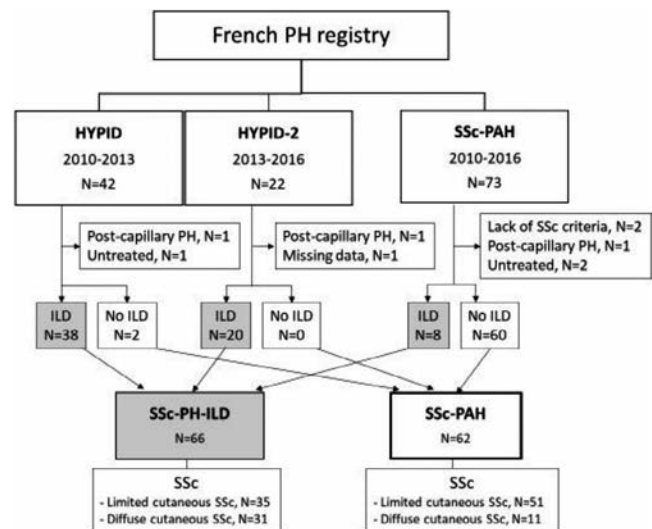


Figure 1. Study population. PH = pulmonary hypertension; HYPID = Pulmonary Hypertension in Interstitial Lung Disease study; SSc-PAH = systemic sclerosis with pulmonary arterial hypertension; ILD = interstitial lung disease.

compared using a log rank test. Overall survival was defined as the difference between date of PH diagnosis and date of death or latest recorded data.

Prognostic factors of overall survival were evaluated with a semiparametric Cox model after verifying the hypothesis of hazard proportionality, first univariable and then multivariable, including the significant factors from univariable analysis and relevant adjustment variables, i.e., age, sex, chronic kidney disease, ILD, and 6-minute walk distance. Longitudinal change in 6-minute walk distance in patients with SSc-PH-ILD and those with SSc-PAH was assessed using a linear mixed effects model, with a linear effect of time, group-by-time interaction, and random intercept and slope.

All statistical tests were bilateral or pairwise when appropriate. *P* values less than 0.05 were considered significant. Hazard ratios (HRs) and 95% confidence intervals (95% CIs) were calculated. For univariable analysis (e.g., Tables 2 and 4), the Bonferroni-Holm correction was applied. Statistical analysis was performed using SAS version 9.4 software.

RESULTS

Study population. One hundred twenty-eight patients were included (Figure 1), with 66 classified in the SSc-PH-ILD group and 62 in the SSc-PAH group. For patients with SSc-PH-ILD, the median time difference between PH diagnosis and the first CT scan was 13 days (IQR 2, 89). Five patients with SSc-PAH without ILD at PH diagnosis were diagnosed as having ILD during follow-up, with a median time between PH diagnosis and ILD diagnosis of 4.1 years (IQR 2.5, 6.1).

The median overall follow-up time was 2.9 years (range 1 month–13.8 years). Four patients with SSc-PH-ILD and

Table 1. Patient characteristics*

	SSc-PAH (n = 62)	SSc-PH-ILD (n = 66)	P
Age, median (IQR) years	71.5 (63, 78)	63.5 (53, 71)	0.0008†
Female	51 (82.3)	41 (62.1)	0.01‡
SSc subtype			0.004‡
Limited	51 (82.3)	35 (53.0)	
Diffuse	11 (17.7)	31 (47.0)	
Autoantibodies			<0.0001§
Anti-Scl-70	0 (0)	27 (40.9)	
Anticentromere	40 (64.5)	9 (13.6)	
Other/unknown	22 (35.5)	30 (45.5)	
6-minute walk test, median (IQR)			
Distance, meters	267.5 (210, 350)	308.5 (237, 350)	0.18
Borg dyspnea score	4 (2, 5)	5 (3, 7)	0.03
SpO ₂ nadir	87 (81, 92)	85 (79, 90)	0.11
SpO ₂ delta	7 (4, 10)	9 (5, 16)	0.02
WHO functional class			0.15§
1–2	24 (39.3)	16 (24.3)	
3	33 (54.1)	42 (63.6)	
4	4 (6.6)	8 (12.1)	
Long-term supplemental oxygen	17 (27.2)	33 (50.0)	0.009‡
Comorbidities			
Arterial hypertension	30 (49.2)	26 (39.4)	0.27‡
Diabetes	5 (8.2)	9 (13.6)	0.33‡
Coronary disease	6 (9.8)	2 (3.0)	0.15§
Chronic kidney disease¶	5 (8.2)	4 (6.1)	0.74§
Obesity#	11 (18.0)	10 (15.2)	0.66‡
Hemodynamics, median (IQR)			
RAP, mm Hg	6 (4, 10)	6 (4, 8)	0.27
Mean PAP, mm Hg	42 (33, 52)	36.5 (30, 42)	0.002
Cardiac index, liter/minute/m ²	2.42 (1.87, 2.96)	2.61 (2.12, 3.07)	0.09
PVR, Wood units	8.70 (5.65, 12.91)	5.70 (4.20, 9.00)	0.0005
PAWP, mm Hg	9 (6, 12)	9 (7, 13)	0.33
Pulmonary function tests			
FVC, % of predicted	100 (84, 116)	68 (57, 81)	<0.0001
FEV ₁ , % of predicted	91 (75, 109)	69 (58, 81)	<0.0001
TLC, % of predicted	92 (83, 102)	67 (58, 74)	<0.0001
DL _{co} , %	40 (31, 51)	25 (18, 35)	0.0005
DL _{co} /VA, %	51 (40, 63)	49 (35, 67)	0.66
Initial PH treatment			0.10
ERA	45 (72.6)**	56 (84.9)††	
PDE5i	9 (14.5)	7 (10.6)	
ERA + PDE5i	7 (11.3)	1 (1.5)	
Prostacyclin analogs	1 (1.6)	2 (3.0)	
Sequential oral combination PH therapy during follow-up	22	15	0.16
ILD treatment at PH diagnosis			NA
None	0	24	
Glucocorticoids alone	0	21	
AZA	0	2	
CYC	66	2	
MMF	0	3	
RTX	0	1	
MMF + CYC	0	3	
CYC + RTX	0	1	
Missing	0	9	

(Continued)

Table 1. (Cont'd)

	SSc-PAH (n = 62)	SSc-PH-ILD (n = 66)	P
Duration of follow-up, median (IQR) years	3.08 (1.03, 6.0)	2.7 (1.2, 5.3)	0.51

* For some categories, data were not available for all 128 patients, as follows: n = 127 for World Health Organization (WHO) functional class, arterial hypertension, diabetes mellitus, coronary disease, chronic kidney disease, obesity, and pulmonary artery wedge pressure (PAWP); n = 126 for cardiac index; n = 125 for pulmonary vascular resistance (PVR) and forced expiratory volume in 1 second (FEV₁); n = 124 for forced vital capacity (FVC); n = 119 for right atrial pressure (RAP); n = 118 for total lung capacity (TLC); n = 114 for 6-minute walk distance; n = 107 for diffusing capacity for carbon monoxide, corrected for alveolar volume (DL_{CO}/VA); n = 103 for Borg dyspnea score and SpO₂ nadir; n = 101 for SpO₂ delta; and n = 84 for DL_{CO}. Except where indicated otherwise, values are the number (%) of patients. SSc-PAH = systemic sclerosis with pulmonary arterial hypertension; SSc-PH-ILD = systemic sclerosis with both pulmonary hypertension and interstitial lung disease; IQR = interquartile range; PAP = pulmonary artery pressure; ERA = endothelin receptor antagonist; PDE5i = phosphodiesterase 5 inhibitor; NA = not applicable; AZA = azathioprine; CYC = cyclophosphamide; MMF = mycophenolate mofetil; RTX = rituximab.

† By Wilcoxon test.

‡ By chi-square test.

§ By Fisher's exact test.

¶ Defined by glomerular filtration rate <60 ml/minute/1.73 m².

Defined by body mass index >30 kg/m².

** Including 8 patients who received ambrisentan and 37 who received bosentan.

†† Including 5 patients who received ambrisentan and 51 who received bosentan.

3 patients with SSc-PAH died before the first follow-up visit. Within one year, 79% of the patients underwent an RHC, and 87% completed a 6-minute walk test.

Baseline characteristics. At baseline, patients with SSc-PH-ILD were more likely to be male, were younger, and more frequently had diffuse cutaneous SSc and anti-Scl-70 antibodies than patients with SSc-PAH (Table 1). Patients with SSc-PAH had more severe PH at the first RHC compared to those with SSc-PH-ILD, with a higher mean PVR and mean PAP, but without significant difference in cardiac index.

Compared to those with SSc-PAH, patients with SSc-PH-ILD had a lower mean FVC, lower diffusing capacity for carbon monoxide (DL_{CO}) (with no difference in DL_{CO} corrected for alveolar volume), and more frequently had supplemental long-term oxygen therapy. Oxygen flow rate did not differ between groups in patients treated with long-term oxygen supplementation (median rate 2 liters/minute). There was no difference between groups in dyspnea at baseline, with ~60% of patients in each group categorized as being in WHO functional class 3. There were also no differences in 6-minute walk distances. First-line PAH-specific therapies were similar in both groups and included endothelin receptor antagonists (80%), phosphodiesterase 5 inhibitors (13%), or a combination of both (6%). Only 3 patients received a prostacyclin analog as initial treatment.

ILD characteristics. Of the 63 CT scans reviewed for patients with SSc-PH-ILD, ILD was extensive in 51 cases (81%) and limited in 12 cases (19%). The most frequent pattern was nonspecific interstitial pneumonia (37%), followed by usual interstitial pneumonia (30%) and undetermined pattern (29%).

Survival. Survival was significantly shorter in patients with SSc-PH-ILD compared to those with SSc-PAH. In SSc-PH-ILD patients, the mortality rates at 1, 2, and 3 years were 8.1%, 21.2%, and 41.5%, respectively, compared to 4.1%, 8.7%, and 21.4% in SSc-PAH patients ($P = 0.04$) (Figure 2).

Among patients with SSc-PH-ILD, immunosuppressive treatment of ILD was associated with a decreased risk of mortality (HR 0.46 [95% CI 0.24–0.89]; $P = 0.02$). Four patients with SSc-PH-ILD underwent lung transplantation after a median time of 3.17 years (IQR 1.85, 4.55), compared to none of the SSc-PAH patients ($P = 0.12$).

In the univariable analysis of the overall population of SSc-PH-ILD and SSc-PAH patients, parameters associated with mortality were chronic kidney disease and lower 6-minute walk distance (Table 2). A nonsignificant trend (with significance set at $P < 0.0025$) toward greater mortality was observed for the presence of ILD, male sex, lower cardiac index, SpO₂, and DL_{CO}. Patients with both ILD of limited extent at the time of CT scan (13) and moderately severe PH (2) had a better prognosis compared to those with either extensive ILD at the time of CT scan and/or severe PH (data not shown).

In the multivariable analysis adjusted for age, sex, and the other significant variables in the univariable analysis, only the presence of ILD, chronic kidney disease, and 6-minute walk distance at baseline were associated with greater mortality (Table 3).

Outcomes of PAH therapy. Upon treatment with PAH-targeted therapy, improvement of WHO functional class (change from class 3–4 to class 1–2) was observed less frequently in patients with SSc-ILD-PH compared to those with SSc-PAH

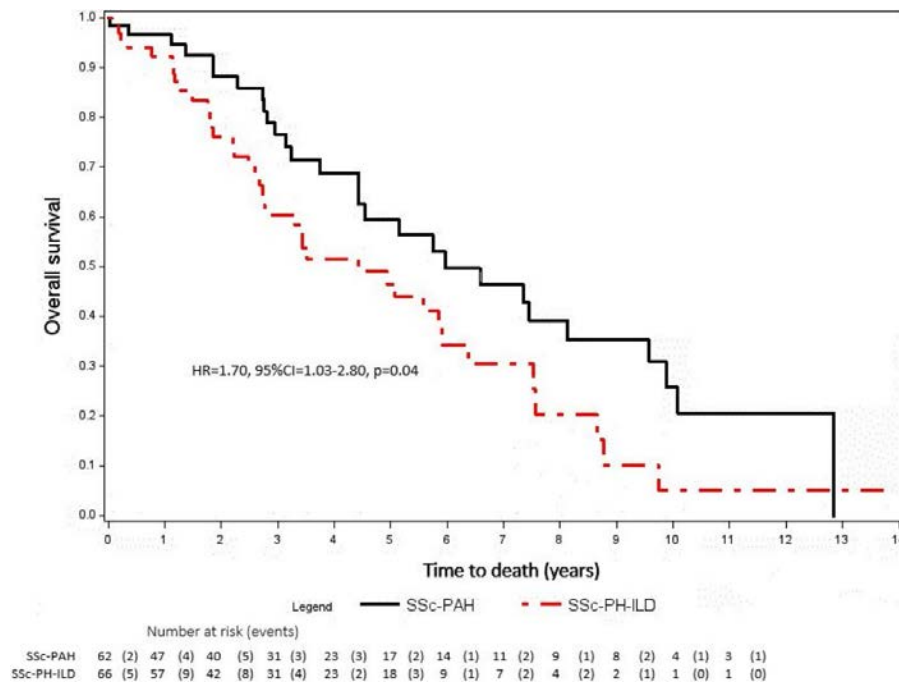


Figure 2. Comparison of survival from PH diagnosis between patients with SSc-PAH and those with SSc-PH-ILD. HR = hazard ratio; 95% CI = 95% confidence interval (see Figure 1 for other definitions).

(13.6% versus 33.3%; $P = 0.02$, not significant after applying the Bonferroni correction) (Table 4). However, upon treatment, there were no significant differences between groups in the variation in hemodynamics, 6-minute walk distance, or proportion of patients who gained >24 meters of 6-minute walk distance (minimal clinically significant difference) (25). Longitudinal change in 6-minute walk distance up to 1 year of follow-up in 115 patients with available data (assessed using linear mixed regression modeling) was not significantly different between groups ($P = 0.48$). No significant difference was found in the number of patients who required initiation of long-term oxygen therapy at the second visit or earlier in patients with SSc-PH-ILD (26%) compared to those with SSc-PAH (15%) ($P = 0.13$).

DISCUSSION

We compared baseline characteristics and outcomes when receiving PAH-targeted therapy between patients with SSc-PAH and those with SSc-PH-ILD. We found a shorter survival in SSc-PH-ILD compared to SSc-PAH. Next, we found no significant differences between groups in change in 6-minute walk distance or hemodynamic response to PAH therapy, mostly using monotherapy, despite less severe hemodynamic impairment in SSc-PH-ILD patients.

In patients with SSc-PH-ILD, hemodynamic improvement was mild yet statistically significant, and not different from that observed in SSc-PAH, although the comparison may have been limited by statistical power. This contrasts with findings

from an earlier study (22), in which only 34 of 70 patients had follow-up RHC available. However, improvement in WHO functional class was obtained in only a minority of patients with SSc-PH-ILD, consistent with these earlier findings (22), and no clinical benefit was therefore demonstrated. Of note, no significant improvement in 6-minute walk distance was observed in patients with SSc-PH-ILD or SSc-PAH. In SSc, 6-minute walk distance is impaired by skin and muscle involvement and may not be an appropriate outcome measure to assess PH (26). Six-minute walk distance may be further confounded by ILD in subjects with SSc-PH-ILD. Whether precapillary PH in patients with SSc-ILD might be managed as SSc-PAH regardless of the presence of ILD requires further evaluation. The present findings may inform future trials of PH therapy in patients with SSc-PH-ILD.

In earlier studies, treatment for PAH was found to be less effective in improving short-term 6-minute walk distance and in reducing the risk of clinical worsening in SSc-PAH compared to idiopathic PAH (27), possibly accounting for a generally more severe outcome (6–9) despite less severe hemodynamic derangements at diagnosis. Patients in the present series mostly received endothelin receptor antagonists and/or phosphodiesterase 5 inhibitors. Very few patients received prostanoid therapy as first-line therapy, although initiation of prostanoids within 6 months of diagnosis was associated with an improved SSc-PH-ILD prognosis in one study (16).

In a recent subgroup analysis of the AMBITION trial, patients with SSc-PAH benefited from initial ambrisentan and tadalafil

Table 2. Univariable analysis of prognostic factors for overall mortality*

Parameter	HR	95% CI	P
Age >60 years	1.78	0.99–3.19	0.05
Male sex	1.81	1.04–3.16	0.04
ILD vs. no ILD	1.70	1.03–2.80	0.04
Limited cutaneous SSc vs. diffuse cutaneous SSc	1.51	0.87–2.63	0.15
Comorbidities			
Arterial hypertension	1.12	0.68–1.83	0.65
Diabetes mellitus	1.85	0.84–4.09	0.13
Coronary disease	1.11	0.35–3.55	0.13
Chronic kidney disease	4.55	2.00–10.35	0.0003
Obesity	0.55	0.26–1.17	0.12
SSc gastrointestinal involvement	0.99	0.53–1.86	0.97
Hemodynamics			
RAP, mm Hg	0.986	0.935–1.040	0.61
Mean PAP, mm Hg	1.018	0.995–1.041	0.13
Cardiac index, liter/minute/m ²	0.576	0.391–0.849	0.005
PVR, Wood units	1.078	0.999–1.164	0.05
Pulmonary function tests			
FVC, % of predicted	0.993	0.928–1.003	0.16
DLco, %	0.968	0.946–0.990	0.005
6-minute walk distance, meters	0.995	0.993–0.998	0.0002
SpO ₂ nadir	0.960	0.924–0.996	0.03
SpO ₂ delta	1.059	1.012–1.109	0.01
Monotherapy vs. combination PH therapy	1.64	0.78–3.44	0.19

* Using the Bonferroni correction, significance was set at $P < 0.0025$. HR = hazard ratio; 95% CI = 95% confidence interval (see Table 1 for other definitions).

combination therapy with a similar magnitude to that observed in the whole trial population (28). In the present study, only 6% of the patients initially received combination therapy, but a greater proportion of patients (29%) later received sequential combination therapy, which became more common practice during the study period and likely contributed to the relatively good outcome in this cohort.

Mortality rates were greater in patients with SSc-PH-ILD than in those with SSc-PAH, consistent with findings from previous studies (17–19). We found ILD to be associated with greater mortality in both univariable and multivariable analyses, even though SSc-PAH patients had more severe hemodynamic impairment at baseline than those with SSc-PH-ILD. It is also noteworthy that SSc-PH-ILD patients were younger than those with SSc-PAH at the time of PH diagnosis and more frequently required long-term oxygen supplementation therapy.

Deterioration in oxygenation frequently occurs during follow-up in patients with SSc-PH-ILD and is associated with mortality (22). It has been suggested that the inhibition by PAH-targeted therapy of hypoxic vasoconstriction in PH associated with ILD could be responsible for an increase in hypoxemia (13,29). Our results do not support this hypothesis, as no significant difference was found between groups in the proportion of patients

in whom oxygen was initiated during follow-up, although numerically there tended to be more frequent initiation of supplemental oxygen in SSc-PH-ILD patients compared to SSc-PAH patients. Our data do not allow us to distinguish between the effect of worsening ILD and that of possible increased right-to-left shunting by PAH-targeted therapy as a cause of deterioration of oxygenation in patients with SSc-PH-ILD, nor do they distinguish between the effects observed according to the specific treatment used for PAH.

Our findings are consistent with those of previous studies demonstrating that low cardiac index and high PVR are associated with increased mortality in SSc-PAH (7,30). In an exploratory subgroup analysis, the patients with the highest mortality had extensive ILD at the time of CT scan and severe PH, and those with the best survival had limited ILD and mild PH, although severity of PH was not related to severity of ILD (data not shown). We speculate that precapillary PH in SSc might develop independently of the presence and severity of ILD.

Male sex was also associated with increased mortality, as previously found in SSc in general (31), in SSc-ILD (32), and in SSc-PAH (7,33,34). It is, however, unclear whether sex can be independently associated with mortality in SSc (35). We also found that chronic kidney disease at baseline was a factor strongly associated with mortality, in both univariable and multivariable analyses, as previously reported in SSc-ILD (36) and PAH (37). We found that both chronic kidney disease and ILD were independently associated with mortality. In other words, SSc-ILD-PH patients had worse mortality than those with SSc-PAH, and both SSc-PAH and SSc-ILD-PH patients were at an increased risk of mortality when chronic kidney disease was present.

Our study has limitations. It is not a randomized trial, and no conclusions can be drawn regarding efficacy of PAH therapy. Due to the small number of patients receiving each class of drug and due to missing data, subgroup analysis by initial treatment category could not be performed. Comparison of SSc-PH-ILD and SSc-PAH groups may be limited by statistical power or be confounded by several factors, as the analysis of prognostic determinants could not be adjusted for disease severity. Patients with SSc-PH-ILD who did not receive PAH-targeted therapy were not available for comparison, and some selection bias, due to patients

Table 3. Multivariable analysis of prognostic factors for overall survival*

Parameter	HR	95% CI	P
Chronic kidney disease	5.22	2.18–12.46	0.0002
ILD	2.11	1.18–3.78	0.01
6-minute walk distance, meters	0.996	0.993–0.998	0.003

* Adjusted for age, sex, and the other variables presented (i.e., for chronic kidney disease, adjustment was made for age, sex, interstitial lung disease [ILD], and 6-minute walk distance). HR = hazard ratio; 95% CI = 95% confidence interval.

Table 4. Outcomes of PAH therapy 3–6 months after baseline*

Parameter	SSc-PAH (n = 62)		SSc-PH-ILD (n = 66)		P, SSc-PAH vs. SSc-PH-ILD
	Change [n]	P	Change [n]	P	
Hemodynamics					
RAP, mm Hg	1.0 (–2.0, 3.0) [45]	0.41†	0.0 (–3.5, 3.0) [44]	0.79†	0.48‡
Mean PAP, mm Hg	–2.0 (–7.0, –2.0) [49]	0.008§	–3.0 (–9.0, –2.0) [47]	0.01§	0.93¶
Cardiac index, liter/minute/m ²	0.2 (–0.2, 0.7) [45]	0.03†	0.2 (–0.2, 0.7) [46]	0.009†	0.45‡
PVR, Wood units	–1.4 (–4.0, 0.0) [46]	<0.001†	–1.0 (–2.6, –0.1) [45]	0.001†	0.47‡
PAWP, mm Hg	2.0 (–1.5, 5.0) [48]	0.007§	0.0 (–3.0, 3.0) [45]	0.85§	0.03¶
6-minute walk distance, meters	14.0 (–31.0, 55.0) [45]	0.25†	–12.0 (–69.0, 51.0) [51]	0.22†	0.11‡
Change in 6-minute walk distance >24 meters, no. (%)	20 (45.5) [44]	NA	18 (32.3) [51]	NA	0.31#
Change in Borg dyspnea score	0 (–1, 2) [37]	0.57†	0 (–2, 0.5) [44]	0.19†	0.16‡
Change in SpO ₂ nadir	0 (–4, 3) [38]	0.83†	0 (–5, 3) [42]	0.68†	0.72‡
Change in SpO ₂ delta	1 (–3, 4) [37]	0.93†	–1 (–3, 4) [41]	0.94†	0.96‡
WHO functional class, no. (%)		0.07**		0.69**	0.02#
3–4 to 1–2	19 (33.3) [47]		8 (13.6) [59]		
1–2 to 3–4	6 (10.5) [47]		4 (6.8) [59]		
Other	32 (56.1) [47]		47 (79.6) [59]		
Initiation or increase of oxygen therapy, no. (%)	9 (15.8) [57]	0.18††	17 (27.4) [62]	0.09††	0.13#
Time to second RHC, months	5.0 (3.9, 7.7) [49]		4.8 (4.1, 6.0) [47]		0.62‡

* Using the Bonferroni correction, significance was set at $P < 0.0038$. Except where indicated otherwise, values are the median (interquartile range). RHC = right-sided heart catheterization (see Table 1 for other definitions).

† By signed rank test.

‡ By nonparametric Wilcoxon test.

§ By Student's paired test.

¶ By Student's parametric test.

By chi-square test.

** By Cochran's Q test.

†† By McNemar's test and kappa test.

diagnosed as having SSc-PAH or those who received treatment, cannot be excluded. Although screening for PH in patients with asymptomatic SSc is largely implemented in France, screening for PH might have been less systematic in patients already diagnosed as having SSc-ILD, potentially biasing the patient cohort; individual indications for RHC (before study enrollment) were not captured.

Only a minority of patients received combination therapy to treat PAH, and the potential effect of treatment with a combination of PH drugs versus monotherapy should be interpreted with caution. Given the current wider use of combination therapy as first-line treatment in PAH, including SSc-PAH, results of our present study may not be applicable to current practice. Data on Pao₂ were not available for all patients, limiting the ability to assess the impact of PAH therapy on oxygenation, although there was no difference between groups in terms of initiation or need to increase supplemental oxygen therapy. The respective roles of PH and ILD on symptoms, oxygenation, and outcomes remain difficult to determine in subjects with SSc-PH-ILD. We defined PH in this study as having a mean PAP of ≥ 25 mm Hg rather than >20 mm Hg (38).

In conclusion, our findings support the notion that SSc-PH-ILD carries a worse prognosis than SSc-PAH. Although no clinical benefit of PAH-targeted therapy was found in patients with SSc-PH-ILD, hemodynamic changes with treatment mostly

using monotherapy did not differ from those in patients with SSc-PAH. These findings emphasize the need to assess the impact of PAH-targeted therapy in randomized controlled trials in patients with SSc-PH-ILD, a vulnerable population of patients who are understudied in clinical trials.

ACKNOWLEDGMENTS

The authors thank Prof. Olivier Sitbon (Paris) and Ms Laurence Rottat for extraction of data from the French PAH registry, and Ms Stephanie Polazzi for managing the database of the HYPID and HYPID-2. The HYPID and HYPID-2 studies were funded by Programme Hospitalier de Recherche Clinique number 27.

AUTHOR CONTRIBUTIONS

All authors were involved in drafting the article or revising it critically for important intellectual content, and all authors approved the final version to be published. Dr. Chauvelot had full access to all of the data in the study and takes responsibility for the integrity of the data and the accuracy of the data analysis.

Study conception and design. Chauvelot, Cottin.

Acquisition of data. Chauvelot, Nieves, Renard, Catella-Chatron, Ahmad, Bertoletti, Camara, Gomez, Launay, Montani, Mornex, Prévot, Sanchez, Schott, Subtil, Traclet, Turquier, Zeghmar, Habib, Reynaud-Gaubert, Humbert, Cottin.

Analysis and interpretation of data. Chauvelot, Gamondes, Berthiller, Cottin.

REFERENCES

- Elhai M, Meune C, Boubaya M, Avouac J, Hachulla E, Balbir-Gurman A, et al. Mapping and predicting mortality from systemic sclerosis. *Ann Rheum Dis* 2017;76:1897–905.
- Galie N, Humbert M, Vachiery JL, Gibbs S, Lang I, Torbicki A, et al. 2015 ESC/ERS guidelines for the diagnosis and treatment of pulmonary hypertension. *Eur Respir J* 2015;46:903–75.
- Simonneau G, Gatzoulis MA, Adatia I, Celermajer D, Denton C, Ghofrani A, et al. Updated clinical classification of pulmonary hypertension. *J Am Coll Cardiol* 2013;62:D34–41.
- Avouac J, Airo P, Meune C, Beretta L, Dieude P, Caramaschi P, et al. Prevalence of pulmonary hypertension in systemic sclerosis in European Caucasians and meta-analysis of 5 studies. *J Rheumatol* 2010;37:2290–8.
- Iudici M, Codullo V, Giuggioli D, Riccieri V, Cuomo G, Breda S, et al. Pulmonary hypertension in systemic sclerosis: prevalence, incidence and predictive factors in a large multicentric Italian cohort. *Clin Exp Rheumatol* 2013;31:31–6.
- Clements PJ, Tan M, McLaughlin VV, Oudiz RJ, Tapson VF, Channick RN, et al, on behalf of the Pulmonary Arterial Hypertension Quality Enhancement Research Initiative Investigators. The Pulmonary Arterial Hypertension Quality Enhancement Research Initiative: comparison of patients with idiopathic PAH to patients with systemic sclerosis-associated PAH. *Ann Rheum Dis* 2012;71:249–52.
- Lefèvre G, Dauchet L, Hachulla E, Montani D, Sobanski V, Lambert M, et al. Survival and prognostic factors in systemic sclerosis-associated pulmonary hypertension: a systematic review and meta-analysis. *Arthritis Rheum* 2013;65:2412–23.
- Condliffe R, Kiely DG, Peacock AJ, Corris PA, Gibbs JS, Vrapai F, et al. Connective tissue disease-associated pulmonary arterial hypertension in the modern treatment era. *Am J Respir Crit Care Med* 2009;179:151–7.
- Ramjug S, Hussain N, Hurdman J, Billings C, Charalampopoulos A, Elliot CA, et al. Idiopathic and systemic sclerosis-associated pulmonary arterial hypertension: a comparison of demographic, hemodynamic, and MRI characteristics and outcomes. *Chest* 2017;152:92–102.
- Launay D, Montani D, Hassoun PM, Cottin V, le Pavec J, Clerson P, et al. Clinical phenotypes and survival of pre-capillary pulmonary hypertension in systemic sclerosis. *PLoS One* 2018;13:e0197112.
- Nihtyanova SI, Schreiber BE, Ong VH, Rosenberg D, Moizadeh P, Coghlan JG, et al. Prediction of pulmonary complications and long-term survival in systemic sclerosis. *Arthritis Rheumatol* 2014;66:1625–35.
- Ryerson CJ, O'Connor D, Dunne JV, Schooley F, Hague CJ, Murphy D, et al. Predicting mortality in systemic sclerosis-associated interstitial lung disease using risk prediction models derived from idiopathic pulmonary fibrosis. *Chest* 2015;148:1268–75.
- Goh NS, Desai SR, Veeraraghavan S, Hansell DM, Copley SJ, Maher TM, et al. Interstitial lung disease in systemic sclerosis: a simple staging system. *Am J Respir Crit Care Med* 2008;177:1248–54.
- Goh NS, Hoyles RK, Denton CP, Hansell DM, Renzoni EA, Maher TM, et al. Short-term pulmonary function trends are predictive of mortality in interstitial lung disease associated with systemic sclerosis. *Arthritis Rheumatol* 2017;69:1670–8.
- Fischer A, Swigris JJ, Bolster MB, Chung L, Csuka ME, Domsic R, et al. Pulmonary hypertension and interstitial lung disease within PHAROS: impact of extent of fibrosis and pulmonary physiology on cardiac haemodynamic parameters. *Clin Exp Rheumatol* 2014;32:S109–14.
- Volkman ER, Sagar R, Khanna D, Torres B, Flora A, Yoder L, et al. Improved transplant-free survival in patients with systemic sclerosis-associated pulmonary hypertension and interstitial lung disease. *Arthritis Rheumatol* 2014;66:1900–8.
- Mathai SC, Hummers LK, Champion HC, Wigley FM, Zaiman A, Hassoun PM, et al. Survival in pulmonary hypertension associated with the scleroderma spectrum of diseases: impact of interstitial lung disease. *Arthritis Rheum* 2009;60:569–77.
- Launay D, Humbert M, Berezne A, Cottin V, Allanore Y, Couderc LJ, et al. Clinical characteristics and survival in systemic sclerosis-related pulmonary hypertension associated with interstitial lung disease. *Chest* 2011;140:1016–24.
- Michelfelder M, Becker M, Riedlinger A, Siegert E, Dromann D, Yu X, et al. Interstitial lung disease increases mortality in systemic sclerosis patients with pulmonary arterial hypertension without affecting hemodynamics and exercise capacity. *Clin Rheumatol* 2017;36:381–90.
- Young A, Vummidi D, Visovatti S, Homer K, Wilhalme H, White ES, et al. Prevalence, treatment, and outcomes of coexistent pulmonary hypertension and interstitial lung disease in systemic sclerosis. *Arthritis Rheumatol* 2019;71:1339–49.
- Sanchez O, Sitbon O, Jais X, Simonneau G, Humbert M. Immunosuppressive therapy in connective tissue diseases-associated pulmonary arterial hypertension. *Chest* 2006;130:182–9.
- Le Pavec J, Girgis RE, Lechtzin N, Mathai SC, Launay D, Hummers LK, et al. Systemic sclerosis-related pulmonary hypertension associated with interstitial lung disease: impact of pulmonary arterial hypertension therapies. *Arthritis Rheum* 2011;63:2456–64.
- Van den Hoogen F, Khanna D, Fransen J, Johnson SR, Baron M, Tyndall A, et al. 2013 classification criteria for systemic sclerosis: an American College of Rheumatology/European League Against Rheumatism collaborative initiative. *Arthritis Rheum* 2013;65:2737–47.
- Montani D, Lau EM, Descatha A, Jais X, Savale L, Andujar P, et al. Occupational exposure to organic solvents: a risk factor for pulmonary veno-occlusive disease. *Eur Respir J* 2015;46:1721–31.
- Mathai SC, Puhon MA, Lam D, Wise RA. The minimal important difference in the 6-minute walk test for patients with pulmonary arterial hypertension. *Am J Respir Crit Care Med* 2012;186:428–33.
- Sanges S, Launay D, Rhee RL, Sitbon O, Hachulla E, Mouthon L, et al. A prospective study of the 6 min walk test as a surrogate marker for haemodynamics in two independent cohorts of treatment-naïve systemic sclerosis-associated pulmonary arterial hypertension. *Ann Rheum Dis* 2016;75:1457–65.
- Rhee RL, Gabler NB, Sangani S, Praestgaard A, Merkel PA, Kawut SM. Comparison of treatment response in idiopathic and connective tissue disease-associated pulmonary arterial hypertension. *Am J Respir Crit Care Med* 2015;192:1111–7.
- Coghlan JG, Galie N, Barbera JA, Frost AE, Ghofrani HA, Hoepfer MM, et al. Initial combination therapy with ambrisentan and tadalafil in connective tissue disease-associated pulmonary arterial hypertension (CTD-PAH): subgroup analysis from the AMBITION trial. *Ann Rheum Dis* 2017;76:1219–27.
- Launay D, Sobanski V, Hachulla E, Humbert M. Pulmonary hypertension in systemic sclerosis: different phenotypes [review]. *Eur Respir Rev* 2017;26:170056.
- Chung L, Domsic RT, Lingala B, Alkassab F, Bolster M, Csuka ME, et al. Survival and predictors of mortality in systemic sclerosis-associated pulmonary arterial hypertension: outcomes from the pulmonary hypertension assessment and recognition of outcomes in scleroderma registry. *Arthritis Care Res (Hoboken)* 2014;66:489–95.
- Fransen J, Popa-Diaconu D, Hesselstrand R, Carreira P, Valentini G, Beretta L, et al. Clinical prediction of 5-year survival in systemic sclerosis: validation of a simple prognostic model in EUSTAR centres. *Ann Rheum Dis* 2011;70:1788–92.
- Winstone TA, Assayag D, Wilcox PG, Dunne JV, Hague CJ, Leipsic J, et al. Predictors of mortality and progression in scleroderma-associated interstitial lung disease: a systematic review. *Chest* 2014;146:422–36.

33. Launay D, Sitbon O, Hachulla E, Mouthon L, Gressin V, Rottat L, et al. Survival in systemic sclerosis-associated pulmonary arterial hypertension in the modern management era. *Ann Rheum Dis* 2013;72:1940–6.
34. Williams MH, Handler CE, Akram R, Smith CJ, Das C, Smee J, et al. Role of N-terminal brain natriuretic peptide (N-TproBNP) in scleroderma-associated pulmonary arterial hypertension. *Eur Heart J* 2006;27:1485–94.
35. Pasarikovski CR, Granton JT, Roos AM, Sadeghi S, Kron AT, Thenganatt J, et al. Sex disparities in systemic sclerosis-associated pulmonary arterial hypertension: a cohort study. *Arthritis Res Ther* 2016;18:30.
36. Bauer PR, Schiavo DN, Osborn TG, Levin DL, St. Sauver J, Hanson AC, et al. Influence of interstitial lung disease on outcome in systemic sclerosis: a population-based historical cohort study. *Chest* 2013;144:571–7.
37. Bitker L, Sens F, Payet C, Turquier S, Duclos A, Cottin V, et al. Presence of kidney disease as an outcome predictor in patients with pulmonary arterial hypertension. *Am J Nephrol* 2018;47:134–43.
38. Simonneau G, Montani D, Celermajer DS, Denton CP, Gatzoulis MA, Krowka M, et al. Haemodynamic definitions and updated clinical classification of pulmonary hypertension. *Eur Respir J* 2019;53:1801913.

Association of Autologous Hematopoietic Stem Cell Transplantation in Systemic Sclerosis With Marked Improvement in Health-Related Quality of Life

Nancy Maltez,¹  Mathieu Puyade,² Mianbo Wang,³ Pauline Lansiaux,⁴ Zora Marjanovic,⁵ Catney Charles,⁴ Russell Steele,⁶ Murray Baron,⁷ Ines Colmegna,⁷  Marie Hudson,⁸ and Dominique Farge,⁹ for the Canadian Scleroderma Research Group and the MATHEC-SFGMTC Network

Objective. To quantify the magnitude, domains, and duration of change in health-related quality of life (HRQoL) in patients with systemic sclerosis (SSc) who underwent autologous hematopoietic stem cell transplantation (HSCT) as compared to SSc patients with similar characteristics who did not undergo autologous HSCT.

Methods. The study was designed as a retrospective study comparing SSc patients who underwent autologous HSCT and SSc patients who met the criteria for transplantation but were treated with conventional care. Outcomes included scores on the 36-item Short Form (SF-36) health survey and the Health Assessment Questionnaire (HAQ) and its disease-specific symptom scales. Differences in scores between the groups were compared using linear models, adjusting for baseline scores and inverse probability of treatment and censoring weights.

Results. In total, 41 SSc patients who underwent autologous HSCT and 65 SSc patients treated with conventional care were compared. In marginal linear weighted models, the SF-36 physical component summary score was a mean \pm SEM 7.02 ± 1.94 points higher at the first annual visit ($P = 0.001$) and 14.40 ± 6.16 points higher at the seventh annual visit ($P = 0.03$) in patients treated with autologous HSCT compared to the conventional care group. HAQ scores were significantly better in the autologous HSCT group compared to the conventional care group during follow-up (mean \pm SEM difference from baseline -0.57 ± 0.13 [$P < 0.001$] at the first annual visit and -0.94 ± 0.49 [$P = 0.07$] at the seventh annual visit). There were no differences in the SF-36 mental component summary scores between the 2 groups either at baseline or during follow-up.

Conclusion. This study provides robust complementary HRQoL data, including overall and event-free survival data, to expand on the standard repertoire of biomedical variables, thus potentially supporting the physical benefits of autologous HSCT in patients with SSc.

INTRODUCTION

Systemic sclerosis (SSc) is a chronic, multiorgan autoimmune disease characterized by progressive fibrosis of the skin

and internal organs (1). The 5-year mortality rate has been estimated to exceed 60% in high-risk patients with early diffuse and rapidly progressive cutaneous disease (2,3). In addition to its involvement in multiple organs leading to significant morbidity,

The Canadian Scleroderma Research Group (CSRG) was supported by the Canadian Institutes of Health Research (CIHR), Scleroderma Canada and its provincial chapters, the Scleroderma Society of Ontario, the Scleroderma Society of Saskatchewan, Sclérodermie Québec, the Cure Scleroderma Foundation, INOVA Diagnostics, Inc., Dr. Fooko Laboratorien GmbH, Euroimmun, Mikrogen GmbH, Fonds de la Recherche en Santé du Québec, and the Canadian Arthritis Network (CAN), and Lady Davis Institute of Medical Research of the Jewish General Hospital. The CSRG has also received educational grants from Pfizer, Actelion, and Mallinkrodt.

¹Nancy Maltez, MD: The Ottawa Hospital, Ottawa, Ontario, Canada; ²Mathieu Puyade, MD, PhD: CHU de Poitiers, CIC 1402, Poitiers, France; ³Mianbo Wang, MSc: Lady Davis Institute, Jewish General Hospital, Montreal, Quebec, Canada; ⁴Pauline Lansiaux, PhD, Catney Charles, BSc: Centre de Référence des Maladies Auto-Immunes Systémiques Rares d'Ile-de-France, AP-HP, Hôpital St. Louis, Université de Paris, Institut de Recherche St. Louis, EA

3518, Paris, France; ⁵Zora Marjanovic, MD: Hôpital St. Antoine, Paris, France; ⁶Russell Steele, PhD: McGill University, Montreal, Quebec, Canada; ⁷Murray Baron, MD, Ines Colmegna, MD: Jewish General Hospital and McGill University Health Center, Montreal, Quebec, Canada; ⁸Marie Hudson, MD, MPH: Lady Davis Institute, Jewish General Hospital, and McGill University, Montreal, Quebec, Canada; ⁹Dominique Farge, MD, MSc, PhD: Centre de Référence des Maladies Auto-Immunes Systémiques Rares d'Ile-de-France, AP-HP, Hôpital St. Louis, Université de Paris, Institut de Recherche St. Louis, EA 3518, Hôpital St. Antoine, Paris, France, and McGill University, Montreal, Quebec, Canada.

Drs. Hudson and Farge contributed equally to this work.

No potential conflicts of interest relevant to this article were reported.

Address correspondence to Nancy Maltez, MD, 1967 Riverside Drive Box 37, Ottawa, Ontario K1H 7W9, Canada. Email: nmaltez@toh.ca.

Submitted for publication February 25, 2020; accepted in revised form September 3, 2020.

SSc is also associated with diminished health-related quality of life (HRQoL), indicated by a decrease in self-reported physical health status scores of more than 1 standard deviation below that in the general population (4).

Treatment options for SSc are limited, with traditional disease-modifying agents having no effects on survival (5,6). In contrast, early phase I/II studies showed that autologous hematopoietic stem cell transplantation (HSCT) allowed a rapid and sustained improvement in skin and lung fibrosis, along with improved long-term survival of up to 7 years after autologous HSCT (7,8). Benefits of autologous HSCT in SSc, in terms of disease progression and survival, were thereafter demonstrated in 3 randomized controlled trials comparing autologous HSCT to monthly intravenous cyclophosphamide, including the ASSIST (Autologous Stem Cell Systemic Sclerosis Immune Suppression Trial) (9), the ASTIS (Autologous Stem Cell Transplantation International Scleroderma) trial (10), and the SCOT (Myeloablative Autologous Stem-Cell Transplantation for Severe Scleroderma) (11) trials. Thus, autologous HSCT has become the best treatment option for early severe SSc (12–15).

Nonetheless, although autologous HSCT is effective, it is associated with significant treatment-related toxicities and mortality in highly fragile patients. This highlights the importance of studying HRQoL (16,17). Our group recently undertook a systematic review of the literature to assess current knowledge of the impacts of autologous HSCT on HRQoL in SSc. We demonstrated a promising improvement in physical HRQoL post-autologous HSCT (18). However, the evidence was limited by the characteristics of the studies, including relatively small sample sizes, lack of details on individual HRQoL domains, and short duration of follow-up (median 1.25–4.5 years). Moreover, most patients were treated in the setting of clinical trials, limiting the generalizability of results to real-world clinical practice (18).

The Maladies Auto-Immunes et Thérapie Cellulaire (MATHEC) (www.mathec.com) is a French network of reference with a mission to improve clinical practice and advance research in the use of cellular therapies for autoimmune diseases, including SSc. The Canadian Scleroderma Research Group (CSRG) has followed up a large cohort of adult patients with SSc longitudinally since 2004. Since autologous HSCT is only rarely performed in Canada, very few patients have undergone autologous HSCT. We therefore proposed to leverage complementary expertise and data sets from French and Canadian scleroderma research teams to study HRQoL in SSc patients treated with autologous HSCT in France compared to Canadian patients who met the criteria for transplantation but did not undergo autologous HSCT.

The purpose of this study was to generate HRQoL data, including data on disease progression and survival, to supplement the standard biomedical variables that are usually emphasized in the medical literature. More specifically, we aimed to quantify the magnitude, domains, and duration of change in HRQoL in SSc patients treated with autologous HSCT compared to patients with

similar characteristics who did not undergo autologous HSCT. We hypothesized that HRQoL would be superior in SSc patients treated with autologous HSCT when compared to those treated with conventional care.

PATIENTS AND METHODS

Ethics considerations. Ethics committee approval for this study was obtained from the Jewish General Hospital in Montreal (approval no. REB 2020-1954). Informed consent was obtained from all patients in accordance with the Declaration of Helsinki and the Guidelines for Good Clinical Practice.

Study population. All consecutive patients who underwent autologous HSCT in the MATHEC cohort from 1999 to 2016 were included in the study. As a comparator group, we selected SSc patients in the CSRG registry who fulfilled the eligibility criteria for autologous HSCT in the ASTIS trial (age >18 years, having diffuse cutaneous SSc according to the American College of Rheumatology 1980 classification criteria for SSc [19], maximum disease duration of 4 years since first non-Raynaud's symptoms, minimum modified Rodnan skin thickness score [MRSS] of 15 [20], and involvement of the heart, lungs, or kidneys or disease duration of ≤2 years with no major organ involvement but with an MRSS of at least 20 and erythrocyte sedimentation rate of >25 mm/hour and/or hemoglobin level of <110 gm/liter) (10) but who had not undergone autologous HSCT. Baseline and annual HRQoL measures were collected prospectively from all patients in the autologous HSCT group and in the CSRG comparator group.

Data collection. Demographic variables, including age, sex, and smoking status, were collected by patient self-report. Disease duration was recorded by study physicians and defined as the interval between the onset of the first non-Raynaud's disease manifestation and baseline study visit. Skin involvement was assessed using the MRSS, a widely used clinical assessment in which the examining physician records the degree of skin thickening with scores ranging from 0 (no involvement) to 3 (severe thickening) in 17 areas (total score range 0–51) (20). Study physicians also recorded information on the patients' history of scleroderma renal crisis, total parenteral nutrition, and body mass index. In addition, laboratory investigations (extracted from the medical records) included the erythrocyte sedimentation rate as well as determination of the levels of hemoglobin, serum creatinine, proteinuria, and serum autoantibodies.

Interstitial lung disease (ILD) was considered present if a high-resolution computed tomography (HRCT) scan of the lung was interpreted by an experienced radiologist as showing ILD. Alternatively, in patients for whom no HRCT scan was available, ILD was identified using a chest radiograph showing either increased interstitial markings (not thought to be due to congestive heart failure) or fibrosis, and/or a study physician report of

the presence of typical “velcro-like crackles” on physical examination (21). Pulmonary function tests were performed in local laboratories working in accordance with the American Thoracic Society standards. The percent predicted value for forced vital capacity (FVC) and lung diffusing capacity for carbon monoxide (DL_{CO}) was extracted from laboratory reports. Transthoracic cardiac echocardiograms were obtained by experienced cardiac sonographers at every site. The systolic pulmonary artery pressure and left ventricular ejection fraction were extracted from the medical reports.

Outcome measures. *Short Form 36 (SF-36).* The SF-36 health survey is a generic HRQoL instrument that consists of 36 questions in 8 domains: physical functioning, bodily pain, physical role functioning, general health, social functioning, mental health, vitality, and emotional role functioning. Each domain can be scored separately, with scores ranging from 0, indicating the worst health state, to 100, indicating the best health state. Domain scores can also be summarized into a physical component summary (PCS) score and a mental component summary (MCS) score. The PCS and MCS are calculated using norm-based scoring, based on a general population sample, to produce T scores for each patient (mean score of 50 with SD of 10). Therefore, for the 2 summary scores, HRQoL is worse than average if it is below 50 and better than average if it is above 50, and each point is one-tenth of an SD (22). This tool has been translated and validated in France and used in studies of SSc (23,24). The minimum clinically important difference (MCID) in the PCS and MCS scores in SSc ranges between 2.5 and 5 points (25). In rheumatoid arthritis, the MCID in the SF-36 domain scores ranges between 5 and 10 points (26).

Health Assessment Questionnaire (HAQ) disability index (DI). The HAQ DI is a self-administered questionnaire specifically validated for functional assessment in SSc (27). It includes 20 questions in 8 categories (dressing and grooming, standing, eating, walking, hygiene, reach, grip, and performing activities). The use of assistive aids and devices to help with function is also recorded. The patient is asked to rate his/her difficulty over the past week in performing the specific tasks in each category on a scale of 0–3 (0 = without difficulty, 1 = with some difficulty, 2 = with much difficulty or with assistance, 3 = unable to perform tasks). The highest scores in each category are added and the total is divided by 8. Scores range from 0 (no disability) to 3 (severe disability). The French version of the HAQ DI has been validated in SSc (28). The MCID in the HAQ DI score in patients with SSc is 0.14 points (25).

In addition to the HAQ, the Scleroderma HAQ (SHAQ) includes disease-specific symptom scales assessing pain, Raynaud's phenomenon, digital ulcers, breathlessness, gastrointestinal symptoms, and overall disease (29). These scales require that patients quantify how much their symptoms interfere with daily activities. The assessments in our study were made using

numeric rating scales ranging from 0 (no activity limitation) to 10 (very severe limitation). The French version of the SHAQ has been validated (25).

Statistical analysis. Baseline characteristics of the patients who underwent autologous HSCT and those who did not undergo autologous HSCT were summarized and compared using descriptive statistics. Differences in the HAQ DI and SHAQ variables and SF-36 domain and summary scores between the study groups were compared using linear models, adjusting for baseline scores and inverse probability of treatment weights (IPTW), calculated as $1/\text{propensity score}$ for the treated subjects and $1/(1 - \text{propensity score})$ for the untreated subjects. Propensity scores were estimated using logistic regression analyses including the following covariates: female sex, age, disease duration, and other variables with *P* values of less than 0.10 in univariate comparisons (presence of ILD, DL_{CO}, history of scleroderma renal crisis, and creatinine levels). In addition, to account for the potential informative censoring between baseline and follow-up visits, the inverse probability of censoring weights (IPCW) was estimated by logistic regression, using the same covariates as in the propensity score model. The outcome model was a marginal linear model including only autologous HSCT, weighted by the product of the IPTW and IPCW.

We also assessed the proportion of patients whose SF-36 PCS score improved by ≥ 5 units and the proportion of patients whose HAQ DI scores improved by ≥ 0.14 units. Based on the proportion of patients whose scores improved at least as much as or more than the MCID, we calculated the number needed to treat in order to achieve, on average, 1 patient with improved physical HRQoL.

Standardized mean differences were computed to assess the balance in distribution of baseline characteristics between patients who underwent autologous HSCT and those who did not, before and after IPTW. A standardized difference of 0.1 represents meaningful balance. Since balance improved for all covariates in the propensity score with re-weighting, except for scleroderma renal crisis, we undertook 2 sensitivity analyses. First, we excluded patients with scleroderma renal crisis in the conventional care group such that none of the subjects in either group had scleroderma renal crisis. Second, since the subjects who underwent autologous HSCT had higher creatinine levels and more proteinuria, we hypothesized that although none had a diagnosis of scleroderma renal crisis, this might simply be a matter of definition. Scleroderma renal crisis is a poorly defined entity and there is considerable ongoing work to develop and validate uniform classification criteria (30). Nevertheless, in the second sensitivity analysis, we excluded scleroderma renal crisis from the propensity score altogether, leaving in creatinine levels only.

Statistical analyses were performed using both SAS version 9.4 and R version 3.6.1 (<http://r-project.org>).

RESULTS

Characteristics of the study patients. Baseline characteristics of the patients treated with autologous HSCT

(n = 41) and those who received conventional care in the comparator group (n = 65) are presented in Table 1. The comparator group consisted of subjects treated with cyclophosphamide (intravenous or oral), azathioprine, methotrexate,

Table 1. Baseline characteristics of the subjects treated with autologous HSCT compared to those treated with conventional care*

	Autologous HSCT (n = 41)	Conventional care (n = 65)
Female, no. (%)	27 (65.9)	50 (76.9)
Age, years	44.7 ± 13.3	53.1 ± 10.7
Smoking status, no. (%)		[1]
Current	3 (7.3)	10 (15.6)
Past	13 (31.7)	26 (40.6)
Never	25 (61.0)	28 (43.8)
Disease duration, years	2.6 ± 1.5	1.5 ± 1.0
MRSS (range 0–51)	25.0 ± 10.5 [1]	27.5 ± 8.1
Interstitial lung disease, no. (%)	38 (92.7)	32 (49.2)
Forced vital capacity, % predicted	78.9 ± 17.5 [4]	83.4 ± 19.8 [2]
Lung DL _{CO} , % predicted	55.2 ± 15.5	62.2 ± 17.6 [4]
History of scleroderma renal crisis, no. (%)	0 [2]	14 (21.5)
ESR, mm/hour	42.8 ± 24.8 [17]	40.7 ± 31.5 [11]
Hemoglobin, gm/dl	12.6 ± 1.2	11.6 ± 2.0
Mean left ventricular ejection fraction, %	38 [3]	61 [3]
Normal left ventricular ejection fraction, %	92.7	98.3
SPAP, mm Hg	33.4 ± 5.7 [4]	34.3 ± 10.7 [21]
Creatinine, μmoles/liter	111.2 ± 34.1	85.0 ± 46.7 [4]
Total parenteral nutrition, no. (%)	1 (2.4)	1 (1.6) [1]
Body mass index, mean ± SD kg/m ²	23.4 ± 4.1	25.1 ± 4.8 [2]
Proteinuria, no. (%)	[4]	[16]
None	26 (70.3)	43 (87.8)
1+	9 (24.3)	5 (10.2)
2+	1 (2.7)	0
≥3+	1 (2.7)	1 (2.0)
SF-36 scores		[2]
Physical function	34.3 ± 11.0	28.5 (9.8)
Role physical	32.7 ± 10.8	31.1 (10.8)
Bodily pain	37.2 ± 10.6	39.2 (9.5)
General health	34.3 ± 7.4	35.0 (9.9)
Vitality	38.1 ± 7.3	39.1 (10.4)
Social function	38.7 ± 12.5	37.8 (13.0)
Role emotional	36.0 ± 13.3	39.7 (14.7)
Mental health	42.4 ± 11.4	45.5 (11.9)
Physical component summary	33.4 ± 10.0	29.7 (8.9)
Mental component summary	41.8 ± 11.7	46.1 (13.0)
HAQ score (range 0–3)	1.4 ± 0.7	1.4 ± 0.7 [2]
SHAQ symptom scales (range 0–10)		
Pain	3.8 ± 2.5	4.7 ± 2.5 [2]
Raynaud's phenomenon	3.8 ± 2.8 [3]	2.6 ± 2.7 [2]
Digital ulcerations	3.1 ± 3.1 [2]	2.0 ± 3.0 [2]
Gastrointestinal involvement	1.4 ± 1.8 [3]	1.3 ± 2.0 [2]
Breathlessness	1.7 ± 2.4 [3]	2.2 ± 2.3 [3]
Overall disease	4.9 ± 2.7	5.1 ± 2.6 [2]
Autoantibodies, no. (%)		[11]
Anticentromere	1 (2.5) [2]	4 (7.4)
Anti-topoisomerase I	26 (65.0) [1]	12 (22.2)
Anti-RNA polymerase III	ND	24 (44.4)
Follow-up time, years	8.4 ± 4.7	4.3 ± 3.1

* Except where indicated otherwise, values are the mean ± SD. Numbers in brackets indicate the number of patients with missing data. HSCT = hematopoietic stem cell transplantation; MRSS = modified Rodnan skin thickness score; DL_{CO} = diffusing capacity for carbon monoxide; ESR = erythrocyte sedimentation rate; SPAP = systolic pulmonary artery pressure; SF-36 = 36-item Short Form; HAQ = Health Assessment Questionnaire; SHAQ = Scleroderma HAQ; ND = not done.

and/or mycophenolate mofetil. The proportions treated with any of those drugs at each visit were as follows: 45% at baseline, 55% at visit 1, 50% at visit 2, 56% at visit 3, 48% at visit 4, 43% at visit 5, 50% at visit 6, and 39% at visit 7. Both groups were predominantly female (65.9% of the autologous HSCT group and 76.9% of the comparator group). Patients in the comparator group were older at the time that they met transplantation criteria (mean ± SD age 53.1 ± 10.7 years) compared to the age at the time of transplantation among patients treated with autologous HSCT (mean ± SD age 44.7 ± 13.3 years). The mean disease duration was somewhat longer in the autologous HSCT group compared to the comparator group (mean ± SD 2.6 ± 1.5 years versus 1.5 ± 1 years), and more subjects in the autologous HSCT group had ILD (92.7% versus 49.2% of the comparators).

Differences in SF-36 scores. Baseline SF-36 domain scores were generally similar between the groups, with the exception of physical function scores, which were higher among patients treated with autologous HSCT (mean ± SD 34.3 ± 11.0 versus 28.5 ± 9.8 among comparators) (Table 1). The PCS and MCS summary scores were a mean ± SD 33.4 ± 10.0 and 41.8 ± 11.7, respectively, among autologous HSCT-treated patients and 29.7 ± 8.9 and 46.1 ± 13.0, respectively, among the comparator subjects.

Differences in SF-36 PCS and MCS summary scores and in SF-36 domain scores at the annual visits from the baseline visit in patients treated with autologous HSCT compared to patients who received conventional care are presented in Figure 1, as well as in Supplementary Figure 1 and Supplementary Tables 1 and 2 (available on the *Arthritis & Rheumatology* website at <http://onlinelibrary>.

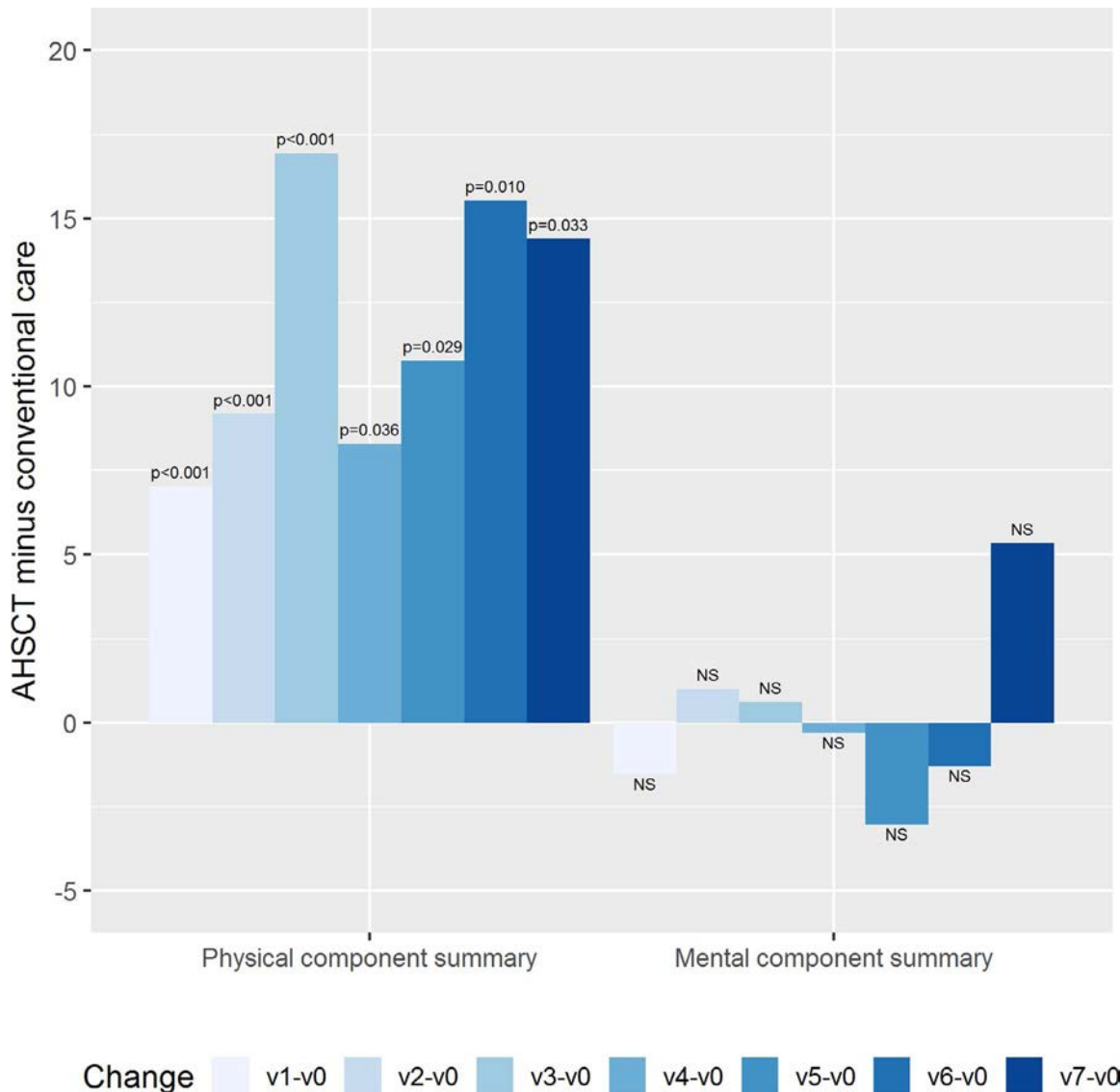


Figure 1. Differences at annual visits 1–7 (v1–v7) from baseline (v0) in physical component summary scores and mental component summary scores on the 36-item Short Form health survey in patients with systemic sclerosis treated with autologous hematopoietic stem cell transplantation (AHSCT) compared to patients who received conventional care. NS = not significant.

wiley.com/doi/10.1002/art.41519/abstract). Values represent differences after weighting for the probability of treatment and censoring. Thus, relative to baseline, the SF-36 PCS scores were a mean \pm SD 7.02 ± 1.94 points higher at the first annual visit ($P = 0.001$) and 14.40 ± 6.16 points higher at the seventh annual visit ($P = 0.03$) in patients treated with autologous HSCT compared to the conventional care group. The SF-36 MCS scores were generally similar between the groups, and this did not change over time.

The results of the SF-36 domain scores were consistent with these findings, with differences generally favoring autologous HSCT in the physical function, role physical, bodily pain, general health, and social function domains, but not in the vitality, role emotional, and mental health domains (see results in Supplementary Table 2 [<http://onlinelibrary.wiley.com/doi/10.1002/art.41519/abstract>]). The largest differences were in physical function, with

higher scores in the autologous HSCT group, ranging from 1 SD to 2 SD above the values in the conventional care group at all time points (all $P < 0.05$).

Differences in HAQ and disease-specific scales. With regard to the HAQ scores of general health status, the mean HAQ score at baseline was 1.4 in both groups (Table 1). Scores on the SHAQ symptom scales were also generally similar between the groups, apart from the score for Raynaud's phenomenon, which was worse among patients in the autologous HSCT group (mean \pm SD 3.8 ± 2.8 versus 2.6 ± 2.7 in the comparator group).

HAQ scores were considerably lower (i.e., indicating better function) at all time points following baseline in patients treated with autologous HSCT compared to comparators (Figure 2 and

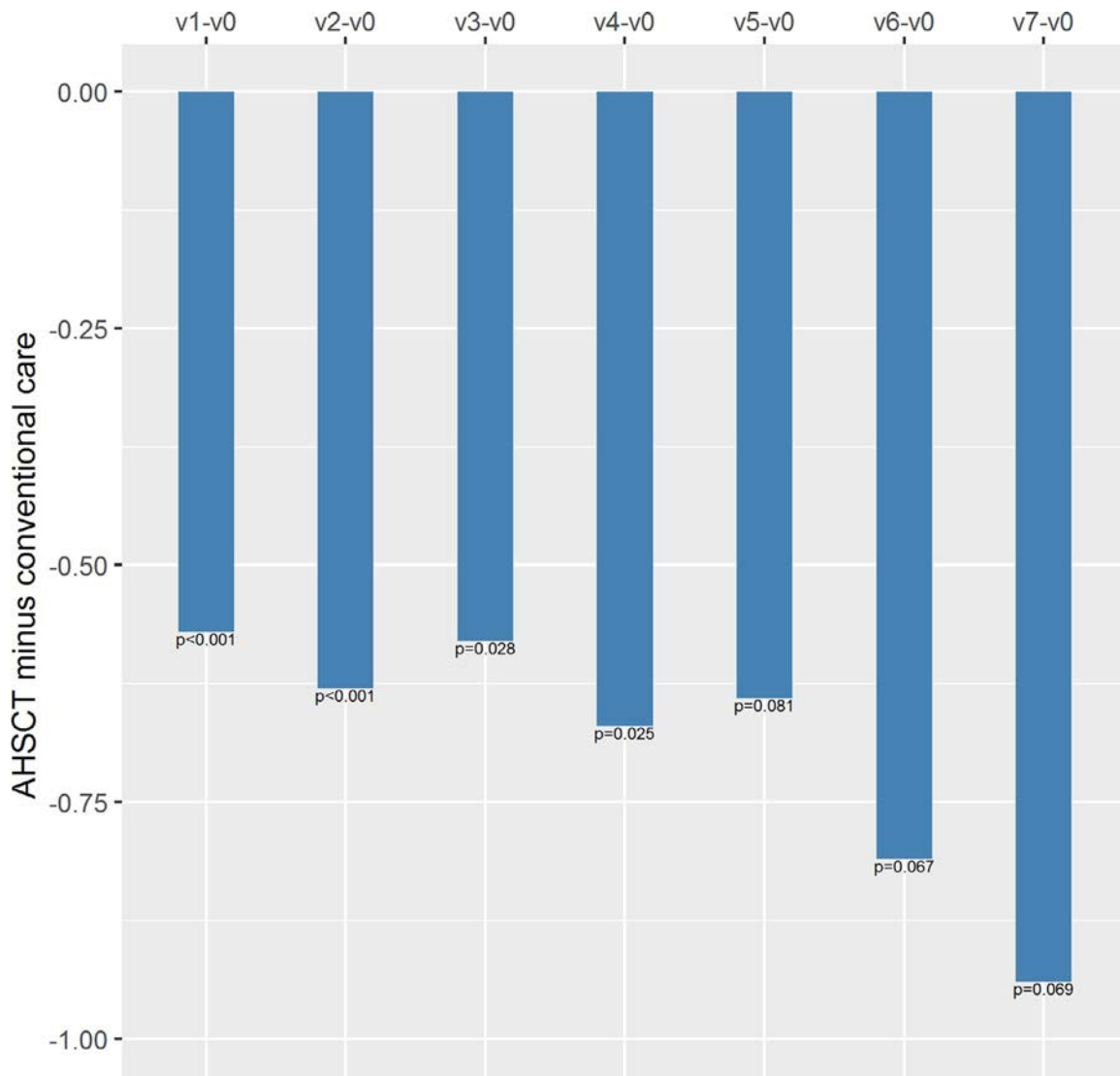


Figure 2. Differences at annual visits 1–7 (v1–v7) from baseline (v0) in Health Assessment Questionnaire scores in patients with systemic sclerosis treated with autologous hematopoietic stem cell transplantation (AHSCT) compared to patients who received conventional care. Color figure can be viewed in the online issue, which is available at <http://onlinelibrary.wiley.com/doi/10.1002/art.41519/abstract>.

Supplementary Table 1 [<http://onlinelibrary.wiley.com/doi/10.1002/art.41519/abstract>]). Again, the HAQ values represent differences between the autologous HSCT-treated patients and comparators at the annual visits compared to the baseline visit, after weighting for the probability of treatment and censoring. In fact, differences from baseline in the HAQ scores appeared to increase in favor of autologous HSCT over time (mean \pm SD difference -0.57 ± 0.13 [$P < 0.001$] at the first annual visit and -0.94 ± 0.49 [$P = 0.07$] at the seventh annual visit).

Differences in disease symptoms assessed with the SHAQ score (scales ranging from 0 to 10) are presented in Figure 3 and Supplementary Table 3 (available on the *Arthritis & Rheumatology* website at <http://onlinelibrary.wiley.com/doi/10.1002/art.41519/abstract>). Results showed marked differences in the SHAQ scores in favor of autologous HSCT, and these differences were early, sustained, and appeared to increase over time. Compared to the baseline visit, the mean \pm SD differences at the first and seventh

annual visits were as follows: for pain scores, -1.02 ± 0.72 ($P = 0.164$) and -3.24 ± 2.50 ($P = 0.033$); for Raynaud's phenomenon, -0.48 ± 0.66 ($P = 0.465$) and -4.00 ± 1.50 ($P = 0.018$); for digital ulcers, 0.06 ± 0.78 ($P = 0.938$) and -1.78 ± 1.74 ($P = 0.323$); for gastrointestinal symptoms, 0.58 ± 0.70 ($P = 0.411$) and -2.53 ± 0.90 ($P = 0.013$); for breathlessness, -1.51 ± 0.51 ($P = 0.005$) and -2.02 ± 1.37 ($P = 0.161$); and for overall disease, -1.62 ± 0.79 ($P = 0.044$) and -4.51 ± 2.02 ($P = 0.041$).

Changes in skin scores and lung function. In post hoc analyses, mechanisms of improvement in HRQoL and physical function were investigated by analyzing changes in skin scores and lung function, using similar linear models and weighting for the probability of treatment and censoring (Table 2). We found that the MRSS scores differed by up to 10 points in favor of subjects treated with autologous HSCT compared to those treated with conventional care, with this difference maintained until the sixth

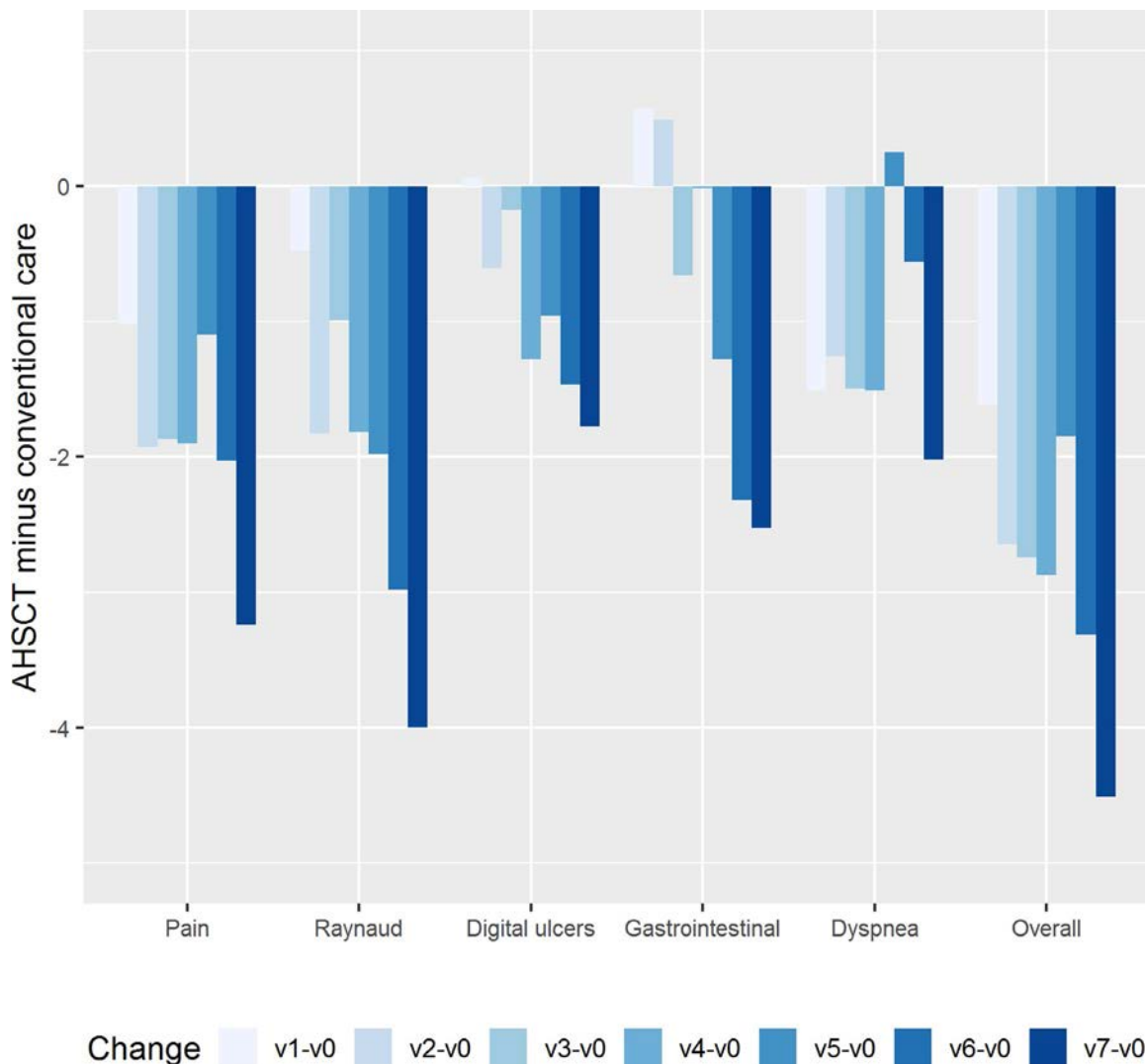


Figure 3. Differences at annual visits 1–7 (v1–v7) from baseline (v0) in Scleroderma Health Assessment Questionnaire symptom scale scores in patients with systemic sclerosis treated with autologous hematopoietic stem cell transplantation (AHSCT) compared to patients who received conventional care. Color figure can be viewed in the online issue, which is available at <http://onlinelibrary.wiley.com/doi/10.1002/art.41519/abstract>.

Table 2. Differences in the MRSS, FVC, and lung DL_{CO} at annual visits from baseline in subjects treated with autologous hematopoietic stem cell transplantation relative to those treated with conventional care*

	MRSS		%FVC		%DL _{CO}	
	$\beta \pm SE$	<i>P</i>	$\beta \pm SE$	<i>P</i>	$\beta \pm SE$	<i>P</i>
v1-v0	-8.77 ± 1.75	<0.001	-1.30 ± 3.00	0.666	-5.33 ± 2.71	0.054
v2-v0	-10.15 ± 2.21	<0.001	3.11 ± 4.00	0.440	-3.03 ± 2.96	0.311
v3-v0	-5.57 ± 2.52	0.031	5.10 ± 4.32	0.243	4.02 ± 3.66	0.278
v4-v0	-7.32 ± 2.70	0.009	2.42 ± 5.44	0.658	2.48 ± 3.79	0.516
v5-v0	-10.51 ± 4.75	0.034	8.98 ± 6.36	0.169	-4.84 ± 4.76	0.318
v6-v0	-8.37 ± 3.71	0.032	12.21 ± 6.59	0.076	-0.48 ± 5.38	0.929
v7-v0	-1.75 ± 4.26	0.685	14.46 ± 8.04	0.088	-8.62 ± 5.83	0.156

* The measures were assessed at baseline (v0) and annual visits 1–7 (v1–v7). MRSS = modified Rodnan skin thickness score; %FVC = forced vital capacity % predicted; %DL_{CO} = diffusing capacity for carbon monoxide % predicted.

annual visit (all *P* < 0.05). Similarly, the difference in the FVC gradually increased, with an increase of up to almost 15% by year 7 in favor of those treated with autologous HSCT, with the difference in FVC as compared to the comparator group approaching statistical significance (*P* = 0.088). There was no consistent difference in the DL_{CO} between subjects treated with autologous HSCT and subjects receiving conventional care over time.

In addition, although improvement in skin scores and lung function were both associated with improvement in HRQoL and function, we found no difference in these associations between treatment groups. Indeed, in linear mixed models aimed at assessing associations between the change in skin scores (MRSS) or lung function (FVC) and outcomes (SF-36 PCS or HAQ scores), interaction terms between predictors (skin scores or FVC) and treatment group (autologous HSCT and conventional care) were not significant (see Supplementary Table 2 [<http://onlinelibrary.wiley.com/doi/10.1002/art.41519/abstract>]).

Numbers needed to treat. We assessed the proportion of patients whose SF-36 PCS score improved by ≥5 units and the proportion of patients whose HAQ DI scores improved by ≥0.14 units, to calculate the number needed to treat in order to achieve, on average, 1 patient with improved physical HRQoL. We found that ~4 subjects needed to be treated with autologous HSCT to have 1 of the subjects experience a clinically meaningful improvement in physical HRQoL and physical function greater than that observed with conventional care (see Supplementary Table 4, available on the *Arthritis & Rheumatology* website at <http://onlinelibrary.wiley.com/doi/10.1002/art.41519/abstract>).

Balance diagnostics and sensitivity analyses. There were differences in baseline characteristics between the 2 study groups. However, a balance in covariates included in the propensity score was achieved for all covariates, except for history of scleroderma renal crisis, after incorporating IPTW (for standardized mean differences in covariates, see Supplementary Table 5, available on the *Arthritis & Rheumatology* website at <http://onlinelibrary.wiley.com/doi/10.1002/art.41519/abstract>).

[library.wiley.com/doi/10.1002/art.41519/abstract](http://onlinelibrary.wiley.com/doi/10.1002/art.41519/abstract)). We therefore undertook 2 separate sensitivity analyses. First, we excluded patients with scleroderma renal crisis from the conventional care group. In these analyses, results were similar to those in the main analyses in terms of between-group differences in the SF-36 PCS, HAQ, and symptom scale scores (data not shown).

Second, we excluded scleroderma renal crisis from the propensity score altogether (leaving in only creatinine levels, which was, if anything, higher in the autologous HSCT group at baseline). Again, similar results as those in the main analyses were obtained for differences in the SF-36 PCS, HAQ, and symptom scale scores (data not shown).

DISCUSSION

In this study, we found that autologous HSCT was associated with early marked improvement, well beyond the MCID, in physical HRQoL and function as compared to that achieved with conventional care, and we observed that this effect was sustained over time. Improvement in specific disease symptoms was also marked and sustained. In fact, differences in disease measures between the groups seemed to increase over time from baseline. However, there were no differences in mental HRQoL scores in subjects treated with autologous HSCT as compared to those receiving conventional care. The improvements in physical HRQoL and function were supported by sustained differences in the MRSS and FVC over time in favor of the subjects treated with autologous HSCT.

These results are consistent with the purported positive impact of autologous HSCT on physical HRQoL in patients with SSc, which was reported in a recent systematic review of the literature (18). In that review, the most robust evidence was found to be from the ASTIS and SCOT trials. The ASTIS trial showed that, at 2 years, subjects who received autologous HSCT had an absolute improvement in HAQ scores of -0.6 ± 1.1 , compared to an absolute score improvement of -0.2 ± 0.8 in those who received cyclophosphamide (*P* = 0.02) (10). Similarly, subjects who

received autologous HSCT had an absolute score improvement in the SF-36 PCS summary score of 10.1 ± 15.8 , compared to an absolute score improvement of 4 ± 11.2 in those who received cyclophosphamide ($P = 0.01$). In the SCOT trial, at 54 months, 53% of the patients treated with autologous HSCT using myeloablative conditioning and total body irradiation showed an improvement of at least 0.4 points in their HAQ scores, compared to 16% of the patients in the comparator arm ($P = 0.01$), and 56% of the patients treated with autologous HSCT showed improvement of at least 10 points in their SF-36 PCS summary scores, compared to 15% in the comparator arm ($P = 0.02$) (11). Our results add to the existing literature by providing long-term data as well as data on specific HRQoL domains and disease symptoms recorded with the SHAQ.

Interestingly, in our study, there was no difference in MCS scores between participants receiving autologous HSCT and those receiving conventional care. This was consistent with the results of the ASTIS trial, which reported no difference in SF-36 MCS scores in subjects who received autologous HSCT compared to those who received cyclophosphamide (difference in score at 2 years 0.3, 95% confidence interval 5.41 to 6.07; $P = 0.91$), and was also consistent with the results of the SCOT trial, which demonstrated that 31% of patients in the autologous HSCT treatment group experienced improvement in their SF-36 MCS scores by at least 10 points, compared to 8% of patients in the cyclophosphamide arm ($P = 0.1$). This is particularly surprising, since patients undergoing autologous HSCT are typically highly motivated individuals. The reasons for the absence of improvement in mental HRQoL with autologous HSCT remain unknown and are likely multifactorial. It is possible that some nonmodifiable factors, such as age, persistent disfigurement, and work disability, may be contributors. In addition, the orthogonal scoring system of the SF-36 PCS and MCS may not adequately reflect mental health functioning in patients with SSc who have either much lower or, in this case, much improved physical functioning (31).

In post hoc analyses, we showed that there was a large difference between treatment groups in terms of functional status and HRQoL (see Supplementary Table 6, available on the *Arthritis & Rheumatology* website at <http://onlinelibrary.wiley.com/doi/10.1002/art.41519/abstract>). Indeed, autologous HSCT was associated with SF-36 PCS summary scores that were 7–8 points higher ($P = 0.009$ – 0.001) and HAQ scores that were 0.52–0.55 points lower ($P = 0.009$ – 0.005) compared to the scores in patients treated with conventional care. Those are large effect sizes and well beyond the MCIDs. These models also showed that skin scores and lung function were significantly associated with functional status and HRQoL, and that this was the same for each treatment group (nonsignificant interaction terms). Separately, we also showed that the magnitude of the effect of autologous HSCT on skin scores and FVC was much higher than that with conventional care (Table 2). Thus, the same amount of change in

skin scores or lung function achieved by either treatment has the same effect on functional status (e.g., for every 1-point decrease in the MRSSs, the HAQ score decreases by 0.03), but because the magnitude of the effect of autologous HSCT on the skin and lungs is so much greater (e.g., decreasing the MRSS score by 5–10 points more than that with conventional care), the overall impact of autologous HSCT on functional status is much larger than conventional care.

Several study limitations must be noted. First, there were differences in baseline characteristics between the 2 study groups. For this reason, we implemented advanced analytical methods that are specifically designed to overcome issues related to confounding by indication and that might result in “quasi-randomization.” After re-weighting, the balance in all covariates included in the propensity score improved, except for history of scleroderma renal crisis; sensitivity analyses in which scleroderma renal crisis was removed from the models did not affect the study results. Nevertheless, we cannot exclude the possibility that there was potential residual confounding in the results.

Second, there was heterogeneity in treatments in the comparator group. Different disease-modifying agents may have varying efficacy and side effect profiles, and this may have impacted participants' experiences. Also, the “cluster effect” needs to be considered. All participants who received autologous HSCT were living in France, and all those treated with conventional care were residents of Canada. Differences in health care systems and access to care may have impacted the study results. These limitations should be weighed against the strengths of the study, which include unique, real-world data and robust statistical modeling.

In summary, the results of this collaborative study add considerable complementary data to the repertoire of traditional biomedical outcome measures, thus further supporting the role of autologous HSCT in patients with SSc. Additional research is needed to understand the trajectories of mental HRQoL in SSc.

AUTHOR CONTRIBUTIONS

All authors were involved in drafting the article or revising it critically for important intellectual content, and all authors approved the final version to be published. Dr. Maltez had full access to all of the data in the study and takes responsibility for the integrity of the data and the accuracy of the data analysis.

Study conception and design. Maltez, Puyade, Wang, Lansiaux, Marjanovic, Baron, Colmegna, Hudson, Farge.

Acquisition of data. Wang, Lansiaux, Charles, Baron, Hudson, Farge.

Analysis and interpretation of data. Maltez, Puyade, Wang, Steele, Hudson, Farge.

REFERENCES

1. Denton CP, Khanna D. Systemic sclerosis. *Lancet* 2017;390:1685–99.
2. Domsic RT, Nihtyanova SI, Wisniewski SR, Fine MJ, Lucas M, Kwok CK, et al. Derivation and external validation of a prediction rule for five-year mortality in patients with early diffuse cutaneous systemic sclerosis. *Arthritis Rheumatol* 2016;68:993–1003.

3. Hao Y, Hudson M, Baron M, Carreira P, Stevens W, Rabusa C, et al. Early mortality in a multinational systemic sclerosis inception cohort. *Arthritis Rheumatol* 2017;69:1067–77.
4. Hudson M, Steele R, Lu Y, Thombs BD, Panopalis P, Baron M. Clinical correlates of self-reported physical health status in systemic sclerosis. *J Rheumatol* 2009;36:1226–9.
5. Volkman ER, Tashkin DP, Sim M, Li N, Goldmuntz E, Keyes-Elstein L, et al. Short-term progression of interstitial lung disease in systemic sclerosis predicts long-term survival in two independent clinical trial cohorts. *Ann Rheum Dis* 2019;7:122–30.
6. Herrick AL, Pan X, Peytrignet S, Lunt M, Hesselstrand R, Mouthon L, et al. Treatment outcome in early diffuse cutaneous systemic sclerosis: the European Scleroderma Observational Study (ESOS). *Ann Rheum Dis* 2017;76:1207–18.
7. Farge D, Marolleau JP, Zohar S, Marjanovic Z, Cabane J, Mounier N, et al. Autologous bone marrow transplantation in the treatment of refractory systemic sclerosis: early results from a French multicentre phase I-II study. *Br J Haematol* 2002;119:726–39.
8. Vonk MC, Marjanovic Z, van den Hoogen FH, Zohar S, Schattenberg AV, Fibbe WE, et al. Long-term follow-up results after autologous haematopoietic stem cell transplantation for severe systemic sclerosis. *Ann Rheum Dis* 2008;67:98–104.
9. Burt RK, Shah SJ, Dill K, Grant T, Gheorghide M, Schroeder J, et al. Autologous non-myeloablative haemopoietic stem-cell transplantation compared with pulse cyclophosphamide once per month for systemic sclerosis (ASSIST): an open-label, randomized phase 2 trial. *Lancet* 2011;378:498–506.
10. Van Laar JM, Farge D, Sont JK, Naraghi K, Marjanovic Z, Larghero J, et al. Autologous hematopoietic stem cell transplantation vs intravenous pulse cyclophosphamide in diffuse cutaneous systemic sclerosis: a randomized clinical trial. *JAMA* 2014;311:2490–8.
11. Sullivan KM, Goldmuntz EA, Keyes-Elstein L, McSweeney PA, Pinckney A, Welch B, et al. Myeloablative autologous stem-cell transplantation for severe scleroderma. *N Engl J Med* 2018;378:35–47.
12. Atkins HL, Muraro PA, van Laar JM, Pavletic SZ. Autologous hematopoietic stem cell transplantation for autoimmune disease—is it now ready for prime time? *Biol Blood Marrow Transplant* 2012;18 Suppl:S177–83.
13. Snowden JA, Saccardi R, Allez M, Ardizzone S, Arnold R, Cervera R, et al. Haematopoietic SCT in severe autoimmune diseases: updated guidelines of the European Group for Blood and Marrow Transplantation. *Bone Marrow Transplant* 2012;47:770–90.
14. Sullivan KM, Majhail NS, Bredeson C, Carpenter PA, Chatterjee S, Crofford LJ, et al. Systemic sclerosis as an indication for autologous hematopoietic cell transplantation: position statement from the American Society for Blood and Marrow Transplantation. *Biol Blood Marrow Transplant* 2018;24:1961–4.
15. Farge D, Burt RK, Oliveira MC, Mousseaux E, Rovira M, Marjanovic Z, et al. Cardiopulmonary assessment of patients with systemic sclerosis for hematopoietic stem cell transplantation: recommendations from the European Society for Blood and Marrow Transplantation Autoimmune Diseases Working Party and collaborating partners. *Bone Marrow Transplant* 2017;52:1495–503.
16. Thombs B, Jewett L, Assassi S, Baron M, Bartlett S, Maia A, et al. New directions for patient-centred care in scleroderma: the Scleroderma Patient-centred Intervention Network (SPIN). *Clin Exp Rheumatol* 2011;30:S23–9.
17. Burt RK, Farge D. Autologous HSCT is efficacious, but can we make it safer? *Nat Rev Rheumatol* 2018;14:189–91.
18. Puyade M, Maltez N, Lansiaux P, Pugno G, Roblot P, Colmegna I, et al. Health-related quality of life in systemic sclerosis before and after autologous haematopoietic stem cell transplant: a systematic review. *Rheumatology (Oxford)* 2019;59:779–89.
19. Subcommittee for Scleroderma Criteria of the American Rheumatism Association Diagnostic and Therapeutic Criteria Committee. Preliminary criteria for the classification of systemic sclerosis (scleroderma). *Arthritis Rheum* 1980;23:581–90.
20. Khanna D, Furst DE, Clements PJ, Allanore Y, Baron M, Czirjak L, et al. Standardization of the modified Rodnan skin score for use in clinical trials of systemic sclerosis. *J Scleroderma Relat Disord* 2017;2:11–8.
21. Steele R, Hudson M, Lo E, Baron M, on behalf of the Canadian Scleroderma Research Group. Clinical decision rule to predict the presence of interstitial lung disease in systemic sclerosis. *Arthritis Care Res (Hoboken)* 2012;64:519–24.
22. Ware J. User's manual for the SF-36v2 health survey: with a supplement documenting SF-12 health survey. 2nd ed. Lincoln (RI): QualityMetric, Inc.; 2007.
23. Georges C, Chassany O, Mouthon L, Tiev K, Marjanovic Z, Meyer O, et al. Évaluation de la qualité de vie par le MOS-SF36 dans la sclérodemie systémique. *Rev Méd Interne* 2004;25:16–21.
24. Hudson M, Thombs BD, Steele R, Panopalis P, Newton E, Baron M, on behalf of the Canadian Scleroderma Research Group. Health-related quality of life in systemic sclerosis: a systematic review. *Arthritis Rheum* 2009;61:1112–20.
25. Khanna D, Furst DE, Wong WK, Tsevat J, Clements PJ, Park GS, et al. Reliability, validity, and minimally important differences of the SF-6D in systemic sclerosis. *Qual Life Res* 2007;16:1083–92.
26. Kosinski M, Zhao SZ, Dedhiya S, Osterhaus JT, Ware JE Jr. Determining minimally important changes in generic and disease-specific health-related quality of life questionnaires in clinical trials of rheumatoid arthritis. *Arthritis Rheum* 2000;43:1478–87.
27. Pope J. Measures of systemic sclerosis (scleroderma): Health Assessment Questionnaire (HAQ) and Scleroderma HAQ (SHAQ), physician- and patient-rated global assessments, Symptom Burden Index (SBI), University of California, Los Angeles, Scleroderma Clinical Trials Consortium Gastrointestinal Scale (UCLA SCTC GIT) 2.0, Baseline Dyspnea Index (BDI) and Transition Dyspnea Index (TDI) (Mahler's Index), Cambridge Pulmonary Hypertension Outcome Review (CAMPHOR), and Raynaud's Condition Score (RCS). *Arthritis Care Res (Hoboken)* 2011;63 Suppl 11:S98–111.
28. Georges C, Chassany O, Mouthon L, Tiev K, Toledano C, Meyer O, et al. Validation of French version of the Scleroderma Health Assessment Questionnaire (SSc HAQ). *Clin Rheumatol* 2005;24:3–10.
29. Steen VD, Medsger TA Jr. The value of the Health Assessment Questionnaire and special patient-generated scales to demonstrate change in systemic sclerosis patients over time. *Arthritis Rheum* 1997;40:1984–91.
30. Butler EA, Baron M, Fogo AB, Frech T, Ghossein C, Hachulla E, et al. Generation of a core set of items to develop classification criteria for scleroderma renal crisis using consensus methodology. *Arthritis Rheumatol* 2019;71:964–71.
31. Hudson M, Thombs B, Baron M. Are the Short Form 36 Physical and Mental Component Summary scores useful measures in patients with systemic sclerosis? Comment on the article by Rannou et al [letter]. *Arthritis Rheum* 2007;57:1339–40.

Cancer in Systemic Sclerosis: Analysis of Antibodies Against Components of the Th/To Complex

Christopher A. Mecoli,  Brittany L. Adler, Qingyuan Yang, Laura K. Hummers, Antony Rosen, Livia Casciola-Rosen,  and Ami A. Shah 

Objective. The aim of this study is to describe 4 of the most common autoantibodies against components of the Th/To complex: human POP1 (hPOP1), RPP25, RPP30, and RPP40. We report their prevalence and clinical characteristics in a systemic sclerosis (SSc) population, and determine whether these specificities are associated with cancer.

Methods. A case–control study was performed using data from the Johns Hopkins Scleroderma Center Cohort. A total of 804 adult patients with SSc were included; 401 SSc patients with no history of cancer after at least 5 years of disease were compared to 403 SSc patients who ever had a history of cancer. Antibodies against hPOP1, RPP25, RPP30, and RPP40 were assayed by immunoprecipitation of ³⁵S-methionine–labeled proteins generated by in vitro transcription/translation. Demographic and clinical characteristics were compared between groups.

Results. Of 804 patients, 67 (8.3%) had antibodies against any component of the Th/To complex. Patients with antibodies to any component were significantly more likely to have limited cutaneous disease, less likely to have tendon friction rubs, and more likely to have findings consistent with interstitial lung disease or pulmonary hypertension. Patients with antibodies against hPOP1, RPP25, RPP30, and/or RPP40 were significantly less likely to develop cancer within 2 years of SSc onset (0% versus 11% of antibody-negative patients; $P = 0.009$).

Conclusion. SSc patients who produce autoantibodies to components of the Th/To complex have a clinical phenotype characterized by limited cutaneous disease and pulmonary involvement. Our findings show that the presence of any Th/To autoantibody may have a protective effect against contemporaneous cancer.

INTRODUCTION

Important new insights into the relationship between systemic sclerosis (SSc; scleroderma) and cancer have emerged over the past decade. Recent research has highlighted that both time and autoantibodies are critical filters in risk-stratifying SSc patients for malignancy (1,2). Whereas some autoantibody specificities have been demonstrated to confer an increased risk of cancer around the time of SSc symptom onset (e.g., anti–RNA polymerase III [anti–RNA Pol III] or anti–RNPC3), others have suggested a protective role (e.g., anticentromere or the combined presence of anti–RNA Pol III and anti–RPA194 antibodies) (2–4). Furthermore, our group has observed that SSc patients lacking antibodies

against centromere, topoisomerase I, and RNA Pol III may have an increased risk of cancer-associated scleroderma (1,4). To address the important question of whether there are additional SSc antibody specificities that are associated with cancer (either protectively or as markers of increased risk), we developed a large, meticulously phenotyped case–control cohort of SSc patients with or without malignancy. In this study, we investigated the relationship between antibodies against 4 well-defined components of the Th/To complex and SSc/cancer status.

The ribonuclease mitochondrial RNA processing complex (RNase MRP) and ribonuclease P (RNase P) are both enzymes that are involved in processing ribosomal, mitochondrial, and transfer RNA. In the early 1980s, sera from SSc patients were found to have

Supported by the National Institute of Arthritis and Musculoskeletal and Skin Diseases, NIH (grants 1K23-AR-075898 and AR-073208) and the Scleroderma Research Foundation. The Rheumatic Diseases Research Core Center is supported by the NIH (grant P30-AR-070254). Dr. Mecoli is a Jerome L. Greene Scholar. Dr. Adler's work was supported by the NIH (grant T32-AR-048522). Drs. Casciola-Rosen and Shah's work was supported in part by the Donald B. and Dorothy L. Stabler Foundation.

Christopher A. Mecoli, MD, MHS, Brittany L. Adler, MD, Qingyuan Yang, MD, PhD, Laura K. Hummers, MD, ScM, Antony Rosen, MBChB, BSc, Livia

Casciola-Rosen, PhD, Ami A. Shah, MD, MHS: Johns Hopkins University, Baltimore, Maryland.

Drs. Casciola-Rosen and Shah contributed equally to this work.

No potential conflicts of interest relevant to this article were reported.

Address correspondence to Livia Casciola-Rosen, PhD, Johns Hopkins University, Division of Rheumatology, Department of Medicine, 5200 Eastern Avenue, Mason F. Lord Building, Center Tower, Suite 5300, Baltimore, MD 21224. Email: lcr@jhmi.edu.

Submitted for publication March 20, 2020; accepted in revised form August 11, 2020.

autoantibodies directed against these complexes (5,6), and the nomenclature evolved to designate “anti-Th” for RNase MRP and “anti-To” for RNase P. In subsequent decades, at least 9 individual proteins associated with each of these complexes have been isolated and characterized (human POP1 [hPOP1], hPOP4, hPOP5, RPP14, RPP20, RPP21, RPP25, RPP30, and RPP40) (7,8). Many components have been described as targets of autoantibodies in SSc, and are collectively referred to as anti-Th/To antibodies. Prior studies have concluded that the prevalence of these antibodies in SSc patients is generally low (5–15%), and the clinical phenotype is consistent with the CREST syndrome (calcinosis, Raynaud’s phenomenon, esophageal dysmotility, sclerodactyly, telangiectasias) or limited cutaneous SSc (9–11). However, those studies were performed in relatively small SSc cohorts and did not assess autoantibodies to individual components of the Th/To complex. Furthermore, how the components relate to one another and their association with cancer has not been explored to date.

In the present report, we describe the prevalence and clinical characteristics of SSc patients who test positive for 4 of the most common autoantibodies of the Th/To complex: hPOP1, RPP25, RPP30, and RPP40. We show that patients with autoantibodies to any of these 4 components of the Th/To complex are protected against cancer-associated SSc and possess a clinical phenotype most notable for pulmonary involvement.

PATIENTS AND METHODS

Patients. A case–control study was performed using data and banked sera from the Johns Hopkins Scleroderma Center Cohort. A total of 804 adult patients with SSc were included, 97% of whom met the American College of Rheumatology/European League Against Rheumatism 2013 classification criteria for SSc (12). A total of 401 SSc patients who had no history of cancer after at least 5 years of disease (median follow-up 14 years [interquartile range (IQR) 9–24]) were compared to 403 SSc patients who ever had a history of cancer. Patient-reported cancer diagnoses were validated by review of medical records and pathology reports when available. Of the 403 patients with cancer, 94 had a nonmelanoma skin cancer (basal and squamous cell carcinomas). The time interval between cancer diagnosis and SSc onset, defined by the first of either the onset of Raynaud’s phenomenon or the first non-Raynaud’s symptom, was calculated. The cancer–SSc interval was further binned into 3 time windows (± 2 , 3, or 5 years) that may suggest the presence of cancer-associated SSc, as previously defined (4,13).

The following clinical variables are prospectively collected in the Johns Hopkins Scleroderma Center Database: Medsger organ-specific scleroderma severity scores (14), modified Rodnan skin thickness score (15), echocardiogram data including ejection fraction (EF) and right ventricular systolic pressure (RVSP), pulmonary function test data including forced vital

capacity (FVC) and diffusing capacity for carbon monoxide (DL_{CO}) (standardized for age and sex and reported as percent predicted [16,17]), cutaneous subtype (18), presence/history of scleroderma renal crisis, tendon friction rubs, myopathy, and synovitis. Patients were referred for right-sided heart catheterization (RHC) at the discretion of the treating rheumatologist as previously described (19). Pulmonary hypertension (PH) was defined as a mean pulmonary artery pressure (PAP) ≥ 21 mm Hg obtained by RHC as recently recommended by the 6th World Symposium on Pulmonary Hypertension (20). Sensitivity analyses were performed using the prior cutoff of a mean PAP of ≥ 25 mm Hg. The Johns Hopkins Institutional Review Board approved this study protocol.

Autoantibody assays. Complementary DNAs encoding full-length FLAG-tagged hPOP1, RPP40, RPP30, and RPP25 were cloned (RPP30) or purchased (RPP40 and POP1 from Origene). DNAs were sequence verified, and used to generate ³⁵S-methionine-labeled proteins by in vitro transcription/translation (IVTT) reactions, per the manufacturer’s protocol (Promega). Immunoprecipitations (IPs) were performed using these products as input; the washed IPs were electrophoresed on 10% sodium dodecyl sulfate–polyacrylamide gel electrophoresis gels and visualized by fluorography (21). An anti-FLAG IP was included in each sample set, and fluorogram exposures were standardized to give anti-FLAG IP bands of similar intensity. All IPs were quantitated by densitometric scanning and normalized to the FLAG IP reference included in the set. Sera from 34 healthy controls

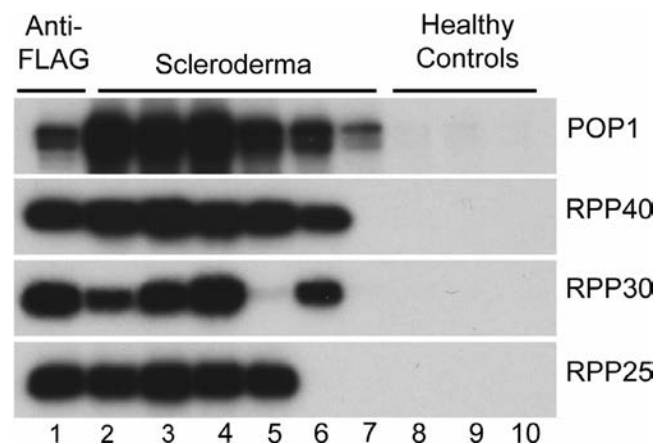


Figure 1. Immunoprecipitation (IP) assay to identify antibodies against 4 different components of the Th/To complex. Sera from 6 scleroderma patients (lanes 2–7) and 3 healthy controls (lanes 8–10) were used for IP analysis of ³⁵S-methionine-labeled human POP1 (hPOP1), RPP40, RPP30, or RPP25 generated by in vitro transcription/translation. The hPOP1 antibodies were detected in all 6 scleroderma patients, RPP40 antibodies were found in 5 (absent in patient 7), RPP30 antibodies were present in 4 (absent in patients 5 and 7), and RPP25 antibodies were present in 4 (absent in patients 6 and 7). An anti-FLAG calibrator IP, performed using an anti-FLAG monoclonal antibody (Sigma), is shown in lane 1 of each set.

Table 1. Demographic and clinical characteristics of the SSc patients without a history of cancer and SSc patients with a history of cancer*

Characteristic	SSc patients without a history of cancer (n = 401)	SSc patients with a cancer history (n = 309)†	P
Sex, female	345 (86)	254 (82)	0.1760
Ethnicity, Hispanic	18 (9)	3 (2)	0.0020
Race			
White	292 (73)	277 (89)	<0.0001
African American	81 (20)	23 (7)	
History of smoking (ever)	185 (47)	161 (52)	0.1490
Age at SSc symptom onset (RP or non-RP), median (IQR)	39.5 (28–49)	48.2 (38–58)	<0.0001
Met ACR 2013 criteria	387 (97)	300 (97)	1.0000
Duration of follow-up, median (IQR) years	14.4 (9–24)	12.6 (6–23)	0.0969
Disease duration upon cohort entry, median (IQR) years	6.5 (2.6–15)	4.9 (1.5–15)	0.0740
Cutaneous subtype			
Scleroderma sine sclerosis	13 (3)	9 (3)	0.2730
Limited	214 (53)	144 (46)	
Type II skin	36 (9)	33 (11)	
Diffuse	138 (34)	124 (40)	
Cutaneous subtype (limited versus diffuse)	138 (34)	124 (40)	0.1170
Maximum modified Rodnan skin thickness score, median (IQR)	6 (3–17)	9 (4–20)	0.0030
History of scleroderma renal crisis	16 (4)	19 (6)	0.2220
Minimum FVC % predicted over follow-up, median (IQR)‡	70 (54–84)	70 (57–84)	1.0000
Maximum RVSP, median (IQR)§	37 (32–50)	40 (33–53)	0.0700
Pulmonary hypertension (mean PAP >20 mm Hg)¶	60 (15)	41 (13)	0.5880
Pulmonary hypertension (mean PAP >24 mm Hg)¶	54 (13)	37 (12)	0.5730
Presence of baseline TFR	35 (9)	41 (13)	0.0660
Presence of synovitis on any examination	84 (21)	68 (22)	0.7820
Deceased	124 (31)	131 (44)	0.0010
Serology			
Any Th/To component (hPOP1, RPP25, RPP30, or RPP40)	36 (9)	23 (7)	0.4950
hPOP1	36 (9)	22 (7)	0.4090
RPP25	23 (6)	12 (4)	0.2970
RPP30	24 (6)	20 (6)	0.8760
RPP40	31 (8)	23 (7)	1.0000

* Except where indicated otherwise, values are the number (%). Patients with a history of cancer were more likely to be white, older at systemic sclerosis (SSc) onset, and have a higher modified Rodnan skin thickness score. RP = Raynaud's phenomenon; IQR = interquartile range; ACR = American College of Rheumatology; FVC = forced vital capacity; RVSP = right ventricular systolic pressure; PAP = pulmonary artery pressure; TFR = tendon friction rub; hPOP1 = human POP1.

† Excluding nonmelanoma skin cancers.

‡ Data were available for 668 patients.

§ Data were available for 590 patients.

¶ Data were available for 148 patients.

banked at the Johns Hopkins site were also tested by IP with each of the IVTT products; an anti-FLAG IP was included in each of these control sets as a reference calibrator. No IP band

Table 2. Number of Th/To subunit specificities in individual patients with SSc*

No. of subunit specificities (hPOP1, RPP25, RPP30, and RPP40)	No. (%) of patients
0	737 (91.67)
1	6 (0.75)
2	4 (0.50)
3	25 (3.11)
4	32 (3.98)
Total	804 (100.00)

* The majority of systemic sclerosis (SSc) patients had antibodies against multiple (>2) subunits. Of the 6 patients with antibodies against only 1 Th/To subunit, most were high-titer positive (+/+/+/+) (4 of 5 with anti-human POP1 [anti-hPOP1] and 0 of 1 with anti-RPP40).

was detected with any of the healthy control sera (see Figure 1 for representative examples). The cutoff for antibody positivity was assigned a calibrated optical density (OD) value of 5 units, which corresponded to the faintest reproducible IVTT-IP band detectable by eye (calibrated OD values ["units"] ranged from 5 to 127). Representative examples of IPs using each of the IVTT products are shown in Figure 1. Cutoffs were defined as follows: negative = <5 units, + = 5–15 units, ++ = >15–50 units, and +++ = >50 units.

Given prior studies demonstrating that the risk of cancer-associated SSc may be modified by the presence of additional immune responses, we were interested in testing whether positivity for any of the anti-Th/To components conferred cancer protection among patients with anti-RNA Pol III antibodies. Anti-RNA Pol III antibody status was determined by line blot assays using the Euroimmun platform (Euroimmun Diagnostics).

Statistical analysis. Statistical analysis was performed using Stata software version 14. The primary analysis excluded nonmelanoma skin cancers (basal and squamous cell carcinomas), with secondary analyses including all cancers. For comparison between groups, Fisher's exact test was used for categorical/binary variables and rank sum test for comparison between continuous variables given a non-normal distribution. Medsger organ-specific severity scores were analyzed as an ordinal variable using the Kruskal-Wallis test. *P* values less than 0.05 were considered significant, adjusting for multiple comparison testing.

RESULTS

Demographic and clinical characteristics of scleroderma patients with or without cancer. The majority of patients were white women, and the mean \pm SD SSc disease duration was 5.9 ± 11 years (Table 1). Comparing SSc patients with a history of cancer (excluding nonmelanoma skin cancer) to those without, patients with cancer were significantly less likely to be Hispanic (2% versus 9%; *P* = 0.002), more likely to be white (89% versus 73%; *P* < 0.0001), and older at SSc symptom onset (median 48.2 years [IQR 38–58] versus 39.5 years [IQR 28–49]; *P* < 0.0001). SSc patients with cancer had an overall higher maximum MRSS (median 9 [IQR 4–20] versus 6 [IQR 3–17]; *P* = 0.003) and had a higher mortality (44% versus 31%; *P* = 0.001). Medsger organ-specific severity scores were comparable between groups, with the notable exception of Raynaud's severity score, which was less severe in the cancer group (*P* = 0.002).

Additional demographic and clinical variables are depicted in Table 1. After adjustment for multiple comparisons (*P* = 0.05/30 variables equates to a significance threshold of <0.002), only ethnicity, race, and mortality remained significant. Similar patterns were observed when comparing SSc patients with any cancer (including nonmelanoma skin cancers; *n* = 403) to patients without cancer with regard to race, ethnicity, and age at onset of SSc (Supplementary Table 1, available on the *Arthritis & Rheumatology* website at <http://onlinelibrary.wiley.com/doi/10.1002/art.41493/abstract>). With the inclusion of nonmelanoma skin cancers, mortality was no longer significantly different, and patients with cancer had a significantly shorter disease duration (5 years versus 6.5 years; *P* < 0.004).

A total of 67 (8.3%) of 804 patients had antibodies against any component of the Th/To complex, with no differences in frequency noted between the cancer and no-cancer groups (Table 1). Of the 67 anti-Th/To-positive patients, 10 (15%) had antibodies against 1 or 2 components, while the majority (57 [85%] of 67) had antibodies targeting 3 or 4 components (Table 2). Given that so few patients produced autoantibodies to only 1 or 2 components, we explored whether these were borderline/low positives. Of the 6 patients with antibodies against only 1 Th/To subunit (5 anti-hPOP1 and 1 anti-RPP40), 4 were moderate/high titer (all were anti-hPOP1).

Clinical phenotype of patients with antibodies against different Th/To components. Patients who were positive for each Th/To antibody specificity (hPOP1, RPP25, RPP30, and RPP40) were compared to all other SSc patients in the cohort with regard to demographic and SSc characteristics (Table 3). Patients with antibodies to any of the 4 components were more likely to have a smoking history, limited cutaneous disease and thus a lower median maximum MRSS, and a lower prevalence of tendon friction rubs.

Upon analyzing associations between Medsger severity scores for individual organ systems and anti-hPOP1 antibodies, significant associations were observed with less severe GI disease (*P* = 0.012) and more severe lung disease (*P* = 0.011). Similarly, patients with antibodies against RPP40 had less severe GI disease (*P* = 0.034) and more severe lung disease (*P* = 0.016). Anti-RPP30-positive patients were more likely to have severe lung disease (*P* = 0.020). No associations between Medsger individual organ system severity scores and anti-RPP25 antibodies were observed.

Given the absence of comprehensive high-resolution computed tomography (CT) scan data in our cohort, we focused on Medsger lung severity scores (which incorporate pulmonary function test parameters and need for supplemental oxygen) as well as RHC data. Patients with antibodies to any of the Th/To components were more likely to have worse pulmonary disease as defined by a higher maximum Medsger lung severity score (*P* = 0.013 by Kruskal-Wallis test). When analyzing for the presence of severe lung disease (defined by an FVC or DL_{CO} <50% predicted or oxygen use required), patients with antibodies against hPOP1, RPP30, or RPP40 had significantly worse lung severity: 60% versus 37% for hPOP1 (*P* = 0.001), 61% versus 37% for RPP30 (*P* = 0.002), and 59% versus 37% for RPP40 (*P* = 0.001). When examining FVC alone as a surrogate for interstitial lung disease (ILD), patients with antibodies to any of the Th/To components were more likely to have severe restriction (FVC <50%) compared to those without antibodies to Th/To components (27% versus 17%; *P* = 0.088). Only anti-hPOP1-positive patients were more likely to develop PH (23% versus 14%; *P* = 0.042). Upon raising the threshold for defining PH to a mean PAP of ≥ 25 mm Hg, anti-hPOP1-positive, anti-RPP30-positive, or anti-RPP40-positive patients were more likely to develop PH (22% versus 12% for hPOP1 [*P* = 0.03], 23% versus 12% for RPP30 [*P* = 0.04], and 21% versus 12% for RPP40 [*P* = 0.04]).

Cancer risk and antibodies against Th/To components.

Among all patients with autoantibodies to at least 1 component of the Th/To complex (*n* = 67), 31 patients had a total of 38 cancers (including nonmelanoma skin cancer). Excluding nonmelanoma skin cancer, 23 patients had a cancer history (with 26 cancers). The presence of antibodies to Th/To components (hPOP1, RPP25, RPP30,

Table 3. Demographic and clinical features of the SSc patients by prevalence of antibodies against various subunits of the Th/T_H complex*

	hPOP1		RPP25		RPP30		RPP40					
	Negative (n = 739)	Positive (n = 65)	Pt	Negative (n = 762)	Positive (n = 42)	Pt	Negative (n = 756)	Positive (n = 48)	Pt	Negative (n = 742)	Positive (n = 62)	Pt
Sex, female	621 (84)	54 (83)	0.8600	640 (84)	35 (83)	0.8310	635 (84)	40 (83)	0.8410	624 (84)	51 (82)	0.7190
Ethnicity, Hispanic	21 (5)	1 (3)	1.0000	21 (5)	1 (5)	0.6130	21 (5)	1 (5)	1.0000	21 (5)	1 (3)	1.0000
Race												
White	609 (82)	52 (80)	0.8860	628 (82)	33 (79)	0.7460	621 (82)	40 (83)	0.8880	609 (82)	52 (84)	0.9440
African American	94 (13)	11 (17)		97 (13)	8 (19)		98 (13)	7 (15)		96 (13)	9 (15)	
Ever smoker	347 (48)	39 (61)	0.0500	358 (48)	28 (68)	0.0100	356 (48)	30 (64)	0.0350	348 (47)	38 (62)	0.0320
Age at SSc symptom onset (RP or non-RP), median (IQR) years	44 (33-55)	42 (32-48)	0.1200	44 (33-55)	43 (37-51)	0.6360	44 (33-55)	44 (32-54)	0.8740	44 (33-55)	43 (32-53)	0.5120
Disease duration upon cohort entry, median (IQR) years	5.6 (1.9-15)	9.8 (4.2-16)	0.1150	5.7 (1.9-15)	9.8 (4.4-15)	0.0760	6 (1.9-15)	10 (3.6-16)	0.0960	5.5 (1.9-15)	10 (4.4-16)	0.0230
Cutaneous subtype												
Sine	26 (4)	1 (2)	<0.0001	26 (3)	1 (2)	<0.0001	26 (3)	1 (2)	<0.0001	26 (4)	1 (2)	<0.0001
Limited	356 (48)	53 (82)		376 (49)	33 (79)		369 (49)	40 (83)		358 (48)	51 (82)	
Type I skin	74 (10)	5 (8)		74 (10)	5 (12)		74 (10)	5 (10)		74 (10)	5 (8)	
Diffuse	283 (38)	6 (9)	<0.0001	286 (38)	3 (7)	<0.0001	287 (38)	2 (4)	<0.0001	284 (38)	5 (8)	<0.0001
Cutaneous subtype (limited versus diffuse)	283 (38)	6 (9)	<0.0001	286 (38)	3 (7)	<0.0001	287 (38)	2 (4)	<0.0001	284 (38)	5 (8)	<0.0001
Maximum MRSS, median (IQR)	8 (4-19)	4 (3-6)	<0.0001	7 (4-19)	4 (2-6)	<0.0001	7 (4-19)	4 (3-6)	<0.0001	8 (4-19)	4 (3-6)	<0.0001
History of SRC	39 (5)	1 (2)	0.2430	39 (5)	1 (2)	0.7160	39 (5)	1 (2)	0.5050	39 (5)	1 (2)	0.3560
Minimum FVC % predicted over follow-up, median (IQR)	72 (56-86)	69 (47-81)	0.7910	72 (56-85)	70 (52-81)	0.7450	72 (56-86)	66 (42-81)	0.4420	72 (56-86)	70 (46-82)	0.6840
Maximum RVSP, median (IQR) mm Hg	38 (32-50)	40 (34-63)	0.2020	38 (32-50)	41 (34-65)	0.3500	38 (32-50)	42 (34-66)	0.2250	38 (32-50)	40 (34-63)	0.1140
PH (mean PAP >20 mm Hg)	100 (14)	15 (23)	0.0420	107 (14)	8 (19)	0.3650	104 (14)	11 (23)	0.0890	101 (14)	14 (23)	0.0590
PH (mean PAP >24 mm Hg)	87 (12)	14 (22)	0.0310	93 (12)	8 (20)	0.2270	90 (12)	11 (23)	0.0400	88 (12)	13 (21)	0.0460
Baseline TFR	81 (11)	0 (0)	0.0010	81 (11)	0 (0)	0.0160	81 (11)	0 (0)	0.0110	81 (11)	0 (0)	0.0020
Presence of synovitis on any examination	153 (21)	14 (22)	0.8740	158 (21)	9 (21)	0.8480	156 (21)	11 (23)	0.7140	155 (21)	12 (19)	0.8710
Deceased	246 (34)	24 (38)	0.5830	256 (34)	14 (34)	1.0000	248 (33)	22 (46)	0.0850	246 (34)	24 (39)	0.4000

* Patients with antibodies against any subunit tended to have limited cutaneous disease, a lower modified Rodnan skin thickness skin (MRSS), and fewer tendon friction rubs (TFRs). Except where indicated otherwise, values are the number (%). SSc = systemic sclerosis; hPOP1 = human POP1; RP = Raynaud's phenomenon; SRC = scleroderma renal crisis; FVC = forced vital capacity; RVSP = right ventricular systolic pressure; PH = pulmonary hypertension; PAP = pulmonary artery pressure.

† By Fisher's exact test for binary and categorical variables; by rank sum test for nonparametric continuous variables.

Table 4. Prevalence of cancer among SSc patients stratified by antibodies against individual Th/To subunits*

	Any component			hPOP1			RPP25			RPP30			RPP40		
	Positive	Negative	P	Positive	Negative	P	Positive	Negative	P	Positive	Negative	P	Positive	Negative	P
Cancer ever	23 (34)	286 (39)	0.514	22 (34)	287 (39)	0.506	12 (29)	297 (39)	0.196	20 (42)	289 (38)	0.648	23 (37)	286 (39)	0.892
Cancer within 5 years	4 (8)	110 (20)	0.055	4 (8.5)	110 (20)	0.078	1 (3)	113 (20)	0.018	4 (13)	110 (19)	0.486	4 (9)	110 (19)	0.109
Cancer within 3 years	2 (2)	83 (16)	0.048	2 (4)	83 (16)	0.047	1 (3)	84 (15)	0.069	2 (7)	85 (15)	0.290	2 (5)	83 (15)	0.069
Cancer within 2 years	0 (0)	58 (11)	0.009	0 (0)	58 (11)	0.016	0 (0)	58 (11)	0.061	0 (0)	58 (11)	0.061	0 (0)	58 (11)	0.025

* In general, antibodies against Th/To subunit(s) appeared to have a protective effect against cancer, with shorter-interval cancers being the most protected. Some analyses were limited by too few cancers in the anti-Th/To-positive group, preventing conclusions about the relationship between the number of anti-Th/To specificities (epitope spreading) and cancer risk. This analysis excluded nonmelanoma skin cancers; other analyses that included nonmelanoma skin cancer in the cancer group or in the cancer-negative group generated similar findings. Values are the number (%). SSc = systemic sclerosis; hPOP1 = human POP1.

and RPP40) conferred a protective effect against cancer-associated scleroderma (excluding nonmelanoma skin cancers from analysis) (Table 4). Patients with antibodies against hPOP1, RPP25, RPP30, and/or RPP40 were significantly less likely to develop cancer within 2 years of SSc onset compared to antibody-negative patients (0% versus 11%; $P = 0.009$). When examining the cancer-scleroderma interval among all patients with cancer, for antibodies against all of the components except RPP25, as the interval between SSc onset and cancer shortened, the protective effect increased. Indeed, no patient with antibodies against any of the 4 components developed cancer within 2 years of SSc onset.

Upon performing secondary analyses including all cancers (that is, including nonmelanoma skin cancer), the magnitude of protection lessened, with only anti-RPP40 antibodies remaining statistically significant as a protective factor against cancer diagnosed within 2 years of SSc symptom onset (3% versus 18% of antibody-negative patients; $P = 0.04$) (Supplementary Table 2, available on the *Arthritis & Rheumatology* website at <http://online.library.wiley.com/doi/10.1002/art.41493/abstract>). We were unable to investigate whether there was a dose-response relationship (e.g., a decreasing prevalence of cancer with an increasing number of autoantibodies to Th/To components) because in the 10 patients with 1 or 2 autoantibodies to Th/To components, only 1 developed cancer (Supplementary Table 3, available on the *Arthritis & Rheumatology* website at <http://onlinelibrary.wiley.com/doi/10.1002/art.41493/abstract>).

Given the association between anti-Th/To antibodies and lung disease, we were interested in investigating the frequency of lung cancer in patients with anti-Th/To antibodies. Of the 31 Th/To antibody-positive patients with a history of cancer, 7 had lung cancer. Limiting the analysis to only the time period within 2, 3, and 5 years surrounding SSc symptom onset, the numbers of lung cancer cases were 0, 0, and 0 (all 7 lung cancers were outside of the ± 5 -year window from SSc symptom onset). Of the 7 patients, all had radiographic ILD on high-resolution CT imaging, and 6 were smokers.

Given the known association of RNA Pol III autoantibodies and cancer risk in SSc, we sought to identify whether any patients produced autoantibodies to both RNA Pol III and one of the Th/To components, and what resulting effect on cancer risk these dual immune responses may have. Nine patients produced both hPOP1 and RNA Pol III autoantibodies, and none had cancer-associated SSc within 3 years. In contrast, patients with RNA Pol III antibodies without antibodies to Th/To components had a significantly increased risk of cancer-associated SSc (24% of SSc patients with RNA Pol III autoantibodies had cancer-associated SSc, defined as cancer excluding nonmelanoma skin cancer, within 3 years of SSc onset compared to 11% without RNA Pol III; $P < 0.0001$). Of the 67 patients with antibodies to at least 1 component of the Th/To complex, few had autoantibodies to the other common SSc specificities: CENP-A (3%; $n = 2$), CENP-B (7%; $n = 5$), or Scl-70 (7%; $n = 5$), as assayed

on a Euroimmun Platform. One patient had both CENP-A and CENP-B antibodies.

DISCUSSION

In this article, we describe the prevalence of autoantibodies to 4 major components of the Th/To complex in SSc patients. This is the largest study performed on Th/To antibodies to date. Our findings highlight the clinical phenotype and negative association of these antibodies with cancer. We reported a prevalence of 8.3% for antibodies against any of the components, with antibody prevalences against the individual complex components ranging from 4% to 9%. These prevalences are consistent with prior research on anti-Th/To prevalence defined by IP in cohorts from Japan (14 [4.6%] of 303) (9), the Netherlands (12 [7%] of 172 SSc patients with nucleolar pattern on antinuclear antibodies) (22,23), and the US (23 [15.4%] of 149) (24). With regard to the clinical phenotype, we have shown that patients with antibodies to any of the 4 components are more likely to have limited cutaneous disease and an increased risk of lung involvement. This finding is also consistent with published findings in SSc cohorts from Japan (5 [36%] of 14 with ILD) (9) and the US (6 [26%] of 23 with ILD) (24). In our study, 19–23% of patients with antibodies to 1 of the 4 components had PH. This finding is similar to the reported prevalence of PH in different SSc cohorts which showed that 33% (63 of 193) of anti-Th/To-positive patients have PH (25).

A main aim of this study was to explore the association with cancer for autoantibodies against each of the 4 Th/To components. Patients with antibodies against hPOP1, RPP25, RPP30, and/or RPP40 were significantly less likely to develop cancer within 2 years of SSc onset (0% versus 11%; $P = 0.009$). This potential protective effect of anti-hPOP1, anti-RPP40, anti-RPP30, and anti-RPP25 antibodies on cancer-associated SSc is a novel observation. Similar observations have been reported by our group regarding anticentromere antibodies protecting against cancer overall in SSc patients (4). Given that so few patients produced autoantibodies to only 1 or 2 components (the majority produced autoantibodies to >2), we were limited in our power to detect any dose-response relationship. Such an observation might support the notion of epitope spreading and warrants further study.

Given prior studies demonstrating that the risk of cancer-associated SSc may be modified by the presence of additional immune responses, we were interested in testing whether positivity to any of the anti-Th/To components conferred cancer protection among patients with anti-RNA Pol III antibodies. Of the 9 patients who produced both anti-Th/To autoantibodies and anti-RNA Pol III antibodies, none had cancer-associated SSc (defined as cancer occurring within 3 years of SSc symptom onset). Although small in number, this observation may signify the ability of anti-Th/To to modify cancer risk conferred by RNA Pol III autoantibodies. Similar findings have been reported with the large subunit of RNA polymerase I (RPA194): in a cohort of patients

with anti-RNA Pol III antibodies, anti-RPA194 was enriched in the group without cancer (18% versus 3.8%; $P = 0.003$) (3). In this context, it is interesting to note that RNase P has been reported to play a role in the transcription of RNA polymerases I and III (26,27), and often forms complexes with both enzymes.

The relationship between autoantibodies to individual components of the RNase MRP and RNase P complexes has been poorly described to date. Several prior studies have described the prevalence of anti-RPP'X' in small numbers of patients ($n < 15$). Adding to the complexity is that different definitions have been used to describe what constitutes anti-Th/To positivity. In one study (9) of 14 anti-Th/To-positive patients (defined by precipitation of a group of 6 proteins ranging in size from 18–120 kd), 12 (86%) were positive for anti-RPP30, and 13 (93%) were positive for anti-hPOP1. Another study of 12 anti-Th/To-positive patients (defined as the ability of serum to immunoprecipitate RNase MRP and RNase P RNA) demonstrated that the majority recognized hPOP1 and/or RPP25, but relatively few recognized RPP40 or RPP30 (22).

Given that there are at least 9 individual proteins comprising the Th/To complex, individuals with autoantibodies to any of the components could technically be considered positive for Th/To antibodies. Based on the literature, we chose to focus on the 4 most prevalent autoantigens of the Th/To complex in the present study. A potential limitation of our study is that because the other components were not assayed, there is a possible risk of misclassifying the Th/To antibody status of some patients. In the present study, using single-input IP of ^{35}S -methionine-labeled proteins generated by IVTT from the relevant DNAs, the majority of patients (85%) had antibodies to 3 or more components of the Th/To complex. Whether these patients also produce autoantibodies to additional components of the Th/To complex (e.g., hPOP5, RPP14, etc.) warrants further study.

A potential limitation of our study is the possibility that cancer status may have been misclassified for those patients who developed cancer beyond the 5-year window. Our case-control study design is also a potential limitation, as it provides a cohort enriched for cancer, potentially biasing the general phenotype of SSc patients under study. However, the large number of patients studied likely mitigates this risk. Our cohort did not have comprehensive data on variables to define ILD radiographically. As such, we presented data on the presence of a severe restrictive ventilatory defect as a surrogate for ILD. In addition, given the small number of patients with antibodies to only 1 or 2 components of the 4 that were studied, we were unable to comment definitively on differences in demographic or disease characteristics based on the different numbers/combinations of anti-Th/To components produced. Future studies investigating the order and timing of antibody generation against different components of the Th/To complex are likely to provide additional important insights into how the immune response evolves.

In this study, we assayed autoantibodies to different components of the Th/To complex in a large, meticulously phenotyped

cohort of SSc patients with and without cancer. Our data demonstrate that most patients produce autoantibodies to multiple components of the complex, and have a phenotype characterized by pulmonary disease. Our findings show, for the first time, that the presence of any Th/To autoantibody may have a protective effect against contemporaneous cancer. Furthermore, patients producing autoantibodies to the Th/To complex should be vigilantly followed up for the development of pulmonary complications of SSc.

AUTHOR CONTRIBUTIONS

All authors were involved in drafting the article or revising it critically for important intellectual content, and all authors approved the final version to be published. Dr. Casciola-Rosen had full access to all of the data in the study and takes responsibility for the integrity of the data and the accuracy of the data analysis.

Study conception and design. Hummers, Rosen, Casciola-Rosen, Shah.

Acquisition of data. Adler, Yang, Casciola-Rosen, Shah.

Analysis and interpretation of data. Mecoli, Casciola-Rosen, Shah.



REFERENCES

- Shah AA, Rosen A, Hummers L, Wigley F, Casciola-Rosen L. Close temporal relationship between onset of cancer and scleroderma in patients with RNA polymerase I/III antibodies. *Arthritis Rheum* 2010;62:2787–95.
- Shah AA, Xu G, Rosen A, Hummers LK, Wigley FM, Elledge SJ, et al. Anti-RNPC-3 antibodies as a marker of cancer-associated scleroderma. *Arthritis Rheumatol* 2017;69:1306–12.
- Shah AA, Laiho M, Rosen A, Casciola-Rosen L. Scleroderma patients with antibodies against the large subunits of both RNA polymerases I and III are protected against cancer. *Arthritis Rheumatol* 2019;71:1571–9.
- Igusa T, Hummers LK, Visvanathan K, Richardson C, Wigley FM, Casciola-Rosen L, et al. Autoantibodies and scleroderma phenotype define subgroups at high-risk and low-risk for cancer. *Ann Rheum Dis* 2018;77:1179–86.
- Hardin JA, Rahn DR, Shen C, Lerner MR, Wolin SL, Rosa MD, et al. Antibodies from patients with connective tissue diseases bind specific subsets of cellular RNA-protein particles. *J Clin Invest* 1982;70:141–7.
- Reddy R, Tan EM, Henning D, Nohga K, Busch H. Detection of a nucleolar 7–2 ribonucleoprotein and a cytoplasmic 8–2 ribonucleoprotein with autoantibodies from patients with scleroderma. *J Biol Chem* 1983;258:1383–6.
- Mahler M, Fritzler MJ, Satoh M. Autoantibodies to the mitochondrial RNA processing (MRP) complex also known as Th/To autoantigen [review]. *Autoimmun Rev* 2015;14:254–7.
- Mattijssen S, Welting TJ, Pruijn GJ. RNase MRP and disease [review]. *Wiley Interdiscip Rev RNA* 2010;1:102–16.
- Kuwana M, Kimura K, Hirakata M, Kawakami Y, Ikeda Y. Differences in autoantibody response to Th/To between systemic sclerosis and other autoimmune diseases. *Ann Rheum Dis* 2002;61:842–6.
- Mahler M, Satoh M, Hudson M, Baron M, Chan JY, Chan EK, et al. Autoantibodies to the Rpp25 component of the Th/To complex are the most common antibodies in patients with systemic sclerosis without antibodies detectable by widely available commercial tests. *J Rheumatol* 2014;41:1334–43.
- Mitri GM, Lucas M, Fertig N, Steen VD, Medsger TA Jr. A comparison between anti-Th/To- and anticentromere antibody-positive

- systemic sclerosis patients with limited cutaneous involvement. *Arthritis Rheum* 2003;48:203–9.
12. Van den Hoogen F, Khanna D, Fransen J, Johnson SR, Baron M, Tyndall A, et al. 2013 classification criteria for systemic sclerosis: an American College of Rheumatology/European League Against Rheumatism collaborative initiative. *Arthritis Rheum* 2013;65:2737–47.
 13. Shah AA, Casciola-Rosen L. Mechanistic and clinical insights at the scleroderma-cancer interface. *J Scleroderma Relat Disord* 2017;2:153–9.
 14. Medsger TA, Bombardieri S, Czirjak L, Scorza R, Rossa AD, Bencivelli W. Assessment of disease severity and prognosis. *Clin Exp Rheumatol* 2003;21:S42–6.
 15. Clements PJ, Lachenbruch PA, Ng SC, Simmons M, Sterz M, Furst DE. Skin score: a semiquantitative measure of cutaneous involvement that improves prediction of prognosis in systemic sclerosis. *Arthritis Rheum* 1990;33:1256–63.
 16. Hankinson JL, Odencrantz JR, Fedan KB. Spirometric reference values from a sample of the general US population. *Am J Respir Crit Care Med* 1999;159:179–87.
 17. Knudson RJ, Kaltenborn WT, Knudson DE, Burrows B. The single-breath carbon monoxide diffusing capacity: reference equations derived from a healthy nonsmoking population and effects of hematocrit. *Am Rev Respir Dis* 1987;135:805–11.
 18. Cottrell TR, Wise RA, Wigley FM, Boin F. The degree of skin involvement identifies distinct lung disease outcomes and survival in systemic sclerosis. *Ann Rheum Dis* 2014;73:1060–6.
 19. Mecoli CA, Shah AA, Boin F, Wigley FM, Hummers LK. Vascular complications in systemic sclerosis: a prospective cohort study. *Clin Rheumatol* 2018;37:2429–37.
 20. Simonneau G, Montani D, Celermajer DS, Denton CP, Gatzoulis MA, Krowka M, et al. Haemodynamic definitions and updated clinical classification of pulmonary hypertension. *Eur Respir J* 2019; 53:1801913.
 21. Fiorentino D, Chung L, Zwermer J, Rosen A, Casciola-Rosen L. The mucocutaneous and systemic phenotype of dermatomyositis patients with antibodies to MDA5 (CADM-140): a retrospective study. *J Am Acad Dermatol* 2011;65:25–34.
 22. Van Eenennaam H, Vogelzangs JH, Lugtenberg D, van den Hoogen FH, van Venrooij WJ, Pruijn GJ. Identity of the RNase MRP- and RNase P-associated Th/To autoantigen. *Arthritis Rheum* 2002; 46:3266–72.
 23. Van Eenennaam H, Jarrous N, Walth H, Jarrous N, van Venrooij WJ, Pruijn GJ. Architecture and function of the human endonucleases RNase P and RNase MRP. *IUBMB Life* 2000;49:265–72.
 24. Falkner D, Wilson J, Medsger TA, Morel PA. HLA and clinical associations in systemic sclerosis patients with anti-Th/To antibodies. *Arthritis Rheum* 1998;41:74–80.
 25. Nunes JP, Cunha AC, Meirinhos T, Nunes A, Araújo PM, Godinho AR, et al. Prevalence of autoantibodies associated to pulmonary arterial hypertension in scleroderma: a review. *Autoimmun Rev* 2018;17:1186–201.
 26. Reiner R, Ben-Asouli Y, Krilovetzky I, Jarrous N. A role for the catalytic ribonucleoprotein RNase P in RNA polymerase III transcription. *Genes Dev* 2006;20:1621–35.
 27. Reiner R, Krasnov-Yoeli N, Dehtiar Y, Jarrous N. Function and assembly of a chromatin-associated RNase P that is required for efficient transcription by RNA polymerase I. *PLoS One* 2008; 3:e4072.

BRIEF REPORT

Calcium Pyrophosphate Dihydrate Crystal Deposition in Gouty Tophi

Hang-Korng Ea,¹  Alan Gauffenic,¹ Quang Dinh Nguyen,² Nhu G. Pham,² Océane Olivier,¹ Vincent Frochot,³ Dominique Bazin,⁴ Nghia H. Le,² Caroline Marty,¹ Agnès Ostertag,¹ Martine Cohen-Solal,¹ Jean-Denis Laredo,⁵ Pascal Richette,¹ and Thomas Bardin⁶ 

Objective. The coexistence of calcium pyrophosphate dihydrate (CPPD) and monosodium urate monohydrate crystals in gouty tophi has rarely been reported. We undertook this study to investigate CPPD crystal deposits in a series of surgically removed gouty tophi and to identify factors associated with these deposits.

Methods. Twenty-five tophi from 22 gout patients were analyzed using polarized light microscopy, field emission scanning electron microscopy (FESEM), and μ Fourier transform infrared (μ FTIR) spectroscopy.

Results. Tophi consisted of multiple lobules separated by fibrous septa and surrounded by a foreign-body giant cell reaction. CPPD crystal aggregates were identified in 9 of 25 tophi from 6 patients. CPPD crystals were dispersed or highly compacted, localized at the edge or inside the tophus lobules, with some lobules completely filled with crystals. Both monoclinic and triclinic CPPD crystal phases were identified using FESEM and μ FTIR. Compared to patients without CPPD, those with CPPD-containing tophi were older (mean 60.5 years versus 47.2 years; $P = 0.009$), and had longer-term gout duration (mean 17.0 years versus mean 9.0 years; $P < 0.05$) and tophi duration (mean 10.0 years versus mean 4.6 years; $P < 0.01$). None of the patients had radiographic chondrocalcinosis of the knee or wrist.

Conclusion. CPPD crystal formation seems to be a late and frequent event of tophus maturation, occurring more frequently with aging, and could contribute to the speed of tophus dissolution and the apparent persistence of tophus sometimes observed even after effective, long-lasting urate-lowering therapy.

INTRODUCTION

The coexistence of monosodium urate monohydrate (MSU) and calcium pyrophosphate dihydrate (CPPD) crystals in synovial fluids has regularly been described, with a prevalence ranging from 0% to 36.1%, depending on the aspirated joint and the use or lack of use of synovial fluid centrifugation (1–3). Age, gout duration, chronic kidney disease, diuretic use, osteoarthritis, and bone erosion have been inconsistently associated with the presence of CPPD and MSU crystals in synovial fluid (1–3). The coexistence of these 2 crystal types in synovial fluid suggests that they may form

at the same place and then be released at the same time into the joint space.

Tophi are the hallmark of chronic and poorly treated gout and consist of ordered MSU crystals surrounded by a foreign-body giant cell reaction (4). Long-standing tophi can appear very dense or calcified, as observed with radiography and computed tomography (CT) (5,6), a finding that could be explained by the coexistence of calcium-containing crystals or by the presence of highly compacted MSU crystals. Although tophi have CT attenuation inferior to calcifications, dense MSU deposits in meniscus and knee cartilage can mimic chondrocalcinosis without the detection

Supported by ART Viggo, Prevention et Traitement des Décalcifications, and the Société Française de Rhumatologie.

¹Hang-Korng Ea, MD, PhD, Alan Gauffenic, MD, Océane Olivier, MD, Caroline Marty, BS, Agnès Ostertag, PhD, Martine Cohen-Solal, MD, PhD, Pascal Richette, MD, PhD: Université de Paris, INSERM UMR 1132, Hôpital Lariboisière, AP-HP, Paris, France; ²Quang Dinh Nguyen, BS, Nhu G. Pham, MD, Nghia H. Le, BS: Vien Gut Medical Center and French-Vietnamese Research Center on Gout and Chronic Diseases, Ho Chi Minh City, Vietnam; ³Vincent Frochot, MD: Hôpital Tenon and Sorbonne Université, UMR S1155, Paris, France; ⁴Dominique Bazin, PhD: Institut de Chimie Physique, Université Paris-Saclay, CNRS UMR 8000, Orsay, France; ⁵Jean-Denis

Laredo, MD: Université de Paris and Hôpital Lariboisière, Paris, France; ⁶Thomas Bardin, MD: Université de Paris, INSERM UMR 1132, Hôpital Lariboisière, AP-HP, Paris, France, and Vien Gut Medical Center and French-Vietnamese Research Center on Gout and Chronic Diseases, Ho Chi Minh City, Vietnam.

No potential conflicts of interest relevant to this article were reported.

Address correspondence to Hang-Korng Ea, MD, PhD, INSERM UMR-S 1132, Hôpital Lariboisière, Centre Viggo Petersen, Third Floor, 2 Rue Ambroise Paré, 75475 Paris Cedex 10, France. Email: korngea@yahoo.fr.

Submitted for publication April 29, 2020; accepted in revised form September 1, 2020.

of calcium-containing crystals by dual-energy CT (DECT) or synovial fluid analysis (6–8). The disappearance of such chondrocalcinosis-mimicking features has been observed after effective urate-lowering therapy, which further suggests that MSU deposition alone could be responsible for chondrocalcinosis-like imaging findings (7). However, the coexistence of MSU crystals and calcification (i.e., calcium-containing crystal deposits) has been described in autopsy studies (5,9).

The nature of the calcium crystals in tophi has seldomly been characterized; one autopsy study identified CPPD crystals (9). Recently, DECT scans revealed CPPD energy attenuation patterns within MSU crystal deposits around the metacarpophalangeal joint of an 82-year-old man with gout and CPPD deposition disease (10). Another study described the presence of CPPD crystals in 5 tophi, without characterizing the type of CPPD crystals and with no data on gout history (11).

The aims of the present study were to assess the frequency of CPPD deposition in gouty tophi, to characterize the type of deposited CPPD crystals, and to identify factors associated with CPPD crystal deposition in tophi.

PATIENTS AND METHODS

Patients. This study was conducted in compliance with Good Clinical Practice and the Declaration of Helsinki and in accordance with Vietnamese law. All patients were informed that surgically removed tophi would be used for diagnostic and research procedures. Patients provided written informed consent. Patient characteristics, comorbidities, treatments, gout history, and laboratory and imaging data were extracted from medical charts.

Histology, sample processing, and CPPD crystal characterization. A total of 25 tophi that were removed from 22 gout patients consecutively operated on at the Vien Gut Medical Center (Hô Chi Minh City, Vietnam) were fixed in 4% paraformaldehyde or 70% alcohol and sent to Lariboisière Hospital, INSERM UMR 1132 (Paris, France). Tophi were embedded in paraffin, and 5- μ m thick sections were deposited on glass slides for sirius red and tartrate-resistant alkaline phosphatase (TRAP) and von Kossa staining. MirrIR low-e microscope slides (Kevley Technologies and Tienta Sciences) were prepared for field emission scanning electron microscopy (FESEM) and μ Fourier transform infrared (μ FTIR) spectroscopy. Tophus sections were systematically analyzed using polarized light microscopy, FESEM, and μ FTIR.

FESEM. FESEM (Zeiss SUPRA55-VP; Goettingen) was used to describe the ultrastructural characteristics of tissue sections. The field-effect gun microscope operates at 0.5–30 kV. High-resolution observations were obtained with 2 secondary electron detectors (Inlens SE and Everhart-Thornley SE). To maintain the integrity of specimens, measurements were obtained at a low voltage (~2 kV) without the usual deposits of carbon at the surface of the sample.

Analysis with μ FTIR. Using the same tissue samples used in the FESEM analyses, μ FTIR was performed to identify the chemical composition of tophus calcifications. All μ FTIR hyperspectral images were recorded with a Spectrum Spotlight 400 μ FTIR imaging system (Perkin–Elmer Life Sciences), with 6.25-mm spatial resolution and 8- cm^{-1} spectral resolution. To determine the proportion of monoclinic CPPD (mCPPD) and triclinic CPPD (tCPPD) in a tissue sample, absorption areas of their specific peaks (mean \pm SD wavelength 936 \pm 4 cm^{-1} and 744 \pm 4 cm^{-1} for mCPPD, and mean \pm SD wavelength 918 \pm 4 cm^{-1} and 764 \pm 4 cm^{-1} for tCPPD) were quantified using ImageJ software and reported for the tissue surface. Five random areas were assessed for each sample.

Radiographic analysis. Standard radiographs were read by a skeletal radiologist (JDL) and rheumatologist (TB). The following semiquantitative scale for tophus opacity was used: 0 = air opacity; 1 = opacity similar to soft tissue; 2 = opacity between soft tissue and bone; 3 = opacity containing high-density granulations.

Statistical analysis. Quantitative variables are described as the mean and the range, and qualitative variables as the number (percentage) of patients. Chi-square test was used to compare qualitative variables (or Fisher's exact test, otherwise) and Mann-Whitney U test was used for quantitative data (or Student's test in case of homoscedasticity, determined by Bartlett's test). *P* values less than 0.05 were considered significant. Data analysis was performed with GraphPad Prism 7.0.

RESULTS

Patient characteristics. We analyzed 25 tophi that were surgically removed from 22 patients. All patients were male, with a mean age of 50.8 years (range 28–66 years) and a mean body mass index of 24.2 kg/m^2 (range 18.9–29.4). Patient characteristics and comorbidities are summarized in Table 1. The mean \pm SD serum urate level was 499 \pm 107 $\mu\text{moles}/\text{liter}$. Overall, 68.2% had stage 2 or 3 chronic kidney disease, 40.9% had dyslipidemia, 22.7% had type 2 diabetes mellitus, 13.6% had hypertension, and 50% were obese. Tophi were removed from great toes ($n = 9$), other toes ($n = 3$), ankles ($n = 3$), knees ($n = 1$), fingers ($n = 4$), elbows ($n = 4$), and tendons ($n = 1$). Resection was performed due to disability induced by tophi, such as difficulty putting on shoes, walking, or other functional limitations.

Identification of rod-like and rhomboid-shaped CPPD crystals within tophus lobules, using polarized light microscopy. Macroscopically and using light microscopy, tophi appeared to contain multiple lobules separated by fibrous septa, which are also shown using sirius red staining (see

Table 1. Characteristics of the patients with and those without CPPD crystal deposition in gouty tophi*

	All (n = 22)	Urate only (n = 16)	Urate and CPPD (n = 6)
Age, years	50.8 (28–66)	47.2 (28–64)	60.5 (56–66)†
Gout duration at surgery, years	11.3 (3–31)	9.0 (3–20)	17.0 (9–31)‡
Tophus duration at surgery, years	6.1 (1–16)	4.6 (1–9)	10.0 (3–16)†
BMI >25 kg/m ² , %	50	56	33
Type 2 DM, %	22.7	31.3	0
Hypertension, %	13.6	18.8	0
Dyslipidemia, %	40.9	43.8	33.3
Stage 2–3 CKD, %	68.2	68.8	66.7
eGFR, ml/minute/1.73 m ²	75.3 (48–116)	75.2 (48–116)	75.5 (60–92)
Serum urate level, μmoles/liter	499 (337–886)	512 (337–886)	466 (404–518)
Bone erosion, %	70	60	80

* Except where indicated otherwise, values are the mean (range). CPPD = calcium pyrophosphate dihydrate; BMI = body mass index; DM = diabetes mellitus; CKD = chronic kidney disease; eGFR = estimated glomerular filtration rate.

† $P < 0.01$ versus patients without CPPD.

‡ $P < 0.05$ versus patients without CPPD.

Supplementary Figure 1, available on the *Arthritis & Rheumatology* website at <http://onlinelibrary.wiley.com/doi/10.1002/art.41515/abstract>). Each lobule contained packed and ordered thin clefts from MSU crystals that had dissolved during sample processing, surrounded by a foreign-body giant cell reaction. MSU crystal-containing tissue appeared acellular and was composed of amorphous amphophilic materials. In 16 samples, most of the multinucleated giant cells expressed TRAP and were localized adjacent to the MSU crystal deposits

within the corona zone, along with numerous mononuclear cells (Supplementary Figure 1C).

CPPD crystals were identified in 9 of 25 retrieved tophi (36%) (3 great toes, 2 fifth toes, 1 third toe, 1 elbow bursa, and 2 fingers) in 6 of 22 patients (27.3%). Three patients had CPPD crystal-containing tophi in 2 different locations. Tophus site distribution did not differ between tophi showing CPPD and those that did not.

Different shapes (long and rod-like, cuboid, and rhomboid) of CPPD crystals were observed using plain and polarized

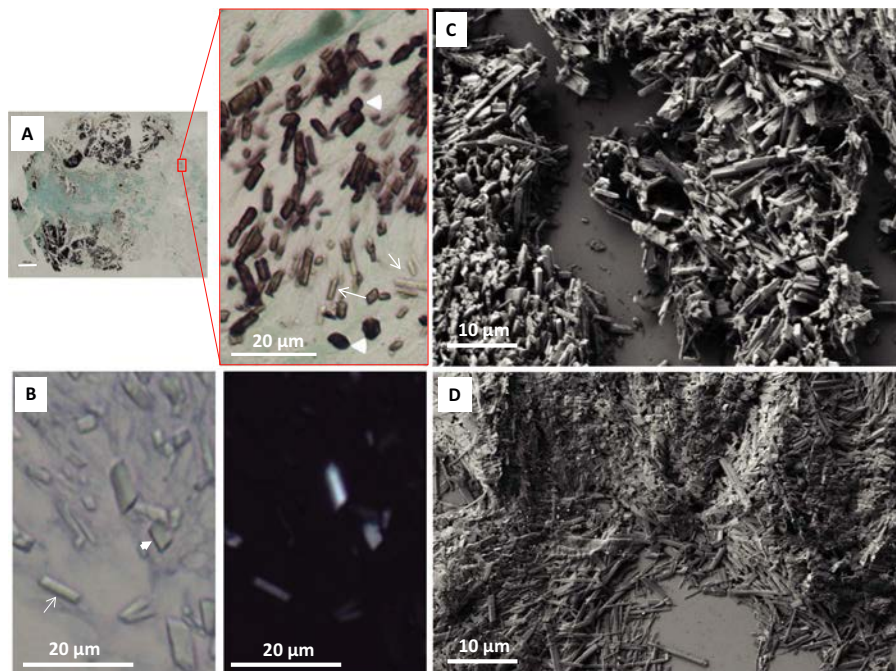


Figure 1. Rod-like calcium pyrophosphate dihydrate (CPPD) crystals and rhomboid CPPD crystals within tophi. **A**, Von Kossa staining shows the presence of dispersed or compacted calcium-containing crystals. Bar in left panel = 400 μm. High-magnification view of dispersed areas shows CPPD crystals with rod-like shapes (**arrows**) and rhomboid shapes (**arrowheads**). **B**, Plain (left) and polarized (right) light microscopy show rod-like CPPD crystals (**arrow**) and rhomboid CPPD crystals (**arrowhead**), with different birefringence. **C**, Field emission scanning electron microscopy (FESEM) shows CPPD crystals. **D**, FESEM of an alcohol-fixed tophus section shows compacted and flat urate crystals. Color figure can be viewed in the online issue, which is available at <http://onlinelibrary.wiley.com/doi/10.1002/art.41515/abstract>.

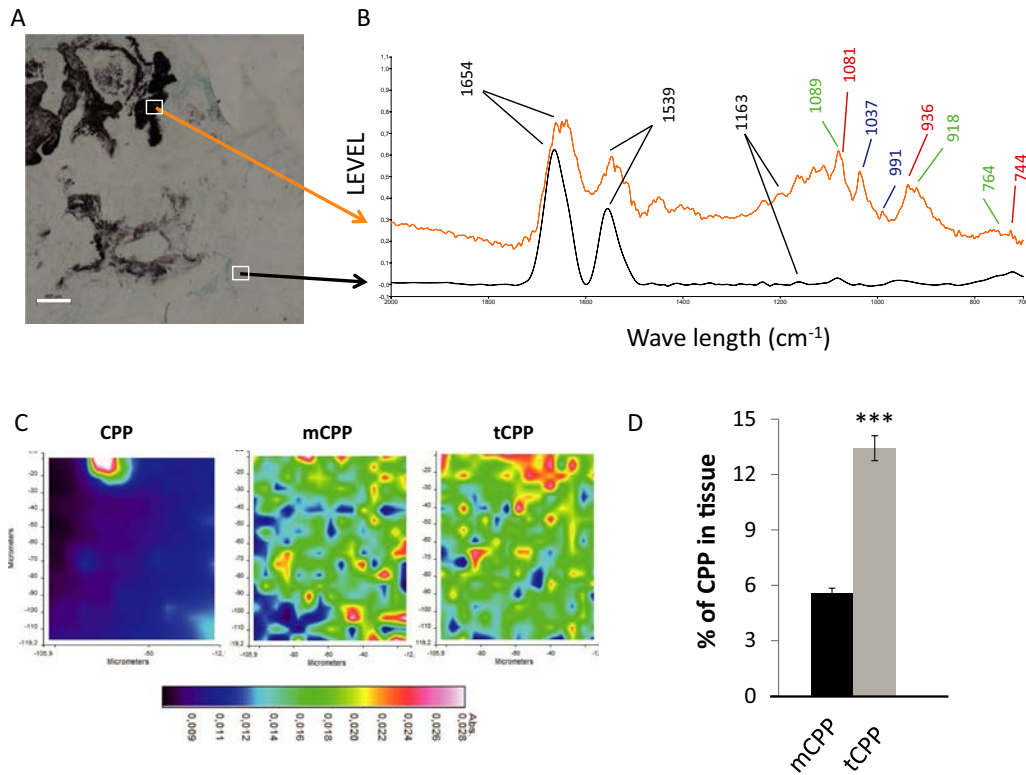


Figure 2. Monoclinic calcium pyrophosphate dihydrate (mCPPD) and triclinic CPPD (tCPPD) crystals detected by μ Fourier transform infrared spectroscopy. **A**, Von Kossa staining of tophus biopsy specimen. Bar = 400 μ m. **B**, Infrared spectra of 2 different lobules: von Kossa-positive lobules (**orange arrow**), showing characteristic peaks for mCPPD phases (red), tCPPD phases (green), and common CPPD crystal peaks (blue); and von Kossa-negative lobules (**black arrow**), showing only mucoproteic matrix peaks (black). **C**, Infrared map of von Kossa-positive areas, showing intense CPPD crystal absorbance (left) containing both mCPPD phases (middle) and tCPPD phases (right). **D**, Ratio of CPPD in tissue containing mCPPD and tCPPD crystals to tissue surface, as quantified with ImageJ. Bars show the mean \pm SEM ($n = 5$ analyzed tophi). *** = $P < 0.001$.

light microscopy and after von Kossa staining (Figures 1A and B, Supplementary Figure 2, and Supplementary Figures 3A and B, <http://onlinelibrary.wiley.com/doi/10.1002/art.41515/abstract>). CPPD crystal depositions were either dispersed or aggregated and highly compacted (Figures 1A and B, Supplementary Figure 2, Supplementary Figures 3A and B, and Supplementary Table 1, <http://onlinelibrary.wiley.com/doi/10.1002/art.41515/abstract>). Within 1 tophus, a variable number of lobules contained CPPD crystals with different deposition patterns and densities. In 6 cases, CPPD crystals completely filled 2–11 tophus lobules (Figure 1A, Supplementary Figure 2A, Supplementary Figures 3A and B, and Supplementary Table 1). CPPD crystals were localized at the edge of and/or inside tophus lobules in close vicinity to MSU crystal sites. No CPPD crystals were observed outside the MSU crystal deposition sites; specifically, no CPPD crystals were observed in the fibrovascular zones.

Characterization of CPPD crystals using FESEM and μ FTIR spectroscopy. FESEM analysis of tophus sections showed variably compacted CPPD crystals of varying morphology (rod-like, cuboid, or rhomboid), size (1–15 μ m), and thickness (Figure 1C). By comparison, FESEM observation of

an alcohol-fixed tophus showed MSU crystals that were flat, thinner, and highly compacted, with a homogenous morphology (Figure 1D). Analysis with μ FTIR confirmed that crystals observed in paraformaldehyde-fixed samples consisted of CPPD with mCPPD and tCPPD phases, characterized by their respective peaks (Figure 2B). Among all samples, tCPPD crystals were the most prevalent phase (Figures 2C and D). No MSU crystals were detected, since they were dissolved by paraformaldehyde fixation (Figure 2B).

Clinical factors associated with CPPD crystals.

Compared to patients with tophi not containing CPPD crystals ($n = 16$), those with CPPD-containing tophi ($n = 6$) were older (mean 60.5 years [range 56–66 years] versus mean 47.2 years [range 28–64 years]; $P = 0.009$) and had a longer duration of gout (mean 17 years [range 9–31 years] versus mean 9 years [range 3–20 years]; $P < 0.05$) and a longer duration of tophus (mean 10.0 years [range 3–16 years] versus mean 4.6 years [range 1–9 years]; $P < 0.01$) (Table 1). None of these 6 patients had radiographic chondrocalcinosis of the knee ($n = 6$) or the wrist ($n = 5$). None of the excised tophi displayed definite calcification on presurgery radiographs. However, 7 of 9 tophi with

CPPD crystal deposits showed dense granulations with a calcium-like density within tophus opacities, which were observed in only 1 tophus without CPPD crystals ($P = 0.02$) (Supplementary Figure 4A, <http://onlinelibrary.wiley.com/doi/10.1002/art.41515/abstract>). The proportions of bone erosion (at the tophus sites) and gout arthropathy were similar between the 2 groups, with no differences in serum urate level (mean \pm SD 466 ± 43 μ moles/liter versus mean \pm SD 512 ± 109 μ moles/liter), estimated glomerular filtration rate (mean \pm SD 75.5 ± 11.9 ml/minute/1.73 m² versus mean \pm SD 75.2 ± 15.7 ml/minute/1.73 m²), or prevalence of comorbidities. None of the 6 patients received diuretics, and their calcium levels were normal.

DISCUSSION

In this series of patients with gouty tophi, we identified a high prevalence (27.3%; 6 of 22 patients) of mCPPD and tCPPD crystal depositions within tophus lobules. The presence of CPPD crystals within tophi occurred preferentially in older patients and in long-lasting gout and tophi, as demonstrated in synovial fluid studies (1–3). CPPD deposition harbored either a dispersed or highly compacted pattern which might reflect the age of their formation. Our findings have enriched those reported by Mohr and Görz, who identified the presence of CPPD crystals in tophi but did not describe the crystal deposition patterns or characterize the crystal phases (11). In our study, tCPPD crystals, the most stable phase, occurred more frequently than mCPPD crystals, as previously reported in CPPD deposition disease (9,12). Three patients had CPPD crystals in 2 tophi at different sites, a scenario noted by Mohr and Görz and in the autopsy study by Grahame et al (9,11). In this latter study, the postmortem examination of a 64-year-old man with gout and hyperparathyroidism-related CPPD crystal disease revealed the coexistence of MSU and CPPD crystals in a metatarsophalangeal tophus, as well as in the sternoclavicular cartilage, knee ligament, and kidney tubules (9). The coexistence of the 2 crystal types in this case was probably promoted by the systemic increase of the serum urate levels and serum calcium levels due to hyperparathyroidism. In contrast, the 6 patients in our study had normal calcemia and showed no chondrocalcinosis on knee and wrist radiographs. Thus, CPPD crystal formation within the tophus core may have been promoted by local cellular and extracellular matrix changes generated by MSU crystal aggregates.

Another possibility may be that mechanisms of CPPD and MSU crystal formation share yet unidentified common factors. Mechanical stress may be one factor, since tophi are preferentially localized in traumatic areas. Mandel et al demonstrated *in vitro* that a denatured collagen matrix containing MSU crystals altered inorganic pyrophosphate diffusion and favored tCPPD crystal formation and growth (13). The authors suggested that MSU crystals might act as a nucleating agent for CPPD formation. Alternatively, the extracellular matrix damage induced by MSU crystals along with the giant cell reaction might facilitate CPPD

crystal formation. Indeed, the fact that CPPD crystal deposition occurred only in some lobules of a given tophus suggested that local environment alterations played a more important role than MSU crystals, *per se*, in CPPD crystal formation. This hypothesis is sustained by the observation of CPPD crystals in 2 and 8 foreign-body granulomas surrounding the suture and particle wears of hip prostheses, respectively (14,15). These observations suggest that the foreign-body giant cell reaction might be sufficient to induce CPPD crystal formation. The underlying mechanisms of this hypothesis need further investigation.

Although the clinical significance of our findings remain hypothetical, the coexistence of CPPD crystals within tophi might explain the following: 1) in some patients, the coexistence of these crystals in synovial fluids; 2) dense or calcified radiologic presentations of long-duration tophi; and 3) allowance of modification of tophus dissolution speed under effective urate-lowering therapy.

Besides its small sample size, this study has limitations. First, we did not rule out metabolic diseases associated with CPPD crystal deposition such as hemochromatosis, hyperparathyroidism, hypomagnesemia, hypophosphatasia, or hereditary CPPD crystal deposition. However, the absence of clinical features of these diseases and the lack of discernible chondrocalcinosis on knee and wrist radiographs provide evidence against a systemic disease responsible for CPPD crystal deposition. Second, we used μ FTIR to characterize CPPD phases instead of x-ray diffraction. However, μ FTIR also allowed semiquantification of mCPPD and tCPPD phases, and has become a routinely used technique in clinical practice. Third, we were unable to precisely describe the exact interactions between MSU crystals and CPPD crystals because of MSU crystal dissolution by the formaldehyde fixator. It would be interesting to know whether MSU crystals were replaced by CPPD crystals in lobules where CPPD crystals were highly compacted. Examination of frozen or alcohol-fixed samples with persistent MSU crystals and the use of DECT and spectral-energy CT technology to distinguish MSU, CPPD, and apatite crystal deposition would help better characterize tophus composition, especially in tophi with dense granulations with a calcium-like density like those seen in the present study (6,10).

In conclusion, CPPD crystal formation appears to be a late and fairly frequent event in tophus maturation. CPPD deposition in tophi might explain the apparent persistence of tophus in some patients even after long-term, effective urate-lowering therapy. The presence of CPPD crystals might decrease tophus dissolution under urate-lowering therapy.

ACKNOWLEDGMENT

This manuscript was edited by Laura Smales (BioMedEditing).

AUTHOR CONTRIBUTIONS

All authors were involved in drafting the article or revising it critically for important intellectual content, and all authors approved the final version to be published. Dr. Ea had full access to all of the data in the study and

takes responsibility for the integrity of the data and the accuracy of the data analysis.

Study conception and design. Ea, Nguyen, Cohen-Solal, Richette, Bardin.

Acquisition of data. Ea, Gauffenic, Pham, Olivier, Frochot, Bazin, Le, Marty, Ostertag, Laredo.


Analysis and interpretation of data. Ea, Gauffenic, Nguyen, Frochot, Bazin, Cohen-Solal, Laredo, Richette, Bardin.

REFERENCES

1. Ankli B, Kyburz D, Hirschmann A, Hügler T, Manigold T, Berger CT, et al. Calcium pyrophosphate deposition disease: a frequent finding in patients with long-standing erosive gout. *Scand J Rheumatol* 2018;47:127–30.
2. Robier C, Neubauer M, Quehenberger F, Rainer F. Coincidence of calcium pyrophosphate and monosodium urate crystals in the synovial fluid of patients with gout determined by the cyto centrifugation technique [letter]. *Ann Rheum Dis* 2011;70:1163–4.
3. Heselden EL, Freemont AJ. Synovial fluid findings and demographic analysis of patients with coexistent intra-articular monosodium urate and calcium pyrophosphate crystals. *J Clin Rheumatol* 2016;22:68–70.
4. Dalbeth N, Pool B, Gamble GD, Smith T, Callon KE, McQueen FM, et al. Cellular characterization of the gouty tophus: a quantitative analysis. *Arthritis Rheum* 2010;62:1549–56.
5. Lichtenstein L, Scott HW, Levin MH. Pathologic changes in gout. *Am J Pathol* 1956;32:871–95.
6. Bousson V, Bardin T, Zeitoun D, Sverzut JM, Ea HK. Monosodium urate deposition in the articular cartilage and meniscus can mimic chondrocalcinosis [letter]. *Joint Bone Spine* 2020;87:95–6.
7. Ottaviani S, Forien M, Dieudé P. A radiographic double contour sign mimicking pseudogout. *J Clin Rheumatol* 2018;24:92.
8. Gerster JC, Landry M, Dufresne L, Meuwly JY. Imaging of tophaceous gout: computed tomography provides specific images compared with magnetic resonance imaging and ultrasonography. *Ann Rheum Dis* 2002;61:52–4.
9. Grahame R, Sutor DJ, Mitchener MB. Crystal deposition in hyperparathyroidism. *Ann Rheum Dis* 1971;30:597–604.
10. Hajri R, Hajdu SD, Hügler T, Zufferey P, Guiral L, Becce F. Dual-energy computed tomography for the noninvasive diagnosis of coexisting gout and calcium pyrophosphate deposition disease. *Arthritis Rheumatol* 2019;71:1392.
11. Mohr W, Götz E. Mixed tophi: calcium pyrophosphate dihydrate crystals in gout tophi. *Z Rheumatol* 2000;59:240–4. In German.
12. Gras P, Ratel-Ramond N, Teychéne S, Rey C, Elkaim E, Biscans B, et al. Structure of the calcium pyrophosphate monohydrate phase (Ca₂P₂O₇·H₂O): towards understanding the dehydration process in calcium pyrophosphate hydrates. *Acta Crystallogr C Struct Chem* 2014;70:862–6.
13. Mandel GS, Halverson PB, Mandel NS. Calcium pyrophosphate crystal deposition: the effect of monosodium urate and apatite crystals in a kinetic study using a gelatin matrix model. *Scanning Microsc* 1988;2:1189–98.
14. Mohr W, Hersener J, Richter R, Buchner F. Fadengranulome mit Kalziumpyrophosphat-Ablagerungen. *Z Orthop Ihre Grenzgeb* 1990;128:134–8.
15. Bos I. Tissue reactions around loosened hip joint endoprostheses. A histological study of secondary capsules and interface membranes. *Orthopade* 2001;30:881–9. In German.

BRIEF REPORT

Imaging-Based Uveitis Surveillance in Juvenile Idiopathic Arthritis: Feasibility, Acceptability, and Diagnostic Performance

Saira Akbarali,¹ Jugnoo S. Rahi,² Andrew D. Dick,³ Kiren Parkash,⁴ Katie Etherton,⁵ Clive Edelsten,⁶ Xiaoxuan Liu,⁷ and Ameenat L. Solebo⁸ 

Objective. Children with juvenile idiopathic arthritis (JIA) need regular examinations for uveitis to avoid visual morbidity from the most common extraarticular manifestation of disease. This study was undertaken to investigate the feasibility, acceptability, and performance of optical coherence tomography (OCT) imaging-based diagnosis of uveitis.

Methods. This observational cross-sectional study included children with and those without uveitis. The children underwent routine clinical examinations and anterior segment OCT scanning of intraocular inflammatory cells. Acceptability of image acquisition was assessed using a visual analog scale and length of time needed to acquire images. Interobserver and intraobserver variability of manual counting of acquired images (Bland-Altman limits of agreement), correlation between imaging and routine assessment, and sensitivity and specificity of anterior segment OCT detection of active inflammation were assessed.

Results. Of the 26 children ages 3–15 years (median age 8 years) who underwent imaging, 12 had active inflammation. All patients rated the acceptability of image acquisition as at least 8.5 on a scale of 0–10. Time taken to acquire images ranged from 1.5 minutes to 22 minutes (median time 8 minutes). There was good positive correlation between clinical assessment and image-based cell quantification ($R^2 = 0.63$, $P = 0.002$). Sensitivity of anterior segment OCT manual image cell count for diagnosis of active inflammation was 92% (95% confidence interval [95% CI] 62–99%), specificity was 86% (95% CI 58–98%), and negative predictive value (ruling out uveitis) was 92% (95% CI 65–99%).

Conclusion. Non-contact, high-resolution imaging for JIA uveitis surveillance is feasible, acceptable to patients, and holds the promise of transforming pediatric practice. Further work is needed to determine the analytic and clinical validity of anterior segment OCT quantification of active inflammation, and the clinical utility and cost-effectiveness of imaging-based disease monitoring.

The views expressed are those of the authors and not necessarily those of the NHS, the NIHR, or the Department of Health and Social Care.

Supported by the NIHR Biomedical Research Centre at Great Ormond Street Hospital for Children NHS Foundation Trust and the Institute of Child Health, University College London. Ms Akbarali's work was supported by a grant from the Great Ormond Street Hospital Charity (grant V0419). Dr. Solebo's work was supported by an NIHR Clinician Scientist award (CS-2018-18-ST2-005). Dr. Rahi's work was supported in part by the NIHR Biomedical Research Centre based at Moorfields Eye Hospital NHS Foundation Trust, University College London Institute of Ophthalmology, and by an NIHR Senior Investigator award.

¹Saira Akbarali, BSc: Great Ormond Street Hospital for Children NHS Foundation Trust, London, UK; ²Jugnoo S. Rahi, PhD, FRCOphth: Great Ormond Street Hospital for Children NHS Foundation Trust, University College London Great Ormond Street Institute of Child Health, NIHR Great Ormond Street Hospital Biomedical Research Centre, NIHR Moorfields Biomedical Research Centre, Moorfields Eye Hospital NHS Foundation Trust, and University College London Institute of Ophthalmology, London, UK; ³Andrew D. Dick, MD, FRCP: NIHR Moorfields Biomedical Research Centre, Moorfields Eye Hospital NHS Foundation Trust, University College London

Institute of Ophthalmology, London, UK, and Bristol Eye Hospital, University Hospitals Bristol NHS Foundation Trust, University of Bristol, Bristol, UK; ⁴Kiren Parkash, MBChB, BMedSci: University of Birmingham Medical School, Birmingham, UK; ⁵Katie Etherton, BSc, MCOptom: Moorfields Eye Hospital NHS Foundation Trust, London, UK; ⁶Clive Edelsten, MD, FRCOphth: Great Ormond Street Hospital for Children NHS Foundation Trust, London, UK, and Ipswich Hospital NHS Foundation Trust, Ipswich, UK; ⁷Xiaoxuan Liu, MBChB: University of Birmingham College of Medical and Dental Sciences and University Hospitals Birmingham NHS Foundation Trust, Birmingham, UK; ⁸Ameenat L. Solebo, PhD, FRCOphth: Great Ormond Street Hospital for Children NHS Foundation Trust, University College London Great Ormond Street Institute of Child Health, NIHR Great Ormond Street Hospital Biomedical Research Centre, London, UK.

No potential conflicts of interest relevant to this article were reported.

Address correspondence to Ameenat Lola Solebo, PhD, FRCOphth, University College London Great Ormond Street Institute of Child Health, 30 Guilford Street, London WC1N 1EH, UK. Email: a.solebo@ucl.ac.uk.

Submitted for publication May 1, 2020; accepted in revised form September 17, 2020.

INTRODUCTION

Juvenile idiopathic arthritis (JIA) is the most common childhood inflammatory rheumatic disorder (1), and uveitis (intraocular inflammation) is the most common extraarticular manifestation of disease (1). Uveitis results in impaired vision in up to one-fifth of affected children, with visual complications typically being a result of delayed diagnosis (2). European and American guidelines recommend a formal uveitis surveillance protocol for all patients in whom a JIA diagnosis is being considered to enable early detection of this often asymptomatic, but potentially blinding, disease (3). Disease activity in anterior uveitis, the most common manifestation of JIA-related uveitis, is currently assessed in a hospital's eye services department using slit-lamp biomicroscopic examination (4), a semiquantitative and subjective assessment.

Imaging-based assessments, such as joint ultrasonography and magnetic resonance imaging (MRI), have provided sensitive, repeatable, and clinically meaningful disease metrics for inflammatory disease, supplementing clinical examination (5). Optical coherence tomography (OCT) is a non-contact, noninvasive, high-speed, high-resolution modality with long-established use for imaging the posterior segment of the eye. It is now by far the most commonly used ophthalmic imaging procedure (6). A relatively recent modification has been used to image the anterior chamber (7), with identification of anterior chamber inflammatory cells as hyper-reflective dots. The feasibility of such image acquisition in children is unclear. We aimed to investigate the feasibility, acceptability, and diagnostic performance of imaging-based disease monitoring for childhood anterior uveitis.

PATIENTS AND METHODS

Children age <18 years with or without uveitis were included in this observational cross-sectional study. The study was approved by the National Health Research Authority (approval no. 18/LO/0252) and local institutional research boards. This research followed the tenets of the Declaration of Helsinki. The study was supported by a Generation R Young Persons Advisory Group and a patient-family advisory group.

Study population. Two groups were recruited. Group 1 comprised children with a diagnosis of chronic anterior uveitis who were recruited from a specialist pediatric uveitis care center in London, England between 2017 and 2018. Group 2 comprised children without a diagnosis of uveitis who were siblings of patients in the outpatient department (where ophthalmology, audiology, and otolaryngology care are provided) for any reason. This latter group enabled an investigation of the normative range of hyper-reflective dots on anterior segment OCT images of patients' eyes.

Children with a history of ocular trauma, any ocular inflammation, or JIA were excluded from group 2. Children ages <2 years, and thus typically unable to undergo a slit-lamp examination without restraint, were excluded from both groups.

Routine clinical assessment of the anterior chamber was carried out by 2 senior ophthalmologists (CE and ALS) using the same Haag Streit BM 900 slit-lamp. The ordinal Standardized Uveitis Nomenclature (SUN) anterior chamber activity cell count grade was used to assess inflammation. The SUN cell grade ranges from 0 to 4+, where 0 = no cells seen within a central 1-mm long beam, 0.5+ = 1–5 cells seen, 1+ = 6–15 cells seen, 2+ = 16–25 cells seen, 3+ = 26–50 cells seen, and 4+ = the highest level of inflammation (>51 cells seen) (4).

Image acquisition. A spectral domain OCT scanner with an axial resolution of 5 microns was used (Optovue AngioVue). Cross-sectional anterior segment OCT scans of the anterior chambers were acquired by an ophthalmologist (ALS), imaging to a depth of 1.96 mm or two-thirds of the average mid-childhood anterior chamber depth (8). Eight cross-sectional images were acquired in an asterisk formation centered on the corneal apex. Children ages ≥ 8 years positioned their head at the machine and were asked to fixate the eye being tested (test eye) on the machine-generated fixation beam. Younger children were asked to fixate the non-test eye on a cartoon played on a smartphone held in a position so as to align the test eye within the scanning window.

Image acquisition time, defined as the duration from the child's first chin placement to successful capture of sufficiently high-quality images to enable image analysis, as judged by 1 trained clinician (ALS), was measured. Acceptability of the acquisition process for the child and accompanying parent or caregiver was captured using the question "What did you think of the scan?" which was completed following reiteration of study aims using a standardized study information leaflet. A 10-cm visual analog scale (VAS) was used, ranging from 0 (not acceptable or crying face) to 10 (completely acceptable or smiling face). The VAS was completed by children ages >6 years, with proxy completion by parents or caregivers only for younger children.

Image analysis. Images were analyzed manually and were reviewed independently by at least 2 examiners, with each examiner undertaking 2 viewings of the stored and anonymized images, separated by at least 2 weeks. All examiners (comprising 1 ophthalmologist, 1 optometrist, and 1 medical student) were trained using a separate set of anterior segment OCT images of confirmed anterior chamber inflammation. Eight cross-sectional images of 3 eyes of 2 children with known anterior chamber inflammation were selected by the study lead (ALS) as training images. There was no other additional training provided.

For manual image analysis, all visible hyper-reflective dots brighter than the background noise and/or >2 pixels were counted. There were no restrictions of size, but any dots with irregular margins suggestive of cell clumping were counted as 2 cells. Hyper-reflective dots immediately anterior to the anterior iris signal were discounted as artefact. Examiners were blinded with regard to the child's identity and the results of clinical assessment. Images were judged ungradable if there were artefacts seen within the viewing envelope formed by the inner surface of the cornea and the superior border of the iris. Total cell count across 8 images and median cell count per image per eye was recorded.

Statistical analysis. Descriptive analysis of all outcome measures was undertaken. Repeatability of manual counting of acquired images was described using the intraclass correlation coefficient (ICC) two-way mixed effect model (intra-observer reliability), Cohen's kappa statistic (interobserver), and the Bland-Altman limits of agreement (intraobserver and interobserver). All analyzed images were used for analyses of count repeatability.

Effectiveness of imaging-based diagnosis of inflammation was assessed using the diagnostic performance of anterior segment OCT detection of active inflammation versus the reference standard of slit-lamp-based assessment. One eye was chosen at random for each child for inclusion within the analysis of OCT as a diagnostic tool versus slit-lamp examination. Only eyes for which

a full set of 8 good quality images were obtained were used for assessment of diagnostic performance. Cases were considered anterior segment OCT positive if any inflammatory cells had been noted on any of the 8 cross-sectional images and were slit-lamp positive if any clinician had graded them as active on biomicroscopic examination of the anterior chamber.

Correlation between imaging-acquired cell count and clinical assessment of inflammation was assessed using a multilevel linear regression model, with correction for within-child correlation to account for the clustered structure of eye-level data for those children who had undergone assessment in both eyes. Accordingly, where data from both eyes were available, both eyes were included in these analyses.

Analyses were undertaken using Stata version 15. Young people and patients co-designed the study to ensure minimization of the burden of participation for patients and their families.

RESULTS

A total of 26 children ages 3–15 years (median age 8 years; 18 female and 8 male) underwent imaging of 52 eyes (Figure 1). This included 19 children with a known diagnosis of uveitis (bilateral in 16), of whom 12 had JIA-associated uveitis. The remaining 7 children had idiopathic uveitis. Of the 19 children, 12 had active anterior inflammation as confirmed by 2 examiners using slit-lamp assessment, with all eyes scoring $\leq 1+$ anterior chamber inflammation on the slit-lamp SUN scale.

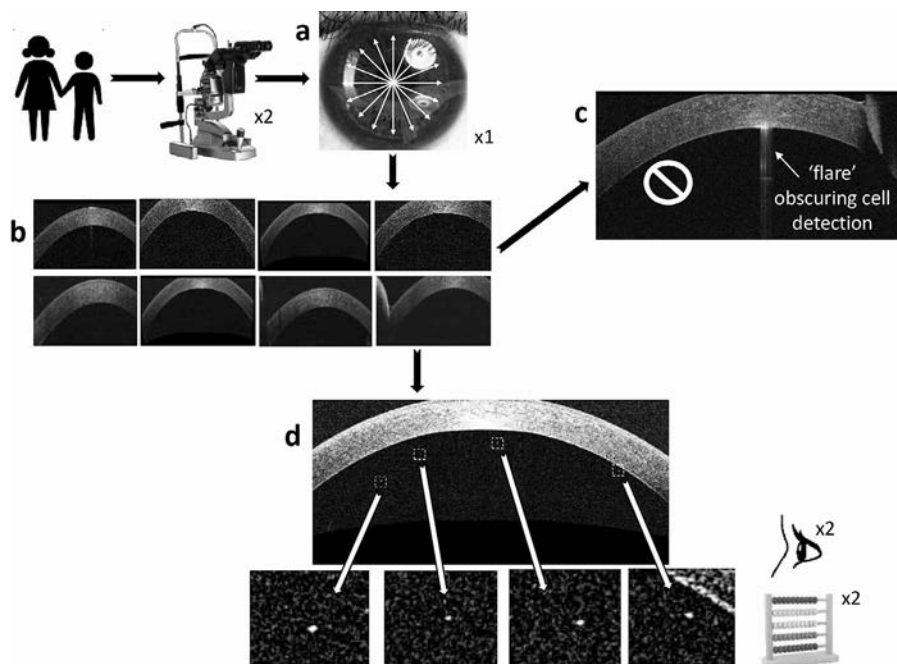


Figure 1. Image acquisition and analysis. After clinical examination and image acquisition, cross-sectional images were subjected to magnification and analysis. **a**, One set of 8 cross-sectional images was acquired from each eye. **b**, Image sets were downloaded to an analysis program and reviewed for quality. **c**, Images with flare were discarded. **d**, Manual analysis of good-quality images was conducted. A full set of good-quality images was available for 44 eyes from 26 children; incomplete sets were available for 8 eyes from 8 children (range 1–6 good-quality images acquired per eye). x2 indicates children were examined by 2 clinicians and counted twice by 2 observers.

Feasibility and acceptability. Time taken to acquire images from both eyes ranged from 1.5 minutes to 22 minutes per child (median time 8 minutes) with a trend toward faster acquisition times as the study progressed (trend $R^2 = 0.4092$, $P < 0.001$) (Supplementary Figure 1, available on the *Arthritis & Rheumatology* website at <http://onlinelibrary.wiley.com/doi/10.1002/art.41530/abstract>). The patient with the longest acquisition time of 22 minutes (patient 3) was 3 years old. The other 2 younger patients (ages 4 years and 5 years) had successful acquisition of images from both eyes within 8 minutes. Of the 52 imaged eyes, a full quota of 8 analyzable images was acquired in 44 eyes (Figure 1), with a total of 377 images undergoing manual cell counting. Patient acceptability scores for the acquisition process were acquired from all those imaged, with 23 older children self-rating and the remaining 3 children having proxy ratings completed by their parents. Acceptability scores ranged from 8.5 to 10 on a scale of 0–10 (median 9.5).

Repeatability of manual counting. Across single images from eyes considered positive for inflammation by manual cell counting, the median cell count per image was 2 (range 1–9). There was good intraobserver image agreement, with an ICC of 0.81 (95% confidence interval [95% CI] 0.63, 0.98) and Bland-Altman limit of agreement indicating agreement of 1 cell across different counts repeated by the same observer (limit of agreement = -1.1 cells [95% CI -1.4 , -0.8] to 1.0 [0.7, 1.4]). There was moderate agreement on cell count between observers ($\kappa = 0.46$ [95% CI 0.28, 0.63]; $P < 0.001$), with evidence of a wider limit of agreement of -2.5 cells (95% CI -3.1 , -1.9) to 1.5 cells (95% CI 0.8, 2.1). There was disagreement between image observers on the presence of intraocular cells in 25 (6.6%) of the 377 reviewed images.

Diagnostic performance indices of anterior segment OCT detection of inflammation. The 44 eyes with a full quota of 8 analyzable images were used in the analysis of diagnostic performance. There was disagreement between image observers on whether cells were detected on OCT imaging in 6 of 44 eyes (Supplementary Table 2, available on the *Arthritis & Rheumatology* website at <http://onlinelibrary.wiley.com/doi/10.1002/art.41530/abstract>). There was disagreement between clinicians on whether an eye was actively inflamed or inactive on SUN slit-lamp grading in 1 of 44 eyes (Supplementary Table 1, <http://onlinelibrary.wiley.com/doi/10.1002/art.41530/abstract>).

No inflammatory cells were detected on anterior segment OCT imaging of the eyes of children without uveitis. Following random selection for inclusion in analysis of 1 eye from each child, of the 12 eyes in which active inflammation was diagnosed on slit-lamp examination, anterior segment OCT images detected inflammatory cells in all but 1 (Table 1). Of the 7 eyes with clinically inactive uveitis (SUN score of 0 for no active inflammation detected on slit-lamp examination), anterior segment OCT

Table 1. Diagnostic accuracy of anterior segment OCT versus slit-lamp examination*

	Positive OCT	Negative OCT	Total
Active inflammation on slit lamp	11	1	12
No active inflammation on slit lamp	2	12	14
Total	13	13	26

* Optical coherence tomography (OCT) had a sensitivity of 91.7 (95% confidence interval [95% CI] 61.5, 99.8), a specificity of 85.7 (95% CI 57.2, 98.2), a positive likelihood ratio of 6.4 (95% CI 1.8, 23.4), a negative likelihood ratio of 0.1 (95% CI 0.01, 0.6), a positive predictive value of 84.6 (95% CI 60.1, 92.3), a negative predictive value of 92.3 (95% CI 64.5, 98.8), and accuracy of 88.5 (95% CI 69.9, 97.6).

detected inflammatory cells in 2 eyes. These cells were detected in children with a known diagnosis of chronic relapsing remitting anterior uveitis.

The negative predictive value of anterior segment OCT manual image cell count for the diagnosis of active inflammation (ruling out inflammation) among the 26 children with or without uveitis was 92% (95% CI 65, 99%) (Table 1).

Correlation of anterior segment OCT cell count and clinical assessment of inflammation. On multilevel regression modeling (thus enabling analysis of both eyes for each child with adjustment for clustering at the participant level), there was good positive correlation between clinical assessment and image-based cell count (correlation coefficient 3.3 [95% CI 1.3, 5.2]) ($R^2 = 0.63$, $P = 0.002$) (Figure 2).

DISCUSSION

In this study, we showed that acquisition of anterior ocular chamber images from children is feasible and acceptable to children and their families. Manual analysis of images is subject to interobserver and intraobserver variability but acquired images can be used to diagnose active inflammation with high levels of sensitivity and specificity.

This study had limitations, including the small sample size and the setting within a quaternary care center. As such, study findings cannot necessarily be extrapolated to the wider population of children at risk of uveitis. However, image acquisition was uniformly viewed to be acceptable by the children undergoing imaging and their families. The same is likely to be true for the wider population. In this study, acceptability of anterior segment OCT as a diagnostic intervention tool has been assessed through the narrow window of the affective attitude of children and families toward image acquisition. A more robust and multifaceted approach to determining the acceptability of this novel diagnostic modality would include measurement of the perceived effectiveness, comparison to existing modalities, opportunity costs, as well as burden (9). The latter has been indirectly captured within our study through the examination of the duration of image acquisition, and

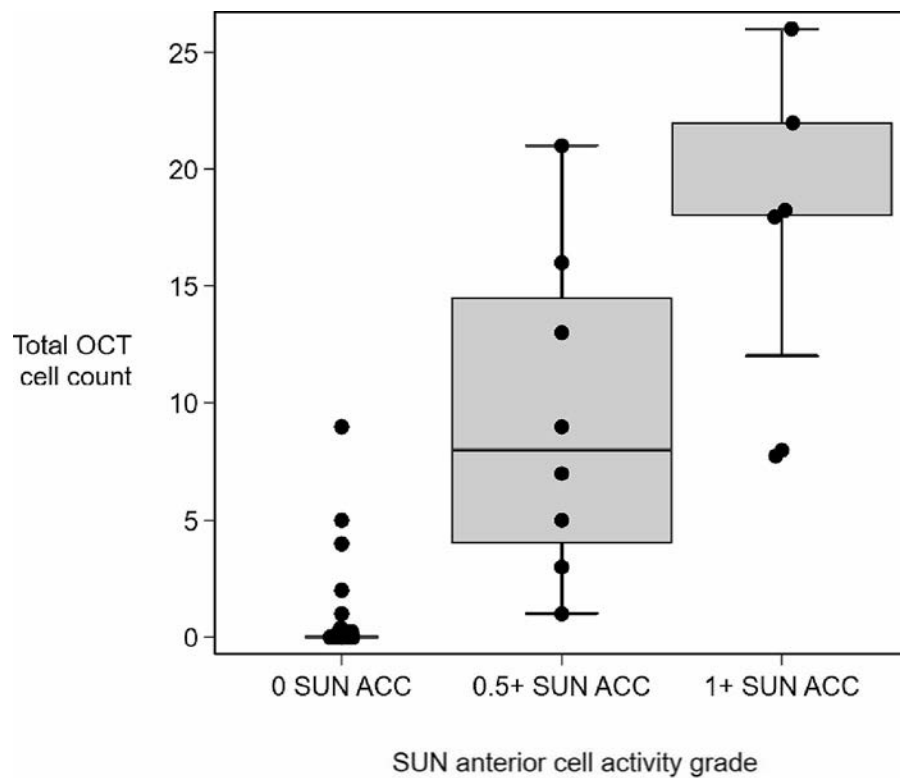


Figure 2. Correlation between Standardized Uveitis Nomenclature (SUN) anterior cell activity (ACC) grade obtained from slit-lamp examination and total cell count obtained by anterior segment optical coherence tomography (OCT). Of the 26 children examined, data for all 44 eyes with full sets of 8 images were included. All eyes of children in the control group who did not have uveitis had 0 affected cells detectable on anterior segment OCT imaging. Data are shown as box plots. Each box represents the 25th to 75th percentiles. Lines inside the boxes represent the median. Lines outside the boxes represent the 10th and 90th percentiles. Circles indicate individual patients.

it is reasonable to presume that the other perceived or experienced aspects of acceptability have influenced participant scores. We were able to show with confidence that the majority of children and families have a strongly positive experience of anterior segment OCT image acquisition within the settings of a feasibility study, which speaks toward acceptability within the broader context of clinical practice.

Poor vision has a significantly negative impact on a child that may be prolonged into adulthood (2,10). The strongest predictor of poor visual outcome for children with JIA-associated uveitis is the presence of established eye complications at diagnosis (11). Early diagnosis, before uncontrolled inflammation has led to structural sequelae, is key to avoiding life-changing visual disability in children at risk. The current diagnostic tool, slit-lamp assessment with quantification of inflammation using the international SUN scale, is subjective, is a semiquantitative measure with wide interobserver variability, and has not been validated for use in children (12). Images such as those successfully acquired in our study are suitable for automated assessment of cell count.

Automated analysis would enable an objective, sensitive measure of the presence and degree of inflammation (7). Laser-based flare-measuring machines have been used to monitor childhood uveitis through objective quantification of

the degree of protein in anterior ocular chamber aqueous fluid. These instruments have not been widely adapted for clinical use because of the time burden of acquisition, cost, and poor clinical utility in other disease areas (11). Conversely, similarly priced OCT machines have been widely adopted in secondary care and primary care settings and across primary care opticians, due to proven clinical utility in a wide variety of common adult eye conditions (13). This wide adoption would support the future implementation of image-based uveitis surveillance and imaging to augment disease monitoring, using images acquired in the community. This would be particularly desirable over the current situation in which uveitis surveillance typically necessitates examination every 3 months within a pediatric eye care center. These centers may be geographically distant from the child's home (14), and there is growing concern about insufficient workforce in pediatric ophthalmology (15). Recent attempts to build OCT machines, which patients can use to self-image, have been successful (16) and pave the way for home-based telemedicine consultations. OCT-based assessments have the additional advantage over slit-lamp examination of enabling the assessor to sit at some distance from the patient, lowering the risk of disease transmission in the coronavirus disease 2019 era.

Results from anterior segment OCT correlate reasonably well with those from slit-lamp examination, but further work is needed to refine anterior segment OCT imaging protocols (particularly for younger children) across the different available OCT machines to automate image analysis in order to further remove variability and to understand the predictive power of imaging for longer term outcomes of interest for clinicians and patients, similar to the work undertaken to demonstrate the utility of MRI measures as early independent predictors of progression in structural joint damage on radiography. This will be particularly key for those children who have detectable inflammation on OCT but no apparent inflammation on slit-lamp examination. Remission is defined as the cessation of a disease or symptoms for a defined period of time. Uveitis specialists now face a challenge familiar to that of other rheumatologists—defining disease cessation—which will require prospective studies able to examine long-term outcomes for children stratified using varying definitions of remission.

Research into outcomes for children with JIA-associated uveitis, or uveitis associated with other autoimmune or autoinflammatory disorders, requires reproducible and child-appropriate outcome measures. Imaging-based metrics for uveitis hold the promise of providing sensitive, robust, validated measurement of disease status which, alongside standardized data sets and patient-centered metrics, can also improve service provision, prognostication, and precision in disease management for affected or at-risk children. Posterior segment OCT imaging for adult retinal disease was initially undertaken only in specialist eye centers, then rapidly adopted across primary care settings, with subsequent automation of analysis across the different imaging platforms (6). A similar trajectory for anterior segment OCT assessment of inflammation will require validation studies to refine acquisition protocols and implement automation of image assessment. These studies will establish the most cost-effective and clinically effective use of anterior segment OCT imaging (cross-platform image acquisition and image analysis) for childhood uveitis, when compared to routine clinical examination. Image-based uveitis surveillance may provide objective and sensitive processes for improving telemedicine care in children with JIA.

ACKNOWLEDGMENTS

We thank Elizabeth Graham, Harry Petrushkin, Sandrine Lacassagne, and Reshma Pattani for their support with this work.

AUTHOR CONTRIBUTIONS

All authors were involved in drafting the article or revising it critically for important intellectual content, and all authors approved the final version to be published. Ms Akbarali had full access to all of the data in the study and takes responsibility for the integrity of the data and the accuracy of the data analysis.

Study conception and design. Rahi, Dick, Liu, Solebo.





Acquisition of data. Akbarali, Edelsten, Solebo.

Analysis and interpretation of data. Akbarali, Parkash, Etherton, Solebo.

REFERENCES

1. Thierry S, Fautrel B, Lemelle I, Guillemin F. Prevalence and incidence of juvenile idiopathic arthritis: a systematic review. *Joint Bone Spine* 2014;81:112–7.
2. Angeles-Han ST, McCracken C, Yeh S, Jenkins K, Stryker D, Rouster-Stevens K, et al. Characteristics of a cohort of children with juvenile idiopathic arthritis and JIA-associated uveitis. *Pediatr Rheumatol Online J* 2015;13:19.
3. Angeles-Han ST, Ringold S, Beukelman T, Lovell D, Cuello CA, Becker ML, et al. 2019 American College of Rheumatology/Arthritis Foundation guideline for the screening, monitoring, and treatment of juvenile idiopathic arthritis-associated uveitis. *Arthritis Care Res (Hoboken)* 2019;71:703–16.
4. Jabs DA, Nussenblatt RB, Rosenbaum JT. Standardization of uveitis nomenclature for reporting clinical data: results of the First International Workshop. *Am J Ophthalmol* 2005;140:509–16.
5. Baker JF, Conaghan PG, Smolen JS, Aletaha D, Shults J, Emery P, et al. Development and validation of modified disease activity scores in rheumatoid arthritis: superior correlation with magnetic resonance imaging-detected synovitis and radiographic progression. *Arthritis Rheumatol* 2014;66:794–802.
6. Fujimoto J, Huang D. Foreword 25 years of optical coherence tomography. *Invest Ophthalmol Vis Sci* 2016;57:OCTi-ii.
7. Liu X, Solebo AL, Faes L, Beese S, Braithwaite T, Round ME, et al. Instrument-based tests for measuring anterior chamber cells in uveitis: a systematic review. *Ocul Immunol Inflamm* 2020;28:898–907.
8. Shimizu Y, Nakakura S, Nagasawa T, Okamoto A, Tabuchi H, Kiuchi Y. Comparison of the anterior chamber angle structure between children and adults. *J AAPOS* 2017;21:57–62.
9. Sekhon M, Cartwright M, Francis JJ. Acceptability of healthcare interventions: an overview of reviews and development of a theoretical framework. *BMC Health Serv Res* 2017;17:88.
10. Cumberland PM, Rahi JS. Visual function, social position, and health and life chances: the UK Biobank Study. *JAMA Ophthalmol* 2016;134:959–66.
11. Rodriguez-Smith J, Yeh S, Angeles-Han S. Improving quick and accurate diagnosis of childhood JIA-uveitis from a pediatric rheumatology perspective. *Expert Rev Ophthalmol* 2020;15:101–9.
12. Kempen JH, Ganesh SK, Sangwan VS, Rathinam SR. Interobserver agreement in grading activity and site of inflammation in eyes of patients with uveitis. *Am J Ophthalmol* 2008;146:813–8.
13. Dabasia PL, Edgar DF, Garway-Heath DF, Lawrenson JG. A survey of current and anticipated use of standard and specialist equipment by UK optometrists. *Ophthalmic Physiol Opt* 2014;34:592–613.
14. Solebo AL, Rahi JS, Edelsten C, Ashworth JL, Dick AD. Management of paediatric ocular inflammatory disease in the UK: national survey of practice [letter]. *Eye (Lond)* 2020;34:591–2.
15. Royal College of Ophthalmologists. Workforce census 2018. URL: <https://www.rcophth.ac.uk/wp-content/uploads/2019/02/RCOphth-Workforce-Census-2018.pdf>.
16. Maloca P, Hasler PW, Barthelmes D, Arnold P, Matthias M, Scholl HP, et al. Safety and feasibility of a novel sparse optical coherence tomography device for patient-delivered retina home monitoring. *Transl Vis Sci Technol* 2018;7:8.

Tapering Canakinumab Monotherapy in Patients With Systemic Juvenile Idiopathic Arthritis in Clinical Remission: Results From a Phase IIIb/IV Open-Label, Randomized Study

Pierre Quartier,¹  Ekaterina Alexeeva,² Tamàs Constantin,³ Vyacheslav Chasnyk,⁴ Nico Wulffraat,⁵ Karin Palmblad,⁶ Carine Wouters,⁷ Hermine I. Brunner,⁸  Katherine Marzan,⁹ Rayfel Schneider,¹⁰ Gerd Horneff,¹¹ Alberto Martini,¹² Jordi Anton,¹³  Xiaoling Wei,¹⁴ Alan Slade,¹⁵ Nicolino Ruperto,¹⁶  and Ken Abrams,¹⁵ in collaboration with the Paediatric Rheumatology International Trials Organisation and the Pediatric Rheumatology Collaborative Study Group

Objective. To evaluate the efficacy and safety of 2 canakinumab monotherapy tapering regimens in order to maintain complete clinical remission in children with systemic juvenile idiopathic arthritis (JIA).

Methods. The study was designed as a 2-part phase IIIb/IV open-label, randomized trial. In the first part, patients received 4 mg/kg of canakinumab subcutaneously every 4 weeks and discontinued glucocorticoids and/or methotrexate as appropriate. Patients in whom clinical remission was achieved (inactive disease for at least 24 weeks) with canakinumab monotherapy were entered into the second part of the trial, in which they were randomized 1:1 into 1 of 2 treatment arms. In arm 1, the dose of canakinumab was reduced from 4 mg/kg to 2 mg/kg and then to 1 mg/kg, followed by discontinuation. In arm 2, the 4 mg/kg dose interval was prolonged from every 4 weeks, to every 8 weeks, and then to every 12 weeks, followed by discontinuation. In both arms, canakinumab exposure could be reduced provided systemic JIA remained in clinical remission for 24 weeks with each step. The primary objective was to assess whether >40% of randomized patients in either arm maintained clinical remission of systemic JIA for 24 weeks in the first part of the study.

Results. In part 1 of the study, 182 patients were enrolled, with 75 of those patients randomized before entering part 2 of the trial. Among the 75 randomized patients, clinical remission was maintained for 24 weeks in 27 (71%) of 38 patients in arm 1 (2 mg/kg every 4 weeks) and 31 (84%) of 37 patients in arm 2 (4 mg/kg every 8 weeks) ($P \leq 0.0001$ for arm 1 versus arm 2 among those meeting the 40% threshold). Overall, 25 (33%) of 75 patients discontinued canakinumab, and clinical remission was maintained for at least 24 weeks in all 25 of these patients. No new safety signals were identified.

Conclusion. Reduction of canakinumab exposure may be feasible in patients who have achieved clinical remission of systemic JIA, but consistent interleukin-1 inhibition appears necessary to maintain this response.

INTRODUCTION

Systemic juvenile idiopathic arthritis (JIA), the most severe category of JIA, is characterized by systemic inflammation and

arthritis. Systemic inflammation is manifested through spiking quotidian fever, maculopapular rash, hepatosplenomegaly, lymphadenopathy, serositis, and elevated serum levels of inflammation markers such as C-reactive protein (CRP), erythrocyte

ClinicalTrials.gov identifier: NCT02296424.

Supported by Novartis Pharma AG.

¹Pierre Quartier, MD: RAISE Reference Centre for Rare Diseases, Necker-Enfants Malades, AP-HP, Imagine Institute, Paris University, Paris, France; ²Ekaterina Alexeeva, MD, PhD: National Medical Research Center of Children's Health of the Ministry of Health of the Russian Federation, Sechenov First Moscow State Medical University of the Ministry of Health of the Russian Federation, Moscow, Russia; ³Tamàs Constantin, MD: Semmelweis University, Budapest, Hungary; ⁴Vyacheslav Chasnyk, MD: St. Petersburg State Pediatric Medical University, St. Petersburg, Russia; ⁵Nico Wulffraat, MD: University Medical Center Utrecht, Utrecht, The Netherlands; ⁶Karin Palmblad, MD, PhD: Karolinska Institutet, Karolinska University Hospital, Stockholm, Sweden;

⁷Carine Wouters, MD, PhD: University of Leuven, Department of Microbiology and Immunology, Laboratory of Adaptive Immunology & Immunobiology, University Hospitals Leuven, Department of Pediatrics, Leuven, Belgium; ⁸Hermine I. Brunner, MD, MSc, MBA: University of Cincinnati, Cincinnati Children's Hospital Medical Center, Cincinnati, Ohio; ⁹Katherine Marzan, MD: Children's Hospital Los Angeles, Los Angeles, California; ¹⁰Rayfel Schneider, MBBCh: University of Toronto and Hospital for Sick Children, Toronto, Ontario, Canada; ¹¹Gerd Horneff, MD: Asklepios Klinik St. Augustin, St. Augustin, Germany, and University Hospital Cologne, Cologne, Germany; ¹²Alberto Martini, MD: Istituto Giannina Gaslini, IRCCS, Genoa, Italy; ¹³Jordi Anton, MD, PhD: Hospital St. Joan de Déu, Esplugues de Llobregat, Spain, and Universitat de Barcelona, Barcelona, Spain; ¹⁴Xiaoling Wei, MSc: China

sedimentation rate, and ferritin (1–5). Systemic JIA is a systemic autoinflammatory disease, and the innate immune system plays a prominent role in its pathophysiology (6,7).

Currently available therapeutic agents for systemic JIA include nonsteroidal antiinflammatory drugs (NSAIDs), glucocorticoids, and disease-modifying antirheumatic drugs (DMARDs), including synthetic DMARDs and biologic DMARDs targeting interleukin-1 (IL-1) and IL-6 (7–14). Tumor necrosis factor (TNF) blockers can also be used, but their efficacy is generally lower in systemic JIA compared to other forms of JIA (15,16). The goal of systemic JIA treatment is to achieve and maintain complete clinical remission in order to avoid complications and improve long-term outcomes (17,18). Therapeutic strategies aiming to minimize exposure to systemic glucocorticoids, and ideally, discontinue them, are of great importance to prevent severe and longstanding side effects associated with the long-term use of these drugs, particularly growth inhibition and obesity (19,20). In recent years, the paradigm of explicitly defining a treatment target and applying tight control and necessary adjustment of therapy to reach it has been incorporated into “treat-to-target” recommendations for several rheumatic diseases, including JIA (17,18). Treat-to-target strategies may include the reduction of exposure to DMARDs, or even discontinuation, for patients with systemic JIA in clinical remission; however, very limited scientific evidence is currently available on the effects of tapering synthetic or biologic DMARDs in patients with systemic JIA.

IL-1 plays a major role in the pathogenesis of systemic JIA (7), and blockade of IL-1 can provide effective therapeutic control of disease activity (8–11,14,21). Canakinumab, a human anti-IL-1 β monoclonal antibody, has shown sustained efficacy in treating systemic JIA patients and allowing the tapering of glucocorticoids (8,10). In a pivotal phase III study of canakinumab in patients with active systemic JIA, the average glucocorticoid dose could be reduced from 0.34 mg/kg to 0.05 mg/kg in patients treated with canakinumab, with 42 (33%) of 128 patients discontinuing glucocorticoids (10). However, limited information is available on the effects of reducing exposure to, or even discontinuation of, canakinumab in patients with systemic JIA in clinical remission. In a long-term extension study, tapering of canakinumab to a reduced dose of 2 mg/kg every 4 weeks was attempted, with 44 (25%) of 177 patients receiving at least 3 reduced doses over a median follow-up

of 25 months (8). The dose reduction in these 44 patients was maintained until study end in 26 (59%) of the patients. Therefore, in this study, we evaluated the efficacy and safety of 2 canakinumab monotherapy tapering schemes in patients with systemic JIA in clinical remission.

PATIENTS AND METHODS

Study design. The present study was designed as a randomized, open-label, 2-part clinical trial. As shown in Figure 1, the trial included 2 cohorts of patients with systemic JIA. Cohort 1 comprised patients with systemic JIA who had inactive disease at their last visit. These patients were included in a previous long-term extension trial of canakinumab preceded by other pivotal studies (8,10) (see Supplementary Figure 1 for a summary of the flow of patients in the clinical trials of the canakinumab development program, available on the *Arthritis & Rheumatology* website at <http://onlinelibrary.wiley.com/doi/10.1002/art.41488/abstract>). Inactive disease was considered achieved when the following criteria were met (22): no joints with active arthritis; no fever due to systemic JIA; no rash, serositis, splenomegaly, hepatomegaly, or generalized lymphadenopathy attributable to systemic JIA; normal CRP serum levels (or, if elevated, not attributable to systemic JIA); and a physician global assessment of disease activity score of ≤ 10 mm (on a 100-mm visual analog scale [VAS]), indicating inactive disease. Cohort 2 comprised newly recruited patients with systemic JIA who had never been treated with canakinumab and who had active disease at the time of enrollment (see the Supplementary Appendix for inclusion and exclusion criteria, available on the *Arthritis & Rheumatology* website at <http://onlinelibrary.wiley.com/doi/10.1002/art.41488/abstract>).

In part 1 of the trial, all patients received 4 mg/kg of open-label canakinumab subcutaneously every 4 weeks. Patients taking systemic glucocorticoids and/or methotrexate (MTX) at the time of study entry were encouraged, at the discretion of the investigator, to taper and discontinue these medications according to protocol-specified guidelines (Supplementary Appendix, available on the *Arthritis & Rheumatology* website at <http://onlinelibrary.wiley.com/doi/10.1002/art.41488/abstract>) at any time after study entry (cohort 1) or to discontinue these medications 8 weeks after study initiation (cohort 2). Patients in whom clinical remission was achieved (which was classified as

Novartis Institutes for Biomedical Research, Ltd, Beijing, China; ¹⁵Alan Slade, PharmD, Ken Abrams, MD: Novartis Pharmaceuticals Corporation, East Hanover, New Jersey; ¹⁶Nicolino Ruperto, MD, MPH: Clinica Pediatrica e Reumatologia, PRINTO, Istituto Giannina Gaslini, IRCCS, Genoa, Italy.

Dr. Quartier has received consulting fees, speaking fees, and/or honoraria from Novartis (less than \$10,000). Dr. Brunner has received consulting fees, speaking fees, and/or honoraria from GlaxoSmithKline (less than \$10,000) and from Roche and Novartis (more than \$10,000 each). Dr. Schneider has received consulting fees from Novartis, NovImmune, Sobi, and Roche (less than \$10,000 each). Dr. Horneff has received consulting fees, speaking fees, and/or honoraria from Eli Lilly, GSK, Novartis, Pfizer, and Sobi (less than \$10,000 each). Dr. Martini has received consulting fees, speaking fees, and/or honoraria from Eli Lilly, EMD Serono, Janssen, Novartis, Pfizer, and AbbVie

(less than \$10,000 each). Dr. Anton has received consulting fees, speaking fees, and/or honoraria from Novartis, Sobi, Roche, Sanofi, AbbVie, Pfizer, and NovImmune (less than \$10,000 each). Dr. Wei owns stock or stock options in Novartis. Dr. Ruperto has received consulting fees from Ablynx, AbbVie, AstraZeneca-Medimmune, Biogen, Boehringer, Bristol Myers Squibb, Eli Lilly, EMD Serono, GlaxoSmithKline, Hoffmann-La Roche, Janssen, Merck, Novartis, Pfizer, R-Pharma, Sanofi, Servier, Sinergie, Sobi, and Takeda (less than \$10,000 each). No other disclosures relevant to this article were reported.

Address correspondence to Pierre Quartier, MD, UIHR, Necker-Enfants Malades Hospital, 149 Rue de Sèvres, 75015 Paris, France. Email: pierre.quartier@aphp.fr.

Submitted for publication January 27, 2020; accepted in revised form August 6, 2020.

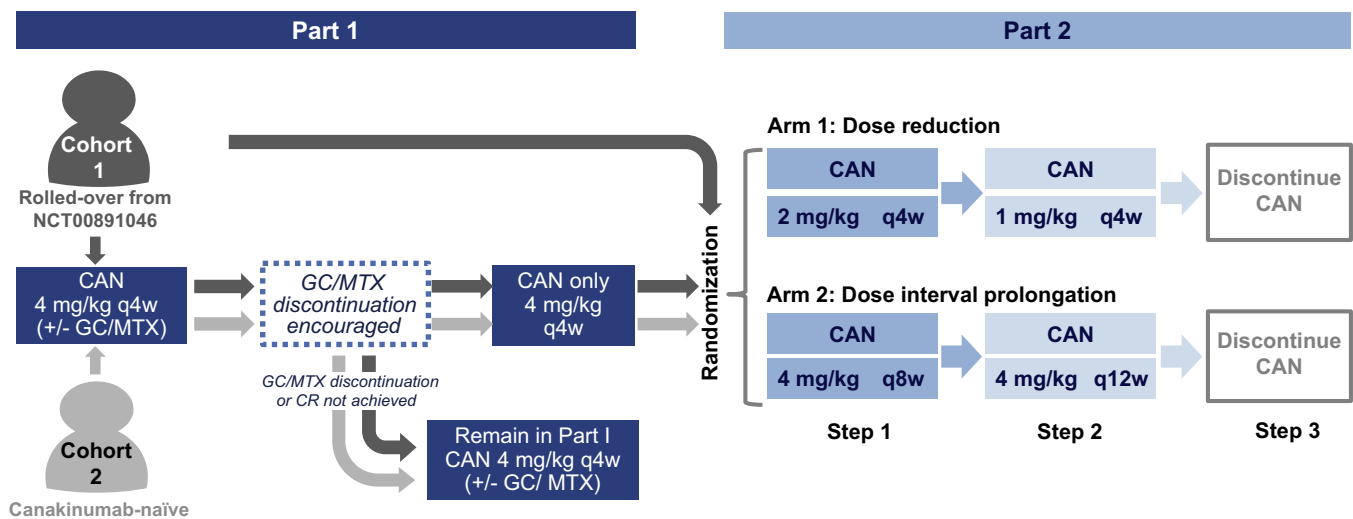


Figure 1. Flow chart of the study design. Cohort 1 comprised patients with systemic juvenile idiopathic arthritis in complete clinical remission (CR) at the last visit of a previous long-term extension trial of canakinumab (CAN) (ClinicalTrials.gov identifier: NCT00891046) (8). Patients in cohort 1 who were already receiving canakinumab monotherapy could enter directly into part 2 of the study. Cohort 2 comprised newly recruited patients with active disease at baseline. Patients in whom clinical remission was achieved with canakinumab monotherapy for at least 4 weeks in part 1 entered part 2 of the study (as long as the randomization period was still open). Patients in whom these criteria were not met, or in whom criteria were met after randomization was closed, remained in part 1 until study end. Randomization was only to achieve balance between the treatment arms as no comparison between the cohorts was planned. GC = glucocorticoid; MTX = methotrexate; q4w = every 4 weeks.

having maintained inactive disease for ≥ 24 weeks) and who had received canakinumab monotherapy for ≥ 4 weeks were considered eligible for randomization in part 2 of the study. A sample size of 76 patients was estimated to be sufficient for the evaluation of the primary objective (sample size calculations are available in the Supplementary Appendix), and therefore randomization was stopped once this predefined target was reached. Patients who met eligibility criteria after this time point did not enter the second part of the study and remained in part 1 until study end. Patients who were eligible to enroll in part 2 were randomized 1:1 into 1 of 2 treatment arms. Randomization was performed only to achieve balance between the treatment arms, and therefore it was not necessary to compare the number of patients deemed eligible before and after this time point.

In both treatment arms, open-label canakinumab exposure was progressively reduced in 3 consecutive steps (24 weeks each) as long as clinical remission was maintained. In the dose reduction arm, the tapering schedule was as follows: reduction from 4 mg/kg of canakinumab every 4 weeks during the first part of the study to 2 mg/kg every 4 weeks (step 1), reduction from 2 mg/kg to 1 mg/kg of canakinumab every 4 weeks (step 2), and then finally discontinuation (step 3). In the dose interval prolongation arm, prolongation of the dose intervals in canakinumab therapy was as follows: prolongation of the 4 mg/kg dose of canakinumab during the first part of the study from every 4 weeks to every 8 weeks (step 1), then to every 12 weeks (step 2), and then finally discontinuation (step 3). At every step, patients were considered as having “regimen failure” and were required to return to a regimen

of 4 mg/kg of canakinumab every 4 weeks if they experienced any of the following: a systemic JIA flare according to the criteria for disease flare in pediatric JIA (10,23), need for up-titration of medication, or need for treatment with systemic glucocorticoids or MTX. In patients with regimen failure, we required that achievement of clinical remission in these individuals be demonstrated again with 4 mg/kg of canakinumab monotherapy every 4 weeks. If clinical remission was maintained in these patients, they were then permitted to attempt tapering again. Finally, patients in whom clinical remission was not maintained and did not experience regimen failure remained in the reduced-dose regimen. If clinical remission was achieved in these patients again, they were allowed to progress to the next tapering step and further reduce or discontinue canakinumab.

The present study was conducted from November 2014 to September 2017 in 45 centers from 16 countries following the ethics principles of the Declaration of Helsinki and the Good Clinical Practice guidelines and was approved by an independent ethics committee for each participating country. Participating centers were members of the Paediatric Rheumatology International Trials Organisation (PRINTO) and the Pediatric Rheumatology Collaborative Study Group (PRCSG) (see Appendix A for the full list of study investigators) (24,25). All patients, parents, or legal guardians of patients provided written informed consent.

Study objectives. The primary objective of the study was to assess whether, on initiation of these regimens in part 2 of the study in patients with systemic JIA in clinical remission

who had been receiving 4 mg/kg of canakinumab monotherapy, at least 40% of patients remained in clinical remission for 24 consecutive weeks after randomization to either the dose reduction arm (dose reduced to 2 mg/kg every 4 weeks) or the dose interval prolongation arm (4 mg/kg dose interval prolonged to every 8 weeks). This 40% threshold was chosen after consultation with a panel of experts from the PRINTO and PRCSG networks and was estimated to be meaningful for clinical practice. The 24-week time point was determined taking into account that 8–12 weeks are required to reach steady-state serum concentrations of canakinumab (26), and 12 additional weeks were estimated to be an appropriate observation period to assess the effect of the drug thereafter. The secondary objective of the study was to assess the long-term safety and tolerability of canakinumab throughout the trial. Additional metrics included the proportion of patients treated with canakinumab who successfully discontinued MTX and glucocorticoids (in part 1 of the study), the efficacy of canakinumab over time as measured according to the American College of Rheumatology (ACR) preliminary definition of improvement in juvenile arthritis (27), and determination of the extent of disease activity according to the Juvenile Arthritis Disease Activity Score (JADAS) (28–30).

Outcome measures. In the present study, the following ACR core set measures adapted for JIA (27) were used to assess active disease: the physician global assessment of disease activity on a 0–100-mm VAS, patient/parent assessment of patient overall well-being, number of joints with active arthritis according to the ACR definition, number of joints with limitation of motion, CRP values (normal range 0–10 mg/liter), the cross-culturally adapted and validated version of the Childhood Health Assessment Questionnaire (C-HAQ) score (31), and fever (defined as having a body temperature of >38°C) in the preceding week due to systemic JIA. Inactive disease status was assessed every 4 weeks and at any point at which the investigators suspected worsening of systemic JIA symptoms.

To assess the extent of disease activity, the JADAS score in 27 joints using the CRP level (JADAS27-CRP) was calculated as previously described (28–30,32,33). Clinical responses were measured according to achievement of 30%, 70%, and 90% levels of improvement in the ACR core set measures adapted for JIA (ACR Pediatric 30 [ACR Pedi 30], ACR Pedi 70, and ACR Pedi 90, respectively), as previously described (27,34), along with the absence of fever.

The safety of canakinumab was assessed in terms of adverse events (AEs) and serious AEs (SAEs) classified according

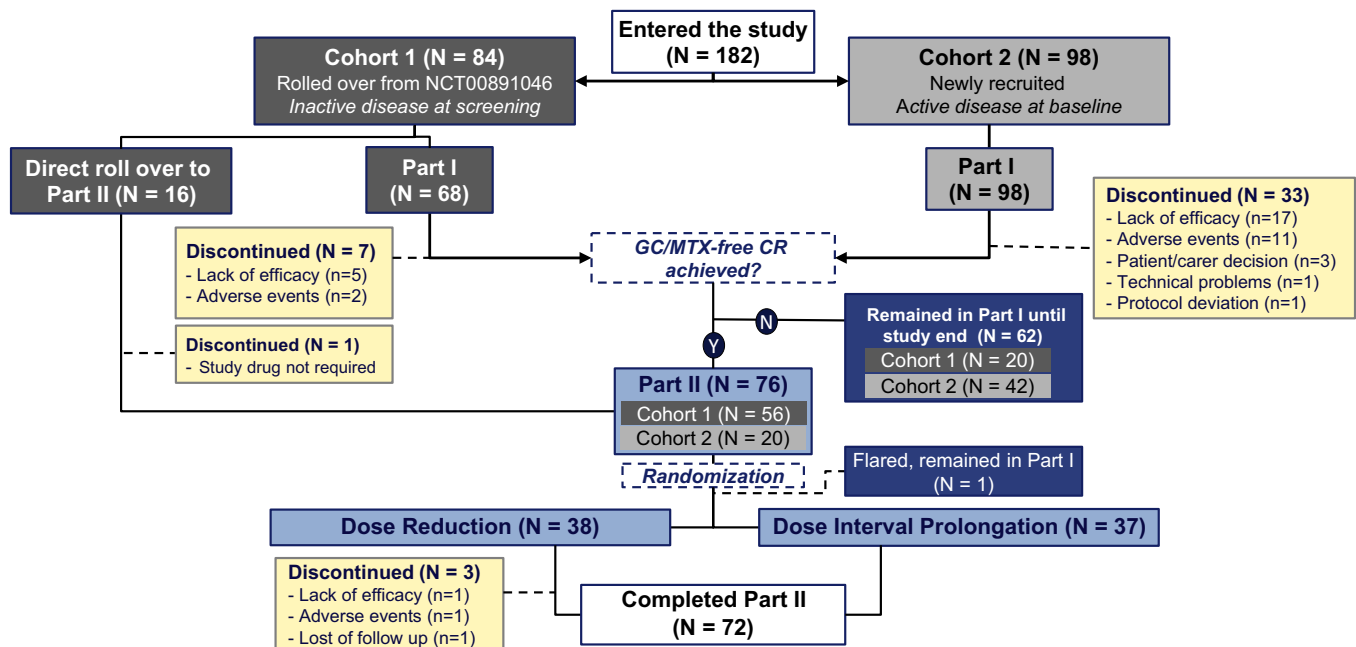


Figure 2. Flow chart of the study population. In total, 182 individuals entered the study, with 44 discontinuing the study and 138 completing it. Sixty-three patients remained in part 1 until study end, and 72 patients completed part 2. After reaching the predefined population of 76 patients for part 2 (patients in whom clinical remission [CR] with canakinumab monotherapy was achieved without glucocorticoids [GCs] or methotrexate [MTX]), randomization enrollment was closed, and patients in whom clinical remission was achieved with canakinumab monotherapy after this time remained in part 1 of the study. Among the 62 patients who were not randomized and remained in part 1 until study end, protocol deviations were reported in 4 patients who were not randomized but progressed to the canakinumab tapering treatment arm, with 1 patient enrolled directly from the long-term extension trial of canakinumab (ClinicalTrials.gov identifier: NCT00891046) (8) and receiving 1 dose according to the dose reduction scheme before discontinuing the study and 3 additional patients in part 1 progressing to the dose interval prolongation treatment arm. These patients were not included in the efficacy analyses of part 2. Y = yes; N = no.

to version 20.1 of the Medical Dictionary for Regulatory Activities. All potential cases of macrophage activation syndrome (MAS), infections classified as SAEs, and malignancies were reviewed and adjudicated by independent adjudication committees that were established for each of these groups of AEs for the entire canakinumab development program (35). The clinical and laboratory assessments included the regular monitoring of hematology, blood chemistry, and urinalysis results as well as regular assessments of vital signs, physical condition, and body weight. Immunogenicity assessments were performed at baseline and every 24 weeks by testing for antidrug antibody concentrations in the serum over time, using a validated electrochemiluminescence immunoassay (36).

Statistical analysis. The study results were reported following the recommendations of the Consolidated Standards of Reporting Trials (CONSORT) statement (37) and the intent-to-treat (ITT) principle for parts 1 and 2 of the study, with imputation of missing data for nonresponders in analyses of the primary variables (as described in the Supplementary Appendix, available on the *Arthritis & Rheumatology* website at <http://onlinelibrary.wiley.com/doi/10.1002/art.41488/abstract>). The full analysis set and the safety set in part 1 were equivalent and consisted of all patients in cohort 1 or cohort 2 who received ≥ 1 dose of the study drug. The full analysis set in part 2 consisted of all patients who were randomized to undergo either dose reduction or dose interval prolongation of the study drug and who received ≥ 1 dose of canakinumab, and the safety set consisted of all patients who received ≥ 1 dose of the study drug.

Statistical hypotheses for the primary end point were tested by exact binomial test at the 2.5% level of significance. As

randomization in part 2 was performed solely for the purpose of avoiding selection bias, no inferential between-treatment comparisons were done. For safety evaluation, exposure-adjusted rates of AEs per 100 patient-days were summarized in part 1 of the study by cohorts and in part 2 by tapering regimen arm overall and for each tapering step within the regimen. Additional details on statistical methods and sample size calculation are provided in the Supplementary Appendix, available on the *Arthritis & Rheumatology* website at <http://onlinelibrary.wiley.com/doi/10.1002/art.41488/abstract>.

RESULTS

Study patients. The distribution of patients assessed in this study is depicted in Figure 2. Additionally, the flow of patients through clinical trials evaluating canakinumab is described in Supplementary Figure 1, available on the *Arthritis & Rheumatology* website at <http://onlinelibrary.wiley.com/doi/10.1002/art.41488/abstract>. Overall, 182 patients were enrolled in the present study. Cohort 1 included 84 (46.2%) of 182 patients, of whom 68 entered the first part of the study. The remaining 16 patients were directly eligible to enroll into the second part of the study, as clinical remission of systemic JIA was achieved in these patients with a canakinumab regimen that did not include glucocorticoids or MTX, and 15 of these patients were subsequently included in the second part of the study. Cohort 2 included 98 (53.8%) of 182 patients.

In the first part of the study, 166 patients were treated with 4 mg/kg of canakinumab every 4 weeks, with tapering and discontinuation of glucocorticoids and MTX allowed and encouraged, as described in the Patients and Methods. Of these individuals, 40

Table 1. Patient demographic and baseline clinical characteristics*

	Part 1			Part 2	
	Cohort 1 (n = 68)	Cohort 2 (n = 98)	Total (n = 166)	Dose reduction arm (n = 38)	Dose interval prolongation arm (n = 37)
Age, years	12 (8–15)	8 (5–12)	9 (6–14)	10.5 (7–15)	11 (9–14)
Female sex, no. (%)	34 (50)	56 (57.1)	90 (54.2)	19 (50)	20 (54.1)
Weight, kg	39.0 (28.4–54.3)	26.5 (19.4–41.8)	31.8 (22–48.4)	35.1 (23.4–55.2)	41.3 (29–54.2)
Parent or patient global assessment of overall well-being, 0–100-mm VAS	2 (0–8)	42 (17–65)	18.5 (2–52)	5 (0–46)	1 (0–10)
Physician global assessment of disease activity, 0–100-mm VAS	0 (0–2)	51 (38–63)	32 (0–54)	0 (0–11)	0 (0–26)
C-HAQ score	0 (0–0.4)	1.3 (0.5–1.8)	0.7 (0–1.5)	0 (0–1)	0.1 (0–0.6)
Number of joints with active arthritis	0 (0–0)	3 (2–8)	1 (0–5)	0 (0–0)	0 (0–0)
Standardized CRP level, mg/liter†	5.6 (0.6–9.7)	88.8 (24.3–255.7)	18.5 (4–114.2)	5.9 (0.5–10)	5.5 (2–10)
Systemic glucocorticoid use at baseline, no. (%)	23 (33.8)	50 (51)	73 (44)	7 (18.4)	10 (27)
Methotrexate use at baseline, no. (%)	31 (45.6)	32 (32.7)	63 (38)	11 (28.9)	4 (10.8)
Prior use of anakinra, no. (%)	22 (32.4)	15 (15.3)	37 (22.3)	16 (42.1)	11 (29.7)
Prior use of tocilizumab, no. (%)	15 (22.1)	20 (20.4)	35 (21.1)	9 (23.7)	5 (13.5)
Prior use of any biologic agents, no. (%)‡	41 (60.3)	36 (36.7)	77 (46.4)	23 (60.5)	15 (40.5)

* Except where indicated otherwise, values are the median (interquartile range). VAS = visual analog scale; C-HAQ = Childhood Health Assessment Questionnaire.

† C-reactive protein (CRP) analyses were performed by local laboratories and standardized for comparison across sites and patients.

‡ Includes anakinra, tocilizumab, abatacept, etanercept, and adalimumab.

patients (7 of 68 in cohort 1 [10.3%] and 33 of 98 in cohort 2 [33.7%]) discontinued the study, and 61 patients entered part 2. The remaining patients did not meet the eligibility criteria to enter the second part of the study before enrollment for randomization was closed, and therefore remained in part 1 until study end. The mean observation time in part 1 was 466 days in cohort 1 and 434 days in cohort 2.

In the second part of the study, 76 patients were randomized to receive canakinumab at either a reduced dose ($n = 38$) or a prolonged dose interval ($n = 38$). One patient randomized to the dose interval prolongation arm experienced a flare just after randomization, and therefore never initiated canakinumab tapering and moved back into part 1 of the study; this individual was not included in the analyses of the results derived from the second part of the study. The mean observation time in part 2 was 597 days for the dose reduction arm and 595 days for the interval-prolongation arm.

Demographics and baseline characteristics. Baseline demographic details and characteristics of patients enrolled in parts 1 and 2 of the study are summarized in Table 1. In part 1, there were more young children (age <6 years) in cohort 2 (17 of 98, or 17%) compared to cohort 1 (6 of 68, or 8.8%). The median values for clinical parameters and disease activity scores at baseline were high among patients in cohort 2, including CRP level, number of joints with active disease, number of joints with limited range of motion, physician global assessment of disease activity scores, parent/patient global assessment of overall well-being, and C-HAQ scores. As expected, those parameters were much lower in cohort 1. In the second part of the study, baseline demographic characteristics were mostly comparable for the 2 treatment arms. At baseline, the mean time of prior exposure to canakinumab in cohort 1 patients was 3.1 years. Of note, only 8 of 84 patients in cohort 1 had previously attempted a dose reduction to 2 mg/kg of canakinumab every 4 weeks in the long-term extension trial of canakinumab (8).

Efficacy. *Tapering of glucocorticoids and MTX and achievement of clinical remission in part 1 of the study.* In cohort 1, discontinuation of glucocorticoids during the first part of the study was achieved in 9 (39%) of 23 patients who had received them at baseline, and MTX was discontinued in 13 (42%) of 31 patients. During the first 24 weeks of part 1, inactive disease was maintained in a relatively constant proportion of the patients in cohort 1 who were receiving canakinumab monotherapy (Figure 3A). In total, clinical remission was achieved in 46 of 68 patients who received canakinumab monotherapy in part 1 of the study and in 41 patients who entered part 2 of the study. Calculated median JADAS27-CRP scores remained low during the first 24 weeks of the study (Figure 3B). Flares of systemic JIA were experienced by 14 (20%) of 68 patients.

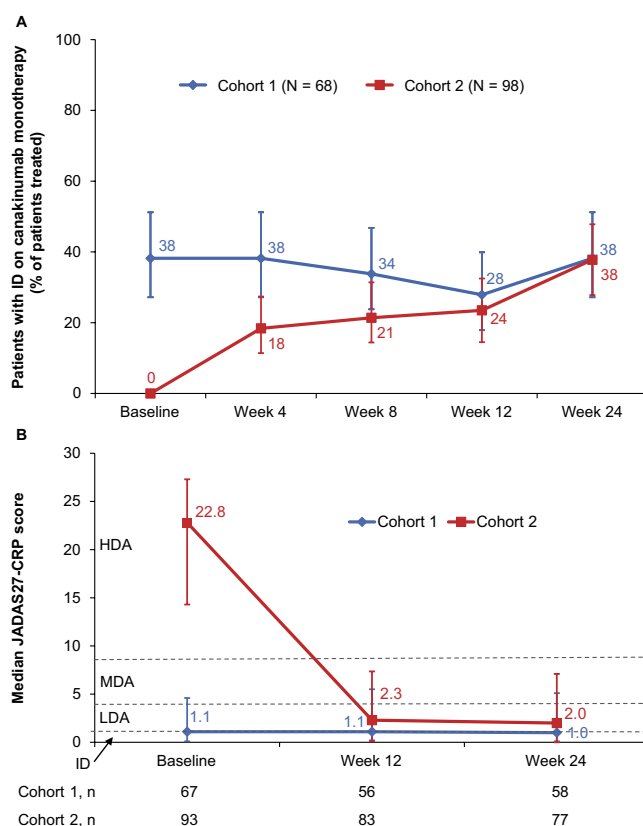


Figure 3. Efficacy of canakinumab in part 1 of the study. **A**, Percentage of systemic juvenile idiopathic arthritis (JIA) patients with inactive disease (ID) following canakinumab monotherapy. Intent-to-treat (ITT) analysis of the full analysis set is shown, with imputation of missing data for nonresponders in the initial 24 weeks of part 1. For each time point, the percentage of patients with inactive disease who received canakinumab monotherapy (with treatment maintained until the end of part 1) is presented. Percentages were calculated from the total ITT population, which included patients who had received glucocorticoids and/or methotrexate. Values indicate percentages, and error bars show the 95% confidence intervals. Of note, no adjustment for multiple comparisons has been performed, and line graphs used are only for descriptive purposes. **B**, Median Juvenile Arthritis Disease Activity Scores in 27 joints using the C-reactive protein level (JADAS27-CRP) in cohorts 1 and 2 ($n = 68$ and $n = 98$, respectively). Numbers under the line graph represent the actual number of patients evaluated at each time point. Values indicate median scores, and error bars show the interval between the first and third quartiles. Horizontal lines represent the JADAS cutoff values for high disease activity (HDA) (>8.5), moderate disease activity (MDA) (3.9–8.5), low disease activity (LDA) (1.1–3.8), and inactive disease (≤ 1). Of note, these cutoff values have been defined for polyarticular JIA and have not been evaluated specifically in systemic JIA.

In cohort 2, of the 50 patients who received glucocorticoids at baseline, glucocorticoids were discontinued in 17 patients (34%) by the end of part 1, whereas MTX was discontinued in 19 (59%) of 32 patients who had received it at baseline. The proportion of patients in cohort 2 in whom inactive disease was able to be maintained with canakinumab monotherapy increased progressively during the first 24 weeks (Figure 3A). The median time from the

first dose of canakinumab to inactive disease achievement was 8 weeks (data not shown). In total, clinical remission was achieved in 49 of 98 patients from cohort 2 who received canakinumab monotherapy in part 1, and among these 49 patients, 20 entered the second part of the study.

A clear decrease was observed in the median JADAS27-CRP scores from baseline to week 4, decreasing from a median score of 22.8 to 2.6, which was maintained until week 24 of the study (Figure 3B). The efficacy of canakinumab was also reflected by ACR Pedi 30, ACR Pedi 70, and ACR Pedi 90 responses observed in patients from cohort 2, with >60% of the patients presenting with ACR Pedi 90 responses at week 24 (Supplementary Figure 2, available on the *Arthritis & Rheumatology* website at <http://onlinelibrary.wiley.com/doi/10.1002/art.41488/abstract>). Flares of systemic JIA were experienced by 34 (35%) of 98 patients in cohort 2 during part 1.

Tapering of canakinumab in part 2 of the study. The proportion of patients in whom clinical remission was achieved for 24 weeks was assessed as a percentage with 97.5% confidence intervals (97.5% CIs) for patients in each group. At the first tapering event in step 1 of part 2 of the study, the proportion of patients in whom clinical remission was achieved for 24 weeks with a reduced dose of canakinumab of 2 mg/kg every 4 weeks was 27 of 38 (71% of patients [97.5% CI 52–86%]), and the proportion of patients in whom clinical remission was achieved with the prolonged dose interval regimen of 4 mg/kg

every 8 weeks was 31 of 37 patients (84% of patients [97.5% CI 66–95%]) (Figure 4). These values significantly exceeded the predefined threshold of 40% ($P \leq 0.0001$), indicating that the primary end point was met.

Analyses using an exact logistic regression model showed that prior exposure to canakinumab (which occurred in cohort 1 but not in cohort 2) did not impact the probability of being able to maintain clinical remission in the patients at step 1 (data not shown). When including patients in whom clinical remission was not maintained after the initial attempt and who underwent a second attempt, the proportions of patients in whom clinical remission was maintained in step 1 were slightly higher, with 29 (76%) of 38 patients in the dose reduction arm and 33 (89%) of 37 patients in the dose interval prolongation arm maintaining clinical remission. Of note, 7 patients (4 in the dose reduction arm and 3 in the dose interval prolongation arm) did not meet the criteria for inactive disease at all visits during the 24-week period in step 1, and were therefore not considered to be responders at the primary end point, but also did not meet the criteria for regimen failure (as defined in the Patients and Methods), and therefore investigators chose to keep those patients in the tapering regimens. A supportive analysis including these patients as responders showed higher success rates for both arms, with 31 (82%) of 38 patients in the dose reduction arm and 34 (92%) of 37 patients in the dose prolongation arm maintaining these regimens for at least 24 weeks during their first attempt in step 1.

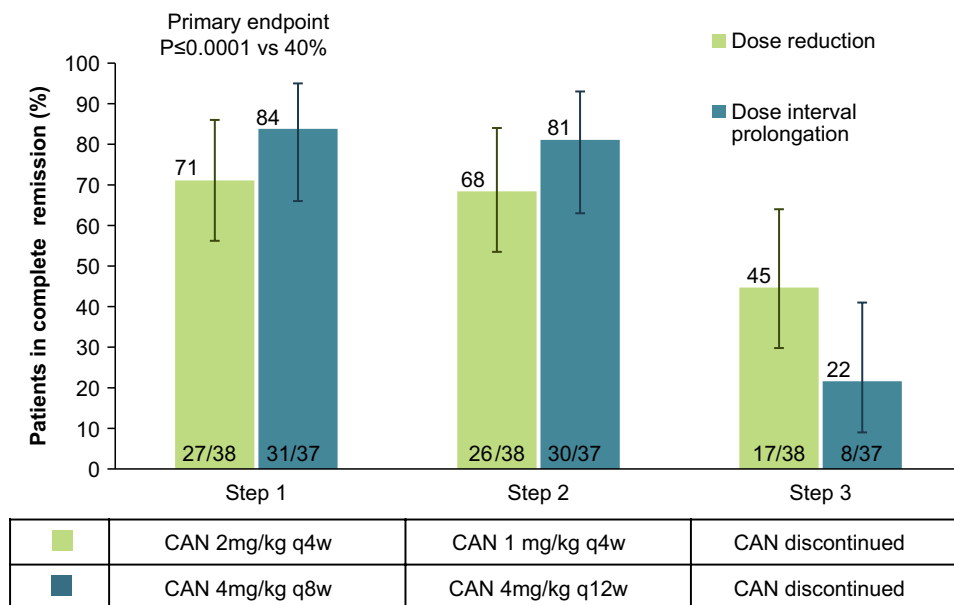


Figure 4. Proportion of patients in whom complete clinical remission (CR) of systemic juvenile idiopathic arthritis was maintained in part 2 of the study. Intent-to-treat (ITT) analysis of the full analysis set with imputation of missing data for nonresponders is shown. Values over bars indicate percentages, values within bars are the number of patients/total number assessed, and error bars show the 97.5% confidence intervals. Only patients in whom clinical remission was maintained for 24 weeks on the first attempt of dose reduction or dose interval prolongation of canakinumab (CAN) were categorized as responders. The proportion of patients in whom clinical remission was maintained in step 1 was significantly higher than the predefined 40% threshold (primary end point) for both treatment arms. No adjustment for multiple comparisons was performed for the remaining data shown, and therefore their presentation is only for descriptive purposes. q4w = every 4 weeks.

Table 2. Incidence of AEs in parts 1 and 2 of the study following adjustment for canakinumab exposure*

	Part 1			Part 2	
	Cohort 1 (n = 68)	Cohort 2 (n = 98)	Total (n = 166)	Dose reduction arm (n = 38)	Dose interval prolongation arm (n = 37)
Total AEs	1.64 (521)	2.45 (1,043)	2.11 (1,564)	1.59 (361)	1.32 (291)
Common AEs†					
Pyrexia	0.04 (13)	0.15 (63)	0.10 (76)	0.07 (17)	0.06 (13)
Nasopharyngitis	0.10 (32)	0.09 (38)	0.09 (70)	0.07 (16)	0.08 (18)
Headache	0.07 (21)	0.09 (37)	0.08 (58)	0.04 (10)	0.07 (16)
Arthralgia	0.04 (14)	0.08 (36)	0.07 (50)	0.07 (15)	0.05 (11)
Diarrhea	0.01 (3)	0.09 (39)	0.06 (42)	0.03 (7)	0.01 (2)
Cough	0.03 (10)	0.07 (29)	0.05 (39)	0.05 (11)	0.01 (3)
Rash	0.02 (5)	0.06 (25)	0.04 (30)	0.02 (4)	0.03 (7)
Upper respiratory tract infection	0.07 (22)	0.04 (18)	0.05 (40)	0.07 (16)	0.03 (6)
Viral infection	0.01 (4)	0.02 (8)	0.02 (12)	0.05 (12)	0.01 (3)
Serious AEs	0.05 (15)	0.08 (34)	0.07 (49)	0.02 (4)	0.01 (2)
Study drug discontinuation due to AEs, no.	3	12	15	1	0

* Except where indicated otherwise, values are the number of adverse events (AEs) per 100 patient-days in the safety set (total number of AEs).

† Common AEs were defined as those with incidence rates of >0.05 per 100 patient-days in either cohort or treatment arm.

In Figure 4, proportions of randomized patients in each arm in whom canakinumab exposure was further decreased at their first attempt in step 2 and who subsequently discontinued canakinumab at their first attempt in step 3 with maintenance of clinical remission for 24 weeks are displayed. Overall, 25 (33%) of 75 patients who were randomized in part 2 discontinued canakinumab and systemic JIA remained in clinical remission in step 3.

The proportion of patients with regimen failure in the dose reduction arm was 7 (18%) of 38, 3 (10%) of 28, and 2 (8.0%) of 25 for steps 1, 2, and 3, respectively. In the dose prolongation arm, these proportions were 1 (2.7%) of 37, 2 (6.1%) of 33, and 4 (15%) of 27. In all patients except 1 (in the dose reduction arm), systemic JIA returned to a state of inactive disease when canakinumab was up-titrated to 4 mg/kg every 4 weeks, according to the study protocol. Overall, 14 (19%) of 75 patients experienced disease flares in part 2, with similar proportions experiencing flares in the 2 treatment arms. The mean number of flares per patient was 0.1 in steps 1, 2, and 3 for the dose reduction arm and 0, 0, and 0.2 for steps 1, 2, and 3 in the dose prolongation arm.

Safety. Incidence of AEs. The mean duration of canakinumab exposure among patients in cohorts 1 and 2 enrolled in part 1 of the study was 466 days and 434 days, respectively. The incidence rate of AEs following adjustment for exposure was higher in cohort 2 (2.45 per 100 patient-days) than in cohort 1 (1.64 per 100 patient-days), with the most commonly reported AEs being pyrexia, nasopharyngitis, headache, arthralgia, and diarrhea (Table 2).

The mean duration of canakinumab exposure for patients randomized for enrollment in part 2 of the study was 489 days for the dose reduction arm and 495 days for the dose prolongation arm. Incidence rates for AEs following adjustment for exposure were 1.59 per 100 patient-days in the dose reduction arm and

1.32 per 100 patient-days in the dose interval prolongation arm (Table 2), with the more commonly reported AEs being pyrexia, nasopharyngitis, upper respiratory tract infection, arthralgia, and headache. Incidence of AEs for each tapering regimen overall as well as for each tapering step is shown in Supplementary Table 1, available on the *Arthritis & Rheumatology* website at <http://online.library.wiley.com/doi/10.1002/art.41488/abstract>. There was no apparent correlation between incidence of AEs and the tapering regimens or tapering steps used in the present study.

Serious AEs and AEs leading to drug discontinuation. Overall, 33 patients (19.9%) in part 1 experienced at least 1 SAE. Incidence rates of SAEs following adjustment for exposure were 0.05 per 100 patient-days in cohort 1 and 0.08 per 100 patient-days in cohort 2 (Table 2). In part 2, SAEs were reported in 4 patients (10.5%) in the dose reduction arm and 1 patient (2.7%) in the dose interval prolongation arm, with exposure-adjusted incidence rates of 0.02 and 0.01 per 100 patient-days, respectively (Table 2). Most SAEs represented isolated events, with infections and infestations being the most commonly reported system organ class affected (Supplementary Table 2, available on the *Arthritis & Rheumatology* website at <http://onlinelibrary.wiley.com/doi/10.1002/art.41488/abstract>). Most SAEs classified as infections or infestations occurred in part 1 of the study, and they were more frequently reported in cohort 2 (9 events, or 0.02 per 100 patient-days) than in cohort 1 (4 events, or 0.01 per 100 patient-days) (Supplementary Table 2). No SAEs of infections were indicated as being opportunistic infections, as adjudicated by an independent committee. Two SAEs related to lung disease were reported, including a mild case of interstitial lung disease and a severe case of alveolar proteinosis that led to study discontinuation for that individual. No deaths were reported during the study.

In part 1, study treatment discontinuation due to AEs occurred in a higher proportion of patients in cohort 2 (12.2%) compared to cohort 1 (4.4%) (Table 2). The most common reasons for discontinuation were disease-related, namely MAS and AEs related to systemic JIA worsening or disease flares. Only 1 patient in part 1 (in the dose reduction arm) experienced an AE (blepharitis) that led to study discontinuation.

Macrophage activation syndrome. In part 1, 5 events were assessed as probable MAS by an independent MAS adjudication committee. These included 2 SAEs of MAS reported in 2 patients in cohort 2 and 3 patients (1 in cohort 1 and 2 in cohort 2) with laboratory abnormalities consistent with MAS (ferritin level of ≥ 500 $\mu\text{g/liter}$ and elevated levels of liver transaminases). In part 2, 1 SAE of MAS in a patient in the dose reduction arm was adjudicated as probable MAS.

Immunogenicity. No antidrug antibodies were detected during the study, except in 1 patient in cohort 1 in whom non-neutralizing antidrug antibodies were detected at an unplanned visit (82 days after last dose of the study drug) and in whom no detectable antibodies were observed at all other visits.

DISCUSSION

In this study, a treat-to-target strategy was used in patients with systemic JIA who were treated with canakinumab. Achievement of clinical remission was chosen as the treatment target, and therapeutic interventions were adjusted to maintain it. Results from this study indicate that systemic JIA patients in whom clinical remission has been maintained with the recommended canakinumab monotherapy regimen of 4 mg/kg every 4 weeks could reduce their exposure to canakinumab either by dose reduction or dose interval prolongation and still be able to maintain clinical remission. No substantial differences between the 2 tapering strategies were apparent, although the study was not designed or powered to compare between the reduced dose and the increased dosing interval therapies, and as such, meaningful comparisons cannot be made.

Clinical remission could be maintained in most patients who were randomized in part 2 of this trial to receive either 2 mg/kg of canakinumab monotherapy every 4 weeks or 4 mg/kg every 8 weeks. Moreover, in almost all patients in whom clinical remission was maintained with 2 mg/kg of canakinumab every 4 weeks, the dose could be further reduced to 1 mg/kg every 4 weeks in step 2. Similarly, in almost all patients in whom clinical remission was maintained with 4 mg/kg of canakinumab every 8 weeks, the dose interval could be further increased to 12 weeks. These results suggest that the progressive tapering methods used in this trial are appropriate to reduce canakinumab exposure in this patient population, with a low incidence of regimen failure, which is defined as occurrence of systemic JIA flares or requirement of canakinumab up-titration or treatment with systemic glucocorticoids or MTX. Nevertheless, only one-third of the patients could

discontinue canakinumab (step 3 in this study) with maintained clinical remission for at least 24 weeks, indicating that a certain level of IL-1 inhibition may be important to maintain clinical remission in the majority of these patients.

The AEs recorded in parts 1 and 2 of this trial were consistent with the known safety profile of canakinumab. Overall, there was no apparent association between progressively tapering canakinumab (either by dose reduction or dose interval prolongation) and the incidence of any class of AEs (including events of MAS) or systemic JIA flares.

Very limited clinical evidence is currently available to support appropriate dose reduction or tapering of DMARDs in patients with systemic JIA or other JIA subtypes. Foell and colleagues compared relapse rates in patients with several types of JIA in clinical remission who discontinued MTX after 6 or 12 months (38). They found no differences between the 2 groups, with ~50% of the patients experiencing a flare within 24 months following study inclusion. Lovell et al reported that discontinuation of anti-TNF treatment in JIA patients resulted in disease flare in 37% of patients by 8 months (39). Results from a previous prospective observational single-center cohort study have demonstrated the efficacy of first-line treatment with IL-1 receptor antagonist anakinra administered daily as monotherapy in 42 patients with newly diagnosed systemic JIA (14). In that study, anakinra was discontinued in patients with an ACR Pedi 90 response for 3 consecutive months (14,34). Results showed that 22 patients had discontinued anakinra and presented with inactive disease after 1 year of follow-up, 25 patients after 3 years, and 18 patients after 5 years.

Part 1 of this trial investigated the efficacy of administering 4 mg/kg of canakinumab every 4 weeks in patients with systemic JIA, to assess whether clinical remission could be achieved without adjunct therapy with glucocorticoids and/or MTX. In treating patients with active disease (cohort 2), efficacy with canakinumab was consistent with the results from previous pivotal phase III trials (10), and clinical remission could be achieved in 50% of the patients receiving canakinumab monotherapy. Also consistent with reported data from the previous pivotal phase III and long-term extension studies was that the discontinuation of glucocorticoids was successful in one-third of the patients who received them at baseline (8,10). These results underline the difficulty in achieving discontinuation of glucocorticoids in patients with systemic JIA. In addition, this study was the first to evaluate the effectiveness of canakinumab in enabling discontinuation of MTX, with nearly 50% of the patients achieving this outcome.

Key limitations of the present study include the open-label nature of canakinumab treatment, lack of a comparator arm in part 2 that included sustained canakinumab monotherapy without tapering, lack of sufficient power to compare between reduced dose and reduced frequency tapering regimens, and the decision to consider the maintenance of 40% of patients in whom clinical remission was achieved as meaningful in clinical practice.

In summary, we observed achievement of clinical remission with canakinumab monotherapy in >50% of the patients in part 1 of the study and maintenance of clinical remission with reduced-exposure canakinumab monotherapy in a high proportion of patients in part 2. We believe that these results are relevant for clinical practice, particularly for designing personalized tapering strategies that can allow an adequate control of disease while minimizing the side effects of certain medications, notably glucocorticoids (17). Our results also show that while clinical remission was maintained in the majority of systemic JIA patients during canakinumab tapering, only a minority of patients could eventually discontinue canakinumab and maintain clinical remission of systemic JIA. Therefore, a certain level of sustained inhibition of the IL-1 pathway seems important for the maintenance of clinical remission in most patients with systemic JIA.

AUTHOR CONTRIBUTIONS

All authors were involved in drafting the article or revising it critically for important intellectual content, and all authors approved the final version to be published. Dr. Quartier had full access to all of the data in the study and takes responsibility for the integrity of the data and the accuracy of the data analysis.

Study conception and design. Quartier, Alexeeva, Constantin, Palmblad, Wouters, Brunner, Martini, Wei, Slade, Ruperto, Abrams.

Acquisition of data. Quartier, Constantin, Chasnyk, Wulffraat, Palmblad, Marzan, Schneider, Horneff, Anton, Wei, Slade, Ruperto, Abrams.

Analysis and interpretation of data. Quartier, Palmblad, Brunner, Horneff, Wei, Slade, Ruperto, Abrams.

ROLE OF THE STUDY SPONSOR

Novartis had no role in the writing of the manuscript or the decision to submit the manuscript for publication. Publication of this article was not contingent upon approval by Novartis. Authors Wei, Slade, and Abrams are employees of Novartis. We thank Rajeeb Ghosh, of Novartis Healthcare, and Marco Migliaccio for medical writing assistance, which was funded by Novartis Pharma AG, Basel, Switzerland.

REFERENCES




- Petty RE, Southwood TR, Manners P, Baum J, Glass DN, Goldenberg J, et al. International League of Associations for Rheumatology classification of juvenile idiopathic arthritis: second revision, Edmonton, 2001. *J Rheumatol* 2004;31:390–2.
- Prakken B, Albani S, Martini A. Juvenile idiopathic arthritis. *Lancet* 2011;377:2138–49.
- Ravelli A, Martini A. Juvenile idiopathic arthritis. *Lancet* 2007;369:767–78.
- Martini A, Ravelli A, di Fuccia G, Rosti V, Cazzola M, Barosi G. Intravenous iron therapy for severe anaemia in systemic-onset juvenile chronic arthritis. *Lancet* 1994;344:1052–4.
- Consolaro A, Giancane G, Alongi A, van Dijkhuizen EH, Aggarwal A, al-Mayouf SM, et al. Phenotypic variability and disparities in treatment and outcomes of childhood arthritis throughout the world: an observational cohort study. *Lancet Child Adolesc Heal* 2019;3:255–63.
- Vastert SJ, Kuis W, Grom AA. Systemic JIA: new developments in the understanding of the pathophysiology and therapy. *Best Pract Res Clin Rheumatol* 2009;23:655–64.
- Pascual V, Allantaz F, Arce E, Punaro M, Banchereau J. Role of interleukin-1 (IL-1) in the pathogenesis of systemic onset juvenile idiopathic arthritis and clinical response to IL-1 blockade. *J Exp Med* 2005;201:1479–86.
- Ruperto N, Brunner HI, Quartier P, Constantin T, Wulffraat NM, Horneff G, et al. Canakinumab in patients with systemic juvenile idiopathic arthritis and active systemic features: results from the 5-year long-term extension of the phase III pivotal trials. *Ann Rheum Dis* 2018;77:1710–9.
- Ruperto N, Quartier P, Wulffraat N, Woo P, Ravelli A, Mouy R, et al. A phase II, multicenter, open-label study evaluating dosing and preliminary safety and efficacy of canakinumab in systemic juvenile idiopathic arthritis with active systemic features. *Arthritis Rheum* 2012;64:557–67.
- Ruperto N, Brunner HI, Quartier P, Constantin T, Wulffraat N, Horneff G, et al. Two randomized trials of canakinumab in systemic juvenile idiopathic arthritis. *N Engl J Med* 2012;367:2396–406.
- Quartier P, Allantaz F, Cimaz R, Pillet P, Messiaen C, Bardin C, et al. A multicentre, randomised, double-blind, placebo-controlled trial with the interleukin-1 receptor antagonist anakinra in patients with systemic-onset juvenile idiopathic arthritis (ANAJIS trial). *Ann Rheum Dis* 2011;70:747–54.
- De Benedetti F, Brunner HI, Ruperto N, Kenwright A, Wright S, Calvo I, et al. Randomized trial of tocilizumab in systemic juvenile idiopathic arthritis. *N Engl J Med* 2012;367:2385–95.
- Ruperto N, Martini A. Current and future perspectives in the management of juvenile idiopathic arthritis. *Lancet Child Adolesc Heal* 2018;2:360–70.
- Ter Haar NM, van Dijkhuizen EH, Swart JF, van Royen-Kerkhof A, el Idrissi A, Leek AP, et al. Treatment to target using recombinant interleukin-1 receptor antagonist as first-line monotherapy in new-onset systemic juvenile idiopathic arthritis: results from a five-year follow-up study. *Arthritis Rheumatol* 2019;71:1163–73.
- Quartier P, Taupin P, Bourdeaut F, Lemelle I, Pillet P, Bost M, et al. Efficacy of etanercept for the treatment of juvenile idiopathic arthritis according to the onset type. *Arthritis Rheum* 2003;48:1093–101.
- Horneff G, Schmeling H, Biedermann T, Foeldvari I, Ganser G, Girschick HJ, et al. The German etanercept registry for treatment of juvenile idiopathic arthritis. *Ann Rheum Dis* 2004;63:1638–44.
- Ravelli A, Consolaro A, Horneff G, Laxer RM, Lovell DJ, Wulffraat NM, et al. Treating juvenile idiopathic arthritis to target: recommendations of an international task force. *Ann Rheum Dis* 2018;77:819–28.
- Magnani A, Pistorio A, Magni-Manzoni S, Falcone A, Lombardini G, Bandeira M, et al. Achievement of a state of inactive disease at least once in the first 5 years predicts better outcome of patients with polyarticular juvenile idiopathic arthritis. *J Rheumatol* 2009;36:628–34.
- Vannucci G, Cantarini L, Giani T, Marrani E, Moretti D, Pagnini I, et al. Glucocorticoids in the management of systemic juvenile idiopathic arthritis. *Pediatr Drugs* 2013;15:343–9.
- Guzman J, Kerr T, Ward LM, Ma J, Oen K, Rosenberg AM, et al. Growth and weight gain in children with juvenile idiopathic arthritis: results from the ReACCh-Out cohort. *Pediatr Rheumatol* 2017;15:68.
- Lovell DJ, Giannini EH, Reiff AO, Kimura Y, Li S, Hashkes PJ, et al. Long-term safety and efficacy of rilonacept in patients with systemic juvenile idiopathic arthritis. *Arthritis Rheum* 2013;65:2486–96.
- Wallace CA, Ruperto N, Giannini E, on behalf of the Childhood Arthritis and Rheumatology Research Alliance, Pediatric Rheumatology International Trials Organization, and the Pediatric Rheumatology Collaborative Study Group. Preliminary criteria for clinical remission for select categories of juvenile idiopathic arthritis. *J Rheumatol* 2004;31:2290–4.
- Brunner HI, Lovell DJ, Finck BK, Giannini EH. Preliminary definition of disease flare in juvenile rheumatoid arthritis. *J Rheumatol* 2002;29:1058–64.

24. Brunner HI, Rider LG, Kingsbury DJ, Co D, Schneider R, Goldmuntz E, et al. Pediatric Rheumatology Collaborative Study Group: over four decades of pivotal clinical drug research in pediatric rheumatology [review]. *Pediatr Rheumatol Online J* 2018;16:45.
25. Ruperto N, Martini A. Networking in paediatrics: the example of the Paediatric Rheumatology International Trials Organisation (PRINTO). *Arch Dis Child* 2011;96:596–601.
26. Sun H, Van LM, Floch D, Jiang X, Klein UR, Abrams K, et al. Pharmacokinetics and pharmacodynamics of canakinumab in patients with systemic juvenile idiopathic arthritis. *J Clin Pharmacol* 2016;56:1516–27.
27. Giannini EH, Ruperto N, Ravelli A, Lovell DJ, Felson DT, Martini A. Preliminary definition of improvement in juvenile arthritis. *Arthritis Rheum* 1997;40:1202–9.
28. Consolaro A, Bracciolini G, Ruperto N, Pistorio A, Magni-Manzoni S, Malattia C, et al. Remission, minimal disease activity, and acceptable symptom state in juvenile idiopathic arthritis: defining criteria based on the juvenile arthritis disease activity score. *Arthritis Rheum* 2012;64:2366–74.
29. Consolaro A, Ruperto N, Bracciolini G, Frisina A, Gallo MC, Pistorio A, et al. Defining criteria for high disease activity in juvenile idiopathic arthritis based on the Juvenile Arthritis Disease Activity Score. *Ann Rheum Dis* 2014;73:1380–3.
30. Consolaro A, Ruperto N, Bazso A, Pistorio A, Magni-Manzoni S, Filocamo G, et al. Development and validation of a composite disease activity score for juvenile idiopathic arthritis. *Arthritis Care Res* 2009;61:658–66.
31. Ruperto N, Ravelli A, Pistorio A, Malattia C, Cavuto S, Gado-West L, et al. Cross-cultural adaptation and psychometric evaluation of the Childhood Health Assessment Questionnaire (CHAQ) and the Child Health Questionnaire (CHQ) in 32 countries: review of the general methodology. *Clin Exp Rheumatol* 2001;19:S1–9.
32. Nordal EB, Zak M, Aalto K, Berntson L, Fasth A, Herlin T, et al. Validity and predictive ability of the juvenile arthritis disease activity score based on CRP versus ESR in a Nordic population-based setting. *Ann Rheum Dis* 2012;71:1122–7.
33. McErlane F, Beresford MW, Baildam EM, Chieng SEA, Davidson JE, Foster HE, et al. Validity of a three-variable Juvenile Arthritis Disease Activity Score in children with new-onset juvenile idiopathic arthritis. *Ann Rheum Dis* 2013;72:1983–8.
34. Vastert SJ, de Jager W, Noordman BJ, Holzinger D, Kuis W, Prakken BJ, et al. Effectiveness of first-line treatment with recombinant interleukin-1 receptor antagonist in steroid-naïve patients with new-onset systemic juvenile idiopathic arthritis: results of a prospective cohort study. *Arthritis Rheumatol* 2014;66:1034–43.
35. Grom AA, Ilowite NT, Pascual V, Brunner HI, Martini A, Lovell D, et al. Rate and clinical presentation of macrophage activation syndrome in patients with systemic juvenile idiopathic arthritis treated with canakinumab. *Arthritis Rheumatol* 2016;68:218–28.
36. Committee for Medicinal Products for Human Use. Guideline on immunogenicity assessment of therapeutic proteins. URL: https://www.ema.europa.eu/en/documents/scientific-guideline/guide-line-immunogenicity-assessment-therapeutic-proteins-revision-1_en.pdf. European Medicines Agency. May 2017.
37. Schulz KF, Altman DG, Moher D, on behalf of the CONSORT Group. CONSORT 2010 statement: updated guidelines for reporting parallel group randomised trials. *BMC Med* 2010;8:18.
38. Foell D, Wulffraat N, Wedderburn LR, Wittkowski H, Frosch M, Gerss J, et al. Methotrexate withdrawal at 6 vs 12 months in juvenile idiopathic arthritis in remission: a randomized clinical trial. *JAMA* 2010;303:1266–73.
39. Lovell DJ, Johnson AL, Huang B, Gottlieb BS, Morris PW, Kimura Y, et al. Risk, timing, and predictors of disease flare after discontinuation of anti-tumor necrosis factor therapy in children with polyarticular forms of juvenile idiopathic arthritis with clinically inactive disease. *Arthritis Rheumatol* 2018;70:1508–18.

APPENDIX A: THE PRINTO AND PRCSG INVESTIGATORS

The PRINTO and PRCSG Investigators are as follows: W. Emminger, A. Ulbrich, S. Fodor (Vienna, Austria), C. Wouters, L. Desomer (Leuven, Belgium), B. Lauwerys, B. Brichard, C. Boulanger, G. Levy, L. Goffin, P.-Q. Le (Brussels, Belgium), M. Bandeira, C. Feitosa Pelajo (Curitiba, Brazil), S. Knupp Feitosa, C. Costa, M. Felix Rodrigues, C. Almeida da Silva, L. Mattei de, K. Kozu (Rio de Janeiro, Brazil), Ronald Laxer (Toronto, Canada), K. Houghton, L. Tucker, K. Morishita (Vancouver, Canada), A. Mogenet, R. Mouy, B. Bader Meunier, C. Meyzer, M. Semeraro, O. Ben-Brahim (Paris, France), I. Kone-Paut, C. Galeotti, L. Rossi, P. Dusser, B. Cherquaoui (Le Kremlin Bicetre, France), A. Belot, A. Duquesne, F. Caroline, L. Audrey, M. Desjonqueres (Bron Cedex, France), I. Foeldvari, A. Kienast, B. Willig, E. Weissbarth-Riedel, A. Froehlich (Hamburg, Germany), D. Barthel, J. Peitz, S. Wintrich, T. Geikowski, A. Schulz (St. Augustin, Germany), M. Hufnagel, M. Hirdes, R. Kubicki, J. Kirschner, A. Janda, A. Jacob, C. Emerich (Freiburg, Germany), A. Raab, G. Ngoumou, K. Minden, M. Lieber, S.-L. von Stuckrad, R. Trauzeddel, D. Haselbusch, H. Kolbeck (Berlin, Germany), J. Kuemmerle Deschner, S. Hansmann, T. Schleich, I. Magunia, J. Riethmuller, N. Anders (Tübingen, Germany), H. Lehmann, J. de Laffolie (Giessen, Germany), T. Lutz, J. Grulich-Henn, J. Pfeil, A. Helling-Bakki (Heidelberg, Germany), A. Ponyi, D. Garan, I. Orban, K. Sevcic (Budapest, Hungary), Y. Butbul, R. Brik, M. Helo (Haifa, Israel), P. Hashkes, O. Toker, R. Haviv (Jerusalem, Israel), Y. Uziel, R. Haviv, V. Moshe, M. Rothschild (Kfar-Saba, Israel), L. Harel, G. Amarillyo, R. Tal, M. Said (Petach-Tikva, Israel), I. Tirosh, S. Spielman, M. Gerstein (Ramat Gan, Israel), A. Ravelli, B. Schiappapietra, G. Varnier, M. Finetti, M. Marasini, R. Caorsi, S. Rosina, S. Federici (Genova, Italy), I. Pontikaki, P. Meroni, V. Gerloni, N. Ughi, T. Ubiali (Milano, Italy), M. Alessio, R. Della Casa (Nepoli, Italy), S. Vastert, J. Swart, A. van Royen-Kerhof, E. Schatorje, G. Van Iperen-Schutte (Utrecht, Netherlands), L. Rutkowska-Sak, I. Szczygielska, M. Kwiatkowska, M. Marusak-Banacka, P. Gietka, (Warsaw, Poland), K. Isaeva, R. Denisova (Moscow, Russia), L. Snegireva, M. Dubko, M. Kostik, N. Buchinskaia, O. Kalashnikova, S. Avrusin, V. Masalova (Saint-Petersburg, Russia), E. Nunez Cuadros, G. Diez, R. Galindo Zavala (Málaga, Spain), R. Bou Torrent, E. Iglesias, J. Calzada, V. Bittermann (Barcelona, Spain), A. Boteanu, M. L. Gamir, D. Clemente Garulo, J. C. Lopez Robledillo, R. Merino, R. Alcobendas, A. Remesal, S. Murias (Madrid, Spain), I. Calvo, B. Lopez, I. Gonzalez, L. Fernandez (Valencia, Spain), Bo Magnusson (Stockholm, Sweden), O. Kasapcopur, K. Barut, A. Adrovic, S. Sahin, M. Erguven, R. Gozdenur Savci (Istanbul, Turkey), S. Ozen, S. Demir, Y. Bilginer, Z. S. Avci, E. D. Batu (Ankara, Turkey), Andreas Reiff, Anusha Ramanatham, Diana Brown, Bracha Shaham, Shirley Parks, Michal Cidon (Los Angeles, California, US), G. Higgins, C. Spencer, J. Rossette, K. Jones, S. Bout Tabaku, S. Farley, S. Akoghanian (Columbus, Ohio, US).

Incidence, Clinical Features, and Outcomes of Late-Onset Neutropenia From Rituximab for Autoimmune Disease

Reza Zonozi,¹  Zachary S. Wallace,¹  Karen Laliberte,¹ Noah R. Huizenga,¹ Jillian M. Rosenthal,¹ Eugene P. Rhee,¹ Frank B. Cortazar,²  and John L. Niles¹

Objective. Late-onset neutropenia (LON) is an underrecognized complication of rituximab treatment. We undertook this study to describe its incidence, risk factors, clinical features, management, and recurrence.

Methods. We conducted a single-center retrospective cohort study of 738 adult patients with autoimmune disease who were treated with rituximab to induce continuous B cell depletion. The primary outcome measure was LON, defined as an unexplained absolute neutrophil count of <1,000 cells/ μ l during B cell depletion. Secondary outcome measures included incidental diagnosis, fever, sepsis, filgrastim use, and recurrent LON. We assessed predictors of LON using Cox proportional hazards regression models. Hazard ratios (HRs) and 95% confidence intervals (95% CIs) were calculated.

Results. We identified 107 episodes of LON in 71 patients. The cumulative incidence at 1 year of B cell depletion therapy was 6.6% (95% CI 5.0–8.7). The incidence rate during the first year was higher compared to thereafter (7.2 cases per 100 person-years [95% CI 5.4–9.6] versus 1.5 cases per 100 person-years [95% CI 1.0–2.3]). Systemic lupus erythematosus and combination therapy with cyclophosphamide were each independently associated with an increased risk of LON (adjusted HR 2.96 [95% CI 1.10–8.01] and 1.98 [95% CI 1.06–3.71], respectively). LON was not observed in minimal change disease or focal segmental glomerulosclerosis. The majority of episodes (59.4%) were asymptomatic. Fever and sepsis complicated 31.3% and 8.5% of episodes, respectively. Most patients (69%) were treated with filgrastim. Rituximab rechallenge occurred in 87% of patients, of whom 21% developed recurrent LON.

Conclusion. LON is common and often incidental. Most cases are reversible and respond well to filgrastim. However, LON can be associated with serious infections and thus warrants vigilant monitoring.

INTRODUCTION

B cell depletion with the anti-CD20 monoclonal antibody rituximab (RTX) has emerged as an important therapeutic strategy for many antibody-mediated autoimmune diseases. A single course of RTX treatment has demonstrated efficacy in inducing remission in antineutrophil cytoplasmic antibody (ANCA)-associated vasculitis (AAV) and rheumatoid arthritis (RA) (1,2). However, relapses are common following cessation of RTX treatment and are often preceded by B cell reconstitution (3,4). For this reason, extended courses of RTX are often used as maintenance therapy (5). However, the increasing use of B cell depletion has led to the emergence of treatment-related complications.

One such complication of B cell depletion therapy is late-onset neutropenia (LON). This entity was originally recognized in lymphoma patients treated with RTX (6–8). Initial studies on the lymphoma population portrayed LON to be rare (9), but later reports demonstrated higher incidences between 5% and 27% (10). More recently, LON has also been recognized in patients with autoimmune disease who were treated with RTX (11–15). However, these reports remain limited in size and scope.

We conducted a single-center retrospective cohort analysis of 738 patients undergoing B cell depletion therapy for autoimmune disease, in order to characterize the incidence, risk factors, clinical features, management, and recurrence of LON. Our study has the greatest number of initial and recurrent LON cases

Dr. Zonozi's work was supported by the National Institute of Diabetes and Digestive and Kidney Diseases, NIH (grant 5T32-DK-007540). Dr. Wallace's work was supported by the National Institute of Arthritis and Musculoskeletal and Skin Diseases, NIH (grants K23-AR-073334 and L30-AR-070520).

¹Reza Zonozi, MD, Zachary S. Wallace, MD, Karen Laliberte, RN, Noah R. Huizenga, BA, Jillian M. Rosenthal, MSN, Eugene P. Rhee, MD, John L. Niles, MD: Massachusetts General Hospital, Boston; ²Frank B. Cortazar,

MD: Massachusetts General Hospital, Boston, and New York Nephrology Vasculitis and Glomerular Center, Albany.

No potential conflicts of interest relevant to this article were reported.

Address correspondence to Reza Zonozi, MD, Vasculitis and Glomerulonephritis Center, Division of Nephrology, Massachusetts General Hospital, 101 Merrimac Street, Boston, MA 02114. Email: rzonozi@yahoo.com.

Submitted for publication January 29, 2020; accepted in revised form August 20, 2020.

published to date. Furthermore, this study has the longest follow-up of continuous B cell depletion published to date.

PATIENTS AND METHODS

Study population. We retrospectively identified patients ≥ 18 years old who were treated with RTX for autoimmune disease between November 8, 2002 and September 30, 2018, at the Vasculitis and Glomerulonephritis Center at the Massachusetts General Hospital. This is a tertiary care referral and treatment center that provides care for a diverse patient population in eastern Massachusetts and the surrounding region. All data were abstracted from the electronic medical record. The study was approved by the Partners HealthCare Human Research Committee. Informed consent was not required due to the retrospective nature of the study.

Treatment regimen and continuous B cell depletion.

All patients received RTX, typically starting with two 1,000-mg intravenous (IV) doses separated by 2–4 weeks. Thereafter, RTX was most commonly administered as a single 1,000-mg IV dose every 4–6 months. This dosing interval has been demonstrated to achieve continuous B cell depletion in $>95\%$ of patients (16–18). If RTX treatment was continued for >2 years, then attempts were made to extend the dosing interval as long as documented B cell depletion was maintained. B cell counts were typically measured every 3 months, including prior to each dose, with peripheral flow cytometry to examine the population of CD19+CD20+ lymphocytes. We defined B cell depletion as a total CD19+CD20+ cell count of <5 cells/ μl . All patients had a complete blood cell count (CBC) with differential that was checked routinely prior to each dose of RTX, for any report of fever, as well as for other clinical indications at the discretion of the treating physician.

Prednisone and other immunosuppressive agents were initially administered with RTX in most patients. Aside from prednisone, a 2-month course of low-dose daily oral cyclophosphamide (CYC) was the most commonly used additional agent, which is part of a standard induction therapy that we have used for AAV, membranous nephropathy (MN), and to treat patients with other conditions (18,19).

Outcome measures. The primary outcome measure was the first episode of LON, which we defined as an unexplained absolute neutrophil count (ANC) of $<1,000$ cells/ μl during the period of B cell depletion. To determine whether patients had another identifiable etiology of neutropenia, medical records surrounding the neutropenia event were reviewed. Resolution of a LON episode was defined as an increase in ANC to a level $\geq 1,000$ cells/ μl .

Secondary outcome measures included incidental diagnosis, chief symptom, nadir ANC, nadir absolute lymphocyte count (ALC), fever, sepsis, source of infection, prednisone dose at the time of event, serum IgG level at the time of event, filgrastim use,

therapeutic antibiotic use, and recurrent LON, defined as a second episode of LON occurring after recovery from the first. Chief symptom was defined as the patient's primary concern. Fever was defined as a single oral temperature of $\geq 38.0^\circ\text{C}$ (100.4°F). Sepsis was defined as the presence of systemic inflammatory response syndrome with a source of infection (20). Determination of infection source was based on available history, examination, imaging, culture data, and treating physician's documentation.

Covariates of LON. The following covariates were examined based on biologic relevance: age, sex, underlying disease, CYC use (never, prior, concurrent), and exposure to other immunosuppressants (methotrexate [MTX], azathioprine [AZA], mycophenolic acid [MPA]) during continuous B cell depletion.

Statistical analysis. Values for continuous variables are presented as the median (interquartile range [IQR]) or as the mean \pm SD, as appropriate. Values for categorical variables are presented as percentages. Person-years at risk of LON were calculated for each patient as time from the index date, defined

Table 1. Characteristics of the study population (n = 738)*

Age, mean \pm SD years	58 \pm 17
Female	392 (53)
Disease	
AAV	529 (72)
SLE	24 (3)
MN	73 (10)
MCD/FSGS	59 (8)
Other	53 (7)
No. of RTX doses, median (IQR)	8 (5–12)
Duration of B cell depletion, median (IQR) years	2.5 (1.4–4.5)
AAV	2.8 (1.4–5.1)
SLE	2.4 (1.8–4.6)
MN	2.2 (1.4–2.6)
MCD/FSGS	2.4 (1.5–3.2)
Other	1.4 (0.7–3.6)
CYC use	
Never	170 (23)
Concurrent†	515 (70)
Prior‡	53 (7)
<6 months of CYC treatment	29 (55)
≥ 6 months of CYC treatment	20 (38)
Other immunosuppressant use	
MPA	59 (8)
AZA	119 (16)
MTX	33 (4)
Glucocorticoids	698 (95)

* Except where indicated otherwise, values are the number (%) of patients. AAV = antineutrophil cytoplasmic autoantibody-associated vasculitis; SLE = systemic lupus erythematosus; MN = membranous nephropathy; MCD/FSGS = minimal change disease/focal segmental glomerulosclerosis; IQR = interquartile range; MPA = mycophenolic acid; AZA = azathioprine; MTX = methotrexate.

† Typically 8 weeks of daily oral cyclophosphamide (CYC) treatment, beginning with the first dose of rituximab (RTX). Dosing was typically 2.5 mg/kg/day for the first week and 1.5 mg/kg/day for 7 weeks, with adjustments made for renal function.

‡ Defined as a course of CYC administered prior to initiation of RTX, as part of a separate remission induction therapy. There were missing data on 4 patients, with unclear duration of CYC exposure.

as the first RTX infusion, through the last documented date of B cell depletion prior to B cell return. If documented B cell return was not available, then we ended the at-risk period 6 months after the last infusion or on the last date of documented B cell depletion, whichever was later. We estimated the cumulative incidence of LON using days from RTX treatment initiation as the time scale and present LON rates per 100 person-years of continuous B cell depletion, with 95% confidence intervals (95% CIs). Poisson regression was used to generate 95% CIs for LON incidence rates. Among patients who sustained an episode of LON, recurrence upon rechallenge was measured from the day of RTX rechallenge to the first day of the second LON episode.

Univariate and multivariate Cox proportional hazards models were used to estimate the hazard ratios and 95% CIs for LON associated with each potential predictor. The multivariable model was adjusted for age, sex, AAV, systemic lupus erythematosus (SLE), MN, other disease category, no CYC exposure, concurrent CYC use, MPA use, AZA use, and MTX use. The model could not accommodate the group of patients with minimal change disease (MCD)/focal segmental glomerulosclerosis (FSGS) due to the absence of any LON events. As such, this group was excluded from the regression model. Instead, a log rank test was used to compare it to other underlying diseases. All analyses were conducted using Stata 15.

RESULTS

Study population. We identified 738 adult patients who had been treated with RTX to induce continuous B cell depletion for autoimmune disease. The mean \pm SD age at initiation of therapy was 58 ± 17 years, and 53% of patients were female. Among the 738 patients, 529 (72%) had AAV, 73 (10%) had MN, 59 (8%) had MCD/FSGS, 24 (3%) had SLE, and 53 (7%) had another autoimmune disease. Underlying diseases included in the "Other" category are listed in Supplementary Table 1, available on the *Arthritis & Rheumatology* website at <http://onlinelibrary.wiley.com/doi/10.1002/art.41501/abstract>.

Of the 529 patients with AAV, 271 (51.2%) had renal involvement, as defined by the presence of hematuria, red blood cell casts, or a rise in serum creatinine level of 30%. The median creatinine level in patients with renal involvement of AAV at the start of RTX treatment was 1.7 mg/dl (IQR 1.11–2.65). All patients with MCD/FSGS had disease that was frequently relapsing, steroid-dependent, or steroid-resistant. All patients with SLE had lupus nephritis. Patient characteristics are presented in Table 1.

Continuous B cell depletion therapy with RTX and other concurrent treatments. All patients were treated with RTX to induce continuous B cell depletion. Patients received a median of 8 doses (IQR 5–12) and were in a state of continuous B cell depletion for a median of 2.5 years (IQR 1.4–4.5). There were a total of 2,214 person-years of follow-up.

A 2-month course of low-dose daily oral CYC was administered concurrently with initiation of RTX in 515 patients (70%). The remaining patients never received CYC (23%; $n = 170$) or had previously received it (7%; $n = 53$). AZA, MPA, and MTX were used in 119 patients (16%), 59 patients (8%), and 33 patients (4%), respectively. Glucocorticoids were used in 698 patients (95%).

Incidence, recurrence, clinical features, and management of LON. *Incidence of LON.* During follow-up, 107 episodes of LON were observed in 71 patients. The cumulative incidences of LON at 1, 2, and 5 years of continuous B cell depletion were 6.6% (95% CI 5.0–8.7), 7.9% (95% CI 6.1–10.2), and 13.5% (95% CI 10.4–17.4), respectively. A Kaplan-Meier curve depicting time to LON episode is shown in Figure 1A. The overall incidence rate of first-time LON was 3.2 cases per 100 person-years (95% CI 2.5–4.0). The incidence rate of LON was higher in the first year following treatment initiation compared to the incidence rate thereafter (7.2 cases per 100 person-years [95% CI 5.4–9.6] versus 1.5 [95% CI 1.0–2.3]). Supplementary Figure 1 (<http://onlinelibrary.wiley.com/doi/10.1002/art.41501/abstract>)

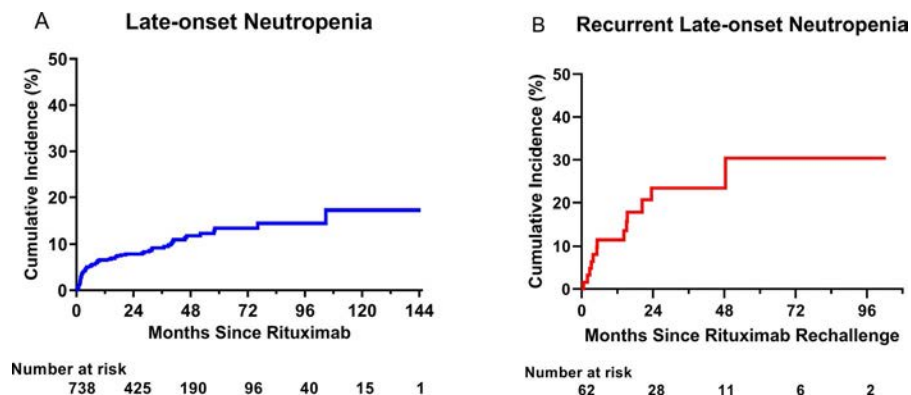


Figure 1. Cumulative incidence of late-onset neutropenia (LON). Kaplan-Meier curves for time to initial LON episode in all patients undergoing continuous B cell depletion therapy with rituximab (A) and time to second episode (recurrence) of LON in patients rechallenged with rituximab treatment (B) are shown.

provides a more detailed version of Figure 1A on the first year of treatment.

Recurrence of LON after RTX rechallenge. Among the 71 patients who experienced LON, 9 patients were not rechallenged. Of these, 4 had second episodes of LON that occurred 19, 54, 66, and 435 days after the first episode, respectively. All remained B cell-depleted at the time of their second episode.

The remaining 62 patients (87%) were rechallenged with RTX. Thirteen of these patients (21%) developed a second LON episode over a median follow-up duration of 2.4 years (IQR 1.3–4.1) of continuous B cell depletion after RTX rechallenge, which corresponds with a recurrent LON incidence rate of 8.5 cases per 100 person-years (95% CI 4.9–14.7) after the date of rechallenge. The cumulative incidence of recurrent LON at 1, 2, and 5 years of continuous B cell depletion after rechallenge was 11.5% (95% CI 5.6–22.6), 23.4% (95% CI 13.8–38.2), and 30.4% (95% CI 16.9–50.9), respectively. A Kaplan-Meier curve for time to recurrent LON is shown in Figure 1B.

Clinical features of LON. Clinical features of LON are shown in Table 2. LON occurred at a median of 4.1 months (IQR 1.6–23.1) after initiating continuous B cell depletion (defined by the first infusion of RTX). Relative to the preceding infusion, LON occurred at a median of 2.3 months (IQR 0.8–4.0). In the subset of patients who developed recurrent LON, the second episode occurred at a median of 5.3 months (IQR 3.3–15.4) after RTX rechallenge. The median nadir ANC for all episodes was 490 cells/ μ l (IQR 12–770), and the median nadir neutrophil percentage was 16.1% (IQR 3.0–32.9). The median nadir ANC for symptomatic episodes was significantly lower than for asymptomatic episodes (128 cells/ μ l [IQR 11–420] versus 700 cells/ μ l [IQR 459–882]; $P < 0.001$) (Table 2). The median ALC and lymphocyte percentage concurrent to the nadir ANC was 775 cells/ μ l (IQR 504–1,440) and 45.5% (IQR 35.5–64.0), respectively. Lymphopenia (defined by an ALC of $<1,000$ cells/ μ l) occurred in 62.3% of the LON episodes. According to chi-square analysis, there was no association between the occurrence of lymphopenia and infections during neutropenia ($P = 0.77$).

Sixty-three episodes of LON (59.4%) were discovered incidentally in asymptomatic patients presenting for routine follow-up. No infections were identified in asymptomatic episodes. In contrast, an infection was identified in all episodes that were symptomatic. Forty-three LON episodes (40.6%) were discovered because a patient reported a symptom, which prompted the treating physician to check the patient's CBC. The most common chief symptom was subjective fever ($n = 30$), followed by gingival soreness ($n = 4$) (Table 2). LON was complicated by sepsis in 8 episodes (8.5%). All sepsis cases resolved with standard therapy. In the entire cohort, 1 patient with multiple relapsing LON died. At the time LON occurred, patients were receiving a median daily prednisone dose of 5 mg (IQR 0–12.5), and the median serum IgG level was 557 mg/dl (IQR 454–733).

Table 2. LON episode characteristics and treatments*

No. of patients with LON	71
No. of LON episodes (initial and recurrent)	107
Time to initial episode, median (IQR) months	4.1 (1.6–23.1)
Nadir ANC for all episodes, median (IQR) cells/ μ l	490 (12–770)
Nadir ANC for asymptomatic episodes	700 (459–882)
Nadir ANC for symptomatic episodes	128 (11–420)
ALC at time of nadir ANC, median (IQR) cells/ μ l	775 (504–1,440)
Febrile neutropenia episodes	30 (31.3)
Sepsis syndrome episodes	8 (8.4)
Chief symptom during episodes	
Asymptomatic/incidental	63 (59.4)
Fever	30 (28.3)
Gum soreness	4 (3.8)
Rash	3 (2.8)
Fall	1 (0.9)
Photophobia	1 (0.9)
Productive cough	1 (0.9)
Pain at tunneled catheter site	1 (0.9)
Nausea/vomiting	1 (0.9)
Malaise	1 (0.9)
Source of infection	
No apparent infection	63 (65.0)
Gingivitis	7 (7.2)
SSTI	7 (7.2)
URI	6 (6.2)
UTI	5 (5.2)
GI (gastroenteritis or colitis)	4 (4.1)
Pneumonia	2 (2.1)
Conjunctivitis	1 (1.0)
Bacteremia	1 (1.0)
Vascular access catheter tunnel infection	1 (1.0)
Prednisone dose at event, median (IQR) mg/day	5 (0–12.5)
Serum IgG level at event, median (IQR) mg/dl†	557 (454–733)
Treatment of LON	
Antibiotic use during episode‡	34 (34.7)
Filgrastim use during episode	70 (69.3)
Filgrastim doses per episode, median (IQR)	1 (1–2)
Duration of episode, median (IQR) days	4 (3–7)

* Except where indicated otherwise, values are the number (%) of patients. Missing data were excluded from calculations. LON = late-onset neutropenia; IQR = interquartile range; ANC = absolute neutrophil count; ALC = absolute lymphocyte count; SSTI = skin and soft tissue infection; URI = upper respiratory infection; UTI = urinary tract infection; GI = gastrointestinal.

† Reference range 614–1,295 mg/dl.

‡ Therapeutic dosing.

Management of LON. Treatments used for LON within our cohort are shown in Table 2. All patients with LON and fever (31.3%; $n = 30$) were hospitalized for management of febrile neutropenia. Therapeutic antibiotics were used in 34.7% of all episodes, most of which were accompanied by fever (81.3%). Filgrastim was used in 83.6% and 69% of LON episodes, with a nadir ANC of <500 cells/ μ l and $<1,000$ cells/ μ l, respectively. Patients who were administered filgrastim had a lower median nadir ANC compared to those who were not (337 cells/ μ l [IQR 50–576] versus 717 cells/ μ l [IQR 472–908]; $P < 0.0001$). In patients treated with filgrastim, a median of 1 dose (IQR 1–2, range 1–8) was administered per LON episode. The median duration of all episodes was 4 days (IQR 3–7).

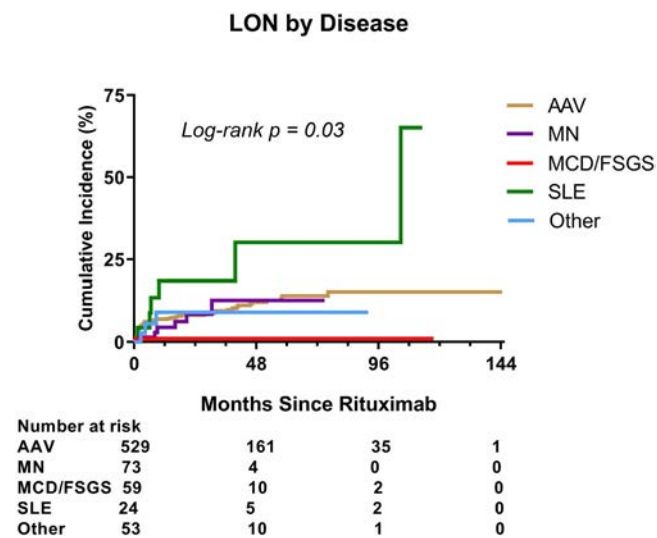


Figure 2. Cumulative incidence of late-onset neutropenia (LON), stratified by disease. Kaplan-Meier curves for time to LON episode are shown. Higher rates of LON were seen in systemic lupus erythematosus (SLE), while no events occurred in minimal change disease (MCD)/focal segmental glomerulosclerosis (FSGS). AAV = antineutrophil cytoplasmic antibody-associated vasculitis; MN = membranous nephropathy.

Effects on LON of underlying disease, CYC treatment, and other covariates. *Effect of underlying disease.* LON occurred more frequently in patients with SLE (25%; $n = 6$) compared to patients with AAV (10.4%; $n = 55$), MN

(8.2%; $n = 6$), or other diseases (7.6%; $n = 4$) ($P = 0.03$ by log rank test) (Figure 2). LON was not observed in any patient with MCD/FSGS. The corresponding crude incidence rates of LON among patients with SLE, AAV, MN, and other diseases were 8.9 cases per 100 person-years (95% CI 4.0–19.7), 3.2 cases (95% CI 2.5–4.2), 4.1 cases (95% CI 1.8–9.1), and 3.5 cases (95% CI 1.1–10.9), respectively. In a multivariable model, the presence of SLE was associated with higher odds of developing LON (adjusted HR 2.96 [95% CI 1.10–8.01]) (Table 3).

Effect of CYC. LON occurred more frequently in patients treated with a combination of CYC and RTX for induction therapy (11.3%; $n = 58$), compared to patients who were never exposed to CYC (5.9%; $n = 10$), or who had CYC exposure prior to the initiation of RTX (5.7%; $n = 3$) ($P = 0.03$ by log rank test). In a multivariable model, treatment with CYC and RTX combination therapy was associated with higher odds of developing LON compared to those who did not receive CYC (adjusted HR 1.98 [95% CI 1.06–3.71]) (Table 3). In a subgroup analysis of patients who received RTX without CYC ($n = 170$), the 12-month cumulative incidence of LON was 3.70% (95% CI 1.68–8.07) (Supplementary Figure 2, <http://onlinelibrary.wiley.com/doi/10.1002/art.41501/abstract>).

Effect of age, sex, and other immunosuppressants. In a multivariable model, age, sex, and exposure to MPA, AZA, or MTX concurrent with RTX treatment were not associated with the development of LON (Table 3).

Table 3. Covariates of late-onset neutropenia*

Variable	Hazard ratio (95% CI)	
	Univariate model	Multivariate model
Age (per 1 year)	1.01 (0.99–1.02)	1.01 (0.99–1.03)
Female	0.92 (0.58–1.47)	0.85 (0.53–1.38)
Disease		
AAV	1.17 (0.66–2.08)	1.0 (referent)
MN	1.01 (0.43–2.34)	0.91 (0.39–2.15)
SLE	2.91 (1.26–6.72)	2.96 (1.10–8.01)
MCD/FSGS	NA	NA
Other	0.93 (0.29–2.95)	0.97 (0.30–3.12)
CYC use		
Never	0.52 (0.27–1.01)	1.0 (referent)
Concurrent	2.23 (1.22–4.08)	1.98 (1.06–3.71)
Prior		
<6 months of CYC treatment	0.26 (0.04–1.90)	–
≥6 months of CYC treatment	0.88 (0.22–3.62)	–
Other concurrent immunosuppressant use		
RTX without MPA/AZA/MTX/CYC	0.68 (0.29–1.57)	1.0 (referent)
MPA	1.44 (0.72–2.91)	1.41 (0.65–3.08)
AZA	0.37 (0.17–0.82)	0.46 (0.20–1.04)
MTX	1.07 (0.39–2.93)	1.24 (0.44–3.54)

* Hazard ratios and 95% confidence intervals (95% CIs) were calculated using a Cox proportional hazards model. The multivariable model was adjusted for age, sex, AAV, SLE, MN, other disease category, no CYC exposure, concurrent CYC use, MPA use, AZA use, and MTX use. The model could not accommodate the MCD/FSGS group due to the absence of any late-onset neutropenia events. As such, it was excluded from the regression model. Instead, the log rank test was used to compare it to other underlying diseases. NA = not applicable (see Table 1 for other definitions).

DISCUSSION

In this retrospective cohort study of 738 patients undergoing B cell depletion therapy with RTX for autoimmune disease, we have provided several key insights into the incidence, risk factors, clinical features, management, and recurrence of LON. First, we have described 71 patients with LON, the largest reported cohort to date, corresponding with a cumulative incidence of 6.6% at 1 year of treatment. Second, we observed that the highest rate of LON occurs in the first year of treatment. Third, we identified SLE and combination therapy with CYC each as positive independent risk factors for the development of LON. Fourth, we expanded on initial observations by others (11–13) on the clinical features of LON, including the often incidental nature of discovery of LON in asymptomatic patients, as well as the potential for serious infectious complications. Fifth, we highlighted the safety and efficacy of filgrastim treatment in this patient population. Finally, we found that RTX rechallenge does not always lead to recurrent LON.

We reported a 6.6% 1-year cumulative incidence of LON. Our findings are consistent with and expand on findings of prior studies on LON, including those that used alternative RTX dosing schedules (10–13,21). By comparison, leukopenia was reported in 3 of 99 patients (3%) in the RTX arm at 6 months in the Rituximab in ANCA-Associated Vasculitis (RAVE) trial, and neutropenia was reported in 2 of 33 patients (6%) in the RTX arm at 12 months in the Rituximab versus Cyclophosphamide in ANCA-Associated Vasculitis (RITUXVAS) trial (1,22). Both trials used a weekly RTX dose of 375 mg/m² for 4 consecutive weeks to treat AAV. Given the long-term, relapsing nature of many antibody-mediated autoimmune diseases, the rising incidence of LON that we observed with extended durations of B cell depletion is of particular concern, underscoring the need for ongoing awareness of neutropenia during remission maintenance therapy.

The mechanism of LON remains unknown. Neutrophils and their precursors do not express CD20, which provides an argument against direct cytotoxicity. Yet, late neutropenic events have been observed after treatment with other anti-CD20 monoclonal antibodies as well as with anti-CD19 chimeric antigen receptor T cells (23,24). These findings support the notion that the state of B cell depletion causes neutropenia. It has been postulated that B cell depletion leads to alterations in hematopoietic growth factors that promote lymphopoiesis and down-regulate granulopoiesis. One such cytokine is BAFF. Serum BAFF levels rise during B cell depletion, with excess levels correlating with neutropenic events (21,25). Another implicated cytokine is stromal cell-derived factor 1 (SDF-1), which promotes early B cell development and regulates neutrophil egress from bone marrow. Perturbations in SDF-1 levels have been shown to correlate with neutropenic events during B cell depletion (24,26). Other hypotheses have been proposed, but additional investigation is needed to more accurately define the mechanism of LON (8,26–30).

Our findings suggest that underlying disease independently informs the risk of LON. Indeed, we found the risk of LON to be 3-fold higher among patients with SLE compared to those with AAV. The interpretation of this association may be limited by sample size and confounding, given that neutropenia is an established manifestation of SLE; however, SLE-associated neutropenia is usually characterized by mild neutropenia (ANC between 1,000 and 1,500 cells/ μ l), which we excluded from our definition of LON. Furthermore, our results are consistent with those of prior studies describing higher rates of LON in SLE (11,21). Distinct roles for BAFF and APRIL have been postulated to explain the unique immunologic phenomenon in SLE (21). In contrast to SLE, we did not observe LON in patients with podocytopathies MCD or FSGS who were treated with RTX, including those who received concurrent CYC. It is possible that urinary loss of RTX in the setting of heavy proteinuria alters its pharmacodynamics (31), or alternatively, that a larger sample size is needed to detect LON in these patients. In a previous study, LON occurred in 11 of 213 pediatric

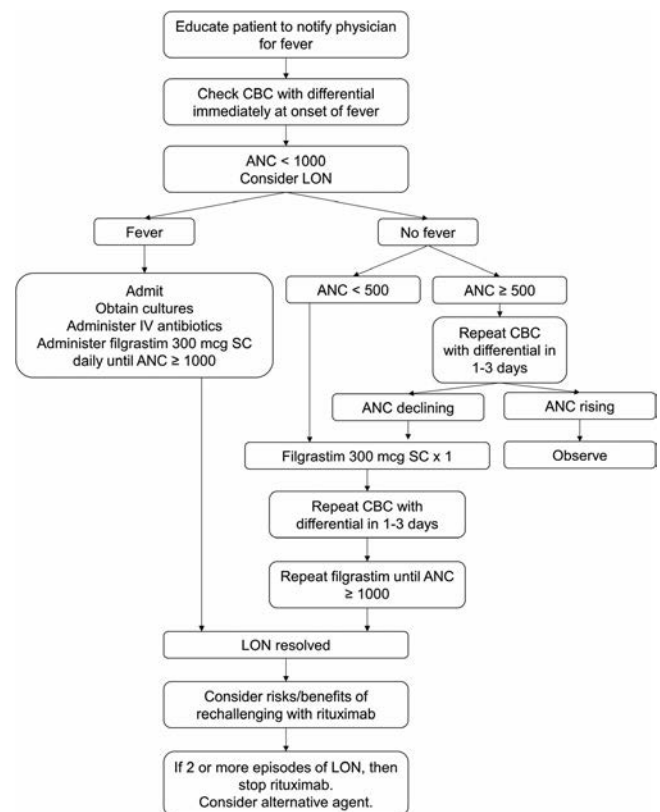


Figure 3. Protocol for management of late-onset neutropenia (LON). The general strategy we use at the Vasculitis and Glomerulonephritis Center at the Massachusetts General Hospital for the management of LON is shown. For any patient with B cell depletion, we advocate obtaining a complete blood cell count (CBC) with differential, at a minimum, for any report of a febrile illness. We advocate filgrastim use in patients with febrile neutropenia or an absolute neutrophil count (ANC) of <500 cells/ μ l. ANC values are expressed in cells/ μ l. IV = intravenous; SC = subcutaneous.

patients (5.2%) treated with RTX for steroid-resistant nephrotic syndrome (32).

CYC can lead to neutropenia in a dose-dependent manner (33). It seems plausible that the combination of RTX and CYC can act synergistically to cause neutropenia. Indeed, in the present study, when low-dose CYC was administered in combination with RTX for induction therapy, we found a 2-fold higher risk of LON compared to those not exposed to CYC. CYC and RTX combination therapy is a regimen used at several large centers (18,34). The basis for using this regimen is that the therapeutic effect of RTX has a delayed onset of action, thus necessitating high doses of glucocorticoids in the first 2 months of therapy (1). The addition of a short course of CYC allows for a more rapid prednisone taper. The steroid minimization and high efficacy of combination therapy in remission induction in AAV need to be weighed against its higher risk of LON.

We described the management of LON in our cohort. We found that most LON episodes were discovered incidentally in asymptomatic patients. Recombinant granulocyte colony-stimulating factor (G-CSF), namely filgrastim, was administered in the majority of episodes that were accompanied by severe neutropenia and/or fever. While there are no data in the literature to suggest that G-CSF impacts morbidity or mortality in LON, data from our cohort suggest a role in shortening its duration. Indeed, the duration of an episode in our cohort (median 4 days) was shorter than those described in prior reports in the literature, which ranged from 9 to 54 days (10,26,29). Importantly, no patient in our cohort had a relapse of their underlying autoimmune disease after receiving filgrastim.

This report provides the largest data set, to date, on RTX rechallenge in patients with LON. Approximately one-fifth of patients in our cohort who sustained LON developed a second episode within 2 years of being rechallenged with RTX, which is more than double the rate of the initial episode. This expands on the findings of a prior study in which a second episode occurred in 16% of retreated patients (12).

Our experience has generated a protocolized approach to the management of LON (Figure 3). For any patient with B cell depletion, we recommend checking a CBC with differential at minimum, for any report of fever. In patients with recurrent LON, RTX should be discontinued, unless ongoing maintenance therapy is deemed essential and there are no reasonable therapeutic alternatives.

The study has several strengths and weaknesses. The greatest strengths are the large size of the cohort receiving continuous B cell depletion, the long duration of follow-up, and the inclusion of patients across a broad spectrum of antibody-mediated autoimmune disease encountered in clinical practice. The main weaknesses are inherent to data collection in retrospective studies, as well as data derived from a single center. Our center is a nephrology-based practice, which explains the low number of patients with certain diseases, specifically RA, and it is possible that rates

of LON are different among those patients. A large majority of patients had AAV, such that comparisons of LON rates based on underlying disease warrant some caution pending larger studies. Finally, CBCs were monitored only at the time of infusions or symptoms, and it is likely that more frequent monitoring would capture more LON episodes.

Since the use of B cell depletion therapy with RTX is likely to increase, it is essential to be aware of the long-term implications of this treatment. LON is common and can be asymptomatic but has the potential to be complicated by serious infection. Further studies are needed to help balance the risks of B cell depletion therapy against the risk of disease relapse.

AUTHOR CONTRIBUTIONS

All authors were involved in drafting the article or revising it critically for important intellectual content, and all authors approved the final version to be published. Dr. Zonozi had full access to all of the data in the study and takes responsibility for the integrity of the data and the accuracy of the data analysis.

Study conception and design. Zonozi, Laliberte, Rhee, Cortazar, Niles.

Acquisition of data. Zonozi, Laliberte, Huizenga, Rosenthal, Cortazar, Niles.

Analysis and interpretation of data. Zonozi, Wallace, Rhee, Cortazar, Niles.

REFERENCES

1. Stone JH, Merkel PA, Spiera R, Seo P, Langford CA, Hoffman GS, et al. Rituximab versus cyclophosphamide for ANCA-associated vasculitis. *N Engl J Med* 2010;363:221–32.
2. Edwards JC, Szczepański L, Szechirński J, Filipowicz-Sosnowska A, Emery P, Close DR, et al. Efficacy of B-cell-targeted therapy with rituximab in patients with rheumatoid arthritis. *N Engl J Med* 2004;350:2572–81.
3. Cartin-Ceba R, Golbin JM, Keogh KA, Peikert T, Sánchez-Menéndez M, Ytterberg SR, et al. Rituximab for remission induction and maintenance in refractory granulomatosis with polyangiitis (Wegener's): ten-year experience at a single center. *Arthritis Rheum* 2012;64:3770–8.
4. Smith RM, Jones RB, Guerry MJ, Laurino S, Catapano F, Chaudhry A, et al. Rituximab for remission maintenance in relapsing antineutrophil cytoplasmic antibody-associated vasculitis. *Arthritis Rheum* 2012;64:3760–9.
5. Guillevin L, Pagnoux C, Karras A, Khouatra C, Aumaitre O, Cohen P, et al. Rituximab versus azathioprine for maintenance in ANCA-associated vasculitis. *N Engl J Med* 2014;371:1771–80.
6. Maloney DG, Grillo-López AJ, White CA, Bodkin D, Schilder RJ, Neidhart JA, et al. IDEC-C2B8 (Rituximab) anti-CD20 monoclonal antibody therapy in patients with relapsed low-grade non-Hodgkin's lymphoma. *Blood* 1997;90:2188–95.
7. McLaughlin P, Grillo-López AJ, Link BK, Levy R, Czuczman MS, Williams ME, et al. Rituximab chimeric anti-CD20 monoclonal antibody therapy for relapsed indolent lymphoma: half of patients respond to a four-dose treatment program. *J Clin Oncol* 1998;16:2825–33.
8. Chaiwatanatorn K, Lee N, Grigg A, Filshie R, Firkin F. Delayed-onset neutropenia associated with rituximab therapy. *Br J Haematol* 2003;121:913–8.
9. Voog E. Neutropenia in patients treated with rituximab [letter]. *N Engl J Med* 2003;348:2691–4.
10. Tesfa D, Palmblad J. Late-onset neutropenia following rituximab therapy: incidence, clinical features and possible mechanisms [review]. *Expert Rev Hematol* 2011;4:619–25.

11. Tesfa D, Ajeganova S, Häggglund H, Sander B, Fadeel B, Hafström I, et al. Late-onset neutropenia following rituximab therapy in rheumatic diseases: association with B lymphocyte depletion and infections. *Arthritis Rheum* 2011;63:2209–14.
12. Salmon J, Cacoub P, Combe B, Sibilia J, Pallot-Prades B, Fain O, et al. Late-onset neutropenia after treatment with rituximab for rheumatoid arthritis and other autoimmune diseases: data from the AutoImmunity and Rituximab registry. *RMD Open* 2015;1:e000034.
13. Monaco WE, Jones JD, Rigby WF. Rituximab associated late-onset neutropenia: a rheumatology case series and review of the literature. *Clin Rheumatol* 2016;35:2457–62.
14. Biotti D, Lerebours F, Bonneville F, Ciron J, Clanet M, Brassat D. Late-onset neutropenia and neurological relapse, during long-term rituximab therapy in myelin oligodendrocyte glycoprotein-antibody spectrum disorder. *Mult Scler* 2018;24:1645–7.
15. Abdulkader R, Dharmapalaiah C, Rose G, Shand LM, Clunie GP, Watts RA. Late-onset neutropenia in patients with rheumatoid arthritis after treatment with rituximab. *J Rheumatol* 2014;41:858–61.
16. Pendergraft WF, Cortazar FB, Wenger J, Murphy AP, Rhee EP, Laliberte KA, et al. Long-term maintenance therapy using rituximab-induced continuous B-cell depletion in patients with ANCA vasculitis. *Clin J Am Soc Nephrol* 2014;9:736–44.
17. Cortazar FB, Pendergraft III WF, Wenger J, Owens CT, Laliberte K, Niles JL. Effect of continuous B cell depletion with rituximab on pathogenic autoantibodies and total IgG levels in antineutrophil cytoplasmic antibody-associated vasculitis. *Arthritis Rheumatol* 2017;69:1045–53.
18. Cortazar FB, Muhsin SA, Pendergraft III WF, Wallace ZS, Dunbar C, Laliberte K, et al. Combination therapy with rituximab and cyclophosphamide for remission induction in ANCA vasculitis. *Kidney Int Rep* 2018;3:394–402.
19. Cortazar FB, Leaf DE, Owens CT, Laliberte K, Pendergraft WF, Niles JL. Combination therapy with rituximab, low-dose cyclophosphamide, and prednisone for idiopathic membranous nephropathy: a case series. *BMC Nephrol* 2017;18:44.
20. Physicians ACoC, Committee SoCCMCC. American College of Chest Physicians/Society of Critical Care Medicine Consensus Conference: definitions for sepsis and organ failure and guidelines for the use of innovative therapies in sepsis [review]. *Crit Care Med* 1992;20:864–74.
21. Parodis I, Söder F, Faustini F, Kasza Z, Samuelsson I, Zickert A, et al. Rituximab-mediated late-onset neutropenia in systemic lupus erythematosus: distinct roles of BAFF and APRIL. *Lupus* 2018;27:1470–8.
22. Jones RB, Cohen Tervaert JW, Hauser T, Luqmani R, Morgan MD, Peh CA, et al. Rituximab versus cyclophosphamide in ANCA-associated renal vasculitis. *N Engl J Med* 2010;363:211–20.
23. Cohen BA. Late-onset neutropenia following ocrelizumab therapy for multiple sclerosis. *Neurology* 2019;92:435–6.
24. Fried S, Avigdor A, Bielora B, Meir A, Besser MJ, Schachter J, et al. Early and late hematologic toxicity following CD19 CAR-T cells. *Bone Marrow Transplant* 2019;54:1643–50.
25. Terrier B, Ittah M, Tourneur L, Louache F, Soumelis V, Lavie F, et al. Late-onset neutropenia following rituximab results from a hematopoietic lineage competition due to an excessive BAFF-induced B-cell recovery. *Haematologica* 2007;92:e20–3.
26. Dunleavy K, Hakim F, Kim HK, Janik JE, Grant N, Nakayama T, et al. B-cell recovery following rituximab-based therapy is associated with perturbations in stromal derived factor-1 and granulocyte homeostasis. *Blood* 2005;106:795–802.
27. Papadaki T, Stamatopoulos K, Stavroyianni N, Paterakis G, Phisphis M, Stefanoudaki-Sofianatou K. Evidence for T-large granular lymphocyte-mediated neutropenia in Rituximab-treated lymphoma patients: report of two cases. *Leuk Res* 2002;26:597–600.
28. Stamatopoulos K, Papadaki T, Pontikoglou C, Athanasiadou I, Stavroyianni N, Bux J, et al. Lymphocyte subpopulation imbalances, bone marrow hematopoiesis and histopathology in rituximab-treated lymphoma patients with late-onset neutropenia [letter]. *Leukemia* 2008;22:1446.
29. Tesfa D, Gelius T, Sander B, Kimby E, Fadeel B, Palmblad J, et al. Late-onset neutropenia associated with rituximab therapy: evidence for a maturation arrest at the (pro) myelocyte stage of granulopoiesis. *Med Oncol* 2008;25:374–9.
30. Fukuno K, Tsurumi H, Ando N, Kanemura N, Goto H, Tanabashi S, et al. Late-onset neutropenia in patients treated with rituximab for non-Hodgkin's lymphoma. *Int J Hematol* 2006;84:242–7.
31. Stahl K, Duong M, Schwarz A, Wagner A, Haller H, Schiffer M, et al. Kinetics of rituximab excretion into urine and peritoneal fluid in two patients with nephrotic syndrome. *Case Rep Nephrol* 2017;2017:1372859.
32. Kamei K, Takahashi M, Fuyama M, Saida K, Machida H, Sato M, et al. Rituximab-associated agranulocytosis in children with refractory idiopathic nephrotic syndrome: case series and review of literature. *Nephrol Dial Transplant* 2014;30:91–6.
33. Langford C. Cyclophosphamide as induction therapy for Wegener's granulomatosis and microscopic polyangiitis. *Clin Exp Immunol* 2011;164:31–4.
34. McAdoo SP, Medjeral-Thomas N, Gopaluni S, Tanna A, Mansfield N, Galliford J, et al. Long-term follow-up of a combined rituximab and cyclophosphamide regimen in renal anti-neutrophil cytoplasm antibody-associated vasculitis. *Nephrol Dial Transplant* 2019;34:63–73.

LETTERS

High prevalence of new-onset or worsening hepatitis C virus-related musculoskeletal symptoms after beginning direct-acting antiviral therapy: a challenging novel observation

To the Editor:

Direct-acting antiviral therapy has revolutionized the management of hepatitis C virus (HCV), and it presents the prospect of an effective cure (1). HCV-related musculoskeletal symptoms are common and can be quite debilitating. It has been reported that joint pain occurs in ~71% of patients with HCV (2). There has been understandable hope that a cure for HCV might mean a cure for related musculoskeletal symptoms. However, in a recent study reported in abstract form, 11.4% of patients with cryoglobulinemic vasculitis experienced vasculitis flares despite remaining HCV-negative by polymerase chain reaction (PCR) (3). Moreover, cases of de novo vasculitis developing even after sustained viral response induced by direct-acting antiviral therapy have been reported (4). We sought to examine whether HCV-infected patients experienced any alteration in musculoskeletal symptoms after beginning direct-acting antiviral therapy (with daclatasavir and sofosbuvir) and becoming HCV-negative by PCR.

Ethics approval for this study was obtained from the Pakistan Kidney and Liver Institute Ethics and Medical Research Committee. All consecutive HCV-infected adult patients who had completed direct-acting antiviral therapy, leading to negative PCR results for HCV, were included in the study. The following features were recorded: demographic characteristics, employment status, level of education, marital status, comorbidities, clinically deformed joints, markers of inflammation, and medications used. Chronic musculoskeletal symptoms were defined as any arthralgias lasting ≥6 weeks and not related to trauma or occupational hazards. Worsening musculoskeletal symptoms were defined as a ≥50% worsening of musculoskeletal symptoms compared with symptoms before beginning direct-acting antiviral therapy. A thorough clinical rheumatologic examination including collecting detailed clinical history was performed. Radiography of the involved joints was performed if clinically indicated.

A total of 250 consecutive HCV-infected patients who had completed direct-acting antiviral therapy and were subsequently HCV-negative by PCR were prospectively evaluated (mean ± SD age 42 ± 9 years [55% female, 45% male]) (Table 1). The mean ± SD duration of follow-up after beginning direct-acting antiviral therapy was 6.5 ± 1.6 months. Of 250 patients, 69 (27.6%) had chronic musculoskeletal symptoms prior to direct-acting antiviral therapy. The rheumatic disease diagnoses are listed in Table 1. Of

these 69 patients, 18 (26%) had stable musculoskeletal symptoms after direct-acting antiviral therapy; however, 51 (74%) of the patients had experienced worsening musculoskeletal symptoms after beginning direct-acting antiviral therapy. Among the 51 patients with worsening symptoms, 22 (43%) had inflammatory arthritis, and the rest had predominantly chronic myofascial pain. We found that 11 patients had developed new-onset musculoskeletal symptoms after direct-acting antiviral therapy, and among them 53% had inflammatory arthropathies (Table 1). No significant association was noted between new-onset or worsening musculoskeletal symptoms and demographic characteristics, employment status, level of education, marital status, or comorbidities (all $P > 0.05$).


Table 1. Demographic characteristics and rheumatic disease features in 250 patients who were negative for hepatitis C virus after treatment*

Age, mean ± SD years	42 ± 9
Female sex	140 (55)
Musculoskeletal symptoms present prior to direct-acting antiviral therapy	69 (27.6)
Stable	18 (26)
Worsening	51 (74)
New onset of musculoskeletal symptoms after direct-acting antiviral therapy	11
Primary rheumatic disease diagnoses among patients experiencing musculoskeletal symptoms prior to direct-acting antiviral therapy	
Rheumatoid arthritis	8 (11.6)
Seronegative inflammatory arthritis	19 (27.5)
Fibromyalgia	38 (55.1)
Other	4 (5.8)
Primary rheumatic disease diagnoses among patients experiencing worsening musculoskeletal symptoms after direct-acting antiviral therapy	
Rheumatoid arthritis	6 (11.8)
Seronegative inflammatory arthritis	16 (31.4)
Fibromyalgia	28 (54.9)
Other	1 (2.0)
Primary rheumatic disease diagnoses among patients experiencing new onset of musculoskeletal symptoms after direct-acting antiviral therapy	
Rheumatoid arthritis	2 (18.2)
Seronegative inflammatory arthritis	5 (45.5)
Fibromyalgia	4 (36.4)

* Except where indicated otherwise, values are the number (%) of patients.

In conclusion, approximately one-quarter of the entire cohort of patients treated with direct-acting antiviral therapy developed new-onset or significant worsening of musculoskeletal symptoms, and these symptoms developed despite persistent negativity for HCV by PCR. To our knowledge, this finding is novel and has not been reported to date; however, more long-term data are needed for confirmation. Moreover, these results suggest that HCV-related musculoskeletal symptoms should be monitored under the direction of a rheumatologist for many months after HCV has resolved.

Dr. Haroon has received consulting fees, speaking fees, and/or honoraria from AbbVie and Celgene (less than \$10,000 each) and has received research support from AbbVie and Pfizer. No other disclosures relevant to this letter were reported.

Muhammad Haroon, MB, MMedSc, PhD, FRCPI, FFSEM, FACR 
 Fatima Memorial Hospital
 FMH College of Medicine and Dentistry
 Khurram Anis, MBBS, MRCPI, FRCPI
 Zara Khan, MBBS
 Naila Nawaz, MSc, MPhil
 Pakistan Kidney and Liver Institute
 Lahore, Pakistan

1. Ara AK, Paul JP. New direct-acting antiviral therapies for treatment of chronic hepatitis C virus infection. *Gastroenterol Hepatol* (N Y) 2015;11:458–66.
2. Ogdie A, Pang WG, Forde KA, Samir BD, Mulugeta L, Chang KM, et al. Prevalence and risk factors for patient-reported joint pain among patients with HIV/hepatitis C coinfection, hepatitis C mono-infection, and HIV mono-infection. *BMC Musculoskelet Disord* 2015. E-pub ahead of print.
3. Tharwat Hegazy M, Fayed A, El Shabony T, Visentini M, Saadoun D, Cacoub P, et al. Relapsing cryoglobulinemic vasculitis following successful HCV eradication by interferon-free direct acting antivirals, an international multicenter study [abstract]. *Arthritis. Rheumatol* 2019; 71 Suppl 10. URL: <https://acrabstracts.org/abstract/relapsing-cryoglobulinemic-vasculitis-following-successful-hcv-eradication-by-interferon-free-direct-acting-antivirals-an-international-multicenter-study/>.
4. Fayed A, El Nokeety MM, Samy Abdelaziz TS, Samir HH, Hamza WM, El Shabony T. Incidence and characteristics of de novo renal cryoglobulinemia after direct-acting antivirals treatment in an Egyptian hepatitis C cohort. *Nephron* 2018;140:275–81.

DOI 10.1002/art.41503

Morning stiffness and neutrophil circadian disarming: comment on the article by Orange et al

To the Editor:

We read with interest the article by Orange et al (1) on their study assessing whether histologic parameters of synovium are related to symptoms of rheumatoid arthritis (RA). They analyzed synovial tissue samples from 176 RA patients who underwent hip or knee arthroplasty. The detection of neutrophils and fibrin in synovial tissue was associated with patient-reported morning

stiffness of ≥ 1 hour. Orange and colleagues suggested that ongoing neutrophil recruitment in synovial tissue may be associated with prolonged morning stiffness.


This interesting observation may provide insights into the mechanisms of one of the most bothersome symptoms of RA. We want to highlight the role of neutrophil circadian disarming as another plausible contributor to synovial neutrophil infiltration and subsequent morning stiffness. Animal studies and retrospective data have revealed that many inflammatory processes manifest circadian periodicity (2). Recent studies demonstrated the release of neutrophils from bone marrow during the night, with peaking in the early morning and gradual degranulation during the day (2,3). Orange and colleagues showed that the presence of neutrophils is the only histologic feature associated with morning stiffness. However, if there is a steady migration of neutrophils to synovium throughout the day, and neutrophils live only for a short duration after infiltrating synovium, why is there joint stiffness only in the morning? We hypothesize that neutrophil circadian disarming may be a plausible explanation of why joint stiffness predominantly occurs during early morning hours. Neutrophils, especially those with higher protein content in their granules, are released in the early morning, are recruited to synovial tissue, and contribute to local inflammation, causing joint stiffness especially in the morning.

Orange et al (1) also report that fibrin deposits along the synovial membrane with enmeshed neutrophils and necrotic neutrophil DNA were less amenable to fibrinolysis. Their findings suggest that this increased stability and rigidity of neutrophil-trapped fibrin deposits in synovium is associated with morning stiffness. There is increased NETosis in synovial fluid and netting neutrophil infiltration in synovial tissue in RA (4). The increased presence of neutrophil extracellular traps (NETs) promotes immune dysregulation and contributes to tissue damage in many inflammatory diseases including RA (5). Furthermore, NETosis leads to fibrin deposition, results in the formation of fibrin networks, and promotes resistance to tissue plasminogen activator-mediated fibrinolysis (6). Hence, it is possible that detected synovial membrane necrotic neutrophil DNA may be related to synovial NETosis, causing fibrin deposition and resistance to degradation. The neutrophils follow a circadian rhythm in their ability to form NETs. In healthy volunteers, granule-loading and the capacity for NET formation by neutrophils are at the highest level around 8:00 AM and gradually decrease later in the day. In summary, the circadian rhythm of neutrophils, NET formation, and the relationship of neutrophils to fibrin may be additional explanations for the relationship between synovial neutrophil infiltration and morning stiffness.

The presence of NETs has been shown to be associated with loss of tolerance to citrullinated antigens and the development of anti-citrullinated protein/peptide antibodies (ACPAs) (7). In addition, rheumatoid factor (RF) and ACPAs may induce neutrophils to form NETs (4). It would be interesting to investigate whether there are any differences in neutrophil infiltration between

ACPA-positive or ACPA-negative and/or RF-positive or RF-negative RA synovium.

Supported by the Intramural Research Program of the National Institute of Arthritis and Musculoskeletal and Skin Diseases, NIH.

Omer Nuri Pamuk, MD 
Sarfraz Hasni, MD
National Institute of Arthritis and Musculoskeletal
and Skin Diseases, NIH
Bethesda, MD

1. Orange DE, Blachere NE, DiCarlo EF, Mirza S, Pannellini T, Jiang CS, et al. Rheumatoid arthritis morning stiffness is associated with synovial fibrin and neutrophils. *Arthritis Rheumatol* 2020;72:557–64.
2. Adrover JM, Aroca-Crevillén A, Crainiciuc G, Ostos F, Rojas-Vega Y, Rubio-Ponce A, et al. Programmed ‘disarming’ of the neutrophil proteome reduces the magnitude of inflammation. *Nat Immunol* 2020;21:135–44.
3. Adrover JM, del Fresno C, Crainiciuc G, Cuartero MI, Casanova-Acebes M, Weiss LA, et al. A neutrophil timer coordinates immune defense and vascular protection. *Immunity* 2019;50:390–402.
4. Khandpur R, Carmona-Rivera C, Vivekanandan-Giri A, Gizinski A, Yalavarthi S, Knight JS, et al. NETs are a source of citrullinated autoantigens and stimulate inflammatory responses in rheumatoid arthritis. *Sci Transl Med* 2013;5:178ra40.
5. Kaplan MJ. Of larks and owls. *Nat Immunol* 2020;21:104–5.
6. Fuchs TA, Brill A, Duerschmied D, Schatzberg D, Monestier M, Myers DD Jr, et al. Extracellular DNA traps promote thrombosis. *Proc Natl Acad Sci USA* 2010;107:15880–5.
7. O’Neil LJ, Kaplan MJ. Neutrophils in rheumatoid arthritis: breaking immune tolerance and fueling disease [review]. *Trends Mol Med* 2019;25:215–27.

DOI 10.1002/art.41505

Reply

To the Editor:

We are grateful for Dr. Pamuk and colleagues’ interest in our article describing synovial histologic features that are associated with patient-reported morning stiffness in RA. Pamuk et al note that neutrophil gene and protein expression, as well as cell counts, fluctuate in the blood in a 24-hour circadian cycle, and the circadian variation in neutrophil function may contribute to morning stiffness. Specifically, circulating neutrophil counts reach a nadir in the early morning, and this is associated with increased expression of CD62L/L-selectin, a cell surface protein important for adhesion or homing (1), as well as increased granularity and tendency for NET formation (2). We agree that it is possible that one of these circadian features of neutrophils may contribute to prolonged morning stiffness in RA. One possibility is that in the morning, neutrophils, with an increased tendency for NET formation, are more likely to extrude DNA into the synovial membrane, and that this then stabilizes fibrin deposits and contributes to patient perception of stiffness. Another possibility is that

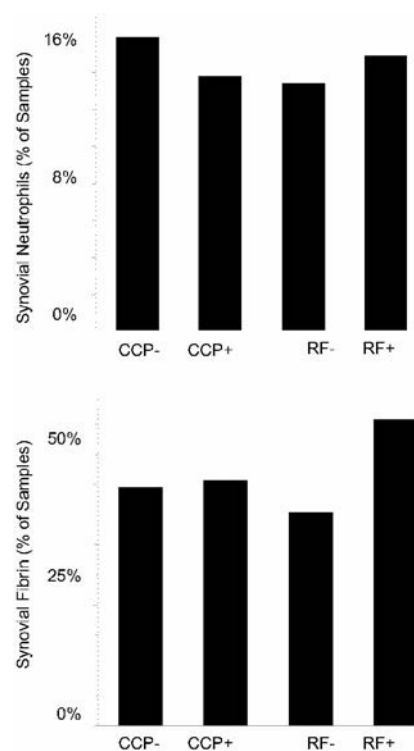





Figure 1. Percentage of synovial samples with infiltrating neutrophils or fibrin deposition according to positivity or negativity for autoantibodies (cyclic citrullinated peptide [CCP] or rheumatoid factor [RF]). There was no significant difference in prevalence of synovial neutrophils or fibrin according to the presence or absence of these autoantibodies.

neutrophils are more likely to traffic and infiltrate inflamed synovium in increased numbers in the morning. We look forward to future studies that might further elucidate the mechanisms of morning stiffness by testing these hypotheses.

Pamuk and colleagues also raise the question of whether there might be a difference in the prevalence of synovial neutrophils in patients with seropositive or seronegative RA, since synovial NETs have been previously shown to be associated with loss of tolerance to citrullinated antigens (3). We did not detect any difference in the frequency of synovial neutrophils or fibrin deposition in patients with seropositive versus seronegative RA (Figure 1). Since neither neutrophils nor fibrin are associated with autoantibodies, we hypothesize that the association between neutrophils, fibrin, and morning stiffness may not be specific to RA and might contribute to the presence of this symptom in other types of inflammatory arthritis, such as seronegative spondyloarthritis.

Dana E. Orange, MD, MS 
Hospital for Special Surgery
and The Rockefeller University
Nathalie E. Blachere, PhD
Mayu O. Frank, NP, PhD
Salina Parveen, MA
Howard Hughes Medical Institute
and The Rockefeller University

Edward F. DiCarlo, MD
 Serene Mirza, BS
 Tania Pannellini, MD, PhD
 Mark P. Figgie, MD
 Vivian P. Bykerk, MD
Hospital for Special Surgery
 Caroline S. Jiang, MS
Rockefeller University Hospital
 New York, NY
 Ellen M. Gravallesse, MD
Brigham and Women's Hospital
 Boston, MA
 Ana-Maria Orbai, MD, MHS 
Johns Hopkins Medicine
 Baltimore, MD
 Sarah L. Mackie, BMBCh
University of Leeds
Leeds NIHR Biomedical Research Centre
and Leeds Teaching Hospitals NHS Trust
 Leeds, UK
 Susan M. Goodman, MD 
Hospital for Special Surgery
 New York, NY

- Adrover JM, del Fresno C, Crainiciuc G, Cuartero MI, Casanova-Acebes M, Weiss LA, et al. A neutrophil timer coordinates immune defense and vascular protection. *Immunity* 2019;50:390–402.
- Adrover JM, Aroca-Crevillén A, Crainiciuc G, Ostos F, Rojas-Vega Y, Rubio-Ponce A, et al. Programmed 'disarming' of the neutrophil proteome reduces the magnitude of inflammation. *Nat Immunol* 2020;21:135–44.
- Khandpur R, Carmona-Rivera C, Vivekanandan-Giri A, Gizinski A, Yalavarthi S, Knight JS, et al. NETs are a source of citrullinated autoantigens and stimulate inflammatory responses in rheumatoid arthritis. *Sci Transl Med* 2013;5:178ra40.

DOI 10.1002/art.41497

Early-onset hydroxychloroquine retinopathy and a possible relationship to blood levels: comment on the article by Petri et al

To the Editor:

Petri et al report that higher blood levels of hydroxychloroquine (HCQ) predicted development of HCQ retinopathy (1). However, in a recent case-control study, HCQ blood levels were not associated with retinopathy (2). The inconsistency may arise from dosage adjustment over time and the timing of blood level testing.

In Japan, height-based HCQ dosing, with a maximum dosage of 6.5 mg/kg ideal weight per day or 400 mg/day, was approved for systemic lupus erythematosus and cutaneous lupus erythematosus in 2015 after a double-blind clinical trial including a pharmacokinetic study demonstrated efficacy and safety (3,4). Dosing based on height and sex is available on the drug package insert so prescribers do not have to calculate. Ophthalmologic screening including both spectral-domain optical coherence tomography and automated visual field assessment is mandatory

Table 1. Characteristics of the 3 patients with HCQ retinopathy at diagnosis*

	Patient 1	Patient 2	Patient 3
Age/sex	37/F	52/F	69/F
Indication	SLE	SLE	SLE
eGFR, ml/minute/1.73 m ²	80–100	23–38	32–54
Liver dysfunction	No	No	No
Use of tamoxifen	No	No	No
Dosage, mg/day	200†	300	300
Height, cm	154	158	155
Real weight, kg	45	45	45
Ideal weight, kg	46	49	47
Dosage, mg/kg real weight/day	4.4	6.7	6.7
Dosage, mg/kg ideal weight/day	4.4	6.1	6.4
Duration of therapy, months	29	29	36
Cumulative dose, gm	182	263	326

* HCQ = hydroxychloroquine; SLE = systemic lupus erythematosus; eGFR = estimated glomerular filtration rate.

† Dosage was temporarily increased to 300 mg/day for 5 months.

before prescription and yearly after initiation. Approximately 20,000 patients have begun HCQ.

As of July 2020, 3 patients had developed HCQ retinopathy (Table 1). HCQ retinopathy was diagnosed 29–36 months after exposure to HCQ. Treatment was maintained at the initial dosage in Patients 2 and 3. In Patient 1, the dosage was temporarily increased to 300 mg/day for 5 months during the total 29-month period of administration. Patients 2 and 3 had impaired renal function. We obtained a blood sample from patient 3 the day after HCQ was discontinued. Liquid chromatography mass spectrometry performed 27 hours after the last dose revealed high whole blood levels of HCQ (2,240 ng/ml).

Petri et al reported a weak correlation (0.32) between HCQ blood levels and weight-based HCQ dosage (0.32) and that the newly recommended maximum daily dosage of 5.0 mg/kg real weight (5) resulted in HCQ blood levels >2,000 ng/ml in some cases (Figure 2 in ref. 1). Measuring HCQ blood levels at the time of retinopathy diagnosis can help in determining the threshold for retinopathy. If HCQ blood levels have a causal relationship to retinopathy, samples obtained at diagnosis should show high levels, and the lowest blood level could be used to estimate the toxicity threshold. For a paradigm shift from weight- or height-based dosing to blood level-based dosing, the therapeutic level should be validated (6).

Dr. Yokogawa's work was supported by a Tokyo Metropolitan Government research grant. Dr. Browning's work was supported by the Diabetic Retinopathy Clinical Research Network. Dr. Ueno has received consulting fees and speaking fees from Sanofi (less than \$10,000). Dr. Shinoda has received consulting fees and speaking fees from Sanofi (less than \$10,000). Dr. Browning owns stock or stock options in Zeiss Meditec. No other disclosures relevant to this letter were reported.

Naoto Yokogawa, MD 
 Akiko Ohno-Tanaka, MD, PhD
 Tokyo Metropolitan Tama Medical Center

Masayuki Hashiguchi, PhD
Keio University
Tokyo, Japan
 Mikiko Shimizu, PhD
Shujitsu University School of Pharmacy
Okayama, Japan
 Hiroko Ozawa, MD
Kawasaki Municipal Hospital
Kanagawa, Japan
 Shinji Ueno, MD, PhD
Nagoya University
Nagoya, Japan
 Kei Shinoda, MD, PhD
Saitama Medical University
Saitama, Japan
 David J. Browning, MD, PhD
Charlotte Eye, Ear, Nose, and Throat Associates
Charlotte, NC

1. Petri M, Elkhalfi M, Li J, Magder LS, Goldman DW. Hydroxychloroquine blood levels predict hydroxychloroquine retinopathy. *Arthritis Rheumatol* 2020;72:448–53.
2. Lenfant T, Salah S, Leroux G, Bousquet E, Le Guern V, Chasset F, et al. Risk factors for hydroxychloroquine retinopathy in systemic lupus erythematosus: a case-control study with hydroxychloroquine blood-level analysis. *Rheumatology (Oxford)* 2020. E-pub ahead of print.
3. Yokogawa N, Eto H, Tanikawa A, Ikeda T, Yamamoto K, Takahashi T, et al. Effects of hydroxychloroquine in patients with cutaneous lupus erythematosus: a multicenter, double-blind, randomized, parallel-group trial. *Arthritis Rheumatol* 2017;69:791–9.
4. Morita S, Takahashi T, Yoshida Y, Yokota N. Population pharmacokinetics of hydroxychloroquine in Japanese patients with cutaneous or systemic lupus erythematosus. *Ther Drug Monit* 2016; 38:259–67.
5. Marmor MF, Kellner U, Lai TY, Melles RB, Mieler WF, American Academy of Ophthalmology. Recommendations on screening for chloroquine and hydroxychloroquine retinopathy (2016 Revision). *Ophthalmology* 2016;123:1386–94.
6. Browning DJ, Yokogawa N, Greenberg PB, Perlman E. Rethinking the hydroxychloroquine dosing and retinopathy screening guidelines. *Am J Ophthalmol* 2020;219:101–6.

DOI 10.1002/art.41521



Reply

To the Editor:

We agree with Dr. Yokogawa and colleagues that in the study by Lenfant et al (1), the lack of findings supporting a relationship between HCQ blood concentration and retinopathy may well have been due to the fact that Lenfant and colleagues selected an adherent control group, which likely inflated the average HCQ levels in their controls relative to typical patients.

Another difference between the 2 studies that may have impacted the findings was the design. Our study was based on a prospective cohort, so patients who developed retinopathy and those who did not develop retinopathy were from the same

cohort. HCQ blood levels were repeatedly measured prior to the onset of retinopathy in all patients. In contrast, the study by Lenfant et al was a case-control study, with cases and controls recruited from different sources, and in the controls, HCQ blood levels were measured only at a single time point (1).

Michelle Petri, MD, MPH 
Johns Hopkins University School of Medicine
Baltimore, MD
 Marwa Elkhalfi, MD, PhD
Alexandria University School of Medicine
Alexandria, Egypt
 Laurence S. Magder, PhD, MPH
University of Maryland School of Medicine
 Jessica Li, MPH
 Daniel W. Goldman, PhD, MCS 
Johns Hopkins University School of Medicine
Baltimore, MD


1. Lenfant T, Salah S, Leroux G, Bousquet E, Le Guern V, Chasset F, et al. Risk factors for hydroxychloroquine retinopathy in systemic lupus erythematosus: a case-control study with hydroxychloroquine blood-level analysis. *Rheumatology (Oxford)* 2020. E-pub ahead of print.

DOI 10.1002/art.41504

To switch or not switch febuxostat: comment on the article by FitzGerald et al




To the Editor:

I read with great interest the 2020 American College of Rheumatology guideline for the management of gout (1). In the guideline, switching to an alternative oral urate-lowering therapy (ULT) agent is conditionally recommended for patients taking febuxostat with a history of cardiovascular disease (CVD) or a new CVD-related event. The limitation of underlying evidence from the US Food and Drug Administration–mandated CARES trial was addressed, i.e., a high dropout rate with a majority of deaths occurring after ULT discontinuation (2). I have 2 additional concerns regarding the recommendation that such patients should switch from febuxostat to an alternative oral ULT agent. First, in these patients, the increased mortality rate within 30 days of febuxostat discontinuation may be due to the abrupt increase in serum uric acid (UA) level with subsequent free urate crystal formation in the cardiovascular system (cardiovascular gout attack) (3). The serum UA level may rebound when treatment is switched from febuxostat to an alternative ULT agent, and it probably takes >1 month to get it under control. Therefore, based on observations from the CARES trial, there may be an increased likelihood of death within the first month if switching from febuxostat to an alternative ULT agent. Second, intolerance to alternative ULT agents and potential inadequate control of UA levels in turn increase the risk of CVD (4). The decision to switch from febuxostat to another treatment should be a shared one that takes into account all of the above-mentioned concerns.

Chuanhui Xu, MD, PhD, MRCP 
*Department of Rheumatology, Allergy, and
Immunology
Tan Tock Seng Hospital
Singapore*

1. FitzGerald JD, Dalbeth N, Mikuls T, Brignardello-Petersen R, Guyatt G, Abeles AM, et al. 2020 American College of Rheumatology guideline for the management of gout. *Arthritis Rheumatol* 2020;72:879–95.
2. White WB, Saag KG, Becker MA, Borer JS, Gorelick PB, Whelton A, et al. Cardiovascular safety of febuxostat or allopurinol in patients with gout. *N Engl J Med* 2018;378:1200–10.
3. Ghang B, Ahn SM, Kim J, Kim YG, Lee CK, Yoo B. Discontinuing febuxostat might cause more deaths than continuing febuxostat: the untold story from the CARES trial. *Rheumatology (Oxford)* 2020;59:1439–40.
4. Pagidipati NJ, Hess CN, Clare RM, Akerblom A, Tricoci P, Wojdyla D, et al. An examination of the relationship between serum uric acid level, a clinical history of gout, and cardiovascular outcomes among patients with acute coronary syndrome. *Am Heart J* 2017;187:53–61.

American College of Rheumatology Guidance for the Management of Rheumatic Disease in Adult Patients During the COVID-19 Pandemic: Version 3

Ted R. Mikuls,¹  Sindhu R. Johnson,²  Liana Fraenkel,³  Reuben J. Arasaratnam,⁴ Lindsey R. Baden,⁵ Bonnie L. Bermas,⁴ Winn Chatham,⁶ Stanley Cohen,⁷ Karen Costenbader,⁵ Ellen M. Gravallesse,⁵ Andre C. Kalil,⁸ Michael E. Weinblatt,⁵ Kevin Winthrop,⁹ Amy S. Mudano,⁶ Amy Turner,¹⁰ and Kenneth G. Saag⁶

Due to the rapidly expanding information and evolving evidence related to COVID-19, which may lead to modification of some guidance statements over time, it is anticipated that updated versions of this article will be published, with the version number included in the title. Readers should ensure that they are consulting the most current version.

Guidance developed and/or endorsed by the American College of Rheumatology (ACR) is intended to inform particular patterns of practice and not to dictate the care of a particular patient. The ACR considers adherence to this guidance to be voluntary, with the ultimate determination regarding its application to be made by the physician in light of each patient's individual circumstances. Guidance statements are intended to promote beneficial or desirable outcomes but cannot guarantee any specific outcome. Guidance developed or endorsed by the ACR is subject to periodic revision as warranted by the evolution of medical knowledge, technology, and practice.

The American College of Rheumatology is an independent, professional medical and scientific society which does not guarantee, warrant, or endorse any commercial product or service.

Objective. To provide guidance to rheumatology providers on the management of adult rheumatic disease in the context of the coronavirus disease 2019 (COVID-19) pandemic.

Methods. A task force, including 10 rheumatologists and 4 infectious disease specialists from North America, was convened. Clinical questions were collated, and an evidence report was rapidly generated and disseminated. Questions and drafted statements were reviewed and assessed using a modified Delphi process. This included asynchronous anonymous voting by email and webinars with the entire panel. Task force members voted on agreement with draft statements using a 1–9-point numerical scoring system, and consensus was determined to be low, moderate, or high based on the dispersion of votes. For approval, median votes were required to meet predefined levels of agreement (median values of 7–9, 4–6, and 1–3 defined as agreement, uncertainty, or disagreement, respectively) with either moderate or high levels of consensus.

Results. Draft guidance statements approved by the task force have been combined to form final guidance.

Conclusion. These guidance statements are provided to promote optimal care during the current pandemic. However, given the low level of available evidence and the rapidly evolving literature, this guidance is presented as a “living document,” and future updates are anticipated.

INTRODUCTION

Since its initial outbreak in Wuhan, China, coronavirus disease 2019 (COVID-19) has rapidly evolved into a worldwide pandemic (1). Caused by infection with severe acute respiratory syndrome coronavirus 2 (SARS-CoV-2), COVID-19 has impacted millions of lives and has contributed to a growing number of deaths worldwide. The pandemic poses a substantial challenge for both rheumatology providers and patients since serious infection is a well-recognized cause of morbidity and mortality across a number of rheumatic diseases. Therefore, there is an urgent need to address important questions regarding COVID-19 risk and prevention as well as the safety surrounding the administration of rheumatic disease treatments.

The American College of Rheumatology (ACR) convened the COVID-19 Clinical Task Force on March 26, 2020, charged by ACR leadership to rapidly provide guidance to rheumatology providers relevant to the management of rheumatic disease in adult patients during the pandemic. Clinical guidance generated from this effort is intended to aid in the care of individual patients, but it is not meant to supplant clinical decision-making. Modifications to treatment plans, particularly in patients with complex conditions, are highly disease-, patient-, geography-, and time-specific and, therefore, must be individualized as part of a shared decision-making process. Although substantial attention has been given to the use of rheumatology treatments (e.g., hydroxychloroquine [HCQ], chloroquine [CQ], interleukin-6 [IL-6] receptor inhibition) in the prevention and management of COVID-19 and associated inflammatory sequelae of infection, the guidance provided in this report is limited to the management of rheumatic disease and does not

address the management of COVID-19 and/or its complications. Furthermore, the guidance herein is presented as a “living” document, recognizing that evidence is evolving rapidly and the ACR anticipates the need for updates of this guidance as such evidence becomes available.

METHODS

Clinical questions. A task force leadership group (TRM, SRJ, LF, KGS) generated initial questions and clinical scenarios to address. Initial questions were informed by review of “Frequently Asked Questions” posted by rheumatology patients on patient-facing websites hosted by the national Arthritis Foundation (2), CreakyJoints (3), and the Global Healthy Living Foundation (4). Questions were categorized into 4 overlapping domains: 1) risk assessment and prevention, 2) use of rheumatic disease treatments in patients at risk for exposure, 3) rheumatic disease treatment immediately following known SARS-CoV-2 exposure (e.g., community-related exposure as defined by the Centers for Disease Control and Prevention [CDC]), and 4) management of rheumatic disease in the context of COVID-19. The task force agreed that the perspective of the guidance should be that of managing clinicians and their individual patients but that some attention should be directed to a societal perspective, when relevant, around potential issues of availability of specific antirheumatic therapies being considered for treatment of COVID-19. Following an initial task force webinar on March 26, 2020, 4 separate subgroups were formed to address and refine questions in each domain. The task force included 14 members from North America and comprised 10 rheumatologists and 4 infectious disease specialists with broad

Supported by the American College of Rheumatology.

¹Ted R. Mikuls, MD, MSPH: University of Nebraska Medical Center, Omaha, and VA Nebraska-Western Iowa Health Care System, Omaha, Nebraska; ²Sindhu R. Johnson, MD, PhD: Toronto Western Hospital, Mount Sinai Hospital, and University of Toronto, Toronto, Ontario, Canada; ³Liana Fraenkel, MD, MPH: Berkshire Health Systems, Pittsfield, Massachusetts, and Yale University, New Haven, Connecticut; ⁴Reuben J. Arasaratnam, MD, MPH, Bonnie L. Bermas, MD: University of Texas Southwestern Medical Center, Dallas; ⁵Lindsey R. Baden, MD, Karen Costenbader, MD, MPH, Ellen M. Gravallesse, MD, Michael E. Weinblatt, MD: Brigham and Women's Hospital, Boston, Massachusetts; ⁶Winn Chatham, MD, Amy S. Mudano, MPH, Kenneth G. Saag, MD, MSc: University of Alabama at Birmingham; ⁷Stanley Cohen, MD: Metroplex Clinical Research Center, Dallas, Texas; ⁸Andre C. Kalil, MD, MPH: University of Nebraska Medical Center, Omaha; ⁹Kevin Winthrop, MD, MPH: Oregon Health and Science University, Portland; ¹⁰Amy Turner: American College of Rheumatology, Atlanta, Georgia.

Dr. Mikuls has received consulting fees, speaking fees, and/or honoraria from Pfizer (less than \$10,000) and research support from Bristol Myers Squibb and Horizon. Dr. Johnson has received consulting fees and/or honoraria from Boehringer Ingelheim and Ikaria (less than \$10,000 each) and research support from GlaxoSmithKline, Corbus, Roche, Merck, Boehringer Ingelheim, and Bayer. Dr. Chatham has received consulting fees, speaking fees, and/or honoraria from ChemoCentryx, Sobi, and Novartis (less than \$10,000 each) and research support from Bristol Myers Squibb, Janssen, and GlaxoSmithKline. Dr. Cohen has received consulting fees, speaking fees, and/or honoraria from Amgen, AbbVie, Bristol Myers Squibb, Eli Lilly, Genentech, Gilead, and Roche (less than \$10,000 each) and from Pfizer (more than \$10,000), and research support from Amgen, AbbVie, Bristol Myers Squibb, Eli Lilly, Gilead, Genentech, Pfizer, and Roche. Dr. Costenbader has received research support

from AstraZeneca, GlaxoSmithKline, Janssen, Eli Lilly, and Merck. Dr. Gravallesse has received salary support from the *New England Journal of Medicine* (more than \$10,000) and has received royalties as an editor for UptoDate and the textbook *Rheumatology*. Dr. Weinblatt has received consulting fees, speaking fees, and/or honoraria from AbbVie, Amgen, Canfite, Crescendo Bioscience, Gilead, GlaxoSmithKline, Horizon, Johnson & Johnson, Merck, Novartis, Pfizer, Roche/Genentech, Samsung, Sanofi, Scipher Medicine, and Setpoint Medical (less than \$10,000 each) and from Bristol Myers Squibb, Corrona, Eli Lilly, and Pfizer (more than \$10,000 each), owns stock or stock options in Lycera, Vorso, Scipher Medicine, Immedix, and Canfite, receives royalties as co-editor of the textbook *Rheumatology*, and has received research support from Amgen, Bristol Myers Squibb, Eli Lilly, Crescendo Bioscience, and Sanofi. Dr. Winthrop has received consulting fees, speaking fees, and/or honoraria from Bristol Myers Squibb, Eli Lilly, Roche, Gilead, Pfizer and GlaxoSmithKline (less than \$10,000 each) and from AbbVie and UCB (more than \$10,000 each) and research support from Pfizer and Bristol Myers Squibb. Dr. Saag has received consulting fees, speaking fees, and/or honoraria from AbbVie, Bayer, GlaxoSmithKline, Behring, Daiichi Sankyo, Gilead, Radius, and Roche/Genentech (less than \$10,000 each) and from Amgen (more than \$10,000) and research support from Amgen and Radius. No other disclosures relevant to this article were reported.

Address correspondence to Ted R. Mikuls, MD, MSPH, University of Nebraska Medical Center, Division of Rheumatology, 986270 Nebraska Medical Center, Omaha, NE 68198. Email: tmikuls@unmc.edu.

Submitted for publication July 7, 2020; accepted July 9, 2020.

No part of this article may be reproduced, stored, or transmitted in any form or for any means without prior permission in writing. For permission information contact permissions@wiley.com. For information about purchasing reprints contact commercialreprints@wiley.com.

Table 1. Timeline in ACR COVID-19 clinical guidance development*

Date(s)	Milestone
2019	
December	Initial cases of novel coronavirus pneumonia identified in Wuhan, China
2020	
January 21	First (travel-related) case of COVID-19 in US (Washington state)
March 11	COVID-19 declared pandemic by World Health Organization
March 26	ACR COVID-19 Clinical Task Force convened—initial webinar
March 26–30	Task force subgroups refine clinical questions and gather evidence
March 31	Evidence report disseminated to task force members
April 1–3	Initial task force vote on statements/questions
April 4	Results of round one voting reviewed, discussed via webinar
April 5–6	Draft statements generated for additional consideration
April 7–8	Second round of task force voting
April 8	Final statements reviewed and refined via webinar
April 9–10	Approved statements concatenated into 25 recommendations and draft guidance document generated
April 11	Guidance document approved by ACR Board of Directors
April 13	Draft guidance posted on ACR website
July 31	Online publication of version 2

* ACR = American College of Rheumatology; COVID-19 = coronavirus disease 2019.

expertise in relevant clinical areas and representing different geographic regions, rheumatic disease specialty areas, and clinical practice settings.

Evidence review. In addition to refining clinical questions addressed, each subgroup was tasked with gathering evidence that addressed questions within the assigned domains. This nonsystematic evidence review included PubMed searches

supplemented by postings from the CDC, US Food and Drug Administration (FDA), and other electronic media sources. Questions and relevant evidence were collated into a single document, which was disseminated by email to the entire task force for review 2 days prior to initial voting. Following initial publication, regular PubMed searches were undertaken, abstracts reviewed by the leadership team with full reports reviewed as appropriate, and new evidence shared with the task force prior to follow-up webinars.

Initial voting. Following the evidence review, an initial round of voting was conducted anonymously by email using a modified Delphi approach as part of the RAND/University of California at Los Angeles (UCLA) appropriateness method (5). The RAND/UCLA appropriateness method has been shown to be highly reproducible (6) and to have content, construct, and predictive validity (7–9). All votes were weighted equally. Task force members were asked to report their level of agreement with 3 general statements in addition to providing graded yes/no responses to 90 clinical questions. Voting was completed using a numerical rating scale of 1–9 for all items. For the 3 general statements, ratings of 9 corresponded to “complete agreement,” 5 corresponded to “uncertain,” and 1 corresponded to “complete disagreement.” Median vote ratings of 1–3, 4–6, and 7–9 were defined a priori and interpreted as disagreement, uncertainty, and agreement, respectively. For yes/no questions, a voting score of 9 indicated that a positive response was expected “to result in a highly favorable benefit to risk ratio” whereas a voting score of 1 strongly favored a negative response and a voting score of 5 corresponded to uncertainty. For questions, median vote ratings of 1–3, 4–6, and 7–9 were interpreted as no, uncertain, and yes responses, respectively. Panel consensus was also assessed and noted to be “low” when ≥ 4 votes fell into the 1–3 rating range with ≥ 4 votes simultaneously falling into the 7–9 rating range. Consensus was deemed to be “high” when all 14 votes fell within a single

Table 2. General guidance for patients with rheumatic disease*

Guidance statement	Level of task force consensus
The risk of poor outcomes from COVID-19 appears to be related primarily to general risk factors such as age and comorbidity.	High
Patients should be counseled on general preventive measures, e.g., social distancing, wearing a mask when social distancing is not possible, and hand hygiene.	High
As part of a shared decision-making process between patients and rheumatology providers, select measures to reduce health care encounters and potential exposure to SARS-CoV-2 (beyond general preventive measures) may be reasonable, e.g., reduced frequency of laboratory monitoring, optimal use of telehealth, increased dosing intervals between intravenous medications.	Moderate to high
If indicated, glucocorticoids should be used at the lowest dose possible to control rheumatic disease, regardless of exposure or infection status.	Moderate to high
Glucocorticoids should not be abruptly stopped, regardless of exposure or infection status.	High
If indicated, ACE inhibitors or ARBs should be continued in full doses or initiated.	Moderate to high

* COVID-19 = coronavirus disease 2019; SARS-CoV-2 = severe acute respiratory syndrome coronavirus 2; ACE = angiotensin-converting enzyme; ARB = angiotensin receptor blocker.

tertile, with all other combinations considered to reflect “moderate” levels of consensus.

Review of initial voting results and generation of draft guidance statements. Results from the first round of voting were reviewed and discussed as part of a task force webinar on April 4, 2020 (Table 1). Discussion was focused on questions and/or statements with median votes reflecting uncertainty and with low or moderate consensus. Panelists were given the opportunity to comment on all of the items presented in the initial voting process. Informed by voting results and discussion, the task force leadership group drafted guidance statements for further consideration.

Second round of voting and guidance approval. Draft statements were sent to task force members and agreement was assessed by email, again using an anonymous voting process as detailed above. Guidance statements receiving a median vote rating of 7–9 with moderate or high consensus were approved as recommendations (10). Results from the second round of voting were presented to the task force during a third webinar on April 8, 2020, and minor revisions to statements were made through an iterative process until consensus was achieved. To minimize redundancy and overlap, the approved statements were combined to generate final guidance statements with the agreement of task force members ascertained via email. The ACR Board of Directors approved these initial recommendations on April 11, 2020. A similar approach was used for changes and/or additions made to the guidance document that followed its initial approval.

RESULTS

Of the 81 guidance statements considered in round 2 voting, 77 received median vote ratings of 7, 8, or 9 and were also

associated with moderate consensus ($n = 36$) or high consensus ($n = 41$), the predefined threshold for approval (Supplementary Tables 1–6, on the *Arthritis & Rheumatology* website at <http://online.library.wiley.com/doi/10.1002/art.41596/abstract>). There were 2 draft statements receiving a median vote rating of <7 (Supplementary Tables 5 and 6) and 2 additional statements with a median vote rating of ≥ 7 that were accompanied by low consensus (Supplementary Tables 2 and 3b). The process resulted in 25 final guidance statements that were posted online by the ACR in draft form on April 13, 2020. These include guidance on 1) general considerations relevant to risk assessment, prevention, and the use of glucocorticoids, angiotensin-converting enzyme (ACE) inhibitors, or angiotensin receptor blockers (ARBs) (Table 2), 2) ongoing treatment of patients with stable rheumatic disease in the absence of infection or SARS-CoV-2 exposure and considerations specific to systemic lupus erythematosus (SLE) (Table 3), 3) treatment of newly diagnosed or active rheumatic disease in the absence of infection or SARS-CoV-2 exposure (Table 4), 4) treatment of rheumatic disease after SARS-CoV-2 exposure (Table 5), and 5) rheumatic disease treatment in the context of documented or presumptive COVID-19 (Table 5).

Following approval and publication of these initial 25 guidance statements, the task force approved 3 additional statements (Supplementary Table 7, on the *Arthritis & Rheumatology* website at <http://onlinelibrary.wiley.com/doi/10.1002/art.41596/abstract>). Two of these statements were combined, leading to a total of 27 guidance statements. Guidance statements specific to the use of HCQ/CQ were revised following initial publication (results of re-voting shown in Supplementary Table 8, on the *Arthritis & Rheumatology* website at <http://onlinelibrary.wiley.com/doi/10.1002/art.41596/abstract>).

Evidence supporting the final recommendations was universally of very low quality: either indirect and/or limited to case

Table 3. Guidance for ongoing treatment of patients with stable rheumatic disease in the absence of infection or known SARS-CoV-2 exposure and in patients with SLE*

Guidance statement	Level of task force consensus
Ongoing treatment in patients with stable rheumatic disease	
HCQ/CQ, SSZ, MTX, LEF, immunosuppressants (e.g., tacrolimus, CSA, MMF, AZA), biologics, JAK inhibitors, and NSAIDs may be continued. (This includes patients with GCA with an indication, in whom IL-6 receptor inhibitors should be continued, if available.)	Moderate to high
Denosumab may still be given, extending dosing intervals to no longer than every 8 months, if necessary to minimize health care encounters.	Moderate
For patients with a history of vital organ-threatening rheumatic disease, immunosuppressants should not be dose-reduced.	Moderate
Treatment of SLE	
For patients with newly diagnosed disease, HCQ/CQ should be started at full dose, when available.	High
For pregnant women with SLE, HCQ/CQ should be continued at the same dose, when available.	High
If indicated, belimumab may be initiated.	Moderate

* SARS-CoV-2 = severe acute respiratory syndrome coronavirus 2; SLE = systemic lupus erythematosus; HCQ = hydroxychloroquine; CQ = chloroquine; SSZ = sulfasalazine; MTX = methotrexate; LEF = leflunomide; CSA = cyclosporin A; MMF = mycophenolate mofetil; AZA = azathioprine; NSAIDs = nonsteroidal antiinflammatory drugs; GCA = giant cell arteritis; IL-6 = interleukin-6.

Table 4. Guidance for the treatment of newly diagnosed or active rheumatic disease in the absence of infection or known SARS-CoV-2 exposure*

Guidance statement	Level of task force consensus
Inflammatory arthritis	
For patients whose disease is well-controlled with HCQ/CQ, this DMARD should be continued when available; when unable to access (including in patients with active or newly diagnosed disease), switching to a different conventional synthetic DMARD (either as monotherapy or as part of combination therapy) should be considered.	Moderate to high
For patients whose disease is well-controlled with an IL-6 receptor inhibitor, this DMARD should be continued when available; when unable to access the agent, switching to a different biologic should be considered.†	Moderate
For patients with moderate-to-high disease activity despite optimal conventional synthetic DMARDs, biologics may be started.†	High
For patients with active or newly diagnosed inflammatory arthritis, conventional synthetic DMARDs may be started or switched.	Moderate
If indicated, low-dose glucocorticoids (≤10 mg prednisone equivalent/day) or NSAIDs may be started.	Moderate to high
Other rheumatic diseases	
For patients with systemic inflammatory or vital organ-threatening disease (e.g., lupus nephritis or vasculitis), high-dose glucocorticoids or immunosuppressants (e.g., tacrolimus, CSA, MMF, AZA) may be initiated.	Moderate
In the context of a drug shortage due to COVID-19, new HCQ/CQ prescriptions for non-FDA-approved indications should be avoided.	High

* SARS-CoV-2 = severe acute respiratory syndrome coronavirus 2; HCQ = hydroxychloroquine; CQ = chloroquine; DMARD = disease-modifying antirheumatic drug; IL-6 = interleukin-6; NSAIDs = nonsteroidal antiinflammatory drugs; CSA = cyclosporin A; MMF = mycophenolate mofetil; AZA = azathioprine; FDA = US Food and Drug Administration.

† The panel noted uncertainty with regard to JAK inhibition in this situation.

series or retrospective cohort studies of COVID-19 patients with limited or no information on underlying rheumatic disease status. Available evidence is summarized below, organized by risk assessment, infection prevention, and rheumatic disease treatments.

Risk assessment. To our knowledge, there is currently no compelling evidence identifying risk factors for poor outcome with COVID-19 that are specific to rheumatic disease. Based on preliminary retrospective cohort studies (11–14), risk factors for poor outcome with COVID-19 include older age (e.g., >65 years)

Table 5. Guidance for the treatment of rheumatic disease following known SARS-CoV-2 exposure and in the context of active or presumptive COVID-19*

Guidance statement	Level of task force consensus
Following SARS-CoV-2 exposure	
SSZ and NSAIDs may be continued.	Moderate to high
HCQ/CQ, immunosuppressants (e.g., tacrolimus, CSA, MMF, AZA), non-IL-6 biologics, and JAK inhibitors should be stopped temporarily, pending 2 weeks of symptom-free observation.†	Moderate to high
In select circumstances, as part of a shared decision-making process, IL-6 receptor inhibitors may be continued.	Moderate
Documented or presumptive COVID-19	
Regardless of COVID-19 severity, HCQ/CQ, SSZ, MTX, LEF, immunosuppressants, non-IL-6 biologics, and JAK inhibitors should be stopped or withheld.	Moderate to high
For patients with severe respiratory symptoms, NSAIDs should be stopped.‡	Moderate
In select circumstances, as part of a shared decision-making process, IL-6 receptor inhibitors may be continued.	Moderate
Reinitiating treatment following COVID-19	
For patients with uncomplicated COVID-19 infections (characterized by mild or no pneumonia and treated in the ambulatory setting or via self-quarantine), consideration may be given to restarting rheumatic disease treatments (e.g., DMARDs, immunosuppressants, biologics, and JAK inhibitors) within 7–14 days of symptom resolution. For patients who have a positive PCR test result for SARS-CoV-2 but are (and remain) asymptomatic, consideration may be given to restarting rheumatic disease treatments (e.g., DMARDs, immunosuppressants, biologics, and JAK inhibitors) 10–17 days after the PCR result is reported as positive.	High
Decisions regarding the timing of reinitiating rheumatic disease therapies in patients recovering from more severe COVID-19-related illness should be made on a case-by-case basis.	High

* SARS-CoV-2 = severe acute respiratory syndrome coronavirus 2; COVID-19 = coronavirus disease 2019; HCQ = hydroxychloroquine; CQ = chloroquine; SSZ = sulfasalazine; NSAIDs = nonsteroidal antiinflammatory drugs; CSA = cyclosporin A; MMF = mycophenolate mofetil; AZA = azathioprine; IL-6 = interleukin-6; MTX = methotrexate; LEF = leflunomide; DMARDs = disease-modifying antirheumatic drugs; PCR = polymerase chain reaction.

† The panel noted uncertainty with regard to temporarily stopping MTX or LEF in this situation.

‡ The panel demonstrated low consensus with regard to stopping NSAIDs in the absence of severe symptoms.

and select comorbidities such as chronic lung disease, hypertension, cardiovascular disease, chronic kidney disease, obesity, and diabetes mellitus, conditions that are frequently overrepresented among patients with rheumatic disease (15–18). Data linking specific rheumatologic treatments to COVID-19 or its complications are either lacking or, when available, conflicting, and are discussed in detail below.

In addition to older age and comorbidity, a number of laboratory measures have been preliminarily associated with poor outcomes from COVID-19 (11,12). Examined in retrospective cohorts of hospitalized patients, biomarkers predictive of poor outcomes have included lymphopenia (particularly, low CD4+ T cell numbers) and elevations in circulating levels of lactate dehydrogenase, C-reactive protein, IL-6, and D-dimer, among others (19–22). Whether lymphopenia portends “preexisting” risk or is a consequence of more severe infection in hospitalized patients is unclear. Defining the precise role different biomarkers might play in predicting COVID-19 outcomes in the context of rheumatic disease will require further study.

General infection prevention. Preventive measures focused on mitigating infection risk and the impact of COVID-19 have been widely publicized by the CDC (23,24) and other public health agencies. The task force acknowledged the importance of these measures, recommending that rheumatic disease patients be provided with guidance around their routine adoption. These focus primarily on optimal hand hygiene, social distancing, and wearing a mask in public when social distancing is not possible, among others. As social distancing has emerged as a focal point in public health strategies aimed at preventing SARS-CoV-2 infection, this may have implications for the delivery of rheumatology care, with efforts to reduce health care encounters as a means of preventing virus spread and preserving the health care workforce (25). The task force acknowledged several relevant strategies that could be applied in the context of rheumatology care, including, but not limited to, optimal use of telehealth, reducing the frequency of routine laboratory surveillance when the associated risk of not testing is deemed to be low, using lower-volume laboratories not located within larger health care facilities, or delaying the initiation or re-dosing of infusion-based treatments when the risk of disease flare is low. The task force endorsed potential temporary delays in performing intravenous administration of zoledronic acid or subcutaneous administration of denosumab (generally given at a health care setting) as two examples (Supplementary Table 4, on the *Arthritis & Rheumatology* website at <http://online.library.wiley.com/doi/10.1002/art.41596/abstract>), recommending that dosing intervals with denosumab not exceed 8 months due to concerns regarding increased vertebral fracture risk following denosumab withdrawal (26).

The task force recognized the importance of social distancing for all patients, including in the workplace when feasible. This may be particularly important for vulnerable patients

at increased risk of poor COVID-19 outcomes (e.g., older patients with multimorbidity) and those at increased risk of SARS-CoV-2 exposure (e.g., health care workers). Workplace accommodations, including appropriate personal protective equipment (PPE), to minimize the spread of infection should be made available, and additional accommodations in the absence of PPE may be needed.

Rheumatic disease treatments. ACE inhibitors and ARBs. Recognizing that ACE2 serves as the cellular receptor for SARS-CoV-2 (27), theoretical concerns have been raised regarding therapies known to increase ACE2 expression (a recognized effect of ACE inhibitors and ARBs) (28). Following acute lung injury, ACE2 levels are down-regulated in local tissue, which may lead to excessive activation of the renin-angiotensin-aldosterone system and worsen underlying pneumonia. This has led to the opposing conjecture that ACE inhibitors or ARBs could be beneficial in the context of active infection (29). To date, however, there are insufficient clinical data to support the notion of either detrimental or beneficial effects of these drugs with respect to COVID-19. The American Heart Association, Heart Failure Society of America, and American College of Cardiology have recommended continuation of ACE inhibitors or ARBs for all patients who have been prescribed these agents, with careful deliberation preceding any change in these treatments (30). A cohort study demonstrated that among patients with hypertension hospitalized with COVID-19, the use of ACE inhibitors or ARBs was associated with significantly improved survival (31). The task force recommended continued use of ACE inhibitors and ARBs per standard of care in rheumatic disease patients who are most likely to benefit from these agents, such as those with a history or risk of scleroderma renal crisis or those with SLE and hypertension (32,33).

Nonsteroidal antiinflammatory drugs (NSAIDs). Although speculation was raised early in the pandemic with regard to NSAID use and possible associations with worse COVID-19 outcomes (34,35), these concerns have yet to be substantiated. The task force endorsed the continued use of these agents and prescription of these medications, when indicated, for newly diagnosed rheumatic disease with the exception that NSAIDs be stopped in those with severe manifestations of COVID-19, such as kidney, cardiac, or gastrointestinal injury, which portend a poor prognosis (36–38). The task force demonstrated low consensus specific to whether NSAIDs should be stopped in the setting of less severe COVID-19, where the use of such agents might provide therapeutic antipyretic and/or antiinflammatory benefit. Others have proposed acetaminophen (or paracetamol) as an alternative to NSAIDs in this situation (39), although appropriate caution is needed as there has been evidence of liver injury accompanying COVID-19 in a proportion of cases (40).

Glucocorticoids. The data related to the effects of glucocorticoid treatment in patients infected with SARS-CoV-2 are mixed. Recognizing potential risks associated with the immunosuppressive effects of glucocorticoids, emerging data suggest that their antiinflammatory properties could theoretically mitigate the impact of COVID-19, particularly during the late phases of infection characterized by hyperinflammation and cytokine storm (11,41). Case series suggest that younger patients with a history of solid organ transplantation and those undergoing cancer chemotherapy living in epidemic areas of Italy, many of whom were receiving glucocorticoids, have not developed severe COVID-19 complications (42). In small hospital-based cohorts, treatment of COVID-19–related acute respiratory distress syndrome with methylprednisolone was associated with improved survival (11) and shorter intensive care unit (ICU) stays (41). In a controlled, open-label study of hospitalized COVID-19 patients, dexamethasone administration was associated with a lower 28-day mortality in a subgroup of patients receiving respiratory support (43).

These limited data suggesting a glucocorticoid benefit in COVID-19 are balanced by indirect data from other viral infections suggesting that there is no meaningful benefit, or even that there may be harm. There are no clinical data, for instance, suggesting benefit from glucocorticoids in the treatment of airway infections related to respiratory syncytial virus, influenza, SARS-CoV-1, or Middle East respiratory syndrome (MERS; caused by a separate coronavirus) (44). Furthermore, in one study of patients with SARS-CoV-1 pneumonia, the use of glucocorticoids was associated with worse outcomes (45). Likewise, glucocorticoid treatment in influenza pneumonia has been associated with significantly worse outcomes including higher mortality, more secondary bacterial infections, and increased length of ICU stay (46). In addition to being associated with reactivation of herpes zoster (47,48), glucocorticoid treatment is associated with a dose-dependent risk of serious bacterial and opportunistic infections (49). This latter concern may be particularly salient, as it was demonstrated in at least one Chinese case series that up to one-half of all COVID-19–related deaths were attributable to secondary bacterial infection (50).

Acknowledging controversies in the available evidence, the task force endorsed continued standard-of-care glucocorticoid administration, avoidance of abrupt treatment withdrawal (given the possibility of hypothalamic–pituitary–adrenal axis suppression [51]), and use of the lowest effective doses to control underlying rheumatic disease manifestations. The panel further endorsed the use of low-dose glucocorticoids when clinically indicated and acknowledged that higher doses in the context of severe, vital organ-threatening disease may be necessary even following SARS-CoV-2 exposure.

Conventional synthetic disease-modifying antirheumatic drugs (csDMARDs). Risks of serious infection with HCQ, CQ, sulfasalazine (SSZ), leflunomide (LEF), and methotrexate (MTX) are relatively small, particularly when given as monotherapies

(52,53). This fact informed the task force's recommendation to continue or initiate these therapies, when needed, in the absence of infection or known SARS-CoV-2 exposure. The task force recommended that SSZ could be continued post-SARS-CoV-2 exposure (expressing uncertainty regarding MTX and LEF in this situation) but recommended temporarily withholding HCQ/CQ, SSZ, LEF, and MTX in the setting of active infection. This latter recommendation specific to SSZ stemmed primarily from concerns that adverse effects from this agent (e.g., gastrointestinal upset, diarrhea, hepatitis, cytopenias, and rarely, pneumonitis) could be confused with signs of COVID-19 infection or could be detrimental, and that temporarily withholding this treatment would be unlikely to result in significant rheumatic disease flares.

Despite lack of support from rigorously conducted clinical trials (54–58), HCQ and CQ have been widely used in the treatment of COVID-19. As a result, supply chain issues for both agents have been reported (59). Recognizing the possibility that antimalarial therapy may not be available for all patients, the task force recommended that other csDMARDs could be used in place of HCQ/CQ in the context of inflammatory arthritis. The task force also recommended that in the setting of concerns regarding drug availability, new prescriptions of HCQ/CQ should be limited to patients with FDA-approved indications. The task force achieved strong levels of agreement and high consensus with regard to the continued use of HCQ/CQ in the management of SLE, when possible. It has been shown that therapeutic drug levels (>500 ng/ml in blood) can be achieved with optimal HCQ dosing strategies and that circulating drug concentrations below this threshold are associated with higher disease activity and increased flare risk in SLE (60,61). In addition to being associated with improved pregnancy outcomes in women with SLE (62), continued use of HCQ in SLE decreases the risk of flare and reduces the risk of longer-term morbidity and mortality (63,64).

The task force recommended temporarily withholding HCQ/CQ following SARS-CoV-2 exposure or infection. This change from prior guidance (Supplementary Table 8, <http://onlinelibrary.wiley.com/doi/10.1002/art.41596/abstract>) stems from emerging reports highlighting the potential for cardiotoxicity (primarily QT prolongation and arrhythmias) that could be heightened in the context of COVID-19 and the receipt of other QT-prolonging agents that are common among hospitalized patients (65–69). Protocols have been proposed for cardiac monitoring to reduce the potential of adverse cardiac events that could be attributable to HCQ/CQ, particularly in the context of severe infection (70). Given the prolonged tissue half-life of antimalarial therapies, such monitoring may be needed in high-risk patients with COVID-19 even in circumstances where these agents have been withheld. As with SSZ, the task force believed that temporary discontinuation of these agents would be unlikely to result in a significant increase in the risk of rheumatic disease flare.

Biologics, immunosuppressants, and JAK inhibitors. Biologics and JAK inhibitors have been associated with an increased risk of serious infection compared to conventional DMARDs (71–77). Most reports to date have focused on the risk of bacterial and opportunistic infections. Less attention has been directed to viral, and particularly viral respiratory, infections. An exception is the increased risk of herpes zoster observed with JAK inhibition (78–80). Although mechanisms linking these agents to the reactivation of herpes zoster are unclear, dampening of innate antiviral effects of type I and type II interferons has been suggested to play a role (81).

Conducted primarily in the context of rheumatoid arthritis, studies examining tapering or discontinuation of biologics or JAK inhibitors suggest that a large proportion of patients experience rheumatic disease flare (82–85). This is relevant because underlying inflammation or disease activity has been implicated as a risk factor for infection (86,87), a risk that may be heightened further in the context of “rescue” glucocorticoids. Although biologic therapies are associated with an increased risk of hospitalization due to serious infection, at least one report in rheumatoid arthritis has suggested that they are associated with a reduced risk of sepsis or fatal outcome, as compared to nonbiologic DMARDs, among patients developing serious infection with these therapies (88). These data provide support for the task force’s recommendation to continue all immunosuppressants (e.g., tacrolimus, cyclosporin A [CSA], mycophenolate mofetil [MMF], or azathioprine), biologics, and JAK inhibitors in patients with stable rheumatic disease in the absence of COVID-19 or SARS-CoV-2 exposure. For patients with inflammatory arthritis in whom optimal csDMARD therapy has been unsuccessful, or those treated with an IL-6 receptor inhibitor facing a potential drug shortage (25), the task force recommended consideration of a biologic treatment but expressed uncertainty with regard to the safety of JAK inhibition in either situation. This uncertainty centered on a reported dampening of innate antiviral pathways with JAK inhibition (80).

In contrast, emerging data suggest that some immunosuppressants, biologics, and/or JAK inhibitors could theoretically mitigate the severe impact of COVID-19, favoring their continued use or initiation in the management of rheumatic disease (89). MMF, for instance, has been associated with improved survival following MERS-CoV infection (90), while CSA inhibits coronavirus replication *in vitro* (91,92). Baricitinib, a JAK inhibitor, interferes with cellular endocytosis and could theoretically impair cellular entry of SARS-CoV-2 (44,93). Whether this property impacts infection risk is unknown. In a small, uncontrolled cohort study of 21 patients with COVID-19 (none with rheumatic disease and all with severe/critical respiratory involvement), tocilizumab administration was associated with marked clinical improvement (94). Recognizing that hyperinflammation and cytokine storm appear to play a central role in severe manifestations of COVID-19 (95), select cytokine inhibitors (along with glucocorticoids and other targeted

small molecules) have been proposed as potential treatments, with many of these agents under active investigation in randomized controlled trials (RCTs) (96–100).

In the absence of robust RCT data to support their continued use, the task force recommended temporarily withholding or stopping all non-IL-6 biologics, immunosuppressants (e.g., tacrolimus, CSA, MMF, and azathioprine), and JAK inhibitors in the context of documented or presumptive COVID-19, as well as after known SARS-CoV-2 exposure. The task force endorsed the notion that, in select circumstances, IL-6 receptor inhibition could be continued in the setting of SARS-CoV-2 infection or following exposure, although corresponding votes achieved only the minimal threshold for approval (both with median vote ratings of 7 and moderate consensus). In discussions relevant to IL-6 receptor inhibition, the panel emphasized the need for shared decision-making between patients and inpatient care teams and endorsed participation in research protocols.

Reinitiating therapies after COVID-19. Following publication of the initial guidance document, the task force approved 3 additional statements specific to reinitiating rheumatic disease treatments withheld following a diagnosis of COVID-19 (Supplementary Table 7, <http://onlinelibrary.wiley.com/doi/10.1002/art.41596/abstract>), which were combined to form 2 additional guidance statements (Table 5). Evidence supporting these is limited. In a small study of 9 patients with uncomplicated COVID-19 (none with rheumatic disease) (101), infectious SARS-CoV-2 (isolation of live virus) was not detected in nasopharyngeal samples from any patient after 8 days of symptoms (102). Moreover, 2 weeks post-symptom onset (often coinciding with symptom resolution in uncomplicated COVID-19), all patients had detectable antibodies to SARS-CoV-2. Some data suggest that the presence of detectable antibodies may provide longer-term protection (102–104). Although evidence supporting the approach is limited, a symptom-free period of at least 3 days has been used as a clinical surrogate for the development of protective adaptive immune responses following COVID-19.

The task force did not endorse routine polymerase chain reaction (PCR) viral testing or SARS-CoV-2 antibody testing to guide the reinitiation of rheumatic disease treatments. PCR results in select patients have remained positive for periods approaching 30 days (102), well after patients are considered infectious. Requiring a negative PCR result before reinitiating treatment could therefore lead to unnecessarily long delays and result in higher risk of rheumatic disease flare.

With the understanding that individuals developing COVID-19 may be infectious for days before symptom onset, longer delays in reinitiating treatment may be warranted in patients who test positive but remain asymptomatic. In patients with severe COVID-19 (~20% of cases), characterized by pneumonia and sometimes requiring hospitalization, symptom duration can exceed 2 weeks. In such cases, the task force believed decisions

regarding reinitiation of rheumatic disease treatment should be made on a case-by-case basis.

DISCUSSION

This ACR guidance document serves as a tool for rheumatology providers to promote optimal care for patients with complex rheumatic disease conditions in the context of the ongoing COVID-19 pandemic. The guidance provided is not intended to be proscriptive nor should it be used to limit treatment options available for patients with rheumatic disease in our current health care climate.

Although the evidence report generated as part of this effort drew on a considerable number of sources, resulting guidance is supported only by very low-quality evidence. In nearly all cases, the evidence identified was indirect and included reports focused on either different infectious etiologies or retrospective cohorts of patients with COVID-19 without consideration of underlying rheumatic disease state. As a result, all of the guidance provided should be considered “conditional” (105,106). However, the literature in this area is rapidly evolving. A PubMed search limited to the time frame from January 1 through March 31 of 2020 resulted in >2,500 citations using the search term “COVID-19.” The same search covering the first half of April resulted in >2,100 citations. As available literature focused on COVID-19 in rheumatic disease populations expands, we anticipate that current knowledge gaps will be addressed.

There are several strengths to this effort that are noteworthy. Responding to the urgency of need, the task force generated guidance over a compressed time frame, while simultaneously leveraging a well-established method of consensus building (modified Delphi in the context of the RAND/UCLA appropriateness method). The panel charged with guidance development included both rheumatologists and infectious disease specialists with broad expertise in relevant clinical areas and representing different regions, disease interests, and practice environments.

We acknowledge limitations in this effort as well. Although the document touches on a broad range of topics, the guidance generated is not comprehensive and does not follow the rigorous guideline methodology routinely used by the ACR when formal clinical practice guidelines are generated. Although this document addresses the administration of many different rheumatology treatments, it does not provide guidance on other medications used in rheumatology practice. Other questions remain. For example, when choosing a new therapy, how should currently available biologics or targeted small molecule therapies be prioritized? What is the impact of COVID-19 on disease activity or function, in both the short- and the long-term? Are rheumatology treatments safe with the coadministration of emerging COVID-19 treatments?

As these and other questions are addressed and new information becomes available, this guidance document will

continue to be revisited, expanded, and perhaps, in some cases, amended. The ACR is committed to maintaining this as a “living document,” allowing needed modifications throughout the pandemic in order to facilitate optimal outcomes in patients with rheumatic disease.

AUTHOR CONTRIBUTIONS

All authors were involved in drafting the article or revising it critically for important intellectual content, and all authors approved the final version to be published. Dr. Mikuls had full access to all of the data in the study and takes responsibility for the integrity of the data and the accuracy of the data analysis.

Study conception and design. Mikuls, Johnson, Fraenkel, Baden, Bermas, Chatham, Costenbader, Gravallesse, Kalil, Weinblatt, Winthrop, Turner, Saag.

Acquisition of data. Mikuls, Johnson, Fraenkel, Arasaratnam, Baden, Bermas, Chatham, Cohen, Costenbader, Kalil, Weinblatt, Winthrop, Mudano, Turner, Saag.

Analysis and interpretation of data. Mikuls, Johnson, Fraenkel, Baden, Bermas, Chatham, Cohen, Costenbader, Gravallesse, Kalil, Weinblatt, Winthrop, Mudano, Turner, Saag.

REFERENCES

- Zhu N, Zhang D, Wang W, Li X, Yang B, Song J, et al. A novel coronavirus from patients with pneumonia in China, 2019. *N Engl J Med* 2020;382:727–33.
- Arthritis foundation. URL: <https://www.arthritis.org/>.
- GHLF Creakyjoints. URL: <https://creakyjoints.org/>.
- Global Healthy Living Foundation. URL: <https://www.ghlf.org/>.
- Brook R. US Agency for Health Care Policy and Research Office of the Forum for Quality and Effectiveness in Health Care clinical practice guideline development: methodology perspectives. In: McCormick MS, Siegel R, editors. *The RAND/UCLA appropriateness method*. Rockville, MD: US Department of Health and Human Services, Public Health Service, Agency for Health Care Policy and Research; 1994: p. 59–70.
- Shekelle PG, Kahan JP, Bernstein SJ, Leape LL, Kamberg CJ, Park RE. The reproducibility of a method to identify the overuse and underuse of medical procedures. *N Engl J Med* 1998;338:1888–95.
- Shekelle PG, Chassin MR, Park RE. Assessing the predictive validity of the RAND/UCLA appropriateness method criteria for performing carotid endarterectomy. *Int J Technol Assess Health Care* 1998;14:707–27.
- Hemingway H, Chen R, Junghans C, Timmis A, Eldridge S, Black N, et al. Appropriateness criteria for coronary angiography in angina: reliability and validity. *Ann Intern Med* 2008;149:221–31.
- Kravitz RL, Laouri M, Kahan JP, Guzy P, Sherman T, Hilborne L, et al. Validity of criteria used for detecting underuse of coronary revascularization. *JAMA* 1995;274:632–8.
- Shekelle PG, MacLean CH, Morton SC, Wenger NS. Assessing care of vulnerable elders: methods for developing quality indicators. *Ann Intern Med* 2001;135:647–52.
- Wu C, Chen X, Cai Y, Xia J, Zhou X, Xu S, et al. Risk factors associated with acute respiratory distress syndrome and death in patients with coronavirus disease 2019 pneumonia in Wuhan, China. *JAMA Intern Med* 2020;180:1–11.
- Zhou F, Yu T, Du R, Fan G, Liu Y, Liu Z, et al. Clinical course and risk factors for mortality of adult in patients with COVID-19

- in Wuhan, China: a retrospective cohort study. *Lancet* 2020;395:1054–62.
13. Yang J, Zheng Y, Gou X, Pu K, Chen Z, Guo Q, et al. Prevalence of comorbidities in the novel Wuhan coronavirus (COVID-19) infection: a systematic review and meta-analysis. *Int J Infect Dis* 2020;94:91–5.
 14. Richardson S, Hirsch JS, Narasimhan M, Crawford JM, McGinn T, Davidson KW, et al. Presenting characteristics, comorbidities, and outcomes among 5700 patients hospitalized with COVID-19 in the New York City area. *JAMA* 2020;323:2052–9.
 15. Nurmohamed MT, Heslinga M, Kitas GD. Cardiovascular comorbidity in rheumatic diseases [review]. *Nat Rev Rheumatol* 2015;11:693–704.
 16. Bichile T, Petri M. Prevention and management of co-morbidities in SLE. *Presse Med* 2014;43:e187–95.
 17. Mikuls TR. Co-morbidity in rheumatoid arthritis. *Best Pract Res Clin Rheumatol* 2003;17:729–52.
 18. Burner TW, Rosenthal AK. Diabetes and rheumatic diseases. *Curr Opin Rheumatol* 2009;21:50–4.
 19. Sarzi-Puttini P, Giorgi V, Sirotti S, Marotto D, Ardizzone S, Rizzardini G, et al. COVID-19, cytokines and immunosuppression: what can we learn from severe acute respiratory syndrome? *Clin Exp Rheumatol* 2020;38:337–42.
 20. Liu Z, Long W, Tu M, Chen S, Huang Y, Wang S, et al. Lymphocyte subset (CD4+, CD8+) counts reflect the severity of infection and predict the clinical outcomes in patients with COVID-19 [letter]. *J Infect* 2020;6:43.
 21. Giwa AL, Desai A, Duca A. Novel 2019 coronavirus SARS-CoV-2 (COVID-19): an overview for emergency clinicians. *Pediatr Emerg Med Pract* 2020;17:1–24.
 22. Terpos E, Ntanasis-Stathopoulos I, Elalamy I, Kastritis E, Sergentanis TN, Politou M, et al. Hematological findings and complications of COVID-19 [review]. *Am J Hematol* 2020;95:834–47.
 23. Centers for Disease Control and Prevention. How to protect yourself & others. 2020. URL: <https://www.cdc.gov/coronavirus/2019-ncov/prevent-getting-sick/prevention.html>.
 24. Centers for Disease Control and Prevention. What to do if you are sick. May 2020. URL: <https://www.cdc.gov/coronavirus/2019-ncov/if-you-are-sick/steps-when-sick.html>.
 25. American College of Rheumatology. COVID-19 practice and advocacy resources. May 2020. URL: <https://www.rheumatology.org/Announcements/COVID-19-Practice-and-Advocacy#Telehealth>.
 26. Tsourdi E, Langdahl B, Cohen-Solal M, Aubry-Rozier B, Eriksen EF, Guañabens N, et al. Discontinuation of denosumab therapy for osteoporosis: a systematic review and position statement by ECTS. *Bone* 2017;105:11–7.
 27. Fang L, Karakiulakis G, Roth M. Are patients with hypertension and diabetes mellitus at increased risk for COVID-19 infection? *Lancet Respir Med* 2020;8:e21.
 28. Danser AH, Epstein M, Batlle D. Renin-angiotensin system blockers and the COVID-19 pandemic: at present there is no evidence to abandon renin-angiotensin system blockers. *Hypertension* 2020;75:1382–5.
 29. Younes A, Samad N. Utility of mTOR inhibition in hematologic malignancies. *Oncologist* 2011;16:730–41.
 30. American Heart Association. Patients taking ACE-i and ARBs who contract COVID-19 should continue treatment, unless otherwise advised by their physician. March 2020. URL: <https://newsroom.heart.org/news/patients-taking-ace-i-and-arbs-who-contrast-covid-19-should-continue-treatment-unless-otherwise-advised-by-their-physician>.
 31. Zhang P, Zhu L, Cai J, Lei F, Qin JJ, Xie J, et al. Association of inpatient use of angiotensin converting enzyme inhibitors and angiotensin II receptor blockers with mortality among patients with hypertension hospitalized with COVID-19. *Circ Res* 2020;126:1671–81.
 32. Tselios K, Koumaras C, Urowitz MB, Gladman DD. Do current arterial hypertension treatment guidelines apply to systemic lupus erythematosus patients? A critical appraisal. *Semin Arthritis Rheum* 2014;43:521–5.
 33. De Vries-Bouwstra JK, Allanore Y, Matucci-Cerinic M, Balbir-Gurman A. Worldwide expert agreement on updated recommendations for the treatment of systemic sclerosis. *J Rheumatol* 2020;47:249–54.
 34. FitzGerald GA. Misguided drug advice for COVID-19. *Science* 2020;367:1434.
 35. US Food and Drug Administration. FDA advises patients on use of non-steroidal anti-inflammatory drugs (NSAIDs) for COVID-19. March 2020. URL: <https://www.fda.gov/drugs/drug-safety-and-availability/fda-advises-patients-use-non-steroidal-anti-inflammatory-drugs-nsaids-covid-19>.
 36. Cheng Y, Luo R, Wang K, Zhang M, Wang Z, Dong L, et al. Kidney disease is associated with in-hospital death of patients with COVID-19. *Kidney Int* 2020;97:829–38.
 37. Shi S, Qin M, Shen B, Cai Y, Liu T, Yang F, et al. Association of cardiac injury with mortality in hospitalized patients with COVID-19 in Wuhan, China. *JAMA Cardiol* 2020;5:802–10.
 38. Wang D, Hu B, Hu C, Zhu F, Liu X, Zhang J, et al. Clinical characteristics of 138 hospitalized patients with 2019 novel coronavirus-infected pneumonia in Wuhan, China. *JAMA* 2020;323:1061–9.
 39. National Institute for Health and Care Excellence. COVID-19 rapid guideline: managing symptoms (including at the end of life) in the community. April 2020. URL: <https://www.nice.org.uk/guidance/ng163>.
 40. Zhang C, Shi L, Wang FS. Liver injury in COVID-19: management and challenges. *Lancet Gastroenterol Hepatol* 2020;5:428–30.
 41. Qin X, Qiu S, Yuan Y, Zong Y, Tuo Z, Li J, et al. Clinical characteristics and treatment of patients infected with COVID-19 in Shishou, China. *Lancet* 2020. URL: <https://ssrn.com/abstract=3541147>.
 42. D'Antiga L. Coronaviruses and immunosuppressed patients: the facts during the third epidemic [letter]. *Liver Transpl* 2020;26:832–4.
 43. RECOVERY Collaborative Group. Dexamethasone in hospitalized patients with COVID-19: preliminary report. *N Engl J Med* 2020. E-pub ahead of print.
 44. Richardson P, Griffin I, Tucker C, Smith D, Oechsle O, Phelan A, et al. Baricitinib as potential treatment for 2019-nCoV acute respiratory disease. *Lancet* 2020;395:e30–1.
 45. Lee N, Chan KC, Hui DS, Ng EK, Wu A, Chiu RW, et al. Effects of early corticosteroid treatment on plasma SARS-associated coronavirus RNA concentrations in adult patients. *J Clin Virol* 2004;31:304–9.
 46. Ni YN, Chen G, Sun J, Liang BM, Liang ZA. The effect of corticosteroids on mortality of patients with influenza pneumonia: a systematic review and meta-analysis. *Crit Care* 2019;23:99.
 47. Pappas DA, Hooper MM, Kremer JM, Reed G, Shan Y, Wenkert D, et al. Herpes zoster reactivation in patients with rheumatoid arthritis: analysis of disease characteristics and disease-modifying antirheumatic drugs. *Arthritis Care Res (Hoboken)* 2015;67:1671–8.
 48. Chen D, Li H, Xie J, Zhan Z, Liang L, Yang X. Herpes zoster in patients with systemic lupus erythematosus: clinical features, complications and risk factors. *Exp Ther Med* 2017;14:6222–8.
 49. Youssef J, Novosad SA, Winthrop KL. Infection risk and safety of corticosteroid use. *Rheum Dis Clin North Am* 2016;42:157–76.
 50. Zhou F, Yu T, Du R, Fan G, Liu Y, Liu Z, et al. Clinical course and risk factors for mortality of adult inpatients with COVID-19 in Wuhan, China: a retrospective cohort study. *Lancet* 2020;395:1054–62.

51. LaRoche GE Jr, LaRoche AG, Ratner RE, Borenstein DG. Recovery of the hypothalamic-pituitary-adrenal (HPA) axis in patients with rheumatic diseases receiving low-dose prednisone. *Am J Med* 1993;95:258–64.
52. Ibrahim A, Ahmed M, Conway R, Carey JJ. Risk of infection with methotrexate therapy in inflammatory diseases: a systematic review and meta-analysis. *J Clin Med* 2018;8:E15.
53. Bernatsky S, Hudson M, Suissa S. Anti-rheumatic drug use and risk of serious infections in rheumatoid arthritis. *Rheumatology (Oxford)* 2007;46:1157–60.
54. Yao X, Ye F, Zhang M, Cui C, Huang B, Niu P, et al. In vitro antiviral activity and projection of optimized dosing design of hydroxychloroquine for the treatment of severe acute respiratory syndrome coronavirus 2 (SARS-CoV-2). *Clin Infect Dis* 2020. E-pub ahead of print.
55. Gautret P, Lagier JC, Parola P, Hoang VT, Meddeb L, Mailhe M, et al. Hydroxychloroquine and azithromycin as a treatment of COVID-19: results of an open-label non-randomized clinical trial. *Int J Antimicrob Agents* 2020:105949. E-pub ahead of print.
56. US Food and Drug Administration. Coronavirus (COVID-19) update: daily roundup. March 2020. URL: <https://www.fda.gov/news-events/press-announcements/coronavirus-covid-19-update-daily-round-up-march-30-2020>.
57. Wang M, Cao R, Zhang L, Yang X, Liu J, Xu M, et al. Remdesivir and chloroquine effectively inhibit the recently emerged novel coronavirus (2019-nCoV) in vitro. *Cell Res* 2020;30:269–71.
58. Gao J, Tian Z, Yang X. Breakthrough: chloroquine phosphate has shown apparent efficacy in treatment of COVID-19 associated pneumonia in clinical studies. *Biosci Trends* 2020;14:72–3.
59. US Food and Drug Administration. FDA drug shortages. April 2020. URL: https://www.accessdata.fda.gov/scripts/drugshortages/dsp_ActiveIngredientDetails.cfm?AI=Hydroxychloroquine+Sulfate+Tablets&st=c&tab=tabs-4&panels=0.
60. Mok CC, Penn HJ, Chan KL, Tse SM, Langman LJ, Jannetto PJ. Hydroxychloroquine serum concentrations and flares of systemic lupus erythematosus: a longitudinal cohort analysis. *Arthritis Care Res (Hoboken)* 2016;68:1295–302.
61. Geraldino-Pardilla L, Perel-Winkler A, Miceli J, Neville K, Danias G, Nguyen S, et al. Association between hydroxychloroquine levels and disease activity in a predominantly Hispanic systemic lupus erythematosus cohort. *Lupus* 2019;28:862–7.
62. Peart E, Clowse ME. Systemic lupus erythematosus and pregnancy outcomes: an update and review of the literature. *Curr Opin Rheumatol* 2014;26:118–23.
63. Canadian Hydroxychloroquine Study Group. A randomized study of the effect of withdrawing hydroxychloroquine sulfate in systemic lupus erythematosus. *N Engl J Med* 1991;324:150–4.
64. Tsakonas E, Joseph L, Esdaile JM, Choquette D, Sénécal JL, Cividino A, et al, for the Canadian Hydroxychloroquine Study Group. A long-term study of hydroxychloroquine withdrawal on exacerbations in systemic lupus erythematosus. *Lupus* 1998;7:80–5.
65. Mercurio NJ, Yen CF, Shim DJ, Maher TR, McCoy CM, Zimetbaum PJ, et al. Risk of QT interval prolongation associated with use of hydroxychloroquine with or without concomitant azithromycin among hospitalized patients testing positive for Coronavirus Disease 2019 (COVID-19). *JAMA Cardiol* 2020;5:1036–41.
66. Bessiere F, Rocca H, Deliniere A, Charriere R, Chevalier P, Argaud L, et al. Assessment of QT intervals in a case series of patients with Coronavirus Disease 2019 (COVID-19) infection treated with hydroxychloroquine alone or in combination with azithromycin in an intensive care unit. *JAMA Cardiol* 2020;5:1067–9.
67. Farre N, Mojon D, Llagostera M, Belarte-Tornero LC, Calvo-Fernandez A, Valles E, et al. Prolonged QT interval in SARS-CoV-2 infection: prevalence and prognosis. *J Clin Med* 2020;9:e2712.
68. Roden DM, Harrington RA, Poppas A, Russo AM. Considerations for drug interactions on QTc in exploratory COVID-19 treatment. *Circulation* 2020;141:e906–7.
69. Bonow RO, Fonarow GC, O’Gara PT, Yancy CW. Association of coronavirus disease 2019 (COVID-19) with myocardial injury and mortality [editorial]. *JAMA Cardiol* 2020;5:751–3.
70. Naksuk N, Lazar S, Peerapattit TB. Cardiac safety of off-label COVID-19 drug therapy: a review and proposed monitoring protocol. *Eur Heart J Acute Cardiovasc Care* 2020;9:215–21.
71. Listing J, Gerhold K, Zink A. The risk of infections associated with rheumatoid arthritis, with its comorbidity and treatment. *Rheumatology (Oxford)* 2013;52:53–61.
72. Tudesq JJ, Cartron G, Riviere S, Morquin D, Lordache L, Mahr A, et al. Clinical and microbiological characteristics of the infections in patients treated with rituximab for autoimmune and/or malignant hematological disorders [review]. *Autoimmun Rev* 2018;17:115–24.
73. Singh JA, Cameron C, Noorbaloochi S, Cullis T, Tucker M, Christensen R, et al. Risk of serious infection in biological treatment of patients with rheumatoid arthritis: a systematic review and meta-analysis. *Lancet* 2015;386:258–65.
74. Singh JA. Infections with biologics in rheumatoid arthritis and related conditions: a scoping review of serious or hospitalized infections in observational studies. *Curr Rheumatol Rep* 2016;18:61.
75. Strangfeld A, Eveslage M, Schneider M, Bergerhausen HJ, Klopsch T, Zink A, et al. Treatment benefit or survival of the fittest: what drives the time-dependent decrease in serious infection rates under TNF inhibition and what does this imply for the individual patient? *Ann Rheum Dis* 2011;70:1914–20.
76. Grijalva CG, Chen L, Delzell E, Baddley JW, Beukelman T, Winthrop KL, et al. Initiation of tumor necrosis factor- α antagonists and the risk of hospitalization for infection in patients with autoimmune diseases. *JAMA* 2011;306:2331–9.
77. Galloway JB, Hyrich KL, Mercer LK, Dixon WG, Fu B, Ustianowski AP, et al. Anti-TNF therapy is associated with an increased risk of serious infections in patients with rheumatoid arthritis especially in the first 6 months of treatment: updated results from the British Society for Rheumatology Biologics Register with special emphasis on risks in the elderly. *Rheumatology (Oxford)* 2011;50:124–31.
78. Zhang N, Wilkinson S, Riaz M, Östör AJ, Nisar MK. Does methotrexate increase the risk of varicella or herpes zoster infection in patients with rheumatoid arthritis? A systematic literature review. *Clin Exp Rheumatol* 2012;30:962–71.
79. Strangfeld A, Listing J, Herzer P, Liebhaber A, Rockwitz K, Richter C, et al. Risk of herpes zoster in patients with rheumatoid arthritis treated with anti-TNF- α agents. *JAMA* 2009;301:737–44.
80. Winthrop KL, Curtis JR, Lindsey S, Tanaka Y, Yamaoka K, Valdez H, et al. Herpes zoster and tofacitinib: clinical outcomes and the risk of concomitant therapy. *Arthritis Rheumatol* 2017;69:1960–8.
81. Winthrop KL. The emerging safety profile of JAK inhibitors in rheumatic disease [review]. *Nat Rev Rheumatol* 2017;13:320.
82. Smolen JS, Nash P, Durez P, Hall S, Ilivanova E, Irazoque-Palazuelos F, et al. Maintenance, reduction, or withdrawal of etanercept after treatment with etanercept and methotrexate in patients with moderate rheumatoid arthritis (PRESERVE): a randomised controlled trial. *Lancet* 2013;381:918–29.
83. Van Vollenhoven RF, Østergaard M, Leirisalo-Repo M, Uhlig T, Jansson M, Larsson E, et al. Full dose, reduced dose or discontinuation of etanercept in rheumatoid arthritis. *Ann Rheum Dis* 2016;75:52–8.
84. Smolen JS, Emery P, Fleischmann R, van Vollenhoven RF, Pavelka K, Durez P, et al. Adjustment of therapy in rheumatoid arthritis on

- the basis of achievement of stable low disease activity with adalimumab plus methotrexate or methotrexate alone: the randomised controlled OPTIMA trial. *Lancet* 2014;383:321–32.
85. Takeuchi T, Genovese MC, Haraoui B, Li Z, Xie L, Klar R, et al. Dose reduction of baricitinib in patients with rheumatoid arthritis achieving sustained disease control: results of a prospective study. *Ann Rheum Dis* 2019;78:171–8.
 86. Au K, Reed G, Curtis JR, Kremer JM, Greenberg JD, Strand V, et al. High disease activity is associated with an increased risk of infection in patients with rheumatoid arthritis. *Ann Rheum Dis* 2011;70:785–91.
 87. Pimentel-Quiroz VR, Ugarte-Gil MF, Harvey GB, Wojdyla D, Pons-Estel GJ, Quintana R, et al. Factors predictive of serious infections over time in systemic lupus erythematosus patients: data from a multi-ethnic, multi-national, Latin American lupus cohort. *Lupus* 2019;28:1101–10.
 88. Richter A, Listing J, Schneider M, Klopsch T, Kapelle A, Kaufmann J, et al. Impact of treatment with biologic DMARDs on the risk of sepsis or mortality after serious infection in patients with rheumatoid arthritis. *Ann Rheum Dis* 2016;75:1667–73.
 89. Favalli EG, Ingegnoli F, de Lucia O, Cincinelli G, Cimaz R, Caporali R. COVID-19 infection and rheumatoid arthritis: faraway, so close! [review]. *Autoimmun Rev* 2020;102523.
 90. Al Ghamdi M, Alghamdi KM, Ghandoor Y, Alzahrani A, Salah F, Alsulami A, et al. Treatment outcomes for patients with Middle Eastern Respiratory Syndrome Coronavirus (MERS CoV) infection at a coronavirus referral center in the Kingdom of Saudi Arabia. *BMC Infect Dis* 2016;16:174.
 91. Tanaka Y, Sato Y, Sasaki T. Suppression of coronavirus replication by cyclophilin inhibitors. *Viruses* 2013;5:1250–60.
 92. De Wilde AH, Zevenhoven-Dobbe JC, van der Meer Y, Thiel V, Narayanan K, Makino S, et al. Cyclosporin A inhibits the replication of diverse coronaviruses. *J Gen Virol* 2011;92:2542–8.
 93. Stebbing J, Phelan A, Griffin I, Tucker C, Oechsle O, Smith D, et al. COVID-19: combining antiviral and anti-inflammatory treatments. *Lancet Infect Dis* 2020;20:400–2.
 94. Xu X, Han M, Li T, Sun W, Wang D, Fu B, et al. Effective treatment of severe COVID-19 patients with tocilizumab. February 2020. URL: <https://www.ser.es/wp-content/uploads/2020/03/TCZ-and-COVID-19.pdf>.
 95. McGonagle D, Sharif K, O'Regan A, Bridgwood C. The role of cytokines including interleukin-6 in COVID-19 induced pneumonia and macrophage activation syndrome-like disease. *Autoimmun Rev* 2020;102537.
 96. ClinicalTrials.gov. National Library of Medicine. Efficacy and safety of emapalumab and anakinra in reducing hyperinflammation and respiratory distress in patients with COVID-19 infection. April 2020. URL: <https://clinicaltrials.gov/ct2/show/NCT04324021>.
 97. ClinicalTrials.gov. National Library of Medicine. Anti-IL6 treatment of serious COVID-19 disease with threatening respiratory failure (TOCIDVID). April 2020. URL: <https://www.clinicaltrials.gov/ct2/show/NCT04322773>.
 98. ClinicalTrials.gov. National Library of Medicine. Tocilizumab vs CRRT in management of cytokine release syndrome (CRS) in COVID-19 (TACOS). April 2020. URL: <https://clinicaltrials.gov/ct2/show/NCT04306705>.
 99. ClinicalTrials.gov. National Library of Medicine. Evaluation of the efficacy and safety of sarilumab in hospitalized patients with COVID-19. April 2020. URL: <https://clinicaltrials.gov/ct2/show/NCT04315298>.
 100. ClinicalTrials.gov. National Library of Medicine. Treatment of moderate to severe coronavirus disease (COVID-19) in hospitalized patients. April 2020. URL: <https://clinicaltrials.gov/ct2/show/NCT04321993>.
 101. World Health Organization. Report of the WHO-China Joint Mission on Coronavirus Disease 2019 (COVID-19). URL: <https://www.who.int/docs/default-source/coronaviruse/who-china-joint-mission-on-covid-19-final-report.pdf>.
 102. Wölfel R, Cormann VM, Guggemos W, Seilmaier M, Zange S, Müller MA, et al. Virological assessment of hospitalized patients with COVID-19. *Nature* 2020;581:465–9.
 103. To KK, Tsang OT, Leung WS, Tam AR, Wu TC, Lung DC, et al. Temporal profiles of viral load in posterior oropharyngeal saliva samples and serum antibody responses during infection by SARS-CoV-2: an observational cohort study. *Lancet Infect Dis* 2020;20:565–74.
 104. Shen C, Wang Z, Zhao F, Yang Y, Li J, Yuan J, et al. Treatment of 5 critically ill patients with COVID-19 with convalescent plasma. *JAMA* 2020;323:1582–9.
 105. Andrews JC, Schünemann HJ, Oxman AD, Pottie K, Meerpohl JJ, Coello PA, et al. GRADE guidelines: 15—going from evidence to recommendation—determinants of a recommendation's direction and strength. *J Clin Epidemiol* 2013;66:726–35.
 106. Andrews J, Guyatt G, Oxman AD, Alderson P, Dahm P, Falck-Ytter Y, et al. GRADE guidelines: 14—going from evidence to recommendations: the significance and presentation of recommendations. *J Clin Epidemiol* 2013;66:719–25.